

METHODOLOGY TOWARDS ACCESSING SMALL MOLECULE HETEROCYCLES FOR
H2OS AND TB PROTEASOME MODULATION

By

Travis Kordero Bethel

A DISSERTATION

Submitted to
Michigan State University
in partial fulfillment of the requirements
for the degree of

Chemistry – Doctor of Philosophy

2018

ABSTRACT

METHODOLOGY TOWARDS ACCESSING SMALL MOLECULE HETEROCYCLES FOR H2OS AND TB PROTEASOME MODULATION

By

Travis Kordero Bethel

This dissertation focused on the development and advancement of methodology for accessing imidazoline scaffolds and other small heterocyclic molecules for biological evaluation. Past research within the Tepe group has correlated functionalized 2-imidazolines to proteasome modulation. Further diversification of the methodology for accessing these 2-imidazoline scaffolds, has allowed for the synthesis of a small library of analogs for SAR evaluation with the h2OS proteasome. These findings were used to further experimentally model and synthesize more efficacious 2-imidazoline derivatives for proteasome modulation. The proteasome is responsible for the degradation of polyubiquitinated proteins in the cell, producing amino acids that can then be used for alternative cellular functions. The introduction of small heterocyclic molecules like 2-imidazolines, bind to the proteasome and lower its efficacy for protein digestion through modulation of its activity.

This dissertation is dedicated to the loving memory of Tamaz Monica Thompson. My best friend, my confidant, my role model, I wouldn't be here without you. This and everything I continue to do will reflect our 26 years of cherished friendship. We will continue this journey together, as each day I carry your heart in my heart.

ACKNOWLEDGMENTS

I would like to take the time out to thank the people truly responsible for motivating me, teaching me as well as shaping me into the person and scientist I am today.

To my committee members:

Dr. Jetze J. Tepe, thank you for being an amazing mentor. I vividly remember our first conversation, in which I sat in your office and asked for the chance to work with you. There was no reason for you to believe in me, and yet without hesitation you accepted me, giving me a position in your research group. At the time when I needed a mentor, you rose to the occasion and have truly taught me everything I know when it comes to teaching and understanding organic chemistry. Thank you for thrusting so much responsibility on me, having that duty made me a more aware researcher and in turn modeled me into better chemist and person. Because of you, I better understand how to approach balancing a successful research group with the responsibilities of teaching chemistry and bringing more people into the fields of STEM. I am able to support my family and help change their life for the better and that is only due to you. You took an immature kid with a desire to prove his worth and transformed him into a chemist whose focus has evolved from proving his worth, to desiring to help others through science. Where I was lacking focus, you helped me find it. Where I was lacking maturity, you helped me develop it. Where I was lacking knowledge, you instilled it. There will never be anything I can do to repay you for the investment in me, my family and our future. Anyone that I am able to inspire to pursue a scientific career, and any impact I am able to achieve in the fields of research are solely due to you taking a risk and

believing in me. To be honest, I don't know what made you believe in me, on that faithful day of our first encounter but I am so grateful that you saw potential in me. I am thankful that through all the stressful times you never gave up on me. I find myself explaining key concepts in organic chemistry to students and having flash backs to when you carefully explained those same things to me. It's memories like those that color my day and motivate me to also teach others and expand their horizons, just like you did for me. Once again Dr. Tepe, my friends, my family and I want to thank you for the amazing experience of being under your tutelage. I will always consider myself a proud member of the Tepe group.

Dr. William D. Wulff, thanks for cultivating my creativity as a synthetic organic chemist. CEM 850 and CEM 852 were pivotal introducing new concepts of organic chemistry to me. It emphasized the creative process of transforming commercially available starting materials to the desired products. It also showed me so many different approaches to developing problem solving skills when synthesizing compounds.

Dr. Robert Maleczka, thank you for demanding the best from students. By setting such a standard of rigor I was able to hone my craft and always push beyond what I thought I was capable of, because I wanted to show you my growth and gain your approval.

Dr. Gary Blanchard, thank you for being a great example of the kind of professor, teacher, an person I aspire to be.

To my family and friends:

Dr. Matthew B. Giletto, thank you for being an amazing lab mate and friend throughout the entirety of our graduate school experience. I have treasured every moment of navigating organic chemistry with your helpful feedback and perfectly timed jokes and impersonations. I look forward to seeing just how much fun we can get into now that we are both done with graduate school.

Corey L. Jones, thank you for the endless laughter and amazing experiences, throughout graduate school. I have truly enjoyed every moment spent as your lab mate. Continue with that same furious passion for science, because I am certain that you have a place amongst the greats of our time. I have always been impressed with both your intellect and your humility. I am sure that you will be an amazing chemist.

Evert Njomen, thank you for being such an amazing balancing force in our lab. I have enjoyed every second of having you as a lab mate. I have learnt so much from you. Your amazing work ethic helped push me to even greater heights. I am so excited to see what the future holds for you.

Dr. Carmin Burrell, thank you for being the most amazing friend a guy could ask for. I am so grateful to MSU for transforming me into a great chemist, but I am more thankful to MSU for introducing me to such an amazing soul. You colour my black and white days with your amazing personality and I am so blessed to have someone like you as my best friend. I look forwards to all our future adventures.

To my sister **Trevisa**, For the longest time it has just been you and I, thank you for being an amazing support system. I have always watched you and have molded my life based on the yours and your experiences. You have single handedly changed my life by having the most amazing kids and making me an uncle. That responsibility has helped to mold me into the man that I am today. Thank you for giving me the two most amazing gifts ever, my niece Maia and my nephew Corey. I look forward to every moment of watching those two grow up into amazing adults, and that is all thanks to you.

To my mom and dad, **Patricia** and **Trevor**. I would like to take the time out to thank my personal heroes, my mom and dad. Thank you for the painstaking work you both put into the development of my sister and me. You have both sacrificed so much for us and given us more than we could have ever imagined. I look back fondly with only good memories of how life has been, and I know that is solely due to you two. I can't imagine what it must have been like, and even now I'm astonished at how much you all have achieved. I only hope that I can be just as successful as you are. Thank you for believing in that 5-year-old child that came to you and said that he wanted to become a scientist. Since that day I have felt nothing but love and support towards this. I can finally say with great excitement that we have done it together.

TABLE OF CONTENTS

LIST OF TABLES	ix
LIST OF FIGURES	x
LIST OF SCHEMES.....	xx
KEY TO SYMBOLS AND ABBREVIATIONS.....	xxiv
CHAPTER ONE – APPROACHES TO 2-IMIDAZOLINE SYNTHESIS	1
CHAPTER TWO – IMIDAZOLINE SAR EVALUATION FOR TB PROTEASOME INHIBITION.....	14
CHAPTER THREE – PROGRESS TOWARDS ACCESSING AGESAMIDES A AND B, AND TRUNCATED ANALOGS	243
CHAPTER FOUR – OLEFIN ACTIVATION OF α,β UNSATURATED SYSTEMS.....	358
CHAPTER FIVE – CONCLUSIONS AND FUTURE WORK.....	421
BIBLIOGRAPHY.....	424

LIST OF TABLES

Table II-I: The effect of N-1 functionalization on potency and specificity in h20S and TB proteasome	26
Table II-II: The effect of N-1 functionalization on potency and specificity in h20S and TB proteasome	36
Table II-III: SAR of N-1 tosylated imidazoline compounds	56
Table III-I: Experimental conditiond of the failed attempts at olefin activation	254
Table III-II: Lewis acids screened for regioselective ring opening of acylated aziridines	278

LIST OF FIGURES

Figure I-I: Imidazole and the structures of its reduced analogs	2
Figure I-II: Group 1 compounds associated with imidazolines synthesis.....	2
Figure I-III: General approach to accessing 2-imidazoline scaffolds from Group 1 compounds...	3
Figure I-IV: Accessing imidazolines molecules from aldehydes and nitrogen sources.....	4
Figure I-V: Cyclization of functionalized N-hydroxyethylbenzamides to yield imidazolines.....	5
Figure I-VI: Synthesis of imidazolines from isocyanoacetates and imines	6
Figure I-VII: Synthesis of imidazolines under photoredox conditions.....	6
Figure I-VIII: Expansion of aziridines in the presence of nitriles with Lewis acids	8
Figure I-IX: Synthesis of imidazoline scaffolds from 1,3 dipolar cycloadditions of azlactones...	9
Figure I-X: Stereochemical outcome of cycloaddition reaction.....	10
Figure I-XI: Different substitution patterns of 2-imidazolines at the 4,5 positions	10
Figure I-XII: The synthesis of disubstituted 2-imidazolines from trisubstituted 2-imidazolines.....	11
Figure I-XIII: Synthesis of cis-imidazolines generated <i>in-situ</i> from trans-imidazolines	12
Figure I-XIV: Synthesis of disubstituted imidazolines from aziridines.....	13
Figure II-I: Shows the h26S proteasome and its components, the h20S and the 19S caps.....	16
Figure II-II: Identified potent structures by screening for proteasome inhibition	18
Figure II-III: Ring expansion of imidoyl aziridines to yield imidazoline scaffolds	20
Figure II-IV: Identifies the positions to be probed by SAR analysis	20
Figure II-V: Identifies the numbering pattern for 2-imidazoline scaffolds.....	21
Figure II-VI: Molecules that were not accessed under reaction conditions.....	32

Figure II-VII: Molecules that were not accessed under reaction conditions.....	35
Figure II-VIII: Identified pathway for radical isomerization of cis imidazolines to trans imidazolines	42
Figure II-IX: Displays the experimentally observed stereoretention of imidazoline products....	42
Figure II-X: Proposed pathway for accessing cis-imidazoline through imidoyl chloride expansion	43
Figure II-XI: A pathway for polar solvent isomerization of cis imidazolines to trans imidazolines	44
Figure II-XII: Shows the steric strain of the cis-isomer and its effect on ring closure.....	45
Figure II-XIII: Pathway to accessing monosubstituted imidazolines.....	51
Figure II-XIV: ZnBr ₂ mediated expansion of 2-pyridyl aziridine	54
Figure II-XV: Proposed monoalkylation conditions using Bn-Cl.....	60
Figure II-XVI: Proposed deprotection of N-1 tosylated imidazolines.....	62
Figure II-XVII: Experimentally shown swap in regiochemistry due to EWG	63
Figure II-XVIII: Proposed expansion of monosubstituted imidazolines.....	63
Figure II-XIX: The ¹ HNMR and ¹³ CNMR for Compound II-I	158
Figure II-XX: The ¹ HNMR and ¹³ CNMR for Compound II-II	159
Figure II-XXI: The ¹ HNMR and ¹³ CNMR for Compound II-III	160
Figure II-XXII: The ¹ HNMR and ¹³ CNMR for Compound II-IV	161
Figure II-XXIII: The ¹ HNMR and ¹³ CNMR for Compound II-V	162
Figure II-XXIV: The ¹ HNMR and ¹³ CNMR for Compound II-VI	163
Figure II-XXV: The ¹ HNMR and ¹³ CNMR for Compound II-VII	164
Figure II-XXVI: The ¹ HNMR and ¹³ CNMR for Compound II-VIII	165
Figure II-XXVII: The ¹ HNMR and ¹³ CNMR for Compound II-IX	166
Figure II-XXVIII: The ¹ HNMR and ¹³ CNMR for Compound II-X	167

Figure II-XXIX: The ¹ HNMR and ¹³ CNMR for Compound II-XI	168
Figure II-XXX: The ¹ HNMR and ¹³ CNMR for Compound II-XII	169
Figure II-XXXI: The ¹ HNMR and ¹³ CNMR for Compound II-XIII	170
Figure II-XXXII: The ¹ HNMR and ¹³ CNMR for Compound II-XIV	171
Figure II-XXXIII: The ¹ HNMR and ¹³ CNMR for Compound II-XV	172
Figure II-XXXIV: The ¹ HNMR and ¹³ CNMR for Compound II-XVI	173
Figure II-XXXV: The ¹ HNMR and ¹³ CNMR for Compound II-XVII	174
Figure II-XXXVI: The ¹ HNMR and ¹³ CNMR for Compound II-XVIII	175
Figure II-XXXVII: The ¹ HNMR and ¹³ CNMR for Compound II-XIX	176
Figure II-XXXVIII: The ¹ HNMR and ¹³ CNMR for Compound II-XX	177
Figure II-XXXIX: The ¹ HNMR and ¹³ CNMR for Compound II-XXI	178
Figure II-XL: The ¹ HNMR and ¹³ CNMR for Compound II-XXII	179
Figure II-XLI: The ¹ HNMR and ¹³ CNMR for Compound II-XXIII	180
Figure II-XLII: The ¹ HNMR and ¹³ CNMR for Compound II-XXIV	181
Figure II-XLIII: The ¹ HNMR and ¹³ CNMR for Compound II-XXV	182
Figure II-XLIV: The ¹ HNMR and ¹³ CNMR for Compound II-XXVI	183
Figure II-XLV: The ¹ HNMR and ¹³ CNMR for Compound II-XXVII	184
Figure II-XLVI: The ¹ HNMR and ¹³ CNMR for Compound II-XXVIII	185
Figure II-XLVII: The ¹ HNMR and ¹³ CNMR for Compound II-XXIX	186
Figure II-XLVIII: The ¹ HNMR and ¹³ CNMR for Compound II-XXX	187
Figure II-XLIX: The ¹ HNMR and ¹³ CNMR for Compound II-XXXI	188
Figure II-L: The ¹ HNMR and ¹³ CNMR for Compound II-XXXII	189
Figure II-LI: The ¹ HNMR and ¹³ CNMR for Compound II-XXXIII	190

Figure II-LII: The ^1H NMR and ^{13}C NMR for Compound II-XXXIV	191
Figure II-LIII: The ^1H NMR and ^{13}C NMR for Compound II-XXXV	192
Figure II-LIV: The ^1H NMR and ^{13}C NMR for Compound II-XXXVI	193
Figure II-LV: The ^1H NMR and ^{13}C NMR for Compound II-XXXVII	194
Figure II-LVI: The ^1H NMR and ^{13}C NMR for Compound II-XXXVIII	195
Figure II-LVII: The ^1H NMR and ^{13}C NMR for Compound II-XXXIX	196
Figure II-LVIII: The ^1H NMR and ^{13}C NMR for Compound II-XL	197
Figure II-LIX: The ^1H NMR and ^{13}C NMR for Compound II-XLI	198
Figure II-LX: The ^1H NMR and ^{13}C NMR for Compound II-XLII	199
Figure II-LXI: The ^1H NMR and ^{13}C NMR for Compound II-XLIII	200
Figure II-LXII: The ^1H NMR and ^{13}C NMR for Compound II-XLIV	201
Figure II-LXIII: The ^1H NMR and ^{13}C NMR for Compound II-XLV	202
Figure II-LXIV: The ^1H NMR and ^{13}C NMR for Compound II-XLVI	203
Figure II-LXV: The ^1H NMR and ^{13}C NMR for Compound II-XLVII	204
Figure II-LXVI: The ^1H NMR and ^{13}C NMR for Compound II-XLVIII	205
Figure II-LXVII: The ^1H NMR and ^{13}C NMR for Compound II-XLIX	206
Figure II-LXVIII: The ^1H NMR and ^{13}C NMR for Compound II-L	207
Figure II-LXIX: The ^1H NMR and ^{13}C NMR for Compound II-LI	208
Figure II-LXX: The ^1H NMR and ^{13}C NMR for Compound II-LII	209
Figure II-LXXI: The ^1H NMR and ^{13}C NMR for Compound II-LIII	210
Figure II-LXXII: The ^1H NMR and ^{13}C NMR for Compound II-LIV	211
Figure II-LXXIII: The ^1H NMR and ^{13}C NMR for Compound II-LV	212
Figure II-LXXIV: The ^1H NMR and ^{13}C NMR for Compound II-LVI	213

Figure II-LXXV: The ¹ HNMR and ¹³ CNMR for Compound II-LVII	214
Figure II-LXXVI: The ¹ HNMR and ¹³ CNMR for Compound II-LVIII	215
Figure II-LXXVII: The ¹ HNMR and ¹³ CNMR for Compound II-LIX	216
Figure II-LXXVIII: The ¹ HNMR and ¹³ CNMR for Compound II-LX	217
Figure II-LXXIX: The ¹ HNMR and ¹³ CNMR for Compound II-LXI	218
Figure II-LXXX: The ¹ HNMR and ¹³ CNMR for Compound II-LXII	219
Figure II-LXXXI: The ¹ HNMR and ¹³ CNMR for Compound II-LXIII	220
Figure II-LXXXII: The ¹ HNMR and ¹³ CNMR for Compound II-LXIV	221
Figure II-LXXXIII: The ¹ HNMR and ¹³ CNMR for Compound II-LXV	222
Figure II-LXXXIV: The ¹ HNMR and ¹³ CNMR for Compound II-LXVI	223
Figure II-LXXXV: The ¹ HNMR and ¹³ CNMR for Compound II-LXVII	224
Figure II-LXXXVI: The ¹ HNMR and ¹³ CNMR for Compound II-LXVIII	225
Figure II-LXXXVII: The ¹ HNMR and ¹³ CNMR for Compound II-LXIX	226
Figure II-LXXXVIII: The ¹ HNMR and ¹³ CNMR for Compound II-LXX	227
Figure II-LXXXIX: The ¹ HNMR and ¹³ CNMR for Compound II-LXXI	228
Figure II-XC: The ¹ HNMR and ¹³ CNMR for Compound II-LXXII	229
Figure II-XCII: The ¹ HNMR and ¹³ CNMR for Compound II-LXXIII	230
Figure II-XCIII: The ¹ HNMR and ¹³ CNMR for Compound II-LXXIV	231
Figure II-XCIV: The ¹ HNMR and ¹³ CNMR for Compound II-LXXV	232
Figure II-XCV: The ¹ HNMR and ¹³ CNMR for Compound II-LXXVI	233
Figure II-XCVI: The ¹ HNMR and ¹³ CNMR for Compound II-LXXVII	234
Figure II-XCVII: The ¹ HNMR and ¹³ CNMR for Compound II-LXXVIII	235
Figure II-XCVIII: The ¹ HNMR and ¹³ CNMR for Compound II-LXXIX	236

Figure II-XCIX: The ¹ HNMR and ¹³ CNMR for Compound II-LXXX	237
Figure II-C: The ¹ HNMR and ¹³ CNMR for Compound II-LXXXI	238
Figure II-CI: The ¹ HNMR and ¹³ CNMR for Compound II-LXXXII	239
Figure II-CII: The ¹ HNMR and ¹³ CNMR for Compound II-LXXXIII	240
Figure II-CIII: The ¹ HNMR and ¹³ CNMR for Compound II-LXXXIV	241
Figure II-CIV: The ¹ HNMR and ¹³ CNMR for Compound II-LXXXV	242
Figure III-I: Structures of FDA approved proteasome inhibitors	244
Figure III-II: Structures of bromopyrrole alkaloids natural products	245
Figure III-III: Isolation of bromoindolophakellin	246
Figure III-IV: bromoindolophakellin bound in the yeast core particle.....	247
Figure III-V: Structures of other bromopyrrolloalkaloids in the same family of dibromophakellin	248
Figure III-VI: Pd mediated N-alkylation in route to accessing Agesamides A and B.....	249
Figure III-VII: Synthesis of the key intermediate to access different pyrrolloalkaloids	251
Figure III-VIII: Proposed retrosynthesis to access desired analogs of Agesamides A and B	251
Figure III-IX: Iodonium catalyzed cyclizations.....	252
Figure III-X: Lewis acid catalyzed brominium opening.....	252
Figure III-XI: Example of resultant aminobromination after nucleophilic ring opening	256
Figure III-XII: Proposed ring opening of halonium intermediate	256
Figure III-XIII: Competing E ₂ mechanism for side product formation	258
Figure III-XIV: Retrosynthetic analysis of analogs of Agesamides A and B.....	259
Figure III-XV: Organocatalytic conjugate addition of benzene systems to α,β unsaturated aldehydes.....	260

Figure III-XVI: Organocatalytic conjugate addition of carbamates to α,β unsaturated aldehydes.....	261
Figure III-XVII: Enantioselective deamination under organocatalytic conditions	263
Figure III-XVIII: Enantioselective aziridination of disubstituted aldehydes	265
Figure III-XIX: Enantioselective aziridination of monosubstituted and aromatic α,β unsaturated aldehydes.....	266
Figure III-XX: Approach towards desired aziridine intermediate	267
Figure III-XXI: Alternative approach to accessing the desired aziridine intermediate	270
Figure III-XXII: Expansion of activated aziridines to give imidazolines	272
Figure III-XXIII: Proposed methodology for controlling ring opening of aziridine intermediates towards accessing desired 6,5,6 fused core	273
Figure III-XXIV: Heine ring expansion of aziridines to yield oxazolines and imidazolines	273
Figure III-XXV: Effect of Lewis acids on aziridine ring opening.....	275
Figure III-XXVI: Proposed coordination of Lewis acid to access desired regioisomer with ring opening.....	276
Figure III-XXVII: Proposed Bronsted acid activation to access desired regioisomer with ring opening.....	278
Figure III-XXVIII: Explanation of difference in stereochemistry based on acidity	280
Figure III-XXIX: Explanation behind expansion of intermediate to undesired regioisomer	281
Figure III-XXX: Modified approach to regio-controlled ring openings of aziridines	281
Figure III-XXXI: Methods of controlling regiochemical outcome of aziridines	283
Figure III-XXXII: Modified approach to regio-controlled ring openings of aziridines.....	283
Figure III-XXXIII: Modified approach to regio-controlled ring openings of aziridines	284
Figure III-XXXIV: Regioselective Lewis acid mediated ring opening.....	286
Figure III-XXXV: Alternative approach to accessing desired regiochemistry.....	287

Figure III-XXXVI: Proposed pathway for N ₁ alkylation	288
Figure III-XXXVII: Proposed pathway for C ₂ alkylation of pyrrole	290
Figure III-XXXVIII: Proposed EDCI coupling to access desired regioisomer	292
Figure III-XXXIX: The ¹ HNMR and ¹³ CNMR for Compound III-I	326
Figure III-XL: The ¹ HNMR and ¹³ CNMR for Compound III-II	327
Figure III-XLI: The ¹ HNMR and ¹³ CNMR for Compound III-III	328
Figure III-XLII: The ¹ HNMR and ¹³ CNMR for Compound III-IV	329
Figure III-XLIII: The ¹ HNMR and ¹³ CNMR for Compound III-V	330
Figure III-XLIV: The ¹ HNMR and ¹³ CNMR for Compound III-VI	331
Figure III-XLV: The ¹ HNMR and ¹³ CNMR for Compound III-VII	332
Figure III-XLVI: The ¹ HNMR and ¹³ CNMR for Compound III-VIII	333
Figure III-XLVII: The ¹ HNMR and ¹³ CNMR for Compound III-IX	334
Figure III-XLVIII: The ¹ HNMR and ¹³ CNMR for Compound III-X	335
Figure III-XLIX: The ¹ HNMR and ¹³ CNMR for Compound III-XI	336
Figure III-L: The ¹ HNMR and ¹³ CNMR for Compound III-XII	337
Figure III-LI: The ¹ HNMR and ¹³ CNMR for Compound III-XIII	338
Figure III-LII: The ¹ HNMR and ¹³ CNMR for Compound III-XIV	339
Figure III-LIII: The ¹ HNMR and ¹³ CNMR for Compound III-XV	340
Figure III-LIV: The ¹ HNMR and ¹³ CNMR for Compound III-XVI	341
Figure III-LV: The ¹ HNMR and ¹³ CNMR for Compound III-XVII	342
Figure III-LVI: The ¹ HNMR and ¹³ CNMR for Compound III-XVIII	343
Figure III-LVII: The ¹ HNMR and ¹³ CNMR for Compound III-XIX	344
Figure III-LVIII: The ¹ HNMR and ¹³ CNMR for Compound III-XX	345

Figure III-LIX: The ¹ HNMR and ¹³ CNMR for Compound III-XXI	346
Figure III-LX: The ¹ HNMR and ¹³ CNMR for Compound III-XXII	347
Figure III-LXI: The ¹ HNMR and ¹³ CNMR for Compound III-XXIII	348
Figure III-LXII: The ¹ HNMR and ¹³ CNMR for Compound III-XXIV	349
Figure III-LXIII: The ¹ HNMR and ¹³ CNMR for Compound III-XXV	350
Figure III-LXIV: The ¹ HNMR and ¹³ CNMR for Compound III-XXVI	351
Figure III-LXV: The ¹ HNMR and ¹³ CNMR for Compound III-XXVII	352
Figure III-LXVI: The ¹ HNMR and ¹³ CNMR for Compound III-XXVIII	353
Figure III-LXVII: The ¹ HNMR and ¹³ CNMR for Compound III-XXIX	354
Figure III-LXVIII: The ¹ HNMR and ¹³ CNMR for Compound III-XXX	355
Figure III-LXIX: The ¹ HNMR and ¹³ CNMR for Compound III-XXXI	356
Figure III-LXX: The ¹ HNMR and ¹³ CNMR for Compound III-XXXII	357
Figure IV-I: The sharpless asymmetric aminohydroxylation reaction	360
Figure IV-II: Hypervalent iodane mediated aminohydroxylation	361
Figure IV-III: Copper-mediated N-tosylaziridination of olefins	362
Figure IV-IV: Electron rich olefin diamination masked as 2-aminoimidazolines	364
Figure IV-V: Aminobromination of neutral olefins	365
Figure IV-VI: Shows the difference in activity based on the presence of 2-aminoimidazoline core	366
Figure IV-VII: The mechanism of the Baylis-Hillman reaction	367
Figure IV-VIII: Proposed pathway towards 2-oxazoline formation	368
Figure IV-IX: Displays difference in stability between aziridine structures	370
Figure IV-X: Identifies one pathway of dimerization of Cbz-guanidine	371

Figure IV-XI: Displays Lewis acid catalysis to form a more reactive Bromonium for cyclization	373
Figure IV-XII: Shows catalytic KI aiding in aminobromination of an α,β unsaturated system	374
Figure IV-XIII: Proposed method of olefin activation in the presence of benzamide.....	375
Figure IV-XIV: Explanation of the difference in regiochemistry based on intermediate stability.....	377
Figure IV-XV: Pathway to accessing imidazolines from activated benzamidines	382
Figure IV-XVI: The mechanism for the mitsunobu reaction	384
Figure IV-XVII: Mechanism for the appel reaction	385
Figure IV-XVIII: Proposed mechanism for appel-like aziridination of olefins	386
Figure IV-XIX: The $^1\text{HNMR}$ and $^{13}\text{CNMR}$ for Compound IV-I	407
Figure IV-XX: The $^1\text{HNMR}$ and $^{13}\text{CNMR}$ for Compound IV-II	408
Figure IV-XXI-: The $^1\text{HNMR}$ and $^{13}\text{CNMR}$ for Compound IV-III	409
Figure IV-XXII: The $^1\text{HNMR}$ and $^{13}\text{CNMR}$ for Compound IV-IV	410
Figure IV-XXIII: The $^1\text{HNMR}$ and $^{13}\text{CNMR}$ for Compound IV-V	411
Figure IV-XXIV: The $^1\text{HNMR}$ and $^{13}\text{CNMR}$ for Compound IV-VI	412
Figure IV-XXV: The $^1\text{HNMR}$ and $^{13}\text{CNMR}$ for Compound IV-VII	413
Figure IV-XXVI: The $^1\text{HNMR}$ and $^{13}\text{CNMR}$ for Compound IV-VIII	414
Figure IV-XXVII: The $^1\text{HNMR}$ and $^{13}\text{CNMR}$ for Compound IV-IX	415
Figure IV-XXVIII: The $^1\text{HNMR}$ and $^{13}\text{CNMR}$ for Compound IV-X	416
Figure IV-XXIX: The $^1\text{HNMR}$ and $^{13}\text{CNMR}$ for Compound IV-XI	417
Figure IV-XXX: The $^1\text{HNMR}$ and $^{13}\text{CNMR}$ for Compound IV-XII	418
Figure IV-XXXI: The $^1\text{HNMR}$ and $^{13}\text{CNMR}$ for Compound IV-XIII	419
Figure IV-XXXII: The $^1\text{HNMR}$ and $^{13}\text{CNMR}$ for Compound IV-XIV	420

LIST OF SCHEMES

Scheme II-I: Synthetic pathway to accessing trans-2,3-diphenyl aziridine starting material	21
Scheme II-II: Synthetic pathway for accessing amide precursors	22
Scheme II-III: Shows the imidoyl chloride formation and resulting expansion to imidazolines	23
Scheme II-IV: Shows the difference in yield when the N-substituent was varied	24
Scheme II-V: Identified expansion products dependence on N-1 alkyl group	24
Scheme II-VI: Highlighted the influence of EDG on acylated aniline expansion	25
Scheme II-VII: The synthesis of amide precursors for probing the 2-position on imidazoline molecules	30
Scheme II-VIII: Synthesis of imidazoline scaffolds with different C-2 groups	31
Scheme II-IX: Example of expansion of amides with mild EWG to imidazolines	32
Scheme II-X: Synthesis of amide precursors to probe Ortho vs Meta vs Para substituent effect	33
Scheme II-XI: Synthesis of imidazolines to probe Ortho vs Meta vs Para substituent effect	34
Scheme II-XII: Synthesis of amide precursors to probe C-2 alkyl substituent and size effect	34
Scheme II-XIII: Synthesis of imidazolines to probe C-2 alkyl substituent and size effect	35
Scheme II-XIV: Synthesis of imidazole from imidazoline	40
Scheme II-XV: Showed the effect of stereochemistry on proteasome inhibition	40
Scheme II-XVI: Synthetic pathway to accessing cis-2,3-diphenyl aziridine starting material	45
Scheme II-XVII: Synthesis of cis imidazolines from aldehydes	46
Scheme II-XVIII: N-I alkylations that did not occur under varied reaction conditions	47
Scheme II-XIX: N-1 alkylation conditions for cis-imidazolines	48

Scheme II-XX: The effect of imidazoline stereochemistry on selectivity and potency of inhibition	50
Scheme II-XXI: Synthesis of tosylated aziridine starting material	52
Scheme II-XXII: Synthesis of tosylated aziridine starting material.....	52
Scheme II-XXIII: Synthesis of N-1 tosylated imidazoline substrates	53
Scheme II-XXIV: Failed expansion reaction conditions.....	55
Scheme II-XXV: Failed N-oxide reaction conditions	55
Scheme II-XXVI: Deprotection conditions for N-1 tosylated imidazolines	58
Scheme II-XXVII: Dialkylation of imidazoline with Bn-Br.....	59
Scheme II-XXVIII: monoalkylation of imidazoline with Bn-Cl	60
Scheme II-XXIX: Synthesis of imidazole from N-I Tosylated imidazolines	61
Scheme II-XXX: Failed deprotection of N-tosylated aziridines	64
Scheme II-XXXI: Pathway to access monosubstituted aziridines for expansion	65
Scheme III-I: Synthesis of 4,5-dibromopyrrole-2-carboxamide	253
Scheme III-II: Failed attempts at olefin activation with 4,5-dibromopyrrole-2-carboxamide	253
Scheme III-III: Failed bromonium catalyzed cyclization	255
Scheme III-IV: Proposed ring opening using the generation of IBr	257
Scheme III-V: Failed attempts at N-alkylation.....	257
Scheme III-VI: Synthesis of the chiral secondary amine catalyst.....	268
Scheme III-VII: Pathway to desired Indole-derivative	269
Scheme III-VIII: Synthesis of desired indole derivative	269
Scheme III-IX: Synthesis of desired aziridine intermediates by EDCI coupling.....	271
Scheme III-X: Transesterification with alkoxide ligands on Lewis acids.....	276

Scheme III-XI: Ring opening of the aziridine in the presence of a Lewis acid to wrong isomer.....	277
Scheme III-XII: Ring opening of the acylated aziridine to wrong regioisomer	279
Scheme III-XIII: Non-selective expansion of aziridine to oxazolines.....	279
Scheme III-XIV: Proposed product of ring opening of aziridine in water.....	280
Scheme III-XV: Accessing derivative to test hypothesis for ring opening	284
Scheme III-XVI: Regiocontrolled ring opening of benzylated aziridines	285
Scheme III-XVII: Results of Lewis acid ring opening of N-benzylated aziridines	287
Scheme III-XVIII: Elimination products of proposed reaction	288
Scheme III-XIX: Regioselective ring opening of N-benzyl aziridines by different electrophiles	289
Scheme III-XX: Failed N ₁ alkylation under basic conditions	289
Scheme III-XXI: Failed C ₂ alkylations of pyrrole	290
Scheme III-XXII: Failed C ₂ alkylations of pyrrole under neutral conditions.....	291
Scheme III-XXIII: Regioselective ring opening of N-benzylated aziridines and failed coupling to indole-2-carboxylic acid	292
Scheme III-XXIV: N ₁ alkylation of Indole under basic conditions	293
Scheme III-XXV: Failed N ₁ alkylations of 2-trichloroacetylpyrrole	294
Scheme III-XXVI: Inseparable mix of products after N ₁ alkylation of pyrrole under basic conditions.....	295
Scheme IV-I: Chiral catalysis synthesis for asymmetric aziridination.....	367
Scheme IV-II: Synthesis of -OR functionalized hydroxyamides	369
Scheme IV-III: Attempts at olefin functionalization using a chiral catalyst.....	369
Scheme IV-IV: Synthesis of Cbz-guanidine and attempted cyclization.....	371
Scheme IV-V: Identified that brominating and cyclization does not occur with only NBS.....	372

Scheme IV-VI: Displays N-bromo-1,3-dimethylurea does not brominate methyl acrylate's olefin	373
Scheme IV-VII: The cyclization of 1,3-dimethyl urea onto an α,β unsaturated system	374
Scheme IV-VIII: Identified the difference in regiochemical outcome with olefin cyclization	376
Scheme IV-IX: Depicts the failed bromination and cyclization of benzamidine under various conditions	378
Scheme IV-X: Shows the failed cyclization of N-Benzylbenzamide	379
Scheme IV-XI: Synthesis of N-bromobenzamide for olefin activation	380
Scheme IV-XII: Failed cyclization of N-bromobenzamide with methyl acrylate	380
Scheme IV-XIII: Lewis acid activation of N-bromobenzamide	381
Scheme IV-XIV: Synthesis of N-methoxy-N'-benzyl benzamide as new lead for olefin activation	382
Scheme IV-XV: Synthesis of new lead compound for olefin activation towards imidazolines	383
Scheme IV-XVI: Attempted azirdination of olefins under appel conditions	386
Scheme IV-XVII: Attempts towards olefin activation using mitsunobu conditions	388
Scheme IV-XVIII: Attempted aziridination of olefins by dehydration of N-hydroxyamides ...	390
Scheme IV-XIX: Attempted aziridination of olefins by dehydration of N-hydroxyamides	391

KEY TO SYMBOLS AND ABBREVIATIONS

Å	Angstrom
Ac	Acetyl
acac	Acetylacetone
ACN	Acetonitrile
aq	Aqueous
Boc	tert-butyloxycarbonyl-
Bn	Benzyl-
Bz	Benzoyl-
°C	Celsius
Cbz	Carboxybenzyl-
Cy	Cyclohexyl-
DCM	Dichloromethane
DDQ	Dichlorodicyanobenzoquinone
DEAD	Diethyl azodicarboxylate
DEE	Diethyl ether
DIAD	Diisopropyl azodicarboxylate
DHQ	Dihydroquinidine
DHQD	Dihydroquinidine
DMAD	Dimethyl acetylenedicarboxylate
DMAP	Dimethylaminopyridine
DMF	Dimethyl formamide

EDCI	Ethyl dimethylaminopropylcarbodiimide
EDG	Electron donating group
Equiv	Equivalent
EtOAc	Ethyl acetate
EWG	Electron withdrawing group
h	Hours
HMDS	Hexamethyldisilazane
h ν	Light
IPA	Isopropyl Alcohol
MM	Multiple Myeloma
mCPBA	m-Chloroperoxybenzoic acid
min	Minute
mol	Mole
MS	Molecular sieves
NBS	N-bromosuccinimide
OTf	Trifluoromethanesulfonate
Ph	Phenyl-
ppy	2-Phenylpyridine
rt	Room temperature
SAR	Structure Activity Relationship
soln	Solution
TB	Tuberculosis
TBAI	Tetrabutylammonium iodide

TBICA	Tribromoisocyanuric acid
TCCA	Trichloroisocyanuric acid
TEA	Triethylamine
TES	Triethylsilyl-
TFA	Trifluoroacetic acid
THF	Tetrahydrofuran
TMS	Trimethylsilyl-
Ts	Tosyl-

CHAPTER ONE – APPROACHES TO 2-IMIDAZOLINE SYNTHESIS

The high demand for imidazoline scaffolds and continued research for developing novel methodology is due to the synthetic versatility of this class of heterocyclic compounds. Applications using imidazoline scaffolds are not limited to a sub-set of organic chemistry but instead are very diverse spanning many scientific fields of interest. Imidazolines have seen applications as homogenous catalysts,¹ surfactants,² anti-corrosion agents,³ and as pharmacophores.⁴⁻⁵ Imidazolines, also known as dihydroimidazoles, are a class of heterocyclic compounds belonging to the imidazole family. Imidazoles when reduced by hydrogen in the presence of a catalyst become one source of the production of imidazolines and imidazolidines. Imidazolines are the products of partial hydrogenation (partial reduction of imidazole). Imidazolidines are the product of complete hydrogenation (full reduction of imidazole). Partial reduction of imidazole gives rise to three imidazoline constitutional isomers, 2-imidazolines, 3-imidazolines, and 4-imidazolines. Of these three constitutional isomers, the most commonly observed and extensively researched isomer is 2-imidazoline. Methods of synthesizing these structures will be addressed through the course of this dissertation. 3-imidazolines and 4-imidazolines are less commonly observed with their chemical behavior being different than that of the 2-imidazolines due to lack of the amidine stability and functionality. Distinguishing between molecules of this family can be done by noting the presence and location of the double bond in each heterocyclic molecule.

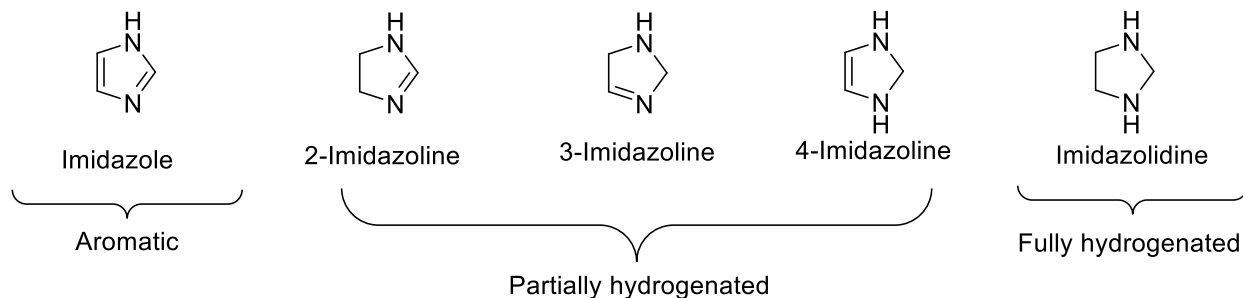


Figure I-I: Imidazole and the structures of its reduced analogs.

The demand for 2-imidazolines have inspired many approaches towards accessing these scaffolds. Classical approaches towards synthesis focused on acyl substitution of amines and diamine molecules with sequential cyclization to yield imidazolines. These reactions are observed with carboxylic acid derivatives (Group 1 carbonyl compounds).

Group 1 carbonyl compounds

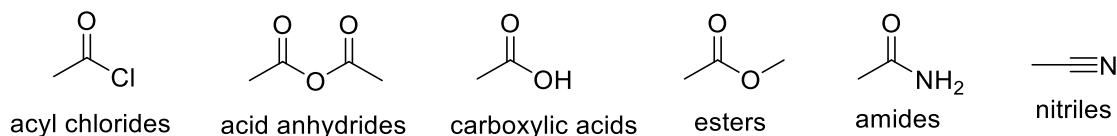


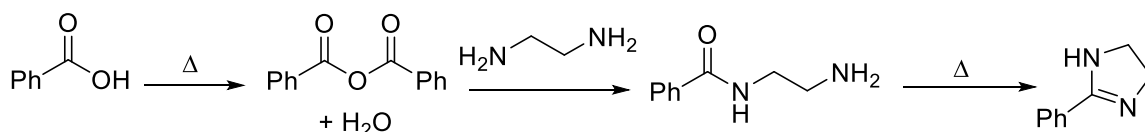
Figure I-II: Group 1 compounds associated with imidazolines synthesis

Group 1 carbonyl compounds

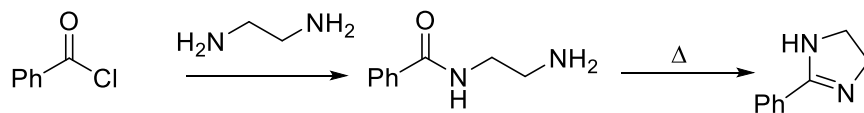
In these carbonyl compounds, the diamine source undergoes a nucleophilic acyl substitution reaction at the carbonyl which displaces the better leaving group and results in an amide. Dehydration by cyclization resulted in the formation of 2-imidazolines scaffolds. Carboxylic acid compounds under heat and pressure generate anhydrides *in-situ*. These molecules

are then sequentially attacked by the diamine nucleophile and the resulting β -amino amide undergoes cyclization to give the 2-imidazoline. Acyl chlorides, esters and nitriles like carboxylic acids derivatives yield the 2-imidazoline by displacement of the leaving group followed by resulting cyclization.⁶⁻⁹

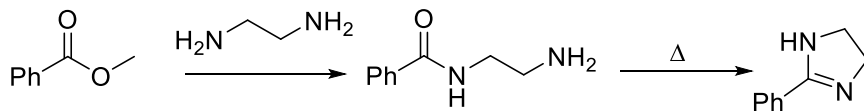
Carboxylic Acids and Anhydrides



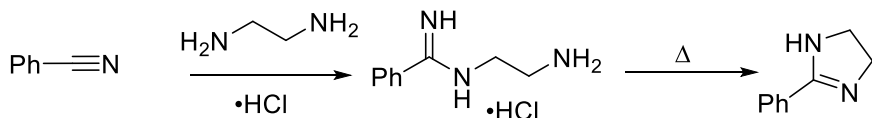
Acyl Chlorides



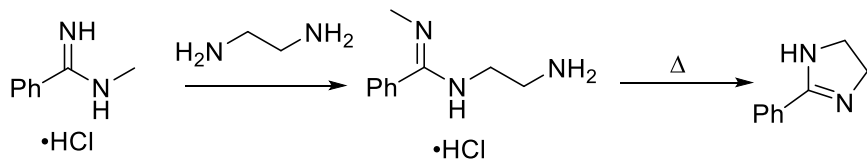
Esters



Nitriles



Amidines



Imidates

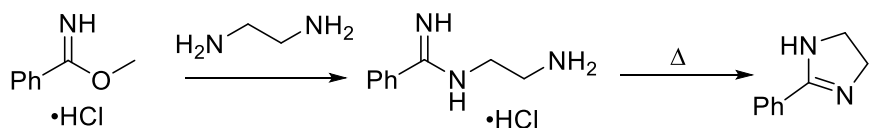
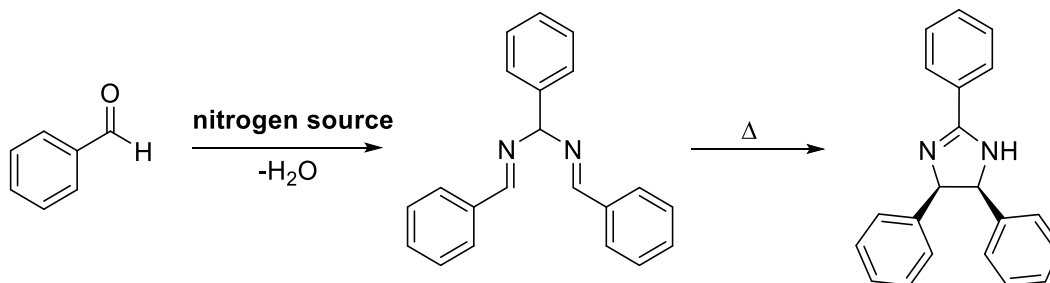


Figure I-III: General approach to accessing 2-imidazoline scaffolds from Group 1 compounds.

Aldehydes

Aromatic aldehydes are distinct derivatives of Group 2 carbonyl compounds and undergo cyclization in the presence of a nitrogen source like ammonia or hexamethyldisilazane. Condensation of the nitrogen source results in the aldimine which undergoes cyclization to give the imidazoline scaffold.¹⁰



Uchida, H.; Shimizu, T.; Reddy, P. Y.; Nakamura, S.; Toru, T.; *Synthesis*, **2003**, 8, 1236 -1240

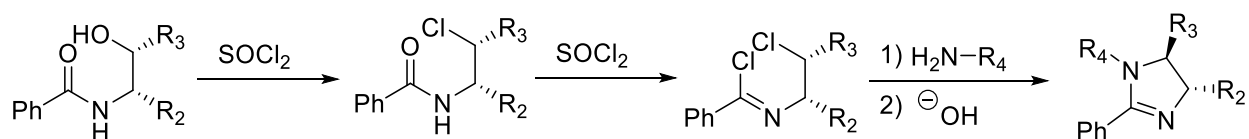
Figure I-IV: Accessing imidazolines molecules from aldehydes and nitrogen sources.

As time progressed the need for synthesizing more chemically diverse analogs of imidazolines for various applications catalyzed new approaches towards imidazoline synthesis. These methods utilize non-classical combinations of reagents to access densely functionalized 2-imidazoline and other imidazoline scaffolds.

Functionalized amide dehydrations

One method of accessing imidazolines stems from sequential transformations of aminoalcohols. Addition of an amino alcohol to an acyl chloride like benzoyl chloride results in

the formation of N-hydroxyethylbenzamide. This functionalized amide can then be dehydrated to the chloroethyl-imidoylchloride. Addition of an amine in the presence of a strong base can give access to disubstituted 2-imidazoline cores.¹¹

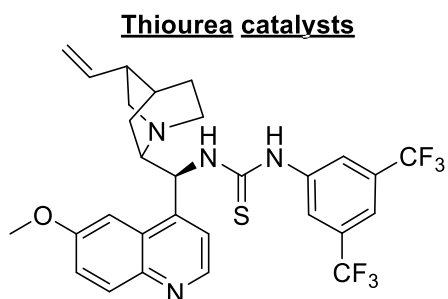
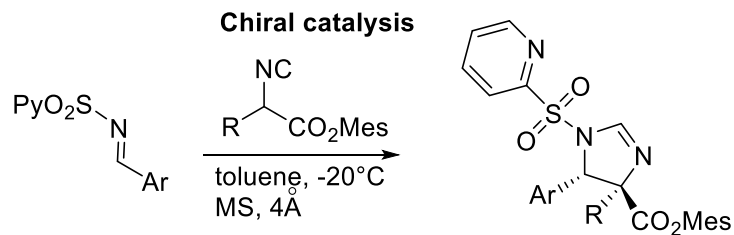


Boland, N. A.; Hynes, S. J.; Matthews, J. W.; Smyth, M. P.; Casey, M.; *J. Org. Chem.*, **2002**, 67, 3919-3922

Figure I-V: Cyclization of functionalized N-hydroxyethylbenzamides to yield imidazolines.

Condensation of imines with isonitriles

Additions of imines in the presence of isonitriles and isocynoacetates yield the formation of imidazolines. In the presence of chiral organocatalyst enantioselective mannich-like reactions occur. Chiral thioureas activate the isonitriles for sequential cycloaddition with the N-sulfonylimines to give the imidazoline scaffold.¹²



Nakamura, S.; Maeno, Y.; Ohara, M.; Yamamura, A.; Funahashi, Y.; Shibata, N.;
Org. Lett., **2012**, *14*, 2960-2963

Figure I-VI: Synthesis of imidazolines from isocyanoacetates and imines.

Direct alkene functionalization

Activation of alkenes can be done by photo-redox conditions in the presence of Ir(ppy)₃ and N-Ts protected 1-aminopyridinium. When this reaction takes place in the acetonitrile, solvent trapping leads to the production of imidazolines.¹³

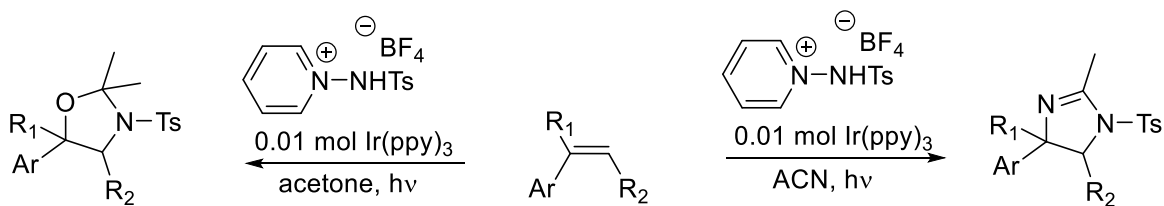
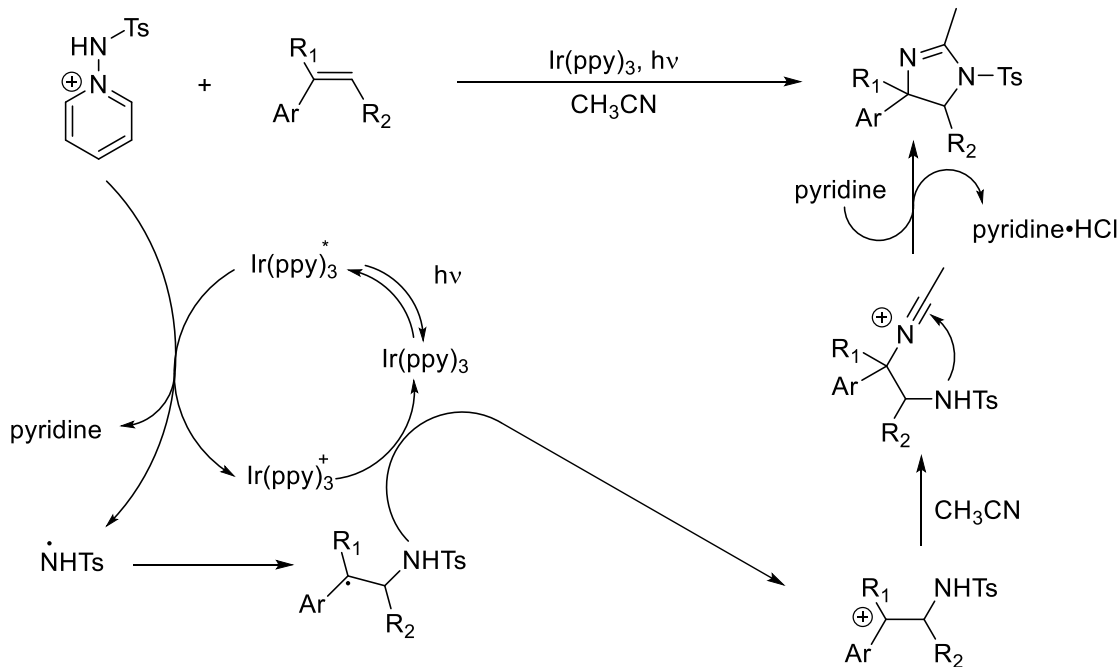


Figure I-VII: Synthesis of imidazolines under photoredox conditions.

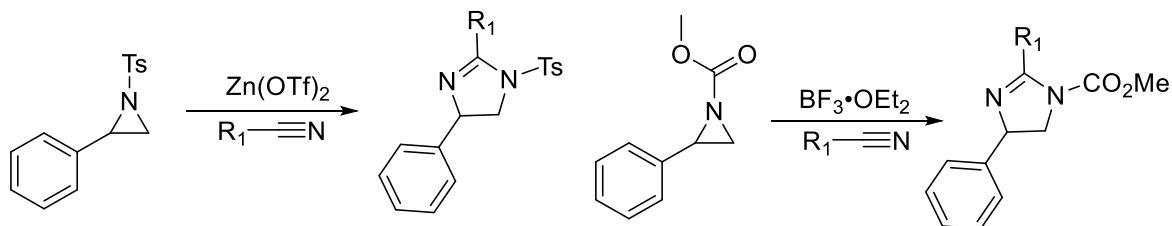
Figure I-VII cont'd



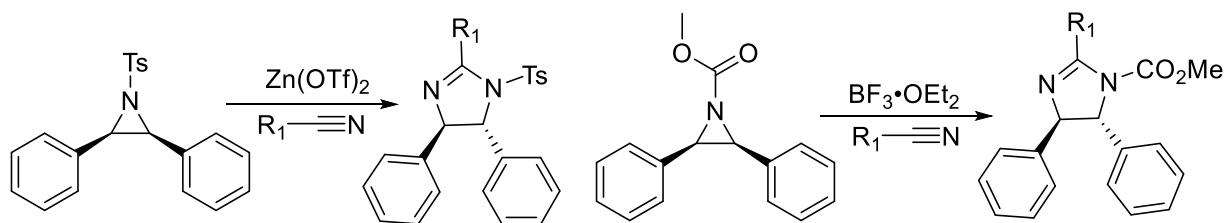
Chen, J.Q.; Yu, W. L.; Wei, Y. L.; Li, T. H.; Xu, P. F.; *J. Org. Chem.*, **2017**, 82, 243-249

Aziridine expansions

Expansions of aziridines in the presence of nitriles and a Lewis acid will give rise to 2-imidazolines in moderate to high yield. Many Lewis acids catalyze this expansion with notable examples being Zn(OTf)₂ and BF₃·OEt₂. The mechanism of this transformation is the Lewis acid mediated ring opening that results in trapping of any carbocation or δ⁺ carbon by the nitrile's nucleophilic nitrogen like in the Ritter reaction. Sequential attack at the nitrile carbonyl results in imidazoline formation.¹⁴⁻¹⁵



Ghosh, K.; Das, K.; Ghorai, M. K.; *Tetrahedron Lett.* **2006**, *47*, 5399-5403

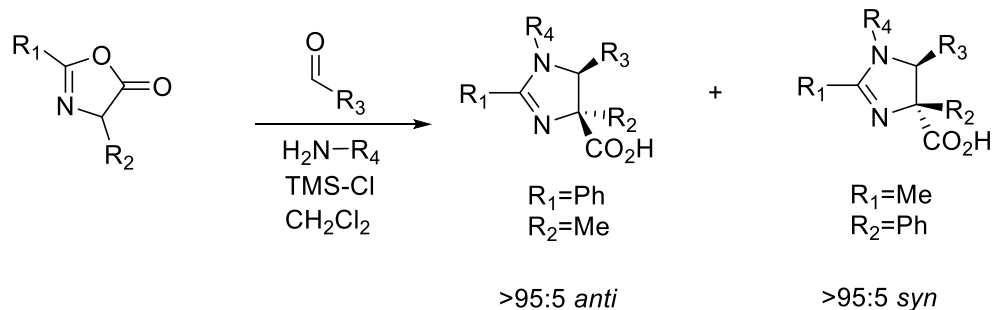


Hiyama, T.; Koide, H.; Fujita, S.; Nozaki, H.; *Tetrahedron*, **1973**, *29*, 3137-3139

Figure I-VIII: Expansion of aziridines in the presence of nitriles with Lewis acids.

Azlactone expansions

Research developed within the Tepe group focused around the synthesis of diverse chemical libraries of imidazolines and other heterocycles from azlactone intermediates. Developing new methodology towards accessing a large library of imidazoline compounds allowed for further biological evaluation of imidazolines and their pharmacophore capabilities. The development of this approach to imidazolines allowed for synthetic tuning of azlactone intermediates to control the stereochemical outcome of the cyclization to imidazolines. This allowed for the synthesis of both the syn- and anti-products of cyclizations, and added diversity to the approach of imidazoline synthesis by identifying a clear pathway to the synthesis of substituted cis-imidazolines. Most methods in literature primarily provide pathways towards trans-imidazolines synthesis as the major product.



Sharma, V.; Tepe, J. J.; *Org. Lett.* **2005**, 7, 5091-5094

Figure I-IX: Synthesis of imidazoline scaffolds from 1,3 dipolar cycloadditions of azlactones.

The reaction involved the generation of an azlactone intermediate from an acylated amino acid. These azlactones when exposed to the Lewis acid TMS-Cl, in the presence of an imine resulted in the cycloaddition reaction to give imidazolines. The addition of TMS-Cl resulted in the formation of a munched azlactone which reacts with the dipolarophile. The stereochemical outcome for producing trans-imidazoline was deduced to be due to the *A-1,3-strain* in the azlactone because of the large substituents. This in turn resulted in the endo approach of the incoming imine, to avoid any addition steric repulsion with the TMS-protected azlactones. Inversion of the stereochemical outcome was done in the presence of a methyl substituent which changes the electronics of the intermediate azlactone.¹⁶

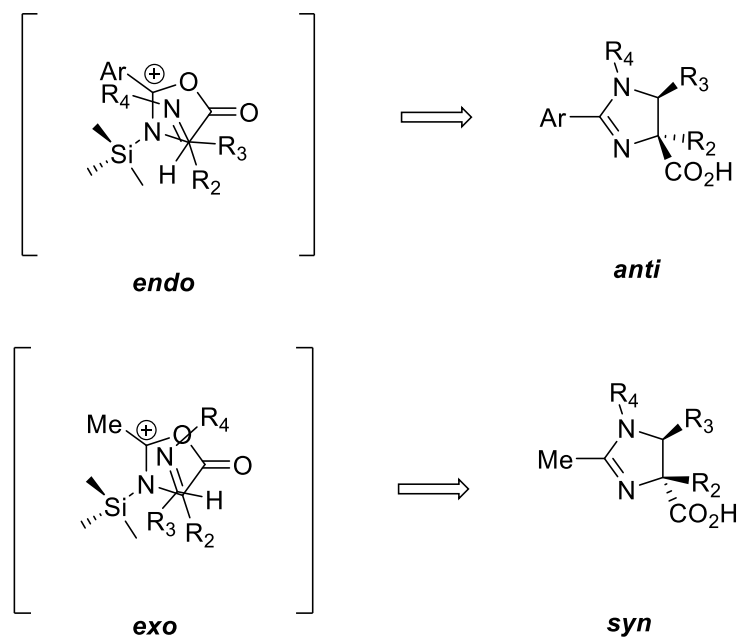


Figure I-X: Stereochemical outcome of cycloaddition reaction.

This methodology accessed tri-substituted imidazoline scaffolds from azlactones. Methodology to access other substitution patterns of 2-imidazoline at the 4 and 5 positions have also been pursued within the Tepe group.

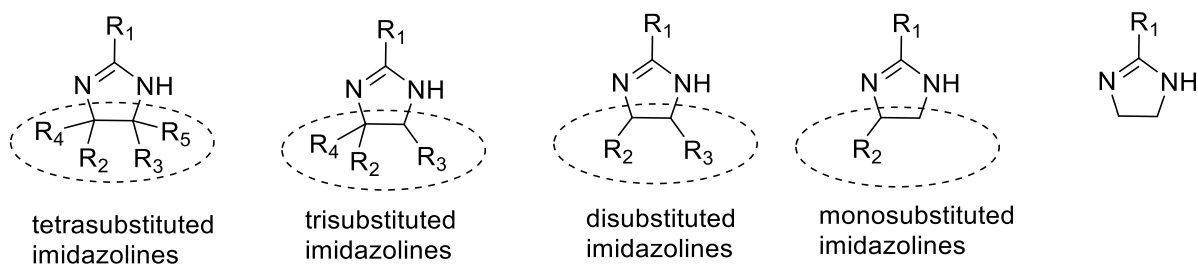
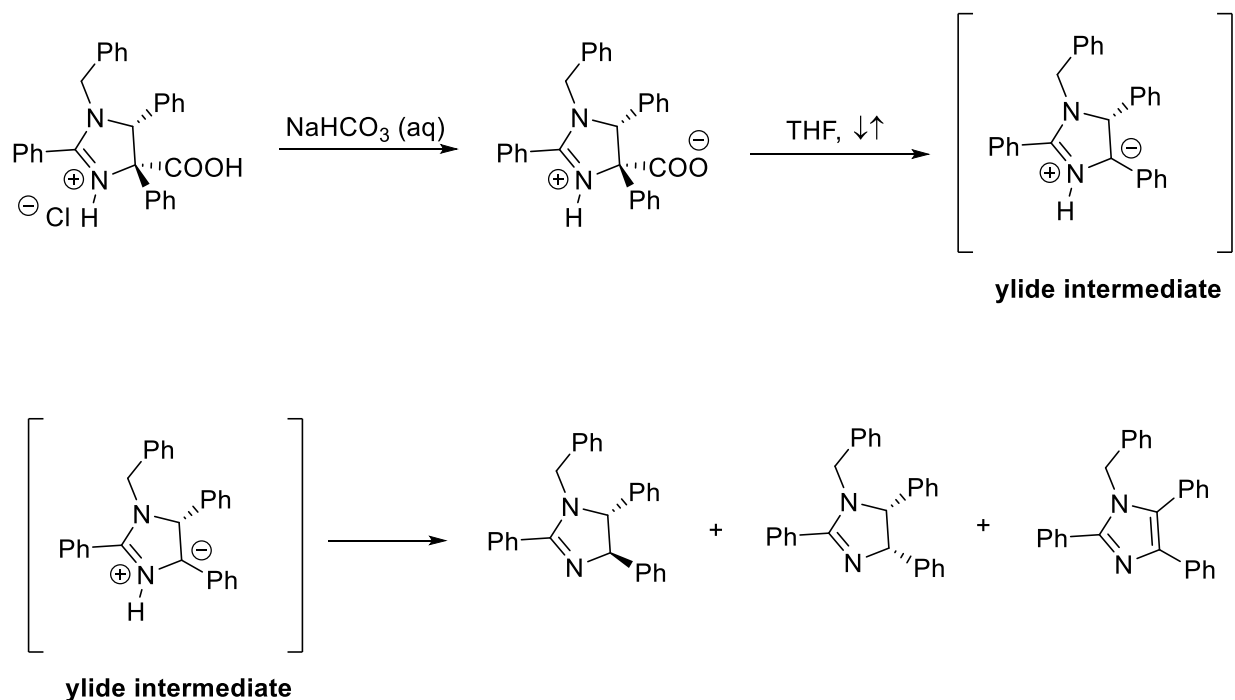


Figure I-XI: Different substitution patterns of 2-imidazolines at the 4,5 positions.

One of these methods utilized the intrinsic basicity of the imidazoline's nitrogen as a method of decarboxylation of the trisubstituted 2-imidazoline scaffolds to the disubstituted analogs. The formation of the stable ylide intermediate resulted in the imidazole, as well as the *cis* and *trans*-imidazolines.¹⁷



Kahlon, D. A.; Lansdell, T. A.; Fisk, J. S., Tepe, J. J. *Bioorg. Med. Chem.* **2009**, *17*, 3093 - 3103

Figure I-XII: The synthesis of disubstituted 2-imidazolines from trisubstituted 2-imidazolines.

In-situ synthesis of disubstituted 2-imidazolines can also be used as nucleophiles to undergo addition or conjugate addition to aldehydes and α,β unsaturated aldehydes respectively. The generation of this azomethine ylide when trapped by an electrophile resulted in the synthesis of *cis*-4,5-diaryl-2-imidazoline scaffolds. This *in-situ* decarboxylation followed by alkylation

resulted in accessing the cis-stereoisomer product, which was inaccessible when R₁= Phenyl in the azlactone cycloaddition. The major product of that reaction was the trans imidazoline.¹⁸

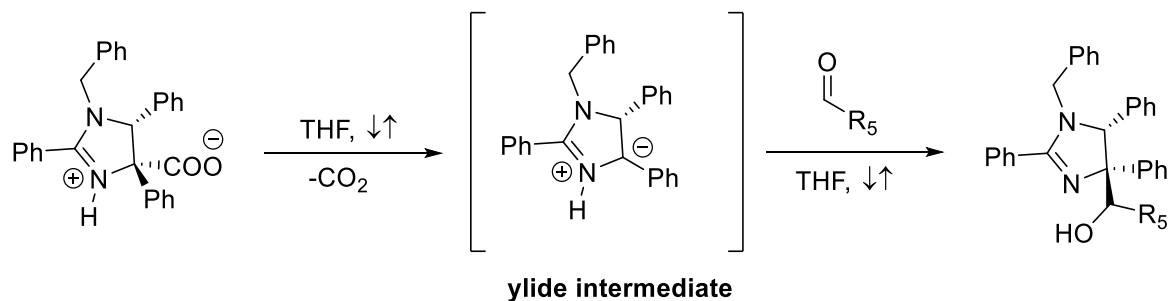
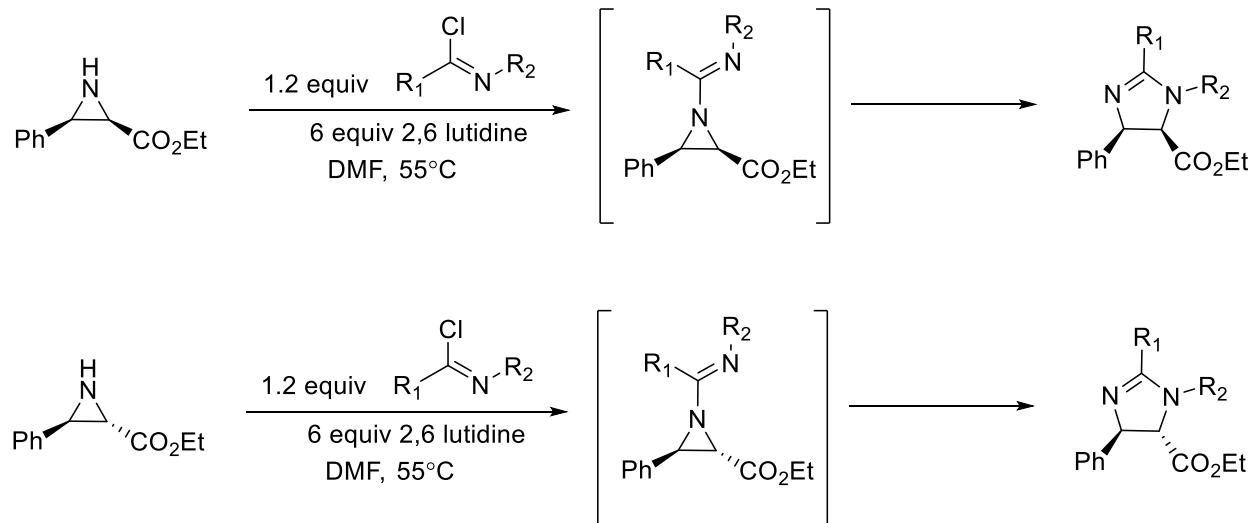


Figure I-XIII: Synthesis of cis-imidazolines generated *in-situ* from trans-imidazolines

Aziridine expansions

The Tepe group has developed methodology towards accessing imidazoline scaffolds from the expansion of aziridines. The generation of imidoyl chlorides from amides in the presence of aziridines result in the formation of imidoylaziridines, which expand under the reaction conditions to give the resulting disubstituted imidazolines.¹⁹



Kuszpit, M. R.; Wulff, W. D.; Tepe, J. J. *J. Org. Chem.* **2011**, *76*, 2913-2919

Figure I-XIV: Synthesis of disubstituted imidazolines from aziridines.

Imidazolines are versatile heterocycle compounds whose industrial applications as surfactants and anti-corrosion agent, catalysis and ligand potential, as well as pharmacophore abilities have motivated researchers towards developing continuous methods for accessing them. These efforts will be further eluded on throughout the dissertation as we show improvements to already known transformations in both yield and potency of pharmacophore properties. New approaches to accessing imidazolines and other small molecule heterocycles will also be shown with explanations into the extent of the capability of the mechanisms behind the transformations.

CHAPTER TWO – IMIDAZOLINE SAR EVALUATION FOR TB PROTEASOME INHIBITION

The overall aim of this research was the further development of innovative imidazoline scaffolds through novel synthesis and published systematic synthetic transformations to access a small library of compounds. These molecules could be used to further elucidate the mechanism of proteasome inhibition observed in the presence of imidazoline compounds. Probing this overall action would further highlight the key factors necessary for increasing efficacy and potency of the imidazoline scaffolds, such as structural diversity, functional group tolerance and molecular recognition to the binding site. It was hypothesized that further exploration into this chemistry would result in the development of enhanced specificity for targeting specific proteasomes in the presence of native ones. Accessing greater potency and specificity would allow for the better treatment of diseases and afflictions that employ the proteasome in their method of activation and persistence such as tuberculosis (TB) and multiple myeloma (MM). The research in this chapter will focus specifically on identifying the key binding motifs in the imidazolines scaffolds with the human 20S proteasome as well as the TB proteasome. The structural activity of the compounds will elucidate what functionalities are necessary for potent inhibition of both proteasomes. Evaluation of structural features will also highlight how selectivity between these two proteasomes can be accessed based on substitution pattern. The final goal of this project is to incorporate both factors, specificity and potency into designing a molecule to inhibit the TB proteasome over the human proteasome (h20S). Achieving proteasome specificity will allow for targeted treatment without undesired side effect of host toxicity.

The proteasome is a protease responsible for maintaining cell viability, homeostasis and regulation of cellular functions. The human proteasome, commonly referred to as the 26S, is comprised of the catalytic 20S core particle and two 19S regulatory caps. When these three groups assemble the 26S proteasome is formed and its function is to cleave proteins marked for degradation into their resulting amino acids. These amino acids can then be recycled by the cell towards other necessary cellular functions. The 19S caps act as recognition sites, identifying proteins that have been polyubiquitinated and funneling them into the catalytic 20S particle for degradation. Developing molecules that specifically target the proteasome result in modulation of proteasome activity when they bind. This modulation changes the rate of peptide degradation done by the proteasome. Imidazolines scaffolds have been experimentally shown to decrease proteasome activity. This decrease effects the degree to which the proteasome can effectively degrade proteins to maintain intercellular processes. Polyubiquitinated proteins begin to accumulate in the cell and result in downstream apoptosis.²⁰⁻²¹

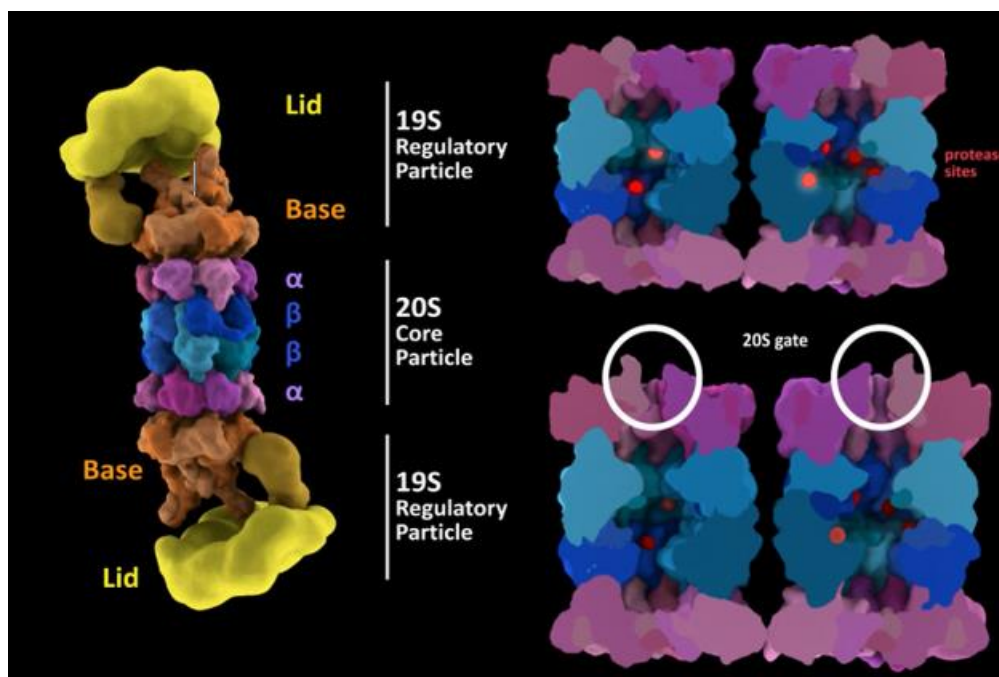


Figure II-I: Shows the h26S proteasome and its components, the h20S and the 19S caps.

Multiple myeloma is a malignant cancer of the plasma cells, found in blood. Although largely incurable, the lifespan of patients can be prolonged through the use of drug therapy. The target of synthetic drugs and polypeptide therapies is the proteasome, which has been identified as the linchpin for activating cell death. Bortezomib, is the one of leading proteasome inhibitors, and has been approved in the U.S. for the treatment of multiple myeloma. Drugs like Bortezomib, exhibit activity through competitive inhibition of the proteasome. This causes proteolysis to stop, thereby causing the accumulation of redundant and damaged proteins in the cell which result in cell death. This ability directly translates to the molecules' potent anticancer activity.²²⁻²³ However over time random mutations occur in cancer cells proteasomes that result in loss of efficacy for Bortezomib and similar therapies.²⁴ Apart from loss of activity, extended use of Bortezomib has resulted in severe off-target effects, due to lack of specificity for the proteasome of cancerous cells. In response to this, research has begun to investigate other methods of proteasome inhibition in an effort to combat the growing resistance to current competitive inhibitors like Bortezomib. Although these mutated cells have developed resistance to the mechanism of competitive inhibition, they are still susceptible to drugs that can target the proteasome through noncompetitive inhibition. Results have shown that off target side effects can be reduced through the use of non-competitive inhibitor causing lowered toxicity to the host.

Tuberculosis is an infectious disease that is spread by *Mycobacterium tuberculosis* (mTB). The emergence of multidrug and extensive drug resistant forms of TB have revitalized the need for novel scaffolds for TB inhibition. TB is highly infectious with approximately 7 million people being diagnosed with new cases of infection on an annual basis. The mode of infection with TB is

one of the compounding issues that is responsible for the large number of infections and deaths due to TB. *Mycobacterium tuberculosis* is transmitted through coughing and sneezing which aerosolizes the bacteria. This allows for one sick patient to infect many people without ever having to come into direct skin to skin contact. The innate nature of the bacteria also affects treatment methods. This mycobacterium possesses a waxy cell wall that protects them from desiccation allowing them to remain viable for up to 6 months as dried aerosol droplets. The slow growth of this bacteria in the body makes treatment difficult because common antimicrobials like penicillin are expelled from the body by the liver before they can have any realistic effect on the bacteria. The last key factor that aids the spread of the TB, is the fact that mTB has two states, active and persistent. The active state is characterized as the initial infection of mTB that the body can recognize and signal for macrophages to engulf and attempt to destroy. In response to this, the mycobacterium can switch to its persistent state to avoid the oxidative stress of nitric oxide that is used by macrophages to destroy foreign bacteria. In its persistent or hibernation state the infection becomes latent, avoiding any body immune responses by hiding in macrophages until the host undergoes an event that causes the immune system to become compromised which reactivates the latent TB infection. The emergence of drug resistant TB stems from a combination of access to treatment options and compliance to medication for the full treatment term in 3rd world countries. Often miseducation about TB and its behavior result in patients abruptly stopping treatments like Isoniazids as soon as visible symptoms disappear, instead of continuing the drug regiment in its entirety. The normal treatment time for a TB infection is 6-8 months to insure there is no secondary infection. One of the key factors that is being targeted in an attempt to combat TB is the inhibition of the proteasome. When mTB switches from its active mode to its passive or persistent mode, it is forced to use different metabolic pathways to survive in a low nutrient environment. One of the

key factors to that survival is the recycling of proteins to make the amino acids available for other cellular operations, which the proteasome is responsible for.²⁵ It has also been seen that when the bacterium has its genes that encode for proteasome activity deleted, the bacteria becomes hypersensitive to the presence of nitric oxide, found in activated macrophages, lowering overall bacterial cell survival. Methods of inhibiting the bacterial proteasome are therefore the best target for aiding in the host body's immune response to destroy this foreign bacteria by disrupting the machinery necessary for maintaining cell viability.²⁶ Targeting the proteasome and changing its reactivity will result in varying the degree to which it can degrade proteins to maintain intercellular processes.²⁷ It is this potential, which we hope to exploit further towards the continued treatment of ailments that heavily rely on proteasome function.

Previous work in the Tepe group accessed large libraries of disubstituted and trisubstituted imidazoline compounds. A large subgroup of those compounds were screened against TB and h20s proteasome for *in vitro* inhibition.^{17, 28} Each molecule's biological activity was evaluated and the screening process identified two key imidazoline scaffolds as synthetic lead compounds. Further synthetic development to those scaffolds was proposed to identify which structural components are necessary for drug viability and specificity.

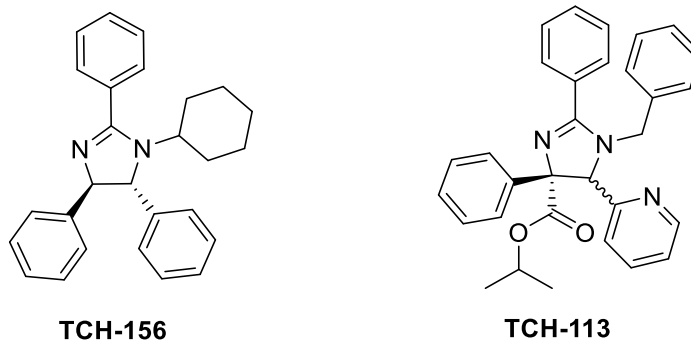
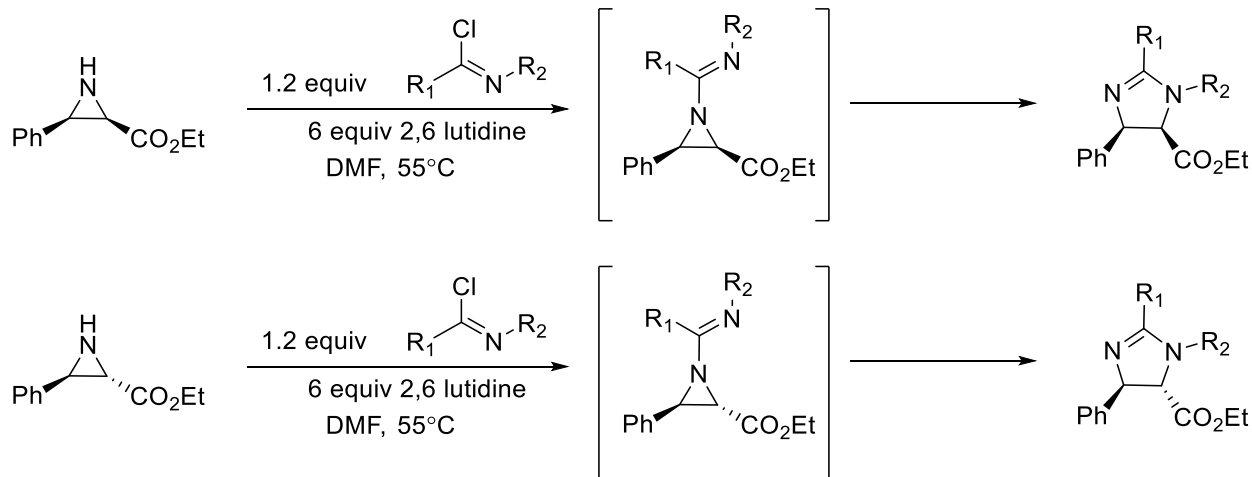


Figure II-II: Identified potent structures by screening for proteasome inhibition.

Those two scaffolds are TCH-156 and TCH-113. TCH-156 was isolated as a racemic mixture and TCH-113 was isolated as a mixture of *cis-trans* isomers. TCH-156 and TCH-113 are both classes of imidazolines but are distinctly different structurally. Despite their structural difference both molecules inhibit the proteasome. This result has further reaffirmed our hypothesis that a library of imidazolines can be structurally tailored to promote potent inhibition. Both molecules highlight distinct functionalities that might be responsible for their inhibition. The initial screen highlighted the fact that TCH-156 was a more potent proteasome inhibitor than TCH-113. Based on this identification, the key functional groups for increased efficacy for TB inhibition of imidazoline scaffolds was proposed for disubstituted imidazolines, like TCH-156.

Within the Tepe group, one of the methods used to access these imidazoline scaffolds is through a regiocontrolled and stereospecific Heine-like ring expansion to yield 2-imidazolines. These imidazolines were accessed from the one pot ring expansion of imidoyl aziridines. This previous work demonstrated that the reactive intermediate, the imidoyl aziridine, can be accessed from the highly reactive imidoyl chloride derivative of a starting amide, made *in-situ* by the addition of oxalyl chloride in the presence various organic bases.¹⁹



Kuszpit, M. R.; Wulff, W. D.; Tepe, J. J. *J. Org. Chem.* **2011**, *76*, 2913-2919

Figure II-III: Ring expansion of imidoyl aziridines to yield imidazoline scaffolds.

The synthesis of an imidazoline library also presented an opportunity to further probe the specifics of the mechanism by which the imidazolyl chlorides expand to imidazolines as well as further clarify the experimental factors necessary to form imidazolines as products. This library would also probe the correlation between functional group and potency of inhibition to highlight any ambiguous motifs tied directly to imidazoline efficacy or specificity for TB's proteasome.

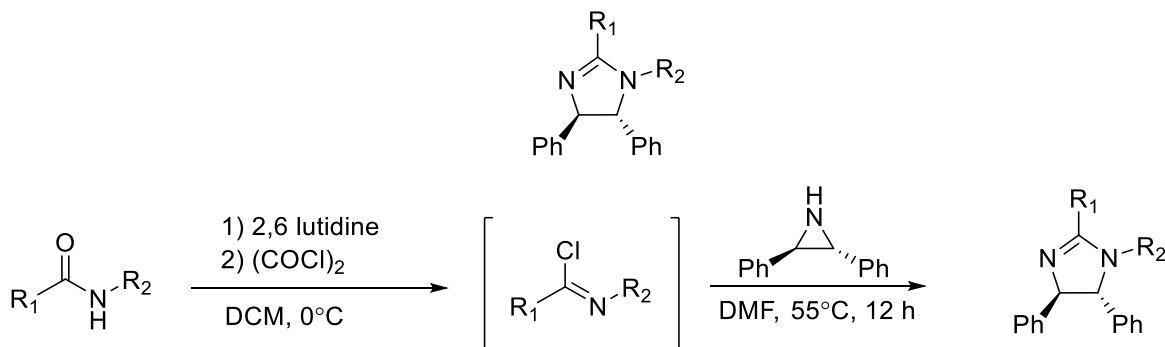


Figure II-IV: Identifies the positions to be probed by SAR analysis.

The imidazolines were formed from the expansion of imidoyl aziridines. The synthesis of trans-2,3-diphenylaziridine was necessary to access the diphenyl substitution pattern of the imidazoline core at the 4 and 5-positions (Figure).

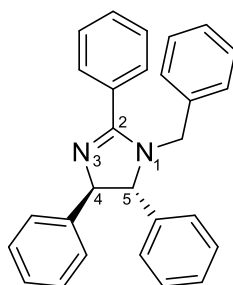
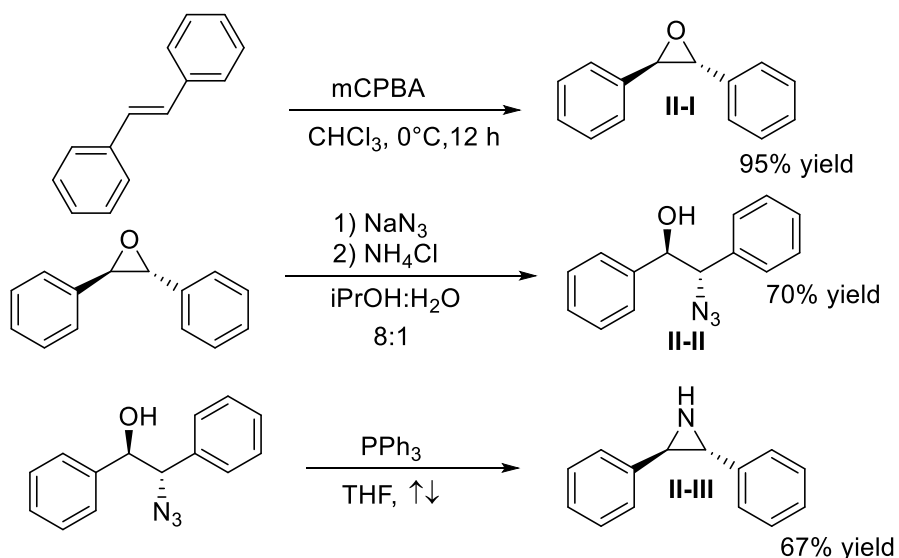


Figure II-V: Identifies the numbering pattern for 2-imidazoline scaffolds.

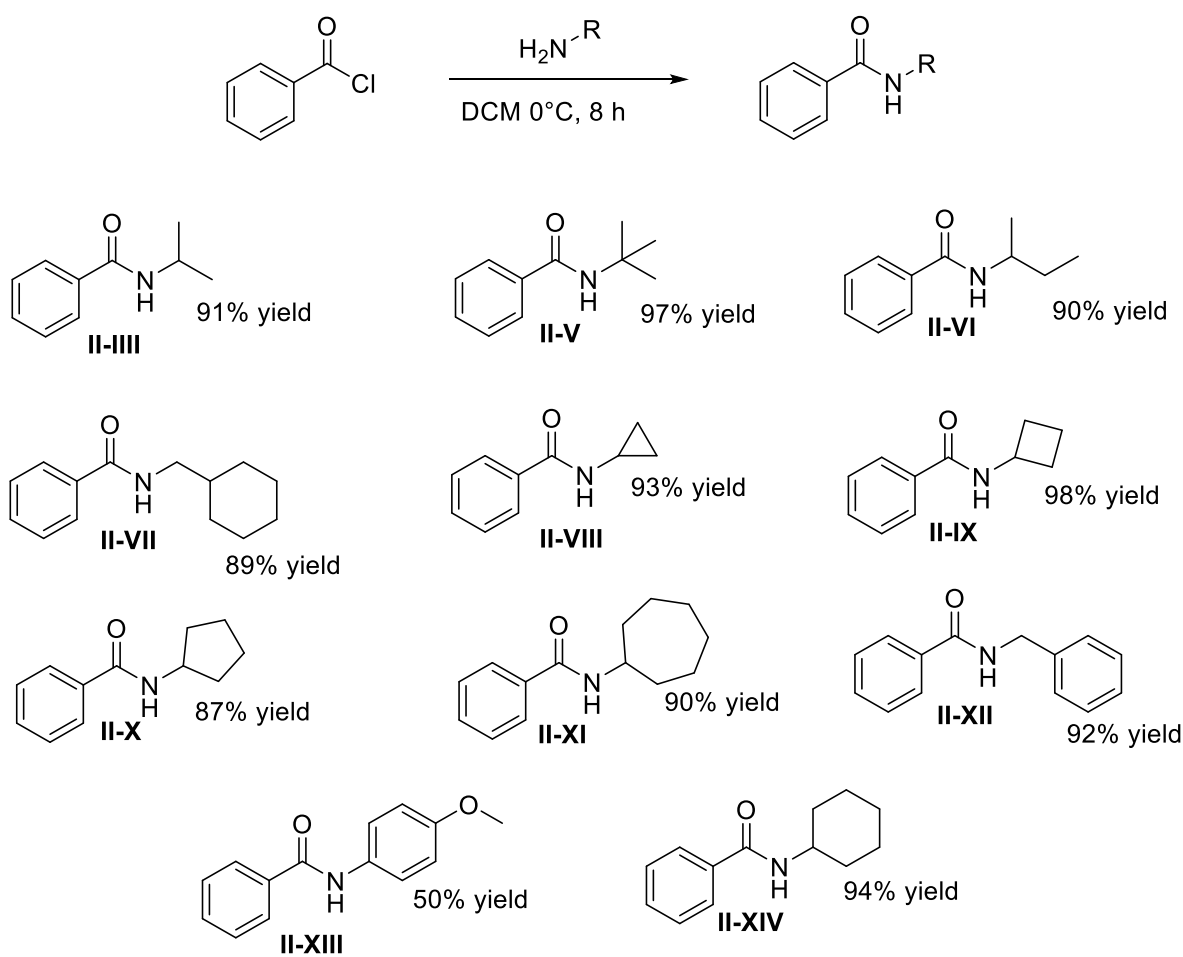
This aziridine was synthesized by the following transformations using the Staudinger reaction.²⁹



Scheme II-I: Synthetic pathway to accessing trans-2,3-diphenyl aziridine starting material.

Initially two points of interest were highlighted for primary screening. The first was the 2-position of the imidazoline. The hypothesis was that the group tethered to the 2-position's

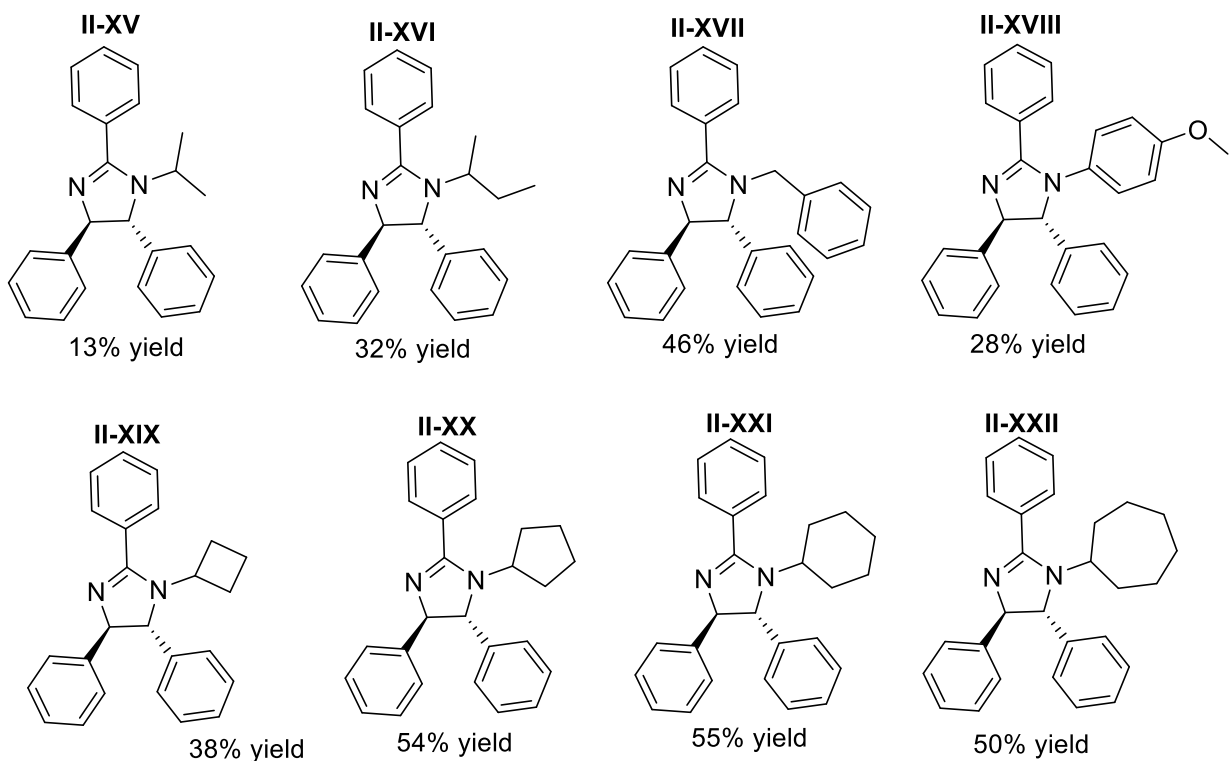
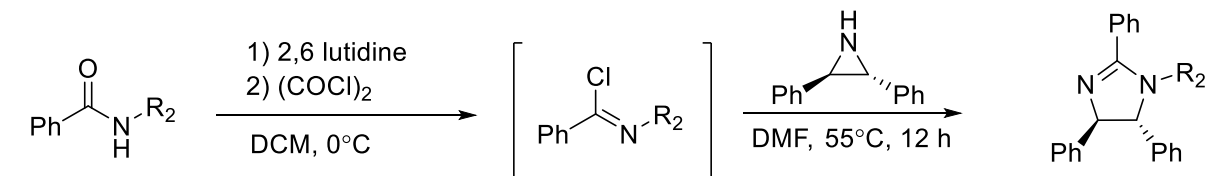
nitrogen of the imidazoline has a direct response in molecule efficacy. To verify this hypothesis, amides were accessed by the Schotten-Baumann reaction. This reaction incorporated amines with various N-alkyl and N-aryl groups with acid chlorides to give N-alkylated and N-aryl amides.



Scheme II-II: Synthetic pathway for accessing amide precursors.

Once these amides were accessed they were exposed to oxalyl chloride in the presence of 2,6 lutidine to generate the reactive imidoyl chloride intermediate (**Figure I-III**). This crude product was isolated and exposed to the trans-2,3-diphenylaziridine in DMF at 55°C for 12-14

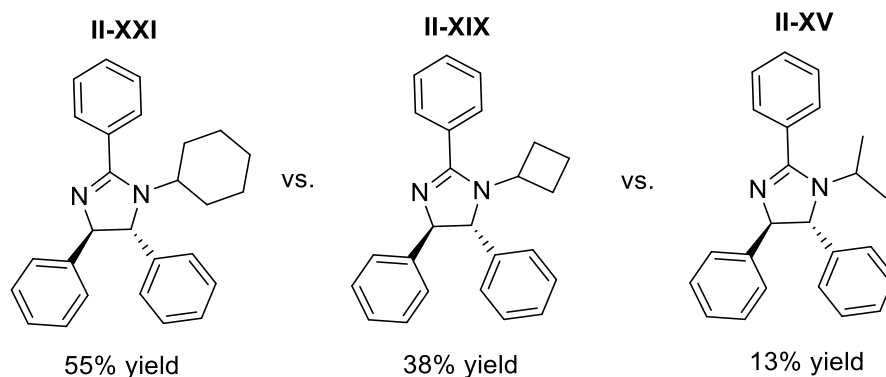
hours after which it was purified under column chromatography to yield the following imidazolines.



Scheme II-III: Shows the imidoyl chloride formation and resulting expansion to imidazolines.

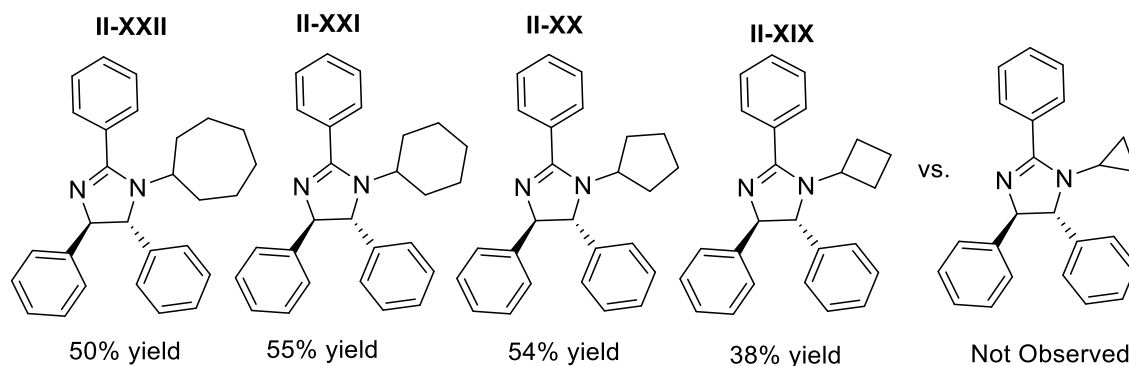
Variation of the 1-position and its resulting expansion illustrated the overall yield of the imidazoline is very dependent on the N-alkyl and N-aryl of the starting amide. This may also elude to each group's effect on the formation of the imidoyl chloride intermediate within the timescale

of the reaction. The expansion tolerated both cycloalkyl and alkyl group but showed a large decrease in yield as the mass of the substituent on the 3-position decreased.



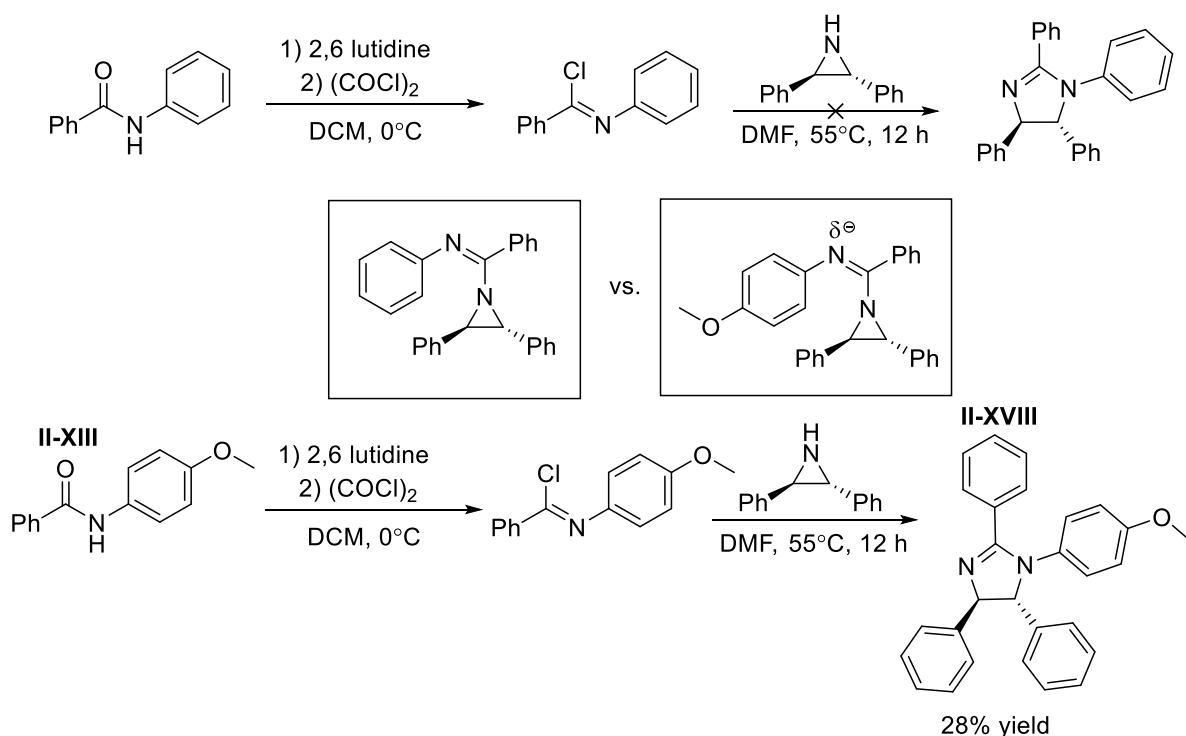
Scheme II-IV: Shows the difference in yield when the N-substituent was varied.

The failed expansion of the N-cyclopropylbenzamide in comparison to the N-cyclobutyl, N-cyclopentyl, N-cyclohexyl and N-cycloheptylbenzamides under the same reaction conditions may suggest the presence of a background radical reaction that occurs in the same timescale as the imidoylaziridine expansion. This implied that the cyclopropyl group was behaving as a radical scavenger and being consumed. This is further supported by the moderate yields of this expansion reaction.



Scheme II-V: Identified expansion products dependence on N-1 alkyl group.

Expansion of the N-benzyl amide was seen in moderate yields. Past research showed that N-phenyl substitution did not allow for ring expansion to the 2-imidazoline. It was hypothesized that this was due to the electron withdrawing group on the amide. This group hindered the formation of the imidoyl chloride and the expansion of the resulting imidoylaziridine was halted because the intermediate's lone pair was stabilized through resonance. This also lowered the nitrogen's nucleophilicity enough to undergo ring expansion to yield the imidazoline. To better probe this the amide of p-anisidine was used because of the donating ability of the p-methoxy group which enhances the nucleophilicity of the anisidine nitrogen in comparison to the aniline derivative.



Scheme II-VI: Highlighted the influence of EDG on acylated aniline expansion.

The proteasome is a quaternary protein structure and therefore has an overall 3-D shape to its structure and its active sites. It was proposed that differences in alkyl group size would give key insight into the molecule's interaction with the proteasome's active site(s) or surface of the proteasome. This is because we proposed that the size of the alkyl functionality was instrumental to evoking a conformational change that would result in modulation of proteasome activity. Changing the size of that alkyl or aryl chain would result in changing the 3-D structure of the overall imidazoline and would cause a difference in the way it interacted with the 3-D structure of the proteasome. This would be reflected in the differences in biochemical activity of the imidazolines with varied N-alkyl and aryl groups at the 3-position. Biological evaluation of the imidazolines was done on a purified protein assay. This assay introduced the imidazolines in varying concentrations to the enzyme (the proteasome) and its response to being exposed to the imidazolines was monitored by the change in the enzyme's ability to digest the substrate (Suc-LLVY-AMC). The results were as followed:

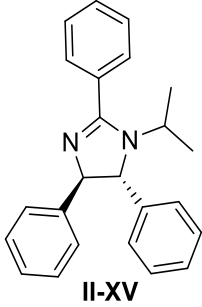
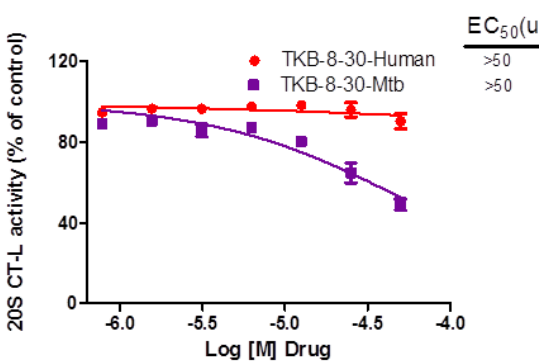
Name/Structure	Dose Response Curve	EC ₅₀ - Human	EC ₅₀ - <i>Mtb</i>	Fold selectivity for <i>Mtb</i>
 <p style="text-align: center;">II-XV</p>		IA	IA	NA

Table II-I: The effect of N-1 functionalization on potency and specificity in h20S and TB proteasome.

Table II-I cont'd

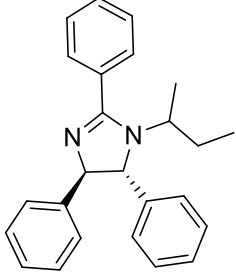
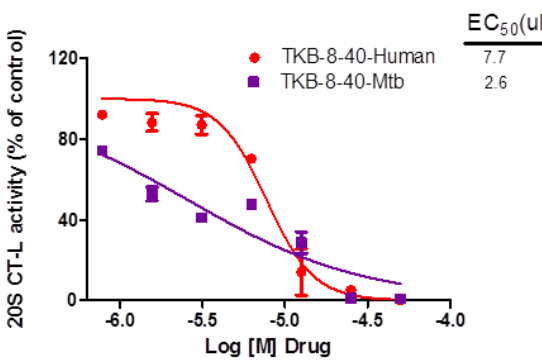
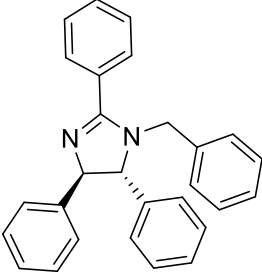
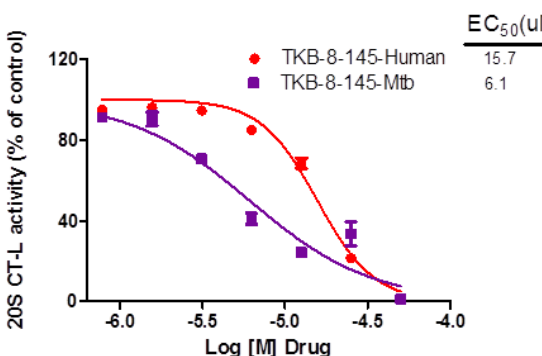
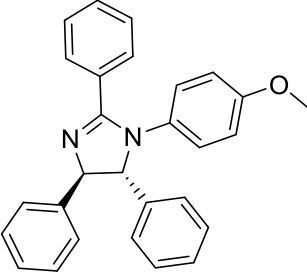
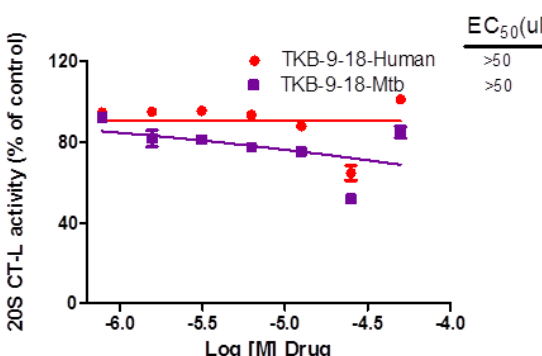
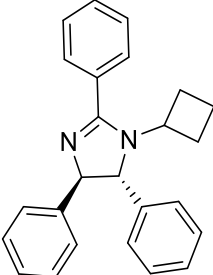
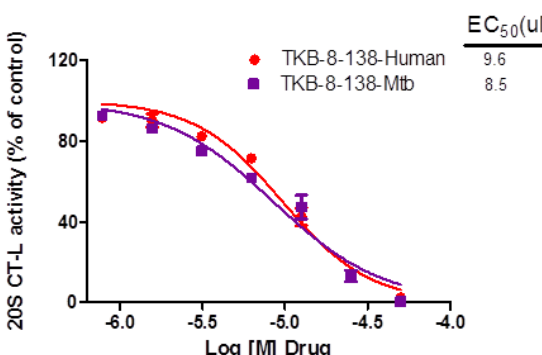
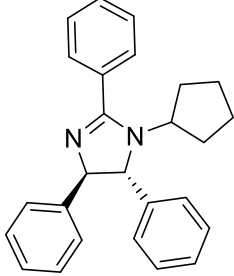
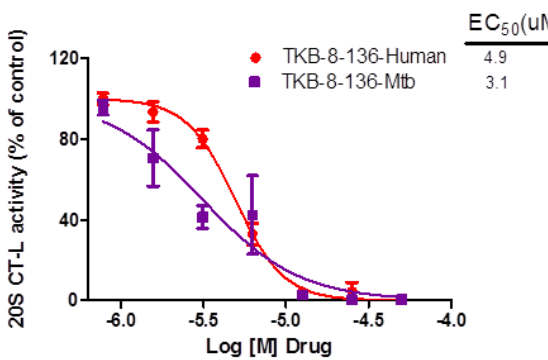
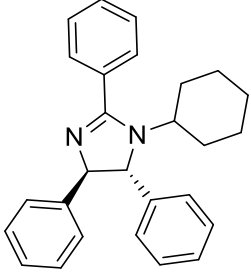
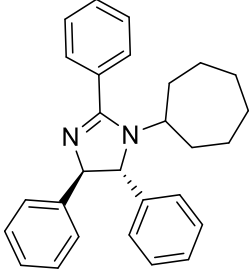
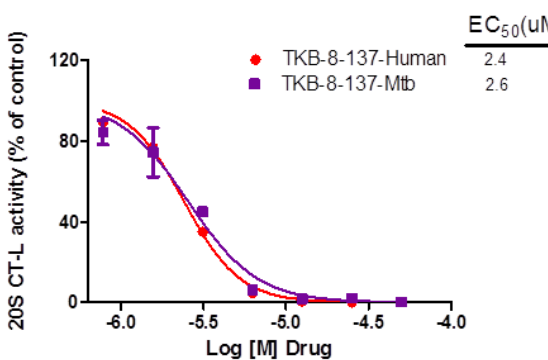
 <p>II-XVI</p>	 <p>EC₅₀(uM)</p> <table border="1"> <tr> <td>TKB-8-40-Human</td> <td>7.7</td> </tr> <tr> <td>TKB-8-40-Mtb</td> <td>2.6</td> </tr> </table>	TKB-8-40-Human	7.7	TKB-8-40-Mtb	2.6	7.7	2.6	3
TKB-8-40-Human	7.7							
TKB-8-40-Mtb	2.6							
 <p>II-XVII</p>	 <p>EC₅₀(uM)</p> <table border="1"> <tr> <td>TKB-8-145-Human</td> <td>15.7</td> </tr> <tr> <td>TKB-8-145-Mtb</td> <td>6.1</td> </tr> </table>	TKB-8-145-Human	15.7	TKB-8-145-Mtb	6.1	15.7	6.1	2.6
TKB-8-145-Human	15.7							
TKB-8-145-Mtb	6.1							
 <p>II-XVIII</p>	 <p>EC₅₀(uM)</p> <table border="1"> <tr> <td>TKB-9-18-Human</td> <td>>50</td> </tr> <tr> <td>TKB-9-18-Mtb</td> <td>>50</td> </tr> </table>	TKB-9-18-Human	>50	TKB-9-18-Mtb	>50	IA	IA	NA
TKB-9-18-Human	>50							
TKB-9-18-Mtb	>50							
 <p>II-XIX</p>	 <p>EC₅₀(uM)</p> <table border="1"> <tr> <td>TKB-8-138-Human</td> <td>9.6</td> </tr> <tr> <td>TKB-8-138-Mtb</td> <td>8.5</td> </tr> </table>	TKB-8-138-Human	9.6	TKB-8-138-Mtb	8.5	9.6	8.5	1.1
TKB-8-138-Human	9.6							
TKB-8-138-Mtb	8.5							

Table II-I cont'd

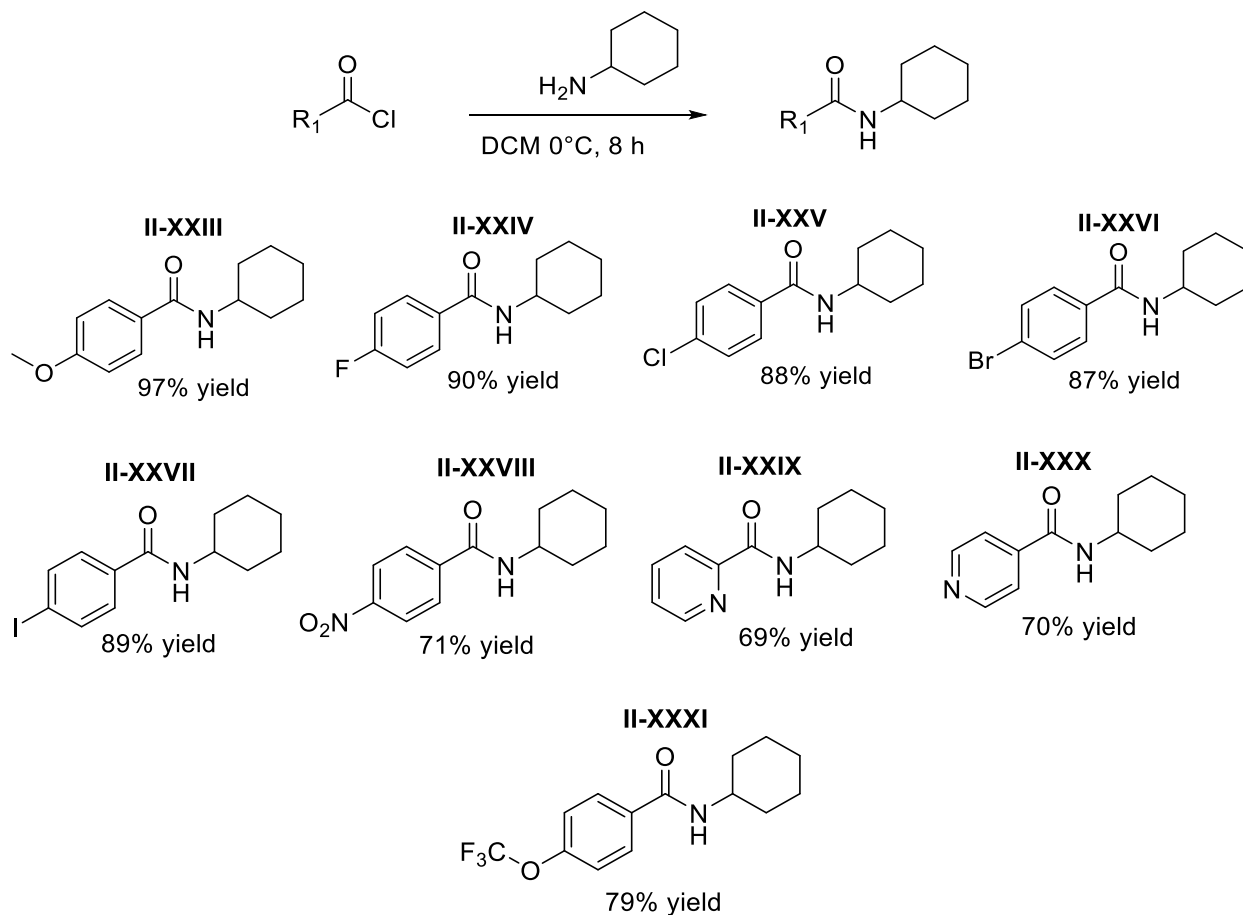
 <p style="text-align: center;">II-XX</p>	 <p style="text-align: right;"> $EC_{50}(\mu M)$ TKB-8-136-Human: 4.9 TKB-8-136-Mtb: 3.1 </p>	4.9	3.1	1.6
 <p style="text-align: center;">II-XXI</p>				
 <p style="text-align: center;">II-XXII</p>	 <p style="text-align: right;"> $EC_{50}(\mu M)$ TKB-8-137-Human: 2.4 TKB-8-137-Mtb: 2.6 </p>	2.4	2.6	0.9

Based on the SAR of the imidazoline compounds there is a direct correlation to the N-alkyl and N-aryl groups and the activity of the compounds towards proteasome inhibition. This result implicated the importance of the 3-D structure of the imidazoline for proper binding with the proteasome. It is this proposed binding that results in a change in conformation, or the lowering of enzyme activity which results in enzyme retardation. This hypothesis was also supposed by computational modelling of the imidazoline structures with the crystal structure of the TB

proteasome. The computational model used the 3-D structure of each imidazoline against the 3-D structure of TB proteasome and calculated the modes of binding to predict the common position for molecule binding as well as binding affinity based on each individual imidazoline. This modeling highlighted that the substituent on the 3-position of the imidazoline is necessary for anchoring the molecule in the subunit of the α -ring in TB. When the N-cyclohexyl derivative was modeled the chair form anchored the imidazoline firmly into the subunit. Modeling of smaller N-alkyl groups showed a decrease in binding affinity that was directly tied to the size of the alkyl group. These molecules had an increased number of lower binding sites, in comparison to the one high binding domain of the N-cyclohexyl derivative which also highlighted the molecules inability to firmly anchor itself to on common site within the subunits.

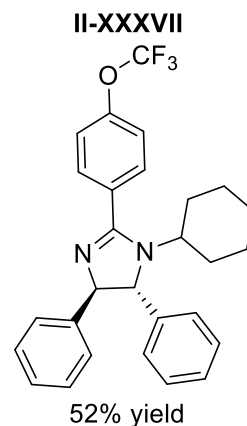
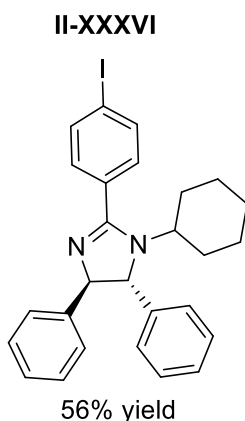
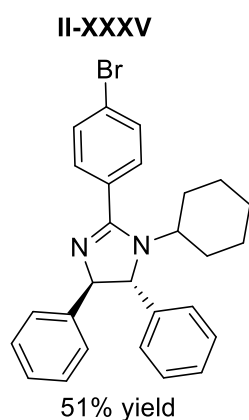
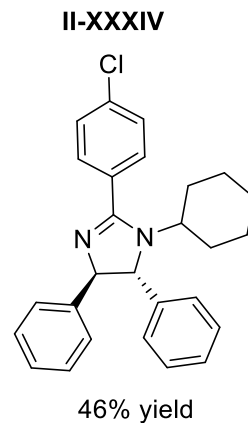
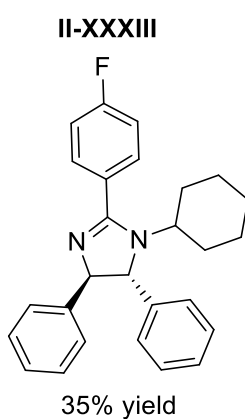
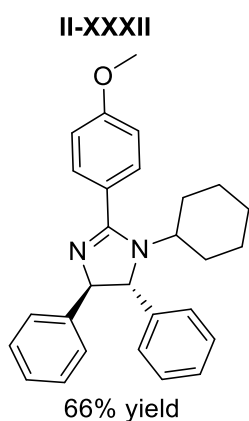
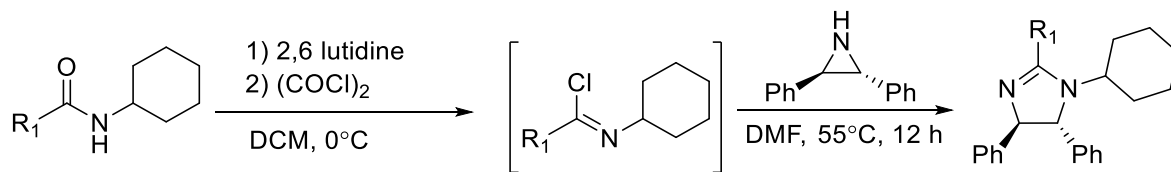
Compiling the data, the N-cyclohexyl group was chosen as the lead N-alkyl group for the 1-position due to its influence on the SAR with the TB proteasome as well the suggested binding of the structure with computational modeling. The computational analysis also spurred interest in further imidazoline scaffolds. These amides were accessed by the Schotten-Baumann reaction, with amines that incorporated various acyl halides and resulted in varied aryl and alkyl groups of the N-cyclohexyl amides. The influence of substitution at the 2-position was then explored further to probe its effect on the expansion reaction. Changing the substituent would influence the potency of imidazoline compounds and allow experimental comparisons between the structural changes and their resulting effects on binding affinity. These experimental results could then be compared to the predictions within the computational model to better understand factors for molecule potency. The primary hypothesis was one of the major factors influencing the activity of the imidazoline compounds towards inhibition was tied to the electron density of the imidazoline ring. Increasing the electron density of the ring through contribution at the 2-position should have

lowered the IC₅₀ value of the compound, reflecting its enhanced potency. The IC₅₀ value is the minimum inhibitory concentration of the molecule responsible for retarding the *in vitro* activity of a biological system by 50 %.



Scheme II-VII: The synthesis of amide precursors for probing the 2-position on imidazoline molecules.

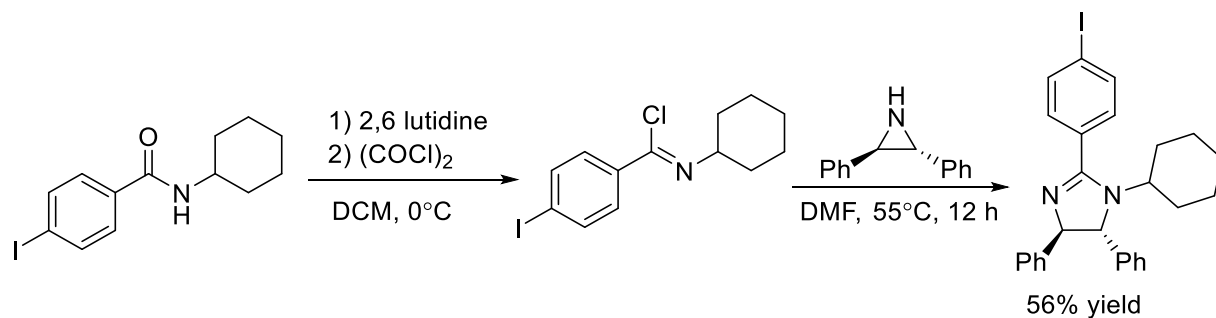
The following amides were exposed to the same reaction conditions for imidazoline expansion, and were used to measure the effect of electron donating groups (EDG) and electron withdrawing groups (EWG) towards intermediate imidoylaziridine generation and product formation.



Scheme II-VIII: Synthesis of imidazoline scaffolds with different C-2 groups.

The following imidazolines were accessed in moderate to good yields and highlighted the effect of substitution on the acyl group of the amide to the resulting imidazoline. EDG's like the 4-methoxy derivative resulted in a greater yield for the imidazoline product. This is likely due to the increased electron density of the imidazolyl aziridine intermediate, which in turn resulted in a larger ratio of expanded product. The effect of EWG was also displayed. Mild EWG's like the 4-iodo and 4-bromo analogs have very little effect on the yield of the overall expansion. Moderate

EWG's like the 4-chloro and 4-fluoro resulted in a lower yield of the expanded imidazolines and this is likely due the lower electron density of the intermediate which results in decreased expansion of the aziridine to the imidazoline.



Scheme II-IX: Example of expansion of amides with mild EWG to imidazolines

This is further supported by the failed expansions of the N-cyclohexylpicolinamide, N-cyclohexylpicolinamide, and N-cyclohexyl-4-nitrobenzamide to their respective imidazolines. These strong electron-withdrawing groups halt either the formation of the imidoyl chloride intermediate or the following expansion of the imidoyl aziridine and only result in starting material recovery or decomposition upon completion of the reaction timeline.

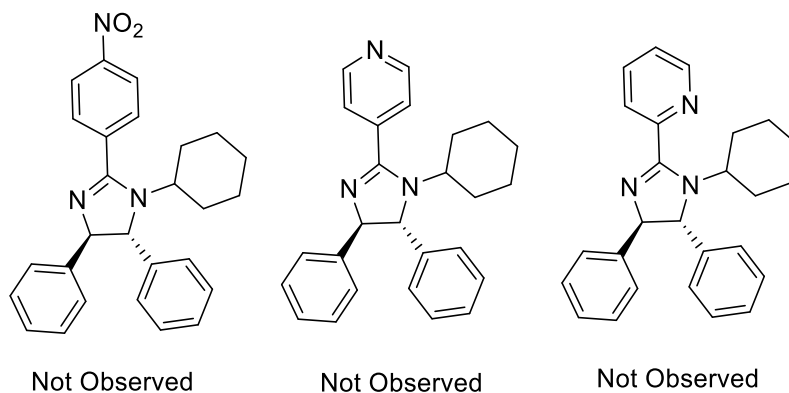
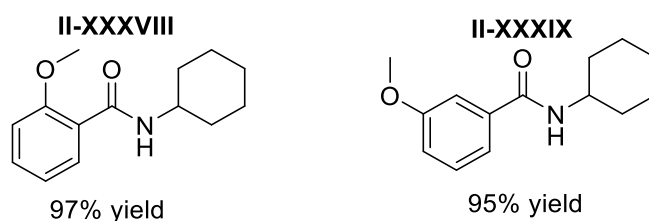


Figure II-VI: Molecules that were not accessed under reaction conditions.

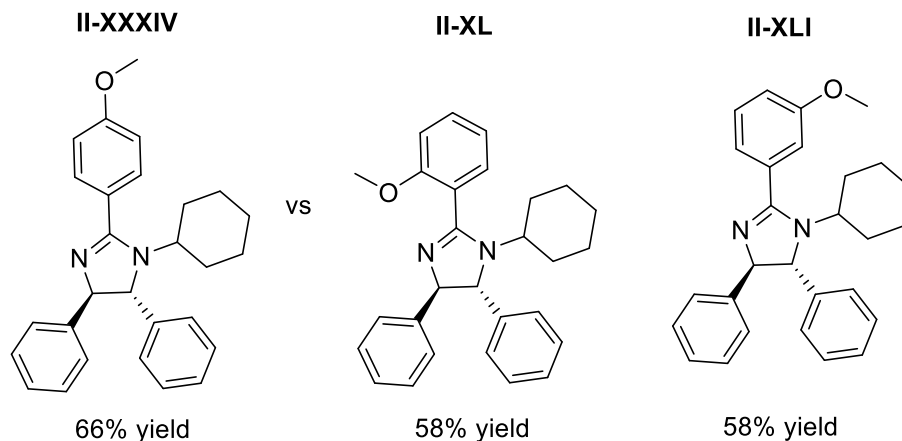
Attempts to synthesis the imidazolines of the N-cyclohexylpicolinamide and N-cyclohexylpicolinamide were done in an effort to modify the current disubstituted imidazoline scaffolds to bare similarity to TCH-113. TCH-113 bares a 2-pyridyl ring in its structure and we wanted to probe whether this functionality could preferentially inhibit the TB proteasome over human proteasome, like TCH-113.

The location of the donating group on the aromatic ring, directly effects its ability to enhance the electron density of the corresponding imidoyl aziridine intermediate. To probe the results of this enhancement the 2-methoxy and 3-methoxy constitution isomers of the N-cyclohexylmethoxy benzamide were accessed via the Schotten-Baumann reaction.



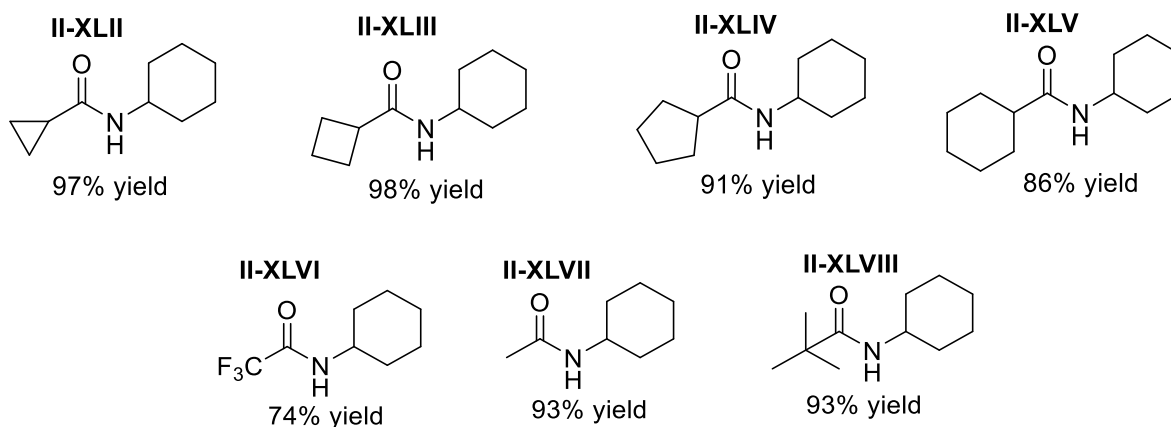
Scheme II-X: Synthesis of amide precursors to probe Ortho vs Meta vs Para substituent effect.

These amides were then exposed to the same reaction conditions to probe the influence of substitution pattern on imidazoline formation. Both constitutional isomers expanded to yield the imidazolines in moderate yield.



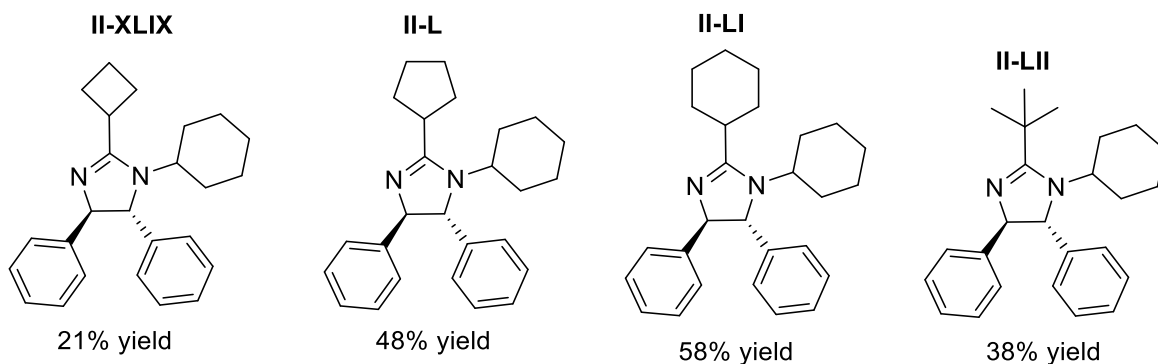
Scheme II-XI: Synthesis of imidazolines to probe Ortho vs Meta vs Para substituent effect.

The versatility of the imidoyl aziridine expansion was further explored to decipher if it tolerated N-alkyl groups amides towards formation of imidazolines with alkyl groups at the 2-position. It was proposed that alkyl groups would donate inductively to the imidazoline ring, increasing its electron density, like what was experimentally observed with EDG in the acyl amide example. To confirm this hypothesis the following amides were accessed:



Scheme II-XII: Synthesis of amide precursors to probe C-2 alkyl substituent and size effect.

These amides were exposed to the reactions conditions and yielded the following imidazolines, in moderate yield:



Scheme II-XIII: Synthesis of imidazolines to probe C-2 alkyl substituent and size effect.

The experimental results re-enforced the same observations noted in the expansion of acyl amides. Strong electron withdrawing groups like the N-cyclohexyl-2,2,2-trifluoroacetamide again caused the expansion to fail. The decomposition of the reaction involving N-cyclohexylcyclopropanecarboxamide again suggested that there might be a background radical reaction occurring in the same timescale as the expansion, with the cyclopropyl group acting as a radical trap. The failed reaction of N-cyclohexylacetamide also reinforced the observation of a direct comparison of the decrease in yield with decreasing size of the functionality.

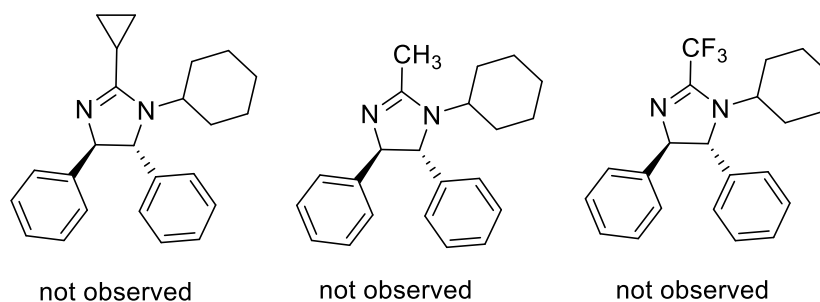


Figure II-VII: Molecules that were not accessed under reaction conditions.

The results of the SAR of the imidazolines were as followed:

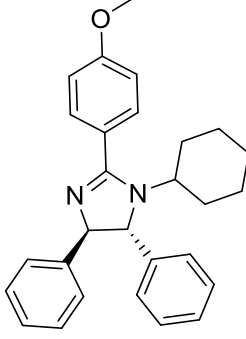
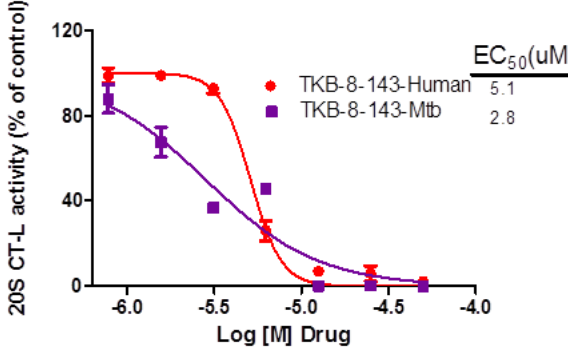
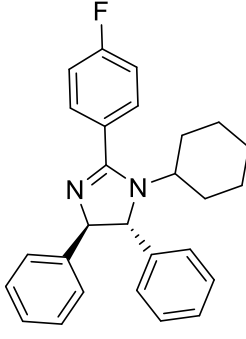
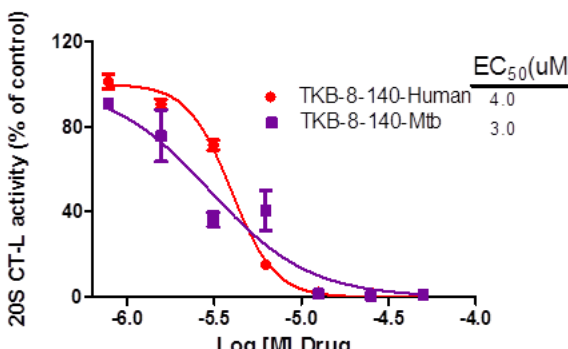
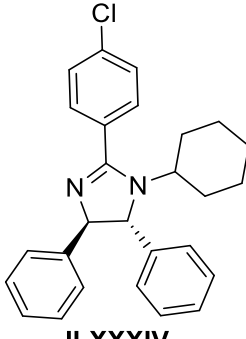
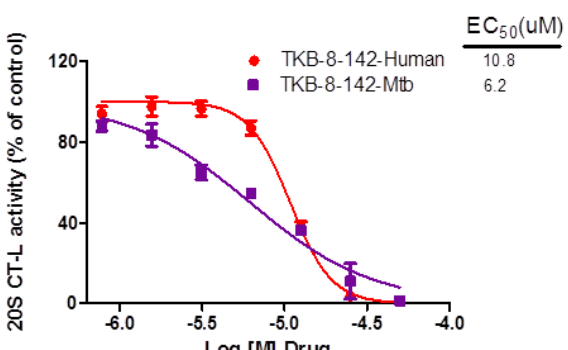
Name/Structure	Dose Response Curve	EC ₅₀ -Human	EC ₅₀ - <i>Mtb</i>	Fold selectivity for <i>Mtb</i>
 <p>II-XXXII</p>		5.1	2.8	1.8
 <p>II-XXXIII</p>		4.0	3.0	1.3
 <p>II-XXXIV</p>		10.8	6.2	1.7

Table II-II: The effect of N-1 functionalization on potency and specificity in h20S and TB proteasome

Table II-II cont'd

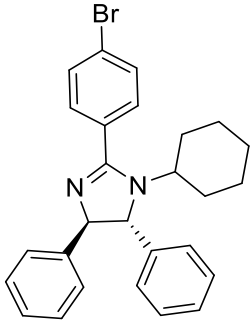
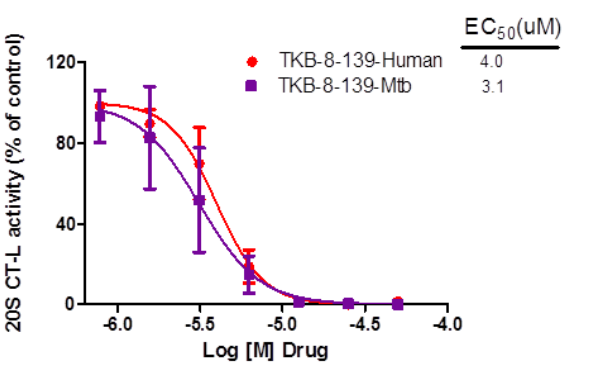
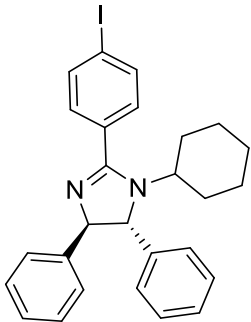
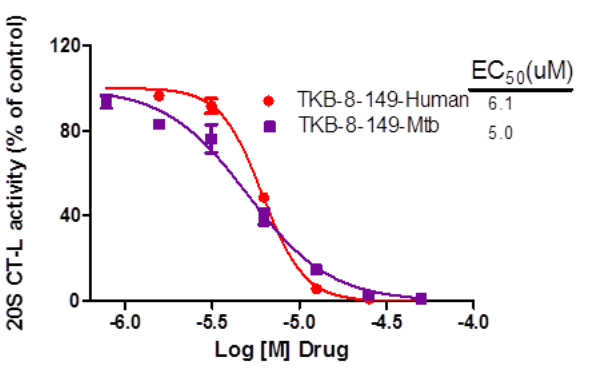
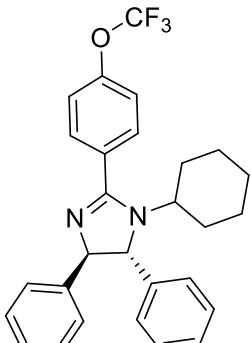
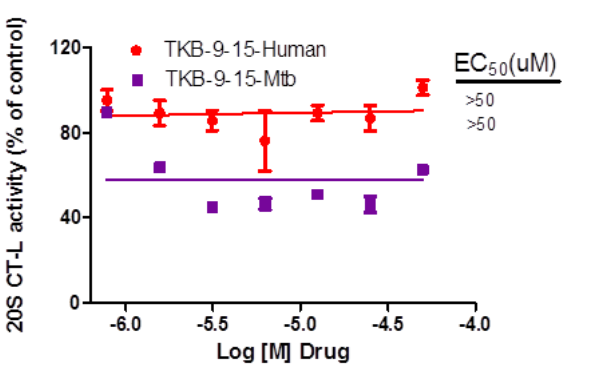
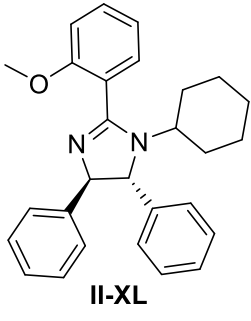
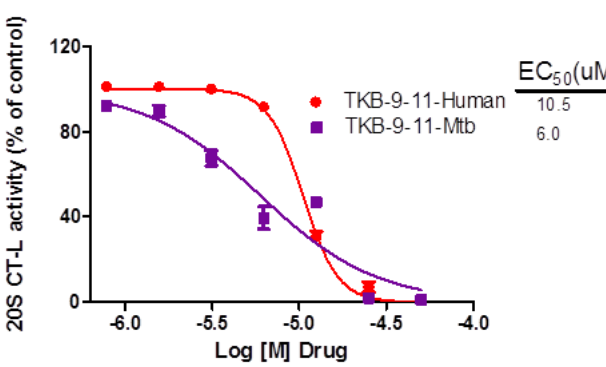
 <p>II-XXXV</p>	 <p>20S CT-L activity (% of control)</p> <p>Log [M] Drug</p> <p> $EC_{50}(uM)$ TKB-8-139-Human 4.0 TKB-8-139-Mtb 3.1 </p>	4.0	3.1	1.3
 <p>II-XXXVI</p>	 <p>20S CT-L activity (% of control)</p> <p>Log [M] Drug</p> <p> $EC_{50}(uM)$ TKB-8-149-Human 6.1 TKB-8-149-Mtb 5.0 </p>	6.1	5.0	1.2
 <p>II-XXXVII</p>	 <p>20S CT-L activity (% of control)</p> <p>Log [M] Drug</p> <p> $EC_{50}(uM)$ TKB-9-15-Human >50 TKB-9-15-Mtb >50 </p>	IA	IA	NA
 <p>II-XL</p>	 <p>20S CT-L activity (% of control)</p> <p>Log [M] Drug</p> <p> $EC_{50}(uM)$ TKB-9-11-Human 10.5 TKB-9-11-Mtb 6.0 </p>	10.5	6.0	1.8

Table II-II cont'd

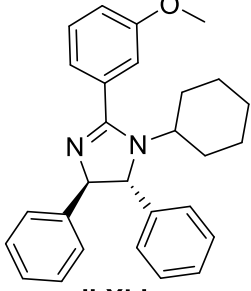
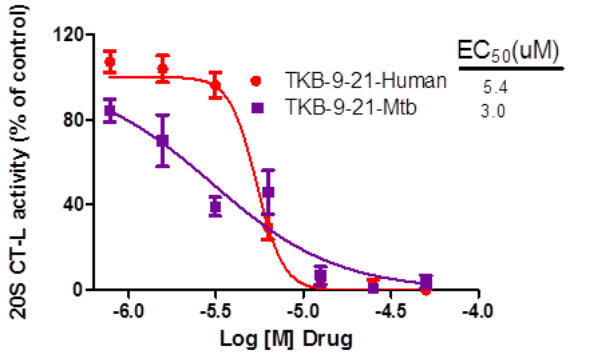
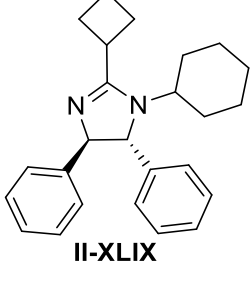
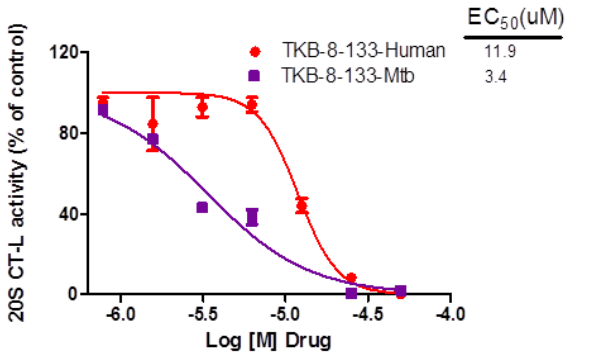
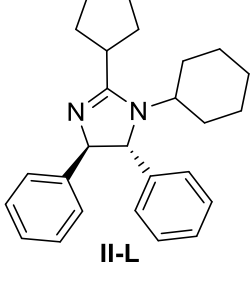
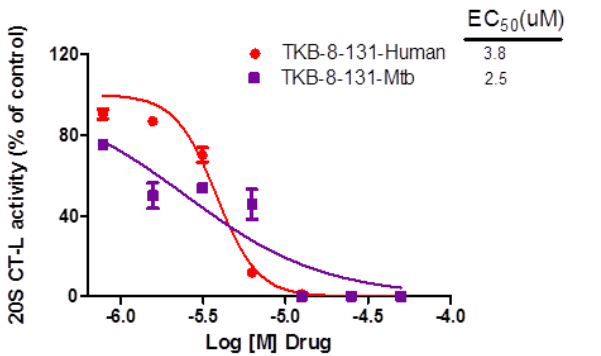
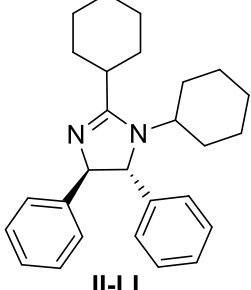
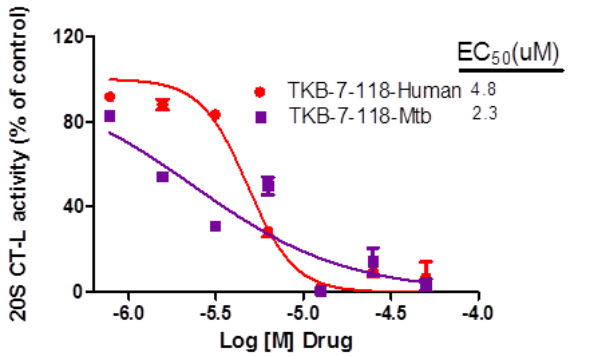
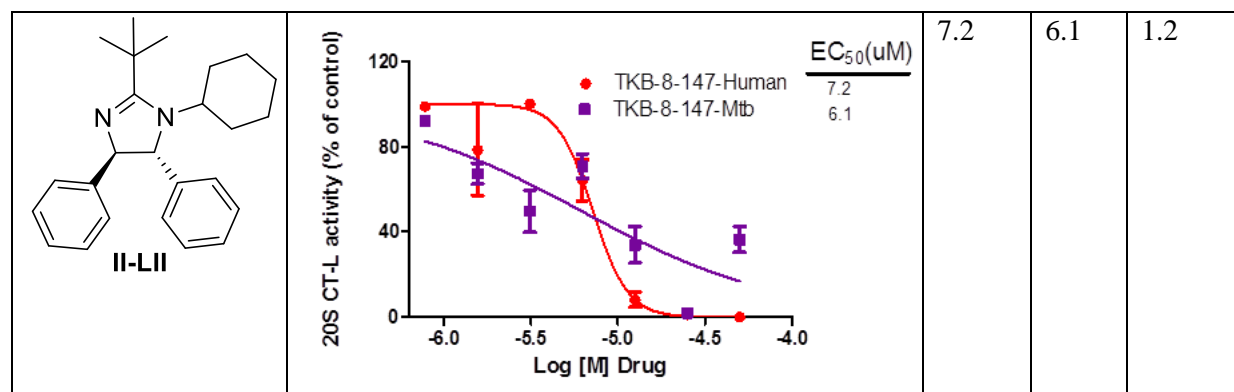
 <p>II-XLI</p>	 <p>20S CT-L activity (% of control)</p> <p>Log [M] Drug</p> <p> $EC_{50}(\mu M)$ TKB-9-21-Human 5.4 TKB-9-21-Mtb 3.0 </p>	5.4	3.0	1.8
 <p>II-XLIX</p>	 <p>20S CT-L activity (% of control)</p> <p>Log [M] Drug</p> <p> $EC_{50}(\mu M)$ TKB-8-133-Human 11.9 TKB-8-133-Mtb 3.4 </p>	11.9	3.4	3.5
 <p>II-L</p>	 <p>20S CT-L activity (% of control)</p> <p>Log [M] Drug</p> <p> $EC_{50}(\mu M)$ TKB-8-131-Human 3.8 TKB-8-131-Mtb 2.5 </p>	3.8	2.5	1.5
 <p>II-LI</p>	 <p>20S CT-L activity (% of control)</p> <p>Log [M] Drug</p> <p> $EC_{50}(\mu M)$ TKB-7-118-Human 4.8 TKB-7-118-Mtb 2.3 </p>	4.8	2.3	2

Table II-II cont'd

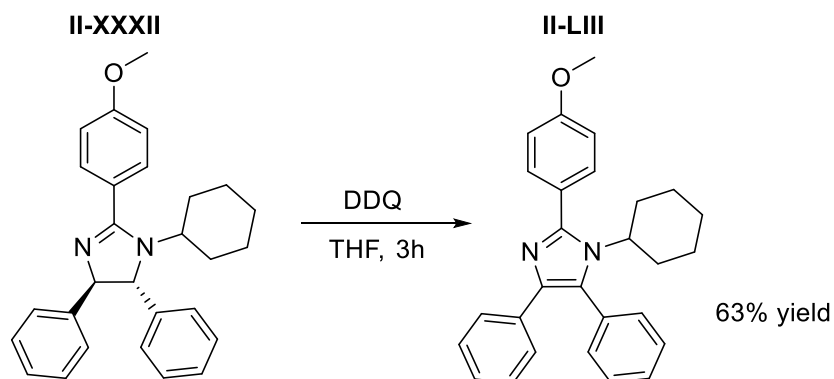


Diversification of the functional groups on the 2-position and 3-position have identified key factors responsible for the inhibition of the proteasome in purified protein assays. Based on the results of the *in vitro* studies, the project was advanced and experiment involving whole cells were analyzed. These *in vitro* studies highlighted another key characteristic for molecule analysis, the ability of drug molecules to permeate the cell wall. The imidazoline compounds would only be able to inhibit the proteasome if they were able to transverse the cellular wall and gain access to the proteasome. This testing would highlight the real-world applications of the *in vitro* analysis done in the Tepe group. These experiments are currently carried out by our collaborators in the Abramovitch lab.

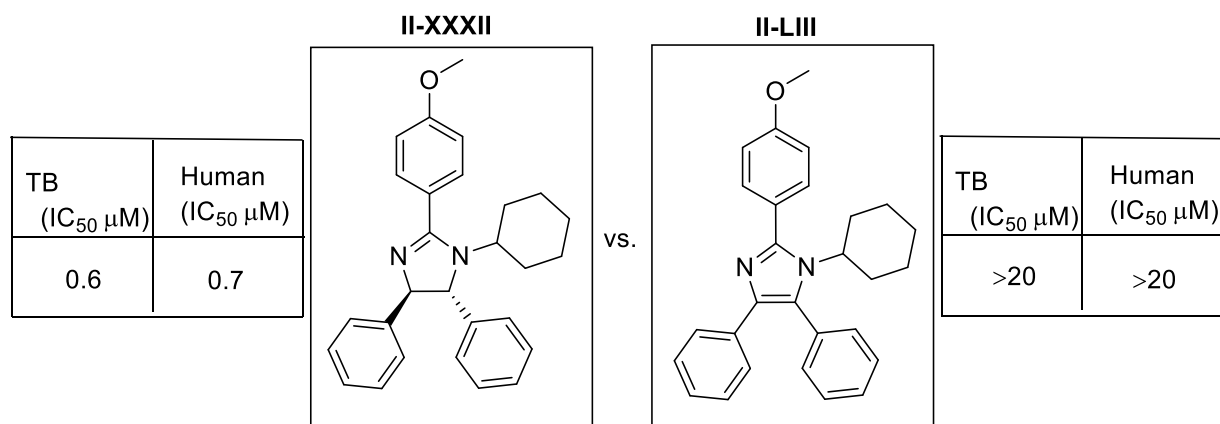
These results have highlighted the complexity of inhibitor design. Some of the molecules tested in purified proteasome assays were shown to be inhibitors but only one of the compounds reactivity was reflected in whole cell assay analysis. This enforces the need for cellular permeability. The increased lipophilicity of **II-LI** resulted in its inability to access the proteasome and cause modulation to its activity.

Further expanding and diversifying the imidazoline synthesis has resulted in accessing a very potent imidazoline compound. Specificity however was not realized, the imidazoline scaffold

displayed inhibition for both the human 20S proteasome as well as the TB proteasome. Oxidation of the imidazoline to the imidazole has shown that stereochemistry plays a critical role in potency of proteasome inhibition. The imidazole compound lost all activity which identifies that the 3-D structure of the molecule is integral for interaction and binding to the proteasome for inhibition to occur.



Scheme II-XIV: Synthesis of imidazole from imidazoline.



Scheme II-XV: Showed the effect of stereochemistry on proteasome inhibition.

Alternative methods of controlling specificity for TB proteasome were proposed and one of the key queries that arose was the contributing factor of the stereochemical relationship of disubstituted imidazolines to their activity. To better understand the relationship that these

configurational isomers and their stereochemistry had on proteasome activity, TCH-113 was closely examined. The cycloaddition reaction that accesses the core functionality of TCH-113 yields an intermediate which is a mixture of epimers, due to the incorporation of the pyridine nitrogen. These compounds are not easily separated into two distinct diastereomers, with HPLC being one of the very few ways to resolve the mixture. Because of this, in the past, the intermediate was further transformed to TCH 113, as a mixture of cis/trans imidazolines.

The high through-put screening identified that TCH-113 at highly concentrations, modulates TB proteasome inhibition. At the same concentration no measurable inhibition of the h20s was observed for TCH-113

The hypothesis was that the contributing factor to this specificity was due to either the potential cis-stereochemistry of the compound or the presence of the Pyridine nitrogen. This query and the recent biological activity data presents another opportunity with imidazolines to further probe the mechanism behind the ring expansion of imido-yl aziridines to access 2-imidazolines. Cis-imidazolines previously synthesized in the past by group members through other synthetic routes. These imidazolines were screened against the human proteasome. Initial results showed inhibition however, this positive result could not be clearly contributed to the cis-imidazolines innate ability. This was due to the fact that these cis-imidazolines can over time or in the presence of light undergo isomerization to form the more stable, trans-imidazoline and these molecules are active against TB.

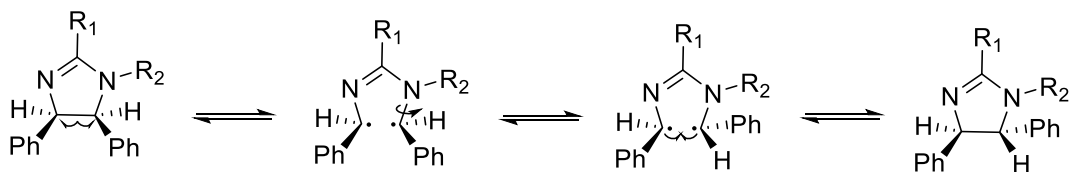
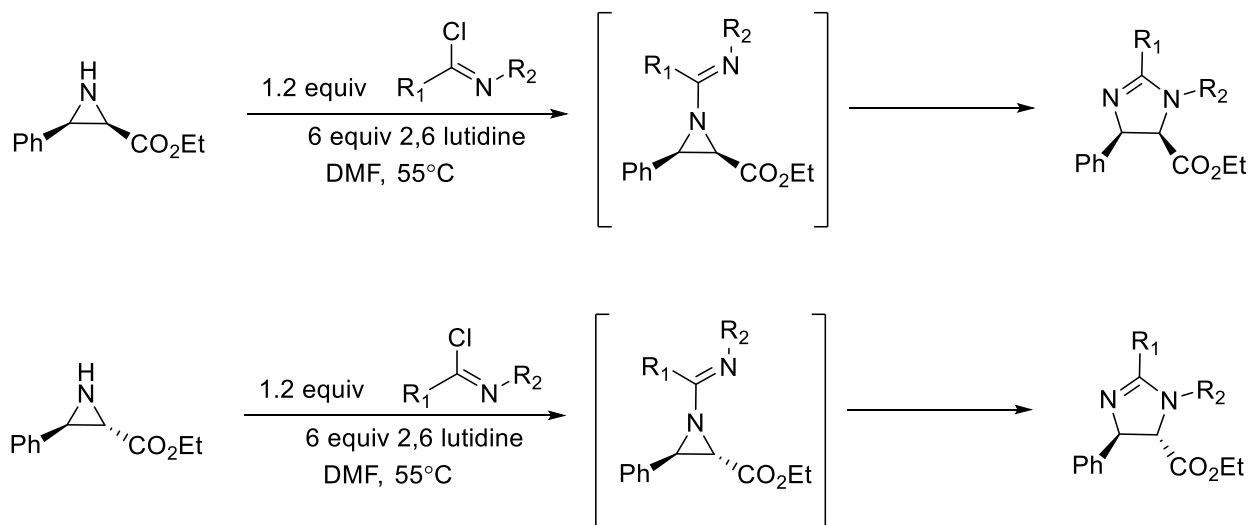


Figure II-VIII: Identified pathway for radical isomerization of cis imidazolines to trans imidazolines.

Past published results in within the group have shown stereoretention of starting aziridines in the production of imidazolines. The cis and trans isomers of ethyl-3-phenyl-aziridine-2-carboxylate were exposed to the same imidoyl chloride intermediate, generating the imidoyl aziridine that ring expanded to the cis and trans products respectively. This was confirmed by NOE studies. This has further demonstrated with the use of trans-2,3-diphenylaziridine which resulted in trans-2-imidazolines.¹⁹



Kuszpit, M. R.; Wulff, W. D.; Tepe, J. J. *J. Org. Chem.* **2011**, *76*, 2913-2919

Figure II-IX: Displays the experimentally observed stereoretention of imidazoline products.

Because of the stereo-retention observed with other substrates, I proposed that starting with the cis-2,3-diphenylaziridine would allow for the attempted synthesis of the cis derivatives of all the previous scaffolds accessed using the cis-2,3-diphenylaziridine. This would allow for further evaluation of the cis-isomer's ability to inhibit TB as well as monitor the rates of conversion of the cis-isomer to the trans-isomer for further analysis of the cis-isomer's viability towards further testing.

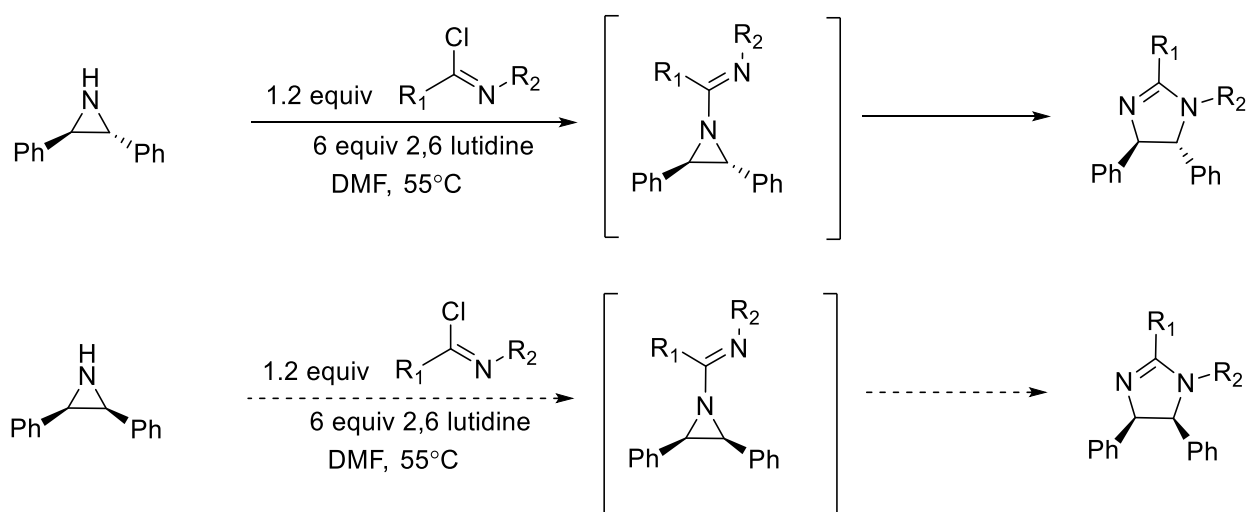


Figure II-X: Proposed pathway for accessing cis-imidazoline through imidoyl chloride expansion.

However, the mechanism for the regio-controlled and stereospecific expansion of trans-aziridines into trans-imidazolines highlights the fact that accessing purely the cis-imidazolines under the current reaction conditions might be challenging.

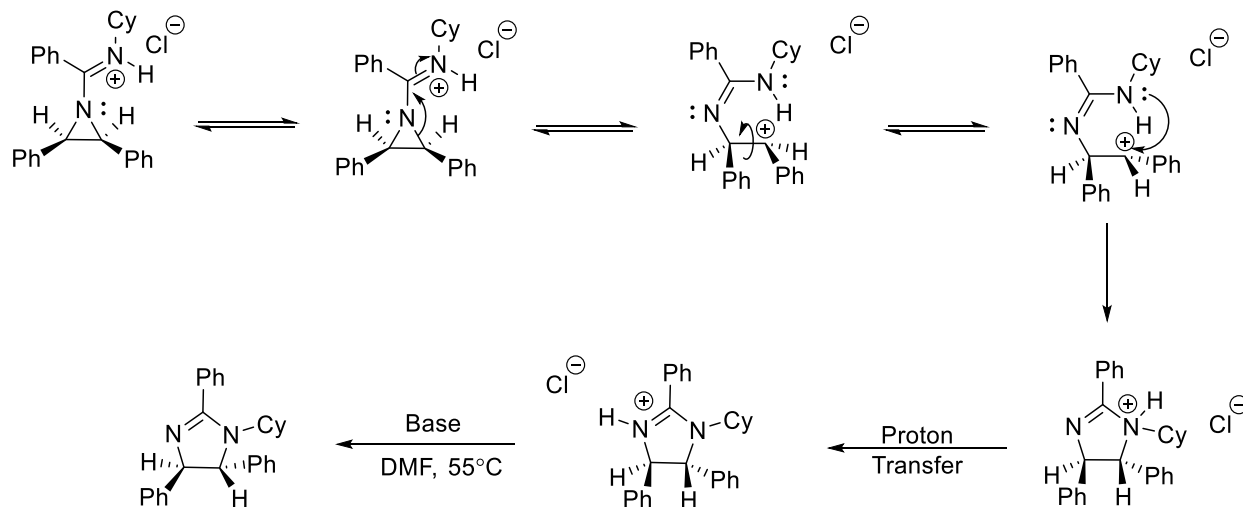
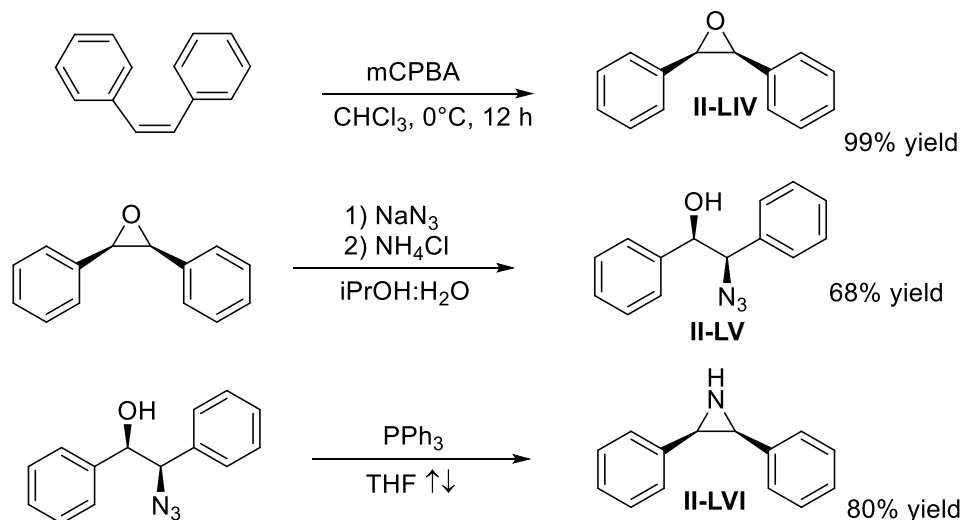


Figure II-XI: A pathway for polar solvent isomerization of cis imidazolines to trans imidazolines.

Under the reaction conditions developed for the synthesis of trans-imidazolines, there is the possibility for complete stereo-convergence from the cis-aziridine to the trans-imidazoline. Protonation of the imidoyl aziridine at either nitrogen can result in aziridine ring opening to yield the benzylic carbocation. Once the benzylic stabilized cation is formed under the thermodynamic conditions of the reaction, carbon-carbon bond rotation towards the more stable trans isomer will occur.

To better understand if the isomerization of the cis-imidazoline to the trans-imidazoline occurs, the cis-2,3-diphenylaziridine was identified as the desired starting material.³⁰ Accessing the cis-imidazoline would experimentally identify the difference configurational isomers of imidazolines would have on TB proteasome inhibition.

Cis-2,3-diphenylaziridine, was synthesized from the epoxidation of cis-Stilbene with mCPBA to yield the cis-2,3-diphenyloxirane. This oxirane was then transformed to the azido alcohol with the addition of NaN₃ and NH₄Cl that underwent an intramolecular Staudinger reaction yield the cis-2,3-diphenylaziridine.²⁹



Scheme II-XVI: Synthetic pathway to accessing cis-2,3-diphenyl aziridine starting material.

Cis-2,3-diphenylaziridine was exposed to the same reaction conditions as the trans isomer. Incorporation of N-cyclohexylbenzamide in DCM with oxalyl chloride was done to give the imidoyl chloride intermediate that cis-2,3-diphenylaziridine was added to. The reaction was refluxed for the same time scale for the standard imidazoline expansion.

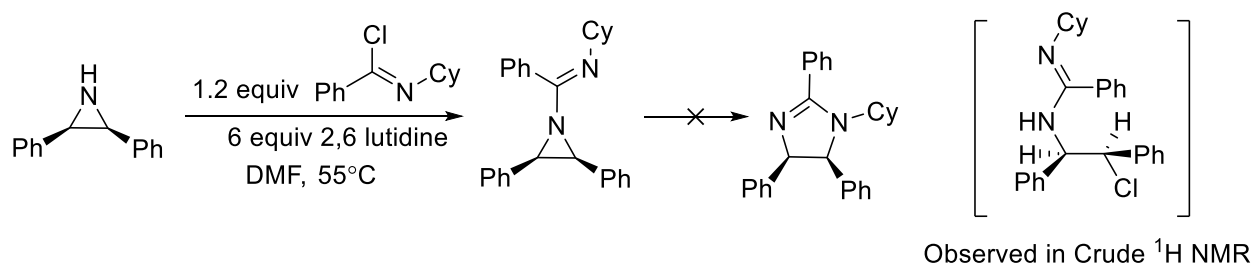
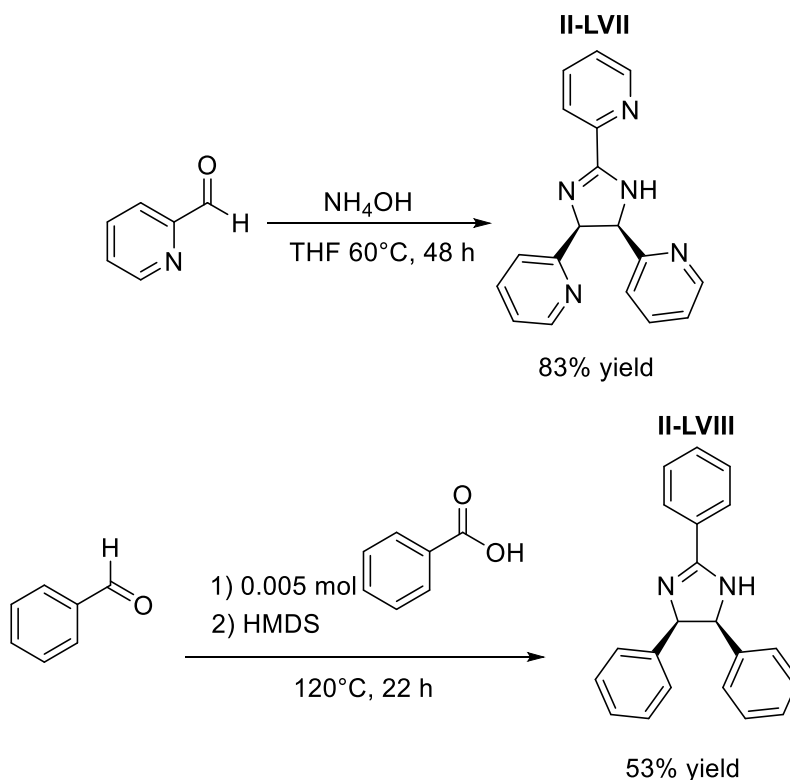


Figure II-XII: Shows the steric strain of the cis-isomer and its effect on ring closure.

Expansion of the cis-2,3-diphenylaziridine did not yield the desired imidazoline, instead a mixture of compounds was isolated at the same Rf with the chloroamidine above being identified as one of the products. This showed that the sterics of the cis-phenyl groups perturb the orientation

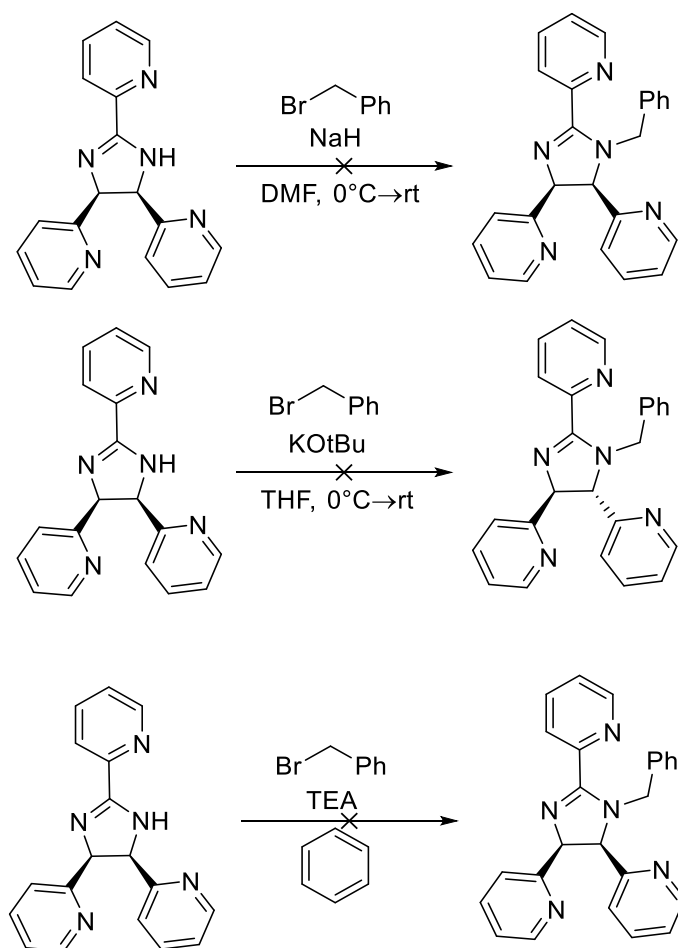
of the reaction intermediate, preventing the correct overlap necessary for the displacement to yield cis-imidazoline compound.

To better understand the effect of cis-stereochemistry in imidazoline compounds for proteasome inhibition two different cis imidazolines accessed through electrocyclic condensation reactions to yield the cis-imidazolines from the starting aldehydes. One factor for selectivity of TCH-113 could be identified as the incorporation of the nitrogen in the pyridine ring which in turn causes a drastic change in the electronics of the system. The presence of the cis stereochemistry may also be a contributing factor for proper molecule alignment in the TB proteasome but improper docking in the human 20S proteasome.



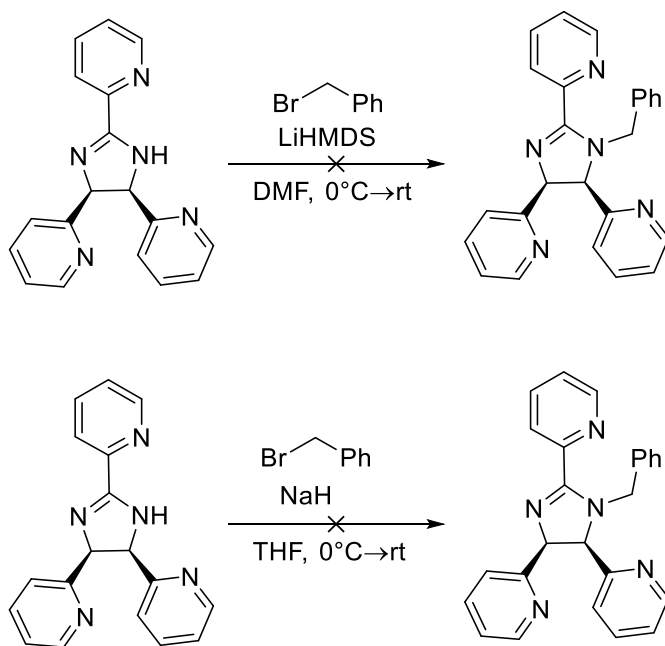
Scheme II-XVII: Synthesis of cis imidazolines from aldehydes.¹⁰

Further modification of the scaffolds was attempted to access molecules with similar or exact R₂ groups as the trans-imidazolines, presently being tested. Alkylation of the 2,2',2''-((4S,5R)-4,5-dihydro-1H-imidazole-2,4,5-triyl)tripyrindine did not occur under any of the experimental conditions tried. This was attributed to the presence of the pyridine nitrogen that prevented proper alkylation of the amidine nitrogen in or the imidazoline core, only starting material was recovered and identified.

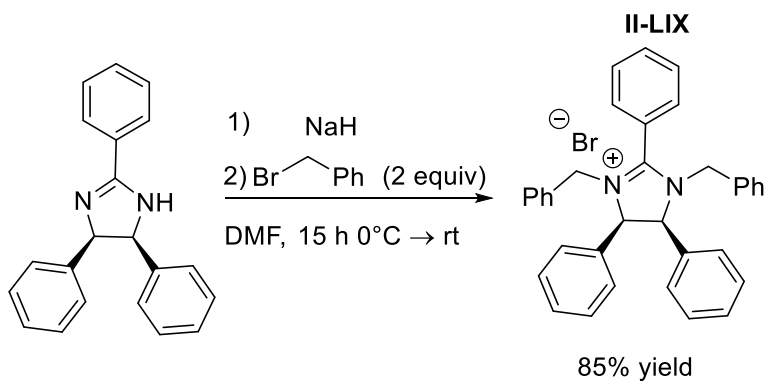


Scheme II-XVIII: N-I alkylations that did not occur under varied reaction conditions

Scheme II-XVIII cont'd

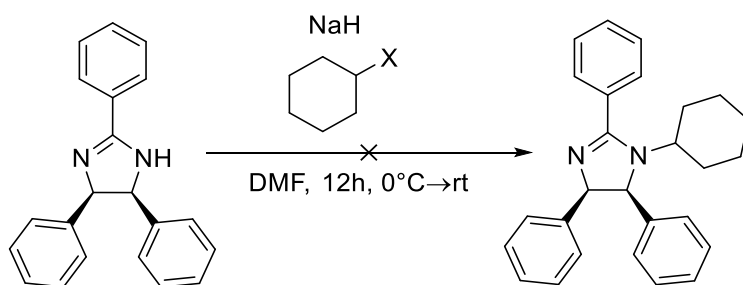
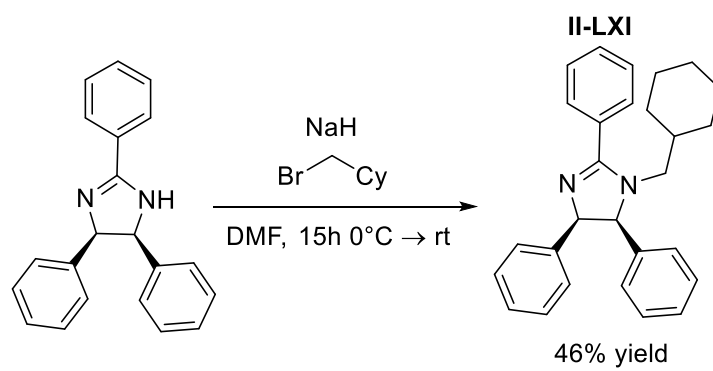
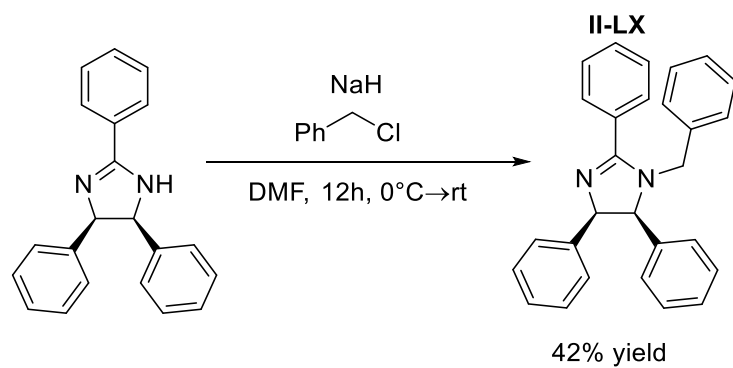


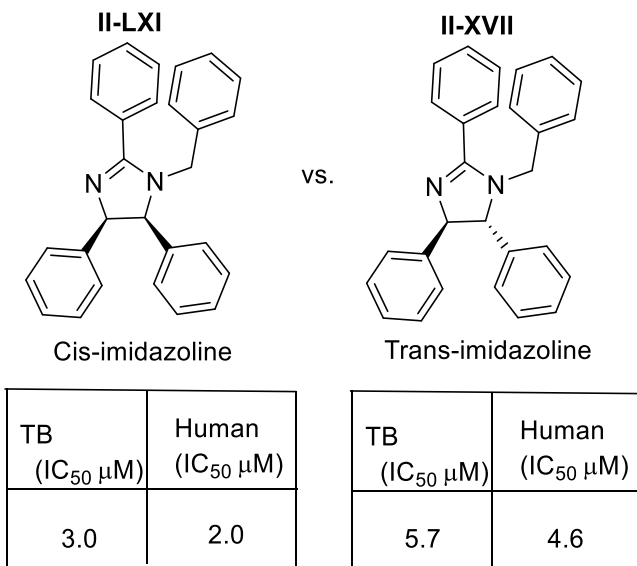
Alkylation of the triphenyl imidazoline occurred in moderate yield only with primary alkyl halides, to give the functionalized scaffolds for evaluation of potency and more notably specificity of one proteasome target over another. When reacted with a secondary alkyl halide the E₂ elimination reaction dominated and resulted in only recovery of starting material in high yield.



Scheme II-XIX: N-1 alkylation conditions for cis-imidazoles

Scheme II-XIX cont'd





Scheme II-XX: The effect of imidazoline stereochemistry on selectivity and potency of inhibition.

Unfortunately, when the molecules were screened, both showed similar inhibition towards the human and the TB proteasome. There was no specificity gained by using one stereoisomer over the other, therefore other approaches to accessing specificity were needed. The unfunctionalized tripyridine imidazoline was not active even at high concentrations.

Another hypothesis was that adding structural diversity can also be incorporated by removal of this cis-trans diphenyl relationship altogether. Modification to the synthesis of the starting aziridine, will clearly identify if both phenyl rings are key structures proteasome inhibition in both the TB and human proteasome, or if some selectivity can be gained towards one over the other. Because of this proposal development of methods towards the synthesis of 2-imidazolines from mono-substituted aziridines. To accomplish this aspect, development of a small library of monosubstituted imidazoline scaffolds using known Lewis acid mediated expansion chemistry was done with the following proposed reaction pathway to yield monosubstituted imidazolines.

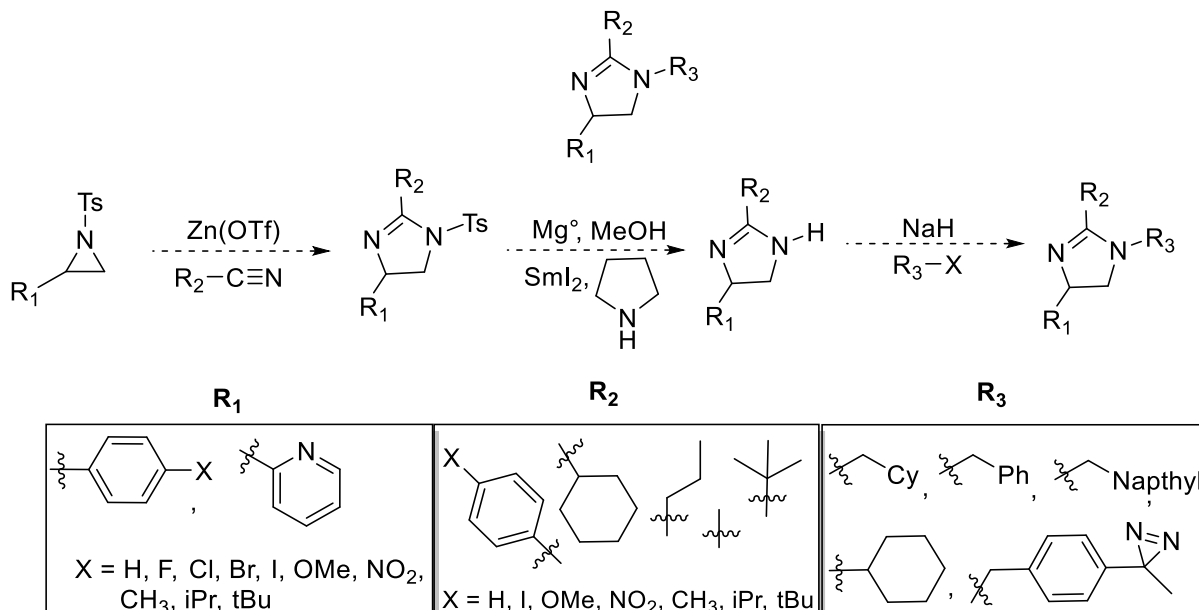
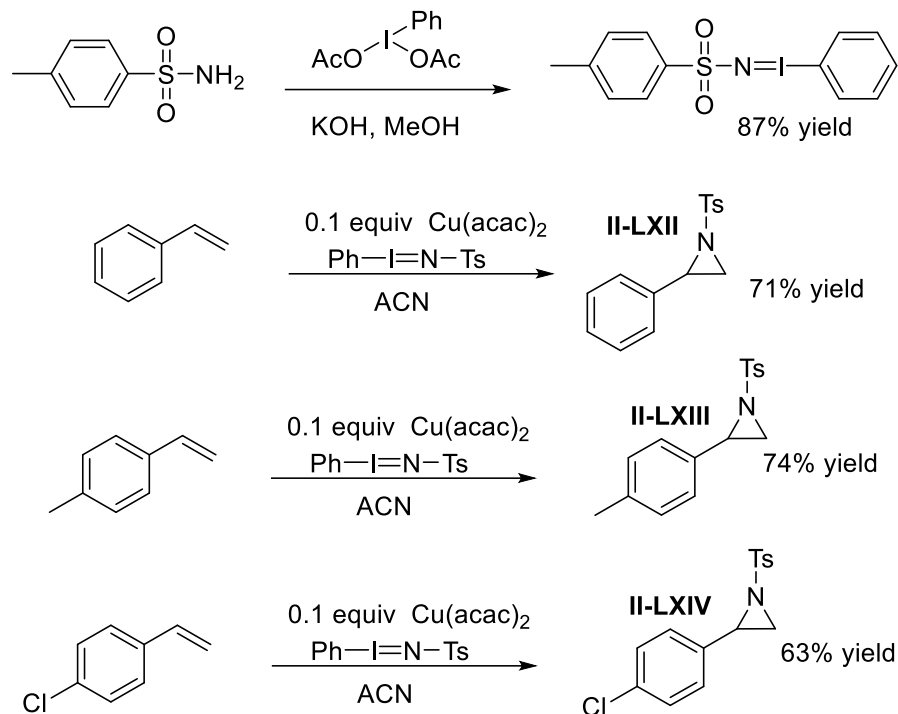


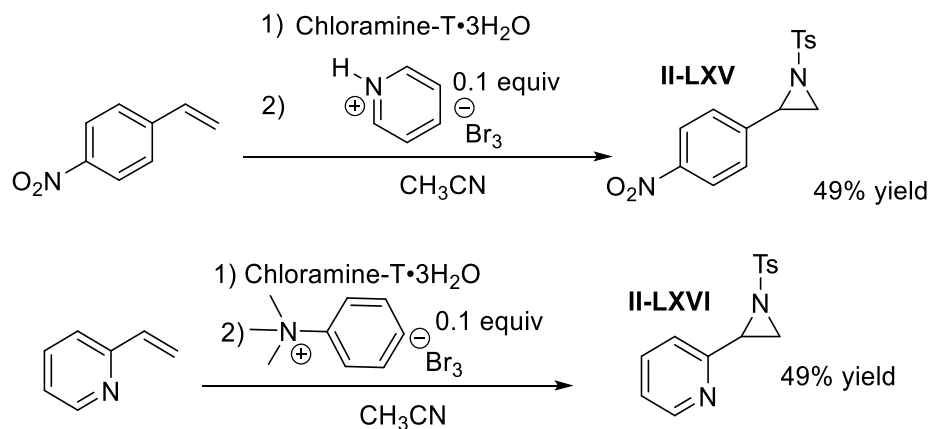
Figure II-XIII: Pathway to accessing monosubstituted imidazolines.

The library would then be screened to identify any key functional groups responsible for inhibition of the TB proteasome. Iodane chemistry was used to access N-tosyl azirindines from the starting olefins, in the presence of $\text{Cu}(\text{acac})_2$.³¹⁻³⁶



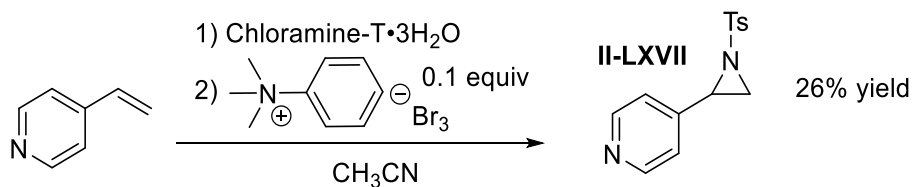
Scheme II-XXI: Synthesis of tosylated aziridine starting material.

To further probe the influence of the pyridine ring and other electron withdrawing groups on specificity to the TB proteasome, like what was observed in TCH-113, the following aziridine's were accessed through tribromide catalyzed expansions.³⁷⁻³⁸

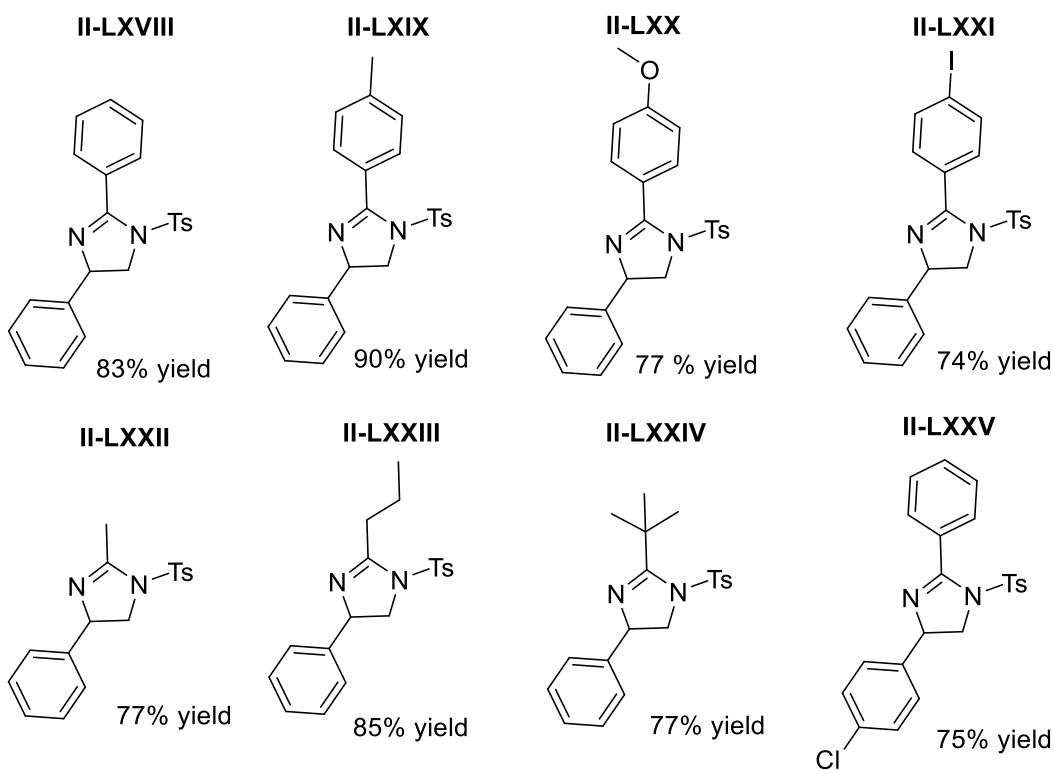
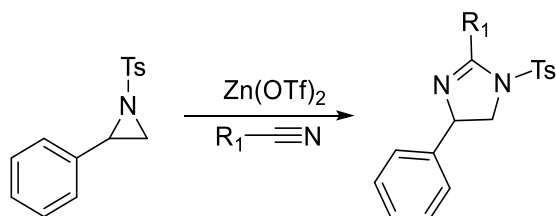


Scheme II-XXII: Synthesis of tosylated aziridine starting material.

Scheme II-XXII cont'd

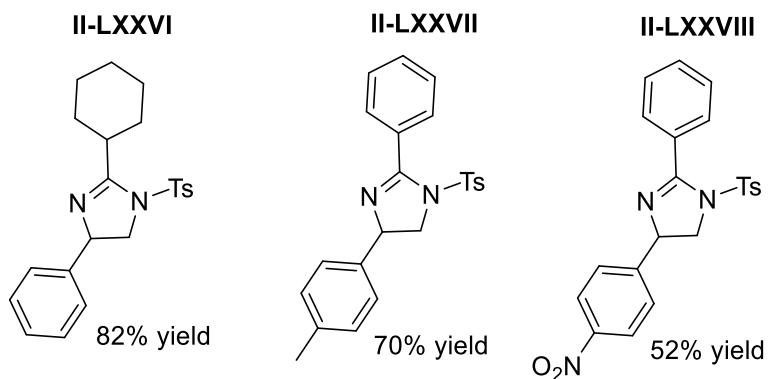


After accessing the aziridines, these intermediates were further functionalized to imidazolines, with most undergoing expansion in good yields with Zn(OTf)₂.³⁹⁻⁴²

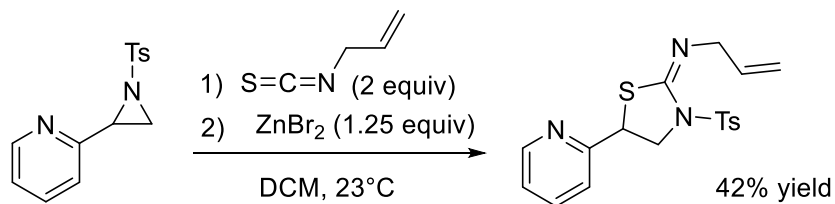


Scheme II-XXIII: Synthesis of N-1 tosylated imidazoline substrates.

Scheme II-XXIII cont'd

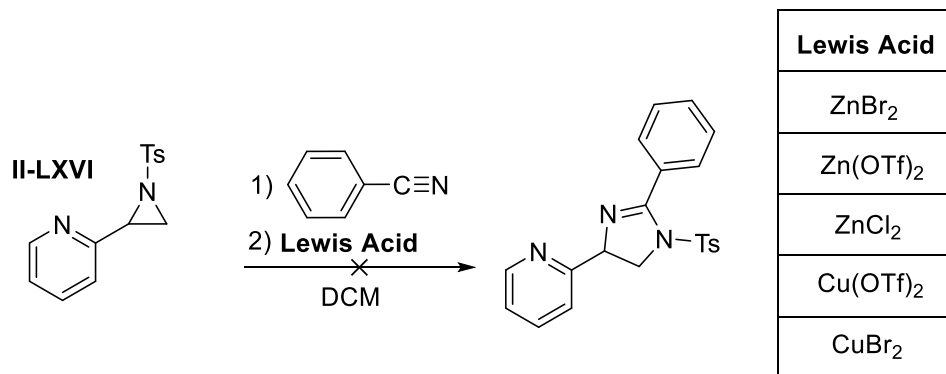


The 4-(1-tosylaziridin-2-yl)pyridine and 2-(1-tosylaziridin-2-yl)pyridine did not expand to imidazolines. Therefore other Lewis acids were screened for acid activated expansion. Previous work in the Stolz group displayed that 2-(1-tosylaziridin-2-yl)pyridine can be expanded in the presence of isothiocyanates to give iminothiazolidines.⁴³



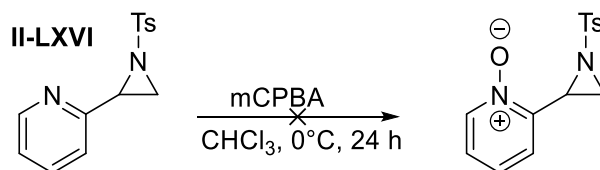
Craig II, R. A.; O'Connor, N. R.; Goldberg, A. F. G.; Stolz, B. M. *Chem. Eur. J.* **2014**, 4806-4813

Figure II-XIV: ZnBr₂ mediated expansion of 2-pyridyl aziridine.



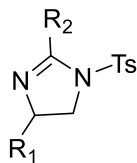
Scheme II-XXIV: Failed expansion reaction conditions.

Screening of these Lewis acids resulted in decomposition of the starting material. The expansion conditions of the isothiocyanates do not tolerate the expansion to the imidazolines. Since the expansion of 2-phenyl-1-tosylaziridine to 2,4-diphenyl-1-tosyl-4,5-dihydro-1H-imidazole was accomplished this suggested that the Lewis acid was being sequestered by the pyridine nitrogen instead of being used to expand the aziridine. To rectify this the concentration of Lewis acid was increased to 3 equiv. but only decomposition was observed. Oxidation of the starting aziridine to the N-oxide, only resulted in decomposition.⁴⁴



Scheme II-XXV: Failed N-oxide reaction conditions.

Some of the initial N-tosyl imidazolines were selected and screened for TB proteasome inhibition. This was done before the subsequent deprotection and N-alkylation to verify if the intermediate structures were also drug candidates for proteasome modulation.

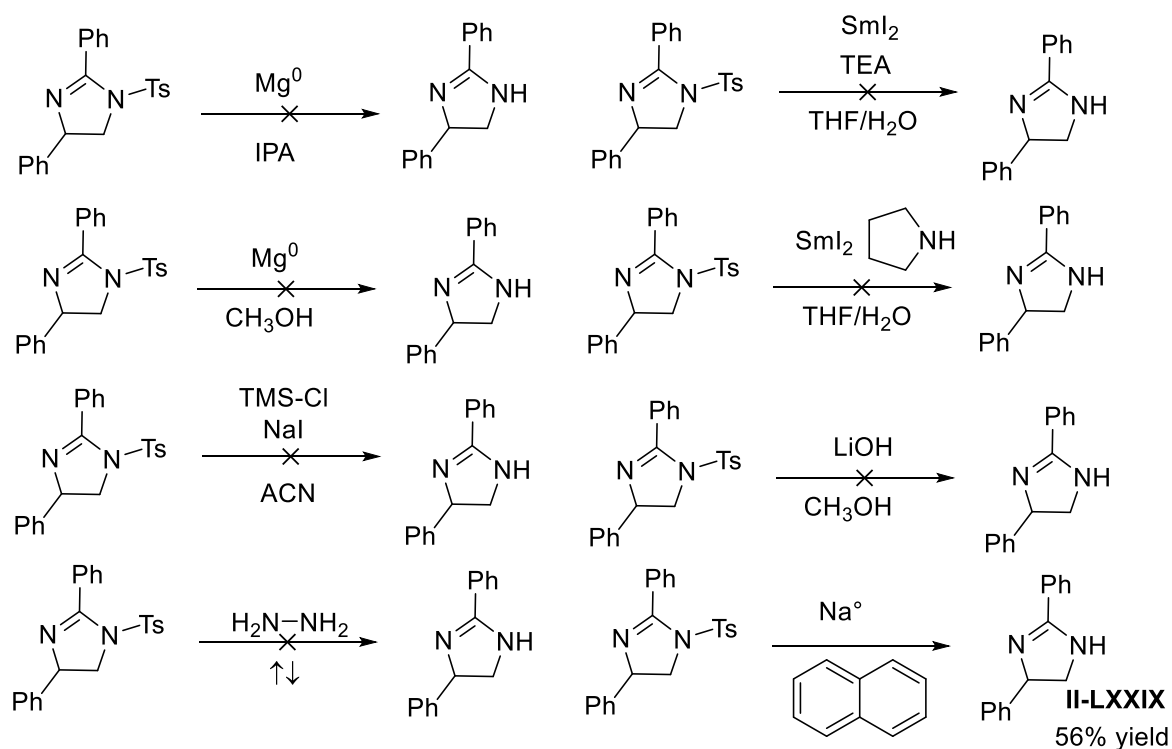
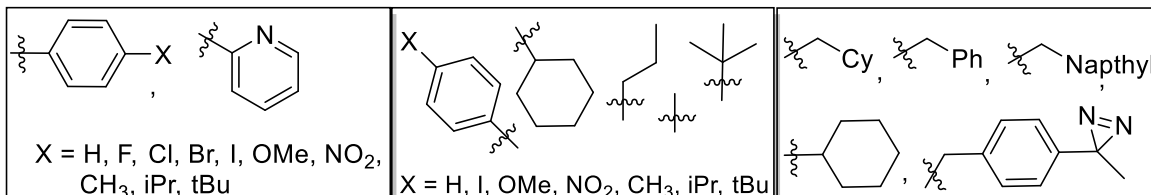
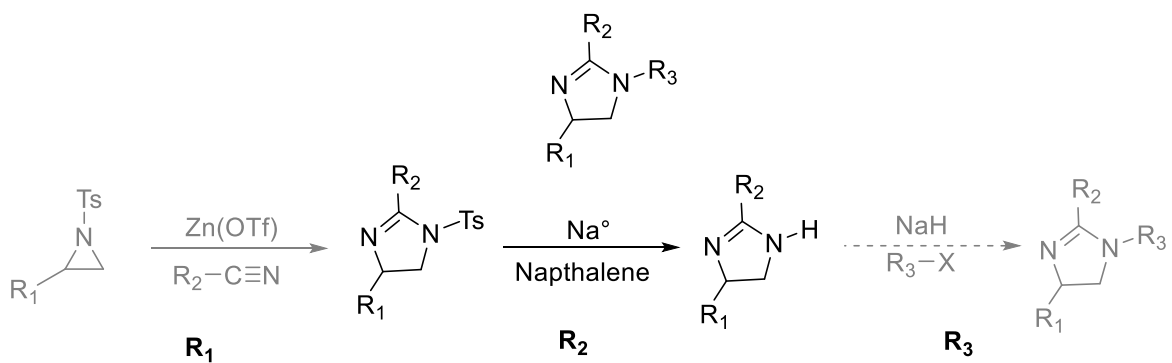


R ₁	R ₂	TB (IC ₅₀ μM)	Human (IC ₅₀ μM)
		>20 μM	>20 μM
		>20 μM	>20 μM
		>20 μM	>20 μM
		>20 μM	>20 μM
		>20 μM	>20 μM
		>20 μM	>20 μM

Table II-III: SAR of N-1 tosylated imidazoline compounds.

The results of the screen showed no inhibition of TB proteasome activity, and based on these results the rest of N-tosyl protected imidazolines were not tested. To clearly identify which of the two factors, being monosubstituted or possessing an electron withdrawing group, were responsible for the loss in activity removal of the tosyl group was attempted. This deprotection would result in an electron rich imidazoline that would then be alkylated with the same R-group present on the

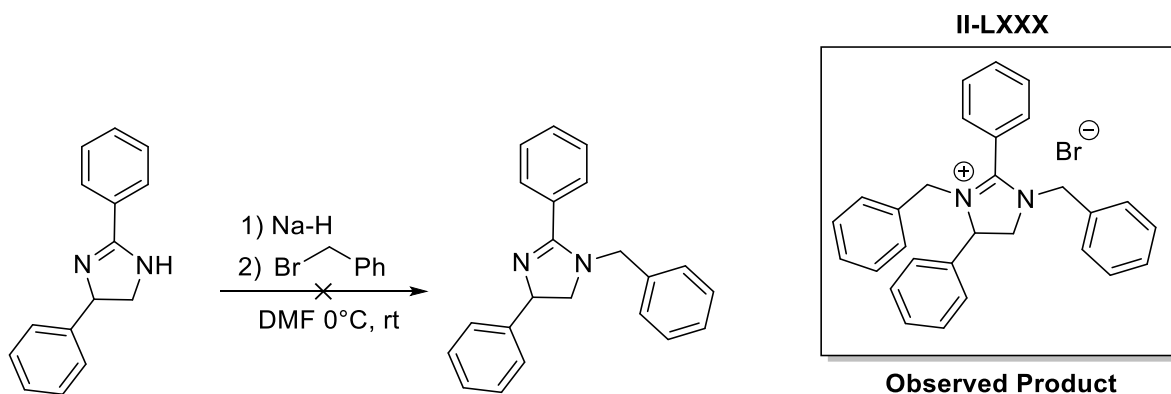
disubstituted derivatives. Alkylation of the monosubstituted derivative would highlight the necessity of a second chiral center in the molecule, result in a better understanding of the three dimensional shape of the imidazolines and its effect on proteasome inhibition. Numerous conditions were attempted for the complete deprotection of the tosyl group from the N-tosyl imidazolines.



Scheme II-XXVI: Deprotection conditions for N-1 tosylated imidazolines.

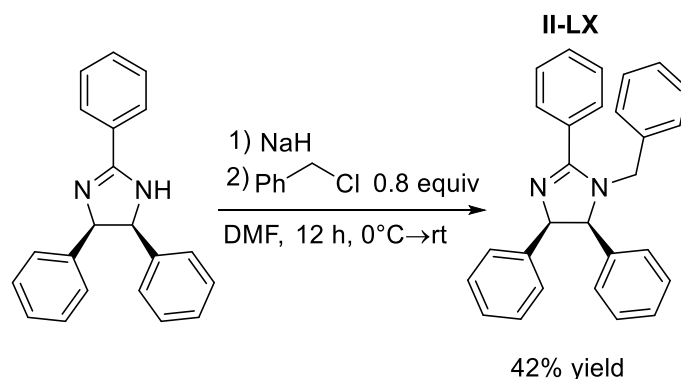
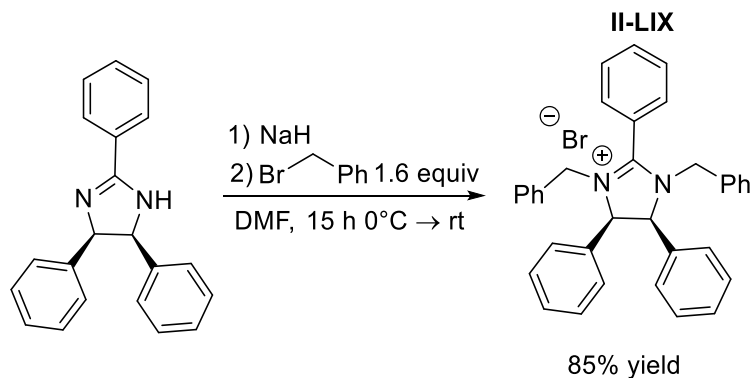
Deprotection did not occur under strongly basic conditions. Refluxing with LiOH in methanol or neat hydrazine gave no product and resulted in only the recovery of starting material. 5 or 10 equivalents of Mg⁰ in MeOH or IPA, resulted in full decomposition of starting material.⁴⁵⁻⁴⁶ That

condition for removal proved too harsh against the imidazoline intermediate. Under acidic conditions the *in-situ* generation of TMSI resulted only in decomposition of imidazoline intermediate.⁴⁷ The use of milder conditions like the SmI_2 failed to detosylate the imidazoline and resulted in full recovery of starting material.⁴⁸⁻⁴⁹ Deprotection only occurred with Na^\ominus in naphthalene and gave the desired imidazoline intermediate in moderate yields.⁵⁰⁻⁵¹ Alkylation is currently being investigated for this imidazoline to give the final structure for TB proteasome inhibition with monosubstituted aziridines.



Scheme II-XXVII: Dialkylation of imidazoline with Bn-Br.

Attempts at alkylation with benzyl bromide only resulted in overalkylation to the dibenzylated species in low yield. Similar results were observed with past attempts of mono alkylation of 2,4,5-triphenyl-4,5-dihydro-1H-imidazole.



Scheme II-XXVIII: monoalkylation of imidazoline with Bn-Cl.

Alkylation with benzyl bromide led to overalkylation, while alkylation with the less reactive alkyl halide, benzyl chloride led to the desired molecule. Therefore, this reaction should be repeated with benzyl chloride to access 1-benzyl-2,4-diphenyl-4,5-dihydro-1H-imidazole. Copper catalyzed N-arylation is another method of imidazoline derivatization that should be approached if the addition of benzyl chloride resulted in over alkylation.⁵²

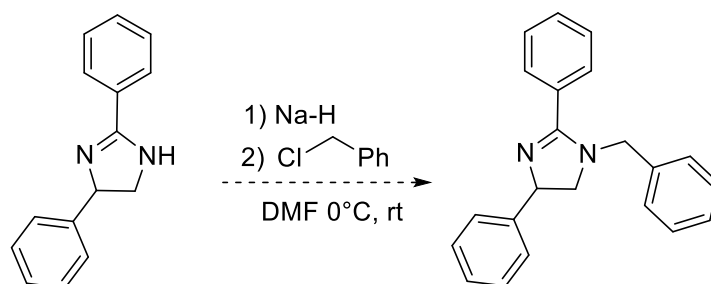
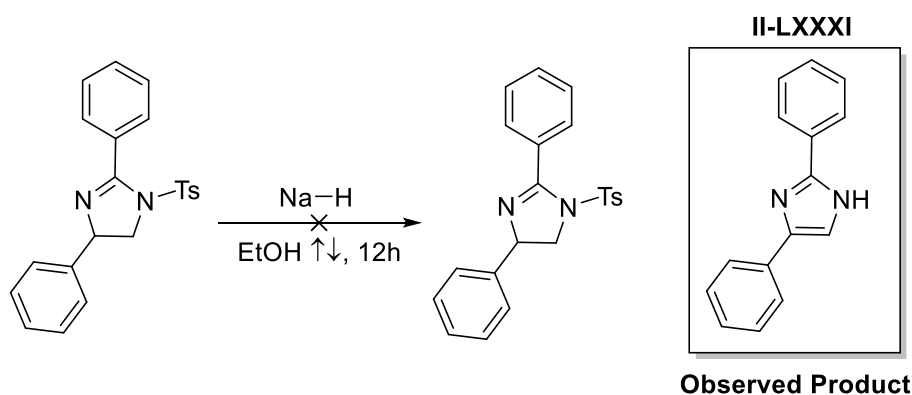
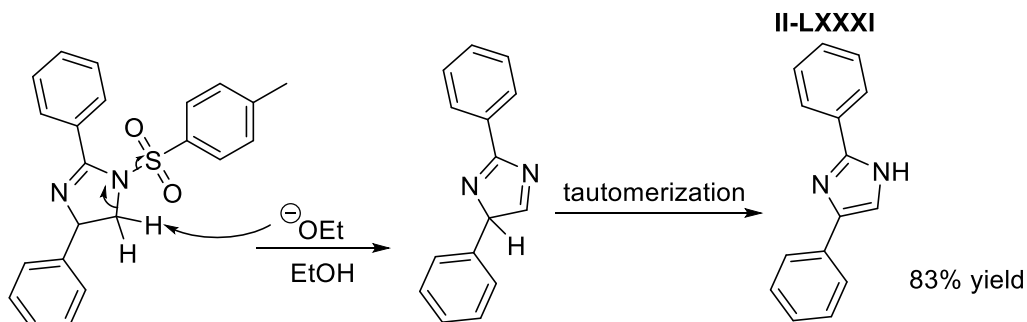


Figure II-XV: Proposed monoalkylation conditions using Bn-Cl

The deprotection of the N-tosylated imidazoline with Na^o in Naphthalene was not repeatable but led to decomposition in subsequent attempts to isolate 2,4-diphenyl-4,5-dihydro-1H-imidazole. Therefore, other basic deprotections are currently being screened to yield the intermediate. When sodium ethoxide was used, the only observed product was the imidazole, 2,4-diphenyl-1H-imidazole.



Mechanism of reaction



Scheme II-XXIX: Synthesis of imidazole from N-I Tosylated imidazolines.

Experimental results suggest strongly basic conditions (Na^o in MeOH, Na^o in Naphthalene, and NaOEt) will only decompose the reaction or lead to over oxidation so milder methods of hydrolysis are next to be screened. One example of mild tosyl deprotection has been the use of HOBt, and

MeOH. This deprotection of the imidazole went in high yield, therefore this method of deprotection should be screened against tosylated imidazolines.⁵³⁻⁵⁴

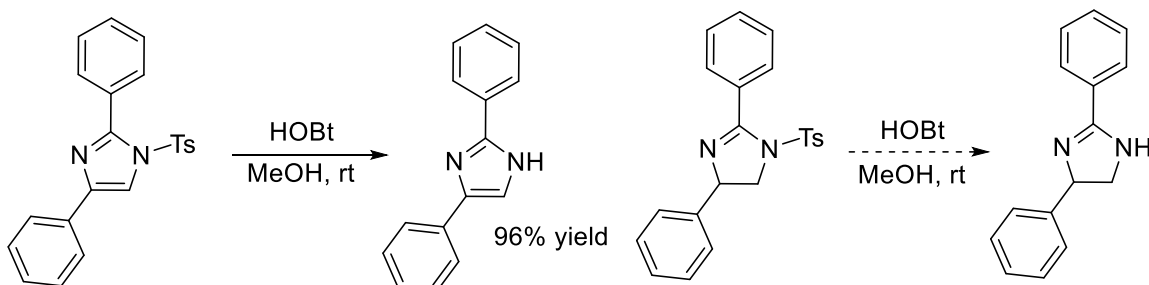


Figure II-XVI: Proposed deprotection of N-1 tosylated imidazolines.

Another method of detosylation of aziridines has been shown in the presence of $\text{BF}_3 \cdot \text{Et}_2\text{O}$ or DMAP. The aziridofullerenes underwent deprotection to yield the cyclized imidazolines.⁵⁵ Based on the sensitivity of tosylated imidazolines towards deprotection, another approach to access monosubstituted imidazolines was implemented, borrowing from past experimental observations. Under the optimized experimental conditions for the formation of disubstituted imidazolines, the only substrate that gave a mixture of regioisomers upon ring expansion was ethyl-3-(4-nitrophenyl)aziridine-2-carboxylate. This was due to electron withdrawing potential of the Nitro group at the 4-position of the phenyl ring that inductively depleted the electron density at the benzylic carbon, causing the expansion to occur at both carbons of the intermediate imidoyl aziridine. With the other substrates, the ring expansion was regioselective and targeted the most electron depleted carbon. Without any strong EWG on the phenyl ring the most electro-positive carbon was the one adjacent to the carboxylate. For example, in the case of ethyl-3-phenyl-2-carboxylate, only one regioisomer is formed by carbon-nitrogen bond formation adjacent to the ester.¹⁹

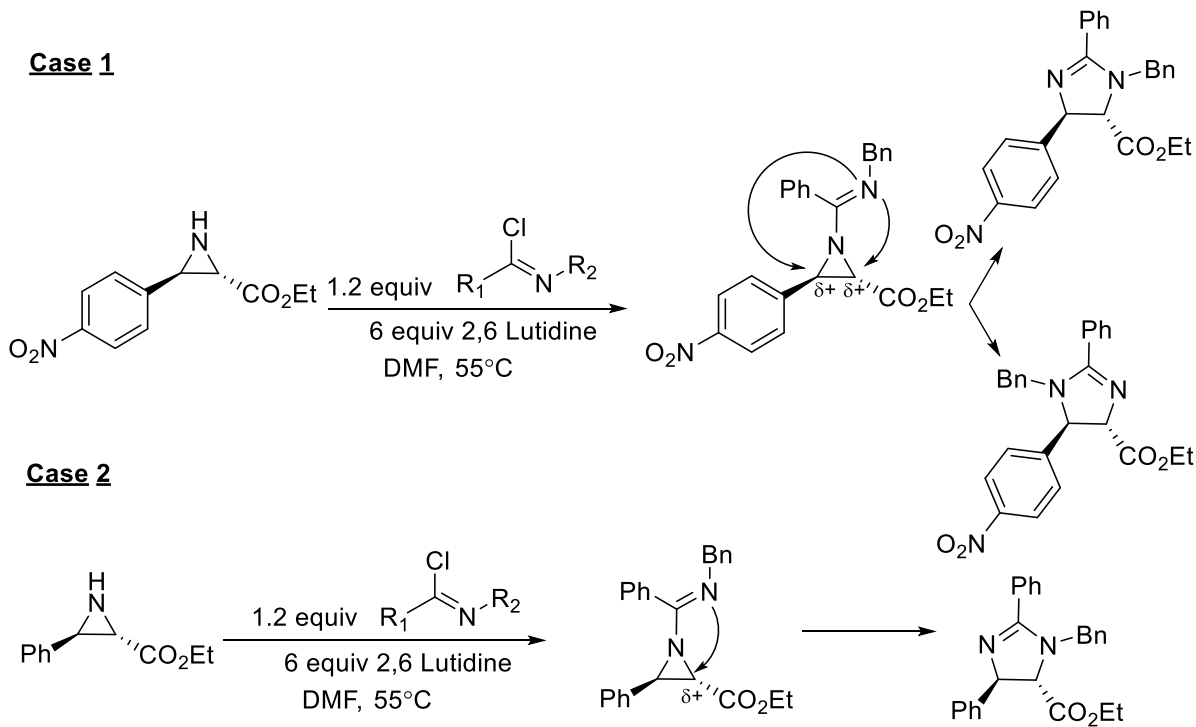


Figure II-XVII: Experimentally shown swap in regiochemistry due to EWG.

The clear difference in electron depletion between one carbon in the aziridine ring in comparison to the other is responsible for the regioselectivity in the disubstituted system. This is the same factor that will be exploited in attempt to produce regioselective monosubstituted imidazolines from imidoylaziridines.

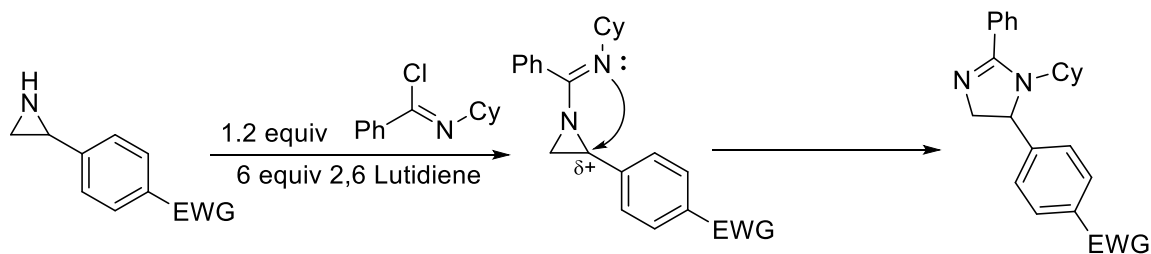
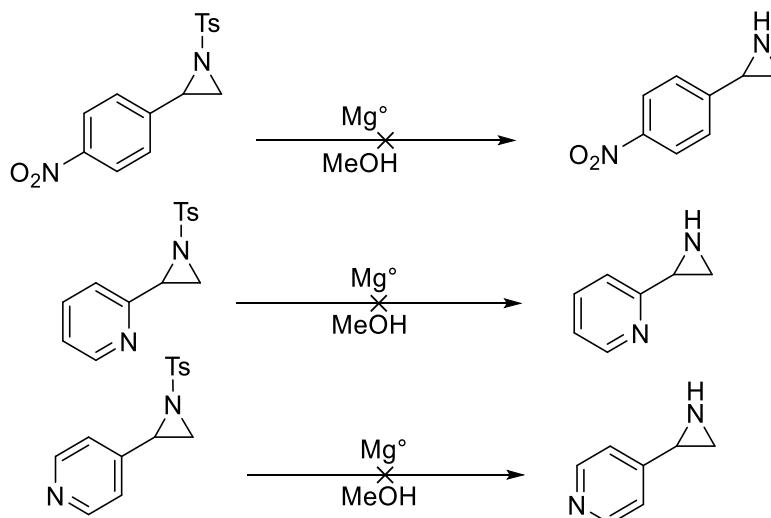


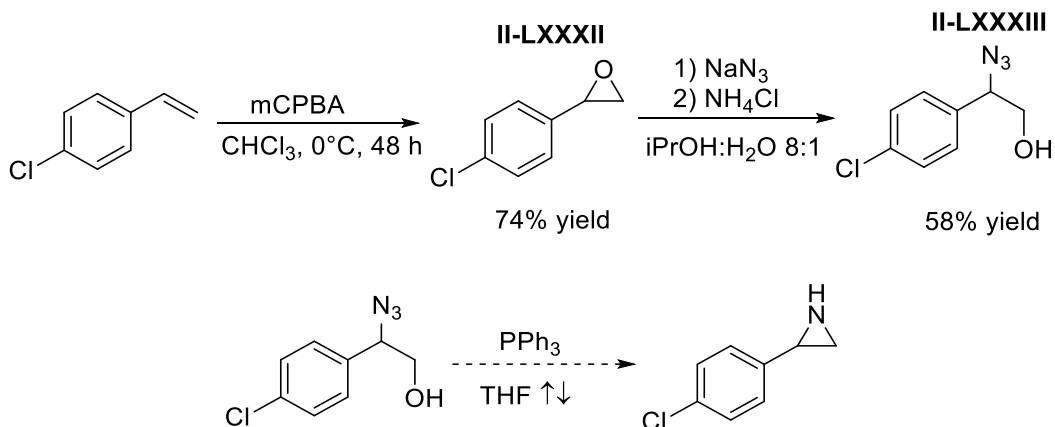
Figure II-XVIII: Proposed expansion of monosubstituted imidazolines.

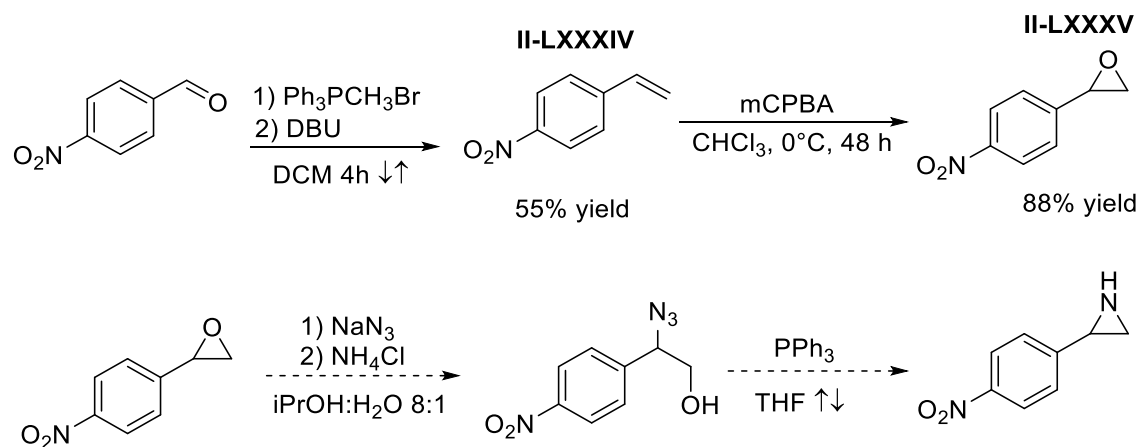
To verify the hypothesis of this expansion tosylated aziridines with strong EWG's were selected as subjected to tosyl-deprotection which resulted in decomposition of the starting material.⁴⁵



Scheme II-XXX: Failed deprotection of N-tosylated aziridines.

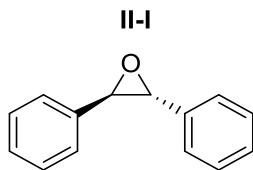
Because of these results accessing the deprotected monosubstituted aziridines by other synthetic routes were pursued using the Staudinger reaction.⁵⁶⁻⁵⁸





Scheme II-XXXI: Pathway to access monosubstituted aziridines for expansion.

With these two aziridines, the expansion of monosubstituted imidazolines should be probed to verify if the presence of an electron withdrawing group can facilitate closure of the intermediate imido-yl aziridine.



Trans-2,3-diphenyloxirane:

Trans-1,2-diphenylethene (5.00 g, 27.74 mmol) was added to a round bottom flask as a solid, and then dissolved in 100 mL of CHCl_3 . The resulting solution was cooled to 0°C by ice bath before the addition of 77% by weight mCPBA (6.84 g, 30.51 mmol) was added as a solid. The solution stirred at 0°C for 1 hour and at 4°C for an additional 23 hours. After which the suspension was washed with 10% Na_2CO_3 (2 x 50 mL), followed by saturated NaCl solution (2 X 50 mL). The organic layers were collected and dried over anhydrous Na_2SO_4 before being reduced *in vacuo* to yield product as a white solid 95 % yield, (5.17 g, 26.39 mmol)

Spectroscopy:

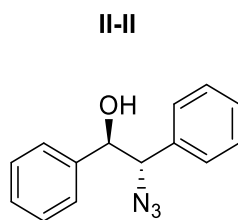
^1H NMR (500 MHz, CDCl_3) δ 7.44 – 7.32 (m, 5H), 3.89 (s, 1H).

^{13}C NMR (125 MHz, CDCl_3) δ 137.11, 128.57, 128.33, 125.50, 62.86.

IR (FT-ATR) cm^{-1} : 3059, 2991, 1603, 1217, 1071

HRMS-ESI (m/z), calculated for $\text{C}_{14}\text{H}_{13}\text{O}$ (M+H) $^+$ 197.0966. Found 197.1003

m.p.: 68.2-68.8 $^\circ\text{C}$



Trans-2-azido-1,2-diphenylethan-1-ol:

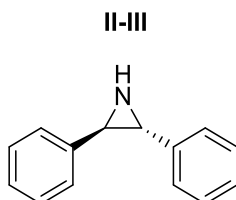
Trans-2,3-diphenyloxirane (2.5 g, 12.74 mmol) was added to a round bottom flask under inert atmosphere (N_2), and to it 100 mL of a (8:1) *i*PrOH:H₂O solution was added. The resulting solution was stirred vigorously as NH₄Cl (1.09 g, 20.38 mmol) was added as a solid. NaN₃ (3.31 g, 50.96 mmol) was then added to the solution and the suspension was refluxed for 12 hours. The reaction was cooled to room temperature and 20 mL of Et₂O and 10 mL of H₂O were added. This solution was poured into 50 mL of Et₂O and washed with (2 X 60 mL) of saturated NaCl solution. The organic layers were collected, dried over anhydrous Na₂SO₄ and reduced in vacuo to give the crude product, which was purified by column chromatography (1:9) THF: Hexanes to give a white solid 70 % yield (2.13 g, 8.90 mmol)

Spectroscopy:

¹H NMR (500 MHz, CDCl₃) δ 7.50 – 7.34 (m, 5H), 7.34 – 7.18 (m, 5H), 4.81 (d, *J* = 6.7 Hz, 1H), 4.71 (d, *J* = 6.7 Hz, 1H), 2.49 (s, 1H).

¹³C NMR (125 MHz, CDCl₃) δ 139.72, 136.06, 136.05, 128.70, 128.66, 128.38, 128.32, 128.15, 127.15, 76.97, 71.21.

HRMS-ESI (*m/z*), calculated for C₁₄H₁₄N₃O (*M*+H)⁺ 240.1137. Found 240.1099.



Trans-2,3-diphenylaziridine:

Trans-2-azido-1,2-diphenylethan-1-ol (1.80 g, 7.52 mmol) was added to a dry round bottom flask under inert atmosphere (N_2). 100 mL of anhydrous THF was added and the resulting solution was stirred vigorously as PPh_3 (2.072 g, 7.90 mmol) was added. The solution was refluxed for 24 hours and then reduced in vacuo to give a clear oil which was cooled to precipitate PPh_3O side product. The crude product as a oil was separated from the solid and purified by column chromatography (9:1 DCM:Hexanes) to yield the product as a clear oil, 67 % yield (0.984 g, 5.03 mmol)

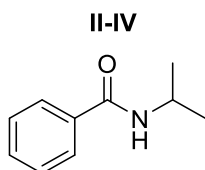
Spectroscopy:

1H NMR (500 MHz, $CDCl_3$) δ 7.40 – 7.32 (m, 4H), 7.32 – 7.24 (m, 6H), 3.11 (s, 2H), 1.56 (s, 1H).

^{13}C NMR (125 MHz, $CDCl_3$) δ 139.53, 128.62, 127.34, 125.48, 43.73.

IR (FT-ATR) cm^{-1} : 3301, 3034, 2978, 1594, 1065, 1054

HRMS-ESI (m/z), calculated for $C_{14}H_{14}N$ (M+H) $^+$ 196.1126. Found 196.1178



N-isopropylbenzamide:

Isopropylamine (1.30 g, 22 mmol) was added by syringe to a 250 mL round bottom flask under inert atmosphere (N_2). 100 mL of anhydrous DCM was then added and the mixture was stirred while triethylamine (3.04 g, 30 mmol) was added by syringe. The resulting solution was cooled to $0^\circ C$ by ice bath before benzoyl chloride (2.81 g, 20 mmol) was added dropwise to the solution, over 10 minutes. The reaction was stirred at $0^\circ C$ for one hour before warming to room temperature and stirring for an additional 8 hours. After which the solution was washed with 0.5 M HCl solution

(2 x 30 mL) followed by saturated NaCl solution (2 x 30 mL). The organic layers were collected and dried over anhydrous Na₂SO₄ and reduced in vacuo before the addition of warm hexanes to precipitate the product as a white solid 91 % yield (2.96 g, 18.14 mmol)

Spectroscopy:

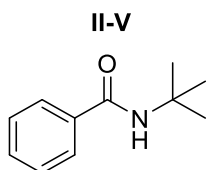
¹H NMR (500 MHz, CDCl₃) δ 7.78 – 7.72 (m, 2H), 7.52 – 7.45 (m, 1H), 7.42 (ddt, *J* = 8.2, 6.6, 1.3 Hz, 2H), 5.92 (s, 1H), 4.29 (m, 1H), 1.26 (d, *J* = 6.5 Hz, 6H).

¹³C NMR (125 MHz, CDCl₃) δ 166.65, 134.96, 131.25, 128.50, 126.77, 41.87, 22.88.

IR (FT-ATR) cm⁻¹: 3291, 3076, 2970, 2874, 1627, 1531, 1488, 1346, 1186

HRMS-ESI (m/z), calculated for C₁₀H₁₄NO (M+H)⁺ 164.1075. Found 164.1056.

M.P.: 96.7°C – 97.5°C



N-(tert-butyl)benzamide:

tert-Butylamine (1.68 g, 23 mmol) was added by syringe to a 250 ml round bottom flask. 100 ml of anhydrous DCM was then added and the mixture was stirred while triethylamine (3.04 g, 30 mmol) was added by syringe. The resulting solution was cooled to 0°C by ice bath before benzoyl chloride (2.81 g, 20 mmol) was added dropwise to the solution, over 10 minutes. The reaction was stirred at 0°C for one hour before warming to room temperature and stirring for an additional 8 hours. After which the solution was washed with 0.5 M HCl solution (2 x 30 mL) followed by saturated NaCl solution (2 x 30 mL). The organic layers were collected and dried over anhydrous

Na₂SO₄ and reduced in vacuo before the addition of warm hexanes to precipitate the product as a white solid 97.0 % yield (3.445 g, 19.44 mmol)

Spectroscopy:

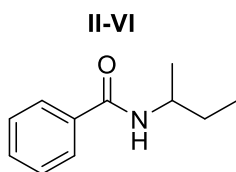
¹H NMR (500 MHz, CDCl₃) δ 7.75 – 7.69 (m, 2H), 7.51 – 7.41 (m, 1H), 7.44 – 7.37 (m, 2H), 5.94 (s, 1H), 1.47 (s, 9H).

¹³C NMR (125 MHz, CDCl₃) δ 166.86, 135.89, 131.06, 128.46, 126.66, 51.59, 28.87.

IR (FT-ATR) cm⁻¹: 3317, 3063, 2964, 2928, 1634, 1530, 1491, 1216,

HRMS-ESI (m/z), calculated for C₁₁H₁₆NO (M+H)⁺ 178.1232. Found 178.1229.

M.P.: 135.8°C – 136.4°C



N-(sec-butyl)benzamide:

sec-Butylamine (3.22 g, 44 mmol) was added by syringe to a 250 ml round bottom flask. 100 ml of anhydrous DCM was then added and the mixture was stirred while triethylamine (6.07 g, 60 mmol) was added by syringe. The resulting solution was cooled to 0°C by ice bath before benzoyl chloride (5.62 g, 40 mmol) was added dropwise to the solution, over 10 minutes. The reaction was stirred at 0°C for one hour before warming to room temperature and stirring for an additional 8 hours. After which the solution was washed with 0.5 M HCl solution (2 x 30 mL) followed by saturated NaCl solution (2 x 30 mL). The organic layers were collected and dried over anhydrous Na₂SO₄ and reduced in vacuo before the addition of warm hexanes to precipitate the product as a white solid 88 % yield (6.26 g, 35.32 mmol)

Spectroscopy:

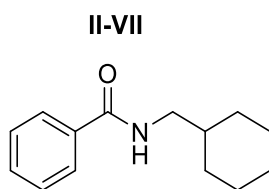
^1H NMR (500 MHz, CDCl_3) δ 7.78 – 7.72 (m, 2H), 7.46 (ddt, $J = 8.4, 6.6, 1.3$ Hz, 1H), 7.43 – 7.35 (m, 2H), 6.07 (d, $J = 8.6$ Hz, 1H), 4.11 (dq, $J = 8.4, 6.6$ Hz, 1H), 1.62 – 1.49 (m, 2H), 1.21 (d, $J = 6.6$ Hz, 3H), 0.94 (t, $J = 7.5$ Hz, 3H).

^{13}C NMR (125 MHz, CDCl_3) δ 166.91, 135.04, 131.19, 128.45, 126.82, 47.08, 29.76, 20.49, 10.45.

IR (FT-ATR) cm^{-1} : 3253, 3067, 2967, 2874, 1627, 1538, 1454, 1297, 1158

HRMS-ESI (m/z), calculated for $\text{C}_{11}\text{H}_{16}\text{NO}$ ($\text{M}+\text{H}$) $^+$ 178.1232. Found 178.1250

M.P.: 80.5°C – 81.2°C



N-(cyclohexylmethyl)benzamide:

Cyclohexylmethylamine (4.98 g, 44 mmol) was added by syringe to a 250 mL round bottom flask. 100 mL of anhydrous DCM was then added and the mixture was stirred while triethylamine (6.07 g, 60 mmol) was added by syringe. The resulting solution was cooled to 0°C by ice bath before benzoyl chloride (5.62 g, 40 mmol) was added dropwise to the solution, over 10 minutes. The reaction was stirred at 0°C for one hour before warming to room temperature and stirring for an additional 8 hours. After which the solution was washed with 0.5 M HCl solution (2 x 30 mL) followed by NaCl solution (2 x 30 mL). The organic layers were collected and dried over anhydrous Na_2SO_4 and reduced in vacuo before the addition of warm hexanes to precipitate the product as a white solid 89 % yield (7.73 g, 35.57 mmol)

Spectroscopy:

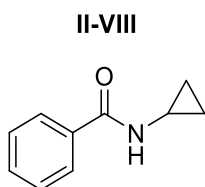
^1H NMR (500 MHz, CDCl_3) δ 7.79 – 7.73 (m, 2H), 7.53 – 7.45 (m, 1H), 7.47 – 7.39 (m, 2H), 6.17 (s, 1H), 3.31 (dd, $J = 6.9, 6.0$ Hz, 2H), 1.83 – 1.74 (m, 2H), 1.78 – 1.71 (m, 1H), 1.75 – 1.64 (m, 1H), 1.59 (tdt, $J = 11.4, 6.9, 3.4$ Hz, 2H), 1.31 – 1.09 (m, 3H), 1.06 – 0.94 (m, 2H).

^{13}C NMR (125 MHz, CDCl_3) δ 167.52, 134.92, 131.29, 128.54, 126.79, 46.22, 38.04, 30.92, 26.39, 25.82.

IR (FT-ATR) cm^{-1} : 3340, 3054, 2937, 2924, 2914, 2845, 1634, 1545, 1492, 1305, 1281, 1149

HRMS-ESI (m/z), calculated for $\text{C}_{14}\text{H}_{20}\text{NO}$ ($\text{M}+\text{H}$) $^+$ 218.1545. Found 218.1599.

m.p.: 100.8°C – 102.0°C



N-cyclopropylbenzamide:

Cyclopropylamine (2.51 g, 44 mmol) was added by syringe to a 250 mL round bottom flask. 100 mL of anhydrous DCM was then added and the mixture was stirred while triethylamine (6.07 g, 60 mmol) was added by syringe. The resulting solution was cooled to 0°C by ice bath before benzoyl chloride (5.62 g, 40 mmol) was added dropwise to the solution, over 10 minutes. The reaction was stirred at 0°C for one hour before warming to room temperature and stirring for an additional 8 hours. After which the solution was washed with 0.5 M HCl solution (2 x 30 mL) followed by saturated NaCl solution (2 x 30 mL). The organic layers were collected and dried over anhydrous Na_2SO_4 and reduced in vacuo before the addition of warm hexanes to precipitate the product as a white solid 93 % yield (6.00 g, 37.22 mmol)

Spectroscopy:

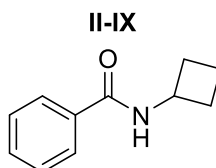
^1H NMR (500 MHz, CDCl_3) δ 7.77 – 7.70 (m, 2H), 7.52 – 7.45 (m, 1H), 7.42 (ddt, $J = 8.2, 6.6, 1.2$ Hz, 2H), 6.27 – 6.23 (m, 1H), 2.91 (tq, $J = 7.0, 3.8$ Hz, 1H), 0.93 – 0.82 (m, 2H), 0.66 – 0.59 (m, 2H).

^{13}C NMR (125 MHz, CDCl_3) δ 168.84, 134.40, 131.46, 128.53, 126.79, 23.10, 6.81.

IR (FT-ATR) cm^{-1} : 3226, 3063, 2998, 2862, 1616, 1551, 1489, 1312, 1025

HRMS-ESI (m/z), calculated for $\text{C}_{10}\text{H}_{12}\text{NO}$ ($\text{M}+\text{H}$) $^+$ 162.0919. Found 162.0916

M.P.: 94.7°C – 95.2°C



N-cyclobutylbenzamide:

Cyclobutylamine (3.13 g, 44 mmol) was added by syringe to a 250 mL round bottom flask. 100 mL of anhydrous DCM was then added and the mixture was stirred while triethylamine (6.07 g, 60 mmol) was added by syringe. The resulting solution was cooled to 0°C by ice bath before benzoyl chloride (5.62 g, 40 mmol) was added dropwise to the solution, over 10 minutes. The reaction was stirred at 0°C for one hour before warming to room temperature and stirring for an additional 8 hours. After which the solution was washed with 0.5 M HCl solution (2 x 30 mL) followed by saturated NaCl solution (2 x 30 mL). The organic layers were collected and dried over anhydrous Na_2SO_4 and reduced in vacuo before the addition of warm hexanes to precipitate the product as a white solid 98 % yield (6.90 g, 39.40 mmol)

Spectroscopy:

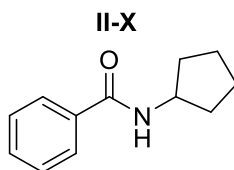
^1H NMR (500 MHz, CDCl_3) δ 7.78 – 7.72 (m, 2H), 7.52 – 7.45 (m, 1H), 7.42 (ddt, $J = 8.3, 6.6, 1.3$ Hz, 2H), 6.24 (s, 1H), 4.66 – 4.54 (m, 1H), 2.51 – 2.38 (m, 2H), 2.02 – 1.89 (m, 2H), 1.82 – 1.71 (m, 2H).

^{13}C NMR (125 MHz, CDCl_3) δ 166.52, 134.59, 131.35, 128.52, 126.83, 45.17, 31.37, 15.18.

IR (FT-ATR) cm^{-1} : 3272, 3062, 2985, 2939, 2866, 1627, 1537, 1491, 1301, 1027

HRMS-ESI (m/z), calculated for $\text{C}_{11}\text{H}_{14}\text{NO}$ ($\text{M}+\text{H}$) $^+$ 176.1075. Found 176.1093.

M.P: 119.5°C – 120.1°C



N-cyclopentylbenzamide:

Cyclopentylamine (1.95 g, 23 mmol) was added by syringe to a 250 mL round bottom flask. 100 mL of anhydrous DCM was then added and the mixture was stirred while triethylamine (3.04 g, 30 mmol) was added by syringe. The resulting solution was cooled to 0°C by ice bath before benzoyl chloride (2.81 g, 20 mmol) was added dropwise to the solution, over 10 minutes. The reaction was stirred at 0°C for one hour before warming to room temperature and stirring for an additional 8 hours. After which the solution was washed with 0.5 M HCl solution (2 x 30 mL) followed by saturated NaCl solution (2 x 30 mL). The organic layers were collected and dried over anhydrous Na_2SO_4 and reduced in vacuo before the addition of warm hexanes to precipitate the product as a white solid 87 % yield (3.28 g, 17.33 mmol)

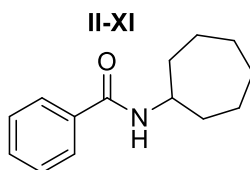
Spectroscopy:

^1H NMR (500 MHz, CDCl_3) δ 7.79 – 7.72 (m, 2H), 7.53 – 7.44 (m, 1H), 7.46 – 7.39 (m, 2H), 6.09 – 6.04 (m, 1H), 4.42 (h, $J = 7.0$ Hz, 1H), 2.17 – 2.04 (m, 3H), 1.80 – 1.59 (m, 3H), 1.57 – 1.44 (m, 2H).

^{13}C NMR (125 MHz, CDCl_3) δ 167.13, 134.93, 131.25, 128.51, 126.80, 51.68, 33.26, 23.81.

HRMS-ESI (m/z), calculated for $\text{C}_{12}\text{H}_{16}\text{NO}$ ($\text{M}+\text{H}$) $^+$ 190.1232. Found 190.1275

M.P.: 160.5°C – 161.1°C

**N-cycloheptylbenzamide:**

Cycloheptylamine (2.60 g, 23 mmol) was added by syringe to a 250 mL round bottom flask. 100 mL of anhydrous DCM was then added and the mixture was stirred while triethylamine (3.04 g, 30 mmol) was added by syringe. The resulting solution was cooled to 0°C by ice bath before benzoyl chloride (2.81 g, 20 mmol) was added dropwise to the solution, over 10 minutes. The reaction was stirred at 0°C for one hour before warming to room temperature and stirring for an additional 8 hours. After which the solution was washed with 0.5 M HCl solution (2 x 30 mL) followed by saturated NaCl solution (2 x 30 mL). The organic layers were collected and dried over anhydrous Na_2SO_4 and reduced in vacuo before the addition of warm hexanes to precipitate the product as a white solid 90 % yield (3.90 g, 17.96 mmol)

Spectroscopy:

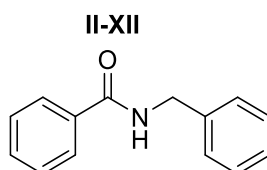
^1H NMR (500 MHz, CDCl_3) δ 7.79 – 7.72 (m, 2H), 7.53 – 7.46 (m, 1H), 7.43 (ddt, $J = 8.2, 6.5, 1.3$ Hz, 2H), 6.03 (d, $J = 7.5$ Hz, 1H), 4.18 (qd, $J = 8.6, 4.3$ Hz, 1H), 2.10 – 2.00 (m, 2H), 1.73 – 1.72 (m, 2H), 1.66 (m, 2H), 1.62 – 1.49 (m, 6H).

^{13}C NMR (125 MHz, CDCl_3) δ 166.32, 135.13, 131.21, 128.51, 126.78, 50.86, 35.21, 28.06, 24.15.

IR (FT-ATR) cm^{-1} : 3237, 3066, 2921, 2858, 1624, 1556, 1488, 1326, 1179

HRMS-ESI (m/z), calculated for $\text{C}_{14}\text{H}_{20}\text{NO}$ ($\text{M}+\text{H}$) $^+$ 218.1545. Found 218.1586.

M.P.: 130.8°C – 131.6°C



N-benzylbenzamide:

Benzylamine (4.72 g, 44 mmol) was added by syringe to a 250 mL round bottom flask. 100 mL of anhydrous DCM was then added and the mixture was stirred while triethylamine (6.07 g, 60 mmol) was added by syringe. The resulting solution was cooled to 0°C by ice bath before benzoyl chloride (5.62 g, 40 mmol) was added dropwise to the solution, over 10 minutes. The reaction was stirred at 0°C for one hour before warming to room temperature and stirring for an additional 8 hours. After which the solution was washed with 0.5 M HCl solution (2 x 30 mL) followed by saturated NaCl solution (2 x 30 mL). The organic layers were collected and dried over anhydrous Na_2SO_4 and reduced in vacuo before the addition of warm hexanes to precipitate the product as a white solid 92 % yield (7.78 g, 36.83 mmol)

Spectroscopy:

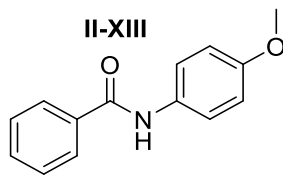
^1H NMR (500 MHz, CDCl_3) 7.83 – 7.76 (m, 2H), 7.52 – 7.45 (m, 1H), 7.44 – 7.37 (m, 2H), 7.34 (d, $J = 4.8$ Hz, 4H), 7.28 (ddd, $J = 9.8, 5.2, 3.5$ Hz, 1H), 6.73 (t, $J = 5.8$ Hz, 1H), 4.61 (d, $J = 5.7$ Hz, 2H).

^{13}C NMR (125 MHz, CDCl_3) δ 167.44, 138.25, 134.35, 131.52, 128.74, 128.55, 127.86, 127.55, 127.01, 44.06.

IR (FT-ATR) cm^{-1} : 3326, 3080, 2919, 2850, 1627, 1529, 1488, 1446, 1327, 1151, 1083

HRMS-ESI (m/z), calculated for $\text{C}_{14}\text{H}_{14}\text{NO}$ ($\text{M}+\text{H}$) $^+$ 212.1075. Found 212.1120.

M.P.: 101.2°C – 101.5°C



N-(4-methoxyphenyl)benzamide:

p-Anisidine (5.17 g, 42 mmol) was added by syringe to a 250 mL round bottom flask. 100 mL of anhydrous DCM was then added and the mixture was stirred while triethylamine (6.07 g, 60 mmol) was added by syringe. The resulting solution was cooled to 0°C by ice bath before benzoyl chloride (4.82 g, 40 mmol) was added dropwise to the solution, over 10 minutes. The reaction was stirred at 0°C for one hour before warming to room temperature and stirring for an additional 8 hours. After which the solution was washed with 0.5 M HCl solution (2 x 30 mL) followed by saturated NaCl solution (2 x 30 mL). The organic layers were collected and dried over anhydrous Na_2SO_4 and reduced in vacuo before the addition of warm hexanes to precipitate the product as a pink solid 50 % yield (4.52 g, 19.88 mmol)

Spectroscopy:

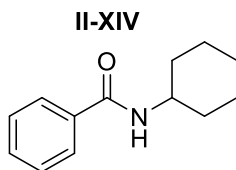
^1H NMR (500 MHz, $\text{DMSO-}d_6$) δ 10.13 (s, 1H), 7.98 – 7.91 (m, 2H), 7.72 – 7.64 (m, 2H), 7.61 – 7.54 (m, 1H), 7.52 (ddt, $J = 8.2, 6.5, 1.3$ Hz, 2H), 6.96 – 6.89 (m, 2H), 3.74 (s, 3H).

^{13}C NMR (125 MHz, $\text{DMSO-}d_6$) δ 165.54, 155.97, 135.50, 132.68, 131.83, 128.80, 127.99, 122.41, 114.17, 55.62.

IR (FT-ATR) cm^{-1} : 3326, 2919, 2850, 1627, 1603, 1577, 1529, 1488, 1327, 1151, 1083

HRMS-ESI (m/z), calculated for $\text{C}_{14}\text{H}_{14}\text{NO}_2$ ($\text{M}+\text{H}$) $^+$ 228.1025. Found 228.1034

m.p: 149.0°C – 150.0°C

**N-cyclohexylbenzamide:**

Cyclohexylamine (2.28 g, 23 mmol) was added by syringe to a 250 mL round bottom flask. 100 mL of anhydrous DCM was then added and the mixture was stirred while triethylamine (3.04 g, 30 mmol) was added by syringe. The resulting solution was cooled to 0°C by ice bath before benzoyl chloride (2.81 g, 20 mmol) was added dropwise to the solution, over 10 minutes. The reaction was stirred at 0°C for one hour before warming to room temperature and stirring for an additional 8 hours. After which the solution was washed with 0.5 M HCl solution (2 x 30 mL) followed by saturated NaCl solution (2 x 30 mL). The organic layers were collected and dried over

anhydrous Na₂SO₄ and reduced in vacuo before the addition of warm hexanes to precipitate the product as a white solid 94 % yield (3.80 g, 18.69 mmol)

Spectroscopy:

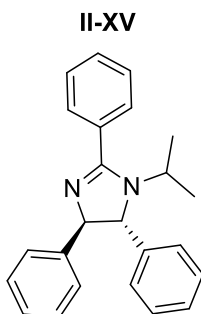
¹H NMR (500 MHz, CDCl₃) δ 7.76 – 7.69 (m, 2H), 6.96 – 6.88 (m, 2H), 5.88 (d, *J* = 8.1 Hz, 1H), 3.97 (tdt, *J* = 11.2, 8.0, 3.9 Hz, 1H), 3.85 (d, *J* = 0.7 Hz, 3H), 2.03 (dt, *J* = 12.4, 4.0 Hz, 2H), 1.76 (dp, *J* = 12.0, 4.0 Hz, 2H), 1.66 (tt, *J* = 8.0, 3.8 Hz, 1H), 1.50 – 1.37 (m, 2H), 1.23 (qd, *J* = 12.0, 3.6 Hz, 3H).

¹³C NMR (125 MHz, CDCl₃) δ 166.07, 135.07, 131.21, 128.48, 126.80, 48.55, 33.33, 25.61, 24.94.

IR (FT-ATR) cm⁻¹: 3296, 3006, 2927, 2853, 2838, 1625, 1605, 1535, 1505, 1252, 1239, 1176, 1027

HRMS-ESI (*m/z*), calculated for C₁₃H₁₈NO (*M*+*H*)⁺ 204.1338. Found 204.1408

m.p: 157.8°C – 158.5°C



Trans-1-isopropyl-2,4,5-triphenyl-4,5-dihydro-1H-imidazole:

N-isopropylbenzamide (0.20 g, 1.23 mmol) was added to a 50 mL flamed dried round bottom flask. 4 mL of anhydrous DCM was added to the flask by syringe. The resulting solution was cooled to 0°C by ice-bath before the addition of 2,6 Lutidine (0.658 g, 6.144 mmol) by syringe. Oxalyl Chloride (0.15 g, 1.23 mmol) was then added over 10 minutes by syringe. The resulting mixture was stirred at 0°C for 1.5 hours after which the solvent was removed to give the

intermediate imidoyl chloride as a brownish-tan solid. This solid was then dissolved in 4 mL of anhydrous DMF and to this solution trans-2,3-diphenylaziridine (0.200 g, 1.024 mmol) was added by syringe. The reaction was then stirred for 12-14 hours at 55°C. The reaction was extracted in EtOAc (2 x 25 mL) and washed with 10 % LiBr solution. After which the organic layers were washed with 0.5 M HCl solution and Saturated NaHCO₃ solution. The organic layers were collected and dried over anhydrous NaSO₄, concentrated and purified by column chromatography (3:7 EtOAc:Hexanes). The product was obtained as a clear oil 13 % yield (0.045 g, 0.13 mmol)

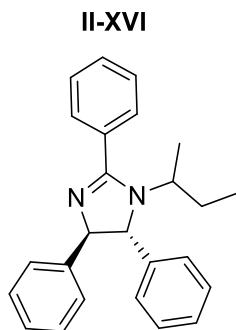
Spectroscopy:

¹H NMR (500 MHz, CDCl₃) δ 7.86 – 7.79 (m, 2H), 7.58 – 7.46 (m, 3H), , 7.42 – 7.35 (m, 6H), 7.39 – 7.26 (m, 4H), 4.92 (d, *J* = 6.8 Hz, 1H), 4.50 (dd, *J* = 6.9, 2.6 Hz, 1H), 4.02 (hept, *J* = 6.8 Hz, 1H), 0.96 (d, *J* = 6.5 Hz, 3H), 0.82 (d, *J* = 6.9 Hz, 3H).

¹³C NMR (125 MHz, CDCl₃) δ 167.43, 129.00, 128.80, 128.78, 128.73, 128.51, 126.77, 126.29, 126.28, 76.75, 69.15, 22.88, , 19.69.

IR (FT-ATR) cm⁻¹: 3067, 3029, 2973, 2928, 1658, 1596, 1495, 1447, 1181, 1026

HRMS-ESI (*m/z*), calculated for C₂₄H₂₅N₂ (M+H)⁺ 341.2016. Found 341.2137.



Trans-1-(sec-butyl)-2,4,5-triphenyl-4,5-dihydro-1H-imidazole:

N-(sec-butyl)benzamide (0.218 g, 1.23 mmol) was added to a 50 mL flamed dried round bottom flask. 4 mL of anhydrous DCM was added to the flask by syringe. The resulting solution was cooled to 0°C by ice-bath before the addition of 2,6 Lutidine (0.658 g, 6.144 mmol) by syringe. Oxalyl Chloride (0.15 g, 1.23 mmol) was then added over 10 minutes by syringe. The resulting mixture was stirred at 0°C for 1.5 hours after which the solvent was removed to give the intermediate imidoyl chloride as a brownish-tan solid. This solid was then dissolved in 4 mL of anhydrous DMF and to this solution trans-2,3-diphenylaziridine (0.200 g, 1.024 mmol) was added by syringe. The reaction was then stirred for 12-14 hours at 55°C. The reaction was extracted in EtOAc (2 x 25 mL) and washed with 10 % LiBr solution. After which the organic layers were washed with 0.5 M HCl solution and Saturated NaHCO₃ solution. The organic layers were collected and dried over anhydrous NaSO₄, concentrated and purified by column chromatography (3:7 EtOAc:Hexanes). The product was obtained as a clear oil 32 % yield (0.116 g, 0.328 mmol)

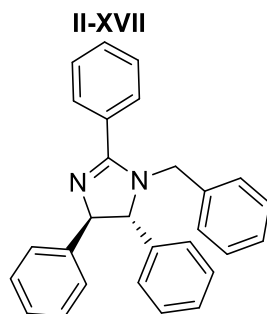
Spectroscopy:

¹H NMR (500 MHz, CDCl₃) δ 7.85 – 7.78 (m, 2H), 7.53 – 7.42 (m, 3H), 7.40 (s, 2H), 7.42 – 7.30 (m, 4H), 7.34 – 7.25 (m, 4H), 4.98 (d, *J* = 6.9 Hz, 1H), 4.43 (d, *J* = 6.9 Hz, 1H), 3.66 (h, *J* = 6.8 Hz, 1H), 1.33 – 1.15 (m, 1H), 1.00 (dq, *J* = 14.1, 7.2 Hz, 1H), 0.92 (d, *J* = 6.6 Hz, 3H), 0.65 (t, *J* = 7.3 Hz, 3H).

¹³C NMR (125 MHz, CDCl₃) δ 168.07, 145.76, 144.62, 131.95, 130.08, 128.76, 128.72, 128.54, 128.48, 127.29, 127.04, 126.65, 126.41, 78.91, 69.27, 54.75, 29.20, 17.39, 11.52.

IR (FT-ATR) cm⁻¹: 3061, 3029, 2965, 2932, 2871, 1615, 1597, 1495, 1447, 1173, 1060, 1027

HRMS-ESI (*m/z*), calculated for C₂₅H₂₇N₂ (M+H)⁺ 355.2174. Found 355.2205.



Trans-1-benzyl-2,4,5-triphenyl-4,5-dihydro-1H-imidazole:

N-benzylbenzamide (0.130 g, 0.615 mmol) was added to a 50 mL flamed dried round bottom flask. 4 mL of anhydrous DCM was added to the flask by syringe. The resulting solution was cooled to 0°C by ice-bath before the addition of 2,6 Lutidine (0.330 g, 3.073 mmol) by syringe. Oxalyl Chloride (0.078 g, 0.615 mmol) was then added over 10 minutes by syringe. The resulting mixture was stirred at 0°C for 1.5 hours after which the solvent was removed to give the intermediate imidoyl chloride as a brownish-tan solid. This solid was then dissolved in 4 mL of anhydrous DMF and to this solution trans-2,3-diphenylaziridine (0.100 g, 0.512 mmol) was added by syringe. The reaction was then stirred for 12-14 hours at 55°C. The reaction was extracted in EtOAc (2 x 25 mL) and washed with 10 % LiBr solution. After which the organic layers were washed with 0.5 M HCl solution and Saturated NaHCO₃ solution. The organic layers were collected and dried over anhydrous NaSO₄, concentrated and purified by column chromatography (3:7 EtOAc:Hexanes). The product was obtained as a clear oil 46 % yield (0.092 g, 0.236 mmol)

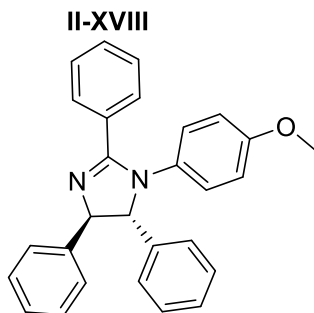
Spectroscopy:

¹H NMR (500 MHz, CDCl₃) δ 7.90 – 7.76 (m, 1H), 7.55 – 7.47 (m, 1H), 7.46 – 7.35 (m, 1H), 7.35 – 7.19 (m, 4H), 7.16 – 7.08 (m, 1H), 7.03 – 6.90 (m, 1H), 5.02 (d, *J* = 8.5 Hz, 1H), 4.73 (d, *J* = 15.6 Hz, 1H), 4.36 (d, *J* = 8.6 Hz, 1H), 3.94 (d, *J* = 15.6 Hz, 1H).

^{13}C NMR (125 MHz, CDCl_3) δ 166.00, 143.78, 141.72, 136.36, 130.27, 128.91, 128.74, 128.69, 128.52, 128.44, 128.00, 127.85, 127.55, 127.21, 127.08, 126.78, 72.56, 49.65.

IR (FT-ATR) cm^{-1} : 3034, 3002, 2987, 2913, 2821, 1605, 1582, 1491, 1423, 1154, 1034, 1011

HRMS-ESI (m/z), calculated for $\text{C}_{28}\text{H}_{25}\text{N}_2$ ($\text{M}+\text{H}$) $^+$ 389.2017. Found 389.2005



Trans-1-(4-methoxyphenyl)-2,4,5-triphenyl-4,5-dihydro-1H-imidazole:

N-(4-methoxyphenyl)benzamide (0.140 g, 0.615 mmol) was added to a 50 mL flamed dried round bottom flask. 4 mL of anhydrous DCM was added to the flask by syringe. The resulting solution was cooled to 0°C by ice-bath before the addition of 2,6 Lutidine (0.330 g, 3.073 mmol) by syringe. Oxalyl Chloride (0.078 g, 0.615 mmol) was then added over 10 minutes by syringe. The resulting mixture was stirred at 0°C for 1.5 hours after which the solvent was removed to give the intermediate imidoyl chloride as a brownish-tan solid. This solid was then dissolved in 4 mL of anhydrous DMF and to this solution trans-2,3-diphenylaziridine (0.100 g, 0.512 mmol) was added by syringe. The reaction was then stirred for 12-14 hours at 55°C . The reaction was extracted in EtOAc (2 x 25 mL) and washed with 10 % LiBr solution. After which the organic layers were washed with 0.5 M HCl solution and Saturated NaHCO_3 solution. The organic layers were collected and dried over anhydrous NaSO_4 , concentrated and purified by column chromatography (3:7 EtOAc:Hexanes). The product was obtained as a clear oil 28 % yield (0.058 g, 0.143 mmol)

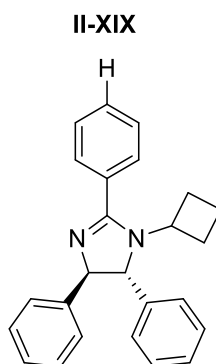
Spectroscopy:

^1H NMR (500 MHz, CDCl_3) δ 9.06 (s, 1H), 7.69 (ddd, $J = 23.8, 7.5, 1.7$ Hz, 4H), 7.53 – 7.46 (m, 1H), 7.50 – 7.37 (m, 2H), 7.41 – 7.30 (m, 4H), 7.31 (s, 2H), 7.33 – 7.27 (m, 1H), 7.31 – 7.25 (m, 3H), 6.95 – 6.87 (m, 3H), 6.24 (d, $J = 6.9$ Hz, 1H), 5.80 (dd, $J = 8.7, 6.9$ Hz, 1H), 3.82 (s, 3H).

^{13}C NMR (125 MHz, CDCl_3) δ 167.83, 159.09, 157.10, 153.19, 137.18, 135.51, 133.81, 131.98, 129.84, 129.04, 128.93, 128.76, 128.62, 128.44, 127.29, 126.98, 126.94, 121.31, 114.25, 81.29, 58.07, 55.47.

IR (FT-ATR) cm^{-1} : 3025, 2983, 2841, 1602, 1594, 1421, 1154, 1092

HRMS-ESI (m/z), calculated for $\text{C}_{28}\text{H}_{25}\text{N}_2\text{O}(\text{M}+\text{H})^+$ 405.1970. Found 405.1983

**Trans-1-cyclobutyl-2,4,5-triphenyl-4,5-dihydro-1H-imidazole:**

N-cyclobutylbenzamide (0.108 g, 0.615 mmol) was added to a 50 mL flamed dried round bottom flask. 4 mL of anhydrous DCM was added to the flask by syringe. The resulting solution was cooled to 0°C by ice-bath before the addition of 2,6 Lutidine (0.330 g, 3.073 mmol) by syringe. Oxalyl Chloride (0.078 g, 0.615 mmol) was then added over 10 minutes by syringe. The resulting mixture was stirred at 0°C for 1.5 hours after which the solvent was removed to give the intermediate imidoyl chloride as a brownish-tan solid. This solid was then dissolved in 4 mL of anhydrous DMF and to this solution trans-2,3-diphenylaziridine (0.100 g, 0.512 mmol) was added by syringe. The reaction was then stirred for 12-14 hours at 55°C . The reaction was extracted in

EtOAc (2 x 25 mL) and washed with 10 % LiBr solution. After which the organic layers were washed with 0.5 M HCl solution and Saturated NaHCO₃ solution. The organic layers were collected and dried over anhydrous NaSO₄, concentrated and purified by column chromatography (3:7 EtOAc:Hexanes). The product was obtained as a clear oil 38 % yield (0.069 g, 0.195 mmol)

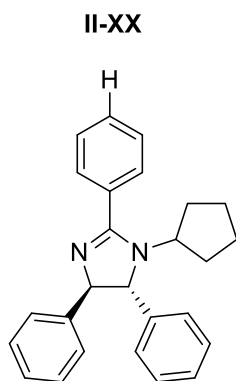
Spectroscopy:

¹H NMR (500 MHz, CDCl₃) δ 7.81 – 7.73 (m, 2H), 7.58 – 7.46 (m, 3H), 7.45 – 7.35 (m, 5H), 7.37 – 7.26 (m, 5H), 4.91 (d, *J* = 6.7 Hz, 1H), 4.72 (d, *J* = 6.7 Hz, 1H), 4.28 – 4.17 (m, 1H), 2.10 (p, *J* = 10.1 Hz, 1H), 1.92 – 1.81 (m, 1H), 1.74 (ddd, *J* = 16.8, 7.6, 4.9 Hz, 1H), 1.71 – 1.63 (m, 1H), 1.45 – 1.20 (m, 2H),.

¹³C NMR (125 MHz, CDCl₃) δ 166.11, 130.21, 128.95, 128.68, 128.65, 128.46, 128.33, 127.46, 127.25, 126.52, 126.18, 70.57, 51.78, 30.42, 29.71, 27.52, 14.57.

IR (FT-ATR) cm⁻¹: 3020, 2977, 1656, 1587, 1448, 1219

HRMS-ESI (m/z), calculated for C₂₅H₂₅N₂ (M+H)⁺ 353.3210. Found 353.3293.



Trans-1-cyclopentyl-2,4,5-triphenyl-4,5-dihydro-1H-imidazole:

N-cyclopentylbenzamide (0.108 g, 0.615 mmol) was added to a 50 mL flamed dried round bottom flask. 4 mL of anhydrous DCM was added to the flask by syringe. The resulting solution was

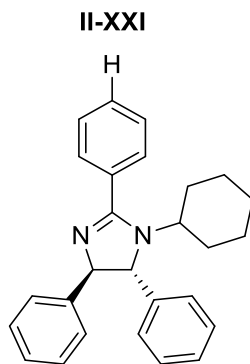
cooled to 0°C by ice-bath before the addition of 2,6 Lutidine (0.330 g, 3.073 mmol) by syringe. Oxalyl Chloride (0.078 g, 0.615 mmol) was then added over 10 minutes by syringe. The resulting mixture was stirred at 0°C for 1.5 hours after which the solvent was removed to give the intermediate imidoyl chloride as a brownish-tan solid. This solid was then dissolved in 4 mL of anhydrous DMF and to this solution trans-2,3-diphenylaziridine (0.100 g, 0.512 mmol) was added by syringe. The reaction was then stirred for 12-14 hours at 55°C. The reaction was extracted in EtOAc (2 x 25 mL) and washed with 10 % LiBr solution. After which the organic layers were washed with 0.5 M HCl solution and Saturated NaHCO₃ solution. The organic layers were collected and dried over anhydrous NaSO₄, concentrated and purified by column chromatography (3:7 EtOAc:Hexanes). The product was obtained as a clear oil 54 % yield (0.100 g, 0.274 mmol)

Spectroscopy:

¹H NMR (500 MHz, CDCl₃) δ 7.86 – 7.79 (m, 2H), 7.59 – 7.45 (m, 3H), 7.44 – 7.35 (m, 6H), 7.36 – 7.26 (m, 4H), 4.88 (d, *J* = 6.8 Hz, 1H), 4.47 (d, *J* = 6.9 Hz, 1H), 4.09 (dq, *J* = 9.8, 7.8 Hz, 1H), 1.56 (dtd, *J* = 14.1, 7.4, 3.3 Hz, 1H), 1.52 – 1.37 (m, 2H), 1.35 (hd, *J* = 5.3, 2.8 Hz, 2H), 1.30 – 1.18 (m, 2H), 1.16 – 1.04 (m, 1H).

¹³C NMR (125 MHz, CDCl₃) δ 167.63, 144.70, 130.11, 128.88, 128.67, 128.64, 128.48, 128.33, 127.27, 127.15, 126.48, 125.97, 69.61, 58.48, 30.96, 27.82, 23.31.

HRMS-ESI (m/z), calculated for C₂₆H₂₇N₂ (M+H)⁺ 367.2172. Found 367.2210.



Trans-1-cyclohexyl-2,4,5-triphenyl-4,5-dihydro-1H-imidazole:

N-cyclohexylbenzamide (0.125 g, 0.615 mmol) was added to a 50 mL flamed dried round bottom flask. 4 mL of anhydrous DCM was added to the flask by syringe. The resulting solution was cooled to 0°C by ice-bath before the addition of 2,6 Lutidine (0.330 g, 3.073 mmol) by syringe. Oxalyl Chloride (0.078 g, 0.615 mmol) was then added over 10 minutes by syringe. The resulting mixture was stirred at 0°C for 1.5 hours after which the solvent was removed to give the intermediate imidoyl chloride as a brownish-tan solid. This solid was then dissolved in 4 mL of anhydrous DMF and to this solution trans-2,3-diphenylaziridine (0.100 g, 0.512 mmol) was added by syringe. The reaction was then stirred for 12-14 hours at 55°C. The reaction was extracted in EtOAc (2 x 25 mL) and washed with 10 % LiBr solution. After which the organic layers were washed with 0.5 M HCl solution and Saturated NaHCO₃ solution. The organic layers were collected and dried over anhydrous NaSO₄, concentrated and purified by column chromatography (3:7 EtOAc:Hexanes). The product was obtained as a clear oil 55 % yield (0.107 g, 0.281 mmol)

Spectroscopy:

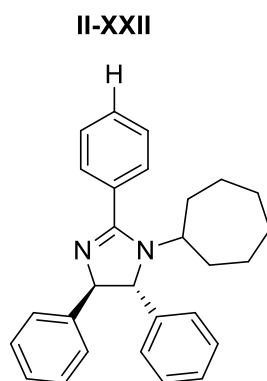
¹H NMR (500 MHz, CDCl₃) δ 7.87 – 7.79 (m, 2H), 7.55 – 7.46 (m, 3H), 7.44 – 7.36 (m, 6H), 7.36 – 7.25 (m, 4H), 4.89 (d, *J* = 6.5 Hz, 1H), 4.54 (d, *J* = 6.5 Hz, 1H), 3.55 (tt, *J* = 11.9, 3.7 Hz, 1H),

1.66 – 1.58 (m, 1H), 1.62 – 1.41 (m, 3H), 1.38 (qd, $J = 12.2, 3.9$ Hz, 1H), 1.28 (s, 1H), 1.09 – 0.93 (m, 2H), 0.93 – 0.77 (m, 2H).

^{13}C NMR (125 MHz, CDCl_3) δ 167.39, 146.21, 144.73, 131.84, 130.14, 128.79, 128.64, 128.63, 128.50, 127.21, 127.12, 126.49, 126.17, 78.60, 69.79, 56.59, 33.59, 30.12, 29.72, 26.09, 25.39, 25.22.

IR (FT-ATR) cm^{-1} : 3060, 3028, 2932, 2854, 1610, 1597, 1495, 1447, 1010

HRMS-ESI (m/z), calculated for $\text{C}_{27}\text{H}_{29}\text{N}_2$ ($\text{M}+\text{H}$) $^+$ 381.2331. Found: 381.2413



Trans-1-cycloheptyl-2,4,5-triphenyl-4,5-dihydro-1H-imidazole:

N-cycloheptylbenzamide (0.134 g, 0.615 mmol) was added to a 50 mL flamed dried round bottom flask. 4 mL of anhydrous DCM was added to the flask by syringe. The resulting solution was cooled to 0°C by ice-bath before the addition of 2,6 Lutidine (0.330 g, 3.073 mmol) by syringe. Oxalyl Chloride (0.078 g, 0.615 mmol) was then added over 10 minutes by syringe. The resulting mixture was stirred at 0°C for 1.5 hours after which the solvent was removed to give the intermediate imidoyl chloride as a brownish-tan solid. This solid was then dissolved in 4 mL of anhydrous DMF and to this solution trans-2,3-diphenylaziridine (0.100 g, 0.512 mmol) was added by syringe. The reaction was then stirred for 12-14 hours at 55°C . The reaction was extracted in EtOAc (2 x 25 mL) and washed with 10 % LiBr solution. After which the organic layers were

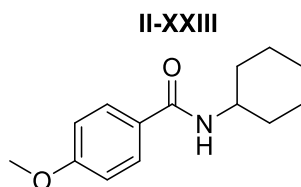
washed with 0.5 M HCl solution and Saturated NaHCO₃ solution. The organic layers were collected and dried over anhydrous NaSO₄, concentrated and purified by column chromatography (3:7 EtOAc:Hexanes). The product was obtained as a yellow oil 50 % yield (0.101 g, 0.256 mmol)

Spectroscopy:

¹H NMR (500 MHz, CDCl₃) δ 7.82 (dd, *J* = 6.7, 3.0 Hz, 2H), 7.58 – 7.45 (m, 3H), 7.43 – 7.36 (m, 6H), 7.31 (ddd, *J* = 7.8, 5.9, 1.9 Hz, 4H), 4.91 (d, *J* = 6.8 Hz, 1H), 4.48 (d, *J* = 6.8 Hz, 1H), 3.69 (dtd, *J* = 10.3, 7.0, 6.6, 4.0 Hz, 1H), 1.65 (ddd, *J* = 13.7, 7.1, 3.7 Hz, 1H), 1.56 – 1.19 (m, 8H), 1.17 – 1.00 (m, 3H).

¹³C NMR (125 MHz, CDCl₃) δ 167.50, 146.28, 144.75, 131.95, 130.09, 128.81, 128.63, 128.58, 128.47, 127.19, 127.06, 126.47, 126.34, 78.84, 70.20, 58.98, 34.92, 32.58, 27.44, 27.10, 24.97, 24.60.

IR (FT-ATR) cm⁻¹: 3065, 3027, 2926, 2856, 1614, 1597, 1494, 1447, 1247, 1027



N-cyclohexyl-4-methoxybenzamide:

Cyclohexylamine (2.28 g, 23 mmol) was added by syringe to a 250 mL round bottom flask. 100 mL of anhydrous DCM was then added and the mixture was stirred while triethylamine (3.04 g, 30 mmol) was added by syringe. The resulting solution was cooled to 0°C by ice bath before 4-methoxybenzoyl chloride (3.41 g, 20 mmol) was added dropwise to the solution, over 10 minutes. The reaction was stirred at 0°C for one hour before warming to room temperature and stirring for

an additional 8 hours. After which the solution was washed with 0.5 M HCl solution (2 x 30 mL) followed by saturated NaCl solution (2 x 30 mL). The organic layers were collected and dried over anhydrous Na₂SO₄ and reduced in vacuo before the addition of warm hexanes to precipitate the product as a white solid 97 % yield (4.52 g, 19.39 mmol)

Spectroscopy:

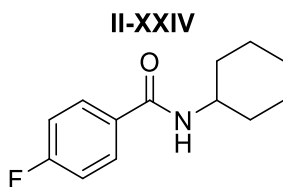
¹H NMR (500 MHz, CDCl₃) 1H NMR (500 MHz, Chloroform-d) δ 7.76 – 7.67 (m, 2H), 6.96 – 6.87 (m, 2H), 5.88 (d, J = 8.1 Hz, 1H), 3.97 (tdt, J = 11.2, 8.0, 3.9 Hz, 1H), 3.85 (d, J = 0.7 Hz, 3H), 2.03 (dt, J = 12.4, 4.0 Hz, 2H), 1.76 (dp, J = 12.0, 4.0 Hz, 2H), 1.66 (tt, J = 8.0, 3.8 Hz, 1H), 1.50 – 1.35 (m, 2H), 1.23 (qd, J = 12.0, 3.6 Hz, 3H).

¹³C NMR (125 MHz, CDCl₃) δ 166.07, 161.95, 128.56, 127.35, 113.65, 55.40, 48.55, 33.33, 25.61, 24.94

IR (FT-ATR) cm⁻¹: 3296, 3006, 2927, 2853, 2838, 1625, 1605, 1535, 1505, 1252, 1239, 1176, 1027

HRMS-ESI (m/z), calculated for C₁₄H₂₀NO₂ (M+H)⁺ 234.1494. Found 234.1516

m.p: 163.4°C – 163.8°C



N-cyclohexyl-4-fluorobenzamide:

Cyclohexylamine (2.28 g, 23 mmol) was added by syringe to a 250 mL round bottom flask. 100 mL of anhydrous DCM was then added and the mixture was stirred while triethylamine (3.04 g,

30 mmol) was added by syringe. The resulting solution was cooled to 0°C by ice bath before 4-fluorobenzoyl chloride (3.17 g, 20 mmol) was added dropwise to the solution, over 10 minutes. The reaction was stirred at 0°C for one hour before warming to room temperature and stirring for an additional 8 hours. After which the solution was washed with 0.5 M HCl solution (2 x 30 mL) followed by saturated NaCl solution (2 x 30 mL). The organic layers were collected and dried over anhydrous Na₂SO₄ and reduced in vacuo before the addition of warm hexanes to precipitate the product as a white solid 90 % yield (3.96 g, 17.91 mmol)

Spectroscopy:

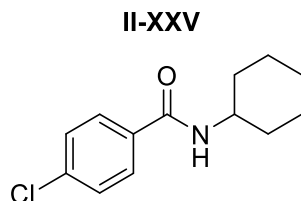
¹H NMR (500 MHz, CDCl₃) 7.79 – 7.70 (m, 2H), 7.14 – 7.03 (m, 2H), 6.03 – 5.82 (m, 1H), 3.95 (dddd, J = 14.8, 10.7, 8.0, 4.0 Hz, 1H), 2.01 (dt, J = 12.2, 3.9 Hz, 2H), 1.81 – 1.70 (m, 2H), 1.65 (dpd, J = 12.8, 3.7, 1.8 Hz, 1H), 1.47 – 1.35 (m, 2H), 1.28 – 1.12 (m, 3H).

¹³C NMR (125 MHz, CDCl₃) δ 164.55, 140.65, 128.03, 123.79, 49.23, 33.13, 25.46, 24.86, 13.19.

IR (FT-ATR) cm⁻¹: 3307, 3096, 2966, 2948, 2932, 2864, 1691, 1554, 1451, 1193, 1150

HRMS-ESI (m/z), calculated for C₁₃H₁₇FNO (M+H)⁺ 222.1294. Found 222.1294

M.P.: 149.1°C – 149.4°C



4-chloro-N-cyclohexylbenzamide:

Cyclohexylamine (4.36 g, 44 mmol) was added by syringe to a 250 ml round bottom flask. 100 ml of anhydrous DCM was then added and the mixture was stirred while triethylamine (6.07 g, 60 mmol) was added by syringe. The resulting solution was cooled to 0°C by ice bath before 4-chlorobenzoyl chloride (7.00 g, 40 mmol) was added dropwise to the solution, over 10 minutes. The reaction was stirred at 0°C for one hour before warming to room temperature and stirring for an additional 8 hours. After which the solution was washed with 0.5 M HCl solution (2 x 30 mL) followed by saturated NaCl solution (2 x 30 mL). The organic layers were collected and dried over anhydrous Na₂SO₄ and reduced in vacuo before the addition of warm hexanes to precipitate the product as a white solid 88% yield (8.4 g, 35.34 mmol)

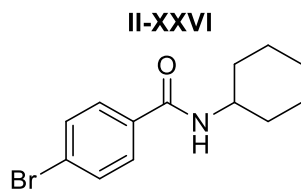
Spectroscopy:

¹H NMR (500 MHz, CDCl₃) δ 7.72 – 7.65 (m, 2H), 7.43 – 7.36 (m, 2H), 5.92 – 5.87 (m, 1H), 3.96 (dddd, *J* = 14.8, 10.7, 8.0, 3.9 Hz, 1H), 2.03 (dt, *J* = 12.6, 4.0 Hz, 2H), 1.76 (dt, *J* = 13.7, 3.8 Hz, 2H), 1.66 (dt, *J* = 12.8, 3.9 Hz, 1H), 1.49 – 1.36 (m, 2H), 1.29 – 1.14 (m, 3H).

¹³C NMR (125 MHz, CDCl₃) δ 165.49, 137.42, 133.41, 128.73, 128.25, 48.81, 33.21, 25.53, 24.88.

IR (FT-ATR) cm⁻¹: 3324, 2901, 2828, 1614, 1576, 1523, 1121, 1048, 1005, 812

HRMS-ESI (*m/z*), calculated for C₁₃H₁₇ClNO (M+H)⁺ 238.0999. Found 238.1027.



4-bromo-N-cyclohexylbenzamide:

Cyclohexylamine (2.28 g, 23 mmol) was added by syringe to a 250 ml round bottom flask. 100 ml of anhydrous DCM was then added and the mixture was stirred while triethylamine (3.04 g, 30 mmol) was added by syringe. The resulting solution was cooled to 0°C by ice bath before 4-bromobenzoyl chloride (4.39 g, 20 mmol) was added dropwise to the solution, over 10 minutes. The reaction was stirred at 0°C for one hour before warming to room temperature and stirring for an additional 8 hours. After which the solution was washed with 0.5 M HCl solution (2 x 30 mL) followed by saturated NaCl solution (2 x 30 mL). The organic layers were collected and dried over anhydrous Na₂SO₄ and reduced in vacuo before the addition of warm hexanes to precipitate the product as a white solid 87 % yield (4.88 g, 17.29 mmol)

Spectroscopy:

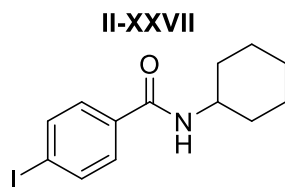
¹H NMR (500 MHz, CDCl₃) δ 7.73 – 7.63 (m, 2H), 7.44 – 7.36 (m, 2H), 6.00 – 5.80 (m, 1H), 3.96 (dddd, J = 14.8, 10.7, 8.0, 3.9 Hz, 1H), 2.03 (dt, J = 12.6, 4.0 Hz, 2H), 1.76 (dt, J = 13.7, 3.8 Hz, 2H), 1.66 (dt, J = 12.8, 3.9 Hz, 1H), 1.48 – 1.36 (m, 2H), 1.28 – 1.13 (m, 3H).

¹³C NMR (125 MHz, CDCl₃) δ 165.57, 133.87, 131.71, 128.45, 125.84, 48.82, 33.21, 25.52, 24.88.

IR (FT-ATR) cm⁻¹: 3283, 2922, 2853, 1631, 1588, 1537, 1152, 1066, 1011, 839

HRMS-ESI (m/z), calculated for C₁₃H₁₇BrNO (M+H)⁺ 282.0498. Found 282.0493

m.p.: 204.1°C – 204.6°C



N-cyclohexyl-4-iodobenzamide:

Cyclohexylamine (2.18g, 22 mmol) was added by syringe to a 250 ml round bottom flask. 100 ml of anhydrous DCM was then added and the mixture was stirred while triethylamine (3.04 g, 30 mmol) was added by syringe. The resulting solution was cooled to 0°C by ice bath before 4-iodobenzoyl chloride (5.62 g, 20 mmol) was added dropwise to the solution, over 10 minutes. The reaction was stirred at 0°C for one hour before warming to room temperature and stirring for an additional 8 hours. After which the solution was washed with 0.5 M HCl solution (2 x 30 mL) followed by saturated NaCl solution (2 x 30 mL). The organic layers were collected and dried over anhydrous Na₂SO₄ and reduced in vacuo before the addition of warm hexanes to precipitate the product as a white solid 89 % yield (5.813 g, 17.66 mmol)

Spectroscopy:

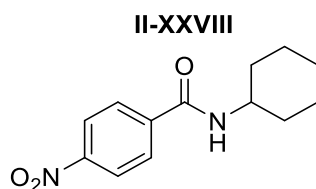
¹H NMR (500 MHz, CDCl₃) δ 7.81 – 7.74 (m, 2H), 7.51 – 7.44 (m, 2H), 5.89 (d, *J* = 7.9 Hz, 1H), 3.96 (dddd, *J* = 14.8, 10.7, 8.0, 3.9 Hz, 1H), 2.02 (dt, *J* = 12.4, 3.9 Hz, 2H), 1.75 (dt, *J* = 13.7, 3.9 Hz, 2H), 1.66 (dt, *J* = 13.0, 3.9 Hz, 1H), 1.49 – 1.36 (m, 2H), 1.22 (qd, *J* = 11.9, 3.2 Hz, 3H).

¹³C NMR (125 MHz, CDCl₃) δ 165.73, 137.67, 134.45, 128.46, 98.05, 48.81, 33.19, 25.52, 24.89.

IR (FT-ATR) cm⁻¹: 3295, 2931, 2852, 1623, 1585, 1537, 1330, 1151, 1006, 712

HRMS-ESI (*m/z*), calculated for C₁₃H₁₇INO (M+H)⁺ 330.0355. Found 330.0379.

M.P.: 206.8°C – 208.1°C



N-cyclohexyl-4-nitrobenzamide:

Cyclohexylamine (2.18 g, 22 mmol) was added by syringe to a 250 ml round bottom flask. 100 ml of anhydrous DCM was then added and the mixture was stirred while triethylamine (3.04 g, 30 mmol) was added by syringe. The resulting solution was cooled to 0°C by ice bath before 4-nitrobenzoyl chloride (3.21 g, 20 mmol) was added dropwise to the solution, over 10 minutes. The reaction was stirred at 0°C for one hour before warming to room temperature and stirring for an additional 8 hours. After which the solution was washed with 0.5 M HCl solution (2 x 30 mL) followed by saturated NaCl solution (2 x 30 mL). The organic layers were collected and dried over anhydrous Na₂SO₄ and reduced in vacuo before the addition of warm hexanes to precipitate the product as a white solid 71 % yield (3.545 g, 14.28 mmol)

Spectroscopy:

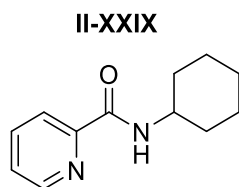
¹H NMR (500 MHz, CDCl₃) δ 8.29 (dd, J = 8.9, 2.2 Hz, 2H), 7.92 (dd, J = 8.9, 2.2 Hz, 2H), 6.01 (d, J = 7.9 Hz, 1H), 4.09 – 3.90 (m, 1H), 2.06 (dd, J = 11.8, 4.8 Hz, 2H), 1.79 (dt, J = 14.4, 3.8 Hz, 2H), 1.74 – 1.62 (m, 1H), 1.45 (tdd, J = 14.0, 8.9, 2.8 Hz, 2H), 1.34 – 1.13 (m, 3H).

¹³C NMR (125 MHz, CDCl₃) δ 164.55, 140.65, 128.03, 123.79, 49.23, 33.13, 25.46, 24.86.

IR (FT-ATR) cm⁻¹: 3316, 3102, 3073, 2937, 2858, 1631, 1600, 1543, 1510, 1454, 1347, 1328, 1107, 1080

HRMS-ESI (m/z), calculated for C₁₃H₁₇N₂O₃ (M+H)⁺ 249.1239. Found 249.1246.

M.P.: 206.2°C – 207.0°C



N-cyclohexylpicolinamide:

Picolinic acid (2.46 g, 20 mmol) was added to a 250 mL round bottom flask. To this 100 mL of anhydrous DCM was added by syringe and to the resulting suspension 1 mL of DMF was added. The suspension was stirred vigorously, while SOCl_2 (13.12 g, 110.27 mmol) was added by syringe over 10 minutes. The solution was then refluxed for 3 hours before reducing in vacuo, to remove excess thionyl chloride and yield the crude carbonyl chloride intermediate. This brown solid was then dissolved in 100 mL of anhydrous DCM and cooled to 0°C by ice bath before the addition of triethylamine (6.07 g, 60 mmol) followed by Cyclohexylamine (3.96 g, 40 mmol). The reaction stirred at 0°C for 2 hours before stirring at room temperature at 10 hours. After which the solution was washed with saturated NH_4Cl solution (2 x 30 mL) followed by NaCl solution (2 x 30 mL). The organic layers were collected and dried over anhydrous Na_2SO_4 and reduced in vacuo to give the crude product as an orange solid and purified on neutral alumina, by column chromatography (1:9 EtOAc:Hexanes) to yield the product as a red-orange solid, 69 % yield, (2.83 g, 13.83 mmol)

Spectroscopy:

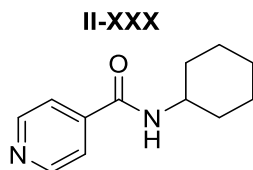
^1H NMR (500 MHz, CDCl_3) δ 8.68 – 8.63 (m, 2H), 7.59 – 7.54 (m, 2H), 6.43 (d, $J = 8.1$ Hz, 1H), 3.92 (dddd, $J = 14.9, 10.8, 8.0, 4.0$ Hz, 1H), 1.98 (dt, $J = 12.2, 3.9$ Hz, 2H), 1.78 – 1.68 (m, 2H), 1.67 – 1.58 (m, 1H), 1.43 – 1.30 (m, 2H), 1.30 – 1.08 (m, 3H).

^{13}C NMR (125 MHz, CDCl_3) δ 163.20, 150.21, 147.90, 137.31, 125.95, 122.20, 48.13, 33.07, 25.59, 24.87.

IR (FT-ATR) cm^{-1} : 3302, 3049, 2933, 2855, 1634, 1538, 1406, 1322, 1083

HRMS-ESI (m/z), calculated for $\text{C}_{12}\text{H}_{17}\text{N}_2\text{O}$ (M+H) $^+$ 205.1341. Found 205.1267.

M.P.: 55.8°C – 56.0°C



N-cyclohexylpicolinamide:

Isonicotinic acid (2.46 g, 20 mmol) was added to a 250 mL round bottom flask. To this 100 mL of anhydrous DCM was added by syringe and to the resulting suspension 1 mL of DMF was added. The suspension was stirred vigorously, while SOCl₂ (13.12 g, 110.27 mmol) was added by syringe over 10 minutes. The solution was then refluxed for 3 hours before reducing in vacuo, to remove excess thionyl chloride and yield the crude carbonyl chloride intermediate. This brown solid was then dissolved in 100 mL of anhydrous DCM and cooled to 0°C by ice bath before the addition of triethylamine (6.07 g, 60 mmol) followed by Cyclohexylamine (3.96 g, 40 mmol). The reaction stirred at 0°C for 2 hours before stirring at room temperature at 10 hours. After which the solution was washed with saturated NH₄Cl solution (2 x 30 mL) followed by NaCl solution (2 x 30 mL). The organic layers were collected and dried over anhydrous Na₂SO₄ and reduced in vacuo to give the crude product as an orange solid and purified by column chromatography (1:1 EtOAc:Hexanes) to yield product as a light yellow solid 70 % yield, (2.83 g, 13.90 mmol)

Spectroscopy:

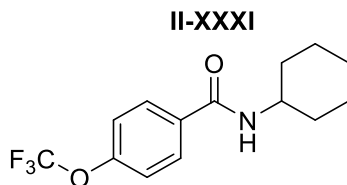
¹H NMR (500 MHz, CDCl₃) δ 8.70 – 8.59 (m, 2H), 7.63 – 7.50 (m, 2H), 6.43 (d, J = 8.1 Hz, 1H), 3.92 (dddd, J = 14.9, 10.8, 8.0, 4.0 Hz, 1H), 1.98 (dt, J = 12.2, 3.9 Hz, 2H), 1.80 – 1.67 (m, 2H), 1.62 (dddd, J = 15.6, 6.2, 3.7, 1.9 Hz, 1H), 1.45 – 1.28 (m, 2H), 1.27 – 1.03 (m, 3H).

¹³C NMR (125 MHz, CDCl₃) δ 164.69, 150.38, 142.12, 120.93, 49.07, 32.99, 25.41, 24.88.

IR (FT-ATR) cm^{-1} : 3340, 3060, 2928, 2850, 1639, 1590, 1567, 1519, 1466, 1429, 1160, 1145, 1084

HRMS-ESI (m/z), calculated for $\text{C}_{12}\text{H}_{17}\text{N}_2\text{O}$ (M+H)⁺ 205.1341. Found 205.1320.

m.p.: 144.2°C – 145.0°C



N-cyclohexyl-4-(trifluoromethoxy)benzamide:

Cyclohexylamine (1.041 g, 10.5 mmol) was added by syringe to a 250 mL round bottom flask. 100 mL of anhydrous DCM was then added and the mixture was stirred while triethylamine (1.518 g, 15 mmol) was added by syringe. The resulting solution was cooled to 0°C by ice bath before 4-(trifluoromethoxy)benzoyl chloride (1.57 g, 10 mmol) was added dropwise to the solution, over 10 minutes. The reaction was stirred at 0°C for one hour before warming to room temperature and stirring for an additional 8 hours. After which the solution was washed with 0.5 M HCl solution (2 x 30 mL) followed by saturated NaCl solution (2 x 30 mL). The organic layers were collected and dried over anhydrous Na_2SO_4 and reduced in vacuo before the addition of warm hexanes to precipitate the product as a white solid 79 % yield (2.26 g, 7.87 mmol)

Spectroscopy:

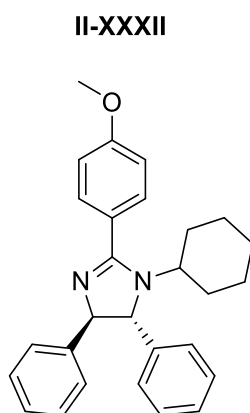
^1H NMR (500 MHz, CDCl_3) δ 7.84 – 7.73 (m, 2H), 7.25 (dq, $J = 7.8, 1.1$ Hz, 2H), 5.98 (d, $J = 8.1$ Hz, 1H), 3.96 (dddd, $J = 14.9, 10.8, 8.0, 3.9$ Hz, 1H), 2.02 (dt, $J = 12.3, 4.0$ Hz, 2H), 1.75 (dp, $J = 11.9, 3.7, 3.1$ Hz, 2H), 1.71 – 1.59 (m, 1H), 1.49 – 1.34 (m, 2H), 1.30 – 1.11 (m, 3H).

^{13}C NMR (125 MHz, CDCl_3) δ 165.31, 151.24, 133.56, 128.69, 121.32, 120.61, 119.27, 48.87, 33.19, 25.50, 24.88.

IR (FT-ATR) cm^{-1} : 3313, 2937 2857, 1629, 1605, 1537, 1500, 1242, 1204, 1149, 1018

HRMS-ESI (m/z), calculated for $\text{C}_{14}\text{H}_{17}\text{F}_3\text{NO}_2$ (M+H) $^+$ 288.1211. Found 288.1251.

m.p: 159.1°C – 160.0°C



Trans-1-cyclohexyl-2-(4-methoxyphenyl)-4,5-diphenyl-4,5-dihydro-1H-imidazole:

N-cyclohexyl-4-methoxybenzamide (0.144 g, 0.615 mmol) was added to a 50 mL flamed dried round bottom flask. 4 mL of anhydrous DCM was added to the flask by syringe. The resulting solution was cooled to 0°C by ice-bath before the addition of 2,6 Lutidine (0.330 g, 3.073 mmol) by syringe. Oxalyl Chloride (0.078 g, 0.615 mmol) was then added over 10 minutes by syringe. The resulting mixture was stirred at 0°C for 1.5 hours after which the solvent was removed to give the intermediate imidoyl chloride as a brownish-tan solid. This solid was then dissolved in 4 mL of anhydrous DMF and to this solution trans-diphenylaziridine (0.100 g, 0.512 mmol) was added by syringe. The reaction was then stirred for 12-14 hours at 55°C. The reaction was extracted in EtOAc (2 x 25 mL) and washed with 10 % LiBr solution. After which the organic layers were washed with 0.5 M HCl solution and Saturated NaHCO_3 solution. The organic layers were

collected and dried over anhydrous NaSO₄, concentrated and purified by column chromatography (4:6 EtOAc:Hexanes). The product was obtained as a clear oil 66 % yield (0.139 g, 0.338 mmol)

Spectroscopy:

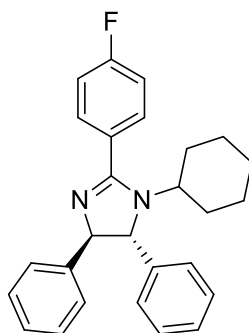
¹H NMR (500 MHz, CDCl₃) δ 7.79 – 7.74 (m, 2H), 7.41 – 7.35 (m, 6H), 7.32 – 7.26 (m, 4H), 7.03 – 6.98 (m, 2H), 4.85 (d, J = 6.2 Hz, 1H), 4.51 (d, J = 6.3 Hz, 1H), 3.89 (s, 3H), 1.63 – 1.53 (m, 3H), 1.47 – 1.40 (m, 2H), 1.27 – 1.25 (m, 1H), 1.06 – 0.99 (m, 2H), 0.89 – 0.82 (m, 2H).

¹³C NMR (125 MHz, CDCl₃) δ 167.05, 161.08, 146.22, 130.16, 128.75, 128.59, 127.16, 127.07, 126.46, 126.12, 116.73, 113.84, 69.68, 56.66, 55.36, 33.58, 30.05, 26.10, 25.40, 25.21.

IR (FT-ATR) cm⁻¹: 3076, 3025, 2932, 2856, 1613, 1512, 1451, 1251, 1220, 1171, 1030

HRMS-ESI (m/z), calculated for C₂₈H₃₁N₂O (M+H)⁺ 411.2437 Found: 411.2500

II-XXXIII



Trans-1-cyclohexyl-2-(4-fluorophenyl)-4,5-diphenyl-4,5-dihydro-1H-imidazole:

N-cyclohexyl-4-fluorobenzamide (0.1361 g, 0.615 mmol) was added to a 50 mL flamed dried round bottom flask. 4 mL of anhydrous DCM was added to the flask by syringe. The resulting solution was cooled to 0°C by ice-bath before the addition of 2,6 Lutidine (0.330 g, 3.073 mmol) by syringe. Oxalyl Chloride (0.078 g, 0.615 mmol) was then added over 10 minutes by syringe. The resulting mixture was stirred at 0°C for 1.5 hours after which the solvent was removed to give

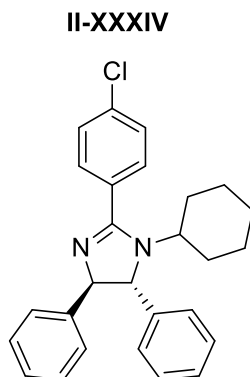
the intermediate imidoyl chloride as a brownish-tan solid. This solid was then dissolved in 4 mL of anhydrous DMF and to this solution trans-2,3-diphenylaziridine (0.100 g, 0.512 mmol) was added by syringe. The reaction was then stirred for 12-14 hours at 55°C. The reaction was extracted in EtOAc (2 x 25 mL) and washed with 10 % LiBr solution. After which the organic layers were washed with 0.5 M HCl solution and Saturated NaHCO₃ solution. The organic layers were collected and dried over anhydrous NaSO₄, concentrated and purified by column chromatography (3:7 EtOAc:Hexanes). The product was obtained as a clear oil 35 % yield (0.071 g, 0.178 mmol)

Spectroscopy:

¹H NMR (500 MHz, CDCl₃) δ 7.86 – 7.78 (m, 2H), 7.44 – 7.32 (m, 6H), 7.35 – 7.22 (m, 4H), 7.23 – 7.14 (m, 2H), 4.87 (d, *J* = 7.0 Hz, 1H), 4.52 (d, *J* = 7.0 Hz, 1H), 3.49 (tt, *J* = 11.7, 3.7 Hz, 1H), 1.66 – 1.51 (m, 2H), 1.49 – 1.30 (m, 2H), 1.23 (d, *J* = 27.7 Hz, 2H), 1.09 – 0.93 (m, 2H), 0.91 – 0.78 (m, 2H).

¹³C NMR (125 MHz, CDCl₃) δ 166.40, 164.83, 162.85, 146.00, 144.52, 130.67, 130.60, 128.81, 128.66, 127.27, 127.18, 126.44, 126.12, 115.74, 115.57, 78.49, 69.82, 56.75, 33.53, 30.06, 26.07, 25.38, 25.17.

HRMS-ESI (*m/z*), calculated for C₂₇H₂₈FN₂ (M+H)⁺ 399.2237 Found: 399.2281



Trans-2-(4-chlorophenyl)-1-cyclohexyl-4,5-diphenyl-4,5-dihydro-1H-imidazole:

4-chloro-N-cyclohexylbenzamide (0.146 g, 0.615 mmol) was added to a 50 mL flamed dried round bottom flask. 4 mL of anhydrous DCM was added to the flask by syringe. The resulting solution was cooled to 0°C by ice-bath before the addition of 2,6 Lutidine (0.330 g, 3.073 mmol) by syringe. Oxalyl Chloride (0.078 g, 0.615 mmol) was then added over 10 minutes by syringe. The resulting mixture was stirred at 0°C for 1.5 hours after which the solvent was removed to give the intermediate imidoyl chloride as a brownish-tan solid. This solid was then dissolved in 4 mL of anhydrous DMF and to this solution trans-2,3-diphenylaziridine (0.100 g, 0.512 mmol) was added by syringe. The reaction was then stirred for 12-14 hours at 55°C. The reaction was extracted in EtOAc (2 x 25 mL) and washed with 10 % LiBr solution. After which the organic layers were washed with 0.5 M HCl solution and Saturated NaHCO₃ solution. The organic layers were collected and dried over anhydrous NaSO₄, concentrated and purified by column chromatography (2:8 EtOAc:Hexanes). The product was obtained as a clear oil 46 % yield (0.098 g, 0.236 mmol)

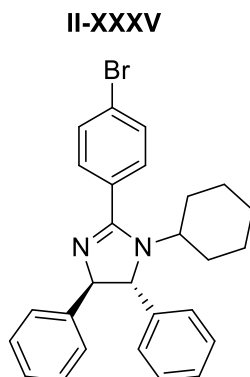
Spectroscopy:

¹H NMR (500 MHz, CDCl₃) δ 7.79 – 7.74 (m, 2H), 7.50 – 7.45 (m, 2H), 7.41 – 7.33 (m, 5H), 7.33 – 7.28 (m, 2H), 7.28 – 7.23 (m, 3H), 4.87 (d, J = 6.6 Hz, 1H), 4.52 (d, J = 6.6 Hz, 1H), 3.47 (tt, J = 11.6, 3.9 Hz, 1H), 1.69 – 1.50 (m, 3H), 1.50 – 1.28 (m, 3H), 1.01 (dq, J = 15.8, 6.2, 3.4 Hz, 2H), 0.91 – 0.74 (m, 2H).

¹³C NMR (125 MHz, CDCl₃) δ 166.35, 145.91, 144.40, 136.12, 129.99, 128.83, 128.82, 128.66, 127.29, 127.21, 126.43, 126.12, 78.58, 69.84, 56.77, 33.51, 30.06, 26.05, 25.35, 25.15.

IR (FT-ATR) cm⁻¹: 3062, 30258, 2932, 2854, 1610, 1598, 1563, 1491, 1451, 1403, 1162, 1112, 1015, 750

HRMS-ESI (m/z), calculated for C₂₇H₂₈ClN₂(M+H)⁺ 415.1941 Found: 415.2004



Trans-2-(4-bromophenyl)-1-cyclohexyl-4,5-diphenyl-4,5-dihydro-1H-imidazole:

4-bromo-N-cyclohexylbenzamide (0.174 g, 0.615 mmol) was added to a 50 mL flamed dried round bottom flask. 4 mL of anhydrous DCM was added to the flask by syringe. The resulting solution was cooled to 0°C by ice-bath before the addition of 2,6 Lutidine (0.330 g, 3.073 mmol) by syringe. Oxalyl Chloride (0.078 g, 0.615 mmol) was then added over 10 minutes by syringe. The resulting mixture was stirred at 0°C for 1.5 hours after which the solvent was removed to give the intermediate imidoyl chloride as a brownish-tan solid. This solid was then dissolved in 4 mL of anhydrous DMF and to this solution trans-2,3-diphenylaziridine (0.100 g, 0.512 mmol) was added by syringe. The reaction was then stirred for 12-14 hours at 55°C. The reaction was extracted in EtOAc (2 x 25 mL) and washed with 10 % LiBr solution. After which the organic layers were washed with 0.5 M HCl solution and Saturated NaHCO₃ solution. The organic layers were collected and dried over anhydrous NaSO₄, concentrated and purified by column chromatography (2:8 EtOAc:Hexanes). The product was obtained as a clear oil 51 % yield (0.120 g, 0.261 mmol)

Spectroscopy:

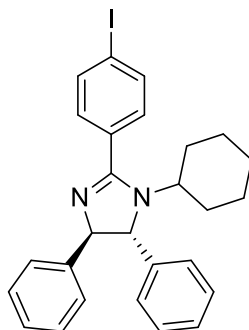
^1H NMR (500 MHz, CDCl_3) δ 7.72 – 7.67 (m, 2H), 7.66 – 7.61 (m, 2H), 7.41 – 7.33 (m, 5H), 7.31 (ddt, $J = 7.8, 5.7, 1.5$ Hz, 2H), 7.24 (d, $J = 1.1$ Hz, 3H), 4.87 (d, $J = 6.6$ Hz, 1H), 4.52 (d, $J = 6.6$ Hz, 1H), 3.47 (tt, $J = 11.6, 3.9$ Hz, 1H), 1.67 – 1.50 (m, 3H), 1.48 – 1.31 (m, 3H), 1.01 (dddd, $J = 16.6, 12.7, 8.1, 3.9$ Hz, 2H), 0.90 – 0.77 (m, 2H).

^{13}C NMR (125 MHz, CDCl_3) δ 166.40, 145.88, 144.36, 131.79, 130.69, 130.22, 128.82, 128.67, 127.30, 127.22, 126.43, 126.12, 124.46, 78.58, 76.76, 69.85, 56.77, 33.51, 30.06, 26.04, 25.35, 25.15.

IR (FT-ATR) cm^{-1} : 3032, 2931, 2853, 1610, 1584, 1488, 1451, 1219, 1112, 1012, 835

HRMS-ESI (m/z), calculated for $\text{C}_{27}\text{H}_{28}\text{BrN}_2$ ($\text{M}+\text{H}$) $^+$ 461.1419 Found: 461.1472

II-XXXVI



Trans-1-cyclohexyl-2-(4-fluorophenyl)-4,5-diphenyl-4,5-dihydro-1H-imidazole:

N-cyclohexyl-4-iodobenzamide (0.203 g, 0.615 mmol) was added to a 50 mL flamed dried round bottom flask. 4 mL of anhydrous DCM was added to the flask by syringe. The resulting solution was cooled to 0°C by ice-bath before the addition of 2,6 Lutidine (0.330 g, 3.073 mmol) by syringe. Oxalyl Chloride (0.078 g, 0.615 mmol) was then added over 10 minutes by syringe. The resulting mixture was stirred at 0°C for 1.5 hours after which the solvent was removed to give the intermediate imidoyl chloride as a brownish-tan solid. This solid was then dissolved in 4 mL of

anhydrous DMF and to this solution trans-2,3-diphenylaziridine (0.100 g, 0.512 mmol) was added by syringe. The reaction was then stirred for 12-14 hours at 55°C. The reaction was extracted in EtOAc (2 x 25 mL) and washed with 10 % LiBr solution. After which the organic layers were washed with 0.5 M HCl solution and saturated NaHCO₃ solution. The organic layers were collected and dried over anhydrous NaSO₄, concentrated and purified by column chromatography (1.5:8.5 EtOAc:Hexanes). The product was obtained as a clear oil 56 % yield (0.145 g, 0.287 mmol)

Spectroscopy:

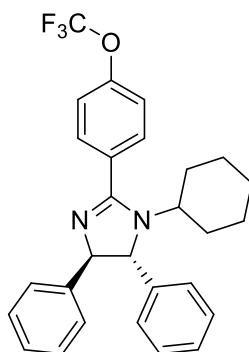
¹H NMR (500 MHz, CDCl₃) δ 7.87 – 7.79 (m, 2H), 7.59 – 7.49 (m, 2H), 7.42 – 7.33 (m, 5H), 7.32 – 7.27 (m, 2H), 7.27 – 7.22 (m, 3H), 4.85 (d, J = 6.7 Hz, 1H), 4.51 (d, J = 6.6 Hz, 1H), 3.52 – 3.39 (m, 1H), 1.69 – 1.50 (m, 3H), 1.46 – 1.34 (m, 3H), 1.01 (qt, J = 12.1, 2.9 Hz, 2H), 0.90 – 0.76 (m, 2H).

¹³C NMR (125 MHz, CDCl₃) δ 166.52, 146.01, 144.46, 137.69, 131.45, 130.28, 128.79, 128.65, 127.25, 127.18, 126.45, 126.12, 96.36, 78.80, 69.83, 56.73, 33.52, 30.03, 26.05, 25.35, 25.16.

IR (FT-ATR) cm⁻¹: 3060, 3028, 2931, 2854, 1608, 1581, 1553, 1484, 1450, 1007, 757, 699

HRMS-ESI (m/z), calculated for C₂₇H₂₈IN₂ (M+H)⁺ 507.1297 Found: 507.1360

II-XXXVII



Trans-1-cyclohexyl-4,5-diphenyl-2-(4-(trifluoromethoxy)phenyl)-4,5-dihydro-1H-imidazole:

N-cyclohexyl-2,2,2-trifluoroacetamide (0.177 g, 0.615 mmol) was added to a 50 mL flamed dried round bottom flask. 4 mL of anhydrous DCM was added to the flask by syringe. The resulting solution was cooled to 0°C by ice-bath before the addition of 2,6 Lutidine (0.330 g, 3.073 mmol) by syringe. Oxalyl Chloride (0.078 g, 0.615 mmol) was then added over 10 minutes by syringe. The resulting mixture was stirred at 0°C for 1.5 hours after which the solvent was removed to give the intermediate imidoyl chloride as a brownish-tan solid. This solid was then dissolved in 4 mL of anhydrous DMF and to this solution trans-2,3-diphenylaziridine (0.100 g, 0.512 mmol) was added by syringe. The reaction was then stirred for 12-14 hours at 55°C. The reaction was extracted in EtOAc (2 x 25 mL) and washed with 10 % LiBr solution. After which the organic layers were washed with 0.5 M HCl solution and Saturated NaHCO₃ solution. The organic layers were collected and dried over anhydrous NaSO₄, concentrated and purified by column chromatography (3:7 EtOAc:Hexanes). The product was obtained as a clear oil 52 % yield (0.124 g, 0.266 mmol).

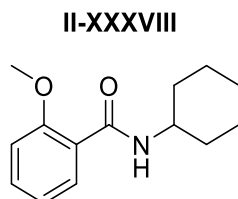
Spectroscopy:

^1H NMR (500 MHz, CDCl_3) δ 7.90 – 7.85 (m, 2H), 7.46 – 7.28 (m, 10H), 7.28 – 7.21 (m, 2H), 4.89 (d, $J = 6.5$ Hz, 1H), 4.55 (d, $J = 6.5$ Hz, 1H), 3.50 (tt, $J = 11.7, 3.8$ Hz, 1H), 1.69 – 1.51 (m, 3H), 1.51 – 1.33 (m, 3H), 1.03 (qdd, $J = 13.9, 8.2, 3.9$ Hz, 2H), 0.86 (dddd, $J = 13.8, 11.8, 10.2, 4.1$ Hz, 2H).

^{13}C NMR (125 MHz, CDCl_3) δ 166.05, 150.59, 144.17, 131.04, 130.36, 128.87, 128.71, 127.40, 127.29, 126.38, 126.11, 121.43, 120.86, 119.37, 69.88, 56.82, 33.52, 30.15, 26.01, 25.34, 25.12.

IR (FT-ATR) cm^{-1} :3063, 3029, 2933, 2856, 1615, 1602, 1578, 1507, 1495, 1452, 1256, 1221, 1164, 1110

HRMS-ESI (m/z), calculated for $\text{C}_{28}\text{H}_{28}\text{F}_3\text{N}_2\text{O}$ ($\text{M}+\text{H}$) $^+$ 465.2154 Found: 465.2212



N-cyclohexyl-2-methoxybenzamide:

Cyclohexylamine (4.36 g, 44 mmol) was added by syringe to a 250 mL round bottom flask. 100 mL of anhydrous DCM was then added and the mixture was stirred while triethylamine (6.07 g, 60 mmol) was added by syringe. The resulting solution was cooled to 0°C by ice bath before 2-methoxybenzoyl chloride (6.82 g, 40 mmol) was added dropwise to the solution, over 10 minutes. The reaction was stirred at 0°C for one hour before warming to room temperature and stirring for an additional 8 hours. After which the solution was washed with 0.5 M HCl solution (2 x 30 mL) followed by saturated NaCl solution (2 x 30 mL). The organic layers were collected and dried over

anhydrous Na₂SO₄ and reduced in vacuo before the addition of warm hexanes to precipitate the product as a white solid 97 % yield (9.02 g, 38.67 mmol)

Spectroscopy:

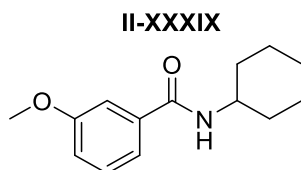
¹H NMR (500 MHz, CDCl₃) δ 8.20 (dd, J = 7.8, 1.9 Hz, 1H), 7.80 (s, 1H), 7.42 (ddd, J = 8.3, 7.3, 1.9 Hz, 1H), 7.12 – 7.03 (m, 1H), 6.96 (dd, J = 8.3, 1.0 Hz, 1H), 4.03 (dddd, J = 13.8, 9.9, 7.9, 3.9 Hz, 1H), 3.96 (s, 3H), 2.05 – 1.93 (m, 2H), 1.78 – 1.55 (m, 4H), 1.43 (ddq, J = 17.8, 10.5, 3.5 Hz, 2H), 1.34 – 1.20 (m, 2H).

¹³C NMR (125 MHz, CDCl₃) δ 164.12, 157.35, 132.41, 132.25, 122.02, 121.31, 111.30, 55.94, 48.00, 33.00, 25.74, 24.66.

IR (FT-ATR) cm⁻¹: 3336, 3070, 2933, 2855, 1628, 1599, 1528, 1486, 1242, 1182, 1027

HRMS-ESI (m/z), calculated for C₁₄H₂₀NO₂ (M+H)⁺ 234.1494. Found 234.1544.

M.P.: 68.7°C – 69.5°C



N-cyclohexyl-3-methoxybenzamide:

Cyclohexylamine (4.36 g, 44 mmol) was added by syringe to a 250 mL round bottom flask. 100 mL of anhydrous DCM was then added and the mixture was stirred while triethylamine (6.07 g, 60 mmol) was added by syringe. The resulting solution was cooled to 0°C by ice bath before 3-methoxybenzoyl chloride (6.82 g, 40 mmol) was added dropwise to the solution, over 10 minutes. The reaction was stirred at 0°C for one hour before warming to room temperature and stirring for

an additional 8 hours. After which the solution was washed with 0.5 M HCl solution (2 x 30 mL) followed by saturated NaCl solution (2 x 30 mL). The organic layers were collected and dried over anhydrous Na₂SO₄ and reduced in vacuo before the addition of warm hexanes to precipitate the product as a white solid 95 % yield (8.87 g, 38.02 mmol)

Spectroscopy:

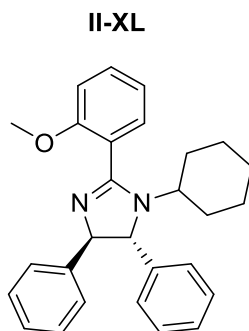
¹H NMR (500 MHz, CDCl₃) δ 7.36 – 7.28 (m, 2H), 7.25 (dt, *J* = 7.6, 1.3 Hz, 1H), 7.02 (ddd, *J* = 8.2, 2.6, 1.0 Hz, 1H), 5.94 (d, *J* = 7.3 Hz, 1H), 4.03 – 3.91 (m, 1H), 3.85 (s, 3H), 2.02 (dt, *J* = 12.3, 4.0 Hz, 2H), 1.80 – 1.70 (m, 2H), 1.66 (ddd, *J* = 13.1, 5.9, 2.1 Hz, 1H), 1.49 – 1.36 (m, 2H), 1.29 – 1.14 (m, 3H).

¹³C NMR (125 MHz, CDCl₃) δ 166.41, 159.77, 136.62, 129.47, 118.47, 117.35, 112.31, 55.44, 48.67, 33.21, 25.56, 24.88.

IR (FT-ATR) cm⁻¹: 3272, 3073, 2934, 2852, 1628, 1586, 1544, 1455, 1248, 1143, 1089, 1032

HRMS-ESI (*m/z*), calculated for C₁₄H₂₀NO₂ (*M*+*H*)⁺ 234.1494. Found 234.1549.

M.P.: 110.7° - 111.2°C



Trans-1-cyclohexyl-2-(2-methoxyphenyl)-4,5-diphenyl-4,5-dihydro-1H-imidazole:

N-cyclohexyl-2-methoxybenzamide (0.144 g, mmol) was added to a 50 mL flamed dried round bottom flask. 4 mL of anhydrous DCM was added to the flask by syringe. The resulting solution was cooled to 0°C by ice-bath before the addition of 2,6 Lutidine (0.330 g, 3.073 mmol) by syringe. Oxalyl Chloride (0.078 g, 0.615 mmol) was then added over 10 minutes by syringe. The resulting mixture was stirred at 0°C for 1.5 hours after which the solvent was removed to give the intermediate imidoyl chloride as a brownish-tan solid. This solid was then dissolved in 4 mL of anhydrous DMF and to this solution trans-2,3 -diphenylaziridine (0.100 g, 0.512 mmol) was added by syringe. The reaction was then stirred for 12-14 hours at 55°C. The reaction was extracted in EtOAc (2 x 25 mL) and washed with 10 % LiBr solution. After which the organic layers were washed with 0.5 M HCl solution and Saturated NaHCO₃ solution. The organic layers were collected and dried over anhydrous NaSO₄, concentrated and purified by column chromatography (5:5 EtOAc:Hexanes). The product was obtained as a clear oil 58 % yield (0.122 g, 0.297 mmol)

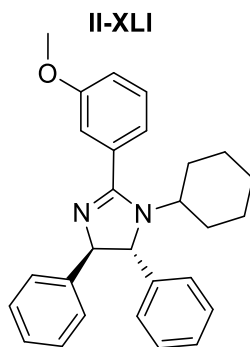
Spectroscopy:

¹H NMR (500 MHz, CDCl₃) δ 7.68 (s, 1H), 7.51 – 7.26 (m, 11H), 7.08 (td, *J* = 7.5, 1.0 Hz, 1H), 7.02 (d, *J* = 8.3 Hz, 1H), 4.86 (s, 1H), 4.55 (d, *J* = 6.1 Hz, 1H), 3.97 (s, 2H), 3.16 (tt, *J* = 12.1, 3.5 Hz, 1H), 1.63 (d, *J* = 13.5 Hz, 1H), 1.39 (qd, *J* = 12.4, 3.7 Hz, 2H), 1.02 (qt, *J* = 13.2, 3.6 Hz, 1H), 0.96 – 0.77 (m, 2H), 0.72 (qd, *J* = 12.9, 3.8 Hz, 1H).

¹³C NMR (125 MHz, CDCl₃) δ 145.17, 128.64, 128.57, 127.11, 126.97, 126.49, 126.30, 120.72, 69.65, 56.10, 55.58, 30.87, 26.12, 25.56, 25.24.

IR (FT-ATR) cm⁻¹: 3063, 3027, 2931, 2853, 1614, 1593, 1494, 1464, 1246, 1026,

HRMS-ESI (*m/z*), calculated for C₂₈H₃₁N₂O (M+H)⁺ 411.2437. Found: 411.2410



Trans-1-cyclohexyl-2-(3-methoxyphenyl)-4,5-diphenyl-4,5-dihydro-1H-imidazole:

N-cyclohexyl-3-methoxybenzamide (0.144 g, 0.615 mmol) was added to a 50 mL flamed dried round bottom flask. 4 mL of anhydrous DCM was added to the flask by syringe. The resulting solution was cooled to 0°C by ice-bath before the addition of 2,6 Lutidine (0.330 g, 3.073 mmol) by syringe. Oxalyl Chloride (0.078 g, 0.615 mmol) was then added over 10 minutes by syringe. The resulting mixture was stirred at 0°C for 1.5 hours after which the solvent was removed to give the intermediate imidoyl chloride as a brownish-tan solid. This solid was then dissolved in 4 mL of anhydrous DMF and to this solution trans-2,3-diphenylaziridine (0.100 g, mmol) was added by syringe. The reaction was then stirred for 12-14 hours at 55°C. The reaction was extracted in EtOAc (2 x 25 mL) and washed with 10 % LiBr solution. After which the organic layers were washed with 0.5 M HCl solution and Saturated NaHCO₃ solution. The organic layers were collected and dried over anhydrous NaSO₄, concentrated and purified by column chromatography (4:6 EtOAc:Hexanes). The product was obtained as a light-yellow oil 58% yield (0.120 g, 0.292 mmol)

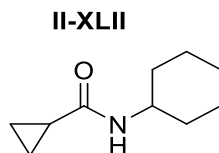
Spectroscopy:

^1H NMR (500 MHz, CDCl_3) δ 7.38 (qt, $J = 7.6, 1.9$ Hz, 9H), 7.33 – 7.24 (m, 4H), 7.09 – 6.99 (m, 1H), 4.87 (d, $J = 7.0$ Hz, 1H), 4.52 (d, $J = 7.0$ Hz, 1H), 3.90 (s, 3H), 3.57 (tt, $J = 11.9, 3.7$ Hz, 1H), 1.66 – 1.49 (m, 3H), 1.49 – 1.32 (m, 3H), 1.02 (dddq, $J = 16.5, 10.0, 6.9, 3.5$ Hz, 2H), 0.91 – 0.77 (m, 2H).

^{13}C NMR (125 MHz, CDCl_3) δ 167.19, 159.59, 146.20, 144.68, 133.19, 129.54, 128.76, 128.60, 127.18, 127.10, 126.50, 126.16, 120.96, 115.90, 114.01, 78.64, 69.79, 56.56, 55.49, 33.58, 30.19, 26.07, 25.40, 25.21.

IR (FT-ATR) cm^{-1} : 3063, 3030, 2934, 2853, 1601, 1576, 1491, 1452, 1286, 1219, 108, 1037

HRMS-ESI (m/z), calculated for $\text{C}_{28}\text{H}_{31}\text{N}_2\text{O}$ ($\text{M}+\text{H}$) $^+$ 411.2437. Found 411.2428

**N-cyclohexylcyclopropanecarboxamide:**

Cyclohexylamine (4.36 g, 44 mmol) was added by syringe to a 250 mL round bottom flask. 100 mL of anhydrous DCM was then added and the mixture was stirred while triethylamine (6.07 g, 60 mmol) was added by syringe. The resulting solution was cooled to 0°C by ice bath before cyclopropanecarbonyl chloride (4.18 g, 40 mmol) was added dropwise to the solution, over 10 minutes. The reaction was stirred at 0°C for one hour before warming to room temperature and stirring for an additional 8 hours. After which the solution was washed with 0.5 M HCl solution (2 x 30 ml) followed by saturated NaCl solution (2 x 30 ml). The organic layers were collected and dried over Na_2SO_4 and reduced in vacuo before the addition of warm hexanes to precipitate the product as a white solid 97 % yield (6.50 g, 38.86 mmol).

Spectroscopy:

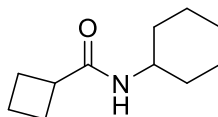
^1H NMR (500 MHz, CDCl_3) δ 5.47 (s, 1H), 3.85 – 3.73 (m, 1H), 1.93 (dt, $J = 12.4, 3.9$ Hz, 2H), 1.77 – 1.67 (m, 2H), 1.67 – 1.58 (m, 1H), 1.46 – 1.24 (m, 3H), 1.25 – 1.08 (m, 3H), 0.99 – 0.92 (m, 2H), 0.76 – 0.66 (m, 2H).

^{13}C NMR (125 MHz, CDCl_3) δ 172.37, 48.28, 33.38, 25.56, 24.92, 14.94, 7.00.

IR (FT-ATR) cm^{-1} : 3306, 2930, 2853, 1632, 1538, 1447, 1403, 1248, 1232, 979

HRMS-ESI (m/z), calculated for $\text{C}_{10}\text{H}_{18}\text{NO}$ ($\text{M}+\text{H}$) $^+$ 168.1388. Found 168.1362.

M.P.: 140.0°C – 140.7°C

II-XLIII**N-cyclohexylcyclobutanecarboxamide:**

Cyclohexylamine (4.36 g, 44 mmol) was added by syringe to a 250 mL round bottom flask. 100 mL of anhydrous DCM was then added and the mixture was stirred while triethylamine (6.07 g, 60 mmol) was added by syringe. The resulting solution was cooled to 0°C by ice bath before cyclobutanecarbonyl chloride (4.74 g, 40 mmol) was added dropwise to the solution, over 10 minutes. The reaction was stirred at 0°C for one hour before warming to room temperature and stirring for an additional 8 hours. After which the solution was washed with 0.5 M HCl solution (2 x 30 mL) followed by saturated NaCl solution (2 x 30 mL). The organic layers were collected and dried over anhydrous Na_2SO_4 and reduced in vacuo before the addition of warm hexanes to precipitate the product as a white solid 98 % yield (7.12 g, 39.27 mmol)

Spectroscopy:

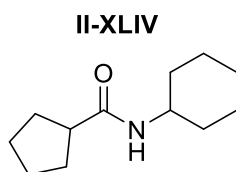
^1H NMR (500 MHz, CDCl_3) δ 5.24 – 5.19 (m, 1H), 3.74 (dddd, $J = 14.8, 10.8, 8.1, 4.0$ Hz, 1H), 2.93 (pd, $J = 8.6, 1.0$ Hz, 1H), 2.24 (pd, $J = 9.1, 2.4$ Hz, 2H), 2.16 – 2.05 (m, 2H), 2.01 – 1.78 (m, 4H), 1.73 – 1.63 (m, 2H), 1.60 (dt, $J = 12.8, 3.8$ Hz, 1H), 1.44 – 1.26 (m, 2H), 1.20 – 1.02 (m, 3H).

^{13}C NMR (125 MHz, CDCl_3) δ 173.88, 47.86, 40.10, 33.27, 25.54, 25.35, 24.88, 18.06.

IR (FT-ATR) cm^{-1} : 3288, 3080, 2975, 2930, 2852, 1637, 1547, 1443, 1252, 1219

HRMS-ESI (m/z), calculated for $\text{C}_{11}\text{H}_{20}\text{NO}$ ($\text{M}+\text{H}$) $^+$ 182.1545. Found 182.1603.

M.P.: 111.8°C -112.2°C

**N-cyclohexylcyclopentanecarboxamide:**

Cyclohexylamine (2.18 g, 22 mmol) was added by syringe to a 250 mL round bottom flask. 100 mL of anhydrous DCM was then added and the mixture was stirred while triethylamine (3.04 g, 30 mmol) was added by syringe. The resulting solution was cooled to 0°C by ice bath before cyclopentanecarbonyl chloride (2.65 g, 20 mmol) was added dropwise to the solution, over 10 minutes. The reaction was stirred at 0°C for one hour before warming to room temperature and stirring for an additional 8 hours. After which the solution was washed with 0.5 M HCl solution (2 x 30 mL) followed by saturated NaCl solution (2 x 30 mL). The organic layers were collected and dried over anhydrous Na_2SO_4 and reduced in vacuo before the addition of warm hexanes to precipitate the product as a white solid 91 % yield (3.565 g, 18.25 mmol)

Spectroscopy:

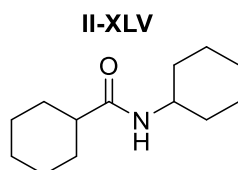
^1H NMR (500 MHz, CDCl_3) δ 5.42 – 5.21 (m, 1H), 3.74 (dddd, $J = 14.7, 10.7, 8.1, 4.0$ Hz, 1H), 2.44 (p, $J = 7.9$ Hz, 1H), 1.89 (dq, $J = 12.3, 4.7, 3.9$ Hz, 2H), 1.86 – 1.62 (m, 8H), 1.63 – 1.48 (m, 3H), 1.42 – 1.29 (m, 2H), 1.12 (dddd, $J = 23.2, 15.6, 9.6, 3.6$ Hz, 3H).

^{13}C NMR (125 MHz, CDCl_3) δ 175.17, 47.93, 46.04, 33.27, 30.46, 25.91, 25.56, 24.89.

IR (FT-ATR) cm^{-1} : 3261, 2916, 2845, 1624, 1544, 1437, 1246, 1153

HRMS-ESI (m/z), calculated for $\text{C}_{12}\text{H}_{22}\text{NO}$ ($\text{M}+\text{H}$) $^+$ 196.1701. Found 196.1736.

M.P.: 160.3°C – 160.8°C

**N-cyclohexylcyclohexanecarboxamide:**

Cyclohexylamine (2.18 g, 22 mmol) was added by syringe to a 250 ml round bottom flask. 100 ml of anhydrous DCM was then added and the mixture was stirred while triethylamine (3.04 g, 30 mmol) was added by syringe. The resulting solution was cooled to 0°C by ice bath before cyclohexanecarbonyl chloride (2.93 g, 20 mmol) was added dropwise to the solution, over 10 minutes. The reaction was stirred at 0°C for one hour before warming to room temperature and stirring for an additional 8 hours. After which the solution was washed with 0.5 M HCl solution (2 x 30 mL) followed by saturated NaCl solution (2 x 30 mL). The organic layers were collected and dried over anhydrous Na_2SO_4 and reduced in vacuo before the addition of warm hexanes to precipitate the product as a white solid 86 % yield (3.60 g, 17.20 mmol)

Spectroscopy:

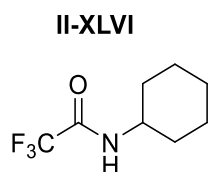
^1H NMR (500 MHz, CDCl_3) δ 5.26 (s, 1H), 3.75 (dddd, $J = 14.6, 10.6, 8.0, 3.9$ Hz, 1H), 2.01 (tt, $J = 11.8, 3.5$ Hz, 1H), 1.94 – 1.73 (m, 6H), 1.73 – 1.54 (m, 4H), 1.49 – 1.29 (m, 4H), 1.29 – 0.95 (m, 6H).

^{13}C NMR (125 MHz, CDCl_3) δ 175.07, 47.67, 45.72, 33.27, 29.74, 25.76, 25.56, 24.85.

IR (FT-ATR) cm^{-1} : 3292, 2916, 2850, 1636, 1543, 1439, 1250, 1212

HRMS-ESI (m/z), calculated for $\text{C}_{13}\text{H}_{23}\text{NO}$ ($\text{M}+\text{H}$) $^+$ 210.1858. Found 210.1876.

M.P.: 172.4°C – 173.0°C

**N-cyclohexyl-2,2,2-trifluoroacetamide:**

Cyclohexylamine (2.18 g, 22 mmol) was added by syringe to a 250 mL round bottom flask. 100 mL of anhydrous DCM was then added and the mixture was stirred while triethylamine (3.04 g, 30 mmol) was added by syringe. The resulting solution was cooled to 0°C by ice bath before 2,2,2-trifluoroacetic anhydride (4.20 g, 20 mmol) was added dropwise to the solution, over 10 minutes. The reaction was stirred at 0°C for one hour before warming to room temperature and stirring for an additional 8 hours. After which the solution was washed with 0.5 M HCl solution (2 x 30 mL) followed by saturated NaCl solution (2 x 30 mL). The organic layers were collected and dried over anhydrous Na_2SO_4 and reduced in vacuo before the addition of warm hexanes to precipitate the product as a white solid 74 % yield (2.88 g, 14.76 mmol)

Spectroscopy:

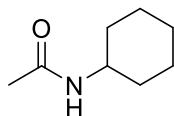
^1H NMR (500 MHz, CDCl_3) δ 6.08 (s, 1H), 3.82 (dddt, $J = 14.9, 11.3, 8.1, 4.0$ Hz, 1H), 1.97 (dt, $J = 12.3, 3.8$ Hz, 2H), 1.80 – 1.71 (m, 2H), 1.70 – 1.60 (m, 1H), 1.39 (dtt, $J = 13.5, 11.9, 3.5$ Hz, 2H), 1.28 – 1.13 (m, 3H).

^{13}C NMR (125 MHz, CDCl_3) δ 49.21, 32.44, 32.41, 25.20, 25.17, 24.58.

IR (FT-ATR) cm^{-1} : 3307, 3096, 2966, 2932, 2864, 1691, 1554, 1451, 1150, 1075, 773

HRMS-ESI (m/z), calculated for $\text{C}_8\text{H}_{13}\text{F}_3\text{NO}$ ($\text{M}+\text{H}$) $^+$ 196.0949. Found 196.0947.

M.P.: 91.5°C – 92.0°C

II-XLVII**N-cyclohexylacetamide:**

Cyclohexylamine (4.36 g, 44 mmol) was added by syringe to a 250 mL round bottom flask. 100 mL of anhydrous DCM was then added and the mixture was stirred while triethylamine (6.07 g, 60 mmol) was added by syringe. The resulting solution was cooled to 0°C by ice bath before acetyl chloride (3.14 g, 40 mmol) was added dropwise to the solution, over 10 minutes. The reaction was stirred at 0°C for one hour before warming to room temperature and stirring for an additional 8 hours. After which the solution was washed with 0.5 M HCl solution (2 x 30 mL) followed by saturated NaCl solution (2 x 30 mL). The organic layers were collected and dried over anhydrous Na_2SO_4 and reduced in vacuo before the addition of warm hexanes to precipitate the product as a white solid 93 % yield (5.24 g, 37.13 mmol).

Spectroscopy:

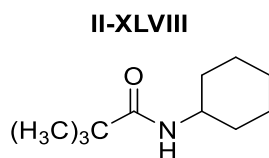
^1H NMR (500 MHz, CDCl_3) δ 5.33 (s, 1H), 3.76 (dddd, $J = 14.7, 10.7, 8.1, 4.0$ Hz, 1H), 1.96 (m, 5H), 1.75 – 1.67 (m, 2H), 1.66 – 1.57 (m, 1H), 1.44 – 1.31 (m, 2H), 1.23 – 1.05 (m, 3H).

^{13}C NMR (125 MHz, CDCl_3) δ 169.02, 48.23, 33.25, 25.53, 24.88, 23.66.

IR (FT-ATR) cm^{-1} : 3286, 2928, 2851, 1636, 1554, 1442, 1253, 1240

HRMS-ESI (m/z), calculated for $\text{C}_8\text{H}_{16}\text{NO}$ ($\text{M}+\text{H}$) $^+$ 142.1232. Found 142.1234.

M.P.: 100.0°C – 100.6°C

**N-cyclohexylpivalamide:**

Cyclohexylamine (4.36 g, 44 mmol) was added by syringe to a 250 mL round bottom flask. 100 mL of anhydrous DCM was then added and the mixture was stirred while triethylamine (6.07 g, 60 mmol) was added by syringe. The resulting solution was cooled to 0°C by ice bath before pivaloyl chloride (4.82 g, 40 mmol) was added dropwise to the solution, over 10 minutes. The reaction was stirred at 0°C for one hour before warming to room temperature and stirring for an additional 8 hours. After which the solution was washed with 0.5 M HCl solution (2 x 30 mL) followed by aqueous saturated sodium chloride solution (2 x 30 mL). The organic layers were collected and dried over anhydrous Na_2SO_4 and reduced in vacuo before the addition of warm hexanes to precipitate the product as a white solid 93 % yield (6.82 g, 37.2 mmol)

Spectroscopy:

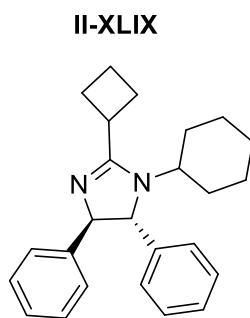
^1H NMR (500 MHz, CDCl_3) δ 5.43 (s, 1H), 3.74 (dddd, $J = 14.6, 10.6, 8.0, 3.9$ Hz, 1H), 1.93 – 1.84 (m, 2H), 1.74 – 1.63 (m, 2H), 1.65 – 1.56 (m, 1H), 1.45 – 1.30 (m, 2H), 1.17 (s, 9H), 1.22 – 1.11 (m, 1H), 1.14 – 1.04 (m, 2H).

^{13}C NMR (125 MHz, CDCl_3) δ 177.40, 47.86, 38.50, 33.15, 27.59, 25.59, 24.86.

IR (FT-ATR) cm^{-1} : 3339, 2931, 2851, 1629, 1531, 1451, 1205, 1095

HRMS-ESI (m/z), calculated for $\text{C}_{11}\text{H}_{22}\text{NO}$ ($\text{M}+\text{H}$) $^+$ 184.1701. Found 184.1739

M.P.: 123.0°C – 123.6°C



Trans-2-cyclobutyl-1-cyclohexyl-4,5-diphenyl-4,5-dihydro-1H-imidazole:

N-cyclohexylcyclobutanecarboxamide (0.111 g, 0.615 mmol) was added to a 50 mL flamed dried round bottom flask. 4 mL of anhydrous DCM was added to the flask by syringe. The resulting solution was cooled to 0°C by ice-bath before the addition of 2,6 Lutidine (0.330 g, 3.073 mmol) by syringe. Oxalyl Chloride (0.078 g, 0.615 mmol) was then added over 10 minutes by syringe. The resulting mixture was stirred at 0°C for 1.5 hours after which the solvent was removed to give the intermediate imidoyl chloride as a brownish-tan solid. This solid was then dissolved in 4 mL of anhydrous DMF and to this solution trans-2,3-diphenylaziridine (0.100 g, 0.512 mmol) was added by syringe. The reaction was then stirred for 12-14 hours at 55°C. The reaction was extracted in EtOAc (2 x 25 mL) and washed with 10 % LiBr solution. After which the organic layers were

washed with 0.5 M HCl solution and Saturated NaHCO₃ solution. The organic layers were collected and dried over anhydrous NaSO₄, concentrated and purified by column chromatography (3:7 EtOAc:Hexanes). The product was obtained as a clear oil 21 % yield (0.039 g, 0.109 mmol)

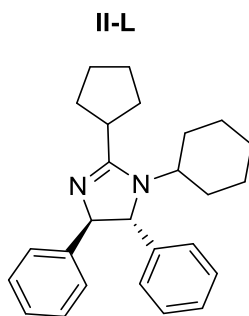
Spectroscopy:

¹H NMR (500 MHz, CDCl₃) δ 7.36 – 7.25 (m, 4H), 7.29 – 7.20 (m, 3H), 7.19 – 7.10 (m, 2H), 4.69 (d, *J* = 6.7 Hz, 1H), 4.36 (d, *J* = 6.8 Hz, 1H), 3.37 – 3.25 (m, 2H), 2.57 (ddq, *J* = 20.9, 11.5, 9.1 Hz, 2H), 2.34 (dtd, *J* = 10.0, 8.4, 3.1 Hz, 2H), 2.09 (dtt, *J* = 11.0, 9.6, 8.4 Hz, 1H), 2.05 – 1.94 (m, 1H), 1.91 – 1.83 (m, 1H), 1.80 – 1.72 (m, 1H), 1.64 (s, 2H), 1.61 – 1.50 (m, 3H), 1.49 – 1.36 (m, 2H), 1.25 (qt, *J* = 13.0, 3.6 Hz, 1H), 1.09 (qt, *J* = 14.1, 3.9 Hz, 1H), 0.86 (dddd, *J* = 16.7, 13.0, 8.6, 3.8 Hz, 1H), 0.69 (qd, *J* = 12.7, 3.6 Hz, 1H).

¹³C NMR (125 MHz, CDCl₃) δ 169.41, 128.57, 128.50, 127.10, 126.95, 126.48, 126.36, 70.62, 55.42, 34.02, 33.41, 30.71, 27.34, 26.72, 26.35, 25.84, 25.31, 18.82.

IR (FT-ATR) cm⁻¹: 3067, 3029, 2973, 2928, 1658, 1596, 1495, 1447, 1181, 1026

HRMS-ESI (m/z), calculated for C₂₅H₃₁N₂ (M+H)⁺ 359.2487. Found 359.2481



Trans-1-cyclohexyl-2-cyclopentyl-4,5-diphenyl-4,5-dihydro-1H-imidazole:

N-cyclohexylcyclopentanecarboxamide (0.120 g, 0.615 mmol) was added to a 50 mL flamed dried round bottom flask. 4 mL of anhydrous DCM was added to the flask by syringe. The resulting

solution was cooled to 0°C by ice-bath before the addition of 2,6 Lutidine (0.330 g, 3.073 mmol) by syringe. Oxalyl Chloride (0.078 g, 0.615 mmol) was then added over 10 minutes by syringe. The resulting mixture was stirred at 0°C for 1.5 hours after which the solvent was removed to give the intermediate imidoyl chloride as a brownish-tan solid. This solid was then dissolved in 4 mL of anhydrous DMF and to this solution trans-2,3-diphenylaziridine (0.100 g, 0.512 mmol) was added by syringe. The reaction was then stirred for 12-14 hours at 55°C. The reaction was extracted in EtOAc (2 x 25 mL) and washed with 10 % LiBr solution. After which the organic layers were washed with 0.5 M HCl solution and Saturated NaHCO₃ solution. The organic layers were collected and dried over anhydrous NaSO₄, concentrated and purified by column chromatography (3:7 EtOAc:Hexanes). The product was obtained as a clear oil 47 % yield (0.090 g, 0.243 mmol)

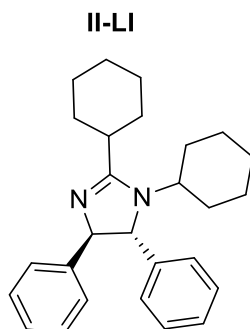
Spectroscopy:

¹H NMR (500 MHz, CDCl₃) δ 7.37 – 7.20 (m, 8H), 7.19 – 7.10 (m, 2H), 4.67 (d, *J* = 6.9 Hz, 1H), 4.36 (d, *J* = 6.9 Hz, 1H), 3.50 (tt, *J* = 11.9, 3.5 Hz, 1H), 2.86 (p, *J* = 8.2 Hz, 1H), 2.23 – 1.97 (m, 4H), 1.95 – 1.80 (m, 2H), 1.82 – 1.40 (m, 7H), 1.29 (qt, *J* = 13.0, 3.6 Hz, 1H), 1.12 (qt, *J* = 14.3, 4.1 Hz, 1H), 0.89 (qt, *J* = 13.2, 4.1 Hz, 1H), 0.76 (qd, *J* = 12.7, 3.6 Hz, 1H).

¹³C NMR (125 MHz, CDCl₃) δ 170.57, 146.15, 144.92, 128.65, 128.51, 128.10, 127.15, 126.97, 126.36, 126.22, 77.75, 70.41, 55.43, 37.78, 33.98, 32.28, 31.04, 30.82, 26.35, 25.84, 25.81, 25.32.

IR (FT-ATR) cm⁻¹: 3068, 3011, 2913, 2856, 1601, 1577, 1484, 1463, 1428, 1264, 1159, 1100

HRMS-ESI (m/z), calculated for C₂₆H₃₃N₂ (M+H)⁺ 373.2644. Found 373.2572



Trans-1,2-dicyclohexyl-4,5-diphenyl-4,5-dihydro-1H-imidazole:

N-cyclohexylcyclohexanecarboxamide (0.129 g, 0.615 mmol) was added to a 50 mL flamed dried round bottom flask. 4 mL of anhydrous DCM was added to the flask by syringe. The resulting solution was cooled to 0°C by ice-bath before the addition of 2,6 Lutidine (0.330 g, 3.073 mmol) by syringe. Oxalyl Chloride (0.078 g, 0.615 mmol) was then added over 10 minutes by syringe. The resulting mixture was stirred at 0°C for 1.5 hours after which the solvent was removed to give the intermediate imidoyl chloride as a brownish-tan solid. This solid was then dissolved in 4 mL of anhydrous DMF and to this solution trans-2,3-diphenylaziridine (0.100 g, 0.512 mmol) was added by syringe. The reaction was then stirred for 12-14 hours at 55°C. The reaction was extracted in EtOAc (2 x 25 mL) and washed with 10 % LiBr solution. After which the organic layers were washed with 0.5 M HCl solution and Saturated NaHCO₃ solution. The organic layers were collected and dried over anhydrous NaSO₄, concentrated and purified by column chromatography (3:7 EtOAc: Hexanes). The product was obtained as a clear oil 58 % yield (0.125 g, 0.297 mmol)

Spectroscopy:

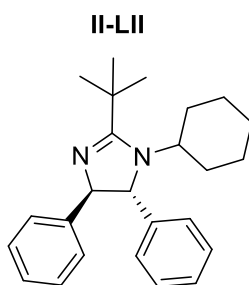
¹H NMR (500 MHz, CDCl₃) δ 7.33 (d, *J* = 7.1 Hz, 3H), 7.33 – 7.23 (m, 2H), 7.23 (d, *J* = 7.7 Hz, 2H), 7.14 (d, *J* = 7.5 Hz, 2H), 4.65 (d, *J* = 6.6 Hz, 1H), 4.33 (d, *J* = 6.6 Hz, 1H), 3.43 (td, *J* = 11.7, 5.8 Hz, 1H), 2.41 (t, *J* = 11.8 Hz, 1H), 2.13 (d, *J* = 13.1 Hz, 1H), 2.05 (d, *J* = 13.2 Hz, 1H), 1.95 –

1.83 (m, 3H), 1.78 (d, $J = 11.3$ Hz, 2H), 1.71 (d, $J = 12.1$ Hz, 1H), 1.58 (q, $J = 16.3, 13.7$ Hz, 3H), 1.50 – 1.33 (m, 4H), 1.36 – 1.25 (m, 1H), 1.14 (qt, $J = 13.9, 3.9$ Hz, 1H), 0.90 (tdd, $J = 13.1, 9.5, 3.9$ Hz, 1H), 0.79 (qd, $J = 12.7, 3.5$ Hz, 1H).

^{13}C NMR (125 MHz, CDCl_3) δ 170.96, 128.63, 128.49, 127.03, 126.91, 126.91, 126.34, 126.07, 70.03, 55.32, 36.99, 33.83, 32.45, 30.97, 30.62, 26.63, 26.31, 26.28, 26.10, 25.79, 25.32.

IR (FT-ATR) cm^{-1} : 3060, 3027, 2928, 2852, 1603, 1581, 1493, 1450, 1411, 1275, 1173, 1130

HRMS-ESI (m/z), calculated for $\text{C}_{27}\text{H}_{35}\text{N}_2$ ($\text{M}+\text{H}$) $^+$ 387.2800 Found: 387.2811



Trans-2-(tert-butyl)-1-cyclohexyl-4,5-diphenyl-4,5-dihydro-1H-imidazole:

N-cyclohexylpivalamide (0.113 g, 0.615 mmol) was added to a 50 mL flamed dried round bottom flask. 4 mL of anhydrous DCM was added to the flask by syringe. The resulting solution was cooled to 0°C by ice-bath before the addition of 2,6 Lutidine (0.330 g, 3.073 mmol) by syringe. Oxalyl Chloride (0.078 g, mmol) was then added over 10 minutes by syringe. The resulting mixture was stirred at 0°C for 1.5 hours after which the solvent was removed to give the intermediate imidoyl chloride as a brownish-tan solid. This solid was then dissolved in 4 mL of anhydrous DMF and to this solution trans-2,3-diphenylaziridine (0.100 g, mmol) was added by syringe. The reaction was then stirred for 12-14 hours at 55°C . The reaction was extracted in EtOAc (2 x 25 mL) and washed with 10 % LiBr solution. After which the organic layers were washed with 0.5 M HCl solution and Saturated NaHCO_3 solution. The organic layers were collected and dried over

anhydrous NaSO₄, concentrated and purified by column chromatography (3:7 EtOAc:Hexanes).

The product was obtained as a clear oil 38 % yield (0.070 g, 0.194 mmol)

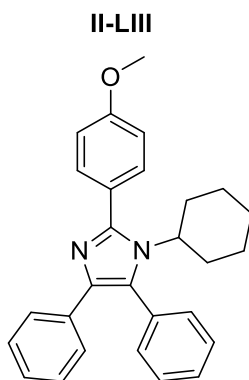
Spectroscopy:

¹H NMR (500 MHz, CDCl₃) δ 7.37 – 7.30 (m, 3H), 7.33 – 7.25 (m, 1H), 7.28 – 7.19 (m, 3H), 7.18 – 7.12 (m, 2H), 4.63 (d, *J* = 4.9 Hz, 1H), 4.34 (d, *J* = 5.0 Hz, 1H), 3.76 (tt, *J* = 11.7, 3.4 Hz, 1H), 1.79 – 1.71 (m, 1H), 1.63 – 1.51 (m, 2H), 1.50 (s, 9H), 1.49 – 1.41 (m, 1H), 1.43 – 1.34 (m, 1H), 1.32 – 1.20 (m, 1H), 1.11 (qt, *J* = 12.6, 3.3 Hz, 1H), 0.87 (qt, *J* = 13.1, 3.5 Hz, 1H), 0.72 (qd, *J* = 12.8, 3.6 Hz, 1H).

¹³C NMR (125 MHz, CDCl₃) δ 172.61, 128.70, 128.49, 126.95, 126.15, 125.74, 69.73, 56.47, 34.24, 33.97, 30.96, 29.42, 26.54, 25.78, 25.25.

IR (FT-ATR) cm⁻¹: 3060, 3027, 2930, 2854, 1594, 1579, 1452, 1400, 1173, 1137

HRMS-ESI (*m/z*), calculated for C₂₅H₃₃N₂ (M+H)⁺ 361.2644. Found 361.2621.



1-cyclohexyl-2-(4-methoxyphenyl)-4,5-diphenyl-1H-imidazole:

Trans-1-cyclohexyl-2-(4-methoxyphenyl)-4,5-diphenyl-4,5-dihydro-1H-imidazole (0.065 g, 0.158 mmol) was added to a round bottom flask with stir bar. 10 mL of anhydrous THF was added to the flask. The resulting solution was stirred while DDQ (0.040 g, 0.174 mmol) was added as a

solid to the flask, and the reaction was refluxed for 2h, then extracted into 30 mL of EtOAc and washed in (3 x 10 mL) saturated NaHCO₃ solution. The organic layers were collected and dried over anhydrous Na₂SO₄ and reduced in vacuo to give the crude product that was purified by column chromatography (3:7 EtOAc: Hexanes) to give the product as a pale yellow solid 63 % yield (0.041 g, 0.099 mmol)

Spectroscopy:

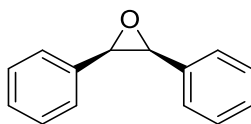
¹H NMR (500 MHz, CDCl₃) δ 7.57 – 7.50 (m, 2H), 7.50 – 7.37 (m, 7H), 7.18 – 7.10 (m, 2H), 7.14 – 7.04 (m, 1H), 7.03 – 6.97 (m, 2H), 3.94 (tt, *J* = 12.3, 3.4 Hz, 1H), 3.88 (s, 3H), 1.87 – 1.80 (m, 2H), 1.66 – 1.42 (m, 5H), 1.04 (qt, *J* = 13.1, 3.4 Hz, 2H), 0.74 (qt, *J* = 13.2, 3.7 Hz, 1H).

¹³C NMR (125 MHz, CDCl₃) δ 160.00, 147.53, 134.73, 132.17, 131.30, 128.90, 128.70, 128.62, 127.86, 126.62, 125.89, 113.72, 58.25, 55.35, 33.57, 26.20, 25.05.

IR (FT-ATR) cm⁻¹: 3028, 2980, 1623, 1568, 1180, 1023

HRMS-ESI (m/z), calculated for C₂₈H₂₉N₂O (M+H)⁺ 408.2204. Found 408.2223

II-LIV



Cis-2,3-diphenyloxirane:

Cis-1,2-diphenylethene (5.00 g, 27.74 mmol) was added to a round bottom flask by syringe, and then dissolved in 100 mL of CHCl₃. The resulting solution was cooled to 0°C by ice bath before the addition of 77% by weight mCPBA (6.84 g, 30.51 mmol) was added as a solid. The solution stirred at 0°C for 1 hour and at 4°C for an additional 23 hours. After which the suspension was washed with 10% Na₂CO₃ (2 X 50 mL), followed by saturated NaCl solution (2 X 50 mL). The

organic layers were collected and dried over anhydrous Na₂SO₄ before being reduced *in vacuo* to yield product as a yellow oil 99 % yield, (5.39 g, 27.46 mmol)

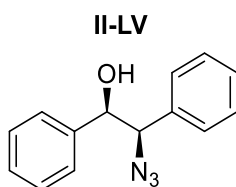
Spectroscopy:

¹H NMR (500 MHz, CDCl₃) δ 7.23 – 7.12 (m, 5H), 4.38 (s, 1H).

¹³C NMR (125 MHz, CDCl₃) δ 134.34, 127.77, 127.50, 126.85, 59.77.

IR (FT-ATR) cm⁻¹: 3059, 2991, 1603, 1217, 1071

HRMS-ESI (m/z), calculated for C₁₄H₁₃O (M+H)⁺ 197.0966. Found 197.0995.



Cis-2-azido-1,2-diphenylethan-1-ol:

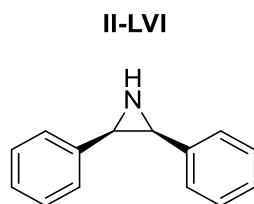
Cis-2,3-diphenyloxirane (2.5 g, 12.74 mmol) was added to a round bottom flask, and to it 100 mL of a (8:1) iPrOH:H₂O solution was added. The resulting solution was stirred vigorously as NH₄Cl (1.09 g, 20.38 mmol) was added as a solid, After which NaN₃ (3.31 g, 50.96 mmol) was added to the solution and the suspension was refluxed for 12 hours. The reaction was cooled to room temperature and 20 mL of Et₂O and 10 mL of H₂O were added. This solution was poured into 50 mL of Et₂O and washed with (2 X 60 mL) of saturated NaCl solution. The organic layers were collected, dried over anhydrous Na₂SO₄ and reduced in vacuo to give the crude product, which was purified by column chromatography (0.5:9.5) THF: Hexanes to give a yellow oil 68 % yield (2.07 g, 8.68 mmol)

Spectroscopy:

^1H NMR (500 MHz, CDCl_3) δ 7.31 – 7.16 (m, 6H), 7.15 – 7.06 (m, 4H), 4.77 (d, $J = 7.9$ Hz, 1H), 4.65 (d, $J = 8.0$ Hz, 1H), 2.79 (s, 1H).

^{13}C NMR (125 MHz, CDCl_3) δ 139.17, 135.96, 128.51, 128.17, 128.15, 127.82, 126.87, 77.99

HRMS-ESI (m/z), calculated for $\text{C}_{14}\text{H}_{14}\text{N}_3\text{O}$ ($\text{M}+\text{H}$) $^+$ 240.1137. Found 240.1114

**Cis-2,3-diphenylaziridine:**

Cis-2-azido-1,2-diphenylethan-1-ol (1.80 g, 7.52 mmol) was added to a dry round bottom flask. 100 mL of anhydrous THF was added and the resulting solution was stirred vigorously as PPh_3 (2.072 g, 7.90 mmol) was added. The solution was refluxed for 24 hours and then reduced in vacuo to give a clear oil which was cooled to precipitate PPh_3O side product. The crude product as an oil was separated from the solid and purified by column chromatography (9:1 DCM:Hexanes) to yield the product as a clear oil 80% yield (1.17 g, 6.01 mmol)

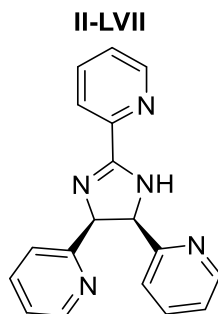
Spectroscopy:

^1H NMR (500 MHz, CDCl_3) δ 7.21 – 7.02 (m, 10H), 3.60 (s, 2H), 1.57 (s, 1H).

^{13}C NMR (125 MHz, CDCl_3) δ 139.53, 128.62, 127.34, 125.48, 43.73.

IR (FT-ATR) cm^{-1} : 3301, 3034, 2978, 1594, 1065, 1054

HRMS-ESI (m/z), calculated for $\text{C}_{14}\text{H}_{14}\text{N}$ ($\text{M}+\text{H}$) $^+$ 196.1126. Found 196.1174.



2,2',2''-cis-4,5-dihydro-1H-imidazole-2,4,5-triyl)tripyrindine:

Picolinaldehyde (10.0 g, 93.3 mmol) was added to a round bottom flask. 60 mL of THF was added to the flask by syringe. Saturated NH₄OH solution (30 mL) was added to the flask and the reaction was stirred at 50°C for 48 hours. The reaction was extracted in EtOAc (80 mL) and washed with saturated NaCl solution (2 x 50 mL). The organic layers were collected and dried over anhydrous NaSO₄, concentrated into a yellow oil, that precipitated product as a yellow solid 83 % yield (7.8 g, 25.88 mmol) upon the addition of warm hexanes.

Spectroscopy:

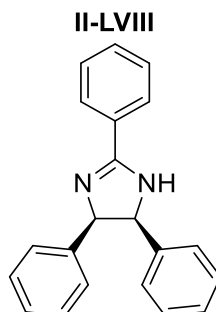
¹H NMR (500 MHz, CDCl₃) δ 8.68 (ddd, *J* = 4.9, 1.8, 1.0 Hz, 1H), 8.39 – 8.28 (m, 3H), 7.85 (td, *J* = 7.7, 1.7 Hz, 1H), 7.44 (ddd, *J* = 7.6, 4.9, 1.2 Hz, 1H), 7.31 (dtd, *J* = 25.2, 7.7, 1.8 Hz, 2H), 7.10 (dt, *J* = 7.8, 1.1 Hz, 1H), 6.97 – 6.86 (m, 3H), 6.70 (s, 1H), 6.05 (d, *J* = 11.1 Hz, 1H), 5.60 (d, *J* = 11.1 Hz, 1H).

¹³C NMR (125 MHz, CDCl₃) δ 165.08, 159.29, 158.63, 148.91, 148.81, 148.44, 148.40, 136.65, 135.67, 135.46, 125.45, 122.88, 122.71, 122.00, 121.75, 121.45, 77.75, 66.30.

IR (FT-ATR) cm⁻¹: 3387, 3124, 2998, 1613, 1574, 1066

HRMS: Product not observed by HRMS-ESI (M+H)⁺

m.p.: 147.5-148.9°C



Cis-2,4,5-triphenyl-4,5-dihydro-1H-imidazole:

Benzaldehyde (10 g, 94.2 mmol) was added to a round bottom flask. Benzoic acid (0.058 g, 0.5 mmol) was added to the flask followed by HMDS (18.2g, 113 mmol). The reaction was then stirred for 12-14 hours at 55°C. The reaction was extracted in EtOAc (50 mL) and washed with saturated NaCl solution (2 x 50 mL). The organic layers were collected and dried over anhydrous NaSO₄, concentrated and purified by column chromatography (5:5 EtOAc:Hexanes). The product was obtained as a yellow oil 53 % yield (4.90 g, 16.43 mmol)

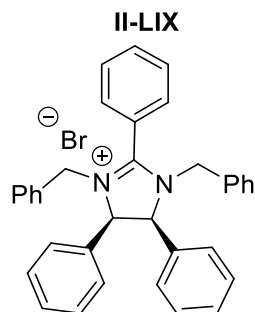
Spectroscopy:

¹H NMR (500 MHz, CDCl₃) δ 8.12 – 8.06 (m, 2H), 7.60 – 7.52 (m, 1H), 7.43 (t, *J* = 7.7 Hz, 2H), 7.04 – 6.95 (m, 6H), 6.87 – 6.80 (m, 4H), 5.34 (s, 2H), 1.30 (s, 1H).

¹³C NMR (125 MHz, CDCl₃) δ 165.16, 136.82, 132.61, 128.91, 128.29, 127.75, 127.36, 127.30, 126.62, 68.58.

IR (FT-ATR) cm⁻¹: 3324, 3048, 2961, 1612, 1583, 1084

HRMS calculated fo C₂₁H₁₉N₂ (M+H)⁺ 299.1548. Found 299.1603.



Cis-1,3-dibenzyl-2,4,5-triphenyl-4,5-dihydro-1H-imidazol-3-ium bromide:

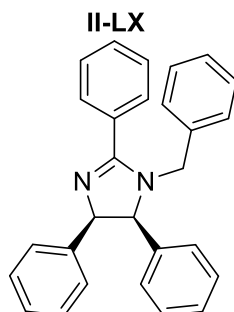
Cis-2,4,5-triphenyl-4,5-dihydro-1H-imidazole 1 (0.175 g, 0.590 mmol) was added to a round bottom flask. 10 mL of anhydrous DMF was added to the flask and the solution was cooled to 0°C by ice bath. 60% by weight NaH (0.035 g, 0.885 mmol) was added to the solution and the suspension was stirred at 0°C for 0.5 hours before the slow addition of Benzyl bromide (0.16 g, 0.91 mmol) by syringe to the flask. The reaction was allowed to warm to room temperature and stirred for 12 hours. After which the solution was extracted in EtOAc (30 mL) and washed with 10 % LiBr solution (3 x 15 mL). The organic layers were gathered and dried over anhydrous Na₂SO₄ and concentrated in vacuo to give the crude product which was purified by column chromatography (1:9 MeOH:DCM) to give the product as a clear oil, 85 % yield (0.230 g, 0.50 mmol)

Spectroscopy:

¹H NMR (500 MHz, CDCl₃) δ 8.36 – 8.30 (m, 1H), 7.89 (d, *J* = 7.3 Hz, 1H), 7.70 – 7.57 (m, 3H), 7.15 – 7.07 (m, 6H), 7.06 – 6.97 (m, 6H), 6.97 – 6.85 (m, 8H), 6.04 (s, 2H), 4.57 (d, *J* = 15.2 Hz, 2H), 4.41 (d, *J* = 15.2 Hz, 2H).

¹³C NMR (125 MHz, CDCl₃) δ 169.25, 132.88, 132.31, 130.78, 130.31, 129.98, 129.09, 128.83, 128.81, 128.74, 128.66, 128.49, 128.43, 122.71, 69.16, 51.12.

HRMS calculated for C₂₈H₂₅N₂ (M+H)⁺ 389.2018. Found 389.2003



Cis-1-benzyl-2,4,5-triphenyl-4,5-dihydro-1H-imidazole:

Cis-2,4,5-triphenyl-4,5-dihydro-1H-imidazole 1 (0.175 g, 0.590 mmol) was added to a round bottom flask. 10 mL of anhydrous DMF was added to the flask and the solution was cooled to 0°C by ice bath. 60% by weight NaH (0.035 g, 0.885 mmol) was added to the solution and the suspension was stirred at 0°C for 0.5 hours before the slow addition of Benzyl chloride (0.097 g, 0.088 mmol) by syringe to the flask. The reaction was allowed to warm to room temperature and stirred for 12 hours. After which the solution was extracted in EtOAc (30 mL) and washed with 10 % LiBr solution (3 x 15 mL). The organic layers were collected, dried over anhydrous Na₂SO₄ and reduced to give the crude product that was purified on neutral alumina (5:5 DCM: Hexanes) to give product as a clear oil 42 % yield (0.096 g, 0.25 mmol).

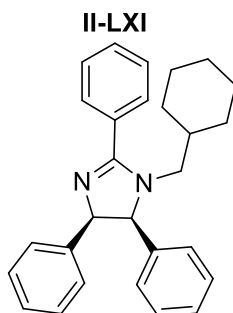
Spectroscopy:

¹H NMR (500 MHz, CDCl₃) δ 7.84 (dd, J = 6.6, 2.9 Hz, 2H), 7.61 – 7.50 (m, 3H), 7.34 – 7.25 (m, 4H), 7.24 – 7.19 (m, 1H), 7.11 – 7.04 (m, 2H), 7.05 – 6.87 (m, 8H), 5.59 (d, J = 11.4 Hz, 1H), 4.96 (d, J = 11.4 Hz, 1H), 4.81 (d, J = 15.6 Hz, 1H), 3.88 (d, J = 15.6 Hz, 1H).

¹³C NMR (125 MHz, CDCl₃) δ 167.23, 131.07, 130.37, 129.06, 128.88, 128.81, 128.78, 128.64, 128.62, 128.60, 128.58, 128.56, 128.13, 128.06, 127.94, 127.91, 127.88, 127.63, 127.37, 127.33, 127.19, 126.76, 126.34, 126.00, 68.44, 49.04, 29.71.

IR (FT-ATR) cm⁻¹: 3058, 3024, 1604, 1598, 1097

HRMS calculated for C₂₈H₂₅N₂ (M+H)⁺ 389.2018. Found 389.1995



Cis-1-(cyclohexylmethyl)-2,4,5-triphenyl-4,5-dihydro-1H-imidazole:

Cis-2,4,5-triphenyl-4,5-dihydro-1H-imidazole 1 (0.175 g, 0.590 mmol) was added to a round bottom flask. 10 mL of anhydrous DMF was added to the flask and the solution was cooled to 0°C by ice bath. 60% by weight NaH (0.035 g, 0.885 mmol) was added to the solution and the suspension was stirred at 0°C for 0.5 hours before the slow addition of (bromomethyl)cyclohexane (0.097 g, 0.088 mmol) by syringe to the flask. The reaction was allowed to warm to room temperature and stirred for 12 hours. After which the solution was extracted in EtOAc (30 mL) and washed with 10 % LiBr solution (3 x 15 mL). The organic layers were collected, dried over anhydrous Na₂SO₄ and reduced to give the crude product that was purified on neutral alumina (5:5 DCM: Hexanes) to give product as a clear oil 46 % yield (0.107 g, 0.27 mmol).

Spectroscopy:

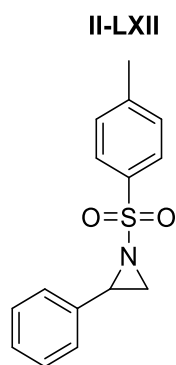
¹H NMR (500 MHz, CDCl₃) δ 7.76 – 7.67 (m, 2H), 7.58 – 7.48 (m, 2H), 7.51 – 7.35 (m, 1H), 7.09 (d, *J* = 6.5 Hz, 1H), 7.09 – 6.98 (m, 5H), 6.97 (dd, *J* = 8.1, 6.1 Hz, 3H), 5.68 (d, *J* = 11.3 Hz, 1H), 5.13 (d, *J* = 11.3 Hz, 1H), 3.14 (dd, *J* = 14.3, 9.1 Hz, 1H), 2.80 (dd, *J* = 14.2, 5.2 Hz, 1H), 1.79 – 1.71 (m, 1H), 1.74 – 1.63 (m, 1H), 1.62 (t, *J* = 3.1 Hz, 1H), 1.59 (s, 1H), 1.48 (dp, *J* = 12.2, 5.3,

4.3 Hz, 2H), 1.33 – 1.23 (m, 1H), 1.25 – 0.97 (m, 3H), 0.70 (qd, $J = 12.1, 3.0$ Hz, 1H), 0.59 (qd, $J = 12.5, 3.6$ Hz, 1H).

^{13}C NMR (125 MHz, CDCl_3) δ 167.62, 139.64, 137.24, 131.78, 129.77, 128.65, 128.47, 128.11, 127.95, 127.73, 127.27, 127.00, 126.15, 73.37, 69.50, 51.62, 36.22, 30.95, 30.52, 26.34, 25.85, 25.82, 25.80.

IR (FT-ATR) cm^{-1} : 3018, 2987, 1628, 1583, 1129

HRMS calculated for $\text{C}_{28}\text{H}_{31}\text{N}_2$ ($\text{M}+\text{H}$) $^+$ 395.2487. Found 395.2489



2-phenyl-1-tosylaziridine:

Styrene (4.18 g, 40.21 mmol) was added to a 100 mL round bottom flask. 45 mL of anhydrous ACN was added by syringe and the resulting solution was stirred vigorously before the addition of 4-methyl-N-(phenyl-13-iodaneylidene)benzene sulfonamide (3.00 g, 8.043 mmol). Copper (II) acetylacetonate (0.162 g, 0.619 mmol) was then added to the suspension and the reaction was stirred at room temperature for 6 hours. The solvent was then removed by vacuum and the crude product was extracted into CHCl_3 (40 mL) and washed with saturated NH_4Cl (2 x 40 mL) followed by saturated NaCl (2 x 40 mL). The organic layers were collected, dried over anhydrous Na_2SO_4 and reduced in vacuo to give the product as a crude solid, purified by column chromatography 3:7 (EtOAc: Hexanes) to give a white solid 71 % yield (1.55 g, 5.71 mmol).

Spectroscopy:

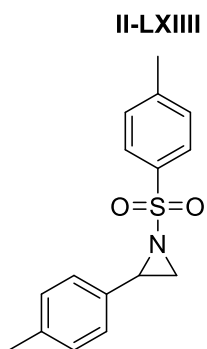
^1H NMR (500 MHz, CDCl_3) δ 7.87 (d, $J = 8.1$ Hz, 2H), 7.36 – 7.25 (m, 5H), 7.22 (dd, $J = 7.5, 2.2$ Hz, 2H), 3.78 (dd, $J = 7.2, 4.5$ Hz, 1H), 2.98 (d, $J = 7.2$ Hz, 1H), 2.45 – 2.36 (m, 4H).

^{13}C NMR (125 MHz, CDCl_3) δ 144.66, 135.03, 134.95, 129.76, 128.55, 128.30, 127.94, 126.55, 41.03, 35.95, 21.66.

IR (FT-ATR) cm^{-1} : 3012, 2977, 1542, 1469, 1413, 1324, 1156, 1128, 1034, 968

HRMS calculated for $\text{C}_{15}\text{H}_{16}\text{NO}_2\text{S}$ ($\text{M}+\text{H}$) $^+$ 274.0902. Found 274.1044

m.p.: 96.1-96.8°C



2-(p-tolyl)-1-tosylaziridine:

1-methyl-4-vinylbenzene (7.92 g, 67.02 mmol) was added to a 100 mL round bottom flask. 45 mL of anhydrous ACN was added by syringe and the resulting solution was stirred vigorously before the addition of 4-methyl-N-(phenyl-13-iodaneylidene)benzene sulfonamide (5.00 g, 13.40 mmol). Copper (II) acetylacetonate (0.270 g, 1.032 mmol) was then added to the suspension and the reaction was stirred at room temperature for 6 hours. The solvent was then removed by vacuum and the crude product was extracted into CHCl_3 (40 mL) and washed with saturated NH_4Cl (2 x 40 mL) followed by saturated NaCl (2 x 40 mL). The organic layers were collected, dried over

anhydrous Na₂SO₄ and reduced in vacuo to give the product as a crude solid, purified by column chromatography 1:9 (EtOAc: Hexanes) to give a white solid 74 % yield (2.86 g, 9.96 mmol).

Spectroscopy:

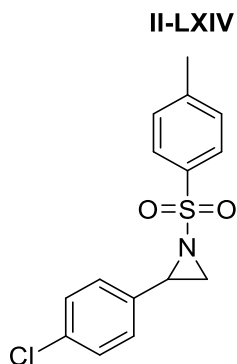
¹H NMR (500 MHz, CDCl₃) δ 7.86 (d, *J* = 8.0 Hz, 2H), 7.32 (d, *J* = 8.0 Hz, 2H), 7.10 (s, 3H), 3.74 (dd, *J* = 7.2, 4.5 Hz, 1H), 2.97 (d, *J* = 7.1 Hz, 1H), 2.43 (s, 3H), 2.38 (d, *J* = 4.5 Hz, 1H), 2.31 (s, 3H).

¹³C NMR (125 MHz, CDCl₃) δ 144.56, 138.15, 135.04, 131.98, 129.76, 129.72, 129.22, 127.91, 126.45, 41.07, 35.81, 21.66, 21.15.

IR (FT-ATR) cm⁻¹: 3017, 2993, 1565, 1498, 1433, 1347, 1168, 1121, 1061, 912

HRMS calculated for C₁₆H₁₈NO₂ (M+H)⁺ 288.1058. Found 288.1180.

m.p.: 135.8-136.4°C



2-(4-chlorophenyl)-1-tosylaziridine:

1-chloro-4-vinylbenzene (9.29 g, 67.02 mmol) was added to a 100 mL round bottom flask. 45 mL of anhydrous ACN was added by syringe and the resulting solution was stirred vigorously before the addition of 4-methyl-N-(phenyl-13-iodaneylidene)benzene sulfonamide (5.00 g, 13.40 mmol). Copper (II) acetylacetonate (0.270 g, 1.032 mmol) was then added to the suspension and the

reaction was stirred at room temperature for 6 hours. The solvent was then removed by vacuum and the crude product was extracted into CHCl_3 (40 mL) and washed with saturated NH_4Cl (2 x 40 mL) followed by saturated NaCl (2 x 40 mL). The organic layers were collected, dried over anhydrous Na_2SO_4 and reduced in vacuo to give the product as a crude solid, purified by column chromatography 2:8 (EtOAc: Hexanes) to give a white solid 63 % yield (2.60 g, 8.45 mmol).

Spectroscopy:

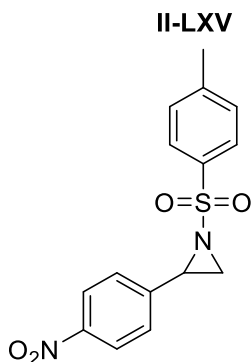
^1H NMR (500 MHz, CDCl_3) δ 7.86 (d, $J = 8.0$ Hz, 2H), 7.34 (d, $J = 8.0$ Hz, 2H), 7.26 (d, $J = 8.3$ Hz, 2H), 7.18 – 7.12 (m, 2H), 3.73 (dd, $J = 7.2, 4.4$ Hz, 1H), 2.98 (d, $J = 7.1$ Hz, 1H), 2.44 (s, 3H), 2.34 (d, $J = 4.4$ Hz, 1H).

^{13}C NMR (125 MHz, CDCl_3) δ 144.81, 134.78, 134.19, 133.62, 129.80, 128.77, 127.93, 127.88, 40.26, 36.06, 21.68.

IR (FT-ATR) cm^{-1} : 3016, 2964, 1567, 1503, 1476, 1389, 1165, 1039

HRMS calculated for $\text{C}_{15}\text{H}_{15}\text{ClNO}_2\text{S}$ ($\text{M}+\text{H}$) $^+$ 308.0512. Found 308.0535

m.p.: 110.8-111.3°C



2-(4-nitrophenyl)-1-tosylaziridine:

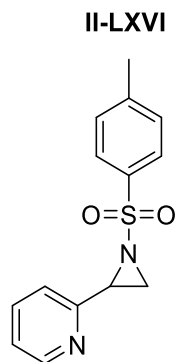
1-nitro-4-vinylbenzene (2.0 g, 13.41 mmol) was added to a 250 mL round bottom flask. 80 mL of ACN was added to the flask by syringe. The resulting solution was stirred vigorously as Chloramine-T·3H₂O (4.155 g, 14.75 mmol) was added, followed by the addition of the 90% technical grade pyridinium tribromide (0.475 g, 1.341 mmol). The reaction was stirred at room temperature for 6 hours. The solvent was then removed in vacuo and the reaction was extracted into 100 mL of CHCl₃. The organic layer was then washed with saturated NaHCO₃ (3 x 20 mL) followed by saturated NaCl (3 x 20 mL). The organic layers were collected, dried over anhydrous Na₂SO₄ and reduced in vacuo. The crude product was purified via column chromatography on silica (3:7 EtOAc: Hexanes) to give the product as a pale yellow solid 49 % yield (2.1 g, 6.57 mmol).

Spectroscopy:

¹H NMR (500 MHz, CDCl₃) δ 8.16 – 8.10 (m, 2H), 7.89 – 7.82 (m, 2H), 7.43 – 7.36 (m, 2H), 7.37 – 7.31 (m, 2H), 3.83 (dd, *J* = 7.2, 4.2 Hz, 1H), 3.04 (d, *J* = 7.2 Hz, 1H), 2.43 (s, 3H), 2.37 (d, *J* = 4.2 Hz, 1H).

¹³C NMR (125 MHz, CDCl₃) δ 147.78, 145.17, 142.51, 134.37, 129.92, 127.98, 127.97, 127.46, 127.44, 123.82, 39.70, 36.56, 21.69.

HRMS calculated for C₁₅H₁₅N₂O₄S (M+H)⁺ 319.0762. Found 319.0787.



2-(1-tosylaziridin-2-yl)pyridine:

2-Vinylpyridine (4.04 g, 38.4 mmol) was added to a 250 mL round bottom flask. 120 mL of ACN was added to the flask by syringe. The resulting solution was stirred vigorously as Chloramine-T·3H₂O (11.90 g, 42.25 mmol) was added, followed by the addition of the Trimethylphenylammonium tribromide (1.44 g, 3.84 mmol). The reaction was stirred at room temperature for 6 hours. The solvent was then removed in vacuo and the reaction was extracted into 100 mL of CHCl₃. The organic layer was then washed with saturated NaHCO₃ (3 x 20 mL) followed by saturated NaCl (3 x 20 mL). The organic layers were collected, dried over anhydrous Na₂SO₄ and reduced in vacuo. The crude product was purified via column chromatography on TEA neutralized silica (4:6 EtOAc: Hexanes) to give the product as a red oil, 49 % yield (5.16 g, 18.816 mmol)

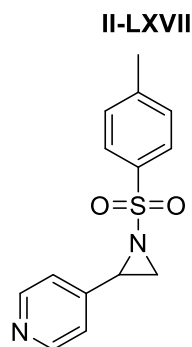
Spectroscopy:

¹H NMR (500 MHz, CDCl₃) δ 8.53 (ddd, *J* = 4.8, 1.8, 0.9 Hz, 1H), 7.90 – 7.78 (m, 2H), 7.63 (td, *J* = 7.7, 1.8 Hz, 1H), 7.40 – 7.24 (m, 3H), 7.20 (ddd, *J* = 7.6, 4.8, 1.2 Hz, 1H), 3.90 (dd, *J* = 7.2, 4.4 Hz, 1H), 2.97 (d, *J* = 7.2 Hz, 1H), 2.66 (d, *J* = 4.3 Hz, 1H), 2.43 (s, 3H).

¹³C NMR (125 MHz, CDCl₃) δ 154.27, 149.62, 144.76, 136.80, 134.51, 129.75, 129.71, 128.14, 126.46, 123.27, 121.78, 41.30, 35.03, 21.66, 21.53.

IR (FT-ATR) cm^{-1} : 3058, 1589, 1467, 1428, 1311, 1200, 1156, 1054, 980

HRMS calculated for $\text{C}_{14}\text{H}_{15}\text{N}_2\text{O}_2\text{S}$ ($\text{M}+\text{H}$)⁺ 275.0854. Found 275.1009.



4-(1-tosylaziridin-2-yl)pyridine:

4-Vinylpyridine (4.04 g, 38.4 mmol) was added to a 250 mL round bottom flask. 120 mL of ACN was added to the flask by syringe. The resulting solution was stirred vigorously as Chloramine-T·3H₂O (11.90 g, 42.25 mmol) was added, followed by the addition of the Trimethylphenylammonium tribromide (1.44 g, 3.84 mmol). The reaction was stirred at room temperature for 6 hours. The solvent was then removed in vacuo and the reaction was extracted into 100 mL of CHCl₃. The organic layer was then washed with saturated NaHCO₃ (3 x 20 mL) followed by saturated NaCl (3 x 20 mL). The organic layers were collected, dried over anhydrous Na₂SO₄ and reduced in vacuo. The crude product was purified via column chromatography on TEA neutralized silica (5:5 EtOAc: Hexanes) to give the product as a red oil, 26 % yield (2.74 g, 9.98 mmol)

Spectroscopy:

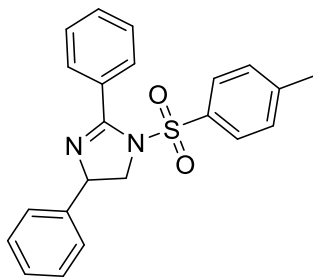
^1H NMR (500 MHz, CDCl_3) δ 8.52 – 8.36 (m, 2H), 7.85 – 7.71 (m, 2H), 7.27 (d, $J = 7.9$ Hz, 2H), 7.13 – 7.02 (m, 2H), 3.65 (dd, $J = 7.2, 4.3$ Hz, 1H), 2.94 (d, $J = 7.2$ Hz, 1H), 2.35 (s, 3H), 2.29 (d, $J = 4.3$ Hz, 1H).

^{13}C NMR (125 MHz, CDCl_3) δ 149.88, 145.07, 144.22, 134.31, 129.87, 127.91, 121.39, 39.22, 36.17, 21.62.

IR (FT-ATR) cm^{-1} : 3028, 1598, 1454, 1428, 1331, 1185, 1147, 1041, 963

HRMS calculated for $\text{C}_{14}\text{H}_{15}\text{N}_2\text{O}_2\text{S}$ ($\text{M}+\text{H}$) $^+$ 275.0854. Found 275.0883.

II-LXVIII



2,4-diphenyl-1-tosyl-4,5-dihydro-1H-imidazole:

2-phenyl-1-tosylaziridine (0.273 g, 1 mmol) was added to a dry 25 mL round bottom flask with stir bar. Benzonitrile (5.00 g, 48.49 mmol) was added to the flask by syringe and the resulting solution was stirred vigorously while $\text{Zn}(\text{OTf})_2$ was added (0.361 g, 1 mmol) as a solid. The solution was stirred at 65°C until all starting aziridine was consumed (3 hours). The reaction was then extracted into CHCl_3 and washed with saturated NaHCO_3 solution (3 x 15 mL). The solution was then washed saturated NaCl (3 x 15 mL) before being dried over anhydrous Na_2SO_4 and reduced *in vacuo* to give crude product purified by column chromatography, 3:7 (EtOAc:Hexanes) to give the product as a clear oil, 85 % yield (0.320 g, 0.850 mmol).

Spectroscopy:

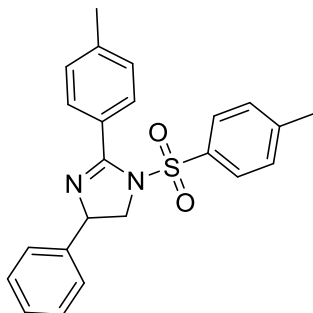
^1H NMR (500 MHz, CDCl_3) δ 7.81 – 7.70 (m, 2H), 7.61 – 7.49 (m, 1H), 7.49 – 7.36 (m, 4H), 7.25 – 7.14 (m, 5H), 7.02 – 6.89 (m, 2H), 5.00 (dd, $J = 9.9, 8.0$ Hz, 1H), 4.44 (dd, $J = 11.4, 9.9$ Hz, 1H), 3.87 (dd, $J = 11.4, 8.0$ Hz, 1H), 2.43 (s, 3H).

^{13}C NMR (125 MHz, CDCl_3) δ 159.98, 144.70, 141.46, 134.40, 131.24, 129.87, 129.79, 128.59, 127.75, 127.62, 127.44, 126.34, 67.74, 56.92, 21.63.

IR (FT-ATR) cm^{-1} : 3022, 2981, 1652, 1575, 1055, 1031.

HRMS calculated for $\text{C}_{22}\text{H}_{21}\text{N}_2\text{O}_2\text{S}$ ($\text{M}+\text{H}$) $^+$ 377.1324. Found 377.1335.

II-LXIX



4-phenyl-2-(p-tolyl)-1-tosyl-4,5-dihydro-1H-imidazole:

2-phenyl-1-tosylaziridine (0.273 g, 1 mmol) was added to a dry 25 mL round bottom flask with stir bar. Tolunitrile (3.51 g, 30 mmol) was added to the flask by syringe and the resulting solution was stirred vigorously while Zn(OTf)₂ was added (0.361 g, 1 mmol) as a solid. The solution was stirred at 65°C until all starting aziridine was consumed (3 hours). The reaction was then extracted into CHCl₃ and washed with saturated NaHCO₃ solution (3 x 15 mL). The solution was then washed saturated NaCl (3 x 15 mL) before being dried over anhydrous Na₂SO₄ and reduced *in vacuo* to give crude product purified by column chromatography, 3:7 (EtOAc:Hexanes) to give the product as a clear oil, 90 % yield (0.340 g, 0.889 mmol).

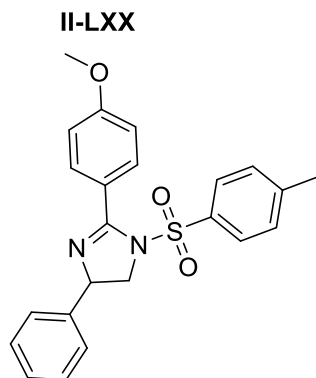
Spectroscopy:

¹H NMR (500 MHz, CDCl₃) δ 7.73 (d, *J* = 7.9 Hz, 2H), 7.45 – 7.39 (m, 2H), 7.26 (d, *J* = 8.0 Hz, 2H), 7.24 – 7.15 (m, 5H), 6.95 (dd, *J* = 6.6, 2.9 Hz, 2H), 4.96 (dd, *J* = 9.9, 7.9 Hz, 1H), 4.42 (dd, *J* = 11.5, 9.8 Hz, 1H), 3.84 (dd, *J* = 11.5, 7.8 Hz, 1H), 2.41 (d, *J* = 19.5 Hz, 6H).

¹³C NMR (125 MHz, CDCl₃) δ 160.00, 144.67, 141.71, 141.60, 134.39, 129.92, 129.82, 129.80, 128.56, 128.49, 127.61, 127.34, 126.35, 67.73, 56.97, 21.69, 21.63.

IR (FT-ATR) cm⁻¹: 3012, 2932, 1646, 1563, 1065

HRMS calculated for C₂₃H₂₃N₂O₂S (M+H)⁺ 391.1480. Found 391.1488.



2-(4-methoxyphenyl)-4-phenyl-1-tosyl-4,5-dihydro-1H-imidazole:

2-phenyl-1-tosylaziridine (0.273 g, 1 mmol) was added to a dry 25 mL round bottom flask with stir bar. 4-methoxybenzonitrile (1.060 g, 8 mmol) was added to the flask by syringe and the resulting solution was stirred vigorously while Zn(OTf)₂ was added (0.361 g, 1 mmol) as a solid. The solution was stirred at 65°C until all starting aziridine was consumed (3 hours). The reaction was then extracted into CHCl₃ and washed with saturated NaHCO₃ solution (3 x 15 mL). The solution was then washed saturated NaCl (3 x 15 mL) before being dried over anhydrous Na₂SO₄ and reduced *in vacuo* to give crude product purified by column chromatography, 2:8 (EtOAc:Hexanes) to give the product as a clear oil, 77 % yield (0.312 g, 0.768 mmol).

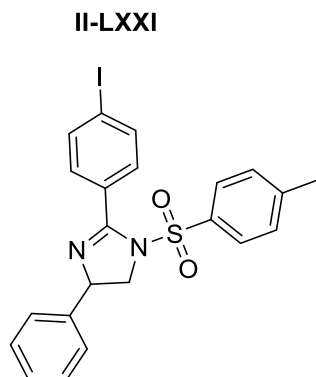
Spectroscopy:

¹H NMR (500 MHz, CDCl₃) δ 7.83 – 7.72 (m, 2H), 7.44 – 7.38 (m, 2H), 7.24 – 7.10 (m, 5H), 7.02 – 6.93 (m, 4H), 4.91 (dd, *J* = 9.7, 8.1 Hz, 1H), 4.43 (dd, *J* = 11.6, 9.8 Hz, 1H), 3.91 – 3.81 (m, 4H), 2.42 (s, 3H).

¹³C NMR (125 MHz, CDCl₃) δ 162.05, 159.68, 144.62, 141.66, 134.45, 131.74, 129.78, 129.70, 128.98, 128.75, 128.54, 128.24, 127.59, 127.33, 127.15, 127.11, 126.99, 126.70, 126.34, 122.30, 113.15, 67.61, 57.09, 55.39, 21.63.

IR (FT-ATR) cm⁻¹: 3012, 2897, 1639, 1455, 1214, 1023, 1012

HRMS calculated for C₂₃H₂₃N₂O₃S (M+H)⁺ 407.1429. Found 407.1439



2-(4-iodophenyl)-4-phenyl-1-tosyl-4,5-dihydro-1H-imidazole:

2-phenyl-1-tosylaziridine (0.273 g, 1 mmol) was added to a dry 25 mL round bottom flask with stir bar. 4-iodobenzonitrile (1.83 g, 8.00 mmol) was added to the flask by syringe and the resulting solution was stirred vigorously while Zn(OTf)₂ was added (0.361 g, 1 mmol) as a solid. The solution was stirred at 65°C until all starting aziridine was consumed (3 hours). The reaction was then extracted into CHCl₃ and washed with saturated NaHCO₃ solution (3 x 15 mL). The solution was then washed saturated NaCl (3 x 15 mL) before being dried over anhydrous Na₂SO₄ and reduced *in vacuo* to give crude product purified by column chromatography, 1.5:8.5 (EtOAc:Hexanes) to give the product as a white paste 74 % yield (0.373 g, 0.74 mmol).

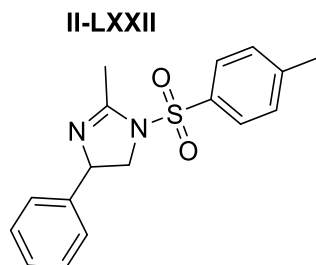
Spectroscopy:

¹H NMR (500 MHz, CDCl₃) δ 7.84 – 7.77 (m, 2H), 7.57 – 7.46 (m, 2H), 7.45 – 7.35 (m, 2H), 7.37 – 7.26 (m, 1H), 7.25 – 7.18 (m, 4H), 6.98 – 6.90 (m, 2H), 4.97 (dd, *J* = 9.9, 8.1 Hz, 1H), 4.47 – 4.38 (m, 1H), 3.89 – 3.81 (m, 1H), 2.44 (s, 3H).

¹³C NMR (125 MHz, CDCl₃) δ 159.27, 144.92, 141.21, 137.01, 134.18, 131.39, 129.92, 129.73, 128.64, 127.58, 127.52, 126.29, 98.20, 67.95, 56.88, 21.66.

IR (FT-ATR) cm^{-1} : 3145, 2988, 1654, 1498, 1088, 1026

HRMS calculated for $\text{C}_{22}\text{H}_{20}\text{IN}_2\text{O}_2\text{S}$ ($\text{M}+\text{H}$)⁺ 503.0290. Found 503.0306.



2-methyl-4-phenyl-1-tosyl-4,5-dihydro-1H-imidazole:

2-phenyl-1-tosylaziridine (0.273 g, 1 mmol) was added to a dry 25 mL round bottom flask with stir bar. Acetonitrile (3.144 g, 76.59 mmol) was added to the flask by syringe and the resulting solution was stirred vigorously while $\text{Zn}(\text{OTf})_2$ was added (0.361 g, 1 mmol) as a solid. The solution was stirred at 65°C until all starting aziridine was consumed (3 hours). The reaction was then extracted into CHCl_3 and washed with saturated NaHCO_3 solution (3 x 15 mL). The solution was then washed saturated NaCl (3 x 15 mL) before being dried over anhydrous Na_2SO_4 and reduced *in vacuo* to give crude product purified by column chromatography, 3:7 (EtOAc:Hexanes) to give the product as a yellow oil, 77 % yield (0.240 g, 0.768 mmol).

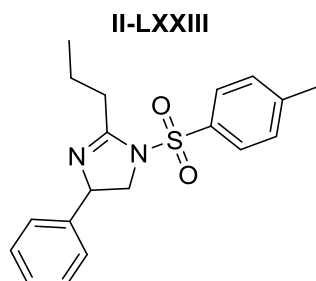
Spectroscopy:

^1H NMR (500 MHz, CDCl_3) δ 7.80 – 7.66 (m, 2H), 7.33 (d, $J = 8.1$ Hz, 2H), 7.29 – 7.19 (m, 3H), 7.08 – 6.93 (m, 2H), 4.97 (ddd, $J = 10.2, 8.0, 1.9$ Hz, 1H), 4.16 (t, $J = 10.1$ Hz, 1H), 3.61 (dd, $J = 9.8, 7.8$ Hz, 1H), 2.44 (s, 3H), 2.38 (d, $J = 1.7$ Hz, 3H).

^{13}C NMR (125 MHz, CDCl_3) δ 156.43, 144.80, 141.55, 135.09, 130.15, 128.69, 127.64, 127.22, 126.40, 66.60, 55.51, 21.62, 16.84.

IR (FT-ATR) cm^{-1} : 3017, 2957, 1637, 1433, 1059, 1024

HRMS-ESI (m/z), calculated for $\text{C}_{17}\text{H}_{19}\text{N}_2\text{O}_2\text{S}$ ($\text{M}+\text{H}$)⁺ 315.1167. Found 315.1196



4-phenyl-2-propyl-1-tosyl-4,5-dihydro-1H-imidazole:

2-phenyl-1-tosylaziridine (0.273 g, 1 mmol) was added to a dry 25 mL round bottom flask with stir bar. butyronitrile (3.00 g, 43.41 mmol) was added to the flask by syringe and the resulting solution was stirred vigorously while $\text{Zn}(\text{OTf})_2$ was added (0.361 g, 1 mmol) as a solid. The solution was stirred at 65°C until all starting aziridine was consumed (3 hours). The reaction was then extracted into CHCl_3 and washed with saturated NaHCO_3 solution (3 x 15 mL). The solution was then washed saturated NaCl (3 x 15 mL) before being dried over anhydrous Na_2SO_4 and reduced *in vacuo* to give crude product purified by column chromatography, 3:7 (EtOAc:Hexanes) to give the product as a clear oil, 85 % yield (0.291 g, 0.850 mmol).

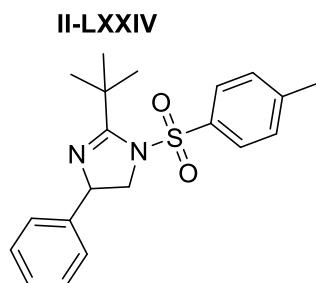
Spectroscopy:

^1H NMR (500 MHz, CDCl_3) δ 7.76 – 7.70 (m, 2H), 7.36 – 7.30 (m, 2H), 7.28 – 7.18 (m, 3H), 7.04 – 6.98 (m, 2H), 4.98 (ddd, $J = 10.1, 7.9, 1.6$ Hz, 1H), 4.15 (t, $J = 10.1$ Hz, 1H), 3.59 (dd, $J = 10.0, 7.8$ Hz, 1H), 2.81 – 2.66 (m, 2H), 2.45 (s, 3H), 1.86 – 1.74 (m, 2H), 1.02 (t, $J = 7.4$ Hz, 3H).

^{13}C NMR (125 MHz, CDCl_3) δ 159.71, 144.65, 141.87, 135.20, 130.07, 128.62, 127.53, 127.22, 126.40, 66.75, 55.69, 31.74, 21.61, 20.21, 13.93.

IR (FT-ATR) cm^{-1} : 3168, 2912, 1627, 1096, 1042

HRMS-ESI (m/z), calculated for $\text{C}_{19}\text{H}_{23}\text{N}_2\text{O}_2\text{S}$ ($\text{M}+\text{H}$)⁺ 343.1480. Found 343.1539



2-(tert-butyl)-4-phenyl-1-tosyl-4,5-dihydro-1H-imidazole:

2-phenyl-1-tosylaziridine (0.273 g, 1 mmol) was added to a dry 25 mL round bottom flask with stir bar. Trimethylacetonitrile (2.49 g, 30 mmol) was added to the flask by syringe and the resulting solution was stirred vigorously while $\text{Zn}(\text{OTf})_2$ was added (0.361 g, 1 mmol) as a solid. The solution was stirred at 65°C until all starting aziridine was consumed (3 hours). The reaction was then extracted into CHCl_3 and washed with saturated NaHCO_3 solution (3 x 15 mL). The solution was then washed saturated NaCl (3 x 15 mL) before being dried over anhydrous Na_2SO_4 and reduced *in vacuo* to give crude product purified by column chromatography, 1.5:8.5 (EtOAc:Hexanes) to give the product as a clear oil, 77 % yield (0.275 g, 0.771 mmol).

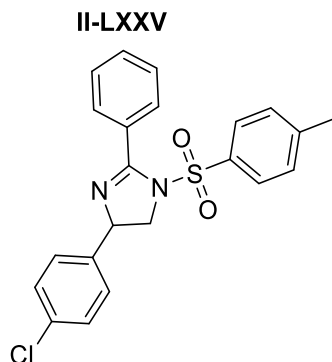
Spectroscopy:

^1H NMR (500 MHz, CDCl_3 -*d*) δ 7.75 – 7.69 (m, 2H), 7.28 – 7.17 (m, 5H), 7.08 – 7.02 (m, 2H), 4.80 – 4.72 (m, 1H), 4.11 (dd, $J = 10.8, 9.4$ Hz, 1H), 3.57 (dd, $J = 10.8, 8.5$ Hz, 1H), 2.41 (s, 3H), 1.54 (s, 9H).

^{13}C NMR (125 MHz, CDCl_3) δ 167.65, 144.29, 141.46, 136.41, 129.84, 128.56, 127.40, 127.19, 126.33, 66.30, 58.34, 36.64, 29.38, 21.57.

IR (FT-ATR) cm^{-1} : 3038, 2857, 1648, 1496, 1063, 1014

HRMS-ESI (m/z), calculated for $\text{C}_{20}\text{H}_{25}\text{N}_2\text{O}_2\text{S}$ ($\text{M}+\text{H}$)⁺ 357.1637. Found 357.1794



4-(4-chlorophenyl)-2-phenyl-1-tosyl-4,5-dihydro-1H-imidazole:

2-(4-chlorophenyl)-1-tosylaziridine (0.308 g, 1 mmol) was added to a dry 25 mL round bottom flask with stir bar. Benzonitrile (5.00 g, 48.49 mmol) was added to the flask by syringe and the resulting solution was stirred vigorously while $\text{Zn}(\text{OTf})_2$ was added (0.361 g, 1 mmol) as a solid. The solution was stirred at 65°C until all starting aziridine was consumed (3 hours). The reaction was then extracted into CHCl_3 and washed with saturated NaHCO_3 solution (3 x 15 mL). The solution was then washed saturated NaCl (3 x 15 mL) before being dried over anhydrous Na_2SO_4 and reduced *in vacuo* to give crude product purified by column chromatography, 3:7 (EtOAc:Hexanes) to give the product as a clear oil, 75 % yield (0.308 g, 0.752 mmol).

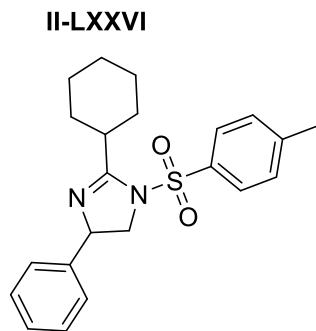
Spectroscopy:

^1H NMR (500 MHz, CDCl_3) δ 7.82 – 7.76 (m, 2H), 7.58 – 7.51 (m, 1H), 7.49 – 7.42 (m, 2H), 7.40 – 7.34 (m, 2H), 7.21 – 7.14 (m, 4H), 6.94 – 6.87 (m, 2H), 4.99 (dd, $J = 10.0, 7.4$ Hz, 1H), 4.43 (dd, $J = 11.5, 10.0$ Hz, 1H), 3.84 (dd, $J = 11.5, 7.4$ Hz, 1H), 2.42 (s, 3H).

^{13}C NMR (125 MHz, CDCl_3) δ 160.35, 144.91, 140.30, 134.30, 133.14, 131.39, 130.00, 129.88, 129.78, 128.67, 127.81, 127.61, 127.54, 66.95, 56.79, 21.62.

IR (FT-ATR) cm^{-1} : 3028, 2932, 1636, 1462, 1031, 1011.

HRMS-ESI (m/z), calculated for $\text{C}_{22}\text{H}_{20}\text{ClN}_2\text{O}_2\text{S}$ ($\text{M}+\text{H}$) $^+$ 411.0934. Found 411.0964.



2-cyclohexyl-4-phenyl-1-tosyl-4,5-dihydro-1H-imidazole:

2-phenyl-1-tosylaziridine (0.273 g, 1 mmol) was added to a dry 25 mL round bottom flask with stir bar. cyclohexanecarbonitrile (3.56 g, 30 mmol) was added to the flask by syringe and the resulting solution was stirred vigorously while $\text{Zn}(\text{OTf})_2$ was added (0.361 g, 1 mmol) as a solid. The solution was stirred at 65°C until all starting aziridine was consumed (3 hours). The reaction was then extracted into CHCl_3 and washed with saturated NaHCO_3 solution (3 x 15 mL). The solution was then washed saturated NaCl (3 x 15 mL) before being dried over anhydrous Na_2SO_4 and reduced *in vacuo* to give crude product purified by column chromatography, 3:7 (EtOAc:Hexanes) to give the product as a clear oil, 82 % yield (0.310 g, 0.82 mmol).

Spectroscopy:

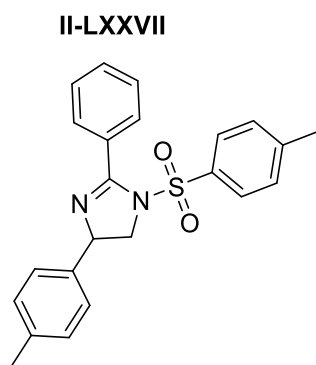
^1H NMR (500 MHz, CDCl_3) δ 7.72 – 7.68 (m, 2H), 7.35 – 7.27 (m, 5H), 7.19 (dd, $J = 7.1, 1.7$ Hz, 2H), 6.39 (d, $J = 7.4$ Hz, 1H), 5.09 – 5.00 (m, 2H), 3.34 – 3.21 (m, 2H), 2.42 (s, 3H), 2.13 (tt, $J =$

11.8, 3.5 Hz, 1H), 1.92 – 1.83 (m, 2H), 1.82 – 1.75 (m, 2H), 1.49 – 1.38 (m, 2H), 1.29 – 1.22 (m, 2H).

^{13}C NMR (125 MHz, CDCl_3) δ 176.48, 143.65, 138.77, 136.76, 129.81, 128.99, 128.00, 126.98, 126.34, 52.35, 48.24, 45.38, 29.63, 29.48, 25.70, 25.66, 21.53.

IR (FT-ATR) cm^{-1} : 3120, 2865 1637, 1462, 1058, 1032

HRMS-ESI (m/z), calculated for $\text{C}_{22}\text{H}_{27}\text{N}_2\text{O}_2\text{S}$ (M+H) $^+$ 383.1793. Found 383.1895.



2-phenyl-4-(p-tolyl)-1-tosyl-4,5-dihydro-1H-imidazole:

2-phenyl-1-tosylaziridine (0.273 g, 1 mmol) was added to a dry 25 mL round bottom flask with stir bar. Benzonitrile (5.00 g, 48.49 mmol) was added to the flask by syringe and the resulting solution was stirred vigorously while $\text{Zn}(\text{OTf})_2$ was added (0.361 g, 1 mmol) as a solid. The solution was stirred at 65°C until all starting aziridine was consumed (3 hours). The reaction was then extracted into CHCl_3 and washed with saturated NaHCO_3 solution (3 x 15 mL). The solution was then washed saturated NaCl (3 x 15 mL) before being dried over anhydrous Na_2SO_4 and reduced *in vacuo* to give crude product purified by column chromatography, 3:7 (EtOAc:Hexanes) to give the product as a clear oil, 70 % yield (0.273 g, 0.700 mmol).

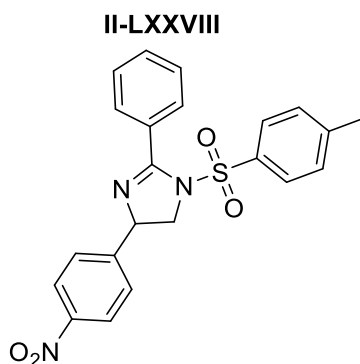
Spectroscopy:

^1H NMR (500 MHz, CDCl_3) δ 7.81 – 7.72 (m, 2H), 7.56 – 7.48 (m, 1H), 7.48 – 7.38 (m, 4H), 7.28 – 7.17 (m, 2H), 7.03 (d, $J = 7.8$ Hz, 2H), 6.89 – 6.83 (m, 2H), 4.95 (dd, $J = 9.9, 8.1$ Hz, 1H), 4.41 (dd, $J = 11.4, 9.9$ Hz, 1H), 3.84 (dd, $J = 11.4, 8.1$ Hz, 1H), 2.43 (s, 3H), 2.31 (s, 3H),

^{13}C NMR (125 MHz, CDCl_3) δ 159.62, 144.63, 138.57, 137.09, 134.48, 131.12, 130.23, 129.84, 129.74, 129.23, 127.71, 127.61, 126.25, 67.70, 56.96, 21.63, 21.10.

IR (FT-ATR) cm^{-1} : 3110, 3056, 2918, 1617, 1069, 1036.

HRMS-ESI (m/z), calculated for $\text{C}_{23}\text{H}_{23}\text{N}_2\text{O}_2\text{S}$ ($\text{M}+\text{H}$) $^+$ 391.1485. Found 391.1498.



4-(4-nitrophenyl)-2-phenyl-1-tosyl-4,5-dihydro-1H-imidazole:

2-(4-nitrophenyl)-1-tosylaziridine (0.319 g, 1 mmol) was added to a dry 25 mL round bottom flask with stir bar. Benzonitrile (4.00 g, 39.00 mmol) was added to the flask by syringe and the resulting solution was stirred vigorously while $\text{Zn}(\text{OTf})_2$ was added (0.361 g, 1 mmol) as a solid. The solution was stirred at 65°C until all starting aziridine was consumed (3 hours). The reaction was then extracted into CHCl_3 and washed with saturated NaHCO_3 solution (3 x 15 mL). The solution was then washed saturated NaCl (3 x 15 mL) before being dried over anhydrous Na_2SO_4 and reduced *in vacuo* to give crude product purified by column chromatography, 3:7 (EtOAc:Hexanes) to give the product as a yellow solid 52 % yield (0.220 g, 0.522 mmol).

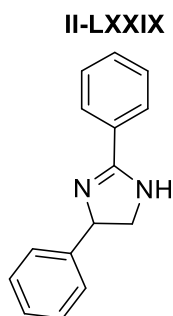
Spectroscopy:

^1H NMR (500 MHz, CDCl_3) δ 8.13 – 8.04 (m, 2H), 7.84 – 7.77 (m, 2H), 7.65 – 7.55 (m, 1H), 7.52 – 7.44 (m, 2H), 7.40 – 7.32 (m, 2H), 7.23 – 7.13 (m, 4H), 5.17 (dd, $J = 10.2, 7.3$ Hz, 1H), 4.59 – 4.49 (m, 1H), 3.95 – 3.82 (m, 1H), 2.41 (s, 3H).

^{13}C NMR (125 MHz, CDCl_3) δ 145.41, 132.10, 130.03, 129.89, 128.00, 127.57, 127.13, 123.86, 56.45, 21.60.

IR (FT-ATR) cm^{-1} : 3094, 2945, 1655, 1595, 1053

HRMS-ESI (m/z), calculated for $\text{C}_{22}\text{H}_{19}\text{N}_3\text{O}_4\text{S}$ ($\text{M}+\text{H}$) $^+$ 422.1175. Found 422.1364.



2,4-diphenyl-4,5-dihydro-1H-imidazole:

Naphthalene (0.577 g, 4.5 mmol) was added to a round bottom flask. Anhydrous THF (30 mL) was added to the flask by syringe and the resulting solution is stirred vigorously as Na° (0.104 g, 4.5 mmol) was added. The reaction was allowed to stir for 1 hour to generate the naphthyl anion after which 2,4-diphenyl-1-tosyl-4,5-dihydro-1H-imidazole (0.376 g, 1 mmol) was added to a 100 mL round bottom flask. The reaction was stirred for 4 hours at room temperature and then the solvent was removed *in vacuo*. 5 mL of H_2O was added and the reaction was adjusted to a pH = 9. The solution was extracted into CHCl_3 (30 mL) and washed with saturated NaCl solution (3 x 20 mL), dried over anhydrous Na_2SO_4 and reduced to give a crude oil purified by column

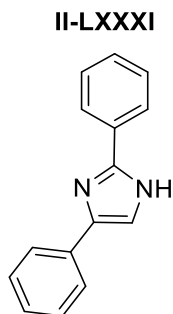
chromatography on TEA neutralized silica (1:9 MeOH:DCM) to give a yellow oil, 56 % yield (0.12 g, 0.564 mmol).

Spectroscopy:

^1H NMR (500 MHz, CDCl_3) δ 8.11 – 7.97 (m, 2H), 7.56 – 7.46 (m, 1H), 7.44 – 7.34 (m, 2H), 7.34 – 7.16 (m, 5H), 6.73 (s, 1H), 5.05 (dd, $J = 11.4, 8.2$ Hz, 1H), 4.14 (t, $J = 11.8$ Hz, 1H), 3.66 (dd, $J = 12.1, 8.2$ Hz, 1H).

^{13}C NMR (125 MHz, CDCl_3) δ 164.46, 141.32, 132.97, 128.92, 128.89, 128.51, 128.18, 126.27, 125.44, 62.18, 55.87.

HRMS-ESI (m/z), calculated for $\text{C}_{15}\text{H}_{15}\text{N}_2$ ($\text{M}+\text{H}$) $^+$ 223.1240. Found 223.1279.



2,4-diphenyl-1H-imidazole:

2,4-diphenyl-1-tosyl-4,5-dihydro-1H-imidazole (0.500 g, 1.33 mmol) was added to a 100 mL round bottom flask. 40 mL of Ethanol was added to the flask by syringe and the resulting solution is stirred vigorously as 60% by weight NaH (0.266 g, 6.65 mmol) was added. The reaction was refluxed for 5 hours. The solvent was removed in vacuo and the crude solid extracted into CHCl_3 (30 mL) and washed with saturated NaCl solution (3 x 20 mL). The organic layers were collected, dried over anhydrous Na_2SO_4 and reduced in vacuo to give a crude

product purified by column chromatography (3:7 EtOAc:Hexanes) to give a white solid 83 % yield (0.243 g, 1.10 mmol).

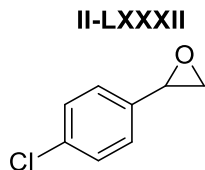
Spectroscopy:

^1H NMR (500 MHz, CDCl_3) δ 7.91 – 7.85 (m, 2H), 7.78 – 7.72 (m, 2H), 7.46 – 7.32 (m, 6H), 7.31 – 7.24 (m, 1H).

^{13}C NMR (125 MHz, CDCl_3) δ 147.00, 129.99, 128.90, 128.81, 128.75, 127.10, 125.27, 124.90.

IR (FT-ATR) cm^{-1} : 3285, 3027, 1602, 1593, 1435, 1020, 994

HRMS-ESI (m/z), calculated for $\text{C}_{15}\text{H}_{13}\text{N}_2$ ($\text{M}+\text{H}$) $^+$ 221.1080. Found 221.1095



2-(4-chlorophenyl)oxirane:

4-Chlorostyrene (5.00 g, 36.08 mmol) was added to a round bottom flask as a solid, and then dissolved in 100 mL of CHCl_3 . The resulting solution was cooled to 0°C by ice bath before the addition of 77% by weight mCPBA (8.89 g, 1.1 mmol) was added as a solid. The solution stirred at 0°C for 1 hour and at 4°C for an additional 23 hours. After which the suspension was washed with 10% Na_2CO_3 (2 X 50 mL), followed by saturated NaCl solution (2 X 50 mL). The organic layers were collected and dried over anhydrous Na_2SO_4 before being reduced *in vacuo* to yield product as a clear oil 74 % yield, (4.10 g, 26.70 mmol)

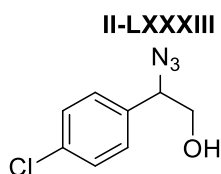
Spectroscopy:

^1H NMR (500 MHz, CDCl_3) δ 7.40 – 7.29 (m, 2H), 7.25 – 7.18 (m, 2H), 3.84 (dd, $J = 4.1, 2.6$ Hz, 1H), 3.15 (dd, $J = 5.5, 4.0$ Hz, 1H), 2.76 (dd, $J = 5.4, 2.5$ Hz, 1H).

^{13}C NMR (125 MHz, CDCl_3) δ 136.14, 133.92, 128.70, 126.82, 51.79, 51.28.

IR (FT-ATR) cm^{-1} : 3025, 2935, 1102, 1043

HRMS-ESI (m/z), calculated for $\text{C}_8\text{H}_8\text{ClO}$ ($\text{M}+\text{H}$) $^+$ 155.0265. Found 155.0284

**2-azido-2-(4-chlorophenyl)ethan-1-ol:**

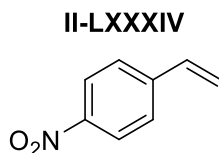
2-(4-chlorophenyl)oxirane (3.7 g, 23.94 mmol) was added to a round bottom flask, and to it 100 mL of a (8:1) $i\text{PrOH}:\text{H}_2\text{O}$ solution was added. The resulting solution was stirred vigorously as NH_4Cl (2.05 g, 38.29 mmol) was added as a solid, after which NaN_3 (6.225 g, 95.74 mmol) was added to the solution and the suspension was refluxed for 12 hours. The reaction was cooled to room temperature and 20 mL of Et_2O and 10 mL of H_2O were added. This solution was poured into 50 mL of Et_2O and washed with (2 X 60 mL) of saturated NaCl solution. The organic layers were collected, dried over anhydrous Na_2SO_4 and reduced in vacuo to give the crude product, which was purified by column chromatography (1:9) $\text{THF}:\text{Hexanes}$ to give a white solid 58 % yield (2.74 g, 20.35 mmol)

Spectroscopy:

^1H NMR (500 MHz, CDCl_3) δ 7.43 – 7.33 (m, 2H), 7.36 – 7.24 (m, 2H), 4.66 (dd, $J = 7.8, 4.9$ Hz, 1H), 3.79 – 3.67 (m, 2H), 1.92 (dd, $J = 7.5, 5.5$ Hz, 1H)

^{13}C NMR (125 MHz, CDCl_3) δ 134.79, 134.61, 129.15, 128.50, 67.09, 66.43.

HRMS: Product was not observed under HRMS-ESI ($\text{M}+\text{H}$) $^+$



1-nitro-4-vinylbenzene:

Methyltriphenylphosphonium bromide (10.65 g, 29.78 mmol) was added to a 250 mL round bottom flask. 100 mL of anhydrous DCM was added by syringe to the flask. To the suspension DBU (5.44 g, 35.73 mmol) was added by syringe and the suspension was refluxed for 2 hours. To this solution, 4-nitrobenzaldehyde (3.24 g, 21.44 mmol) was dissolved in 10 mL of anhydrous DCM and added by syringe. The reaction was refluxed for 20 hrs. The solution was washed with saturated NH_4Cl (2 x 50 mL) followed by saturated NaCl solution (2 x 50 mL). The organic layers were collected, dried over anhydrous Na_2SO_4 and reduced to give the crude product purified by column chromatography to give product as a yellow oil, 55 % yield (1.6 g, 10.72 mmol).

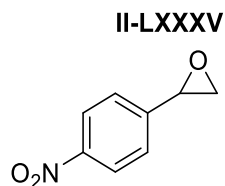
Spectroscopy:

^1H NMR (500 MHz, CDCl_3) δ 8.23 – 8.16 (m, 2H), 7.57 – 7.50 (m, 2H), 6.78 (dd, $J = 17.6, 10.9$ Hz, 1H), 5.93 (d, $J = 17.6$ Hz, 1H), 5.50 (d, $J = 10.9$ Hz, 1H).

^{13}C NMR (125 MHz, CDCl_3) δ 147.15, 143.78, 134.96, 126.79, 123.95, 118.59.

IR (FT-ATR) cm^{-1} : 3065, 1580, 1474

HRMS: Product was not observed under HRMS-ESI ($\text{M}+\text{H}$) $^+$



2-(4-nitrophenyl)oxirane:

4-Nitrostyrene (1.20 g, 8.15 mmol) was added to a round bottom flask as a solid, and then dissolved in 100 mL of CHCl_3 . The resulting solution was cooled to 0°C by ice bath before the addition of 77% by weight mCPBA (3.65 g, 21.2 mmol) was added as a solid. The solution stirred at 0°C for 1 hour and at 4°C for an additional 23 hours. After which the suspension was washed with 10% Na_2CO_3 (2 X 50 mL), followed by saturated NaCl solution (2 X 50 mL). The organic layers were collected and dried over anhydrous Na_2SO_4 before being reduced *in vacuo* to yield product as a pale yellow solid 88 % yield, (1.18 g, 7.15 mmol)

Spectroscopy:

^1H NMR (500 MHz, CDCl_3) δ 8.24 – 8.17 (m, 2H), 7.48 – 7.39 (m, 2H), 3.96 (dd, $J = 4.1, 2.4$ Hz, 1H), 3.23 (dd, $J = 5.5, 4.1$ Hz, 1H), 2.78 (dd, $J = 5.5, 2.5$ Hz, 1H).

^{13}C NMR (125 MHz, CDCl_3) δ 145.22, 126.21, 123.81, 51.70, 51.46.

IR (FT-ATR) cm^{-1} : 3023, 2963, 1474, 1204, 1156

HRMS-ESI (m/z), calculated for $\text{C}_8\text{H}_8\text{NO}_3$ ($\text{M}+\text{H}$) $^+$ 166.0508. Found 166.0598.

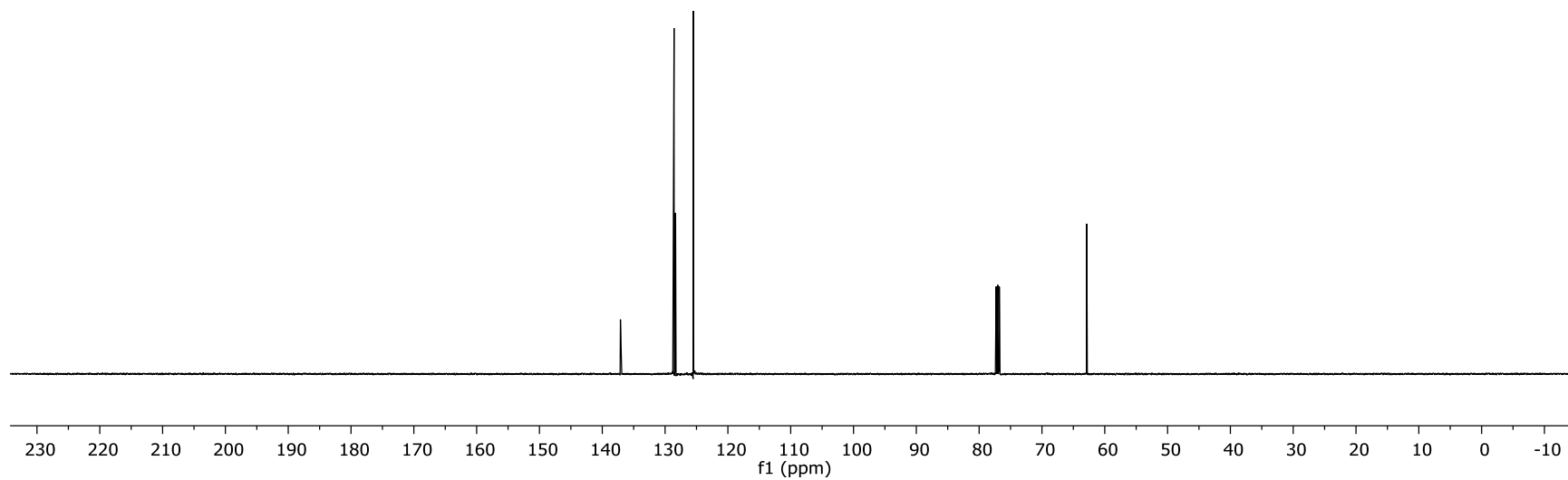
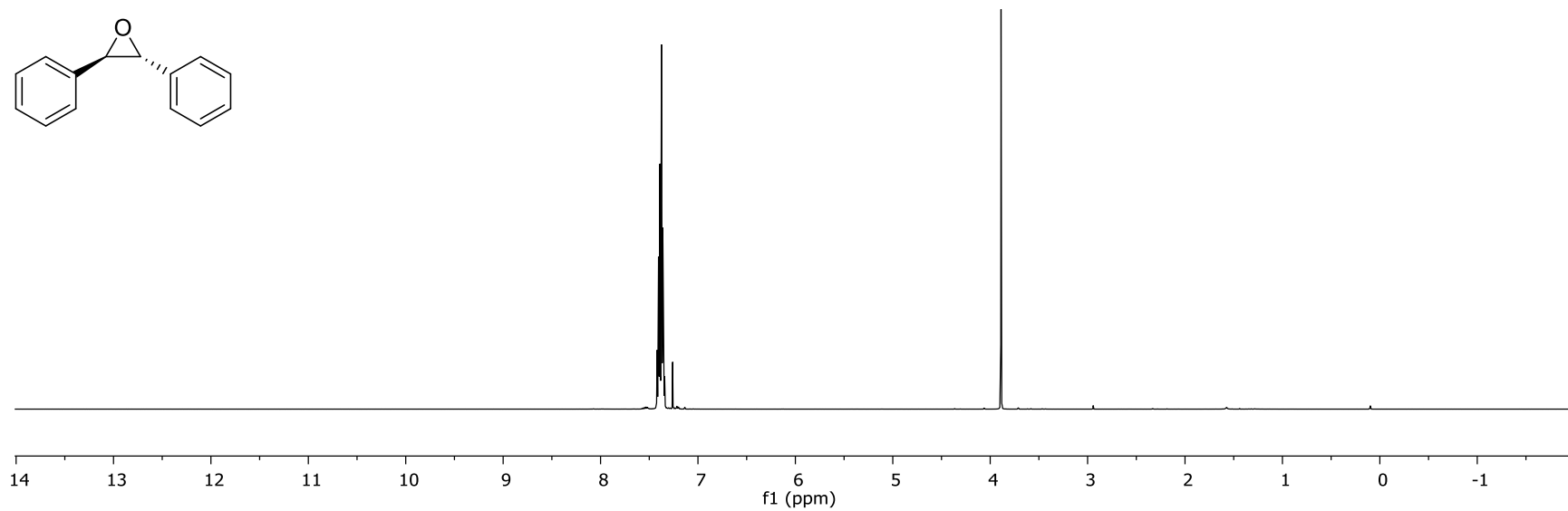
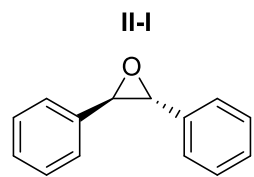


Figure II-XIX: The $^1\text{H NMR}$ and $^{13}\text{C NMR}$ for Compound II-I

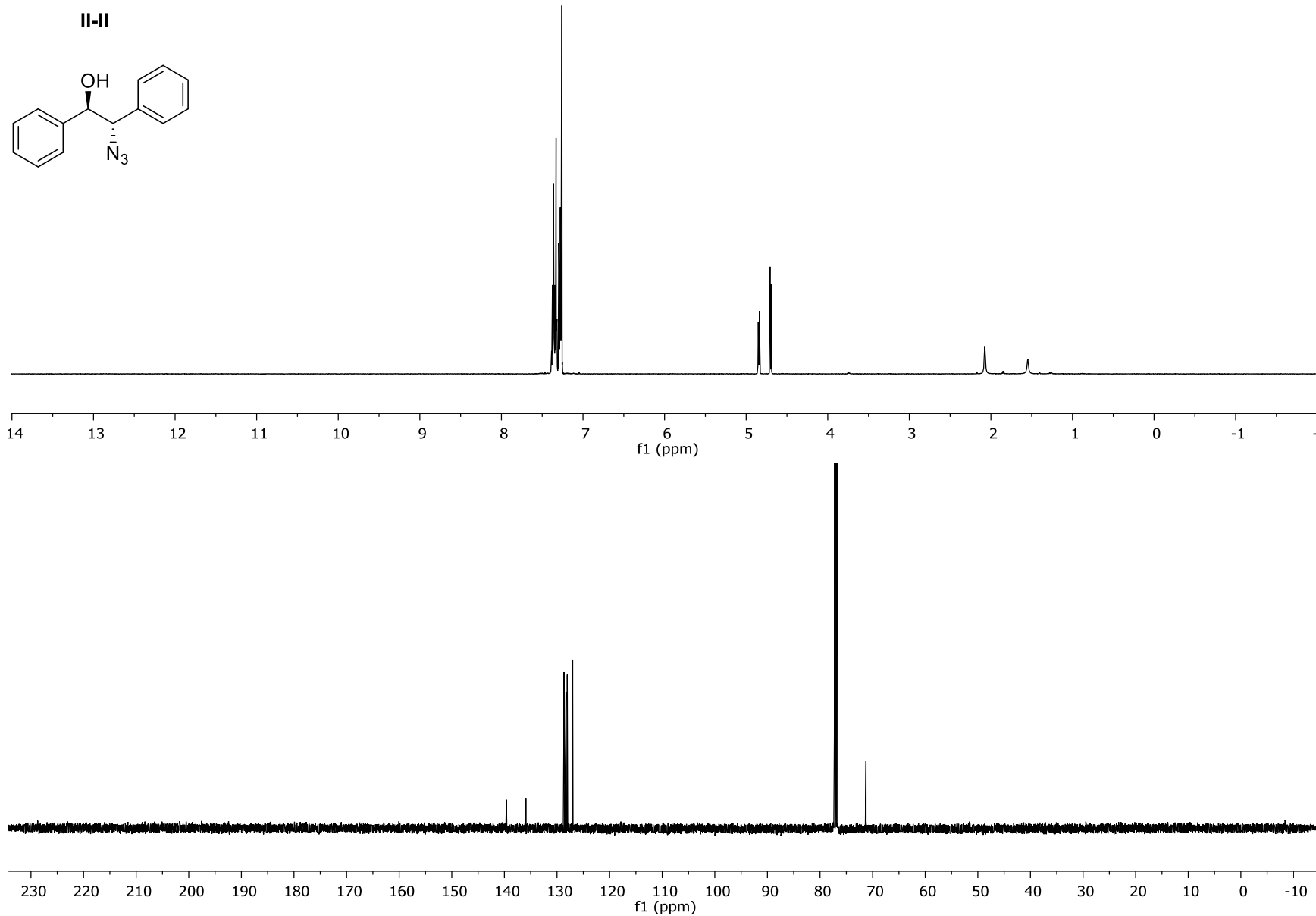


Figure II-XX: The ^1H NMR and ^{13}C NMR for Compound II-II

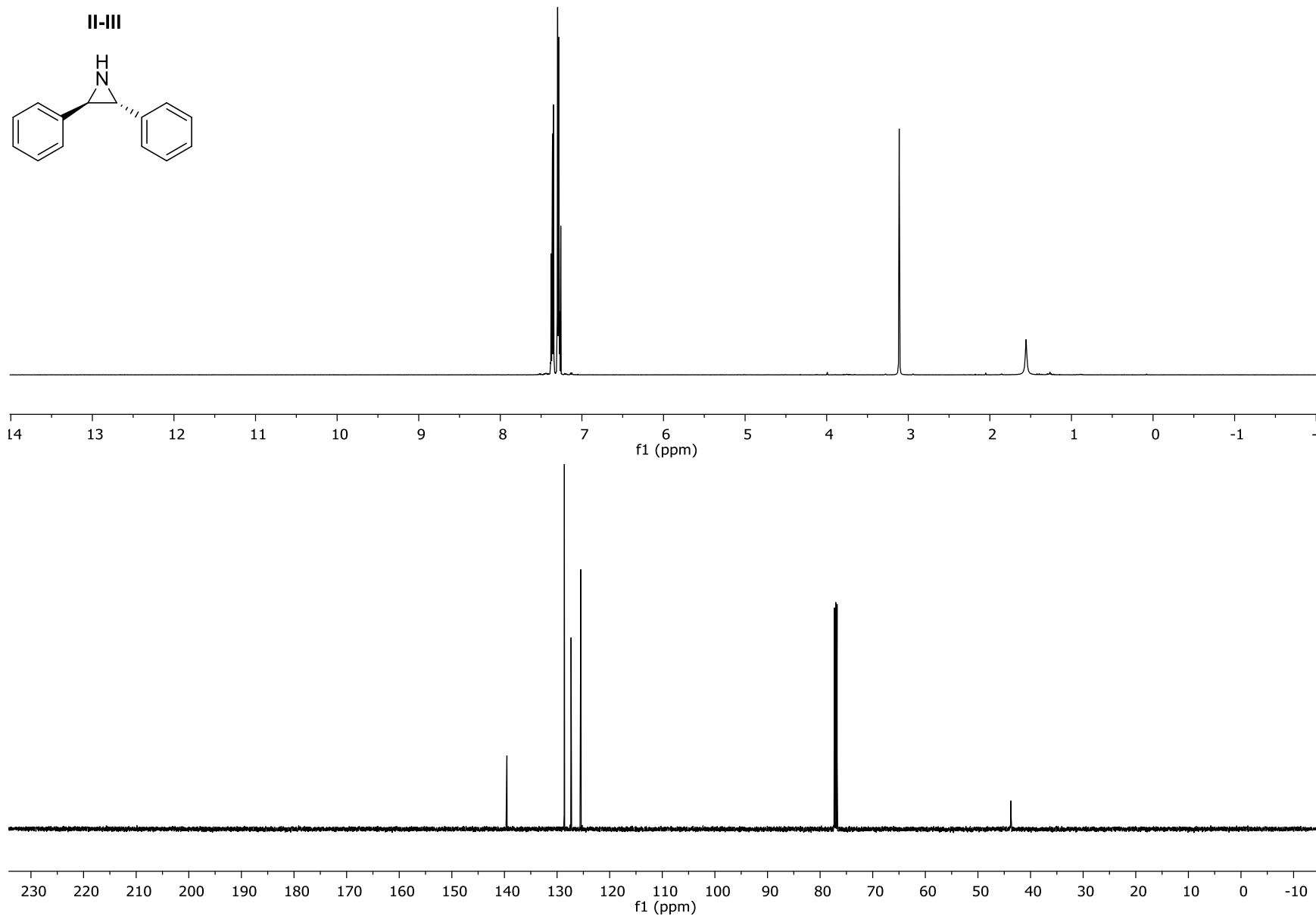


Figure II-XXI: The ^1H NMR and ^{13}C NMR for Compound **II-III**

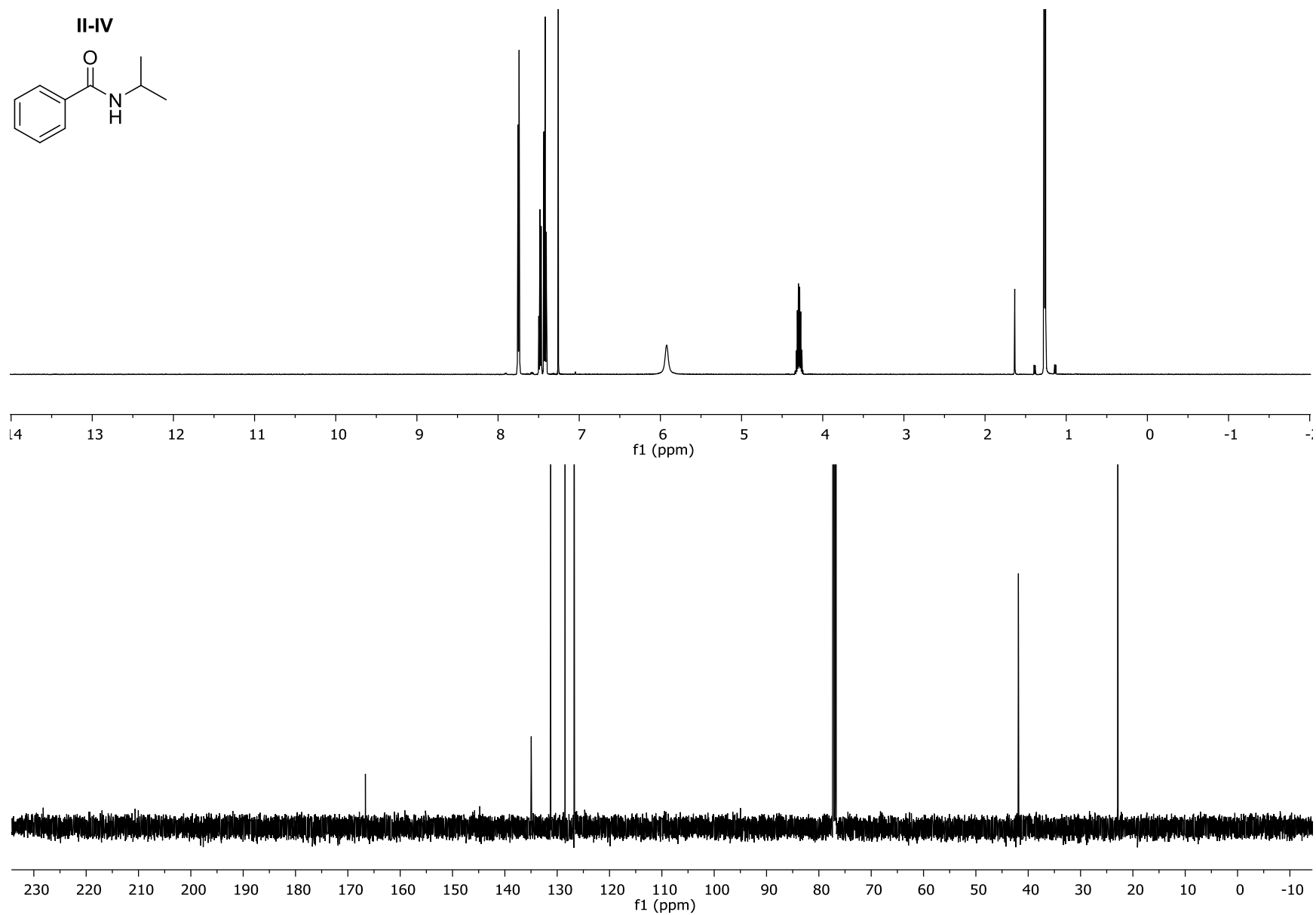
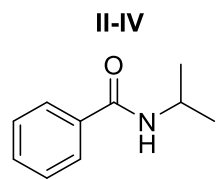


Figure II-XXII: The ^1H NMR and ^{13}C NMR for Compound II-IV

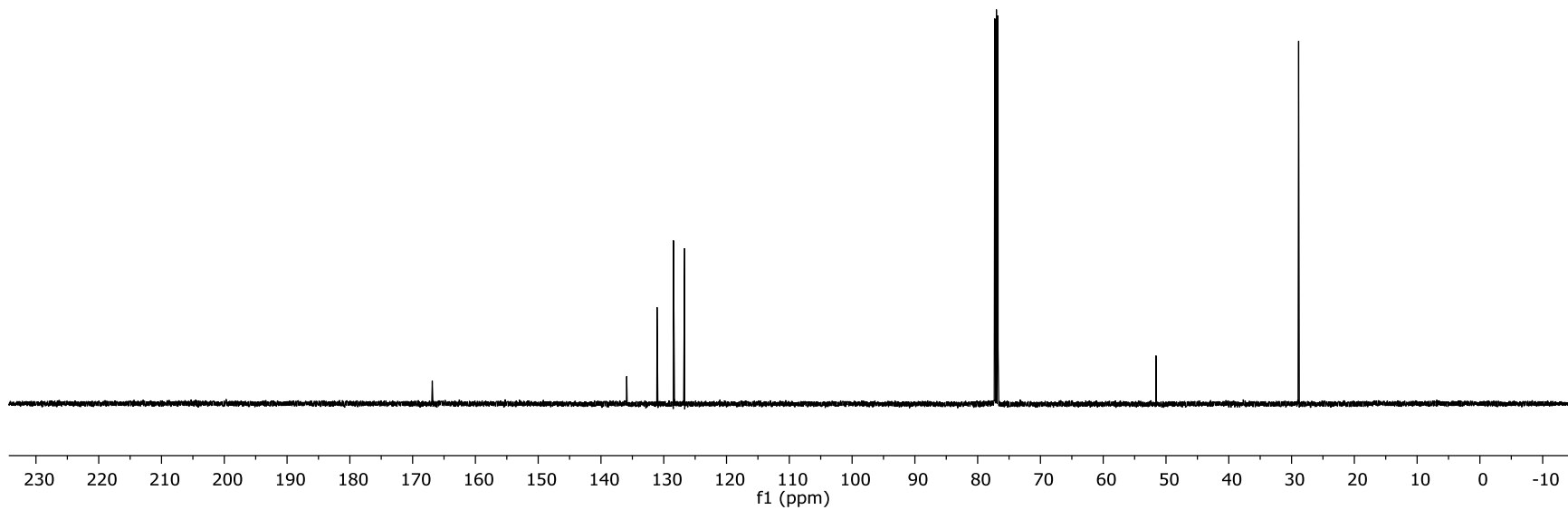
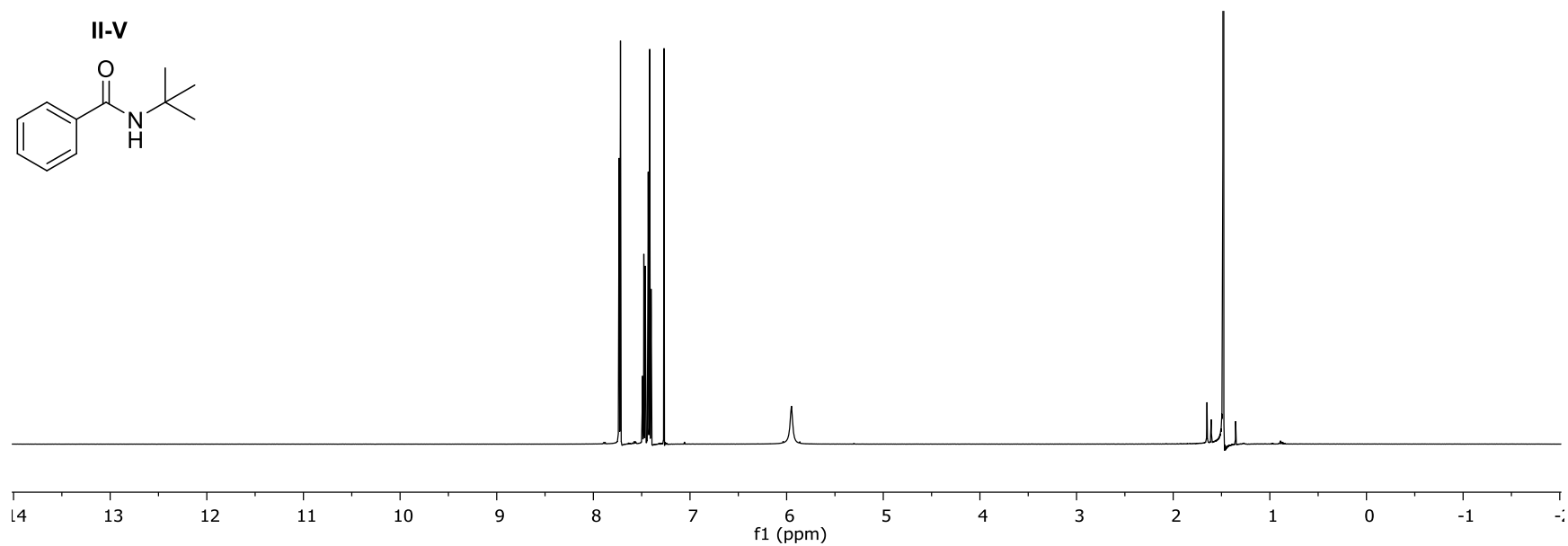
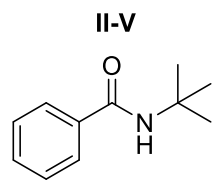


Figure II-XXIII: The $^1\text{H NMR}$ and $^{13}\text{C NMR}$ for Compound II-V

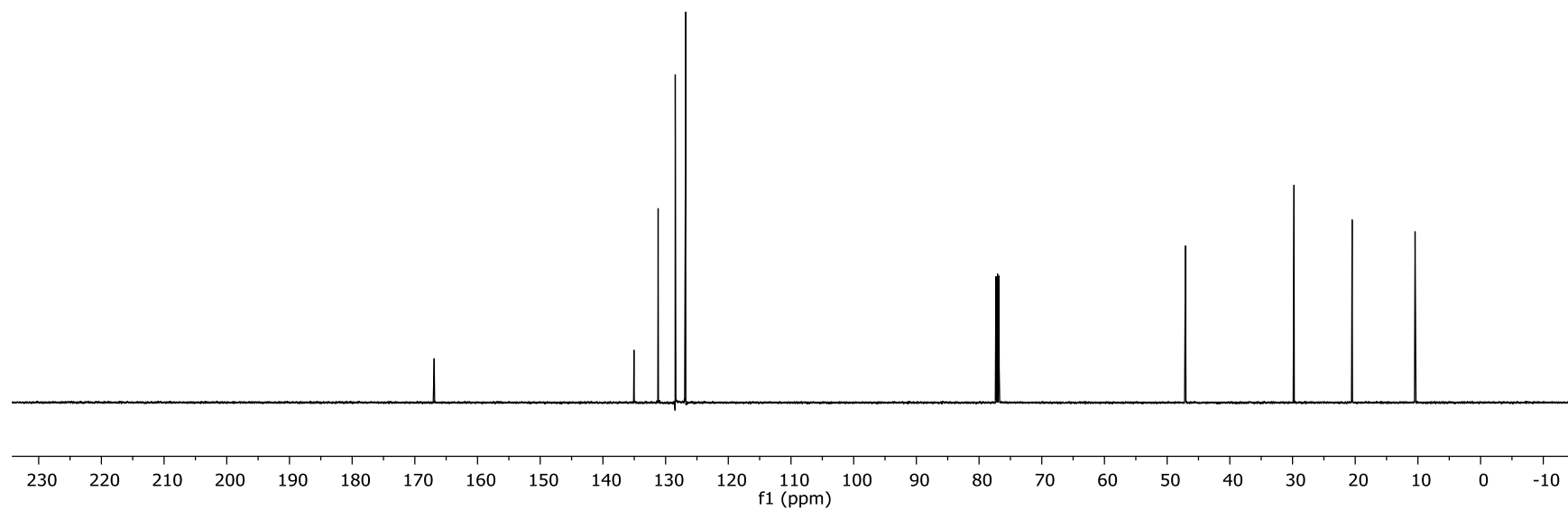
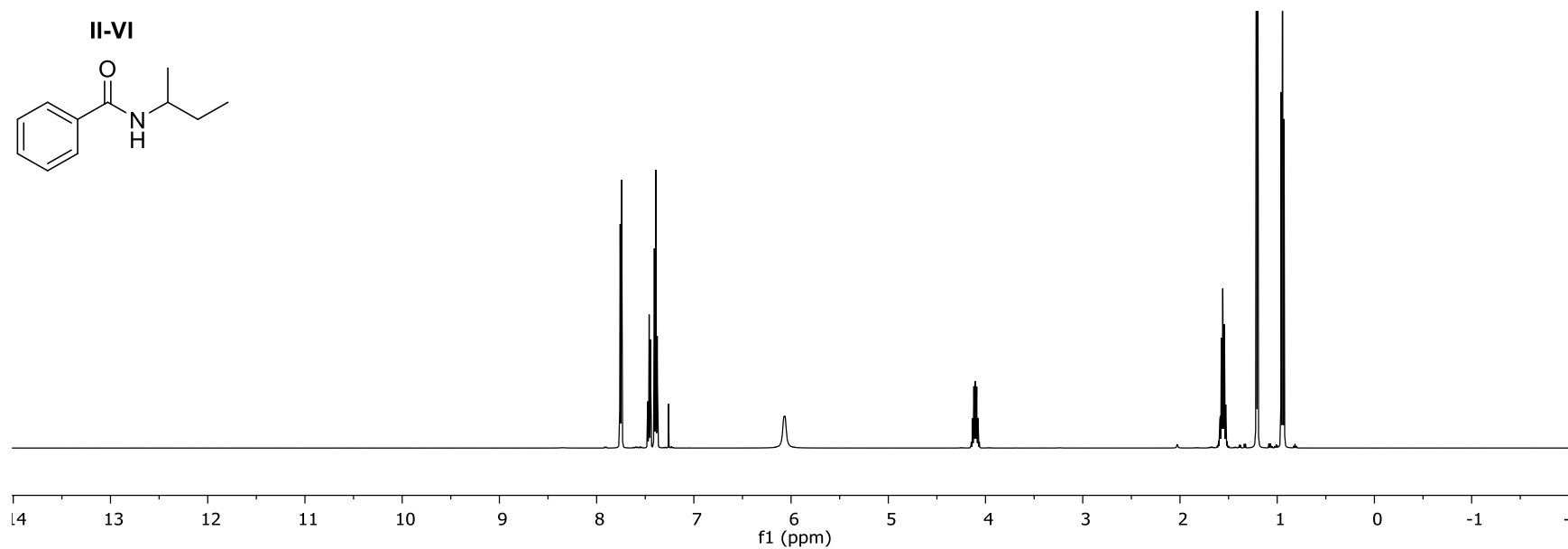
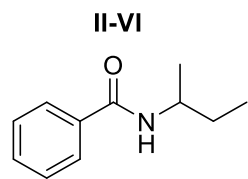


Figure II-XXIV: The ^1H NMR and ^{13}C NMR for Compound II-VI

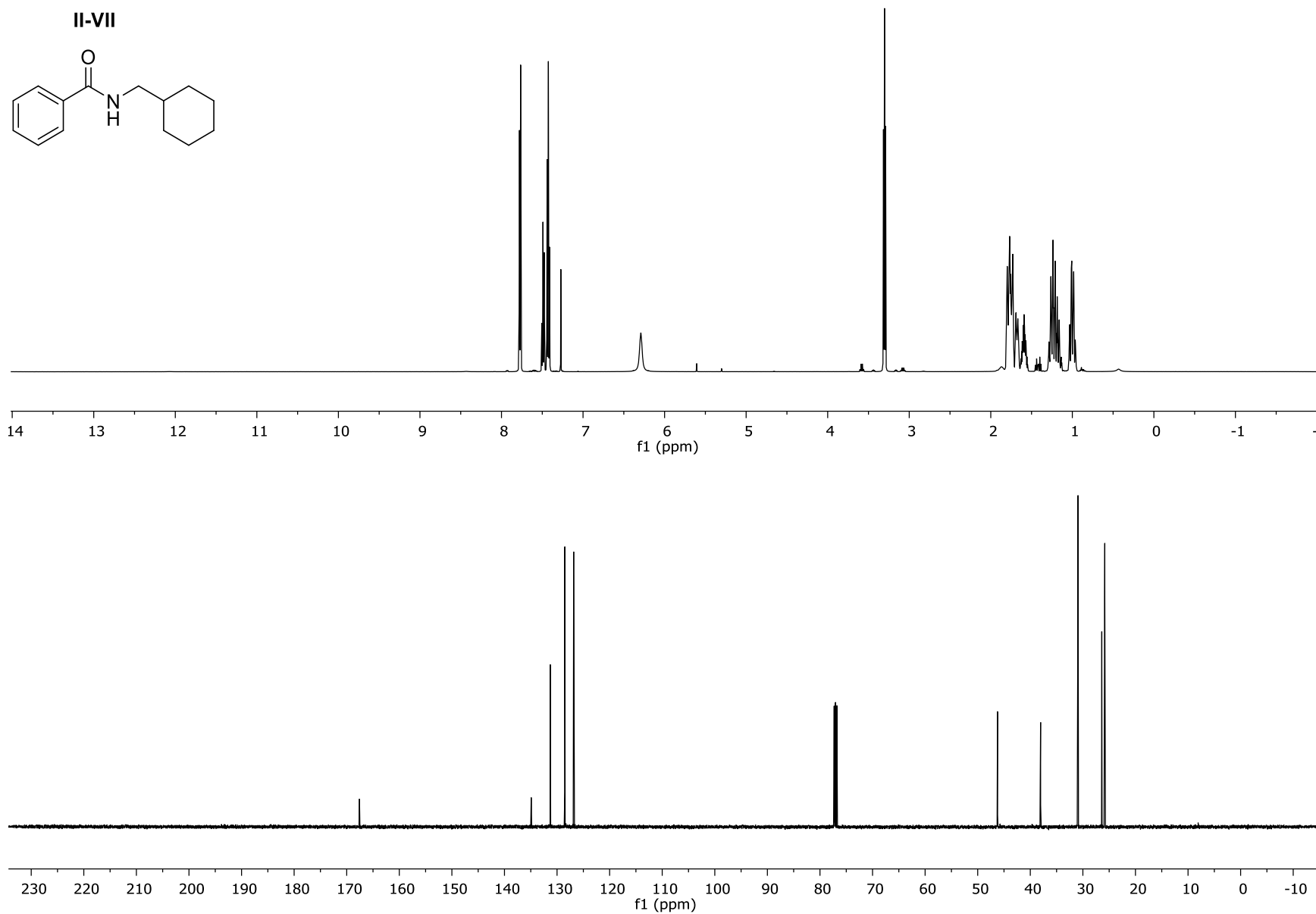


Figure II-XXV: The ^1H NMR and ^{13}C NMR for Compound II-VII

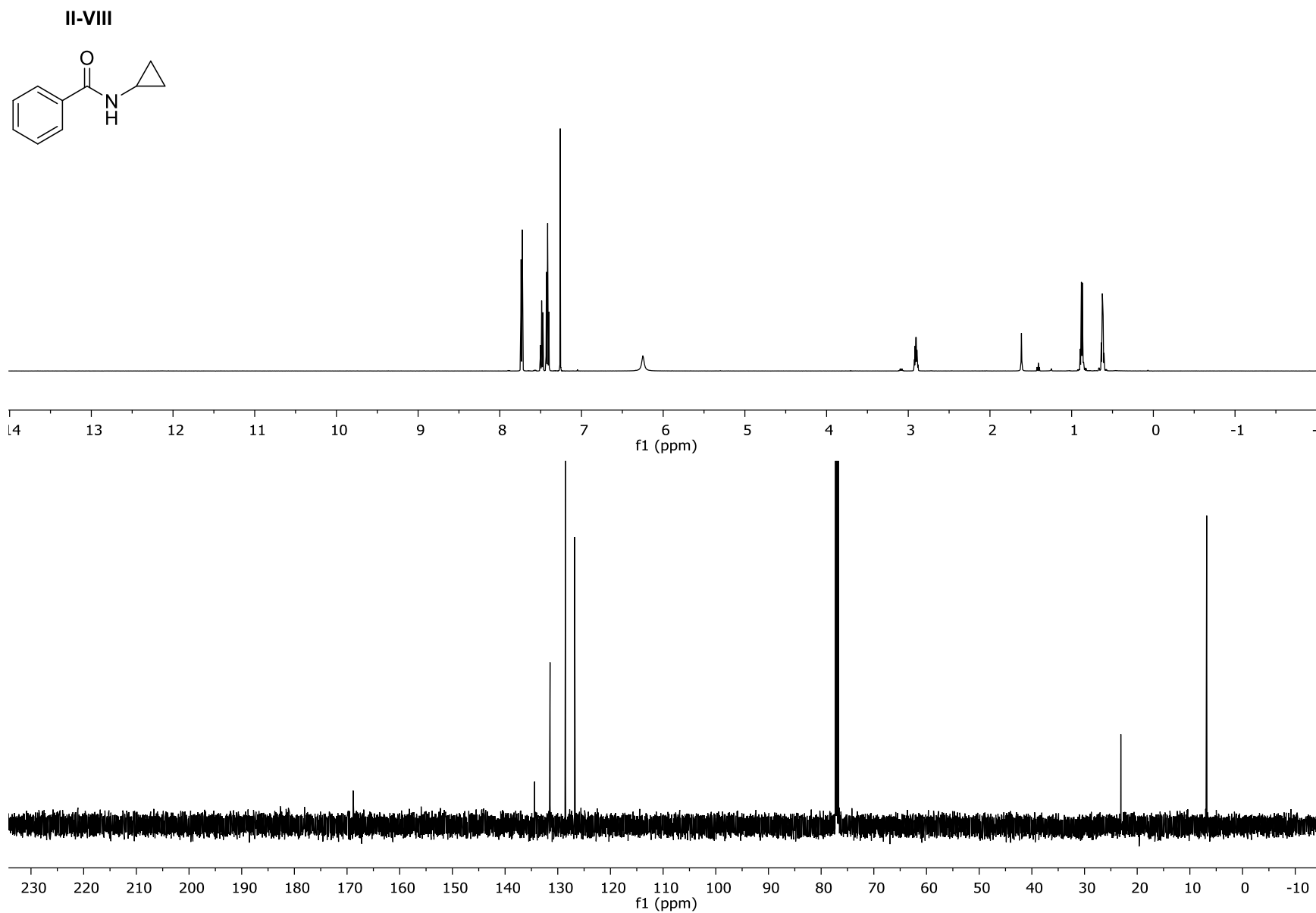


Figure II-XXVI: The ^1H NMR and ^{13}C NMR for Compound II-VIII

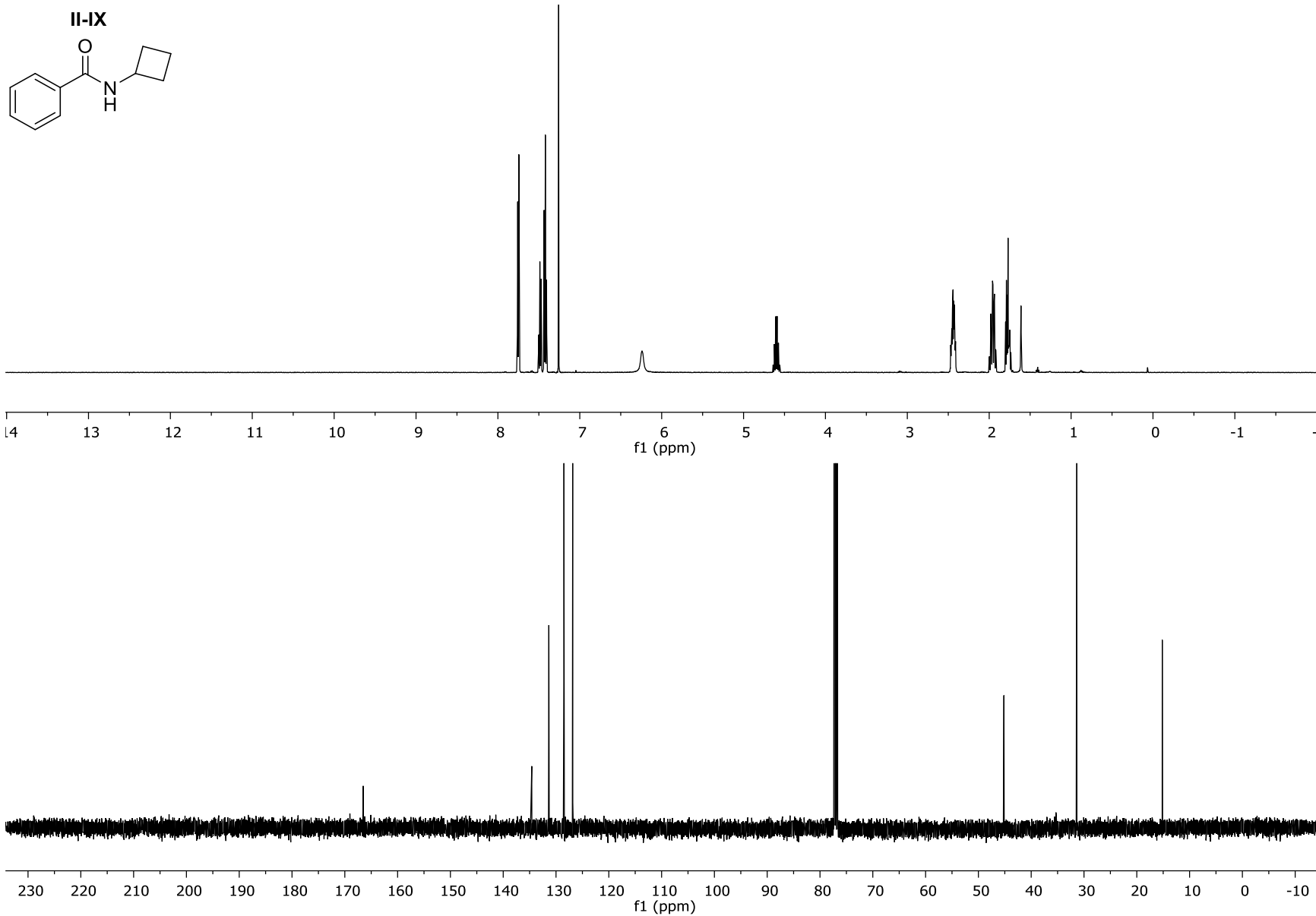


Figure II-XXVII: The ¹H NMR and ¹³C NMR for Compound II-IX

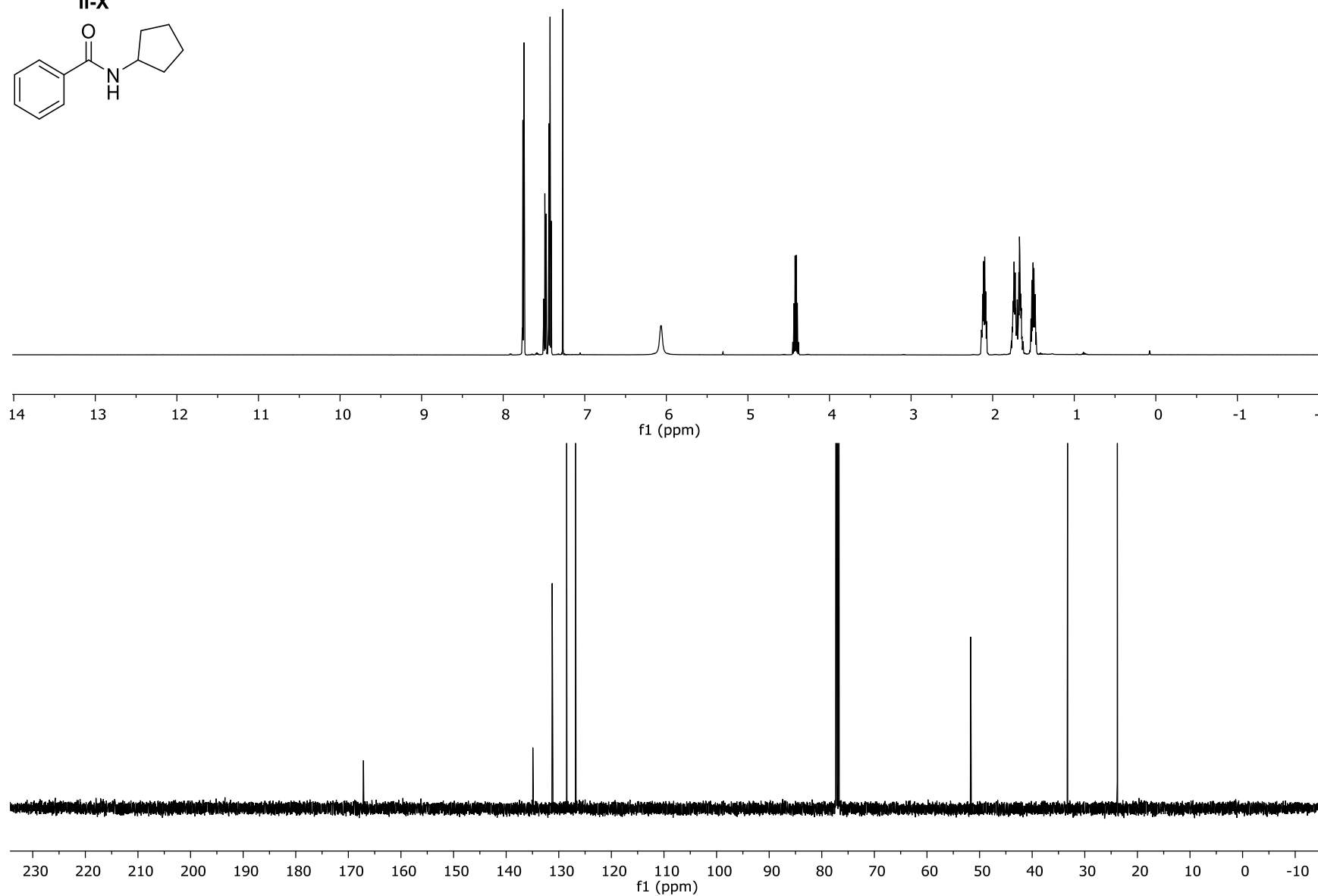
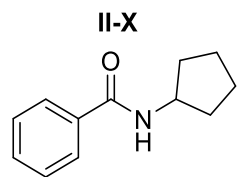


Figure II-XXVIII: The ^1H NMR and ^{13}C NMR for Compound **II-X**

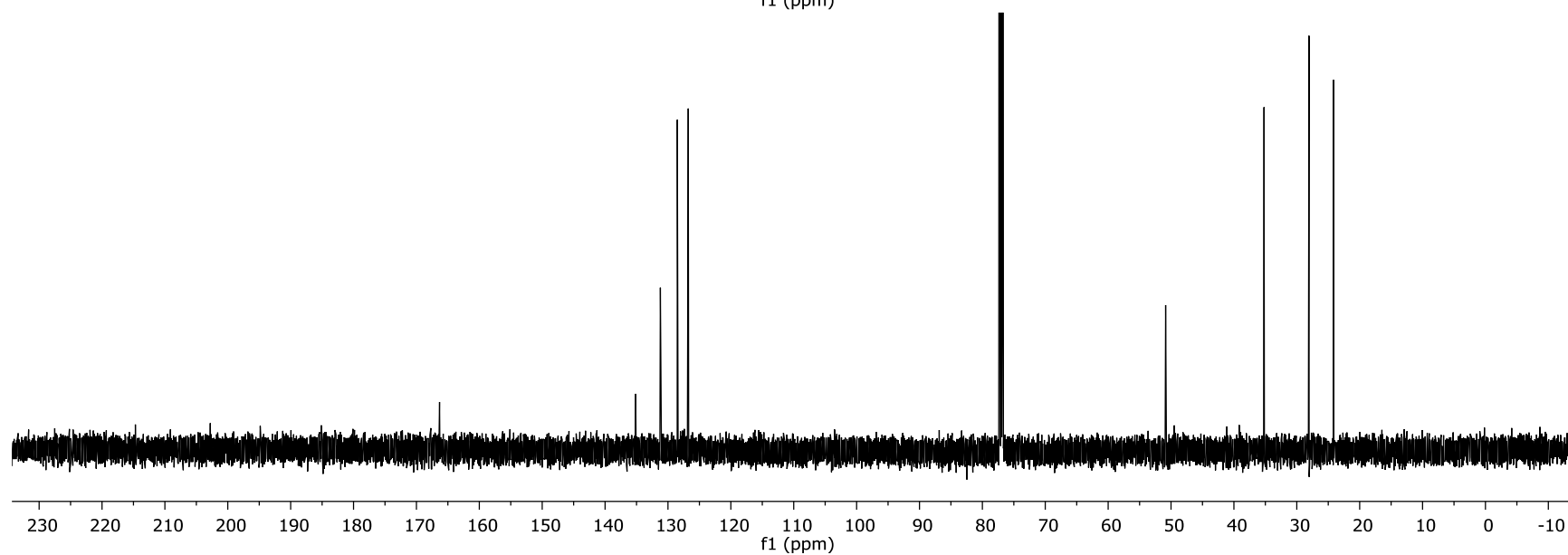
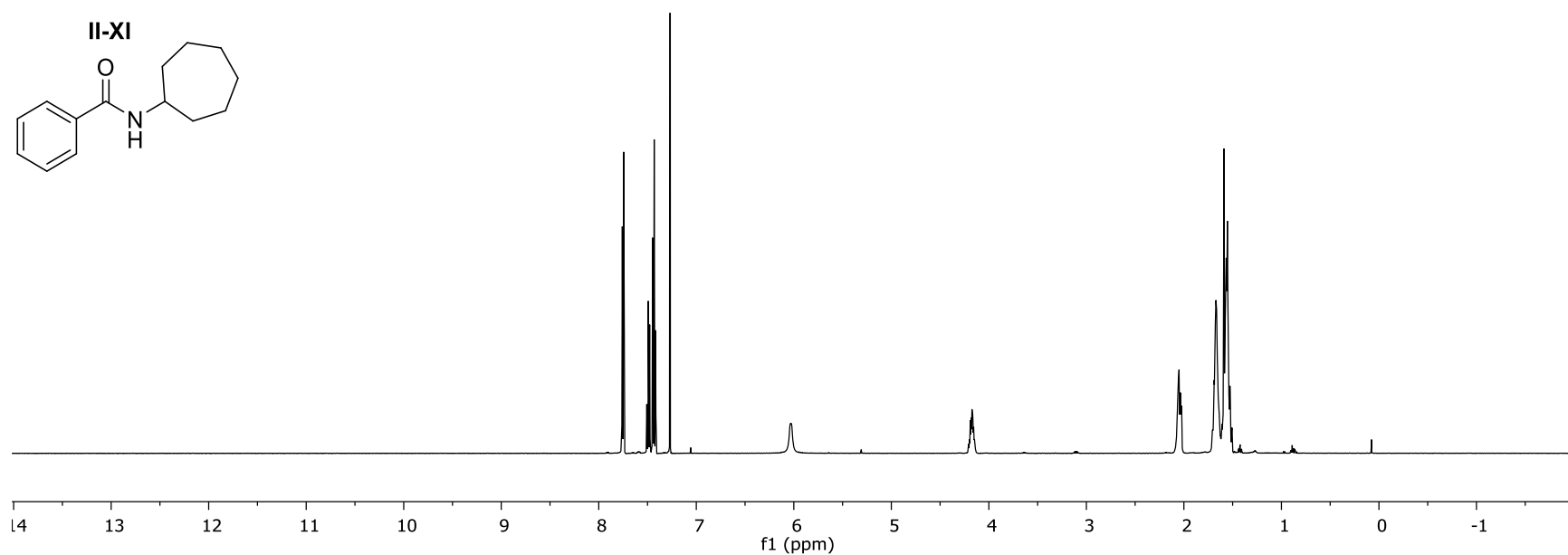
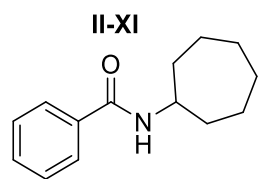


Figure II-XXIX: The ^1H NMR and ^{13}C NMR for Compound **II-XI**

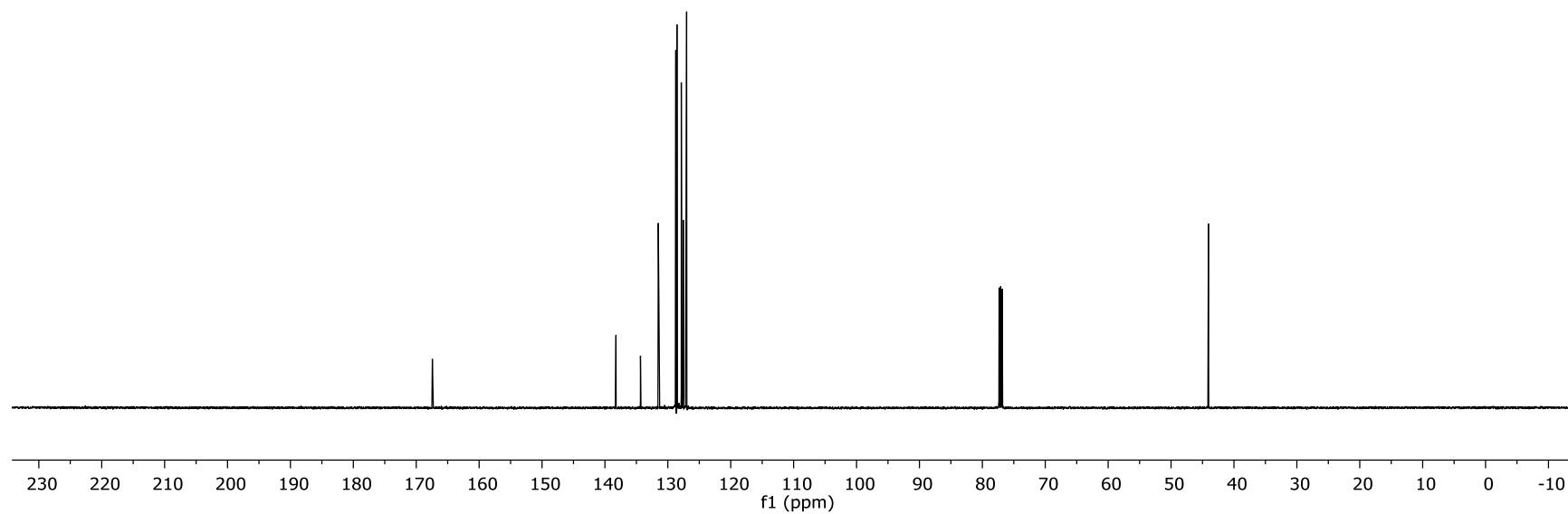
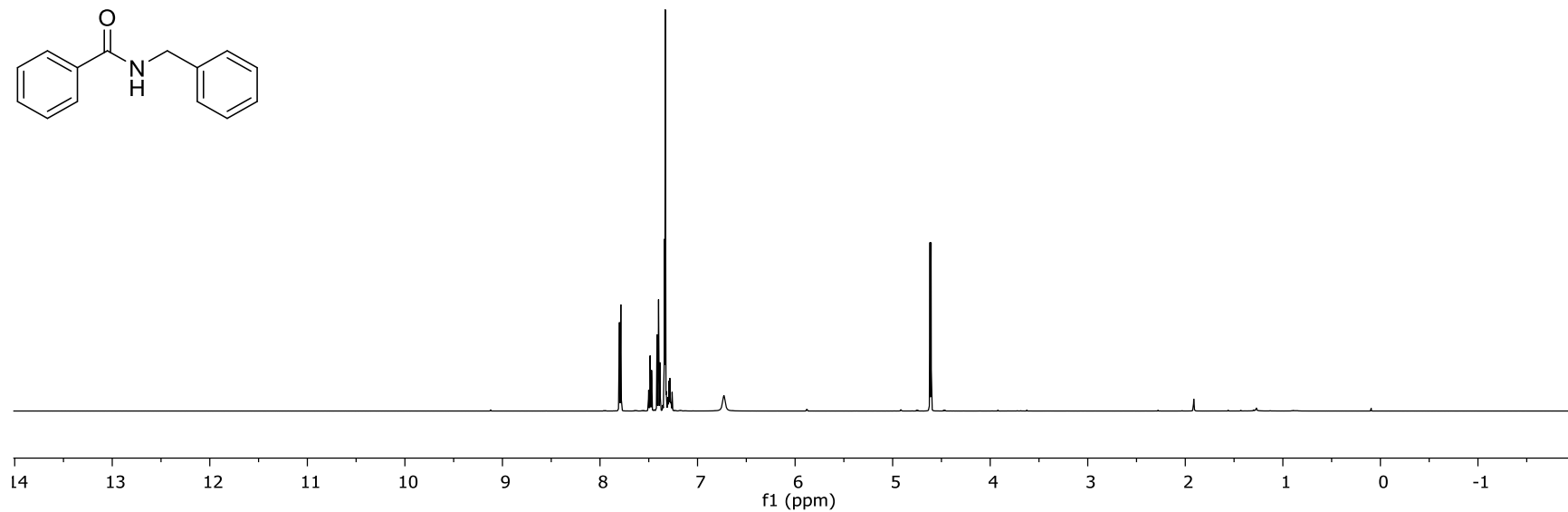
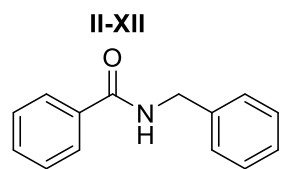


Figure II-XXX: The $^1\text{H NMR}$ and $^{13}\text{C NMR}$ for Compound II-XII

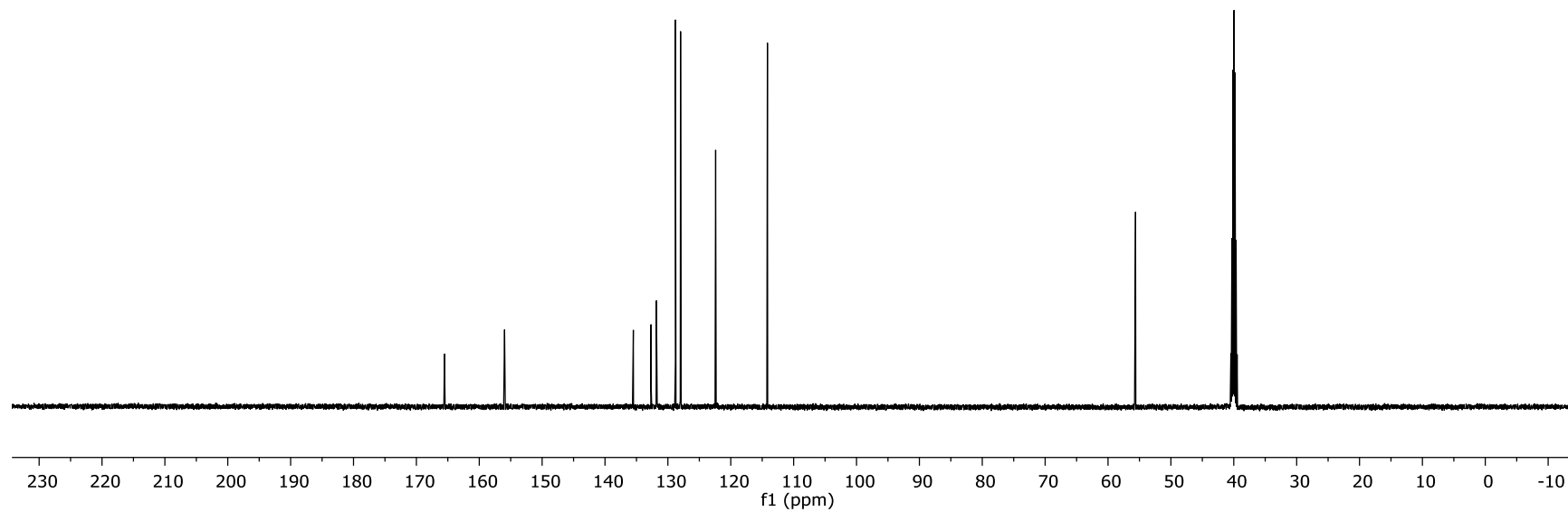
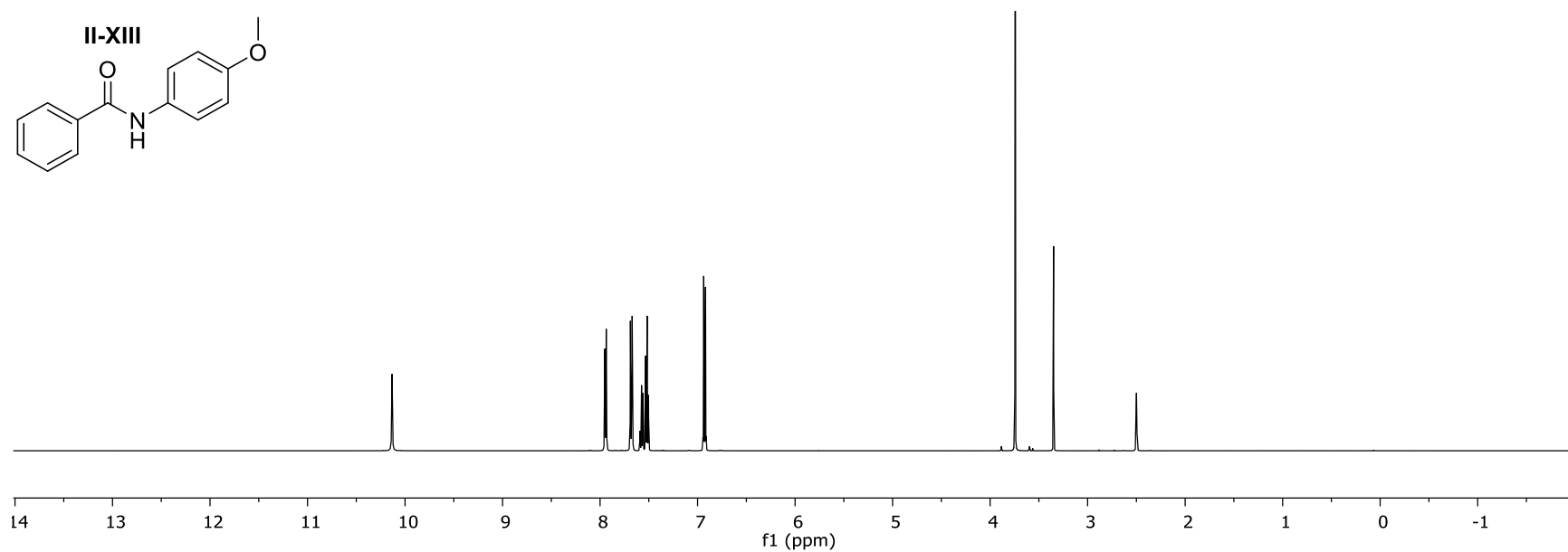
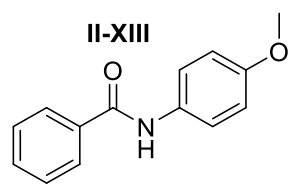


Figure II-XXXI: The ^1H NMR and ^{13}C NMR for Compound II-XIII

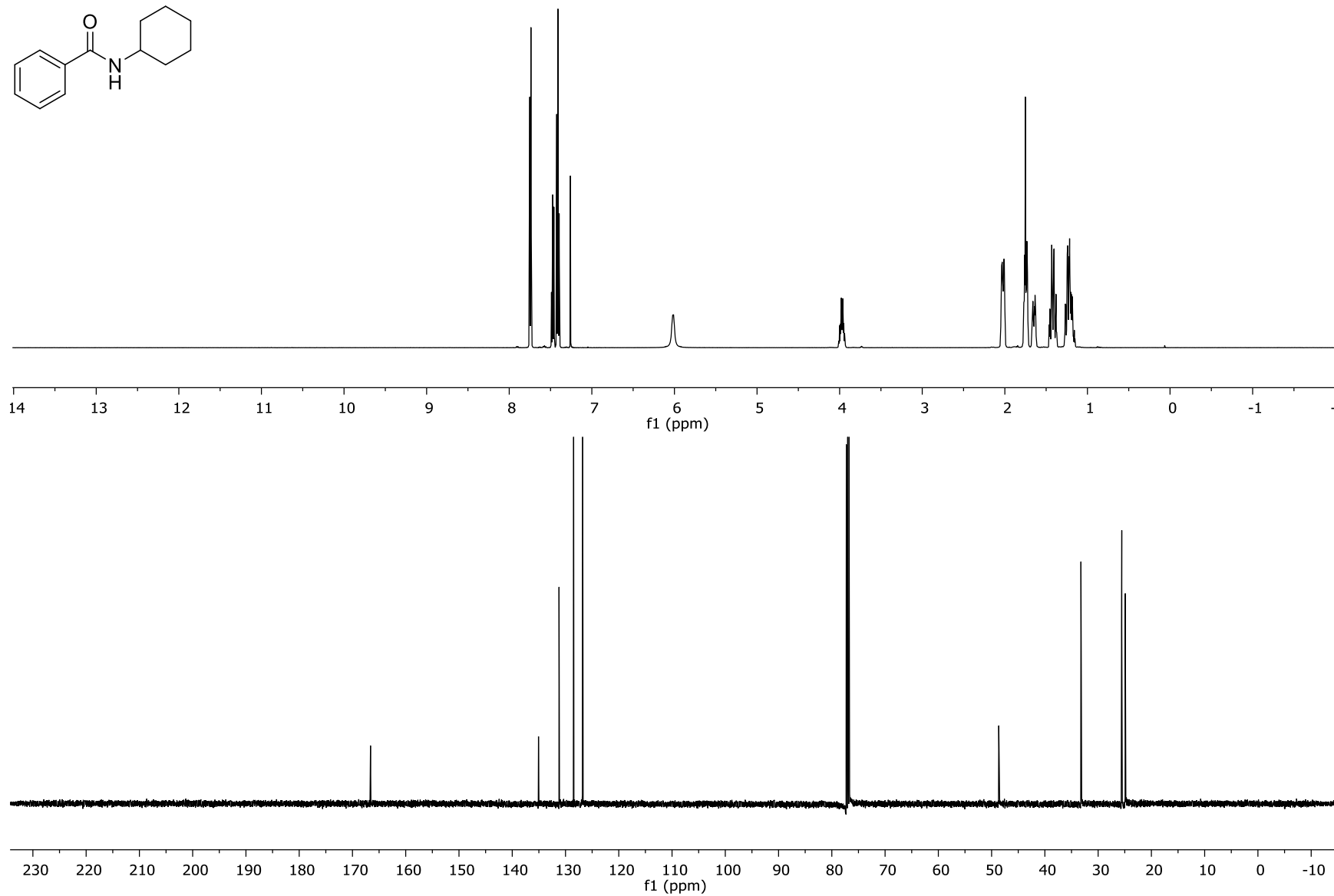
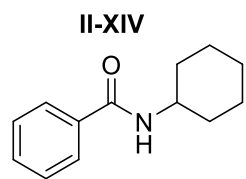


Figure II-XXXII: The ^1H NMR and ^{13}C NMR for Compound **II-XIV**

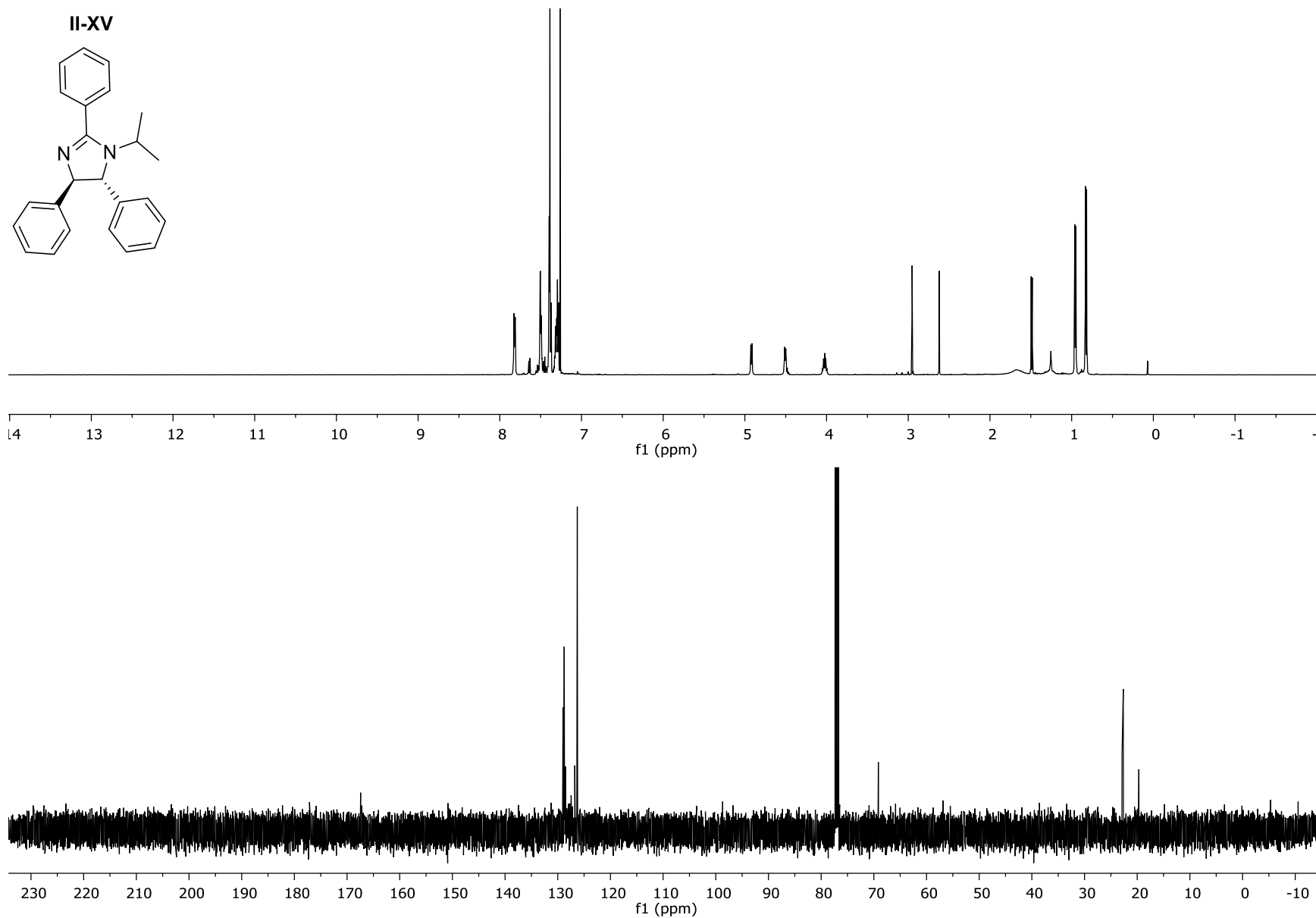


Figure II-XXXIII: The ^1H NMR and ^{13}C NMR for Compound **II-XV**

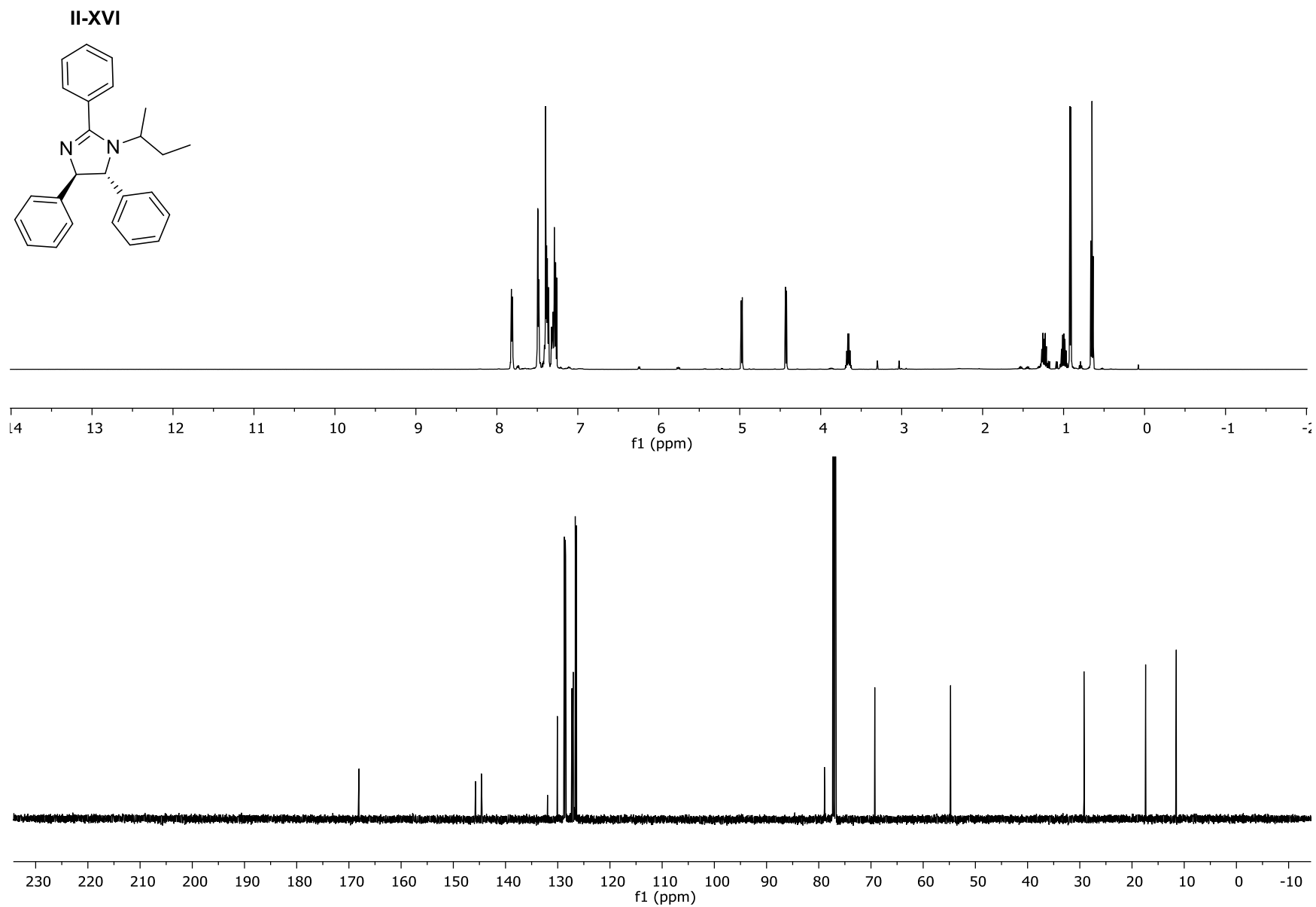


Figure II-XXXIV: The ^1H NMR and ^{13}C NMR for Compound **II-XVI**

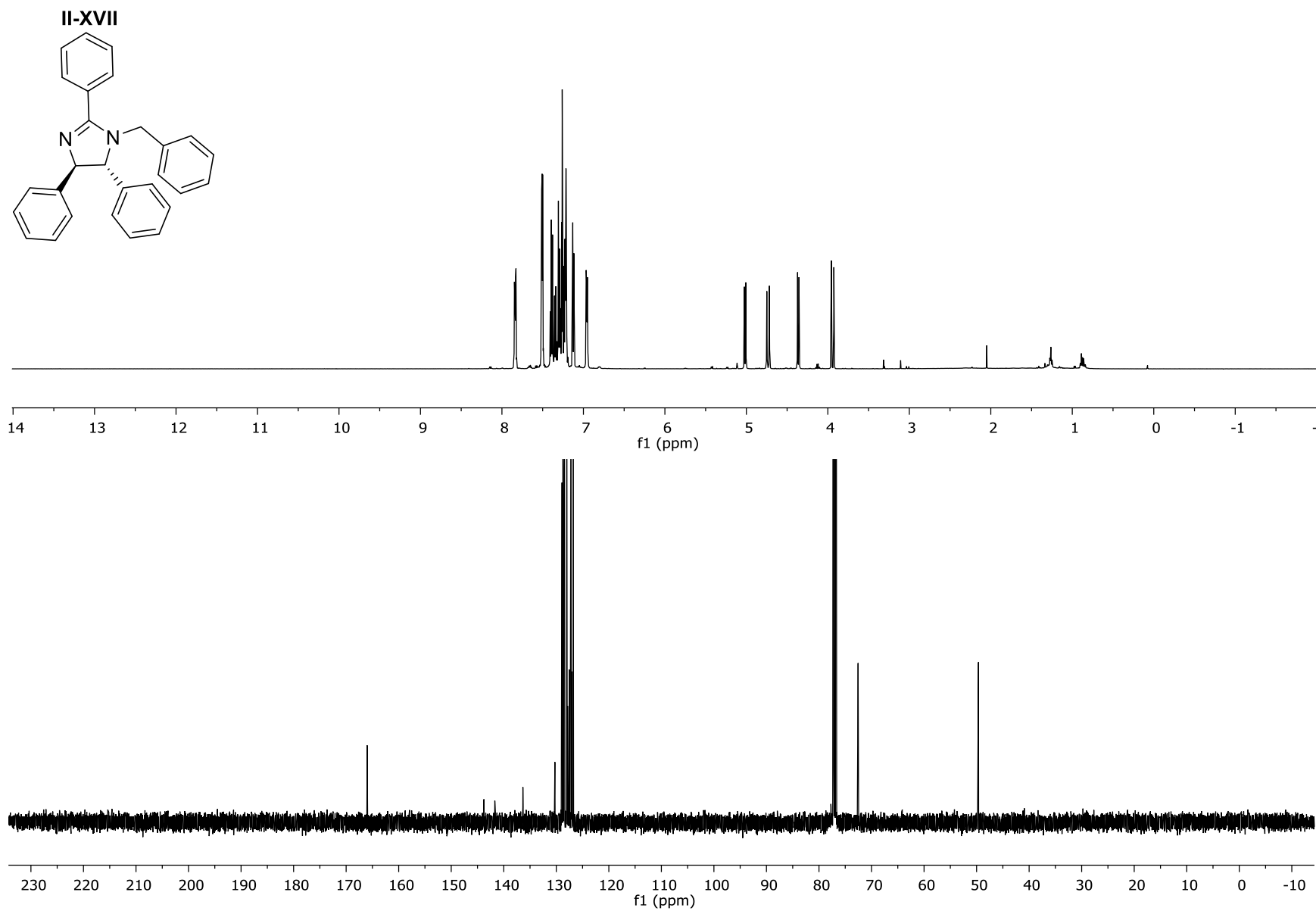


Figure II-XXXV: The ^1H NMR and ^{13}C CNMR for Compound **II-XVII**

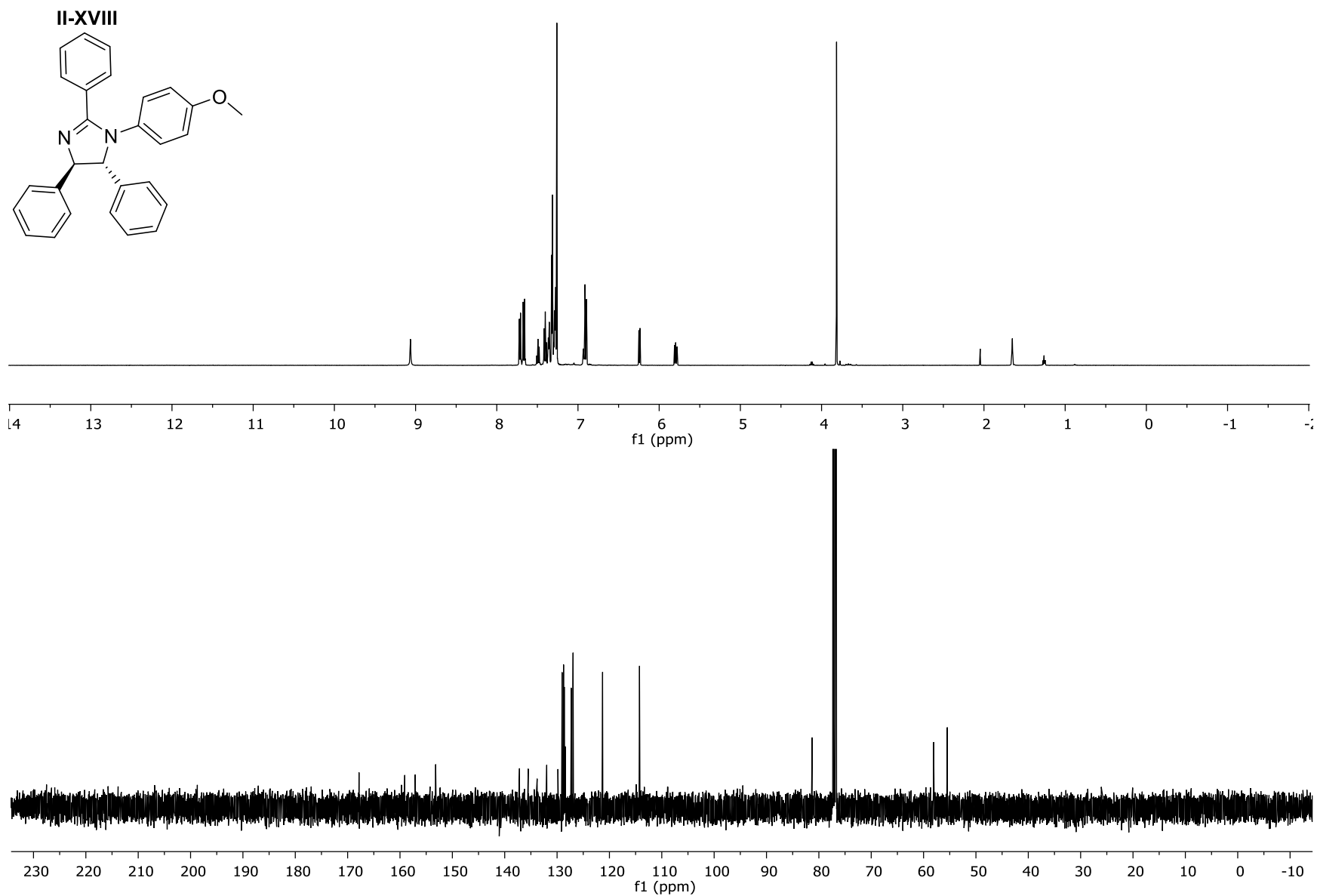


Figure II-XXXVI: The ^1H NMR and ^{13}C NMR for Compound **II-XVIII**

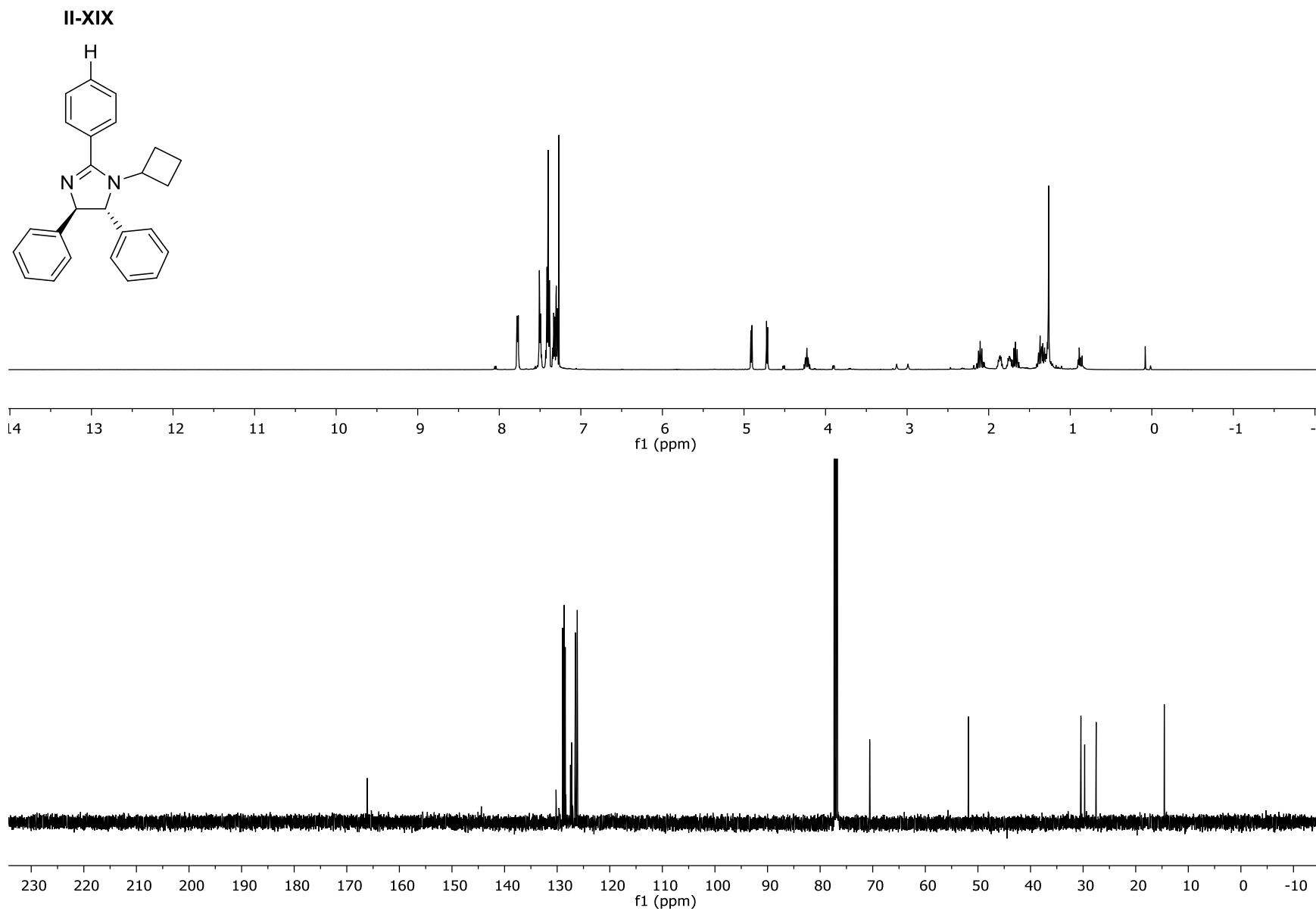


Figure II-XXXVII: The ^1H NMR and ^{13}C NMR for Compound **II-XIX**

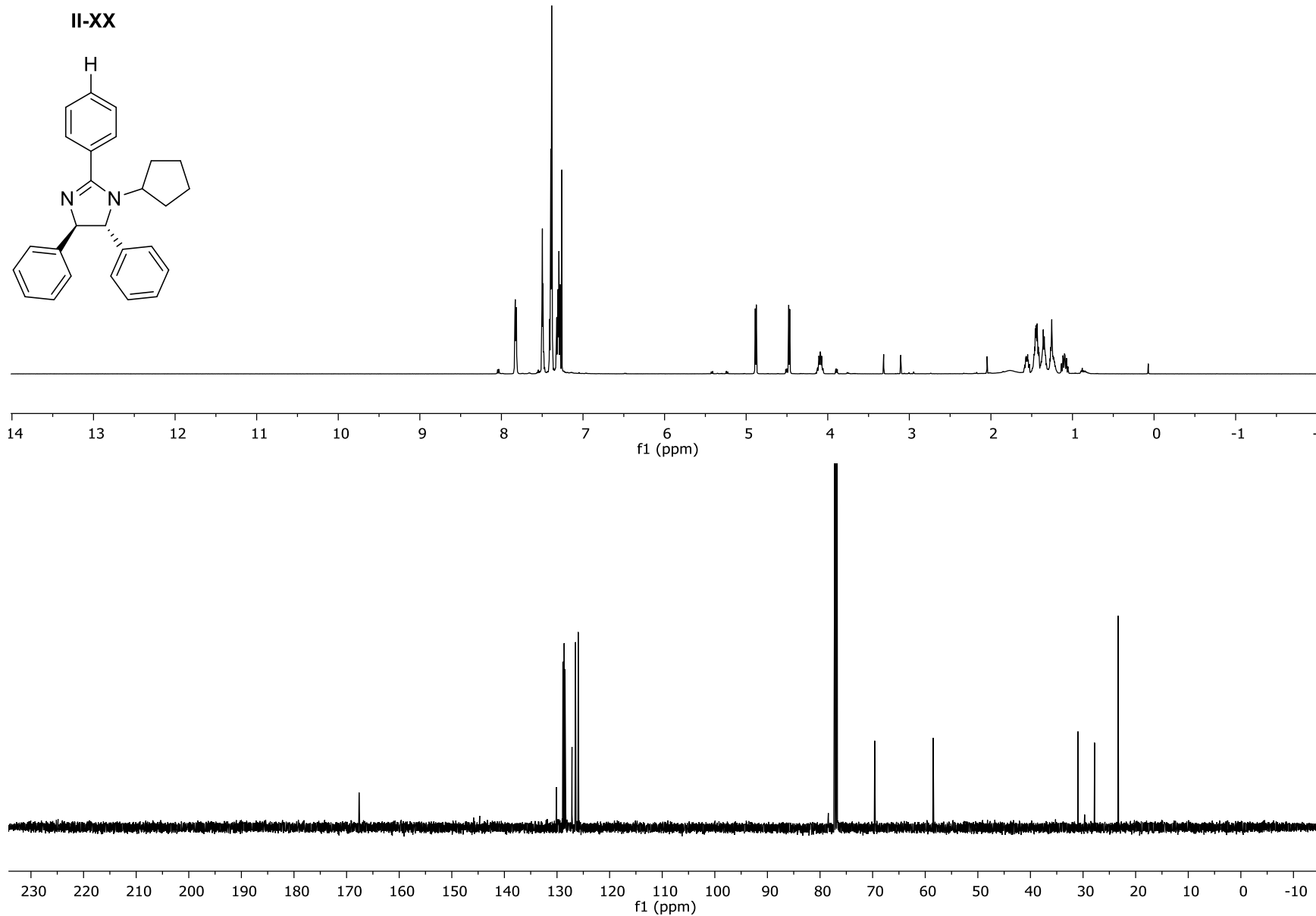


Figure II-XXXVIII: The ^1H NMR and ^{13}C NMR for Compound II-XX

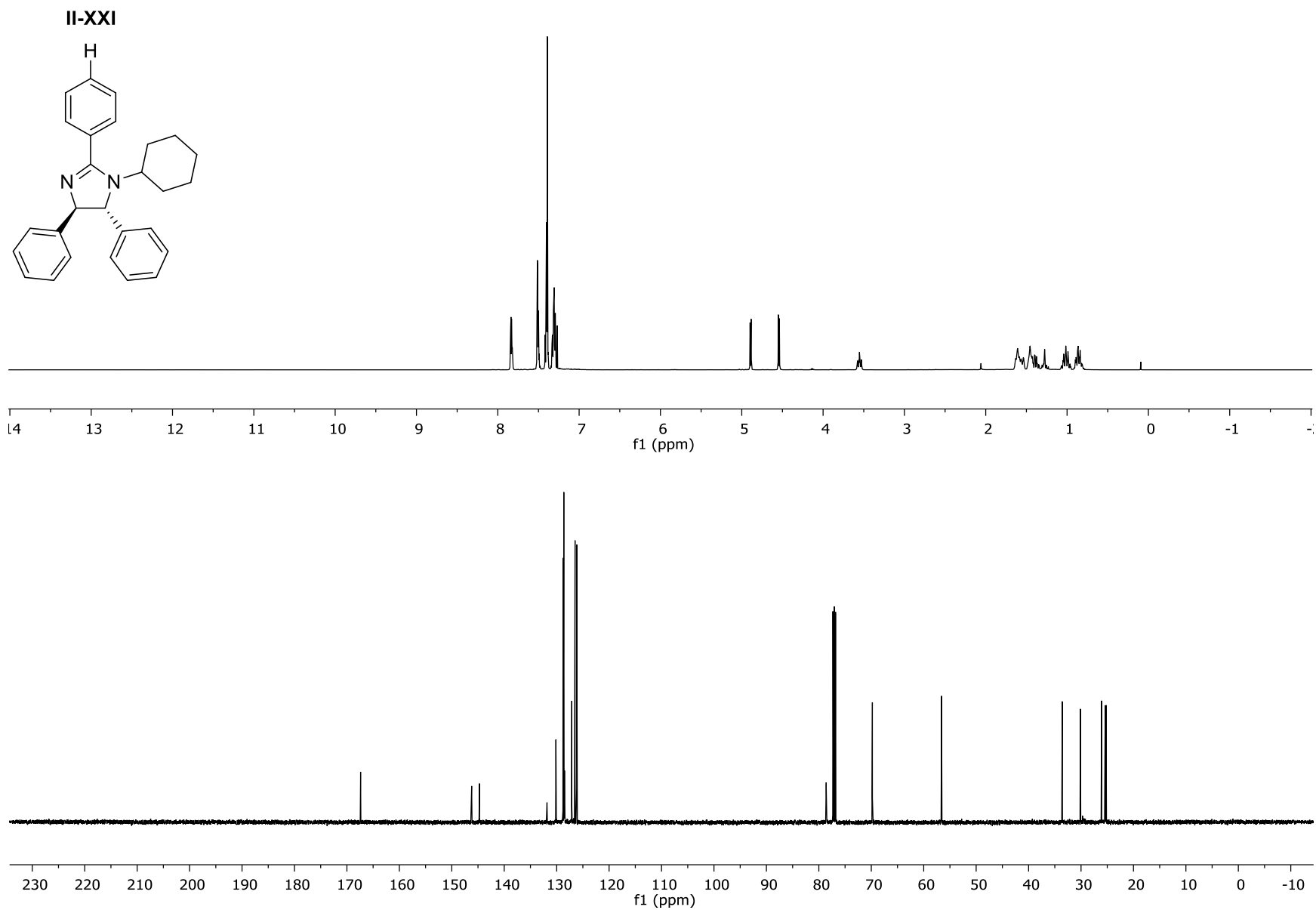


Figure II-XXXIX: The ^1H NMR and ^{13}C NMR for Compound **II-XXI**

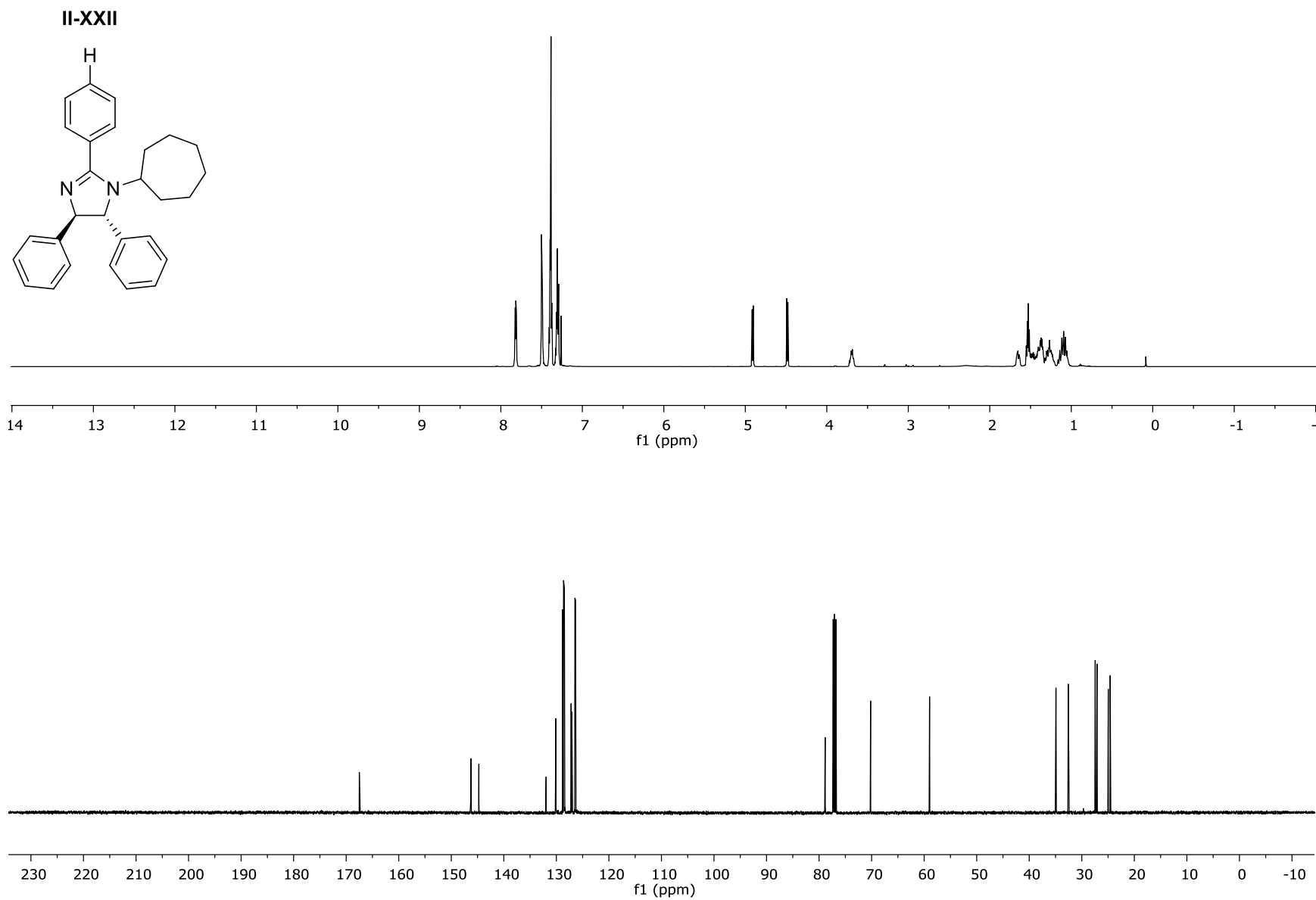


Figure II-XL: The ^1H NMR and ^{13}C NMR for Compound **II-XXII**

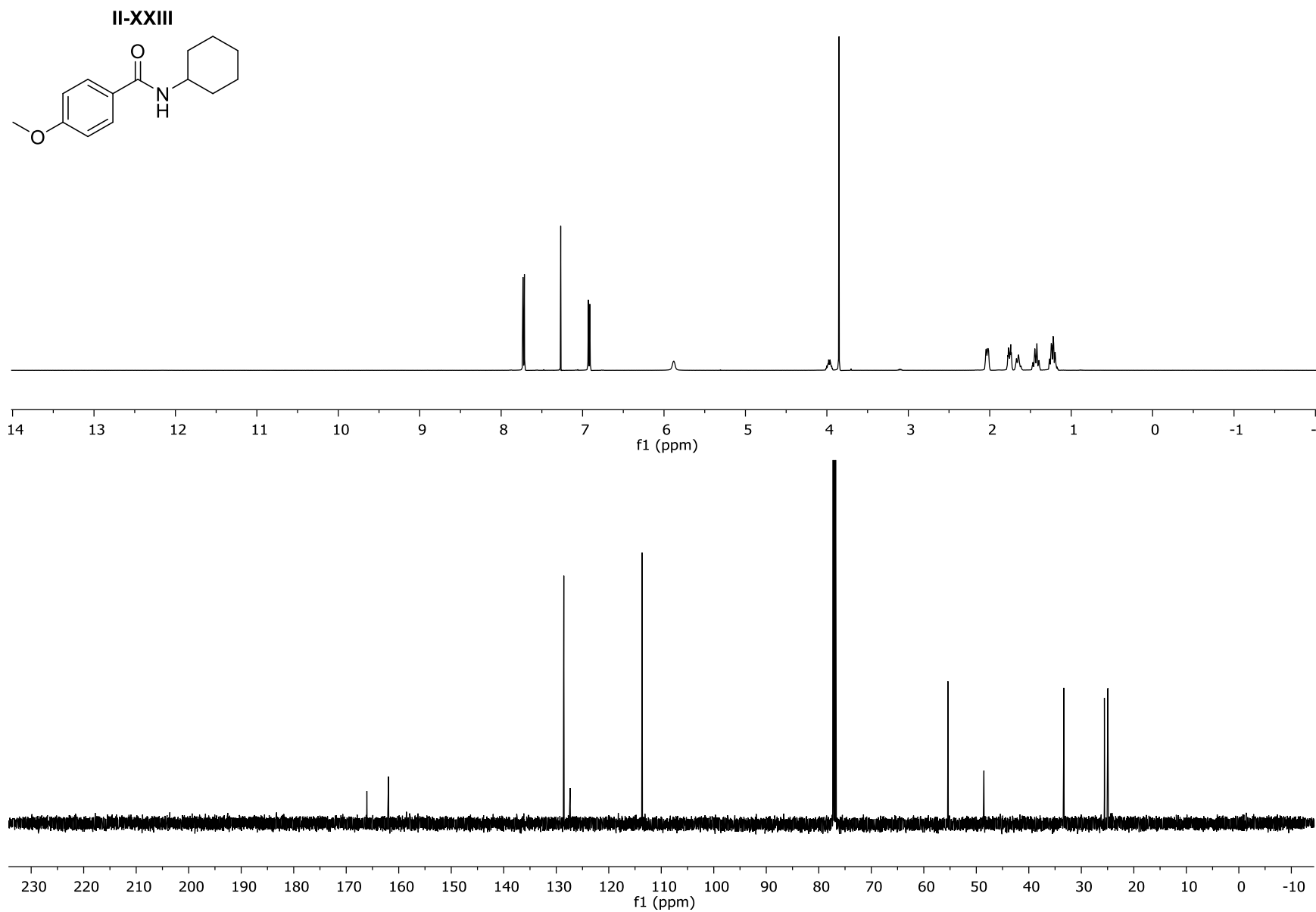


Figure II-XLI: The ^1H NMR and ^{13}C CNMR for Compound **II-XXIII**

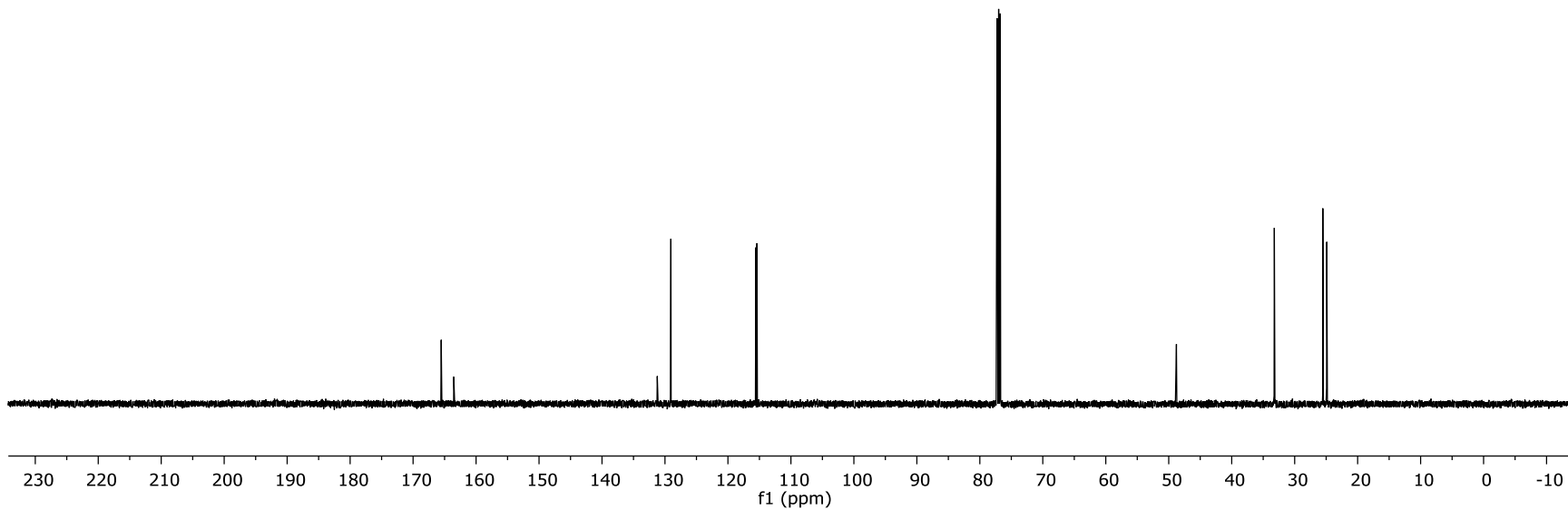
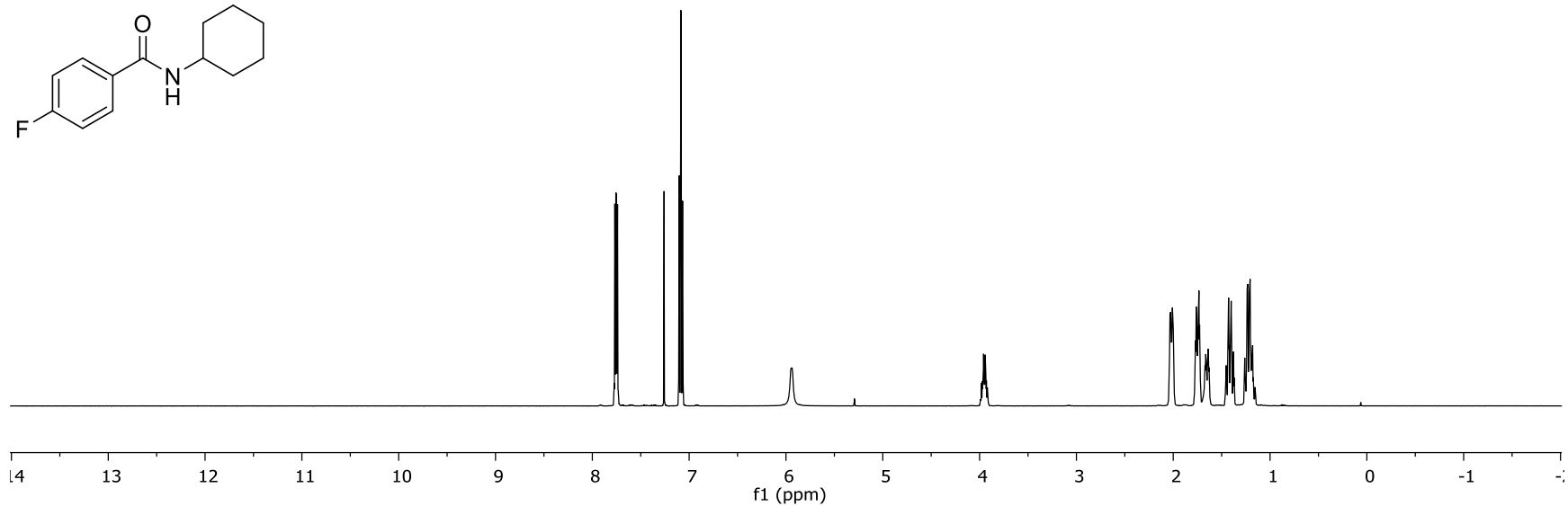
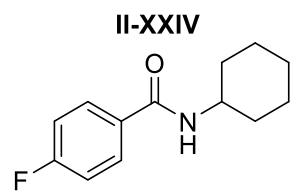


Figure II-XLII: The $^1\text{H NMR}$ and $^{13}\text{C NMR}$ for Compound II-XXIV

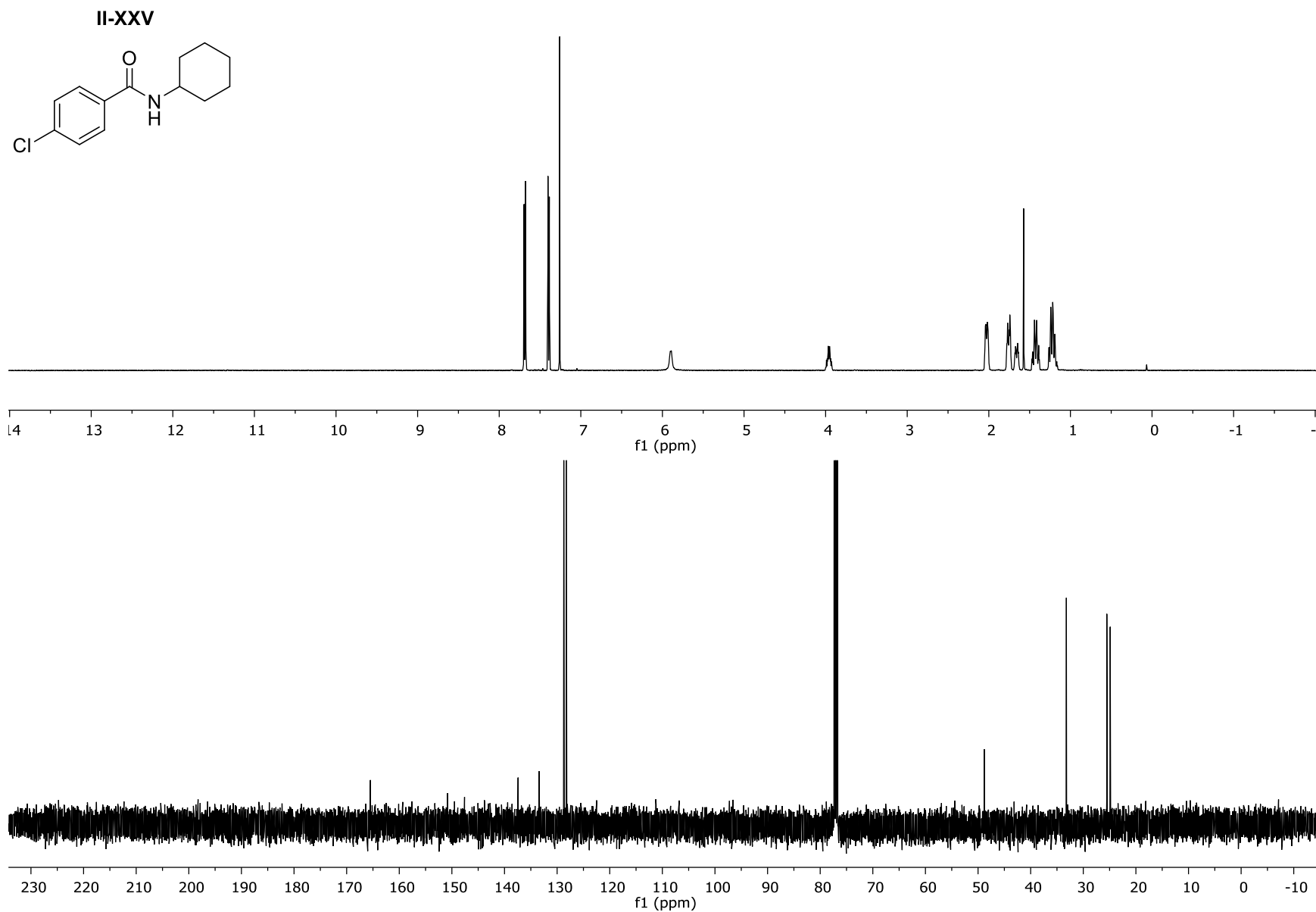


Figure II-XLIII: The ^1H NMR and ^{13}C NMR for Compound **II-XXV**

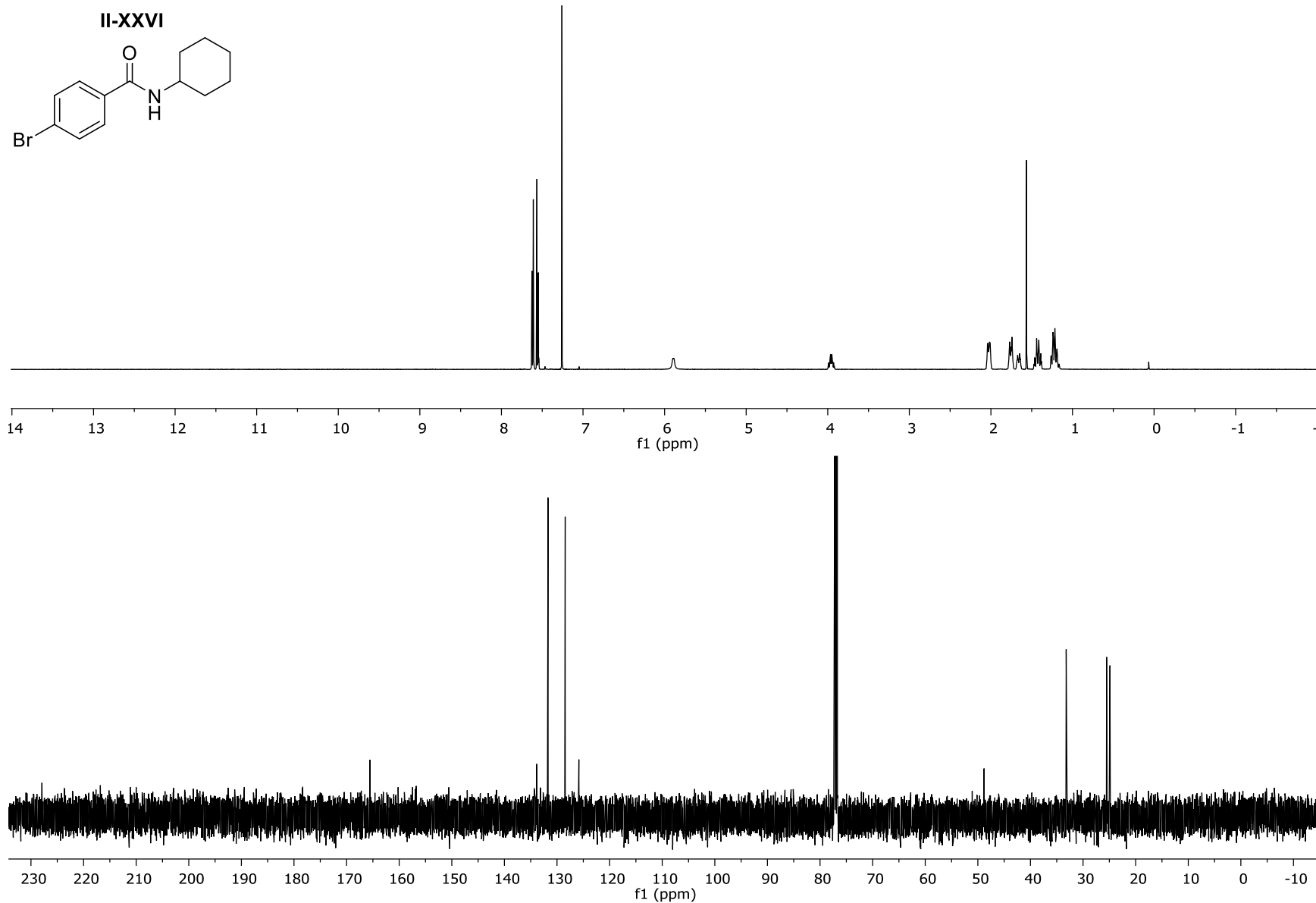


Figure II-XLIV: The ^1H NMR and ^{13}C NMR for Compound **II-XXVI**

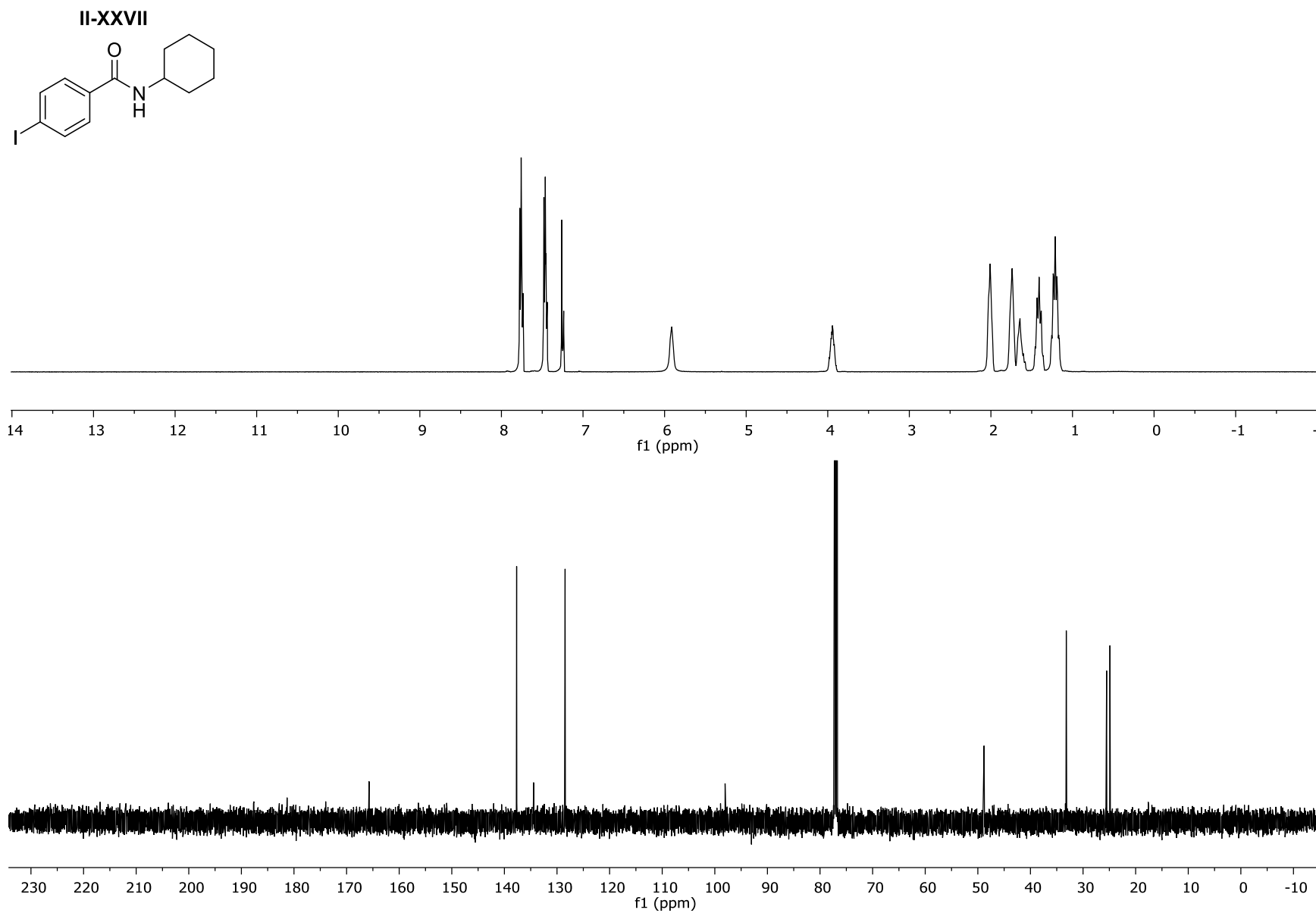


Figure II-XLV: The ^1H NMR and ^{13}C NMR for Compound **II-XXVII**

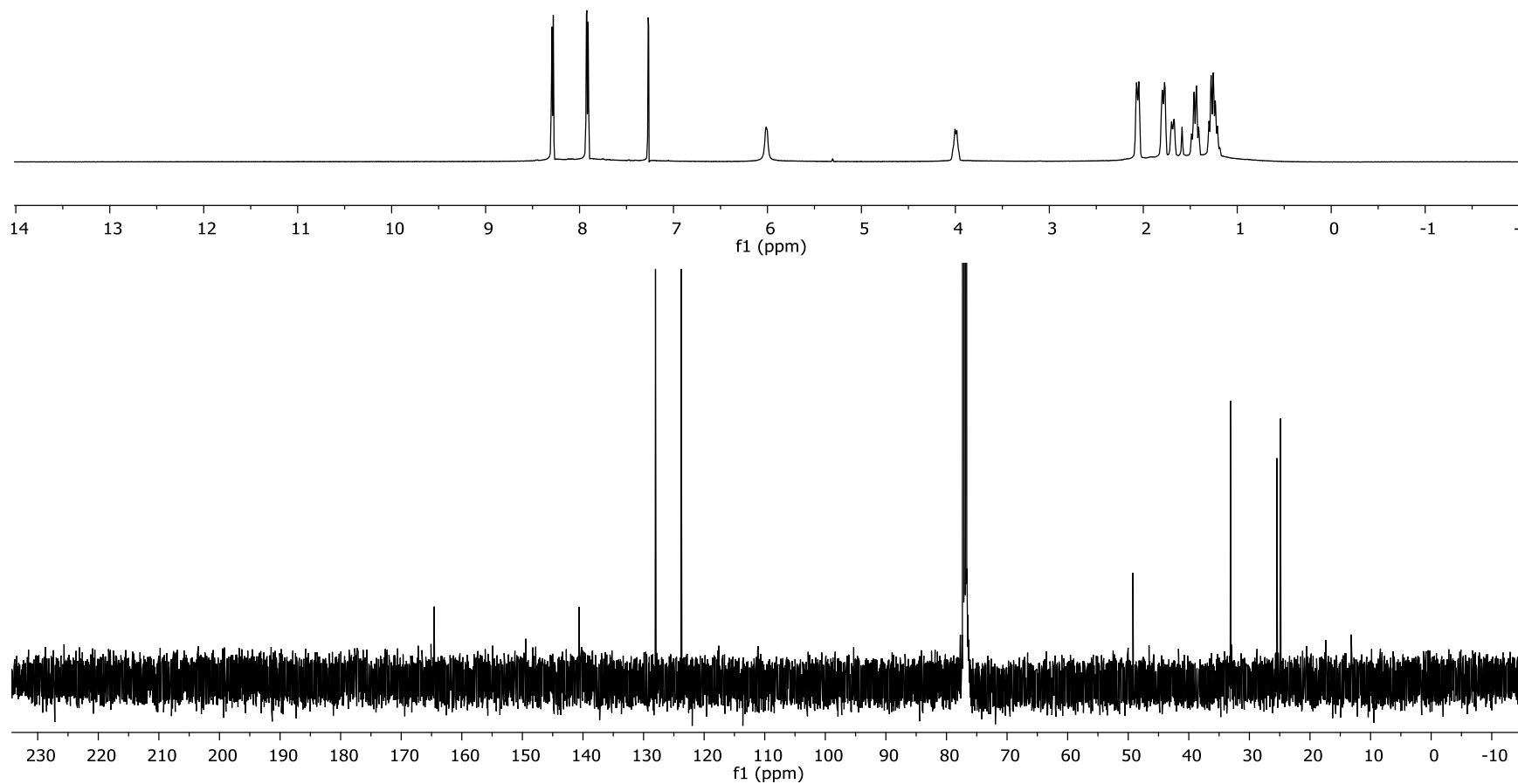
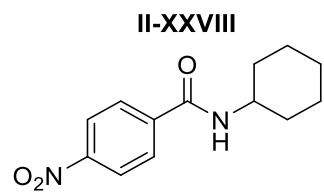


Figure II-XLVI: The ^1H NMR and ^{13}C NMR for Compound II-XXVIII

II-XXIX

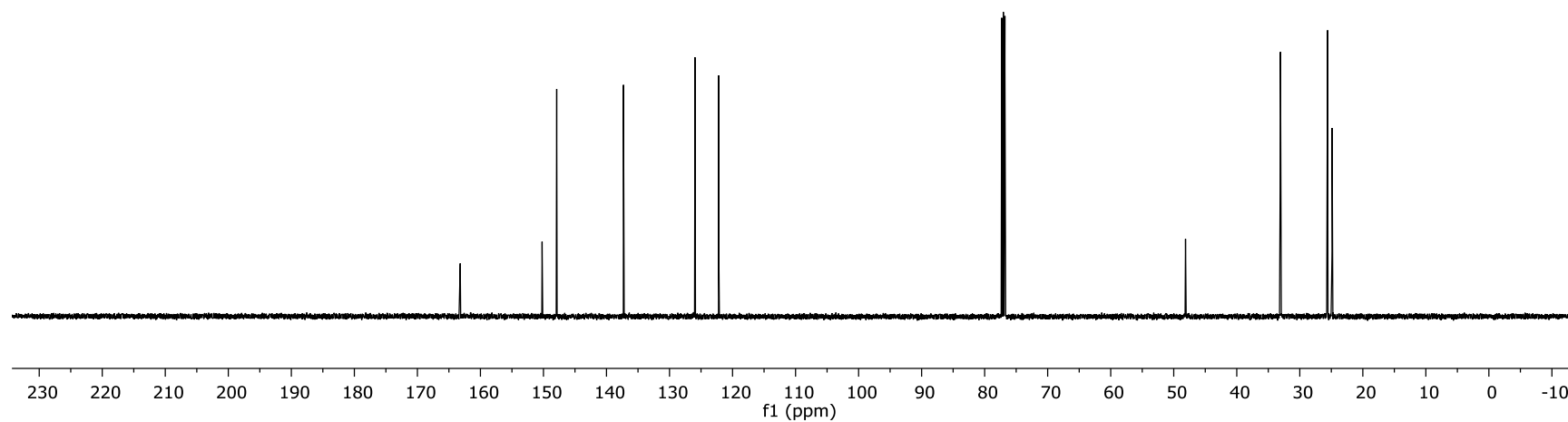
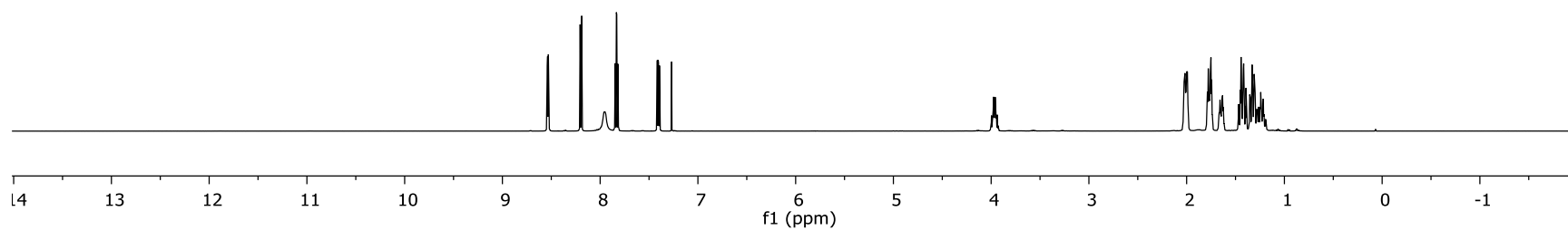
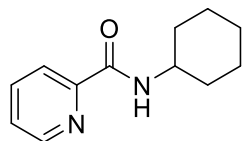


Figure II-XLVII: The ¹H NMR and ¹³C NMR for Compound II-XXIX

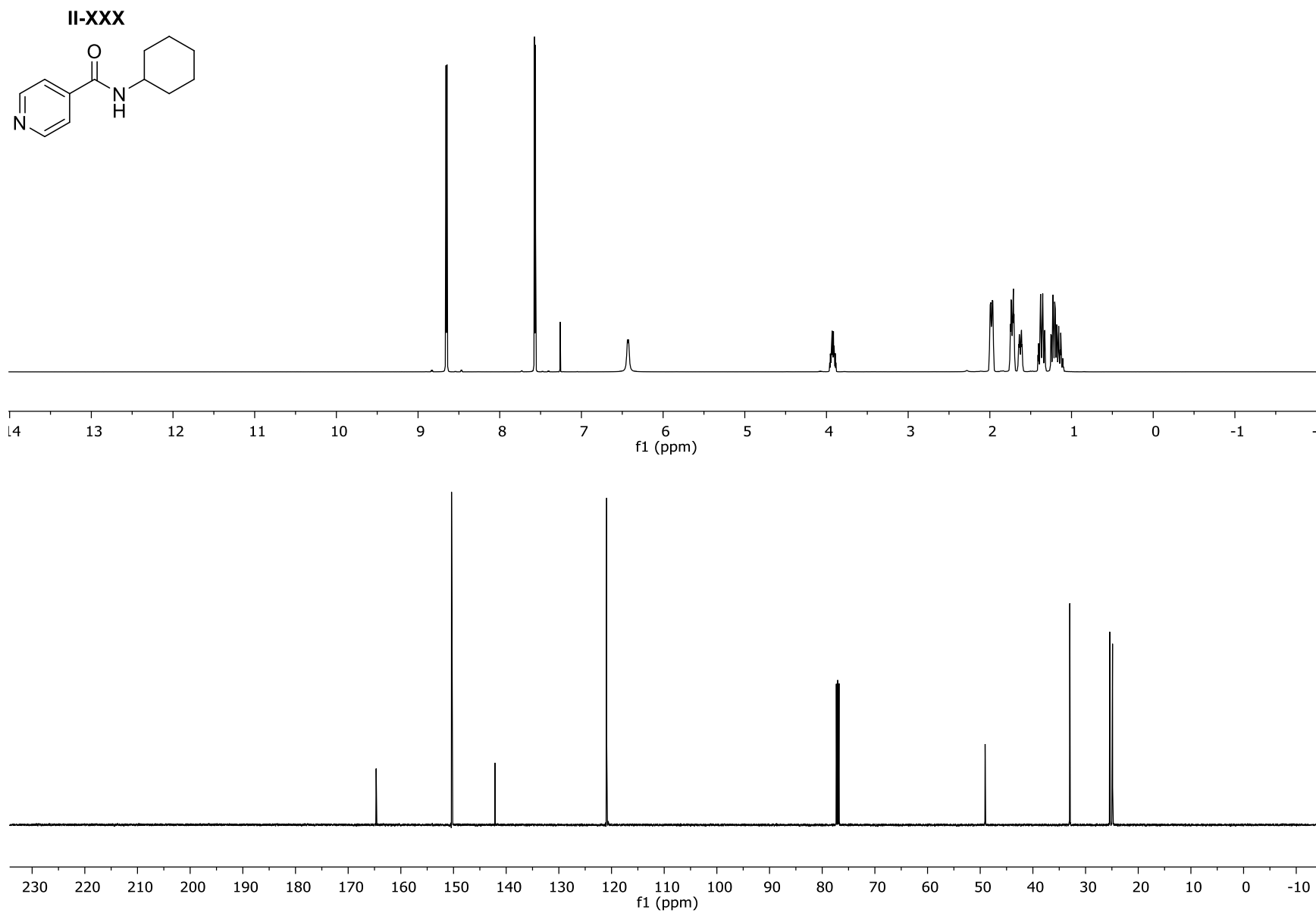


Figure II-XLVIII: The ^1H NMR and ^{13}C NMR for Compound **II-XXX**

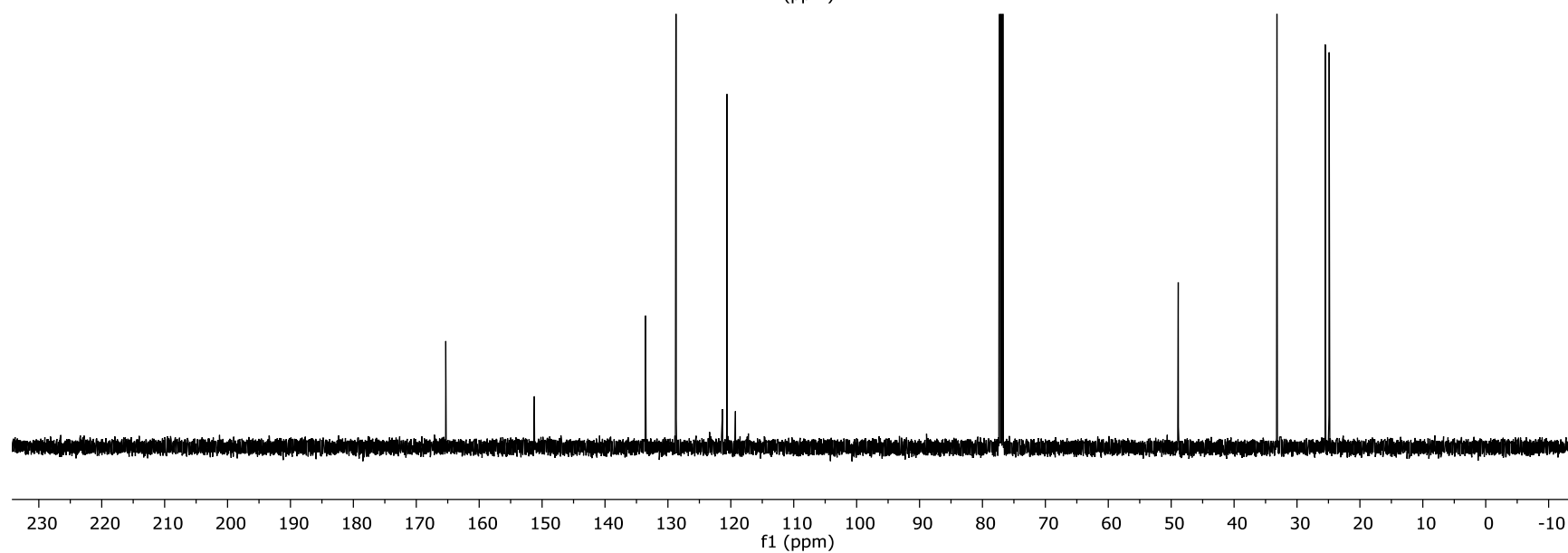
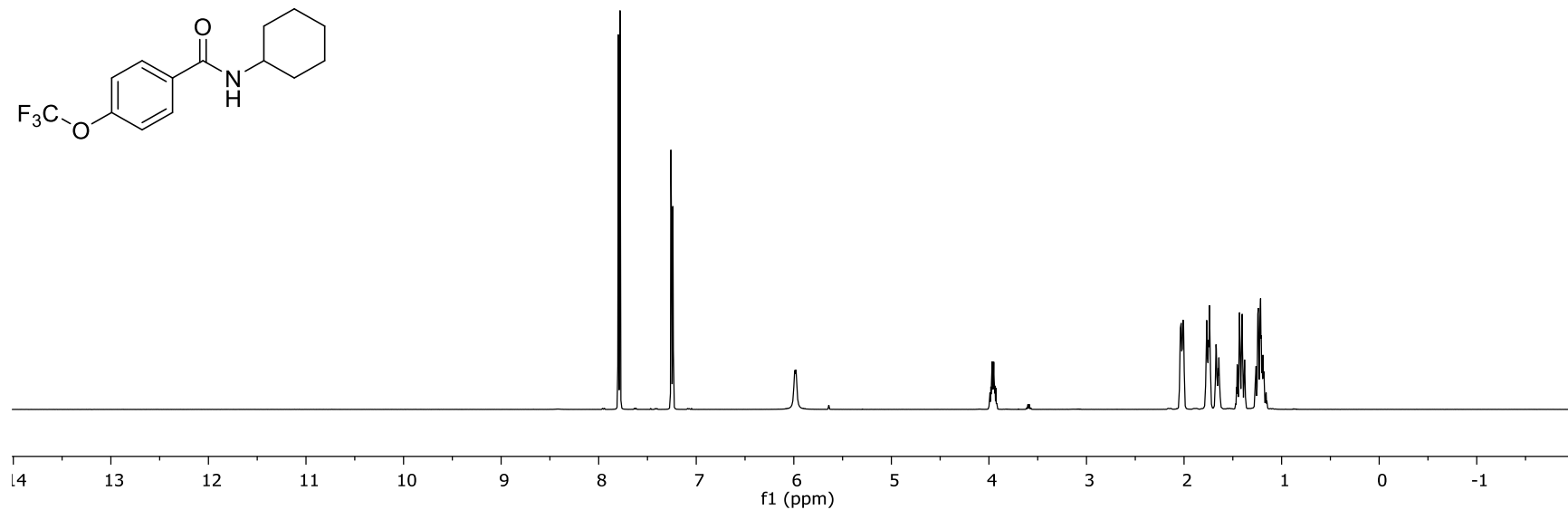
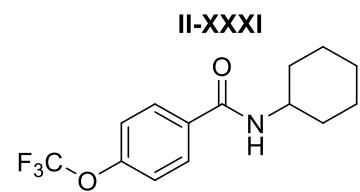


Figure II-XLIX: The ^1H NMR and ^{13}C NMR for Compound **II-XXXI**

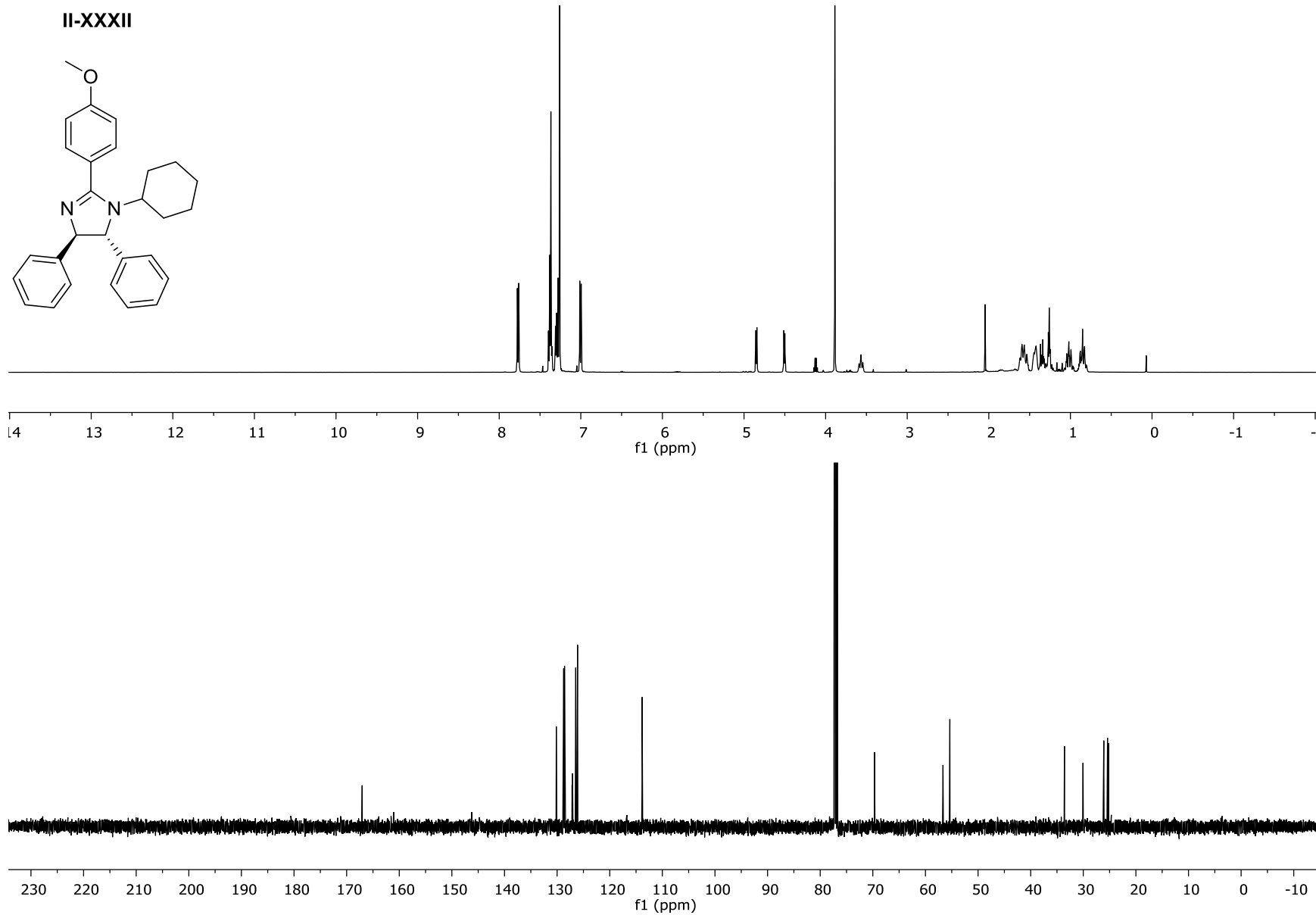


Figure II-L: The ^1H NMR and ^{13}C NMR for Compound **II-XXXII**

II-XXXIII

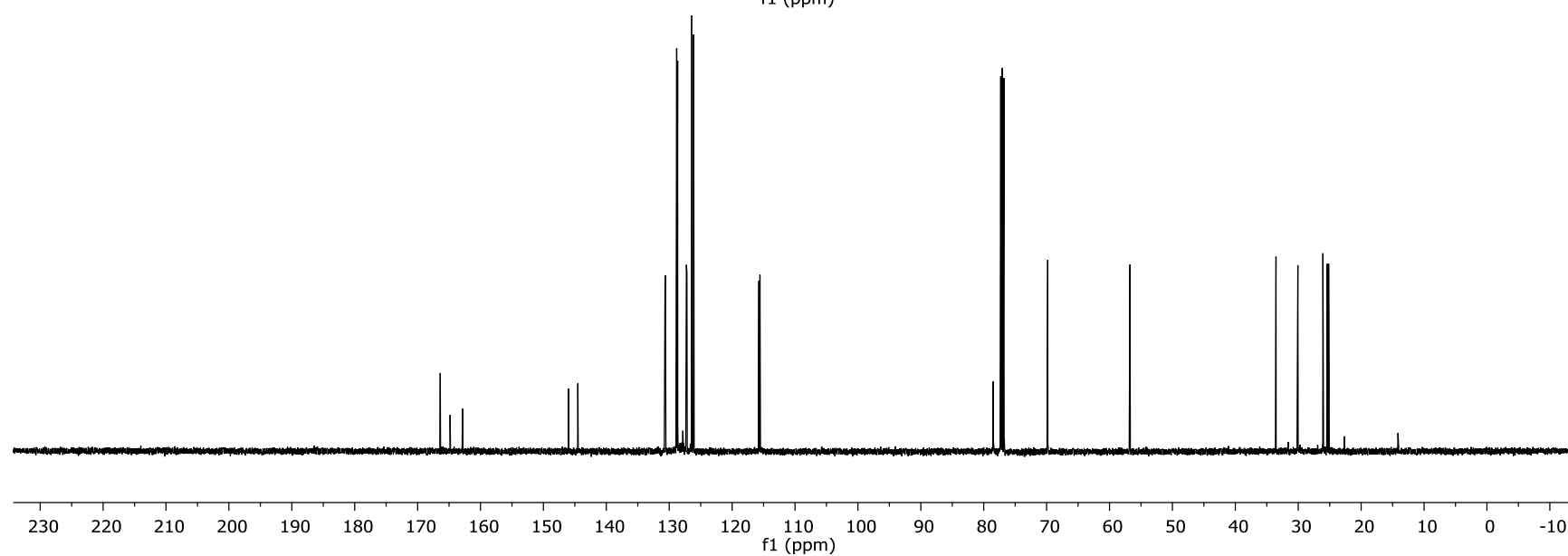
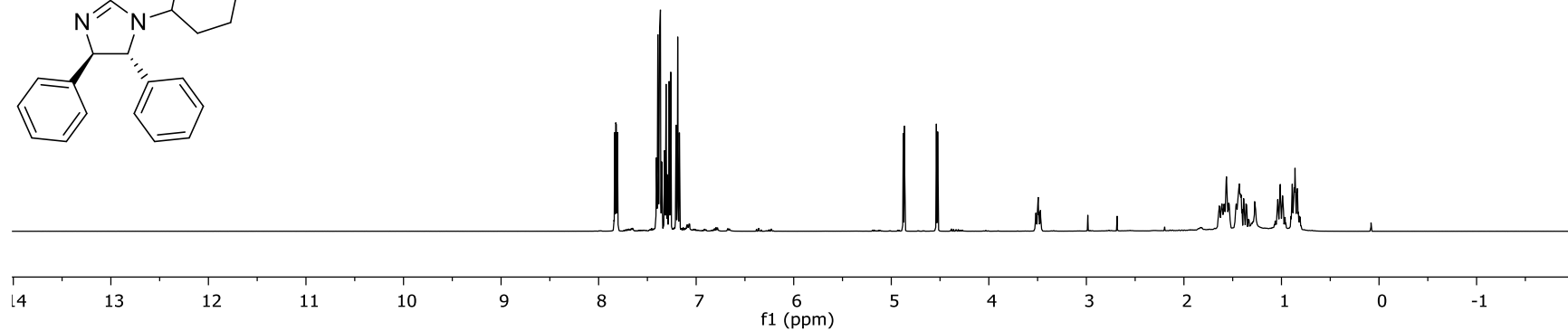
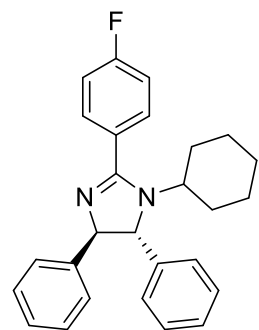


Figure II-LI: The ^1H NMR and ^{13}C NMR for Compound II-XXXIII

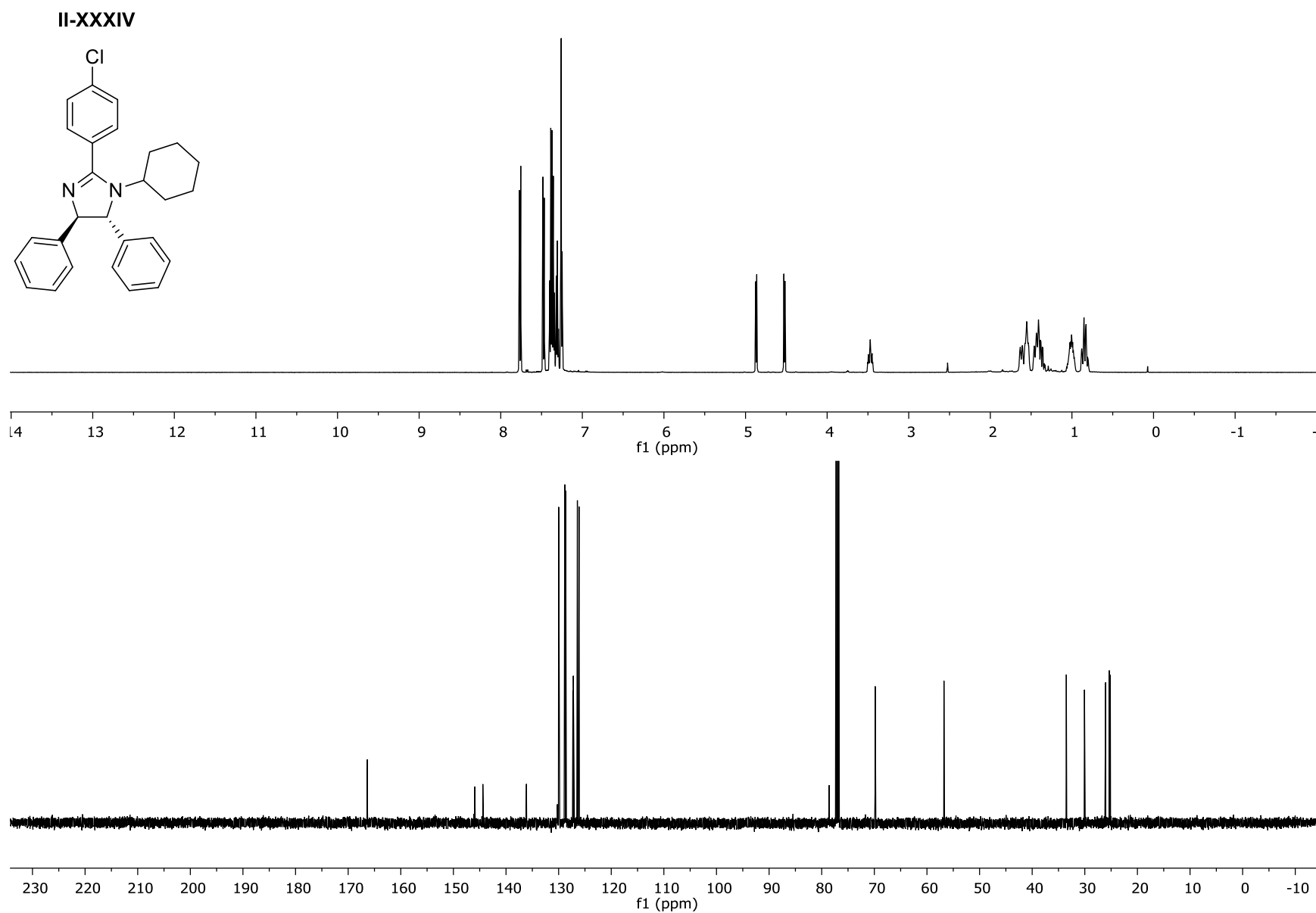


Figure II-LII: The ^1H NMR and ^{13}C NMR for Compound **II-XXXIV**

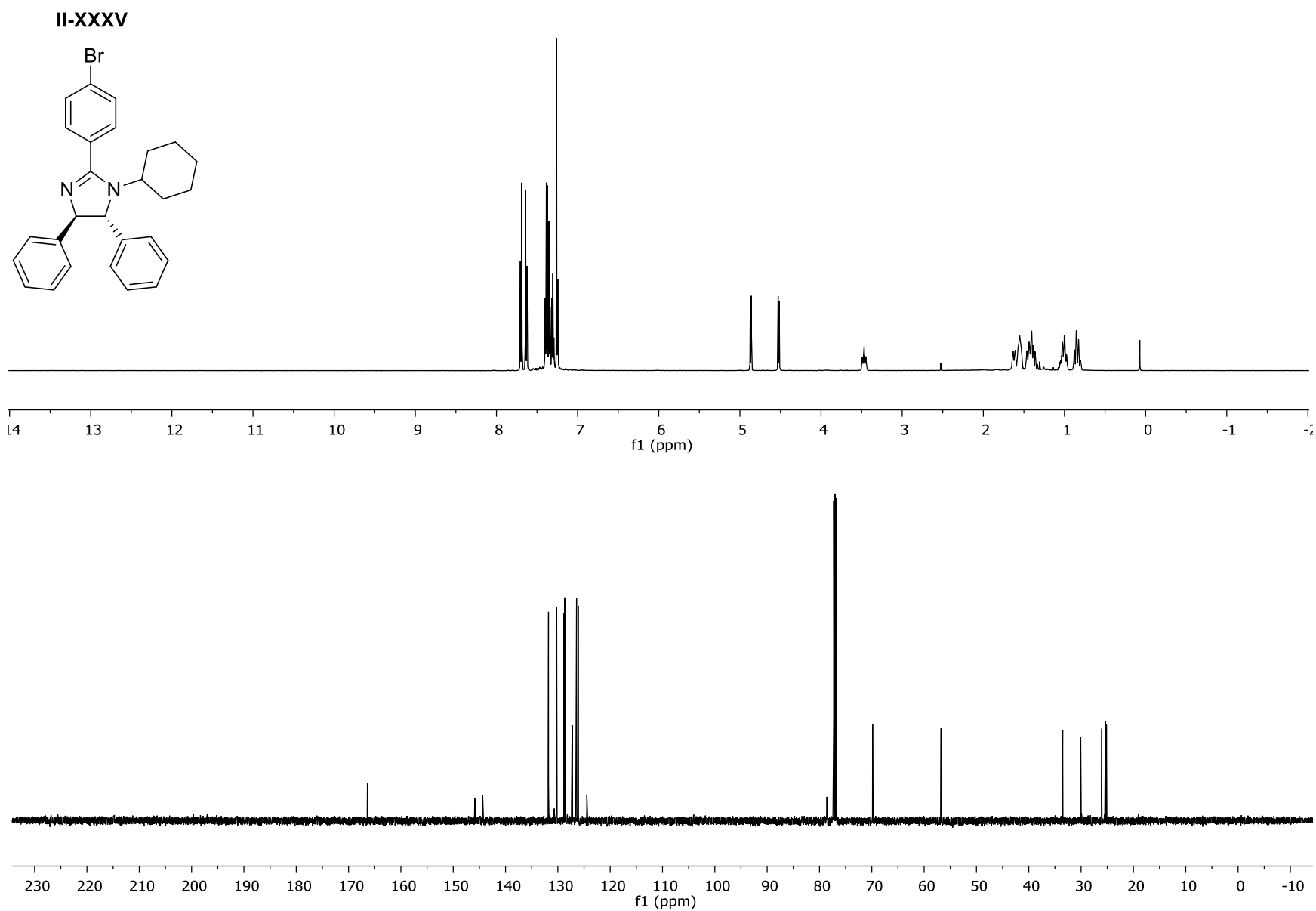


Figure II-LIII: The ^1H NMR and ^{13}C CNMR for Compound **II-XXXV**

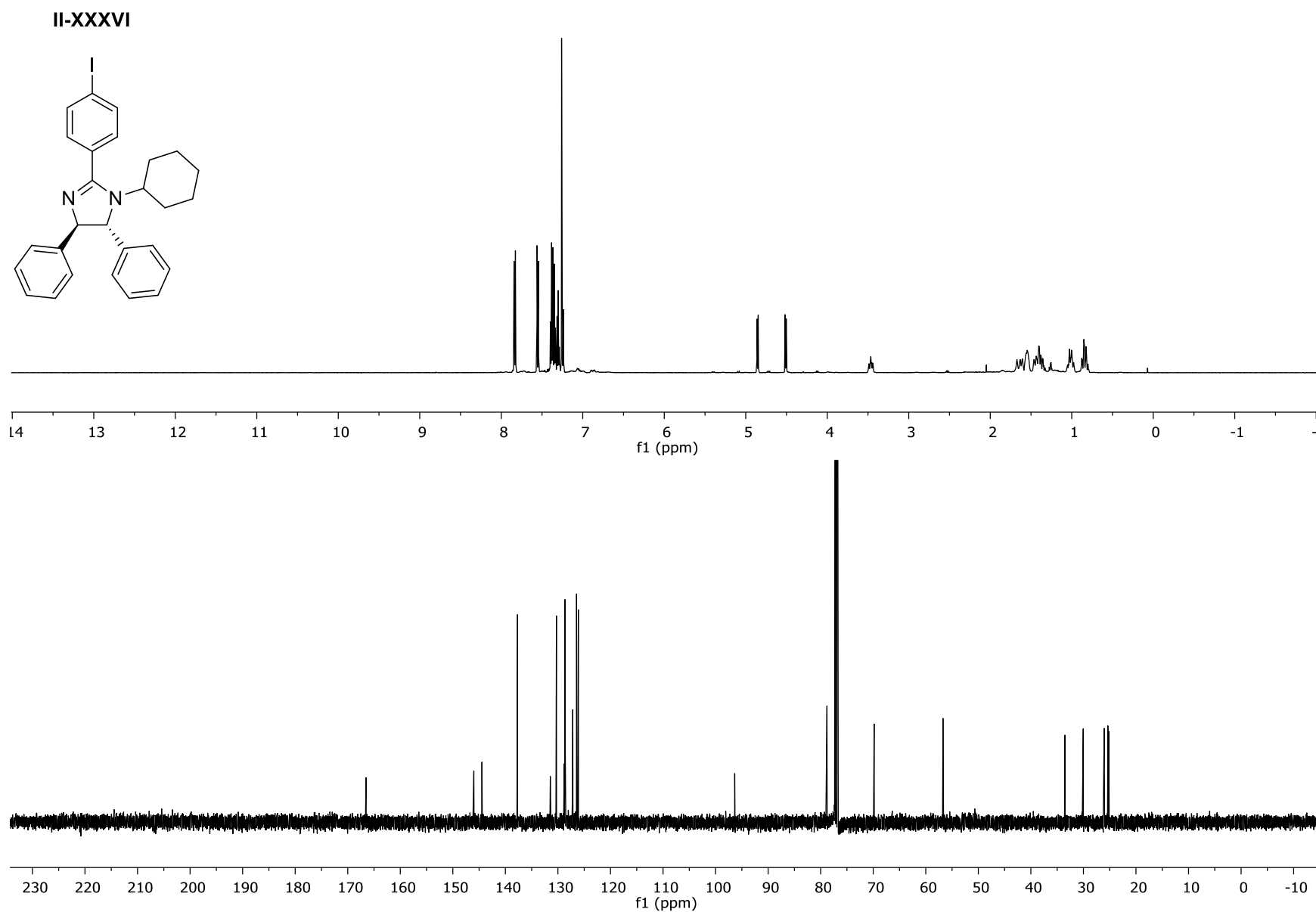


Figure II-LIV: The ^1H NMR and ^{13}C CNMR for Compound **II-XXXVI**

II-XXXVII

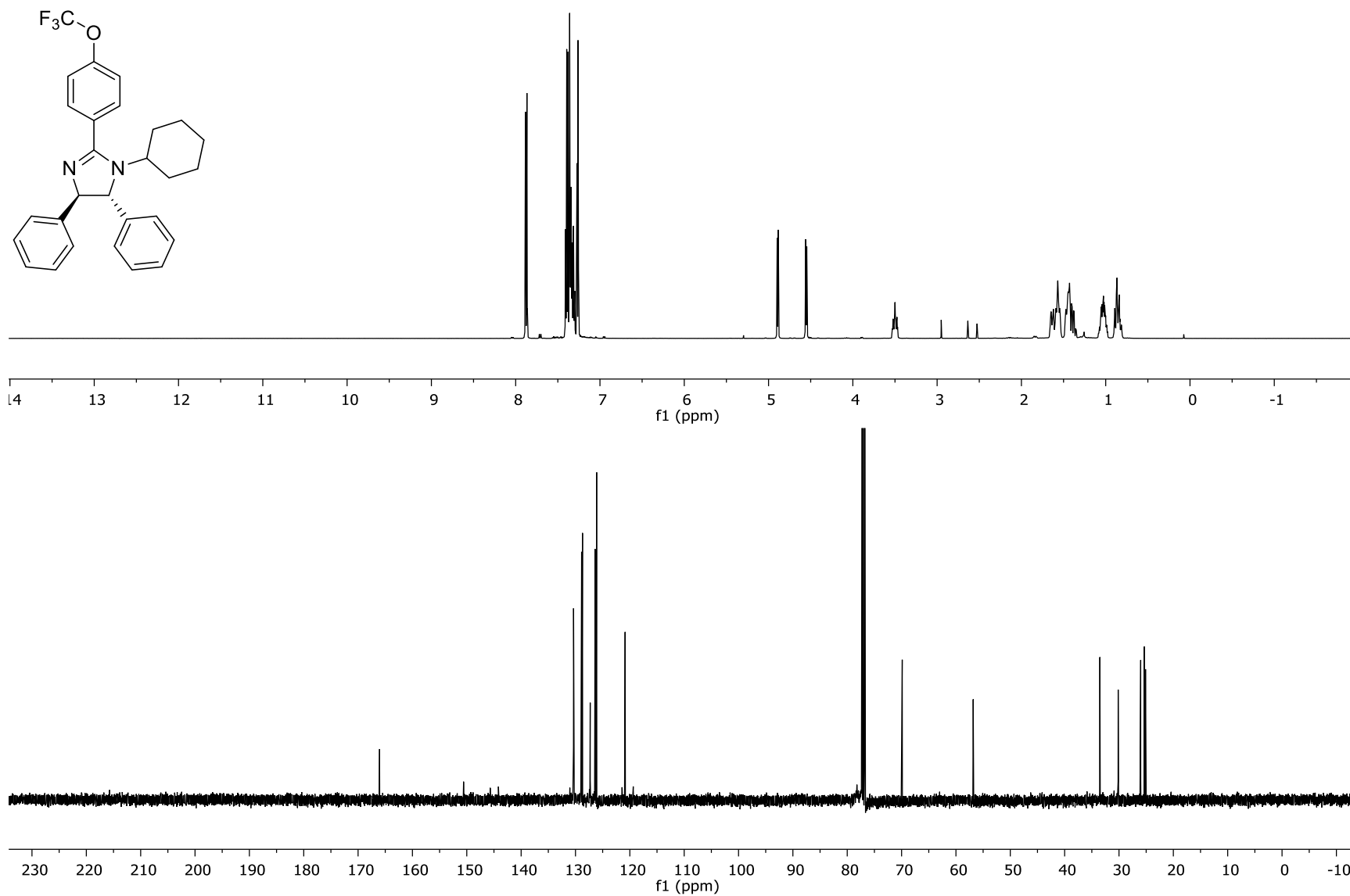


Figure II-LV: The ¹H NMR and ¹³C NMR for Compound **II-XXXVII**

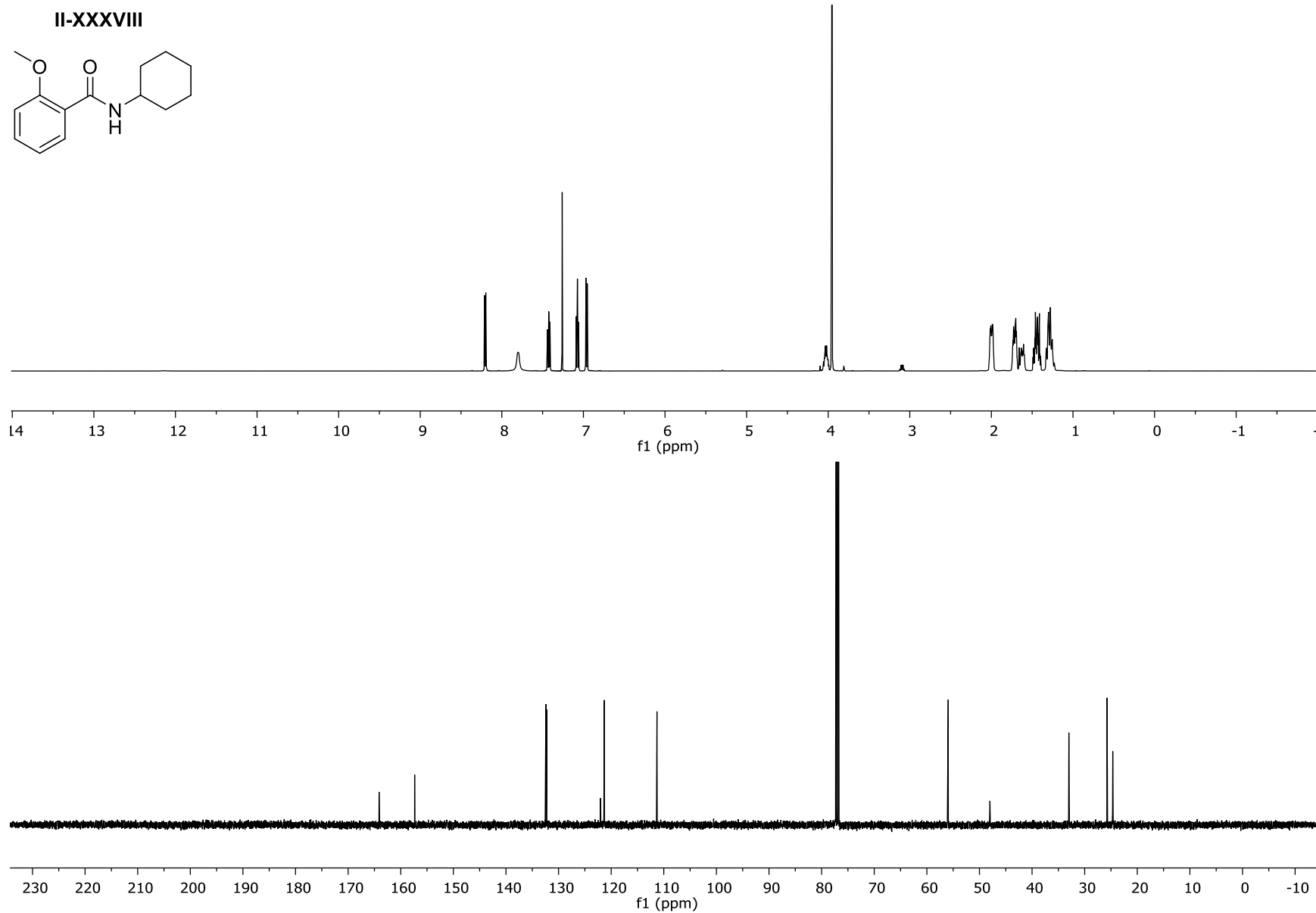


Figure II-LVI: The ^1H NMR and ^{13}C CNMR for Compound **II-XXXVIII**

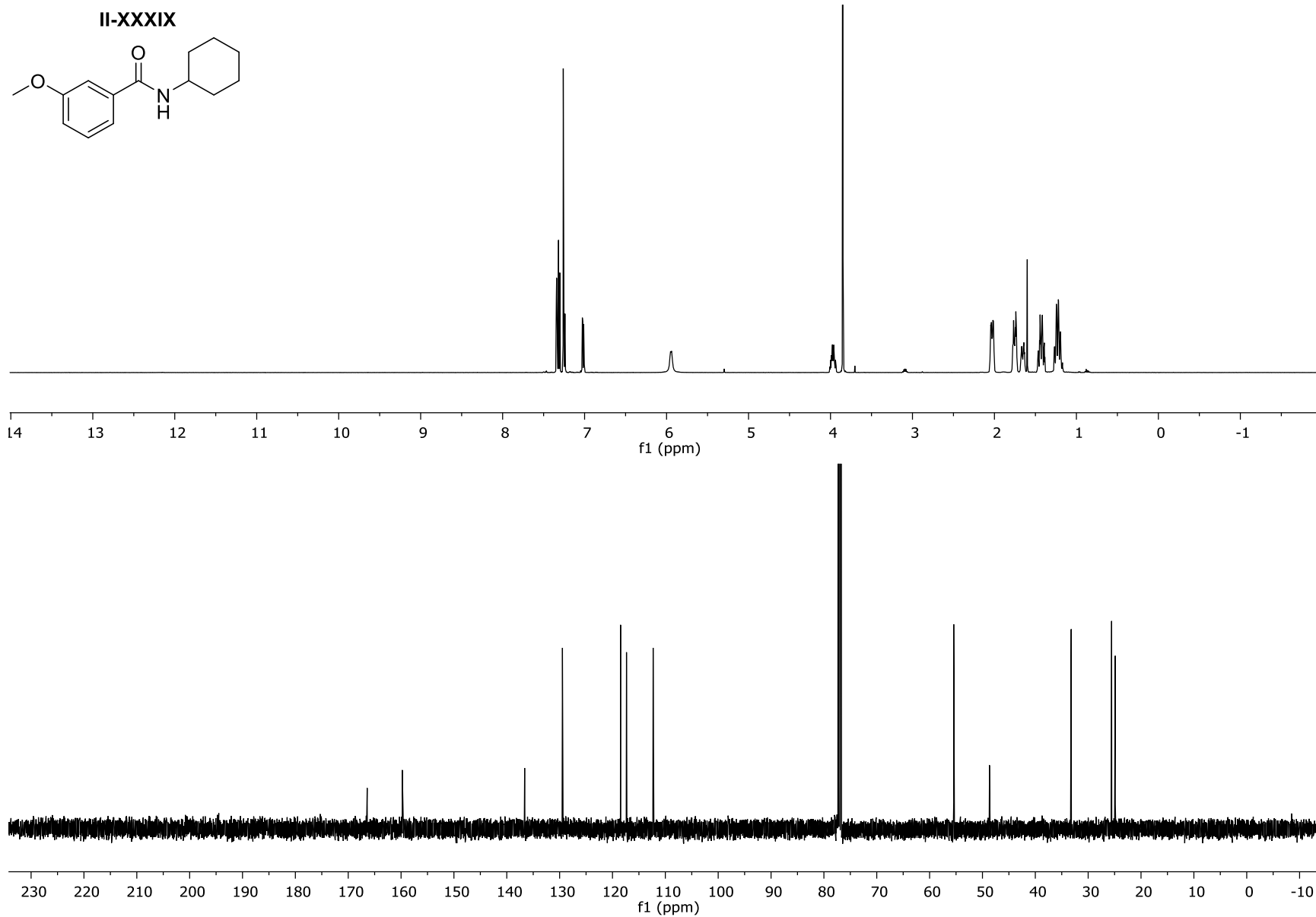


Figure II-LVII: The ^1H NMR and ^{13}C NMR for Compound **II-XXXIX**

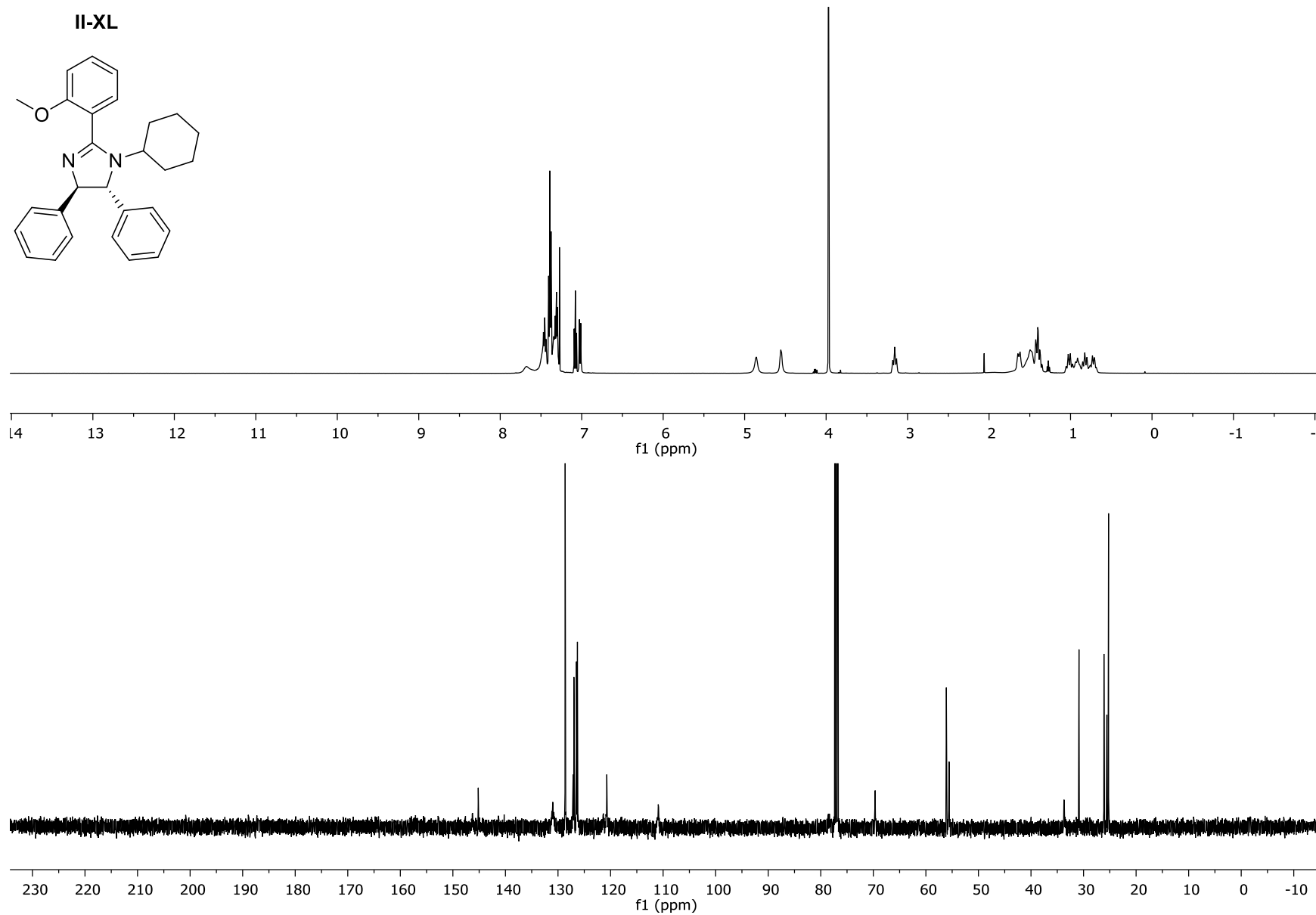


Figure II-LVIII: The ^1H NMR and ^{13}C NMR for Compound **II-XL**

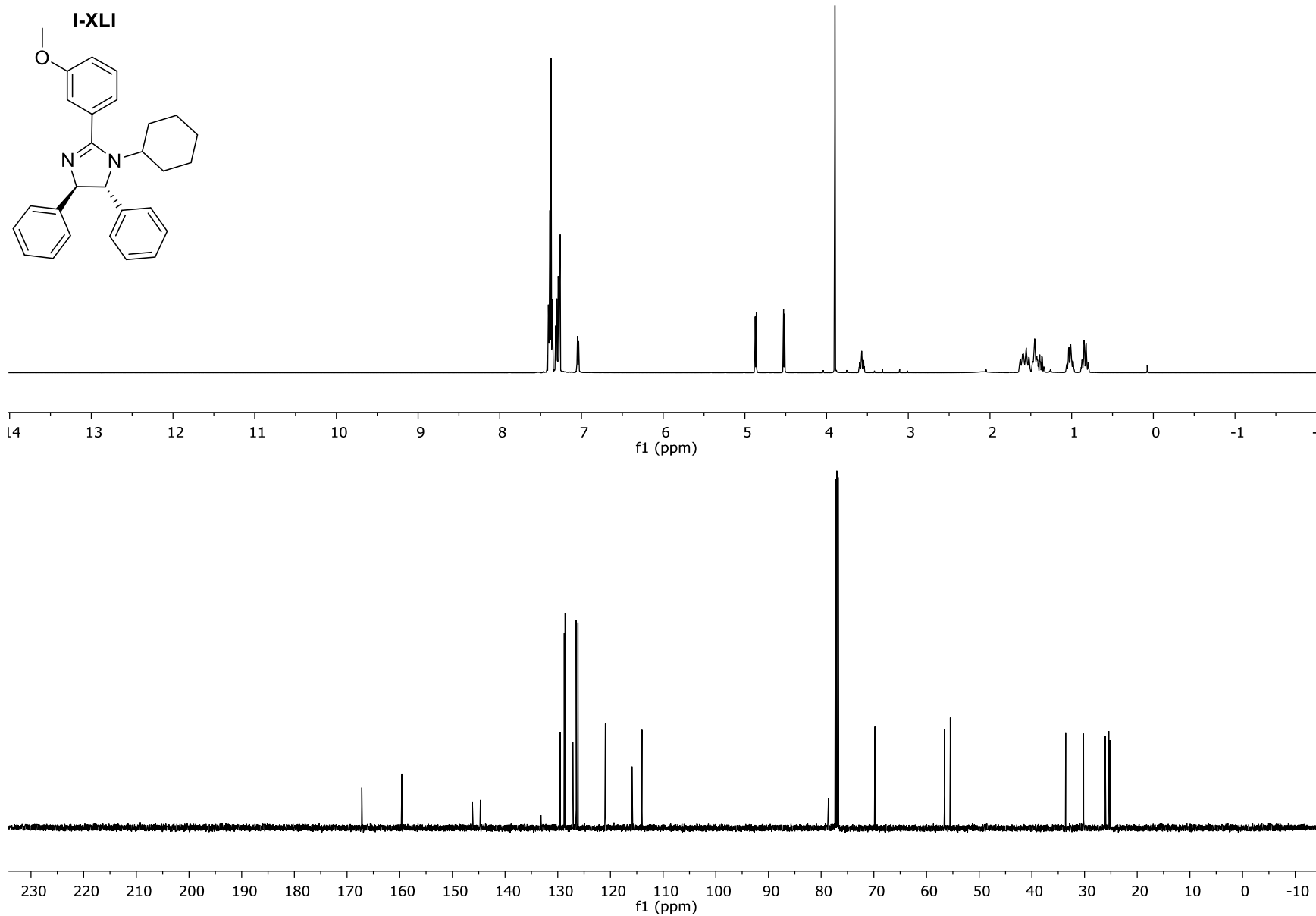


Figure II-LIX: The ^1H NMR and ^{13}C CNMR for Compound **II-XLI**

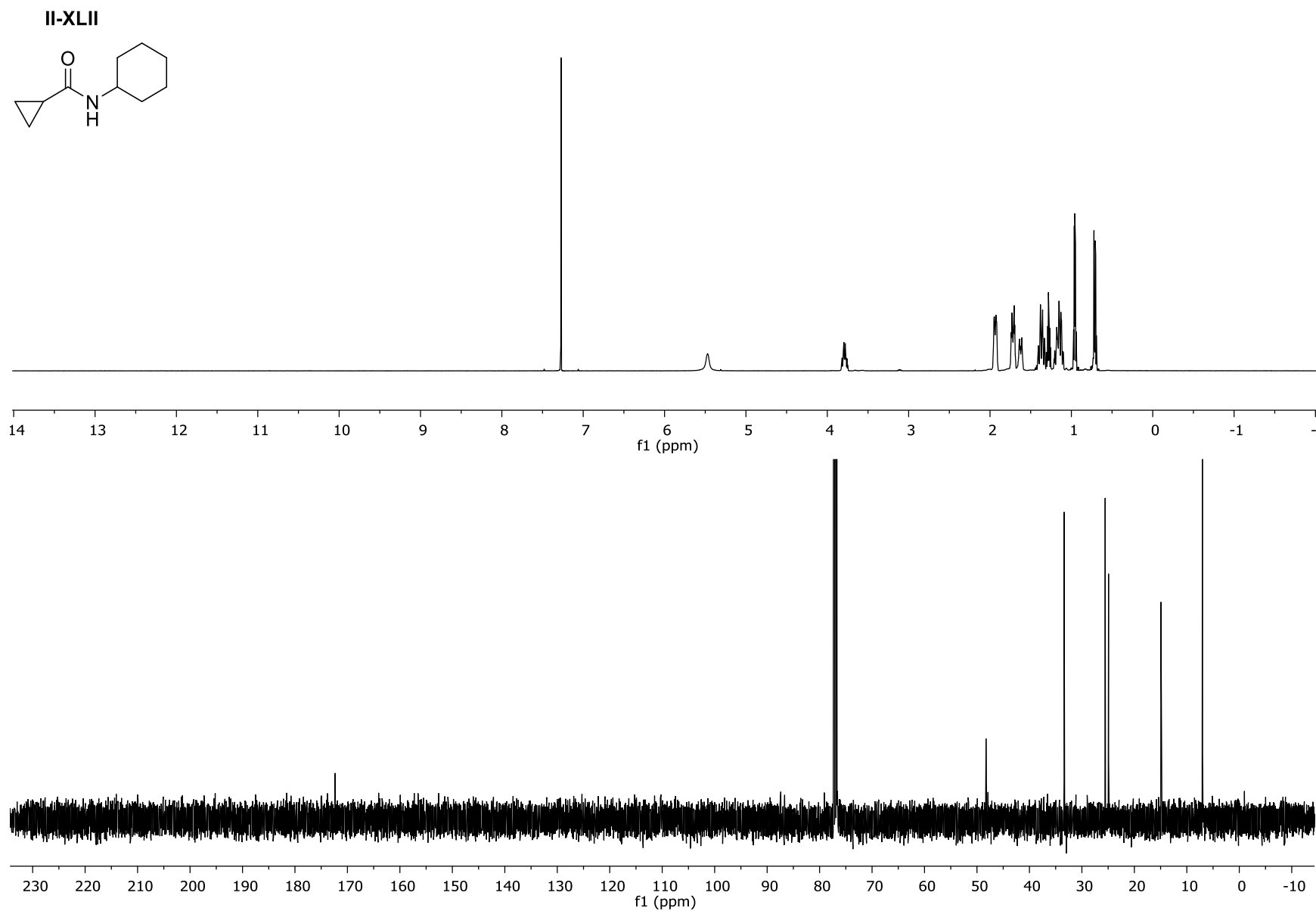


Figure II-LX: The ^1H NMR and ^{13}C NMR for Compound II-XLII

II-XLIII

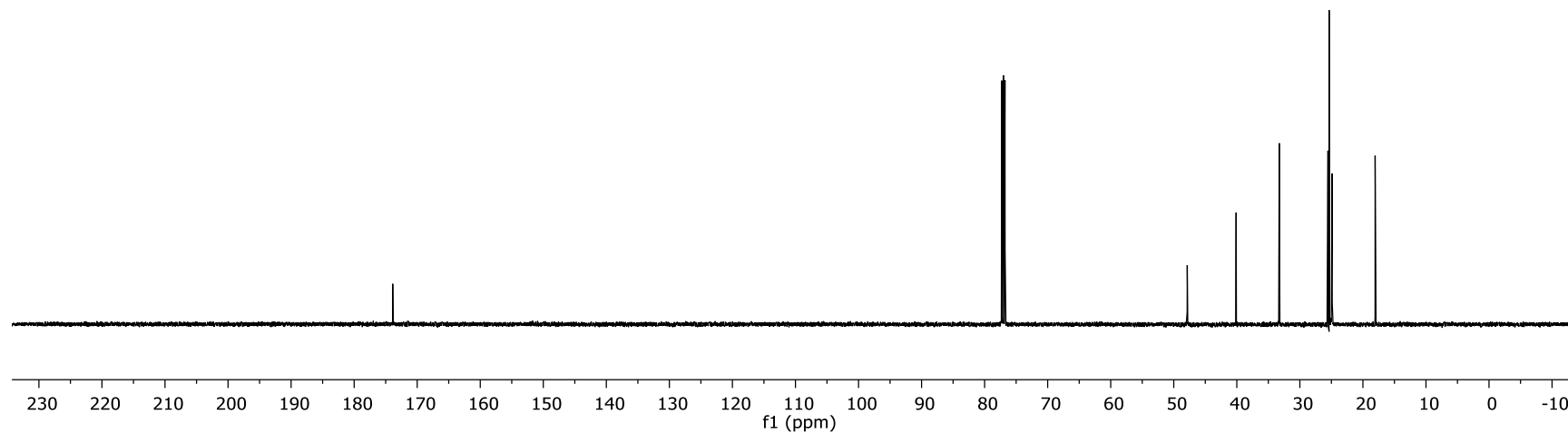
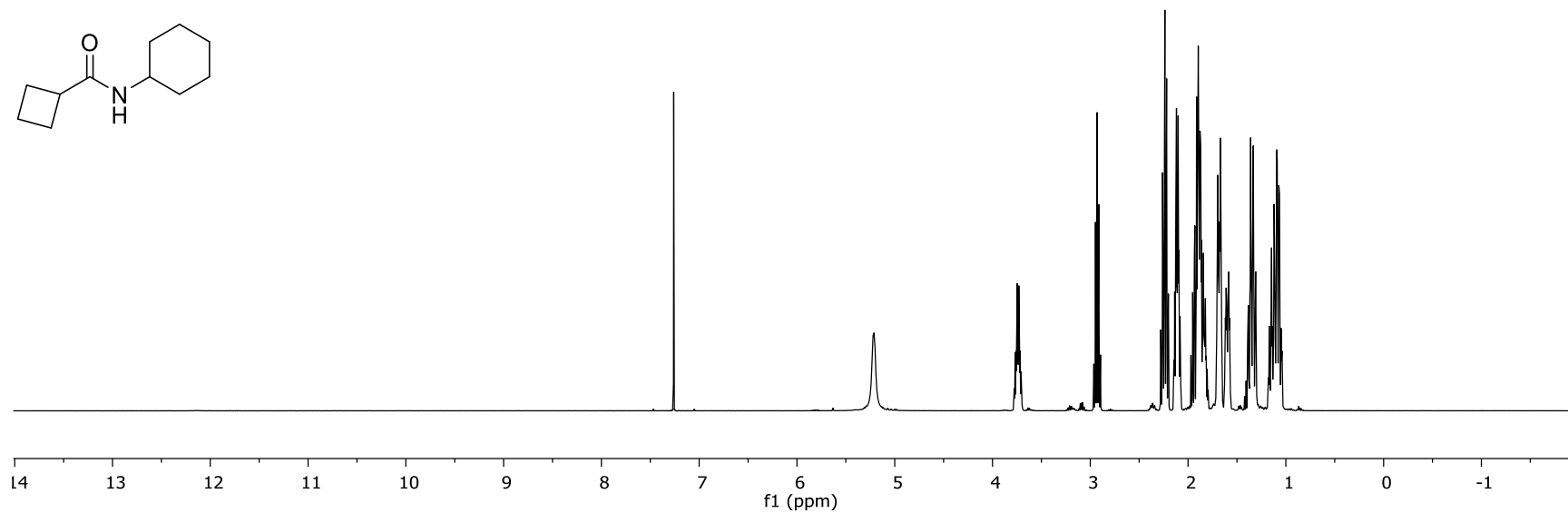
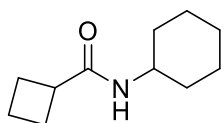


Figure II-LXI: The ^1H NMR and ^{13}C CNMR for Compound II-XLIII

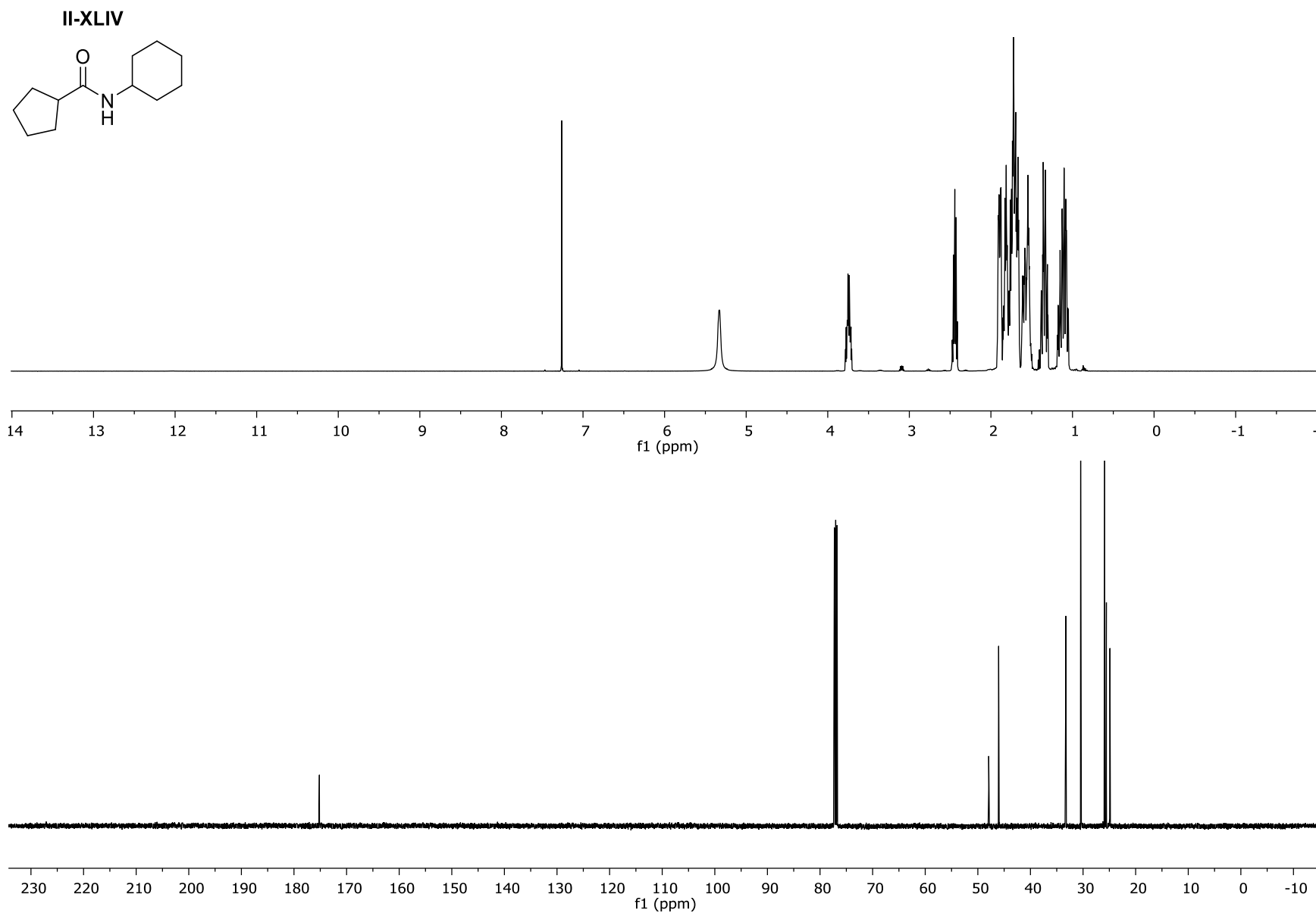


Figure II-LXII: The ^1H NMR and ^{13}C NMR for Compound **II-XLIV**

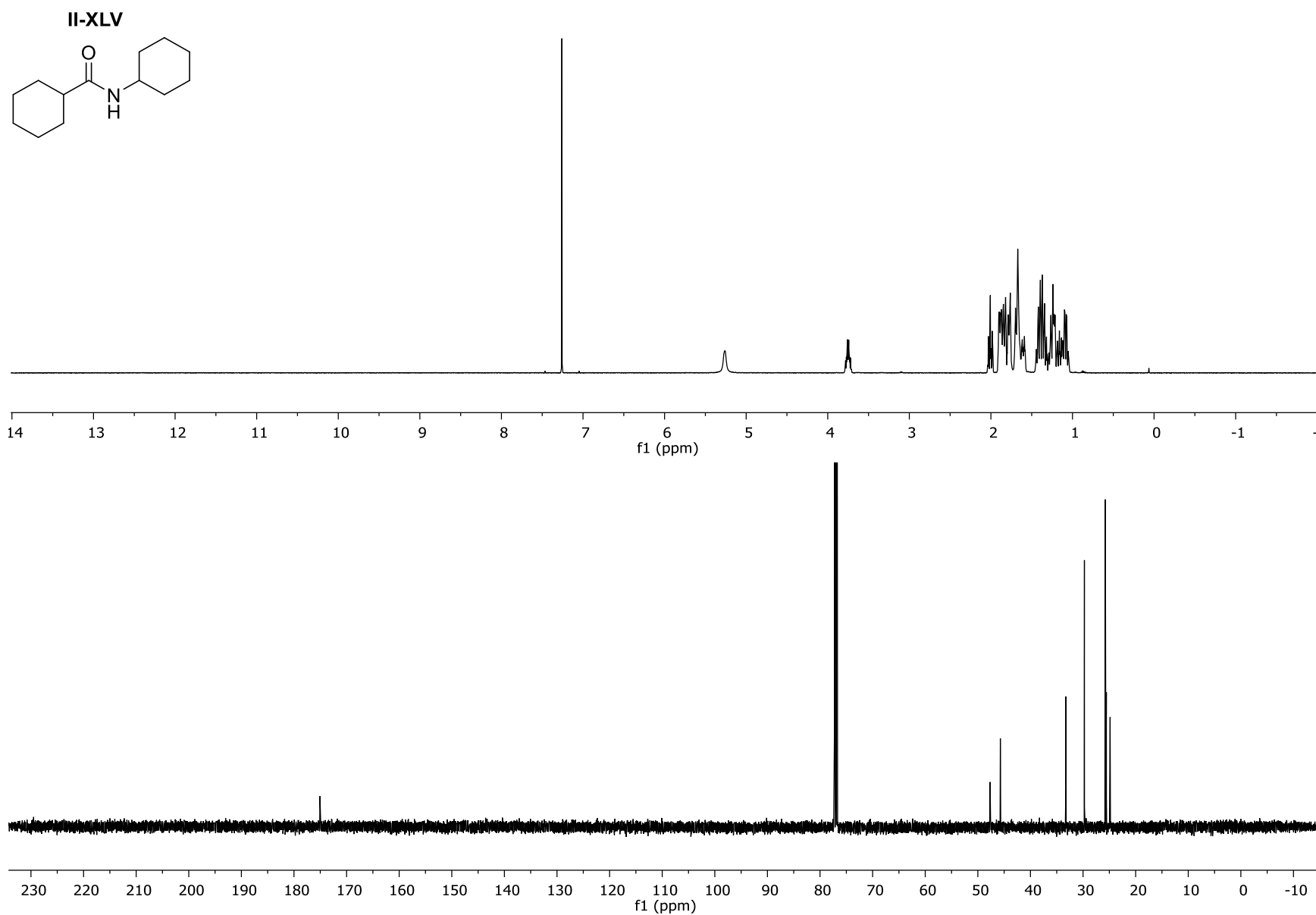


Figure II-LXIII: The ^1H NMR and ^{13}C NMR for Compound **II-XLV**

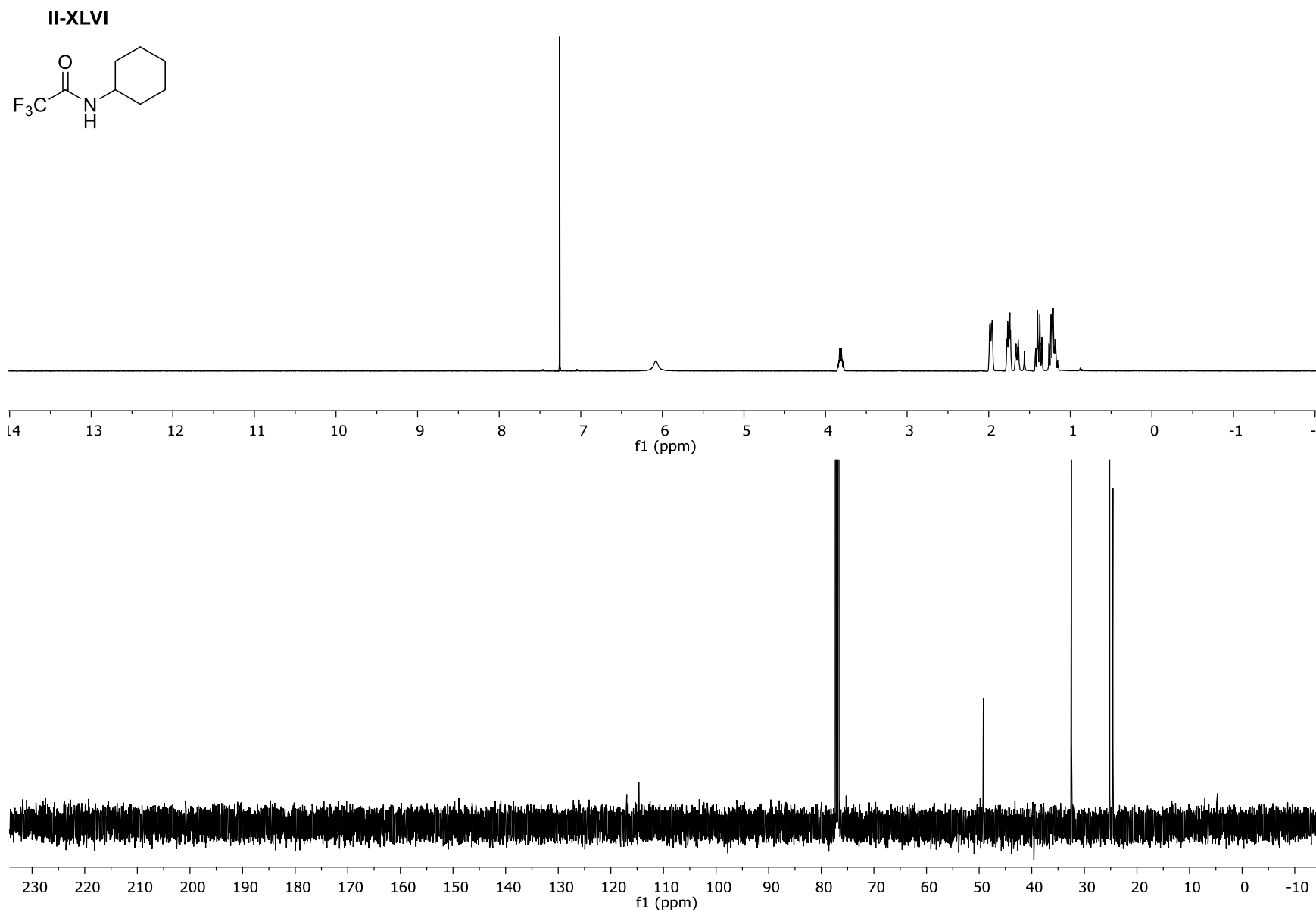


Figure II-LXIV: The ^1H NMR and ^{13}C NMR for Compound **II-XLVI**

II-XLVII

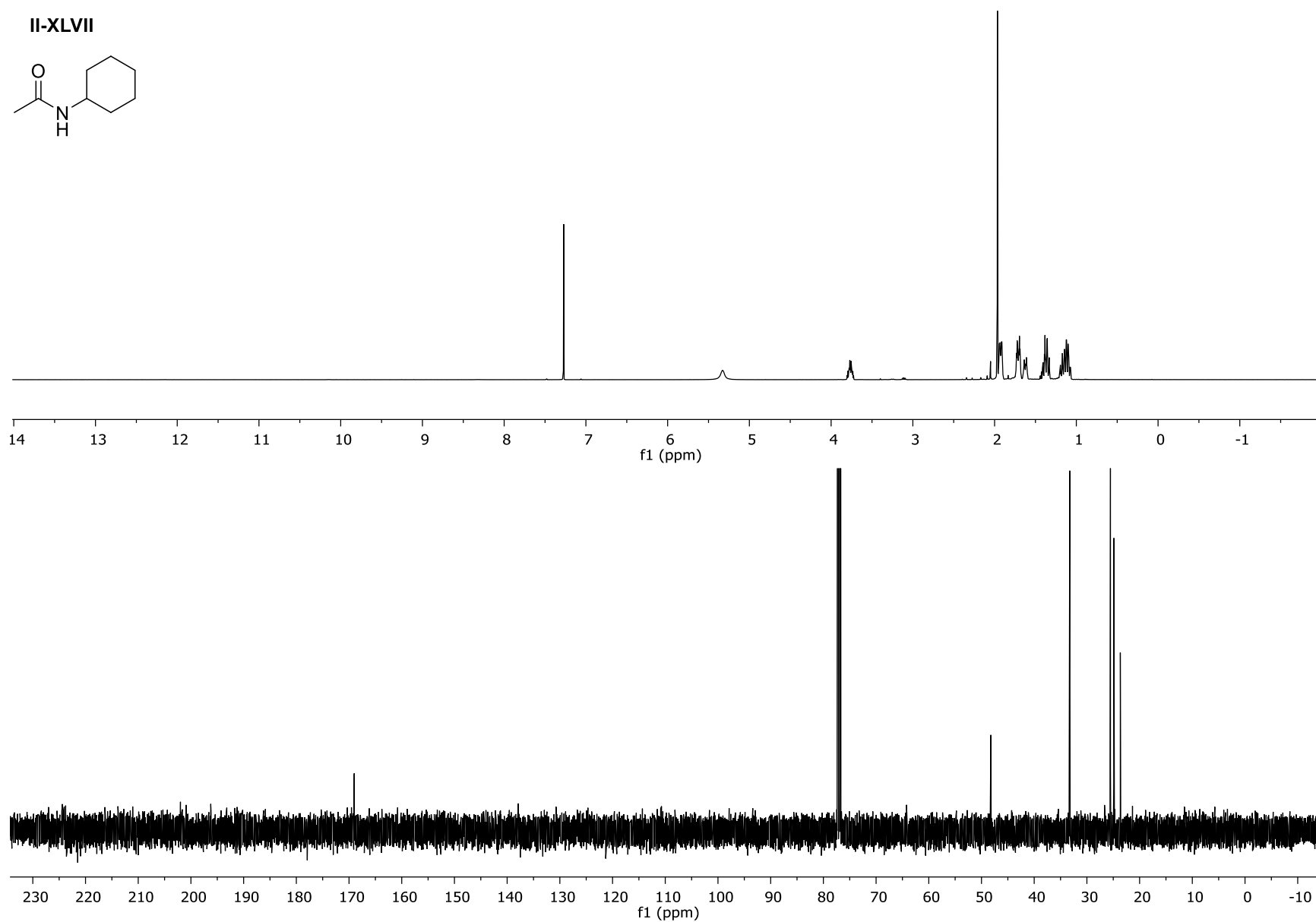
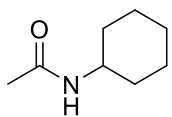


Figure II-LXV: The ^1H NMR and ^{13}C NMR for Compound II-XLVII

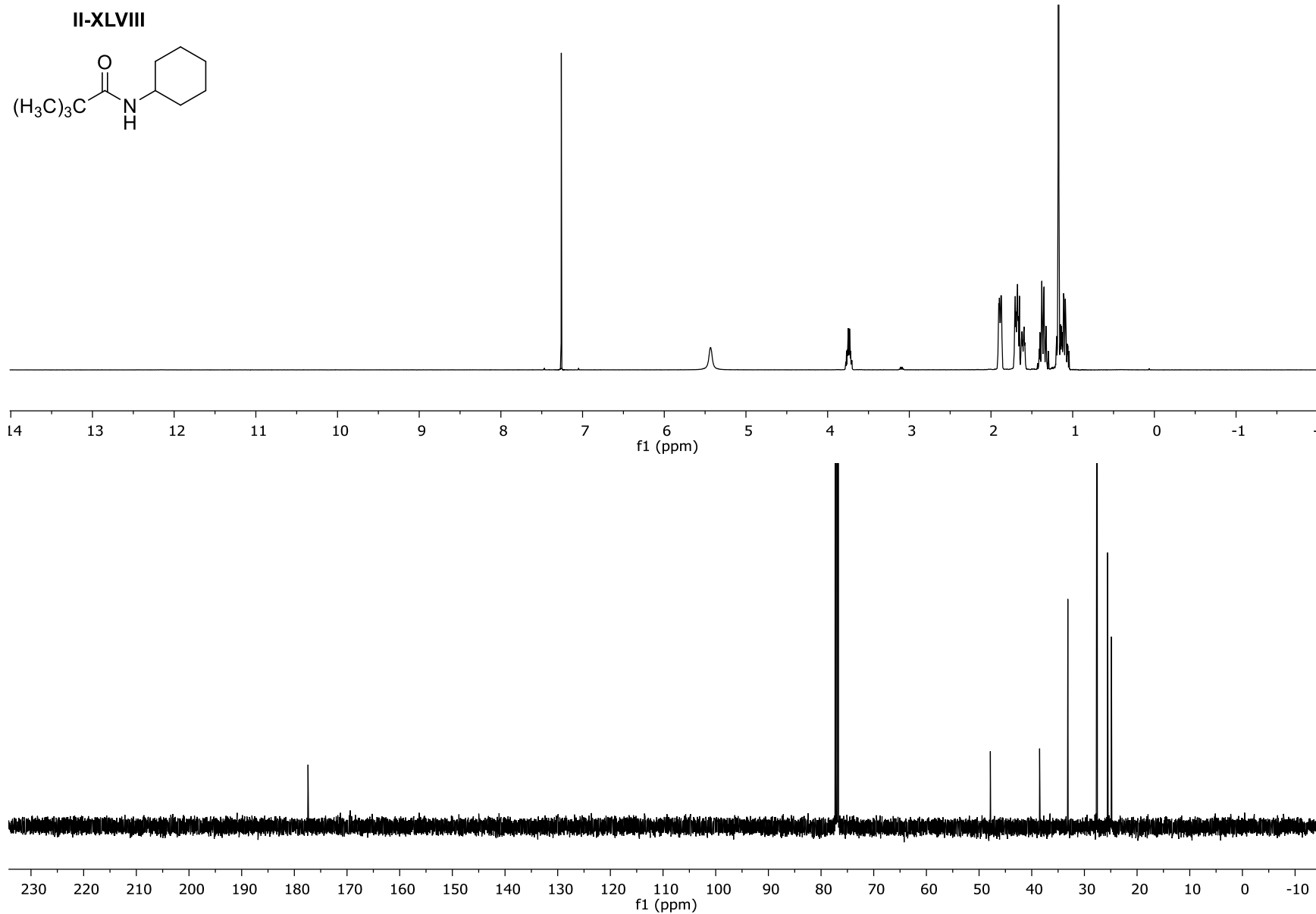


Figure II-LXVI: The ¹H NMR and ¹³C NMR for Compound II-XLVIII

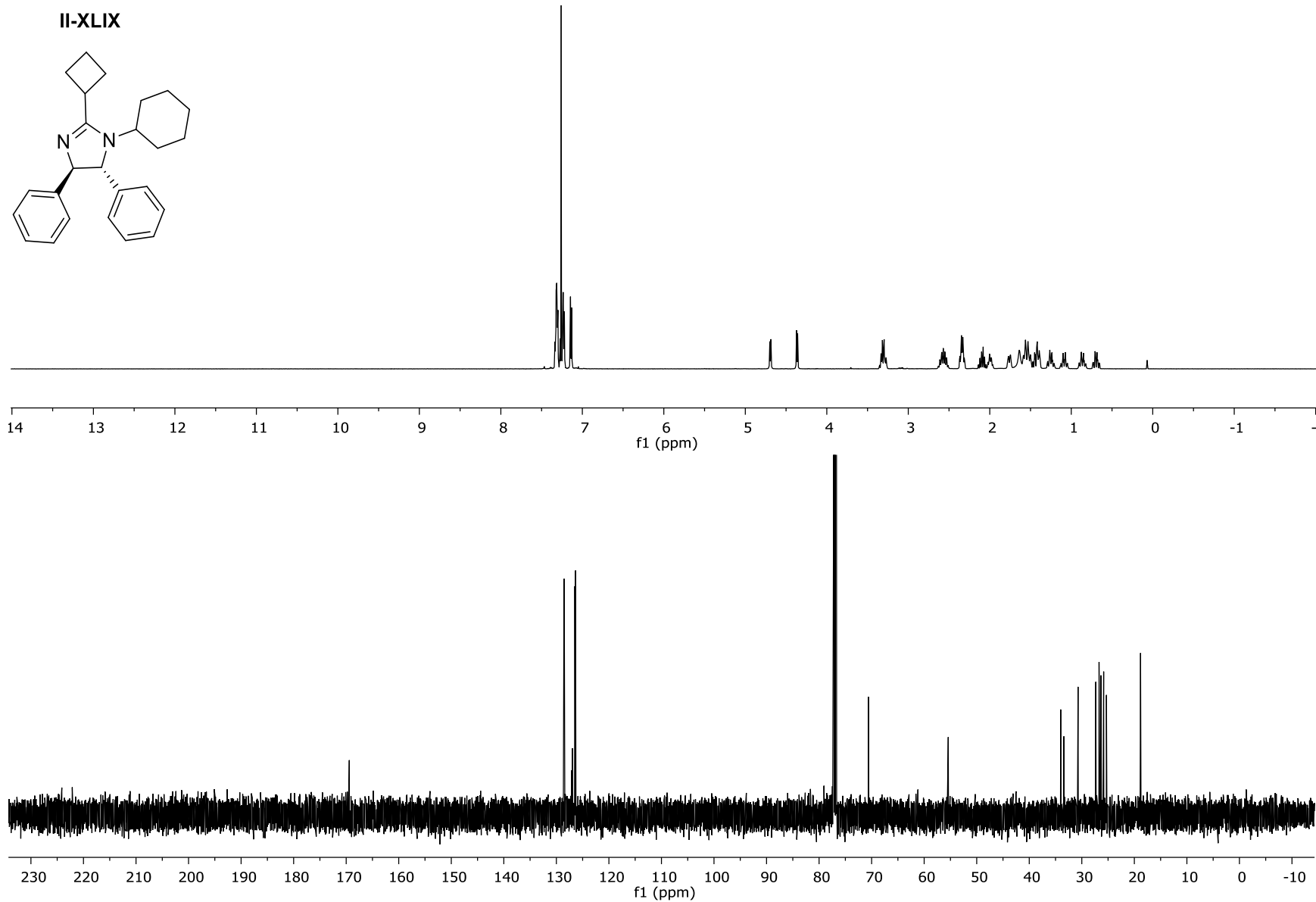


Figure II-LXVII: The ^1H NMR and ^{13}C NMR for Compound **II-XLIX**

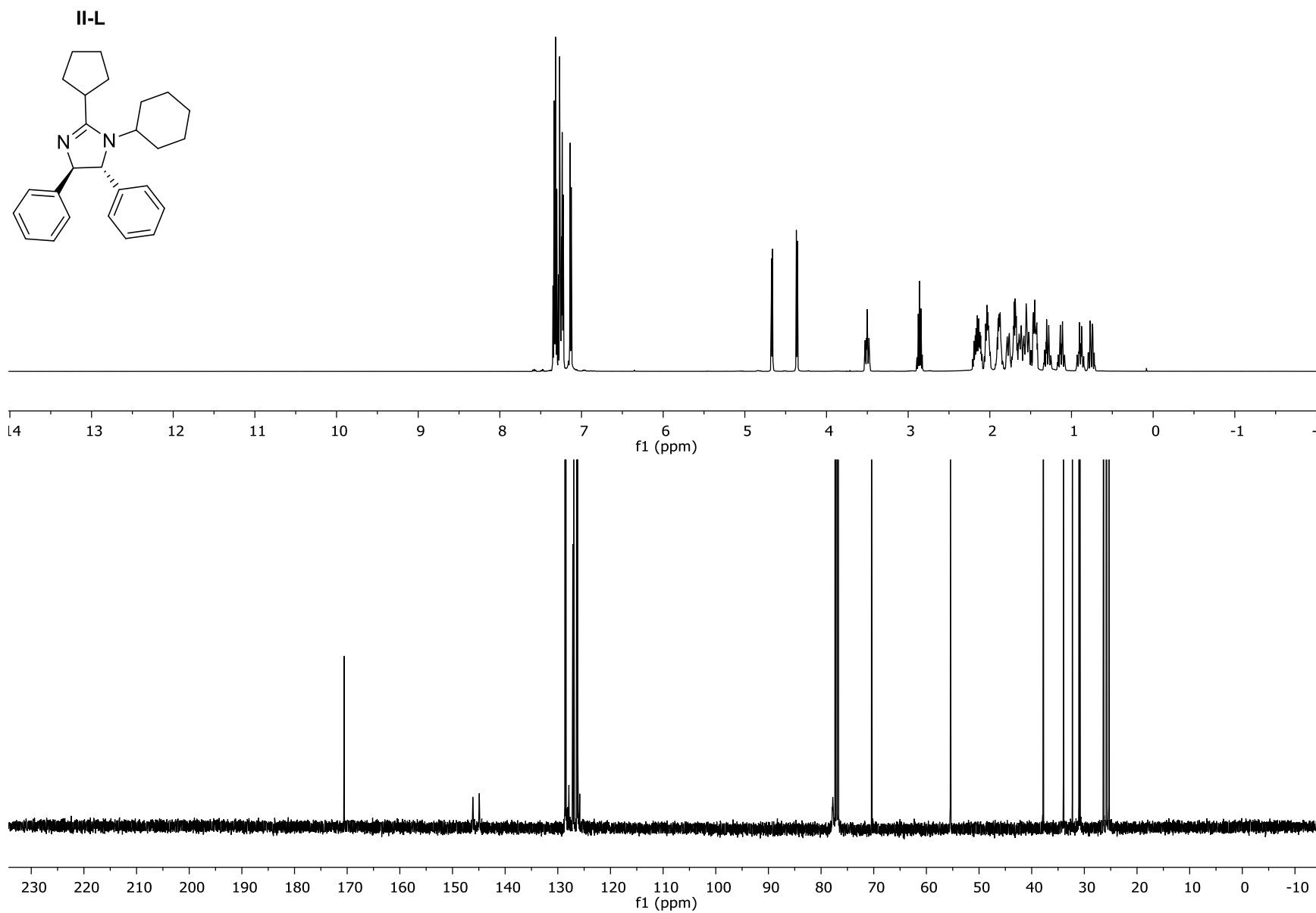


Figure II-LXVIII: The ^1H NMR and ^{13}C NMR for Compound II-L

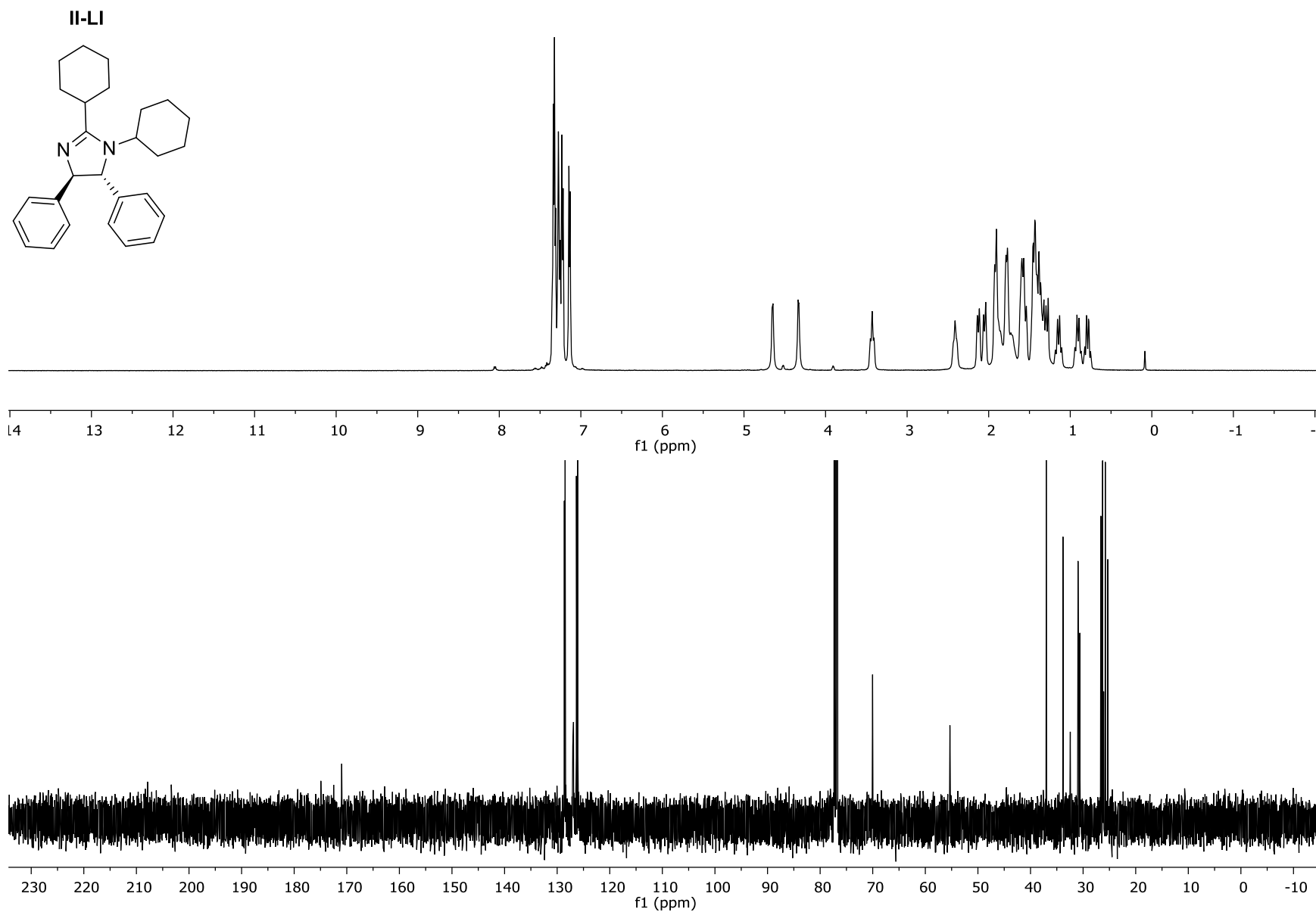


Figure II-LXIX: The ^1H NMR and ^{13}C NMR for Compound II-LI

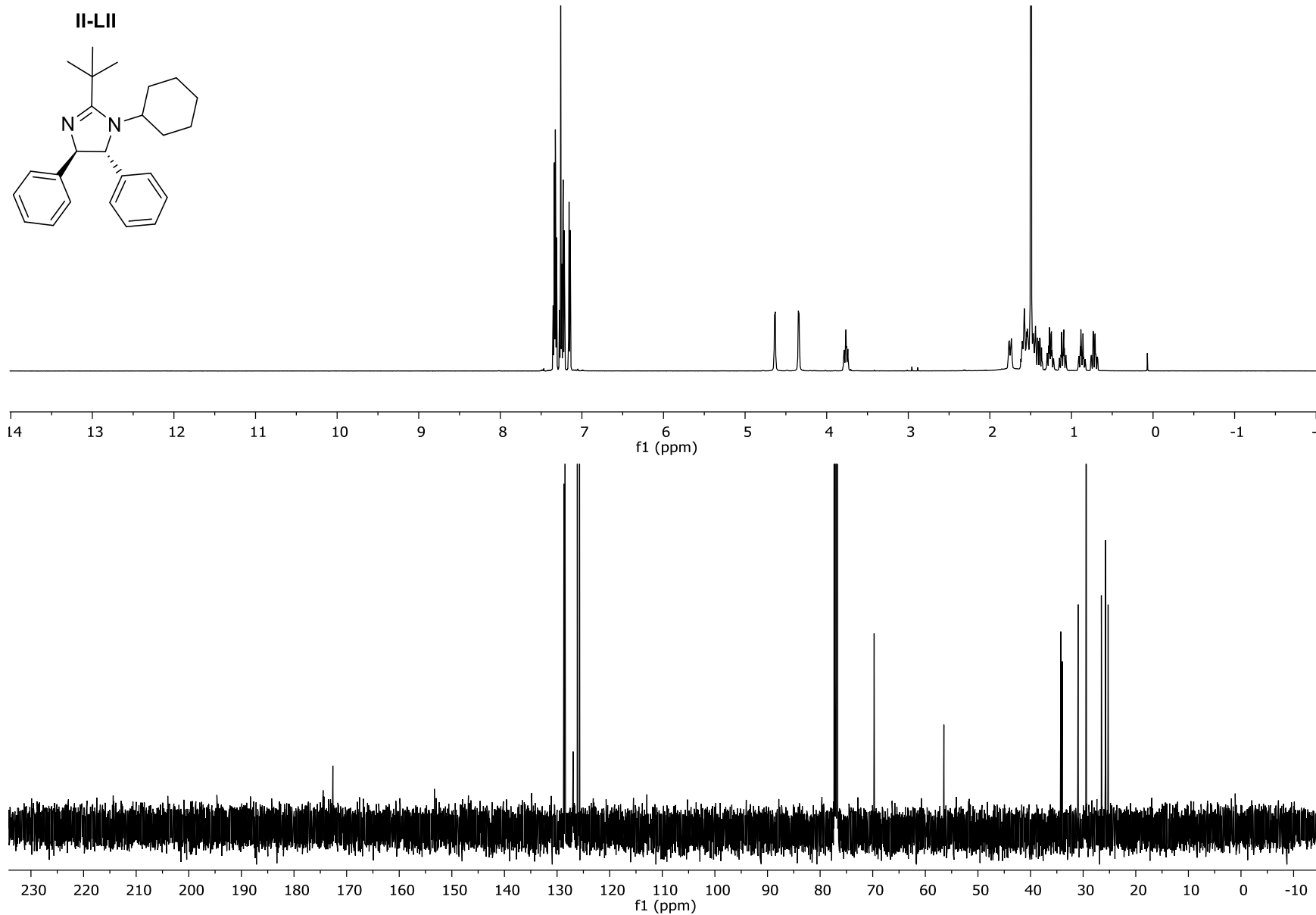


Figure II-LXX: The ^1H NMR and ^{13}C NMR for Compound **II-LII**

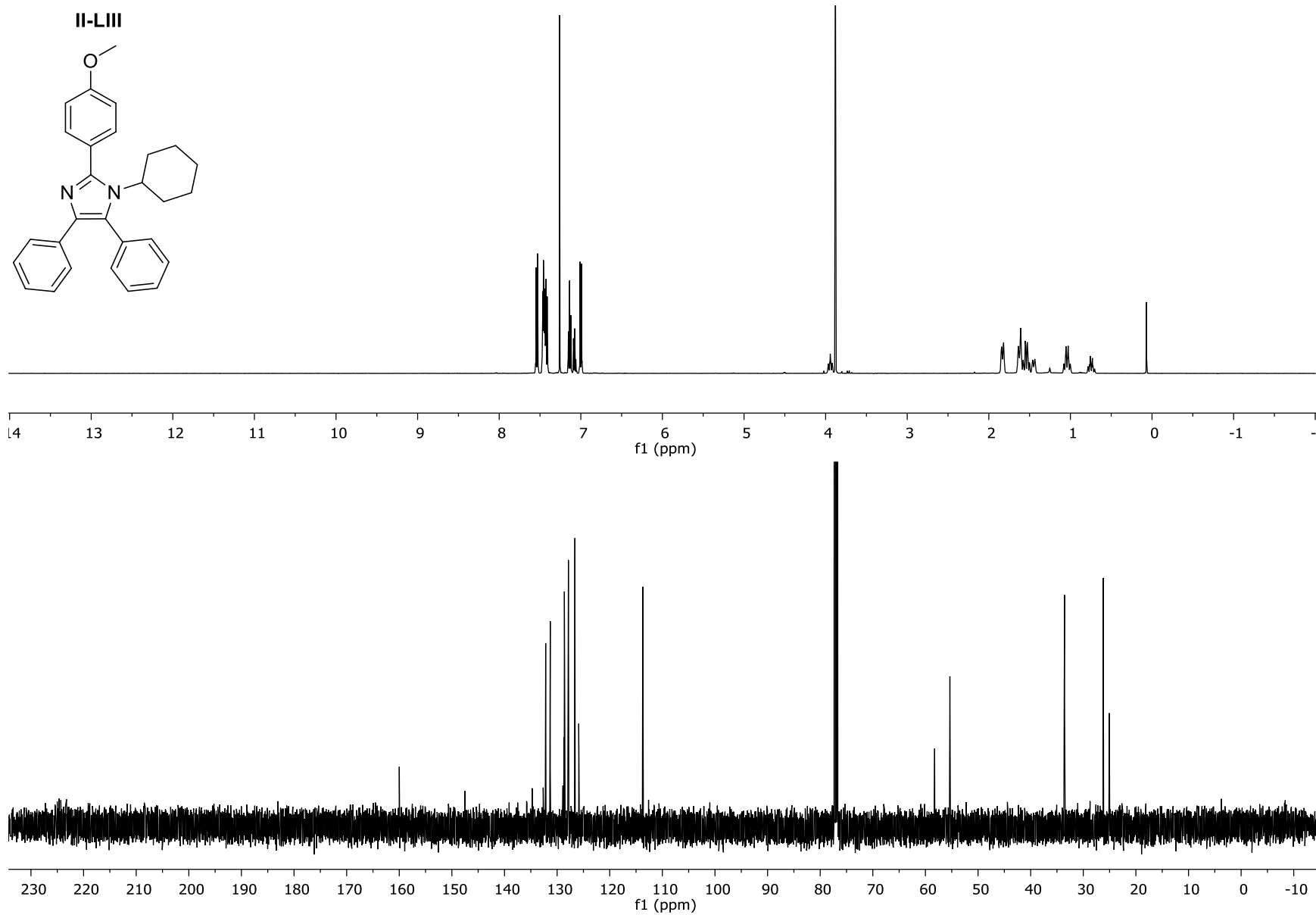


Figure II-LXXI: The ^1H NMR and ^{13}C NMR for Compound **II-LIII**

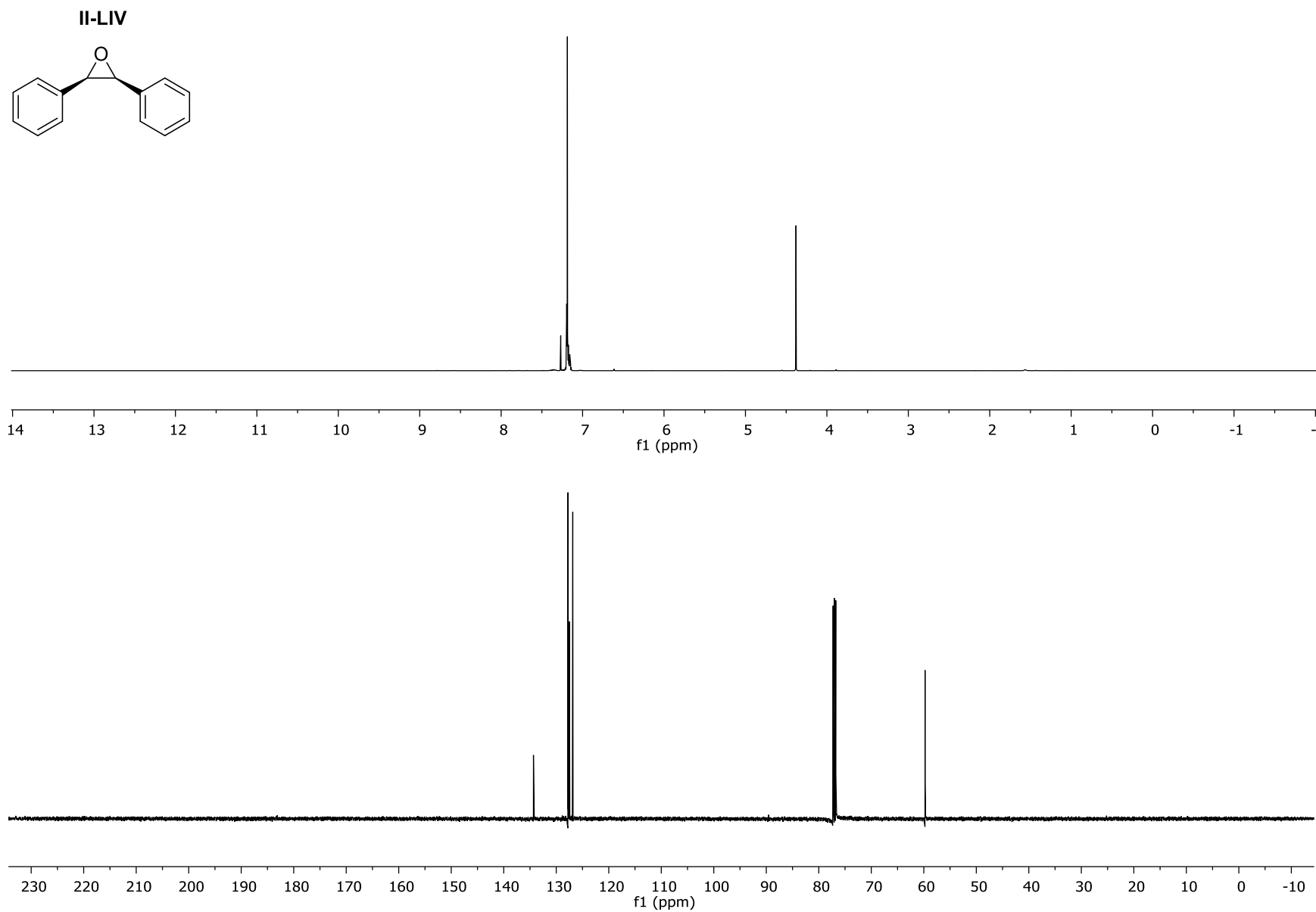


Figure II-LXXII: The ^1H NMR and ^{13}C CNMR for Compound **II-LIV**

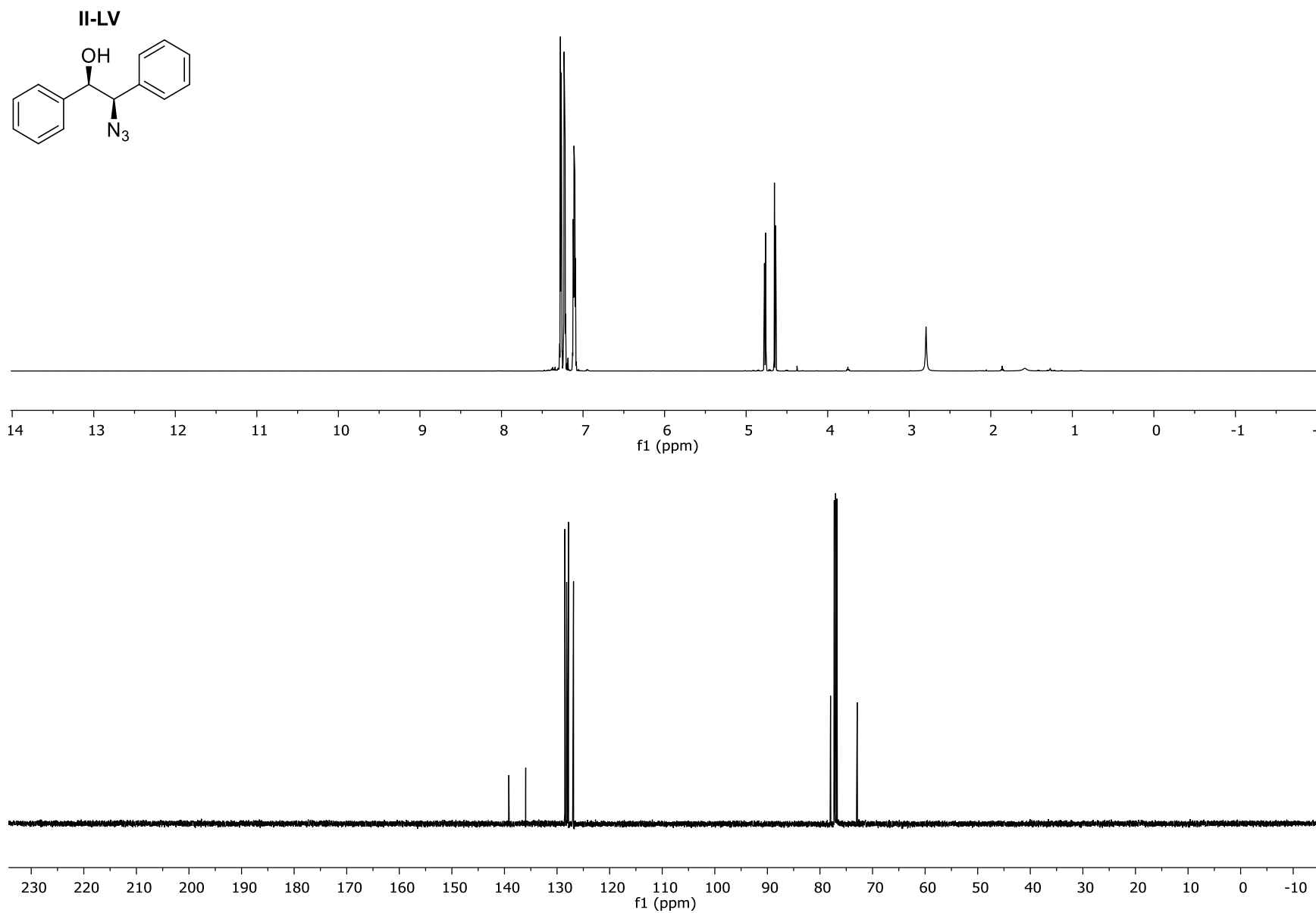


Figure II-LXXIII: The ^1H NMR and ^{13}C NMR for Compound II-LV

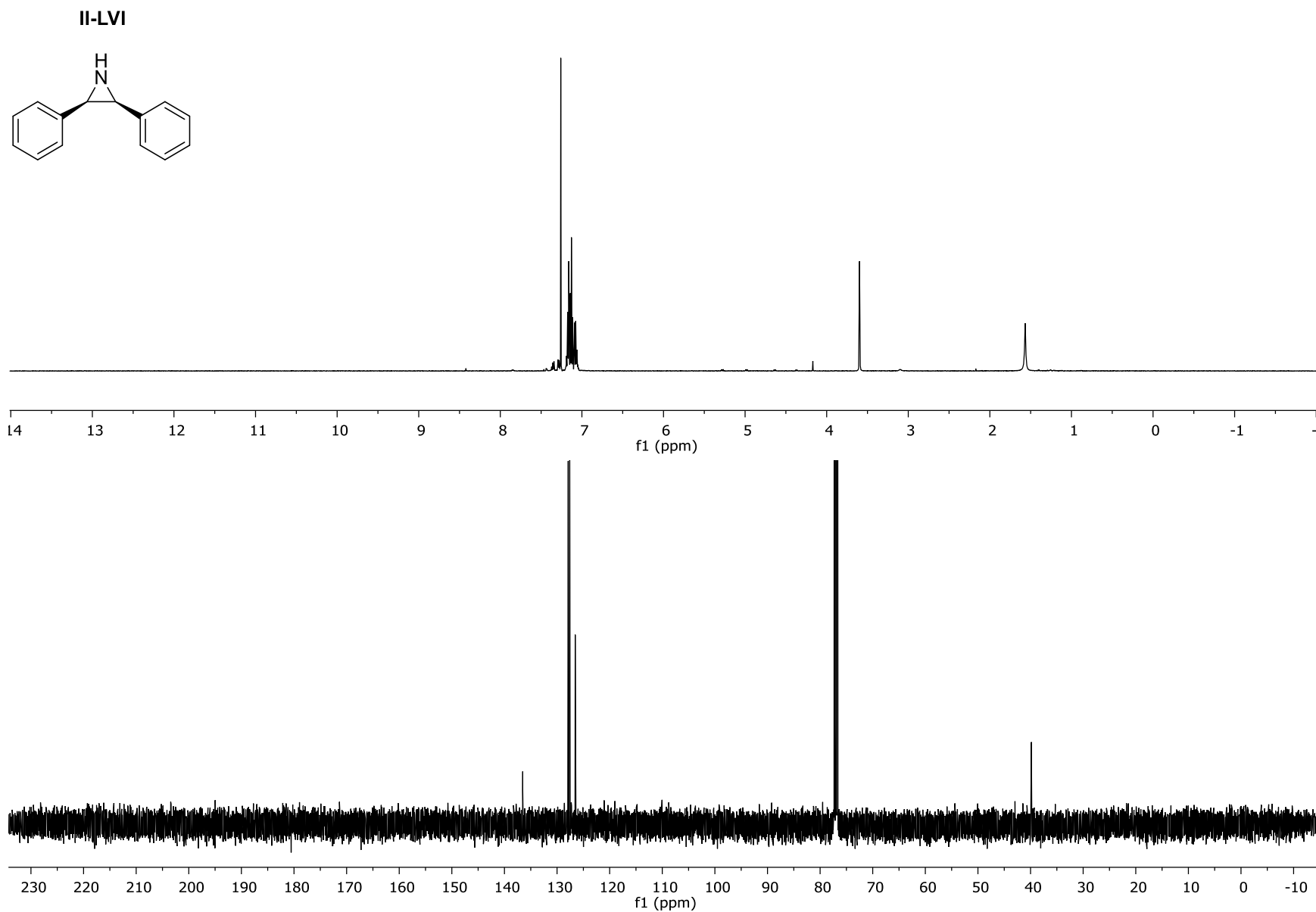


Figure II-LXXIV: The ^1H NMR and ^{13}C NMR for Compound **II-LVI**

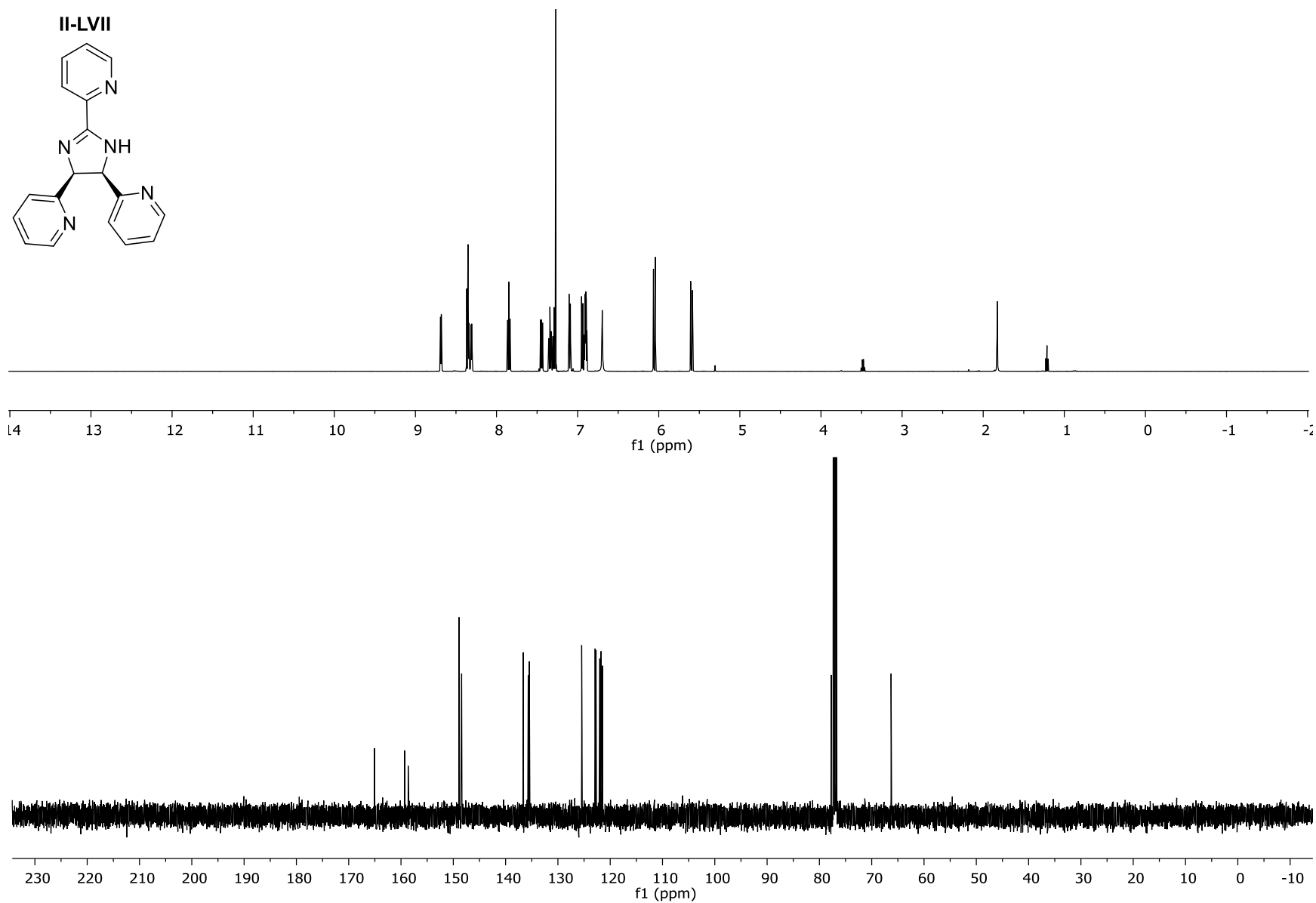


Figure II-LXXV: The ^1H NMR and ^{13}C NMR for Compound **II-LVII**

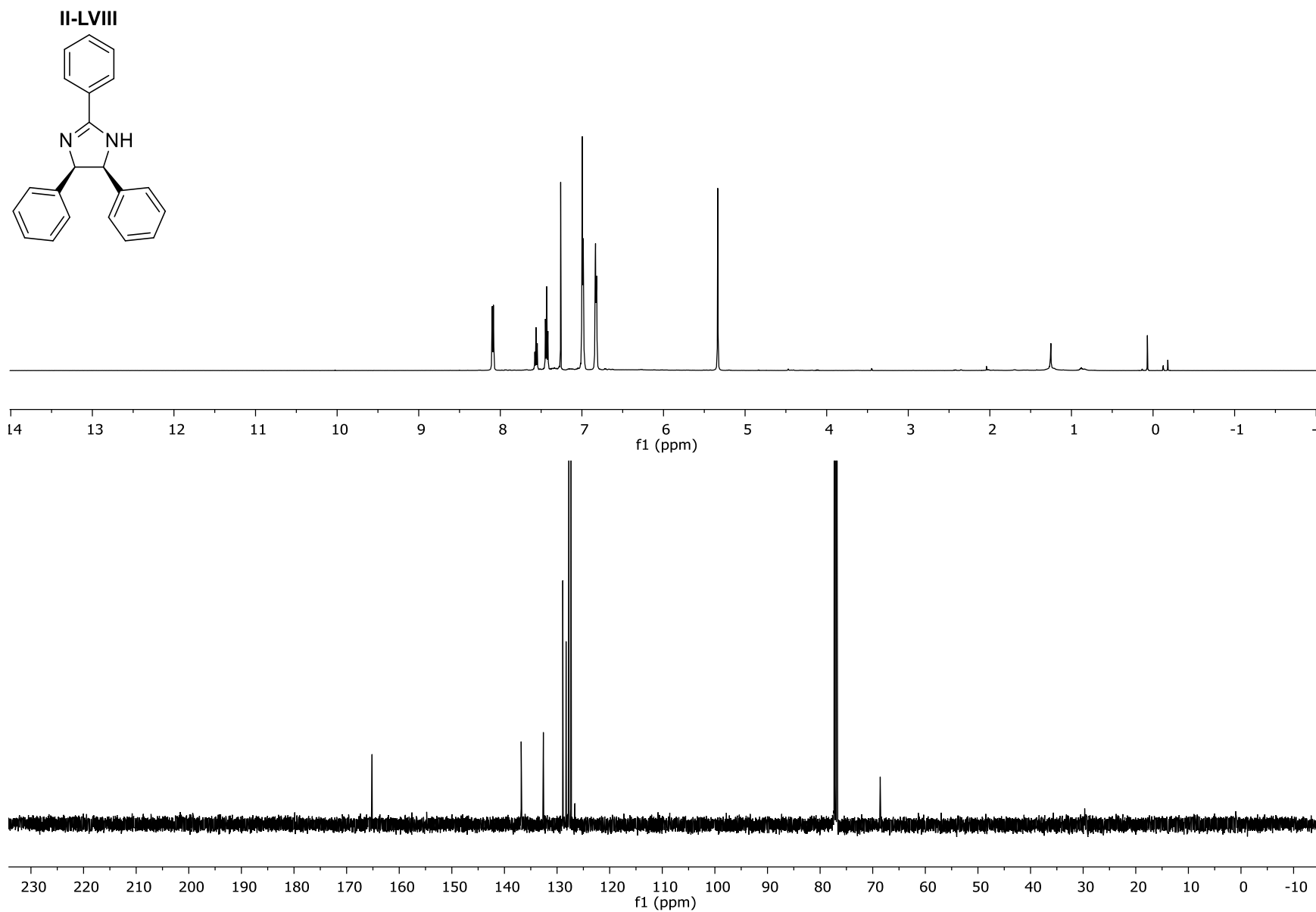


Figure II-LXXVI: The ^1H NMR and ^{13}C NMR for Compound **II-LVIII**

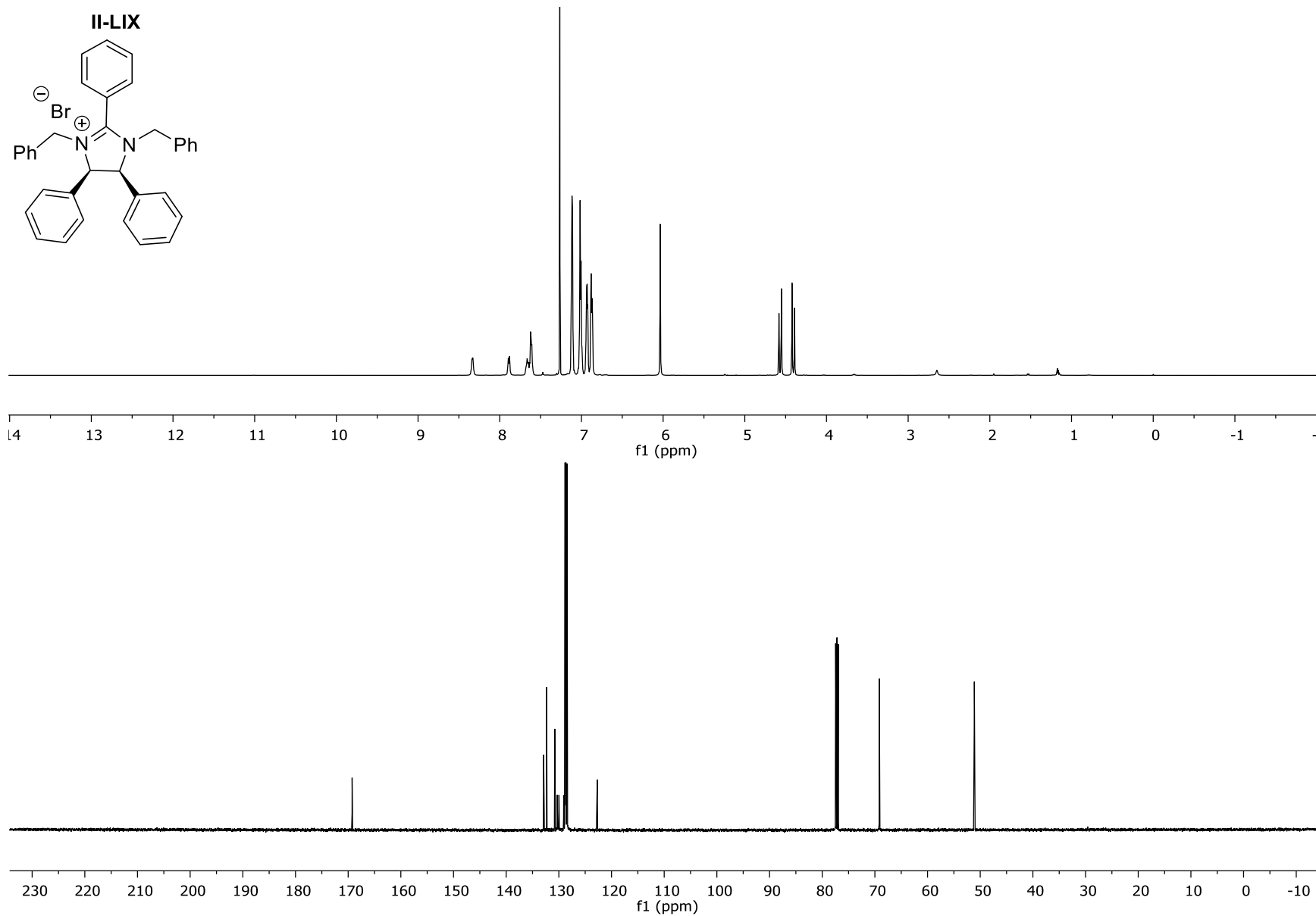


Figure II-LXXVII: The ^1H NMR and ^{13}C NMR for Compound **II-LIX**

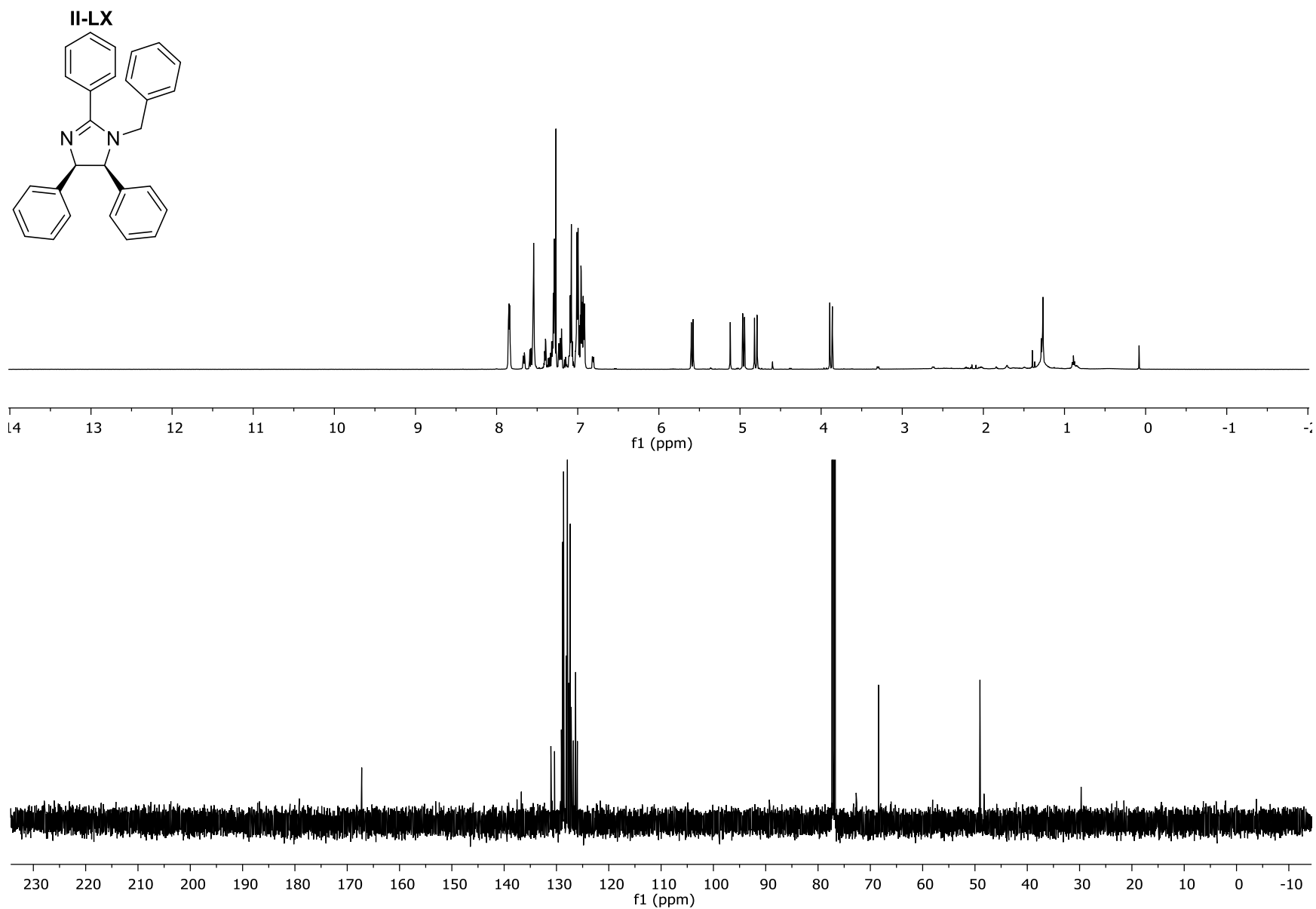


Figure II-LXXVIII: The ^1H NMR and ^{13}C NMR for Compound II-LX

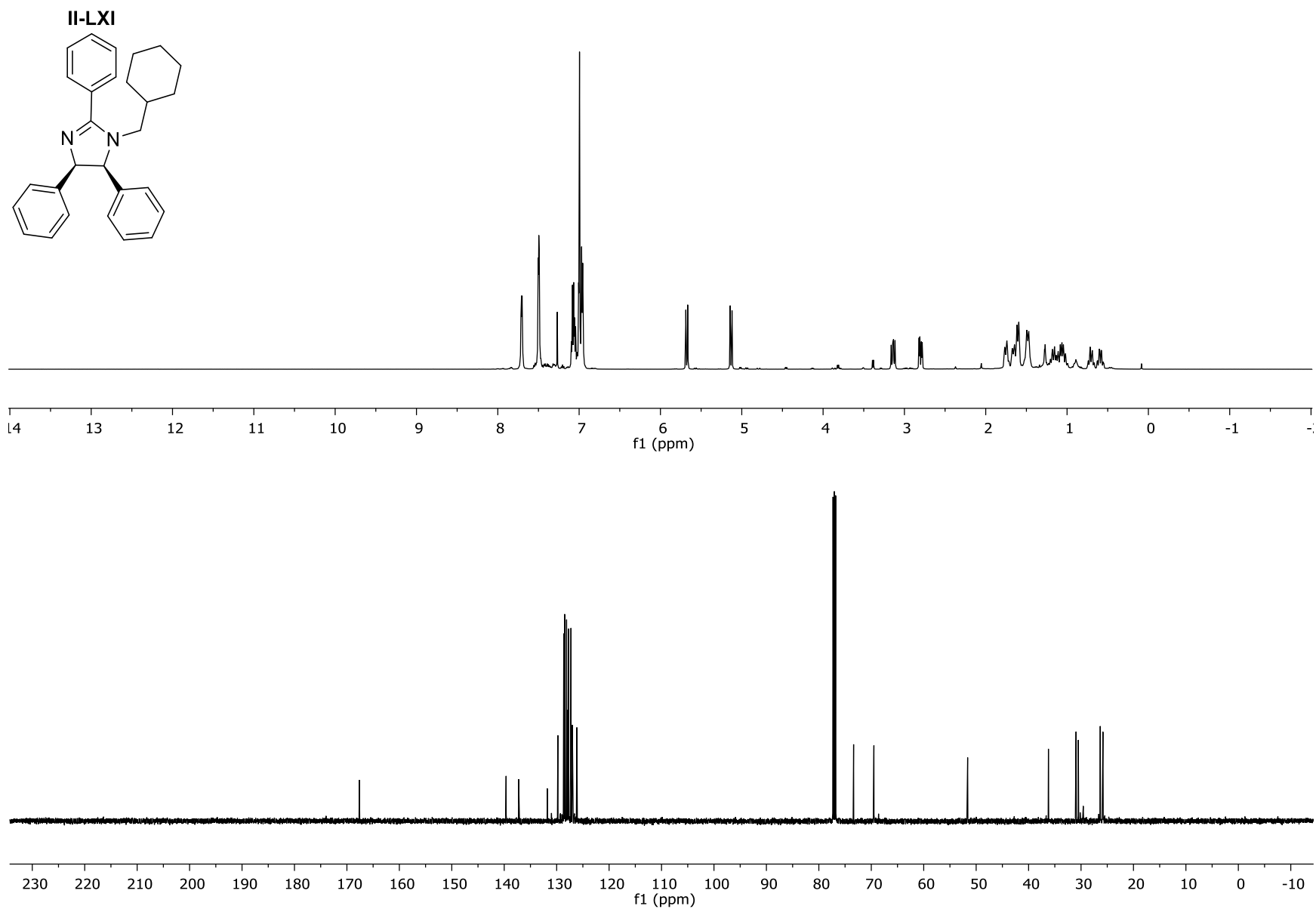


Figure II-LXXIX: The ^1H NMR and ^{13}C NMR for Compound **II-LXI**

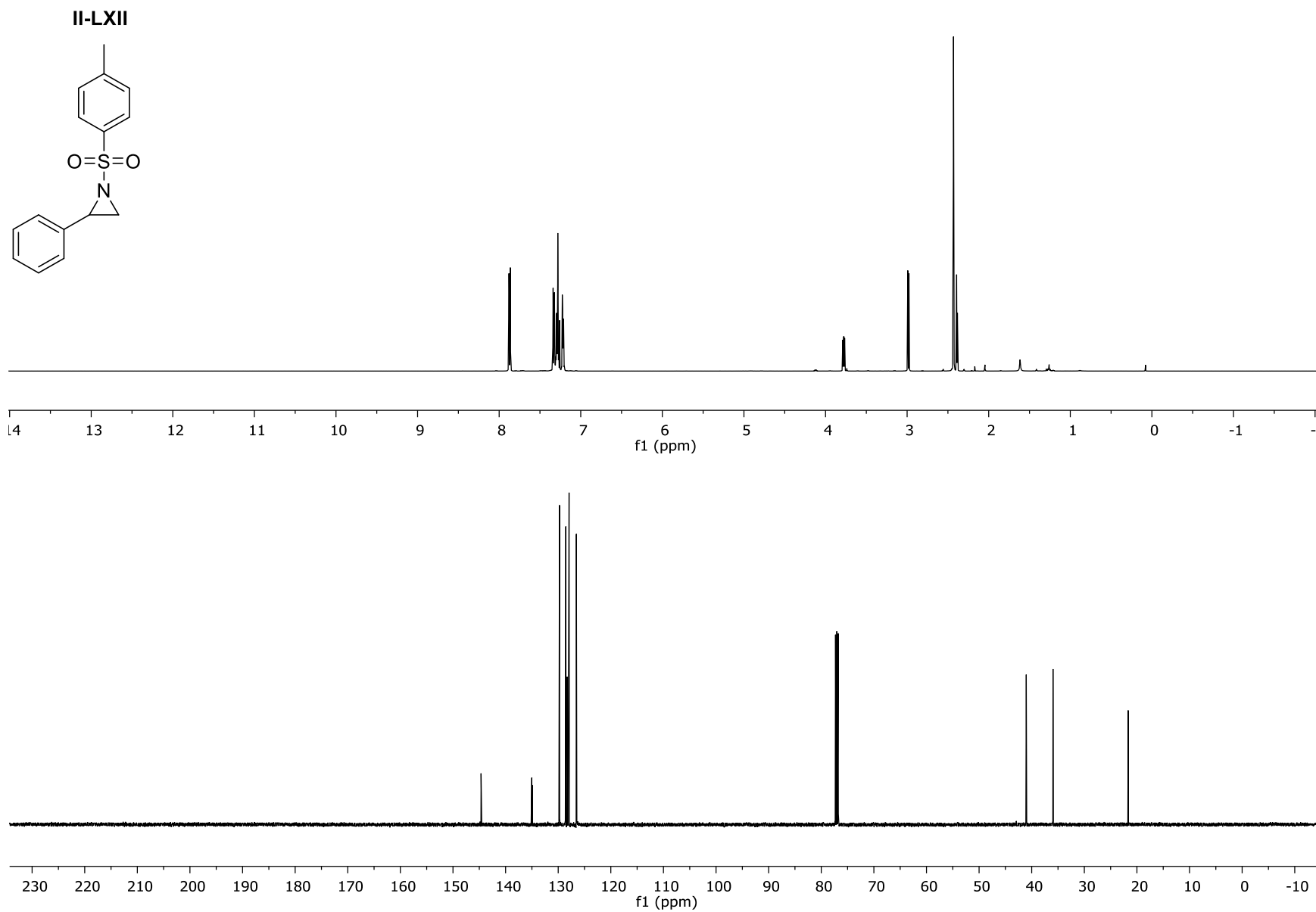


Figure II-LXXX: The ¹H NMR and ¹³C NMR for Compound **II-LXII**

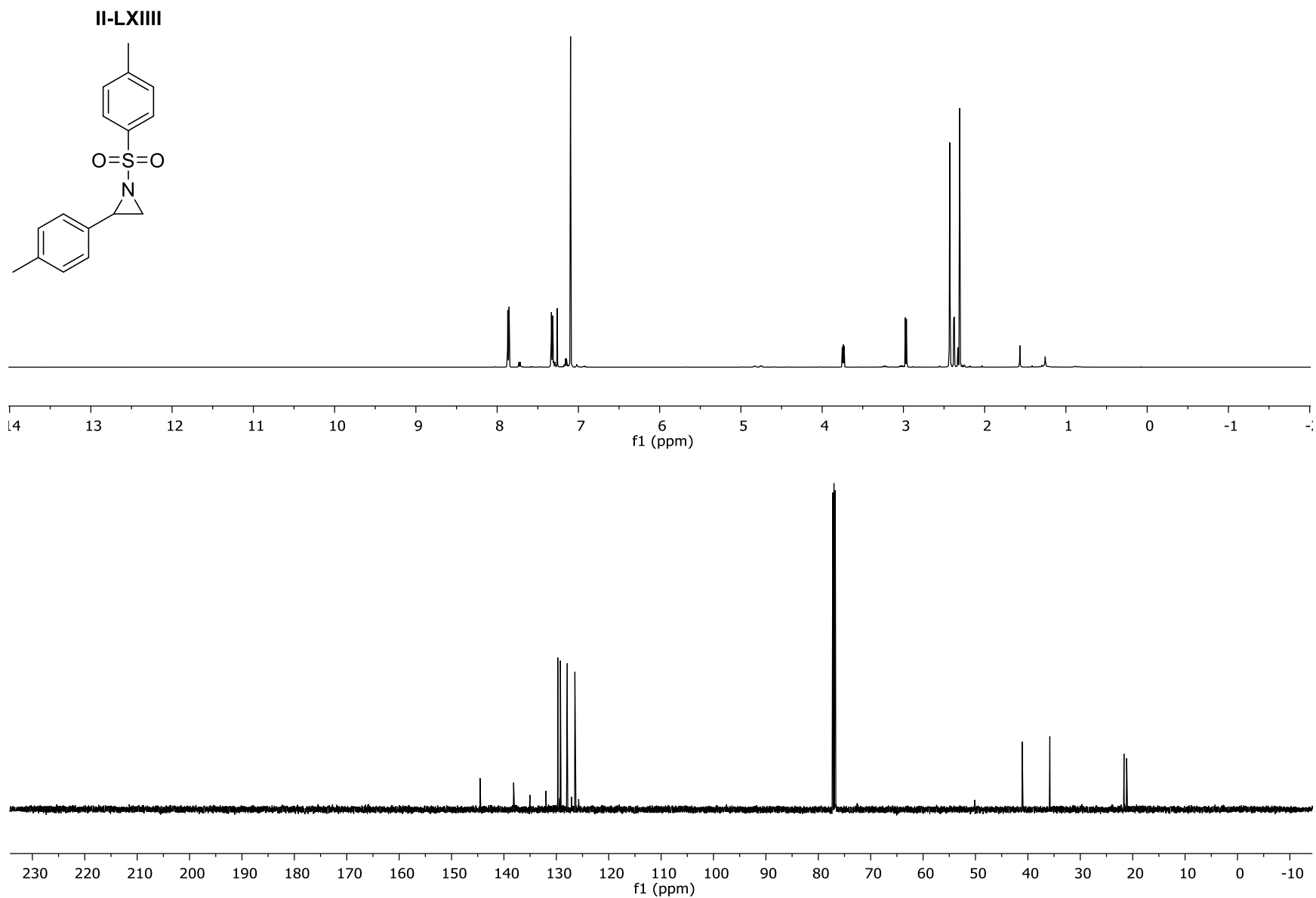


Figure II-LXXXI: The ^1H NMR and ^{13}C NMR for Compound **II-LXIII**

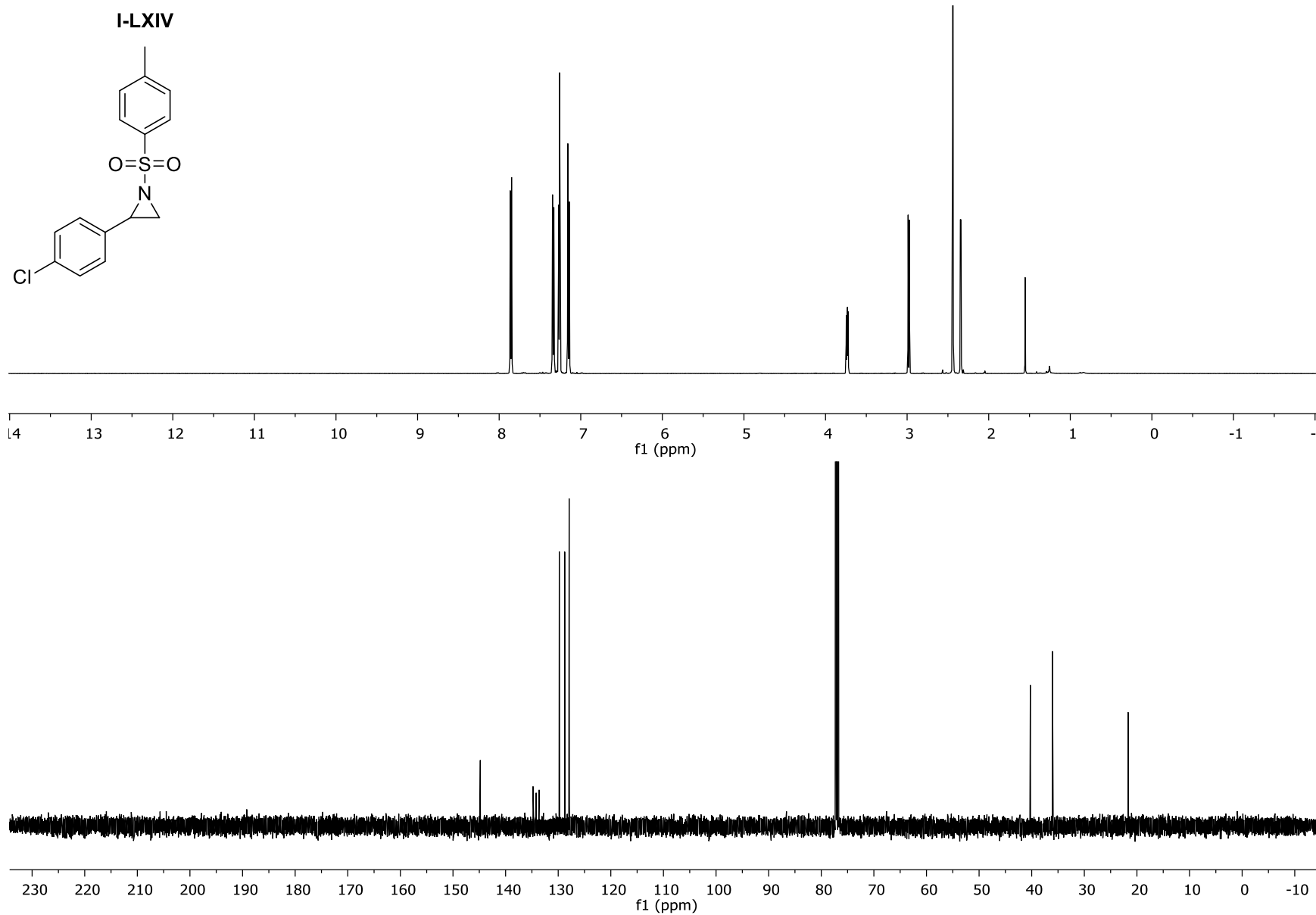


Figure II-LXXXII: The ^1H NMR and ^{13}C NMR for Compound **II-LXIV**

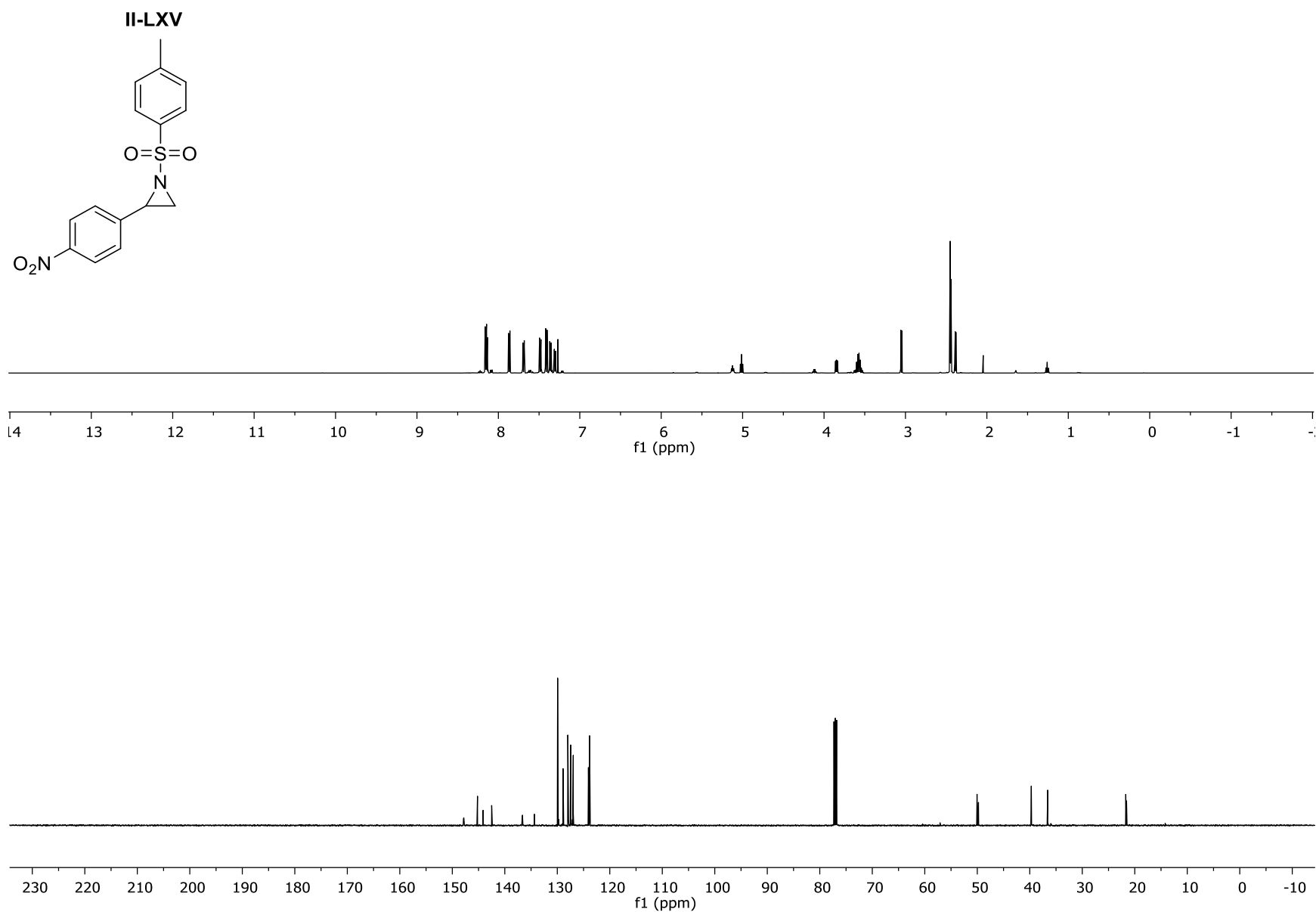


Figure II-LXXXIII: The ¹H NMR and ¹³C NMR for Compound **II-LXV**

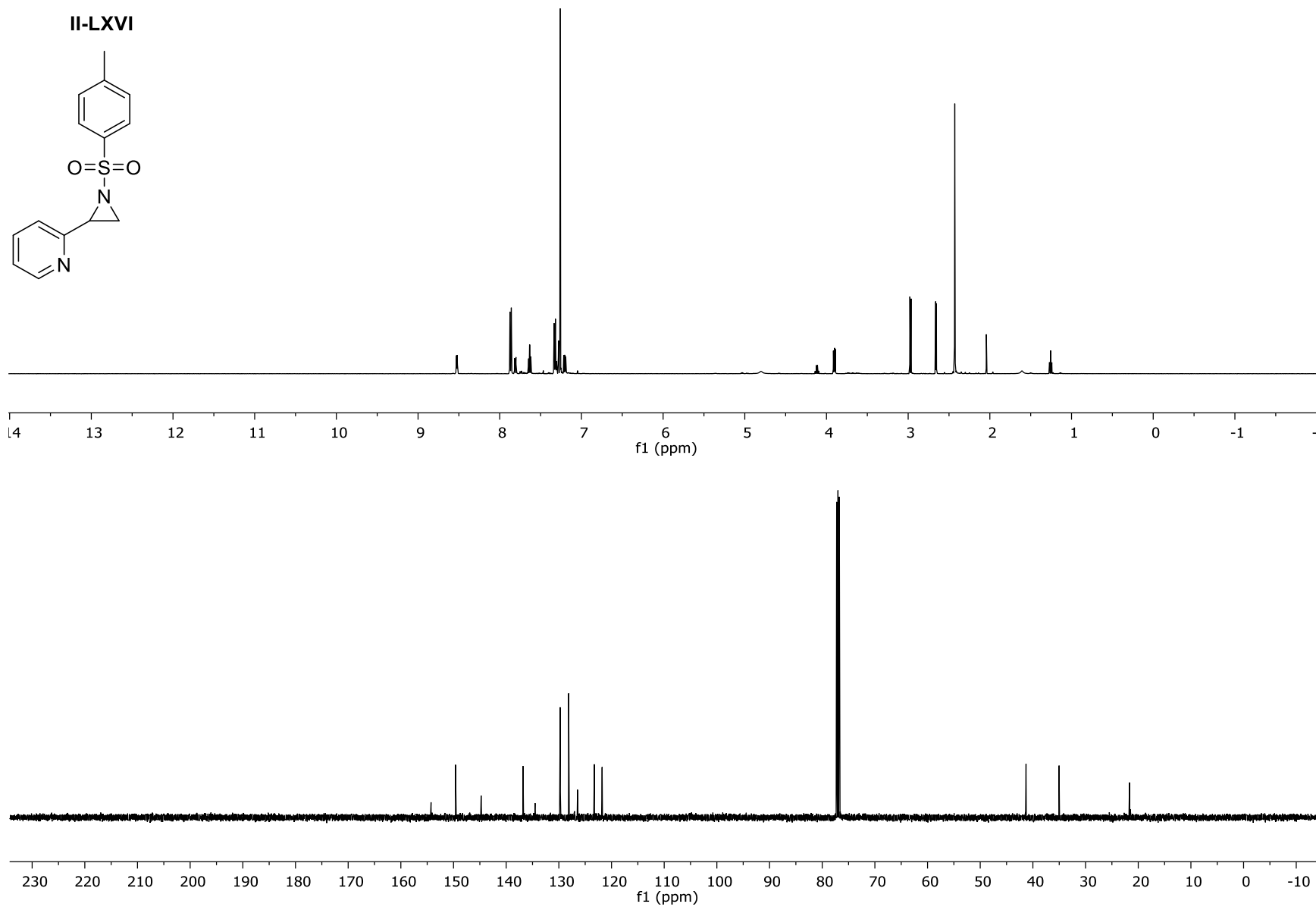


Figure II-LXXXIV: The ^1H NMR and ^{13}C NMR for Compound **II-LXVI**

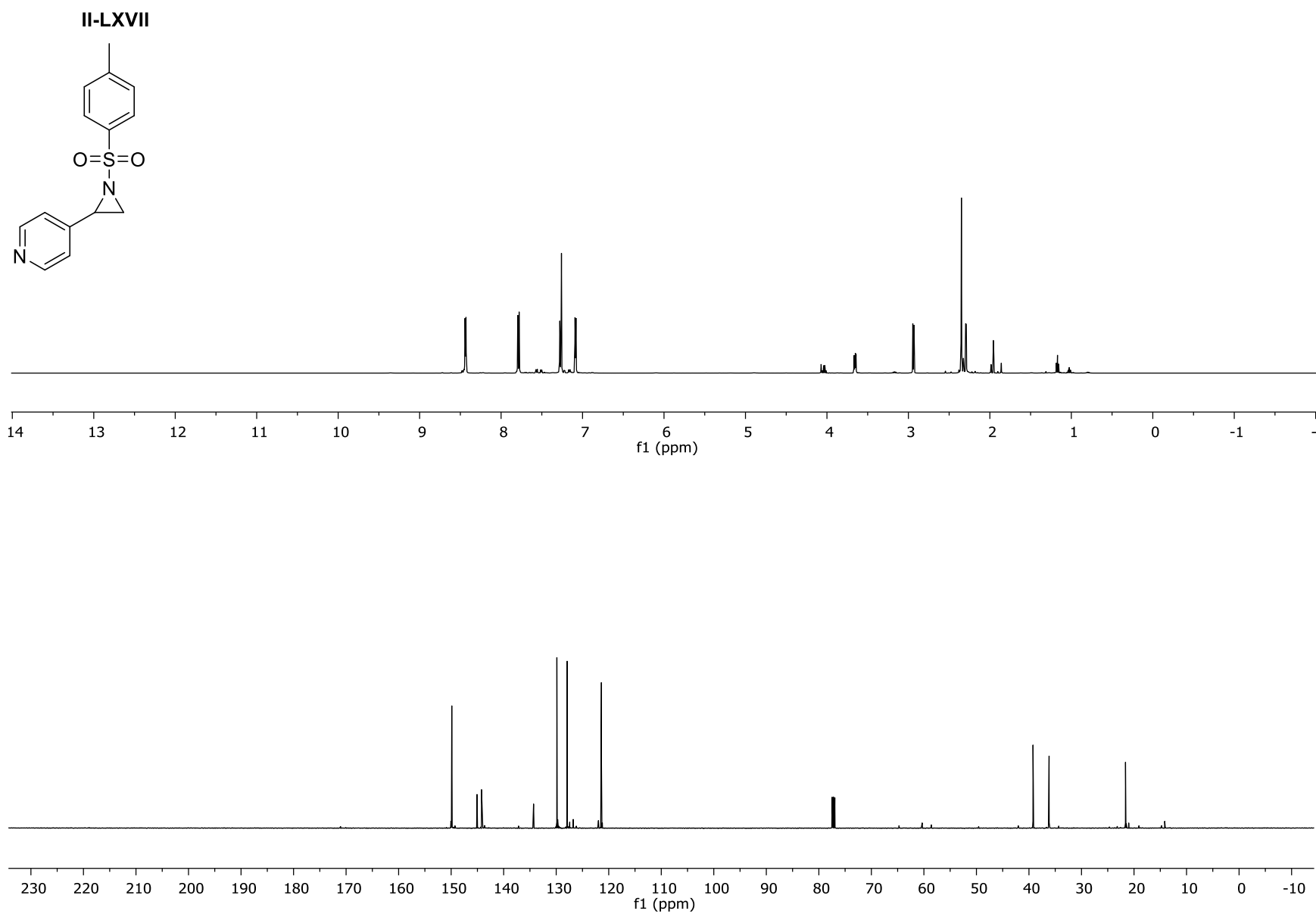


Figure II-LXXXV: The ¹H NMR and ¹³C NMR for Compound **II-LXVII**

II-LXIX

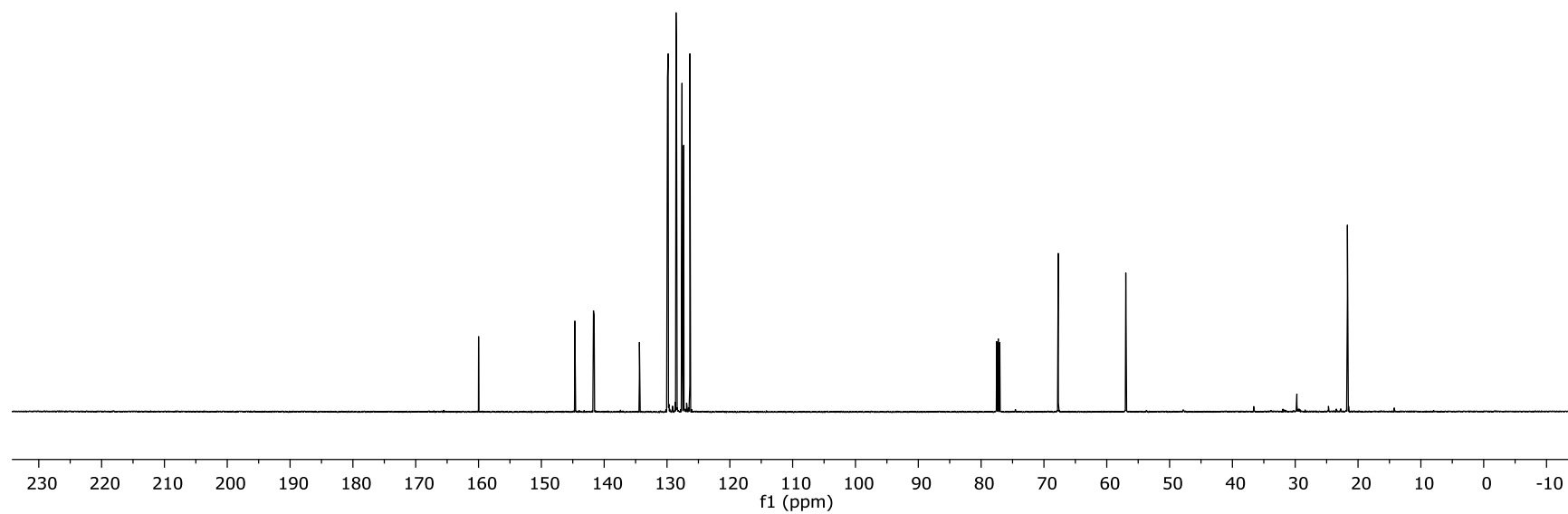
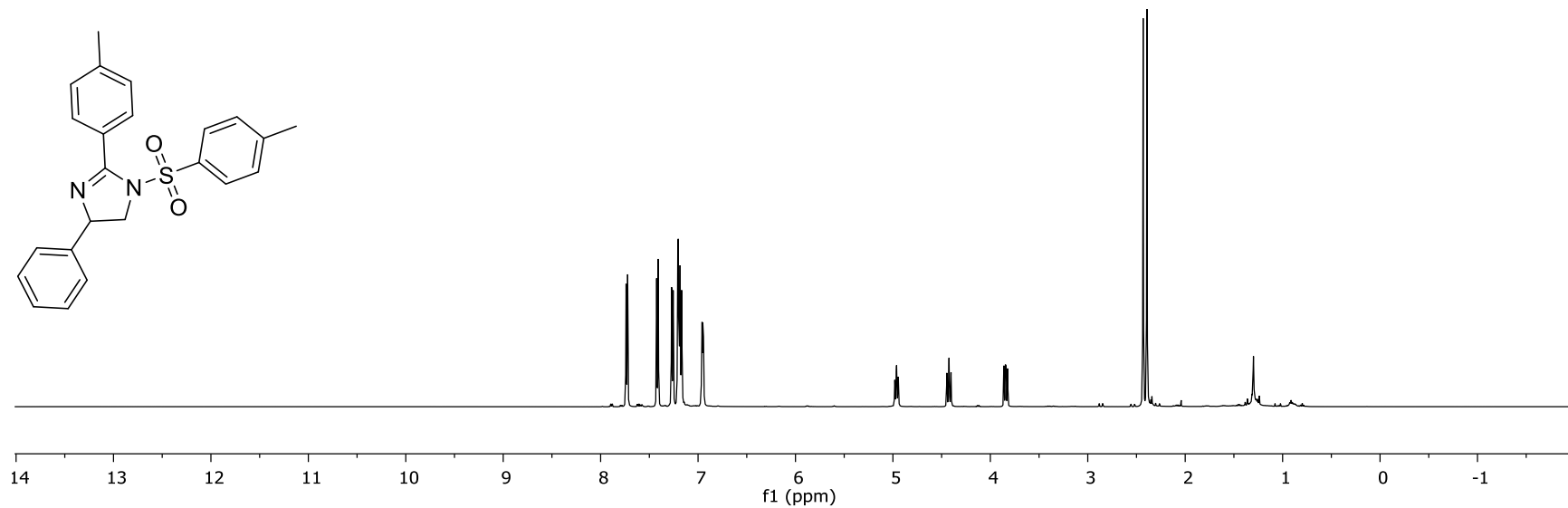
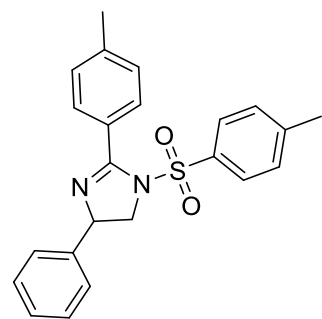


Figure II-LXXXVII: The $^1\text{H NMR}$ and $^{13}\text{C NMR}$ for Compound II-LXIX

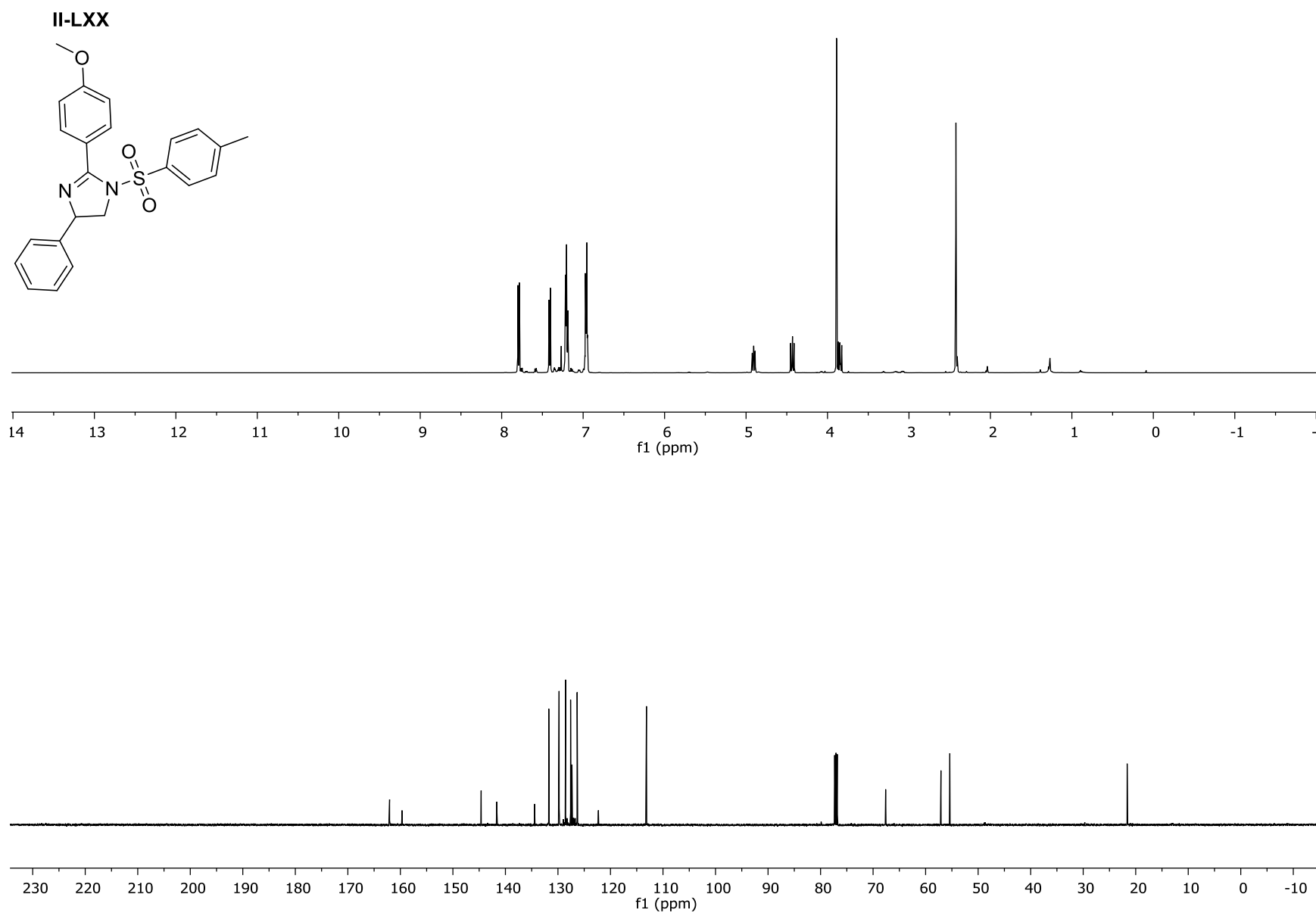


Figure II-LXXXVIII: The ^1H NMR and ^{13}C NMR for Compound **II-LXX**

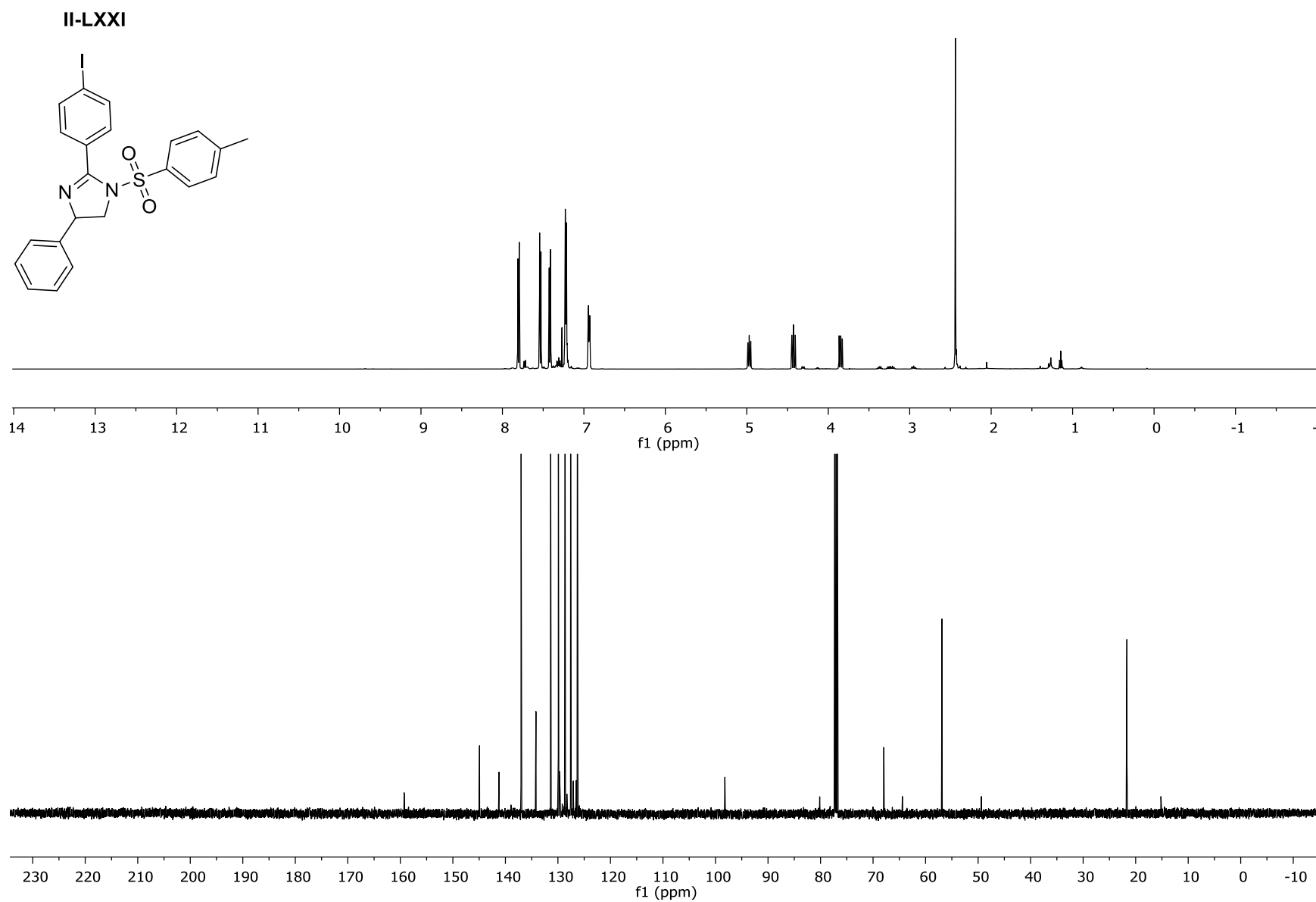


Figure II-LXXXIX: The ^1H NMR and ^{13}C NMR for Compound **II-LXXI**

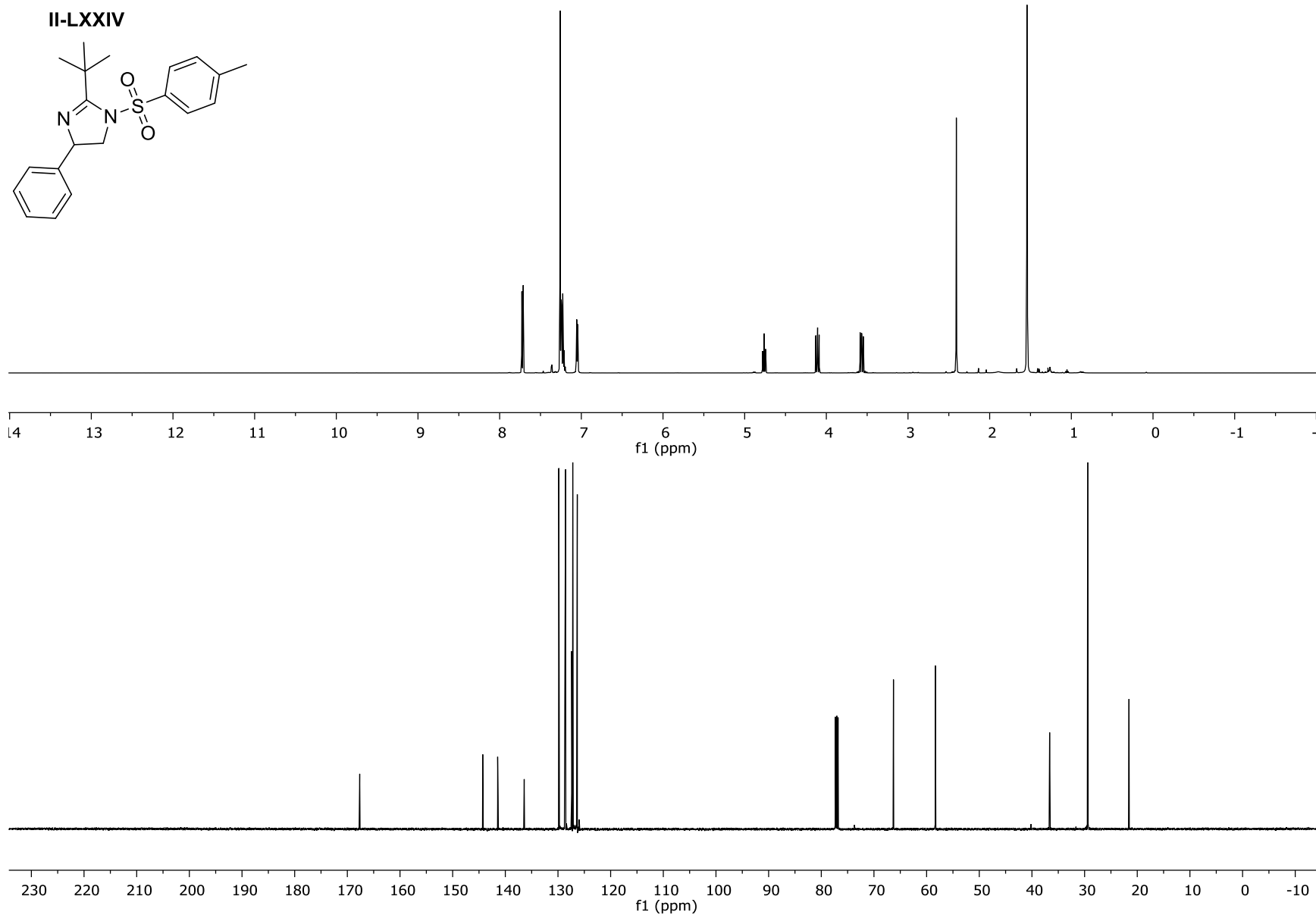


Figure II-XCIII: The ^1H NMR and ^{13}C NMR for Compound **II-LXXIV**

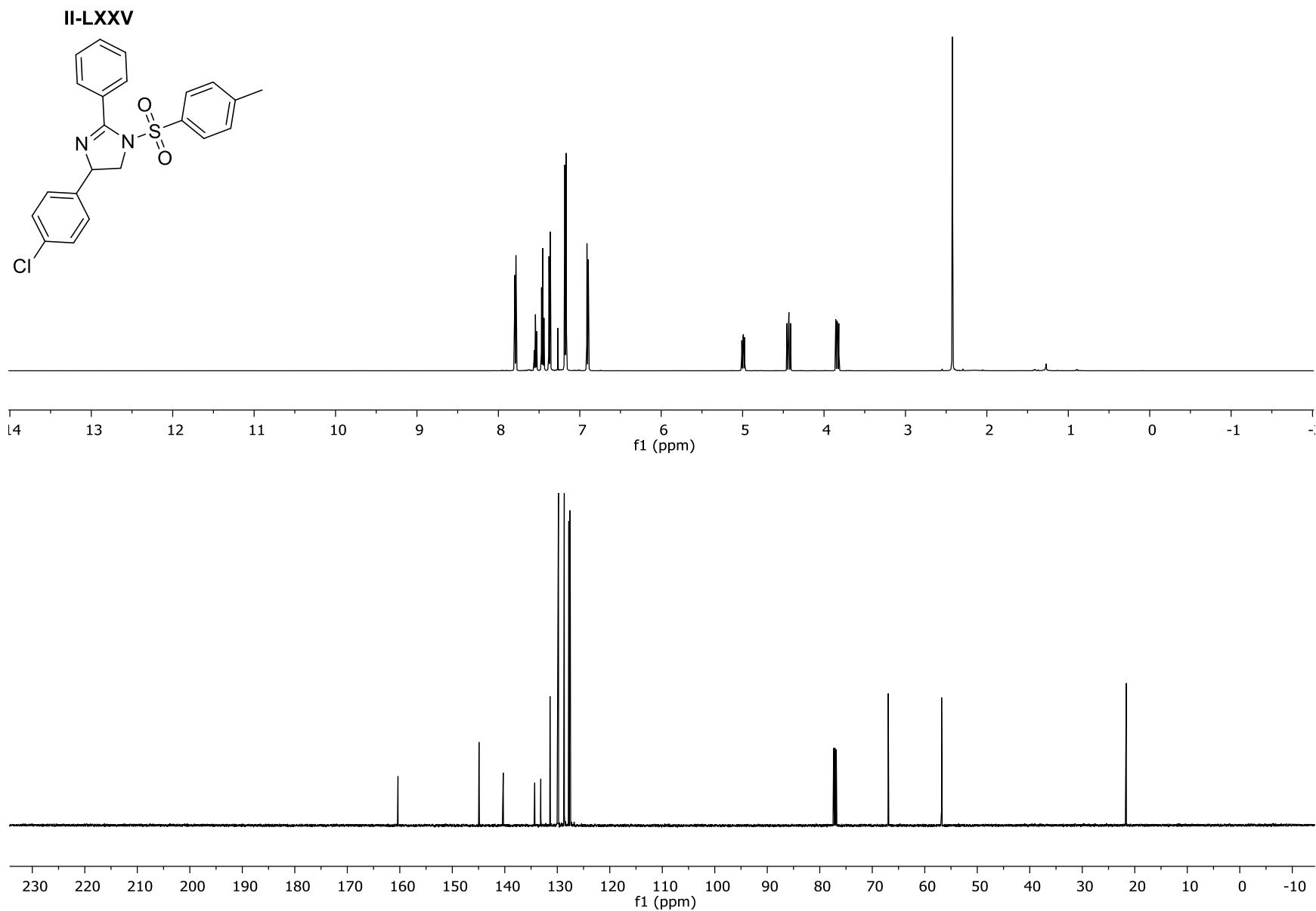


Figure II-XCIV: The ^1H NMR and ^{13}C NMR for Compound II-LXXV

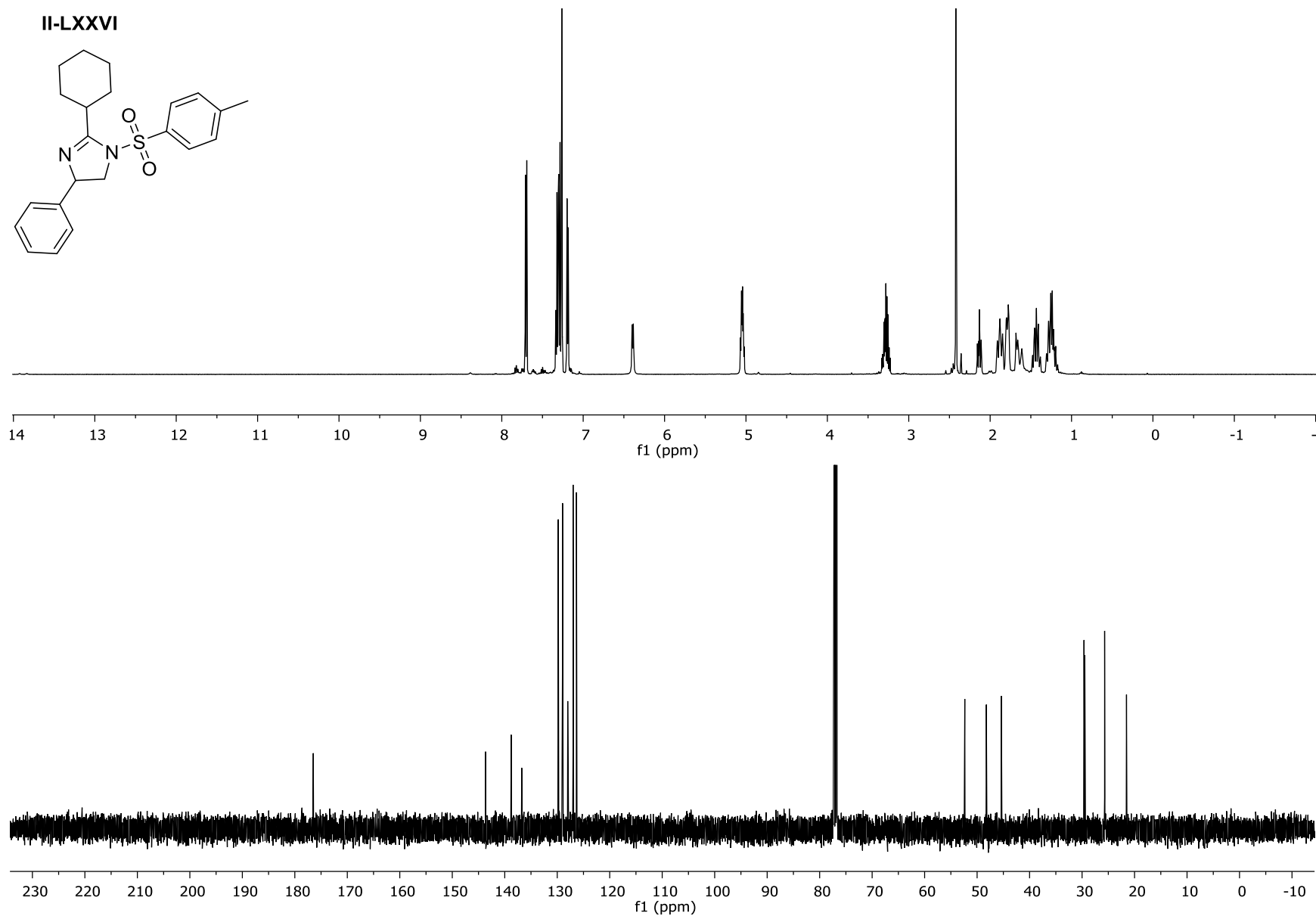


Figure II-XCV: The ^1H NMR and ^{13}C NMR for Compound **II-LXXVI**

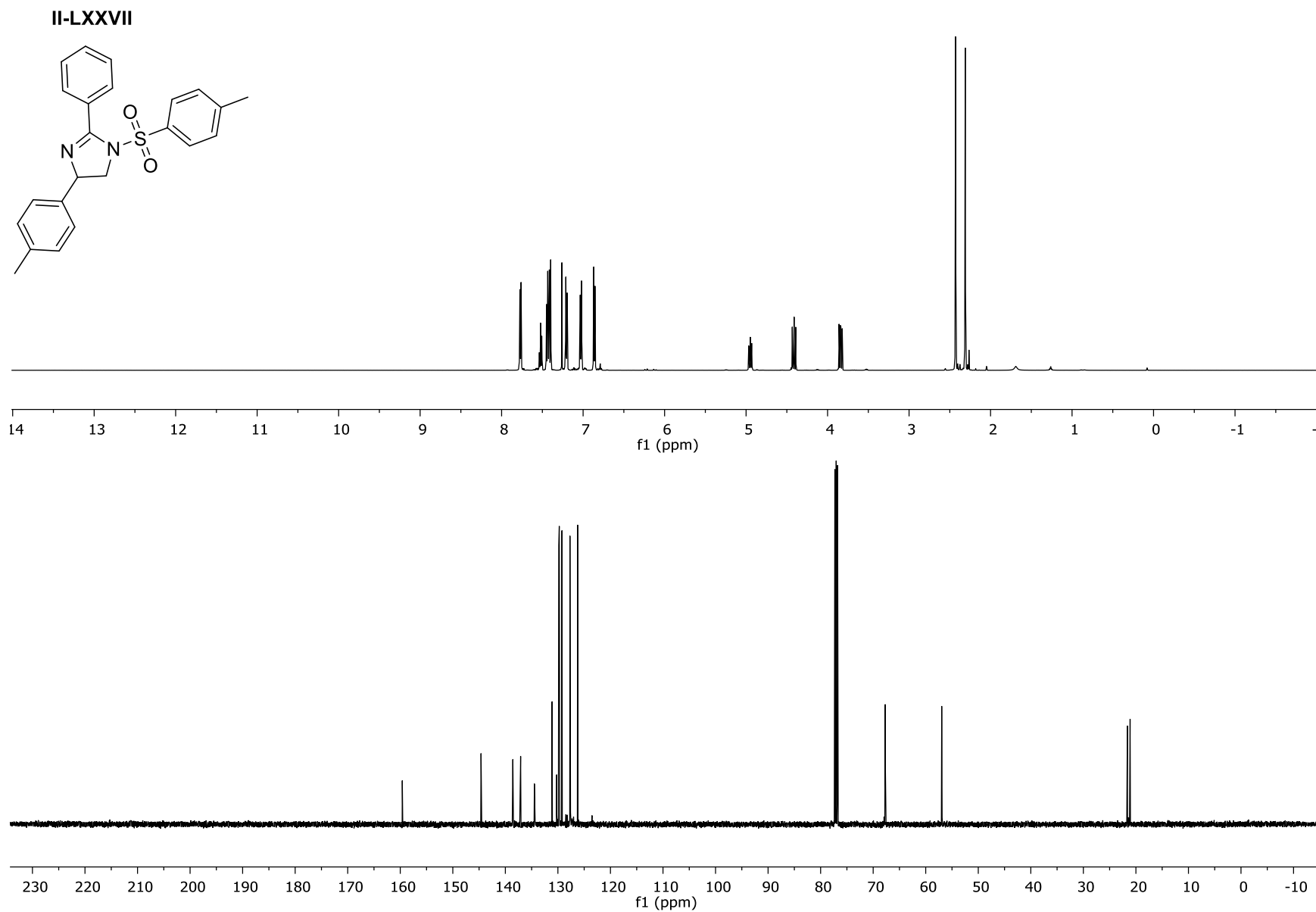


Figure II-XCVI: The ^1H NMR and ^{13}C NMR for Compound II-LXXVII

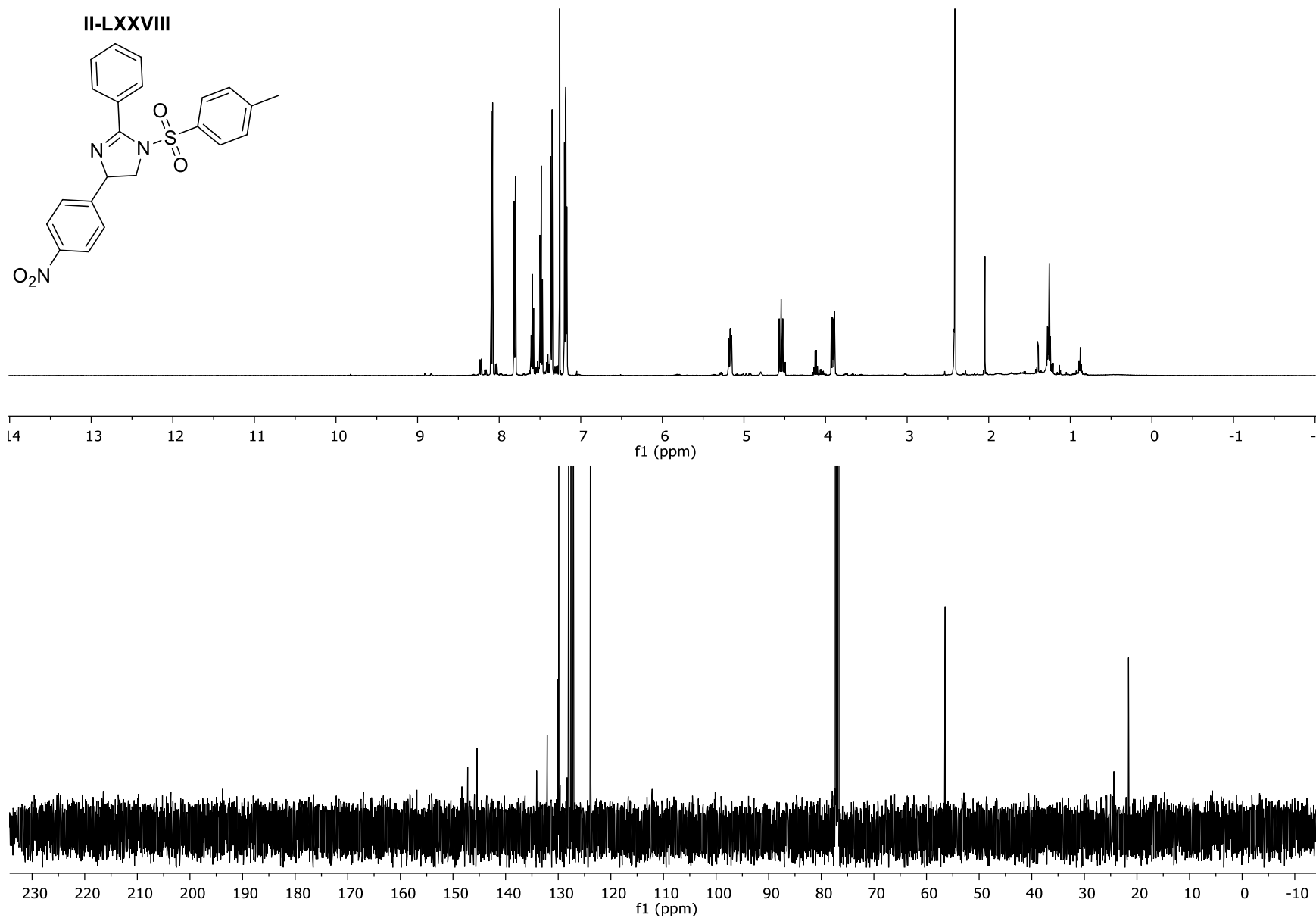


Figure II-XCVII: The ¹H NMR and ¹³C NMR for Compound II-LXXVIII

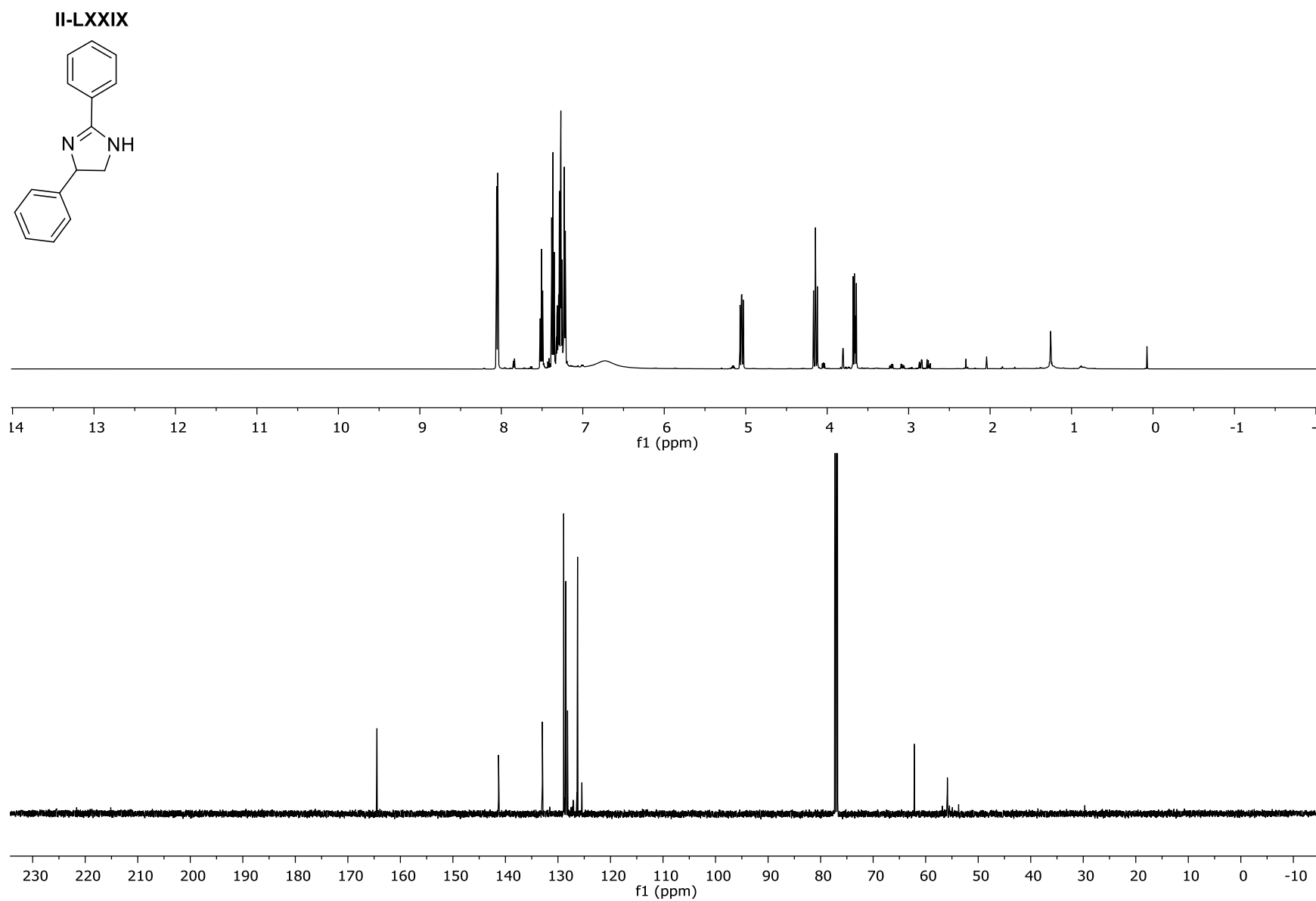


Figure II-XCVIII: The ^1H NMR and ^{13}C NMR for Compound **II-LXXIX**

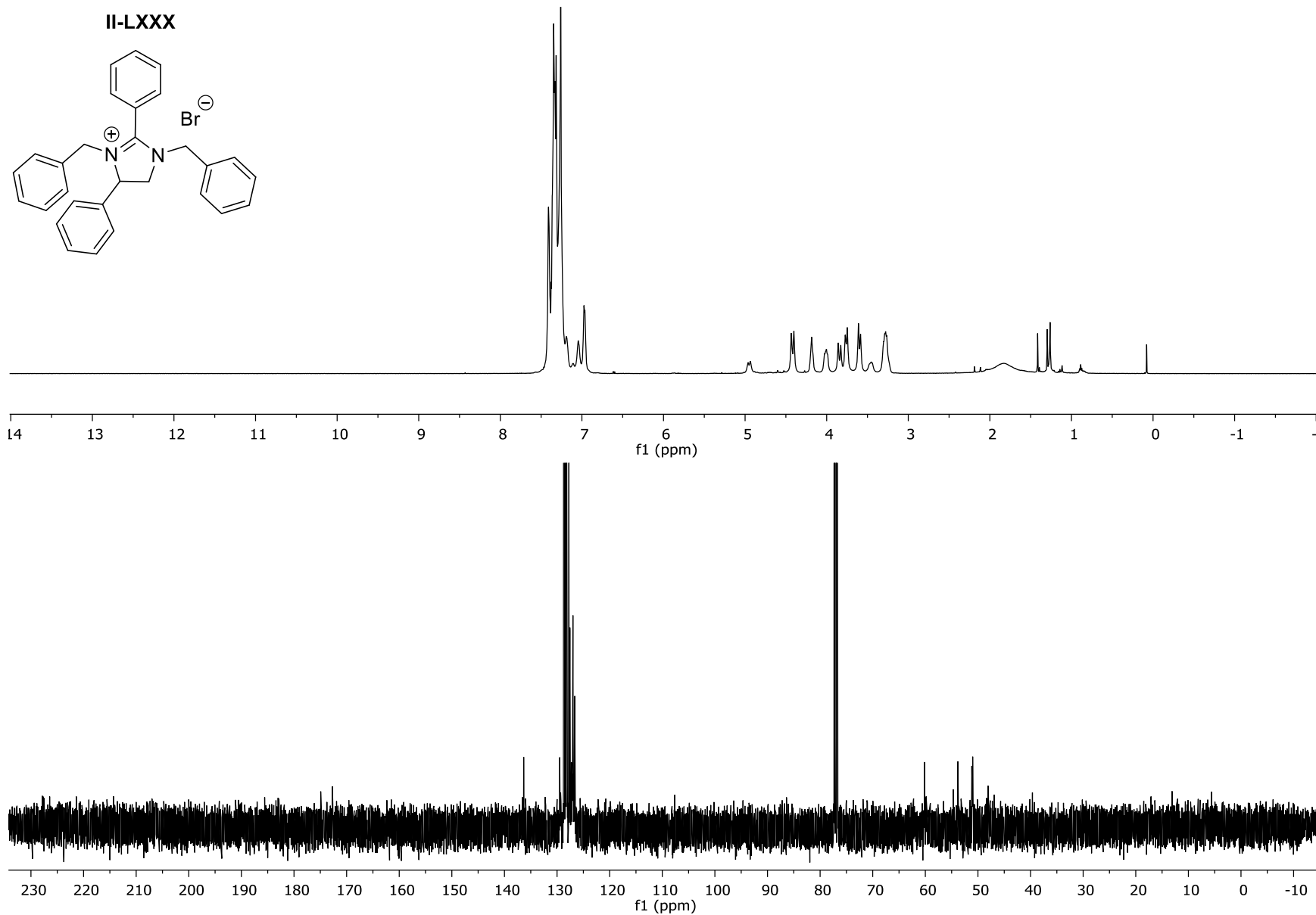


Figure II-XXIX: The ¹H NMR and ¹³C NMR for Compound II-LXXX

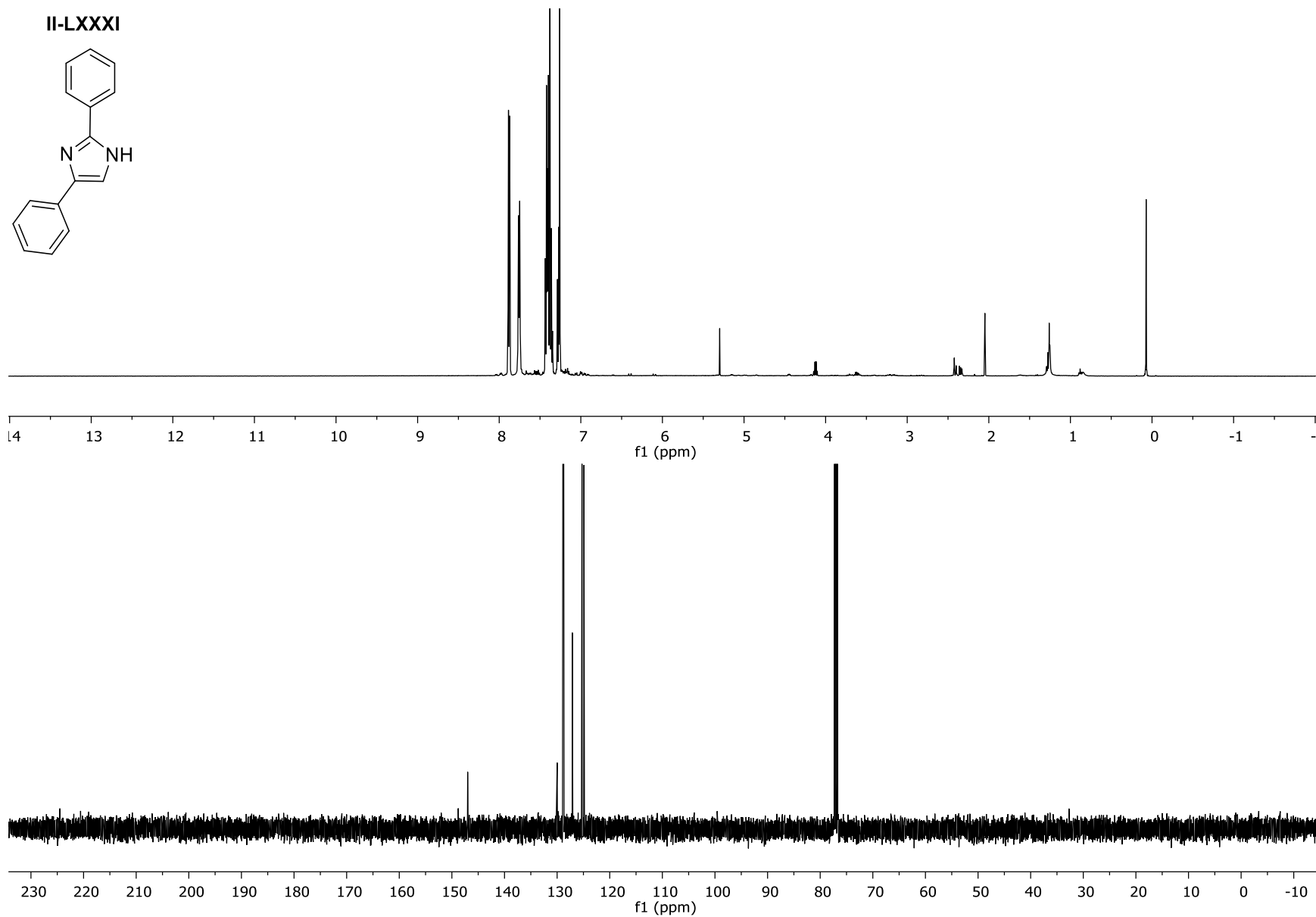


Figure II-C: The ^1H NMR and ^{13}C NMR for Compound **II-LXXXI**

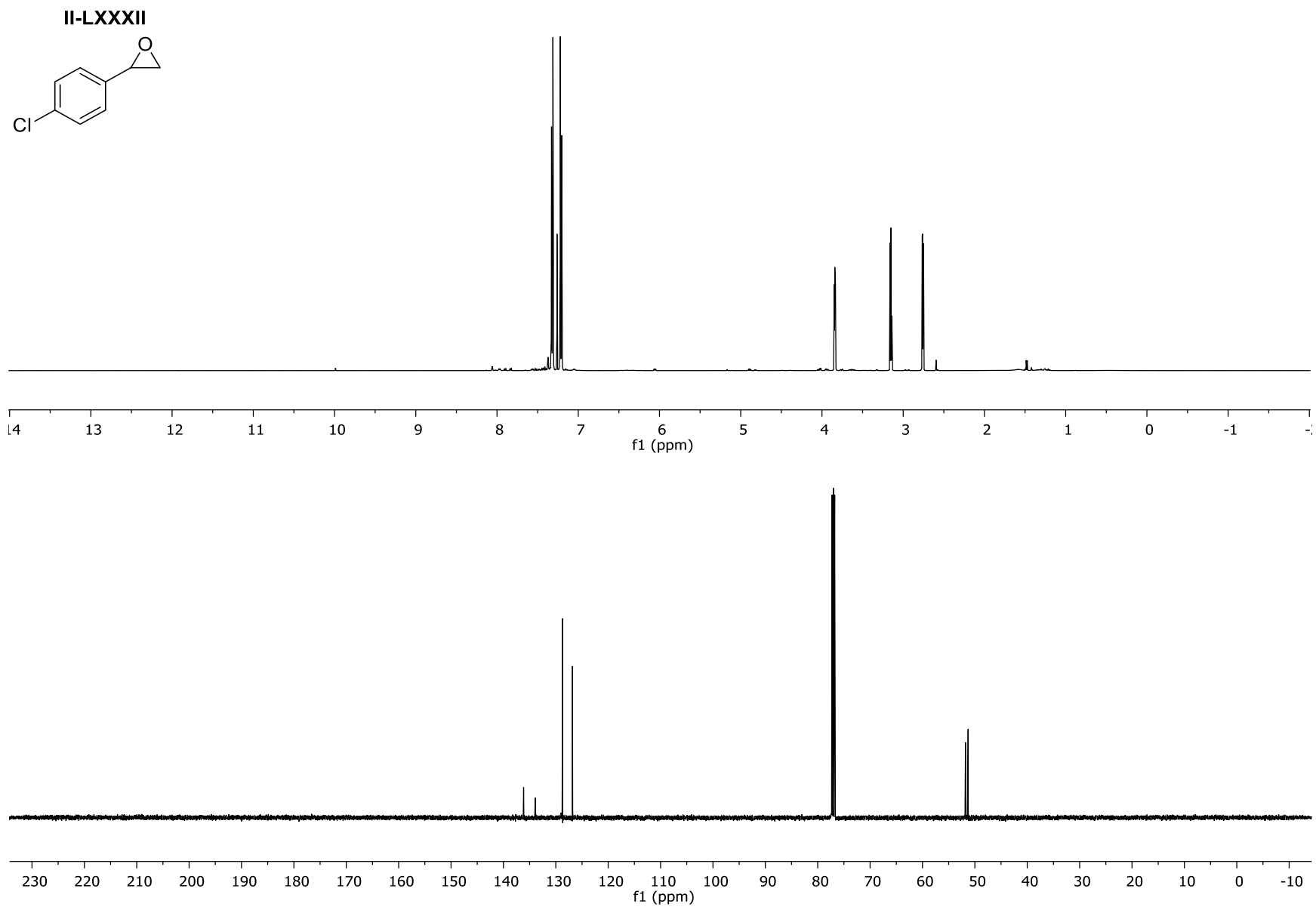


Figure II-CI: The ^1H NMR and ^{13}C NMR for Compound **II-LXXXII**

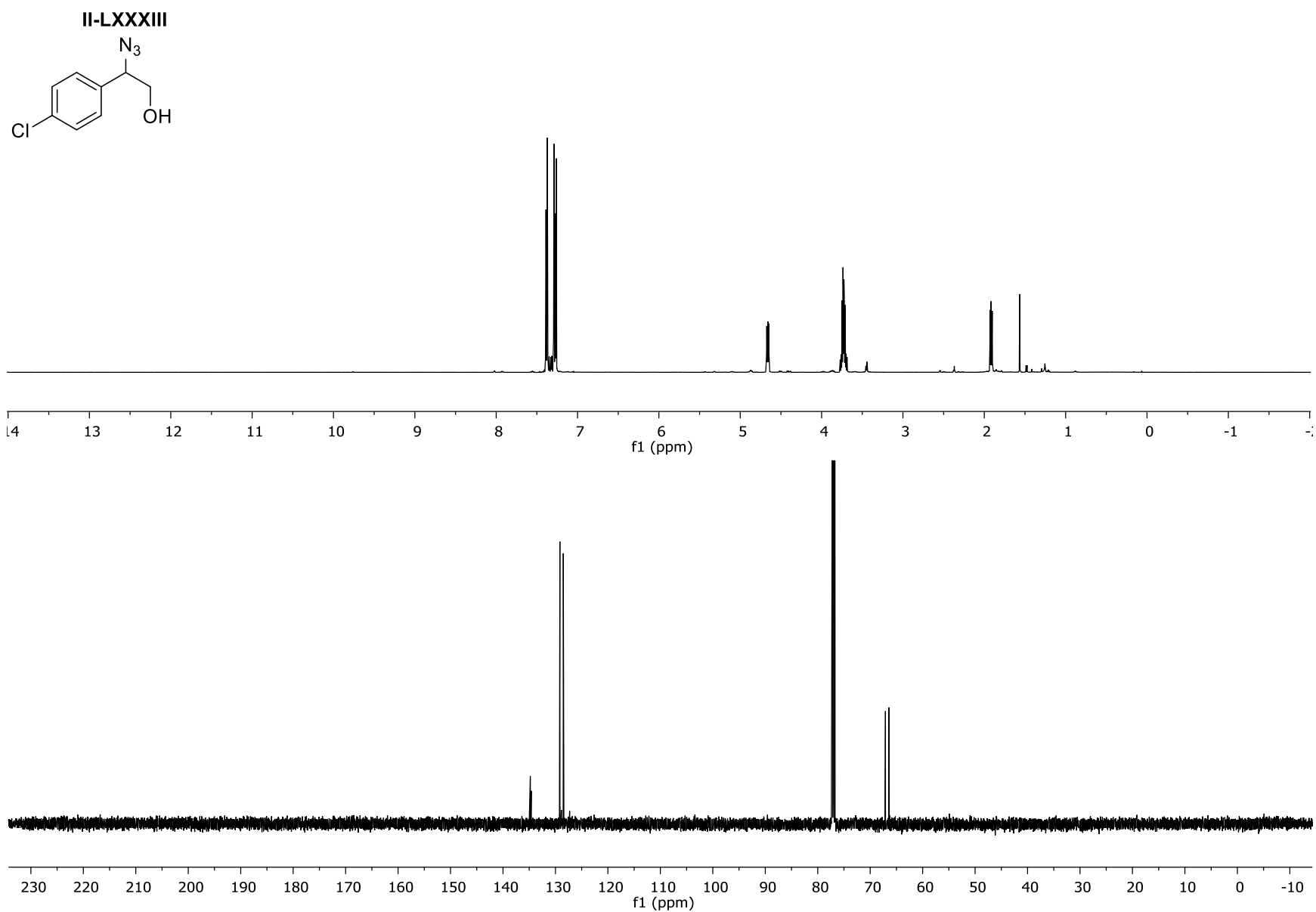


Figure II-CII: The ^1H NMR and ^{13}C NMR for Compound **II-LXXXIII**

II-LXXXIV

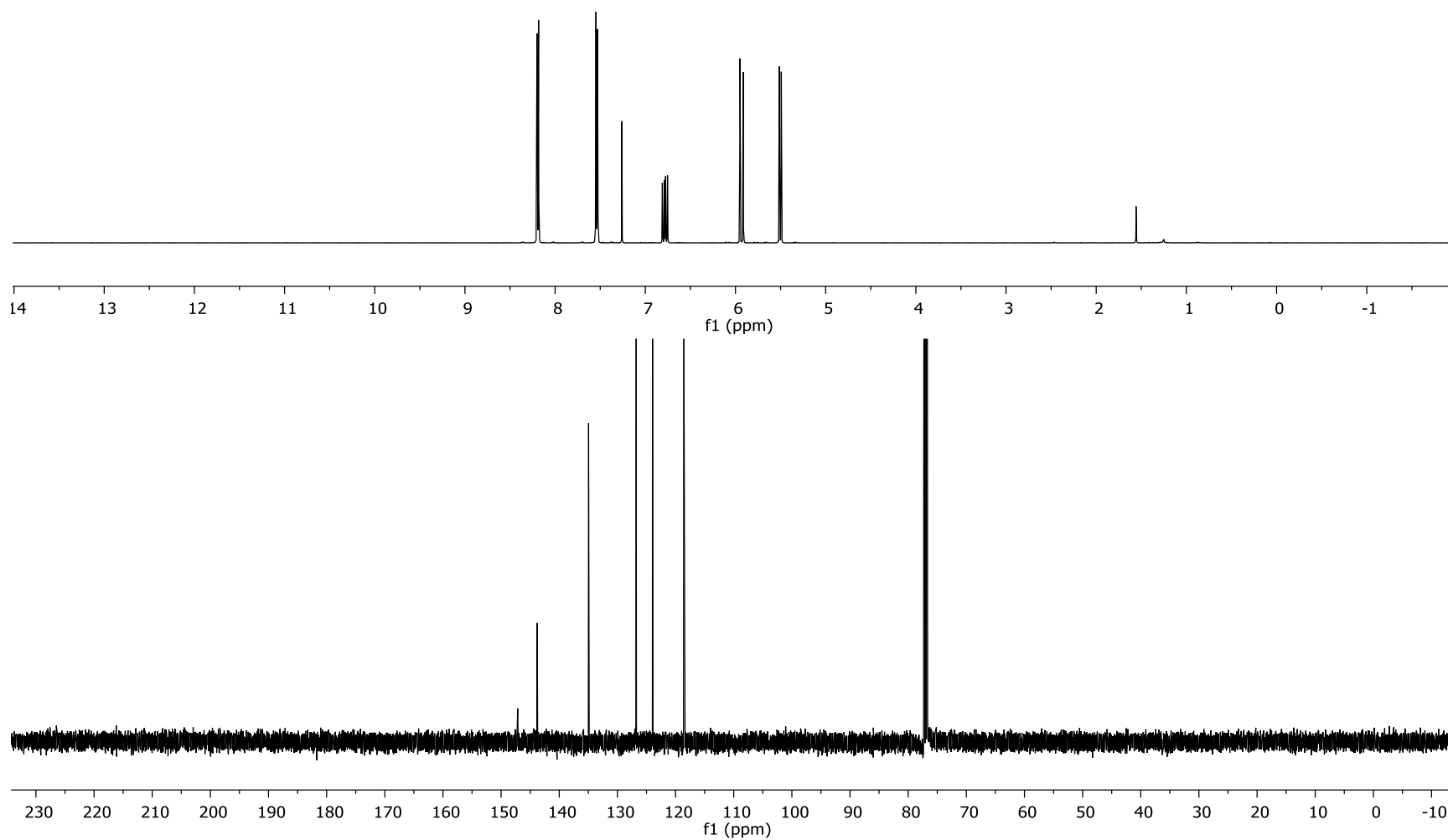
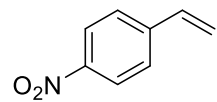


Figure II-CIII: The ^1H NMR and ^{13}C NMR for Compound II-LXXXIV

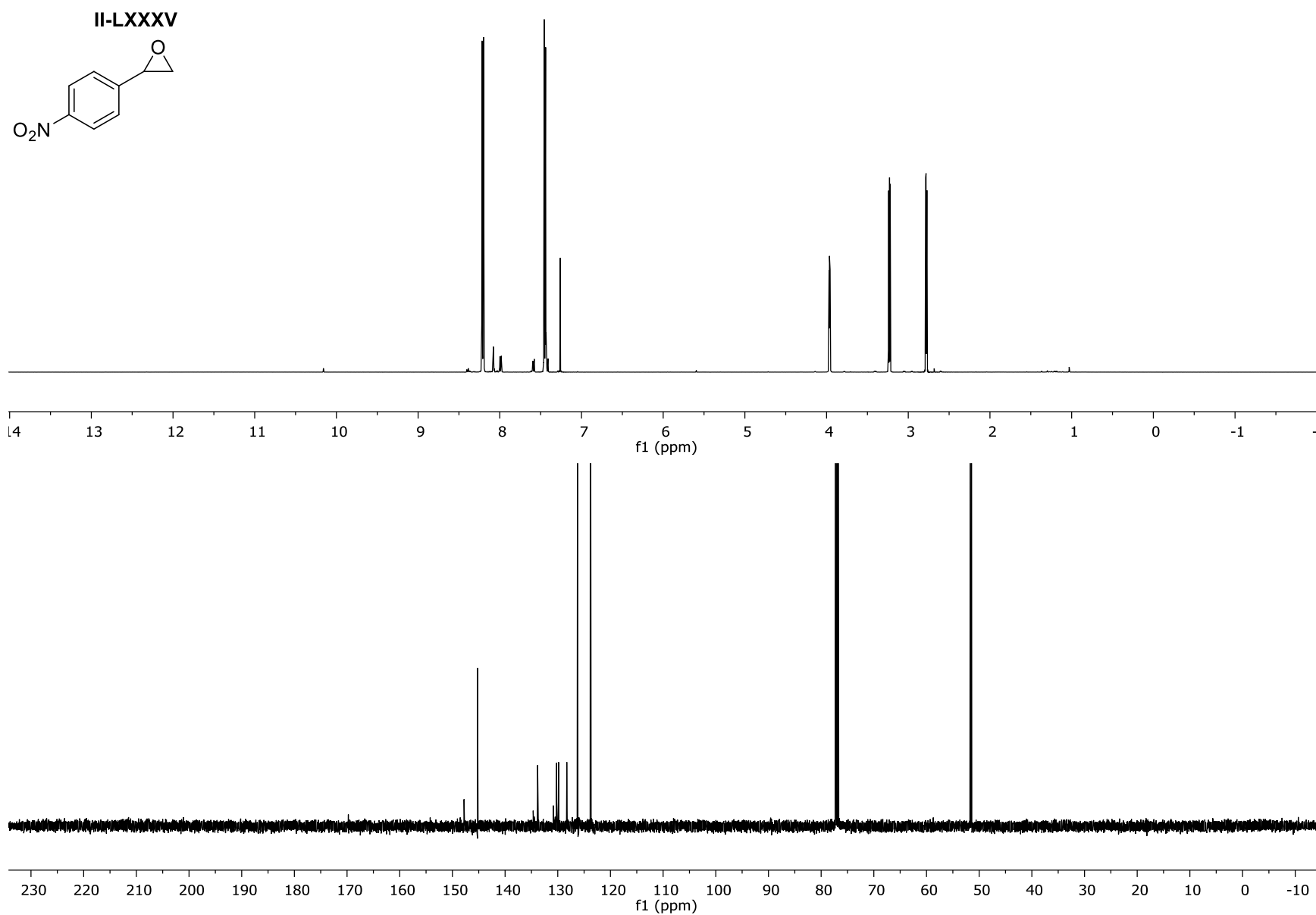


Figure II-CIV: The ^1H NMR and ^{13}C CNMR for Compound **II-LXX**

CHAPTER THREE – PROGRESS TOWARDS ACCESSING AGESAMIDES A AND B, AND TRUNCATED ANALOGS

Modulation of proteasome activity is not just regulated to imidazoline scaffolds. Proteasome modulation has been observed to occur from other diverse substrates, with each acting in a manner based on either their 3-D morphology, functional group reactivity or hydrogen-bonding potential. An example of this is seen in the front-line treatment for Multiple Myeloma (MM). Due to the bone's micro-environment which enhances MM cancer cell growth, aggressive treatments like proteasome inhibition are used to combat cell division and metastasis. Bortezomib is one of the leading proteasome inhibitors and is a polypeptide approved for MM treatment. It exhibits its activity through competitive inhibition of the proteasome which prevents all proteolysis, and results in accumulation of proteins in the cell that promotes apoptosis. This ability directly translates to the molecule's potent anti-cancer activity.

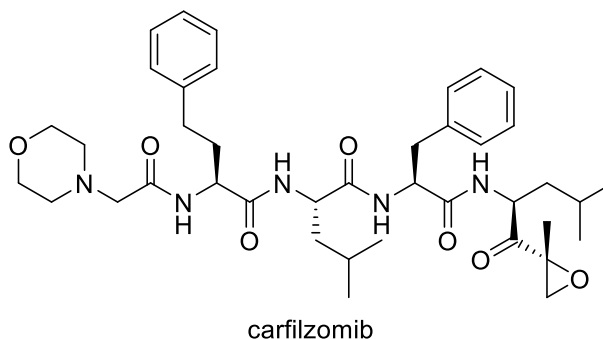
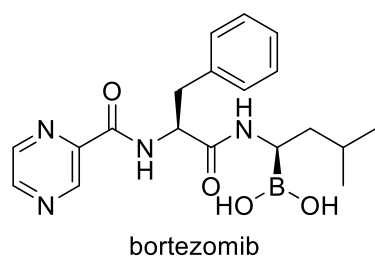


Figure III-I: Structures of FDA approved proteasome inhibitors.

Bortezomib's boronic acid functionality binds to the hydroxy group of the N-terminal Threonine residue in the catalytic site of the proteasome and that action modulates activity, bringing it to a halt. However, over time random mutations occur in amino acid residues around the area of the catalytic site in cancer cells proteasomes. That results in a loss of efficacy for Bortezomib and similar therapies because the molecule can no longer reach the threonine residue due to steric repulsion. Apart from loss of activity, extended use of Bortezomib has resulted in severe off-target effects, such as peripheral neuropathy in patients' due to lack of specificity for the proteasome of cancerous cells over proteasomes in healthy cells. In response to this, research has begun to investigate other methods of proteasome inhibition in an effort, to combat the growing resistance to current competitive inhibitors like Bortezomib.⁵⁹ Although these mutated cells have developed resistance to the mechanism of competitive inhibition, they are still susceptible to drugs that can target the proteasome through other pathways, like noncompetitive inhibition. Published results have shown that off target side effects can be reduced through the use of non-competitive inhibitors which overall lowered toxicity to the host. Based on this, one of the focuses in methods of proteasome inhibition was directed towards natural products and similar synthetic analogs that were proposed to use a non-competitive mode of inhibition to modulate proteasome activity. This lead to further investing phakellin and phakellstatin like scaffolds for biological testing.⁶⁰ These molecules are members of the oroidin family of alkaloids, which are secondary metabolites, isolated from marine sponges like the Agelas. This class of alkaloids is identified by their characteristic pyrrole-2-carboxamide and 2-aminoimidazole motifs.⁶¹⁻⁶² One of the most commonly identified members of this family is the alkaloid palau'amine. The complex structural

features of palau'amine prevented the total synthesis until recently when the Baran lab reported the overall synthesis of palau'amine.⁶³ The synthesis of palau'amine itself has been a focus of many research groups due to its' potent cytotoxic and immunosuppressant ability in near physiological pH's of 7-7.5.⁶⁴ Unfortunately palau'amine's structural stability is highly pH dependent showing degradation when exposed to pH's outside the physiological range.⁶⁰ Phakellin and phakellstain systems possess many of the same structural motifs as palau'amine such as the tetracyclic backbone including a cyclic guanidine or urea. Due to this similarity, it was hypothesized that phakellin and phakellstain may exhibit similar cytotoxicity as palau'amine with increased structural stability for biological evaluation.

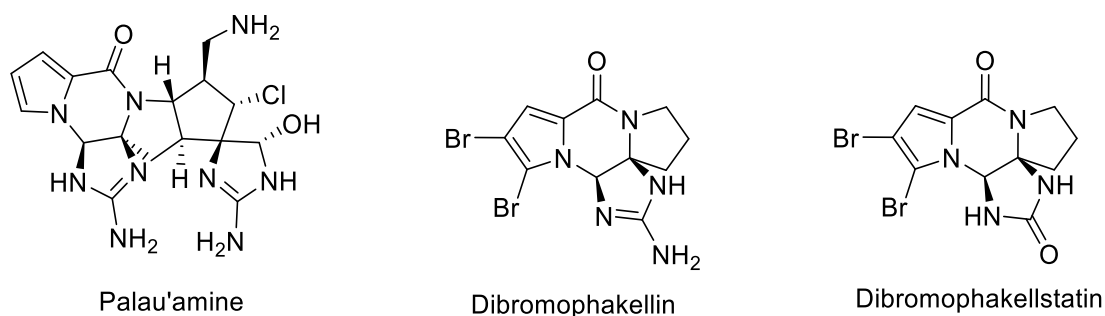


Figure III-II: Structures of bromopyrrole alkaloids natural products

These molecules and their analogs were synthesis by Dr. Nicole Hewlett and the biological results highlighted proteasome modulation, with the cyclic guanidine ring being the key motif for activity.⁶⁵

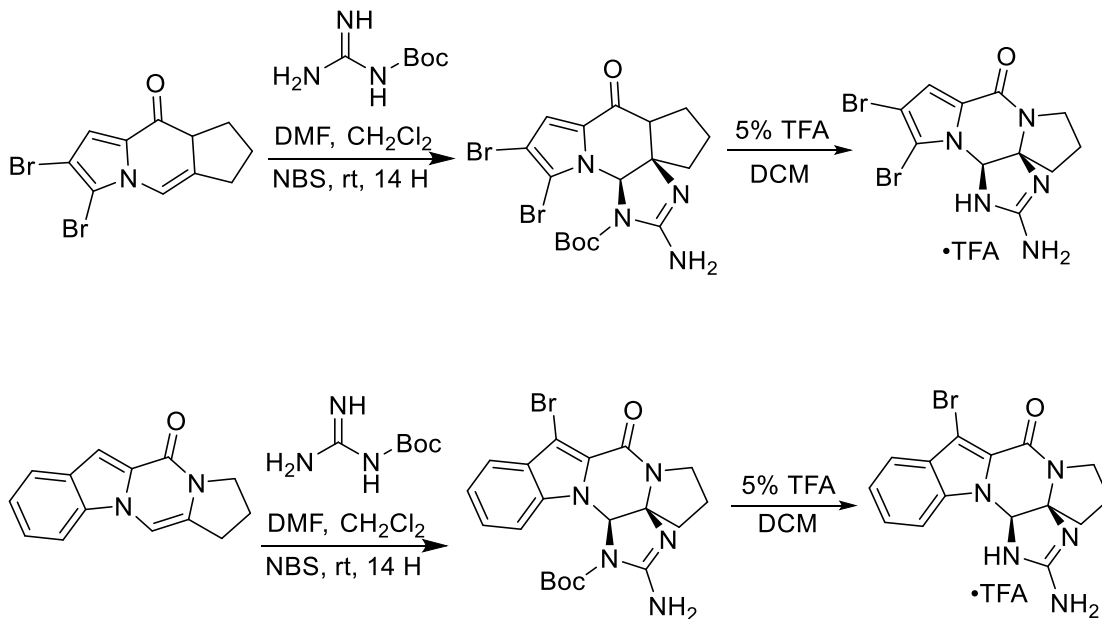
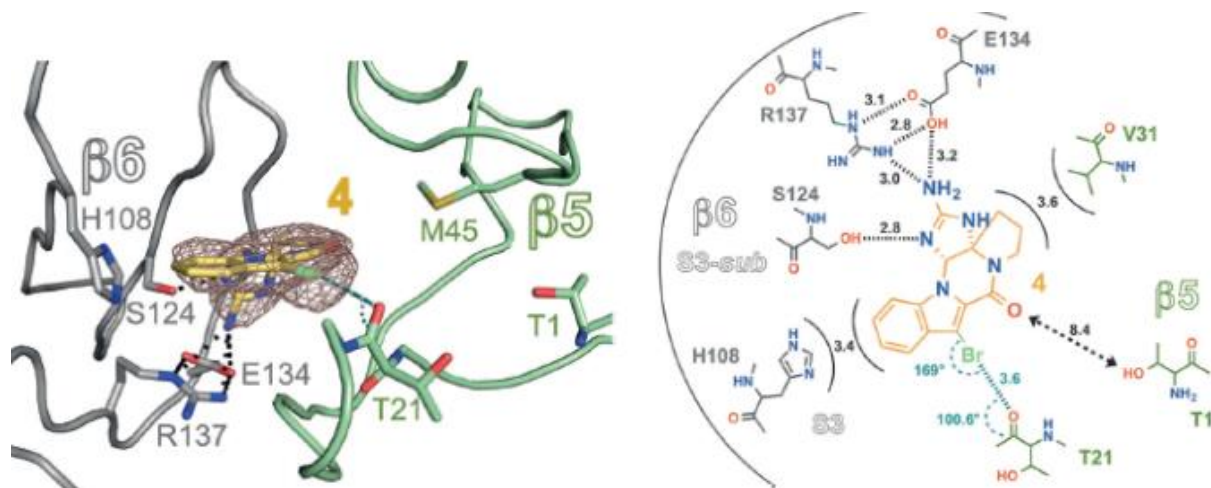


Figure III-III: Isolation of bromoindolophakellin

These results have been further confirmed by the recent work done in the Groll lab in collaboration with the Tepe group. Within the Tepe lab, the 3-bromoindolophakellin derivative was synthesized and based on its potent activity towards proteasome inhibition, sent to the Groll lab along with other analogs for co-crystallization. This co-crystallization would elucidate the mode of proteasome inhibition within the Phakellin class of marine alkaloids. Groll recently published the crystal structure of this indoloalkaloid derivative of the dibromophakellin bound within the γ CP (yeast core particle).⁶⁶ In the publication, it was shown that the highly rigid structure of the mono brominated pentacyclic alkaloid exclusively interacted and binded within the S_3 pocket within the B_5 subunit of the core particle, in the yeast proteasome. It was found that the highly rigid structure with its cyclic 2-aminoimidazoline had strong interactions with the hydrophilic residues along one side on the S_3 pocket, while the planar nature of the molecule formed Van der Waals interactions with flanking side chains perfectly orients the indolo-alkaloid within the pocket towards the formation of a coordination bond with its bromine and a carbonyl

present within the side chain in the pocket. This key interaction is responsible for the electron density mapping that lead to the overall discovery of the bound system.



Beck, P.; Lansdell, T. A.; Hewlett, N. M.; Tepe, J. J.; Groll, M *Angew. Chem. Int. Ed.* **2015**, *54*, 2830-2833

Figure III-IV: bromoindolophakellin bound in the yeast core particle

Coupled with the experimental results of inhibition in the purified protein assays, this crystallization has lent more validity to exploiting this class of natural product scaffolds towards the development of more potent proteasome inhibitors. With this the Oroidin class of molecules, especially the phakellins and phakellstatin have gained a larger focus within the Tepe lab, acting as the spiritual successor to the imidazoline compounds originally synthesized towards proteasome inhibition.^{65, 67-68} This has led to exploring other members of the Oroidin family of marine alkaloids such as Agesamides A and B and similar products like Hanishin, Longamide B and Cyclooroidin.⁶⁹⁻⁷³

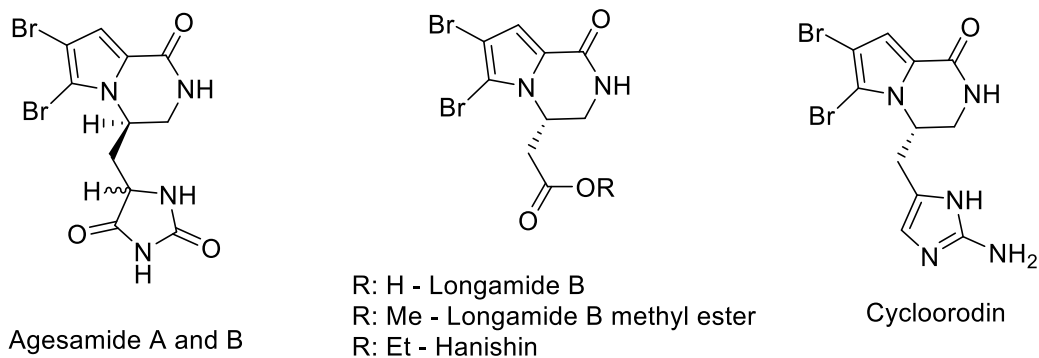
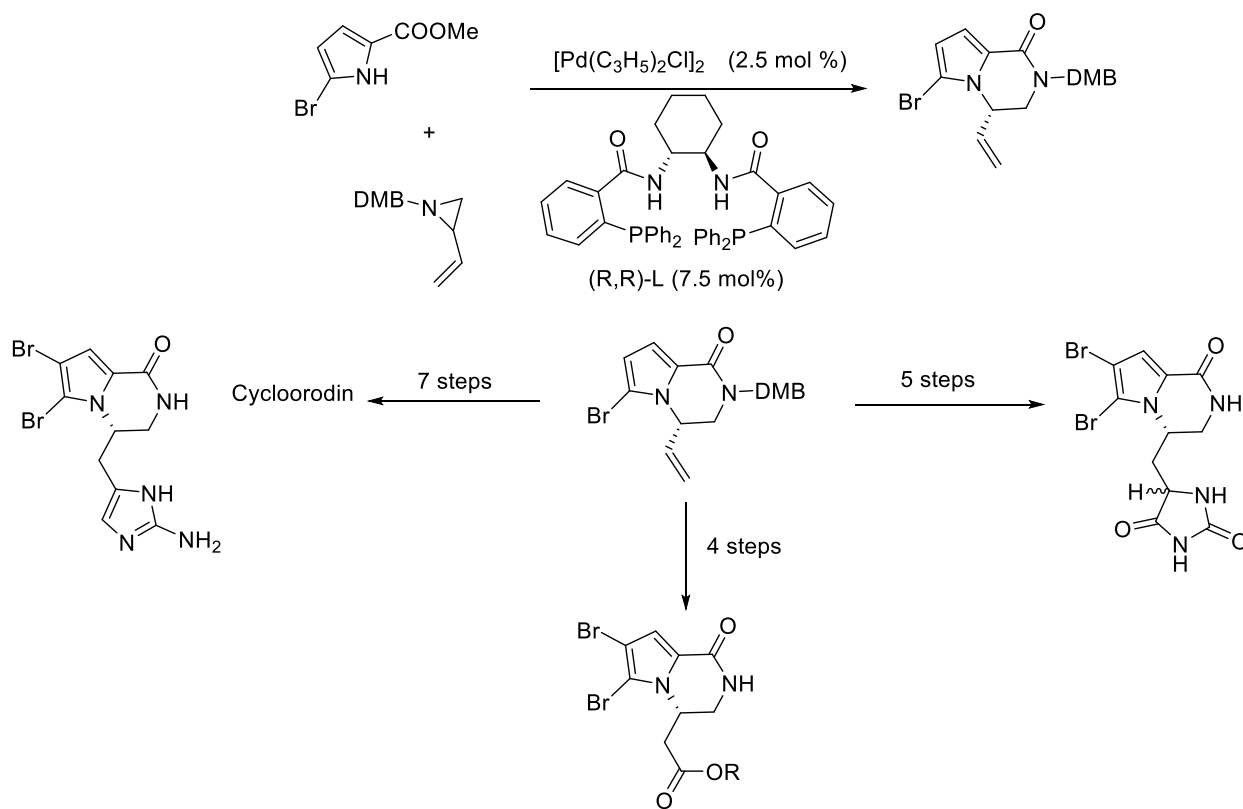


Figure III-V: Structures of other bromopyrroloalkaloids in the same family of dibromophakellin

The examined crystal structure of the bromo-indolophakellin also highlighted the important interaction between the bromine atom and the carbonyl in the proteasome active site. Because of this truncated indole analogs of the Agesamides A and B were also pursued based on their 3-D similarity to bromoindolophakellin when modelled in Pymol. To accommodate both the synthesis of these highly diverse truncated analogs as well as the structurally demanding oroidin natural products, new synthetic methodologies were explored to give direct access to these truncated systems. The intent was that these versatile synthetic intermediates would be further functionalized to the natural products in a few synthetic transformations and result in quickly accessing a large library of oroidin-like compounds for biological evaluation.

To better ascertain the function group tolerance of this class of compounds the current synthetic methods of accessing these oroidin class of compounds were reviewed. These showed the various approaches to accessing these bromo-pyrrole alkaloids. Work done in the Trost lab focused around using Palladium (Pd) to control regiochemistry as well as enforce stereoselectivity towards the formation of their key intermediate. From this common structure, it was proposed that a small library consisting of very similar bromopyrroloalkaloids in the family of Agesamides A

and B could be accessed. The chiral Pd complex catalyzed an asymmetric annulation between the starting aziridine and the pyrrole carboxylate ester through the formation of a Pd-allyl complex.⁷⁴



R = Me: Longamide B methyl ester
R = Et: Hanishin

Dong, G.; Trost, B. *Org. Lett.* **2007**, 9,12, 2357-2359

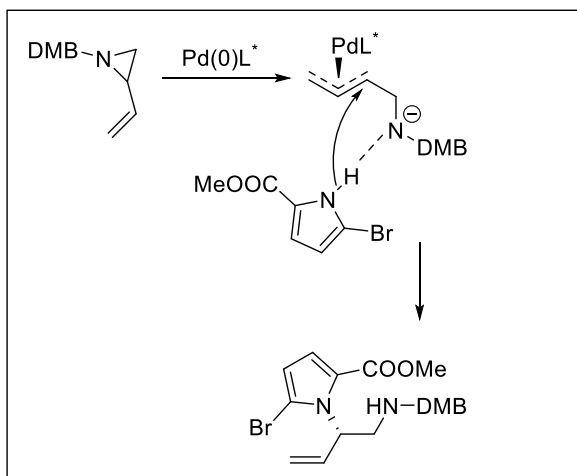
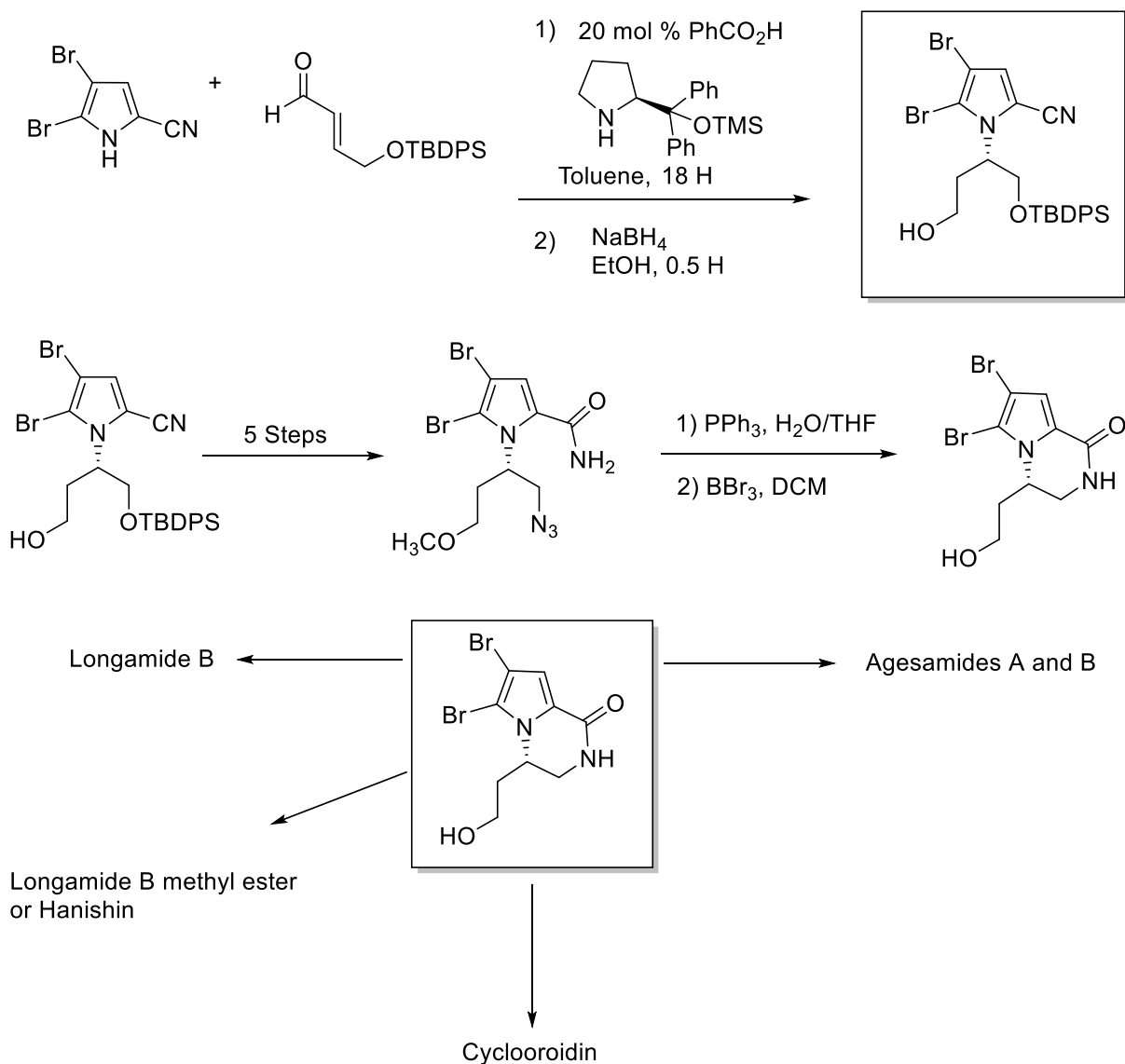


Figure III-VI: Pd mediated N-alkylation in route to accessing Agesamides A and B

Work done in the Cho lab focused on accessing numerous pyrrole alkaloids from one similar intermediate through the use of a chiral secondary amine catalyst. Addition of the chiral catalyst to an α,β unsaturated aldehyde resulted in an iminium complex that underwent enantioselective conjugate aza-michael addition install the key pyrrole functionality. Sequential transformations of that intermediate lead to the proposed synthesis of agesamides a and b, cyclooroidin, longamide b, and hanishin.⁷⁵



Lee, S., Youn, S., Cho, C. *Org. Biomol. Chem.* **2011**, 9, 7734-7741

Figure III-VII: Synthesis of the key intermediate to access different pyrroloalkaloids.

Approach 1 – Halogenation of electron deficient olefins towards aminohalogenation.

Based on literature precedence and motivated by their noted bioactivity multiple approaches to accessing these bromopyrrole analogs pursued. The first approach focused on olefin activation of α,β unsaturated systems to yield either the amino halogenation product or the acylated aziridine. Either product was speculated to give rise to the truncated analogs and natural products.

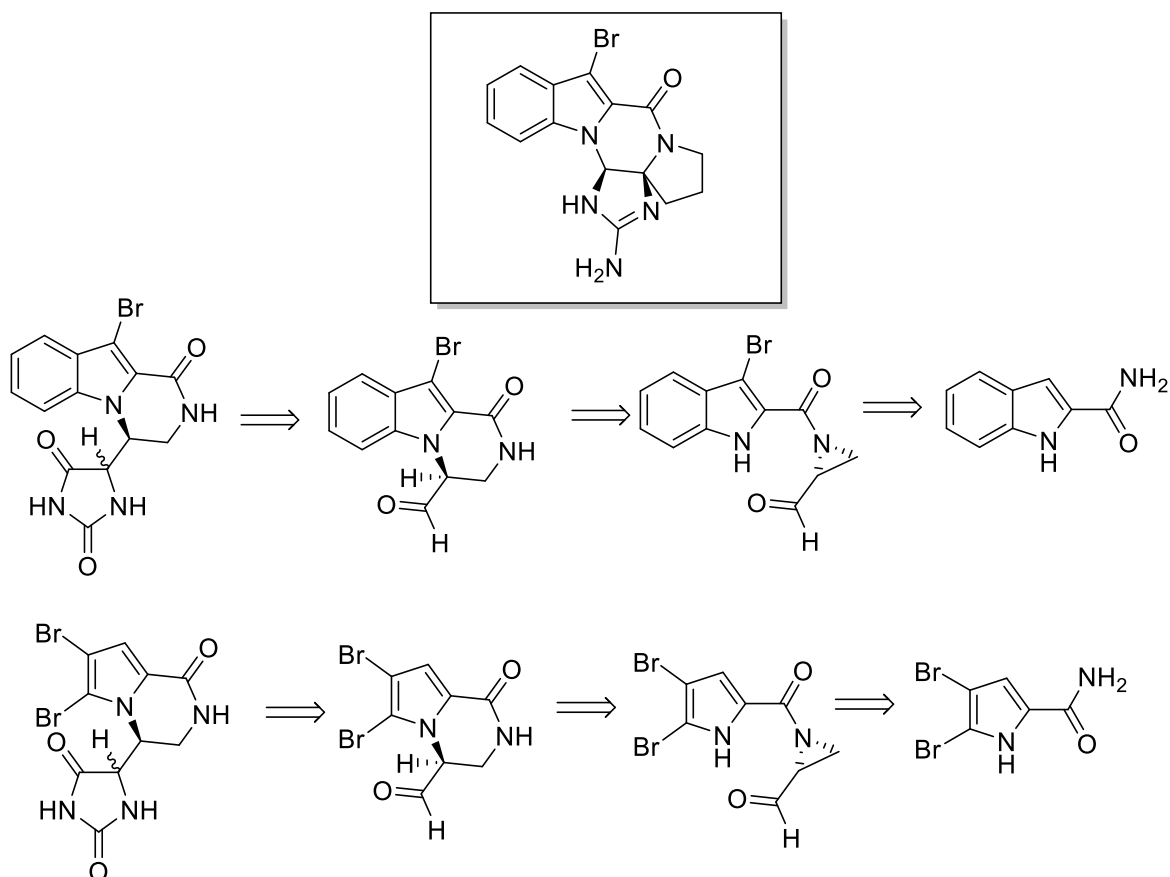


Figure III-VIII: Proposed retrosynthesis to access desired analogs of Agesamides A and B.

Olefin activation of electron depleted olefins like methyl acrylate has been shown to occur in moderate yield based on the formation of a reactive halonium source. The generation of in-situ IBr and ICl was done from the addition of halonium reagents with potassium iodide (KI). The resulting IBr generated was very electrophilic and promoted attack by the olefin and resulted in an iodonium intermediate that was opened by amide or urea to give the cyclized product.

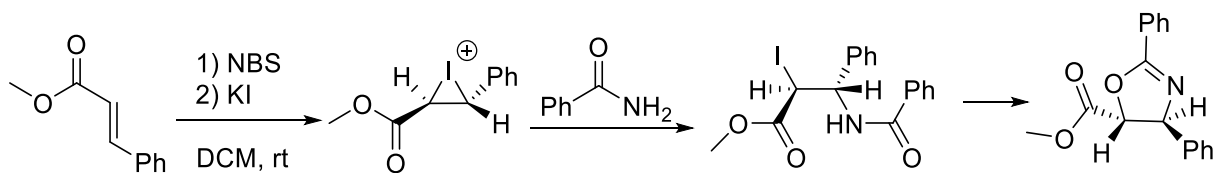


Figure III-IX: Iodonium catalyzed cyclizations

Recently published data in the Tepe group, further identified the generation of a bromonium and sequential opening by an imide to be a method of effective aminohalogenation in moderate yields.⁷⁶ Based on these findings, it was proposed that in the presence of a generated iodonium species that nucleophilic ring opening by a functionalized pyrrole or indole could lead to a key synthetic intermediate for further testing and transformation.

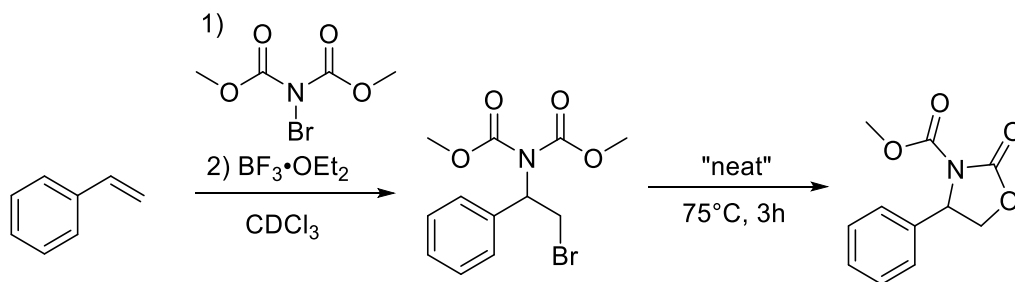
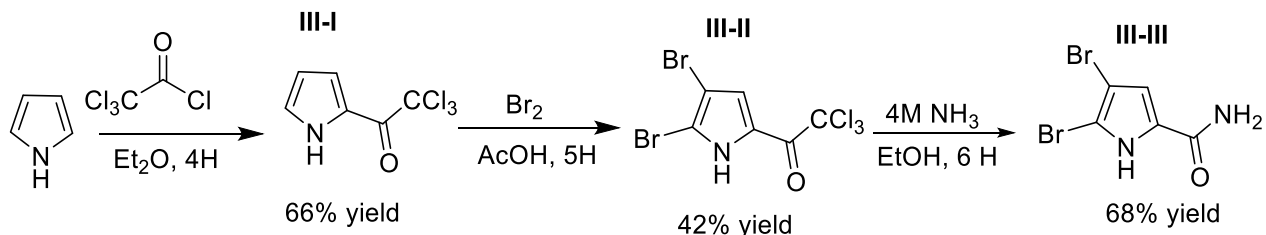


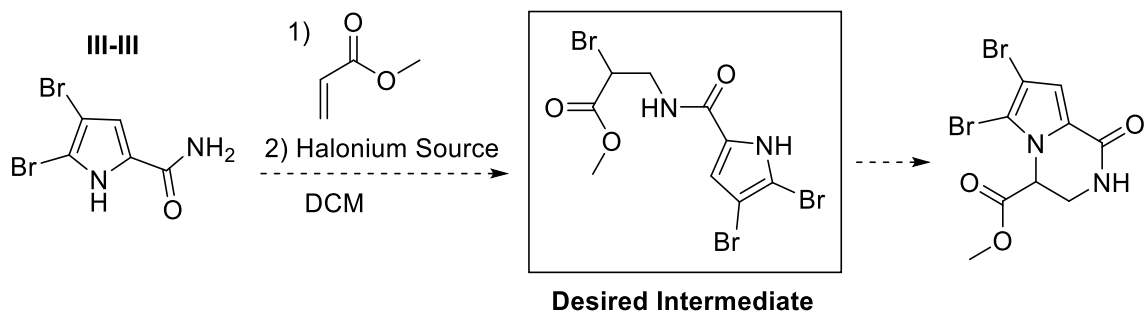
Figure III-X: Lewis acid catalyzed brominium opening.

The functionalized molecule was accessed in three steps, from pyrrole. The first step was the Friedel-Crafts acylation towards formation trichloroacetyl pyrrole, followed by dibromination of this pyrrole with Br₂ in AcOH to give the dibromo-trichloroacetyl pyrrole, which was then reacted with ammonia in methanol to give the proposed pyrrole.⁷⁷⁻⁷⁸



Scheme III-I: Synthesis of 4,5-dibromopyrrole-2-carboxamide

The slow addition of different halonium sources to the pyrrole in the presence of an α,β unsaturated system were carried out and the results are below.



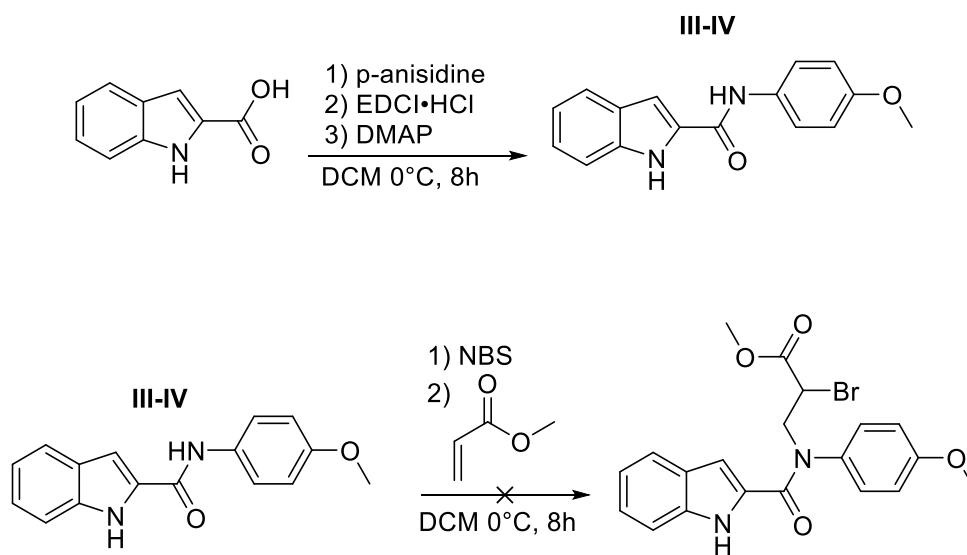
Scheme III-II: Failed attempts at olefin activation with 4,5-dibromopyrrole-2-carboxamide.

Additive	Halonium Source	Base	Observation
–	TBICA	–	S.M. observed
3 equiv KI	TBICA	–	Decomposition
1 equiv KI	TBICA	–	Decomposition
1 equiv KI	TBICA	NaHCO ₃	S.M. observed
–	ICl	NaHCO ₃	S.M. observed
1 equiv KI	ICl	NaHCO ₃	S.M. observed
1 equiv KI	NBS	–	Decomposition
–	TCCA	–	S.M. observed
3 equiv KI	TCCA	–	S.M. observed
1 equiv KI	TCCA	–	S.M. observed
–	IBr	NaHCO ₃	S.M. observed

Table III-I: Experimental condition of the failed attempts at olefin activation.

Addition to the olefin did not occur under varied reaction conditions. The generation of IBr just resulted in decomposition of the starting material. The decomposition of this reaction was suspected to be the generation of the IBr which generates an equivalent of concentrated acid as a bi-product of the halogenation reaction. To probe this, inorganic bases were introduced to the reaction. Organic bases are incompatible with IBr and when exposed undergo rapid halogenation in a very exothermic reaction. The addition of inorganic bases did not result in product formation. Commercial reagent and *in-situ* generated ICl did not react and starting material was recovered. Milder halonium sources did not react with the reagents and only starting material was observed. In many of the synthesis of these oroidin analogs, intermediate steps identify that N-protection of the amide was necessary for sequential transformation. To further probe whether the functionalization of the amide or the pyrrole intermediate was the cause of reaction failure, indolo-

derivatives were used. The indole derivatives were used because of their increased stability to better explore what reaction conditions were necessary to access the desired intermediate. The EDCI coupling of p-anisidine to indole resulted in a PMP-protected indole-2-carboxamide. This substrate was used to probe both the pyrrole and halonium intermediate's contribution to product formation.



Scheme III-III: Failed bromonium catalyzed cyclization.

N-alkylation was not observed when NBS was introduced to N-(4-methoxyphenyl)-1H-indole-2-carboxamide and pre-equilibrated before the addition of methyl acrylate. It was proposed that installation of the PMP group as an EDG would increase nucleophilicity of the carboxamide nitrogen and aid in N-Br formation on the N-(4-methoxyphenyl)-1H-indole-2-carboxamide. The brominated amide would transfer the bromonium to the α,β unsaturated ester and result in bromonium ring opening by the in-situ generated amide anion, similarly to the hydroxyamination of olefins previously published by Tepe group.

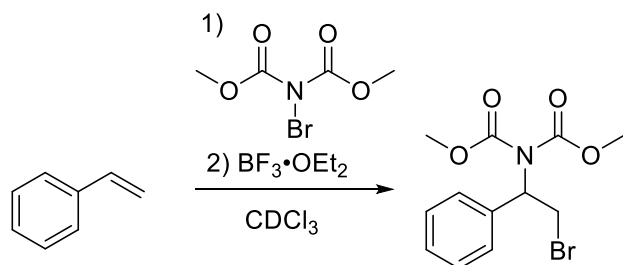


Figure III-XI: Example of resultant aminobromination after nucleophilic ring opening

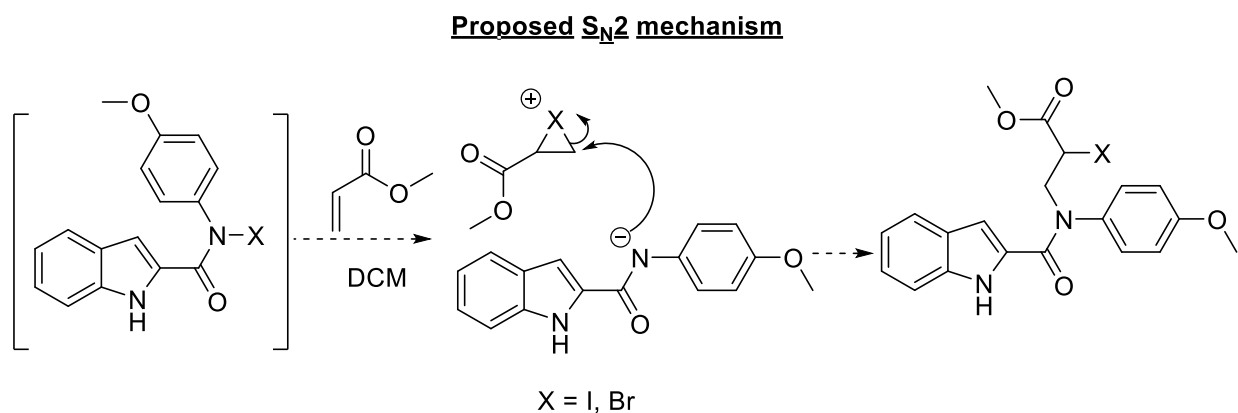
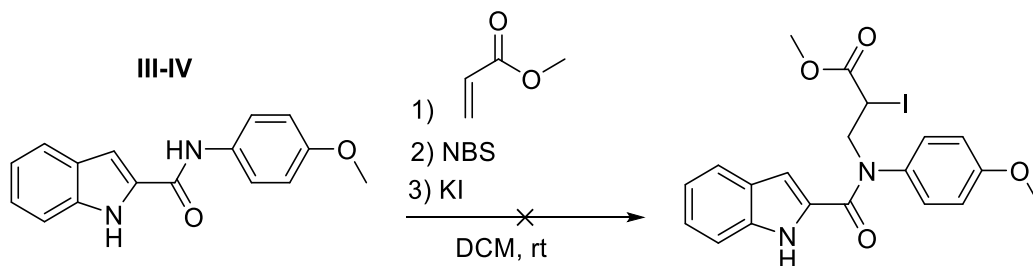


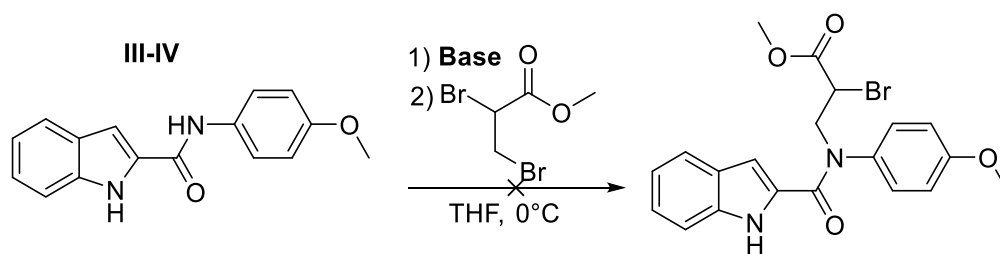
Figure III-XII: Proposed ring opening of halonium intermediate.

The observation of only starting material re-enforced the experimental results observed in the cyclization of benzamide that only strongly electrophilic halonium reagents are reactive enough to undergo iodonium intermediate formation with the electron depleted olefins. IBr was generated in-situ from the addition of NBS in DCM with KI. The formation of IBr did not lead to product formation, starting material was recovered without decomposition. This experimental result confirmed that IBr was not compatible with the pyrrole intermediate.



Scheme III-IV: Proposed ring opening using the generation of IBr.

To ensure that the olefin was being activated, methyl acrylate was first brominated with Br₂ in CCl₄ to give the methyl 2,3-dibromopropanoate. This intermediate was then used to probe which conditions would result in N-alkylation.



<u>Base</u>
NaOEt
LiHMDS
NaH
n-BuLi

Scheme III-V: Failed attempts at N-alkylation

Deprotonation of the starting material indole did not result in N-alkylation, instead starting material was observed which suggested that E₂ elimination occurred to protonate the basic amide intermediate and liberate vinyl bromide as a side product which is a volatile gas. Because of this result this approach of amino-halogenation was abandoned acknowledging the evaporation of the side products, methyl 2-bromoacrylate or methyl 2-iodoacrylate would shift the chemical equilibrium to favor generation of it removing any chance of desired S_N2 product formation.⁷⁹

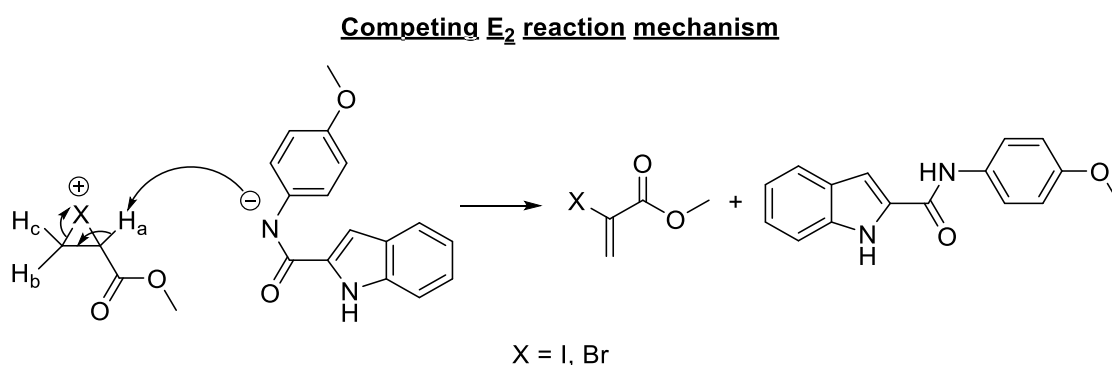


Figure III-XIII: Competing E₂ mechanism for side product formation.

Approach 2 – Iminium/Enamine cascade of secondary amines towards aziridine synthesis

Due to the low functional group tolerance and large amount of side product formation the aminohalogenation of electron depleted olefins was eliminated as a method of accessing these natural products. One of the other approaches used towards accessing these class of compounds was influenced by aziridine formation and expansions. It was proposed that the aziridine intermediate could be selectively opened to yield the reactive intermediates and lead to natural product formation.

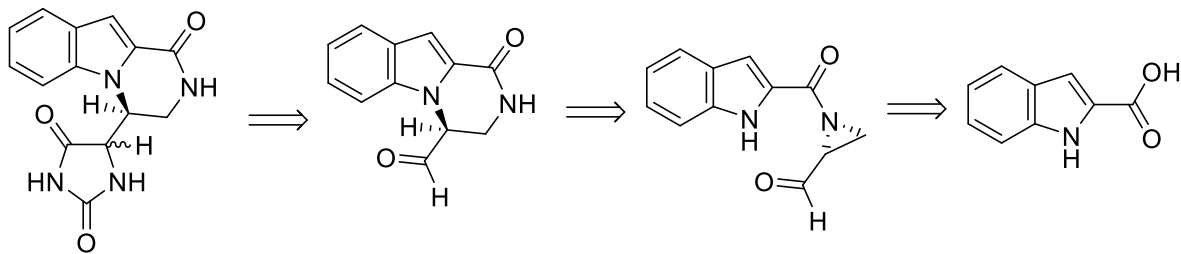
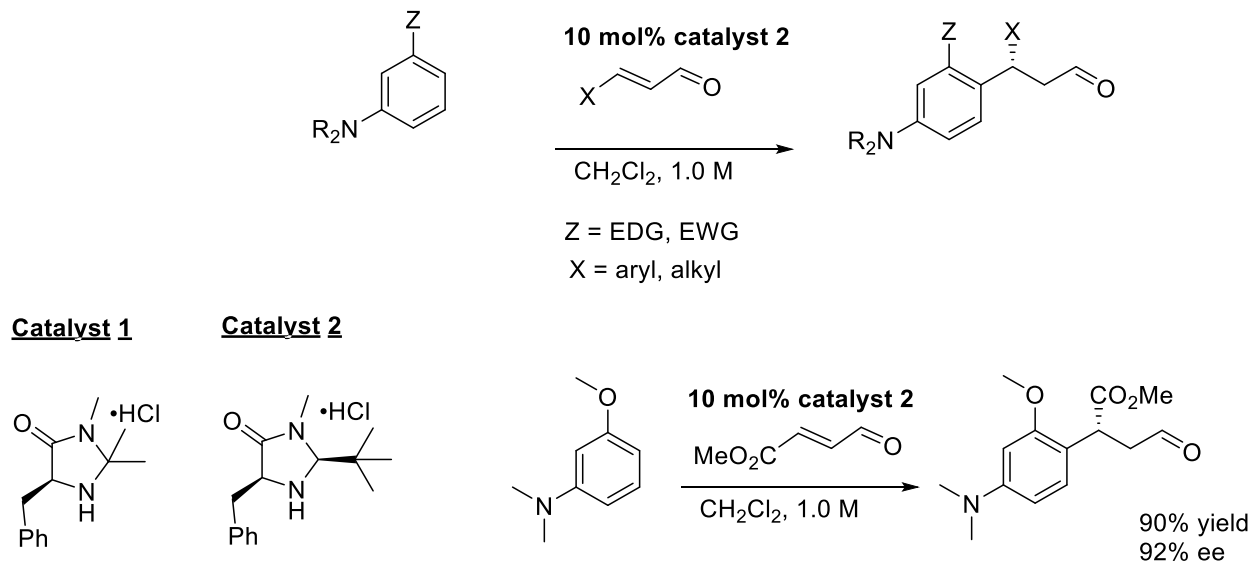


Figure III-XIV: Retrosynthetic analysis of analogs of Agesamides A and B

This work was influenced by the experimental findings of MacMillan and Jørgenson groups who used a tandem iminium/enamine system to promote β -functionalization of α,β unsaturated systems. This research highlighted how secondary amines can be used as organocatalysts to promote nucleophilic attacks on α,β unsaturated systems. This was the desired N-alkylation that wasn't observed with previous attempts using IBr.

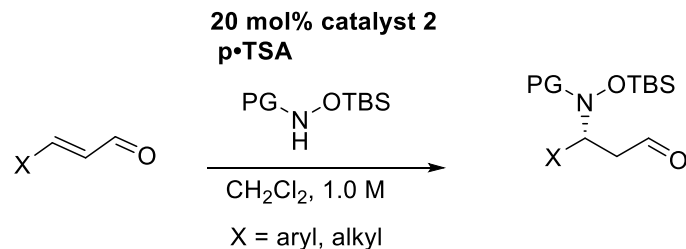
Pioneering work in the MacMillan lab, used influences from the Hajos-Parrish reaction to develop an enantioselective approach to 1,4 addition of α,β unsaturated aldehydes. MacMillan and co-workers utilized the reversible nature of iminium ions to activate α,β unsaturated aldehydes into α,β unsaturated iminium complexes. These reactive systems then underwent conjugate addition in the presence of electron rich benzene ring towards the formation of new C-C bonds. This research group proposed that the use of chiral secondary amines would influence the approach of the incoming benzylic nucleophile. Development of two amine catalyst known as MacMillan's catalyst 1 and catalyst 2 allowed for organocatalytic enantioselective benzene alkylations. Probing of the reaction scope identified that this chemistry tolerated both anilines with EDG and EWG present on the ring, with all reactions proceeding in moderate to high yield.⁸⁰⁻⁸⁵



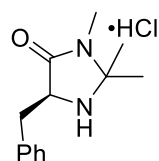
Paras, N. A.; MacMillan, D. A. C.; *J. Am. Chem. Soc.* **2002**, *124*, 7894-7895

Figure III-XV: Organocatalytic conjugate addition of benzene systems to α,β unsaturated aldehydes.

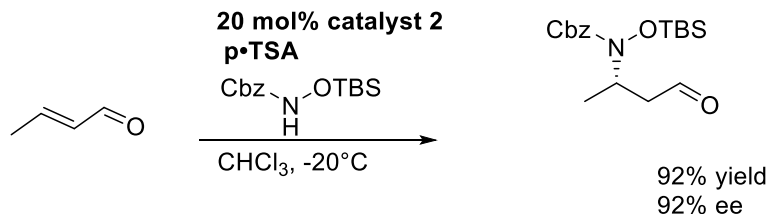
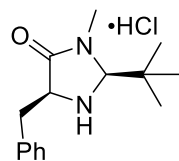
MacMillan and associated furthered their influence on the field of iminium catalyst by demonstrating the versatility of nucleophiles that can be incorporated to α,β iminium complexes. These complexes were generated by the incorporation of a chiral secondary amine catalyst to an α,β unsaturated aldehyde. Previous research demonstrated incorporation of electron rich benzene rings to the β -position of α,β unsaturated aldehydes. These reaction conditions were further modified to allow for the enantioselective conjugated addition of functionalized carbamates to give C-N bond formation. This demonstrated that molecules with lower nucleophilicities could still be incorporated to these activated iminium species in high yield and high enantioselectivity.



Catalyst 1



Catalyst 2

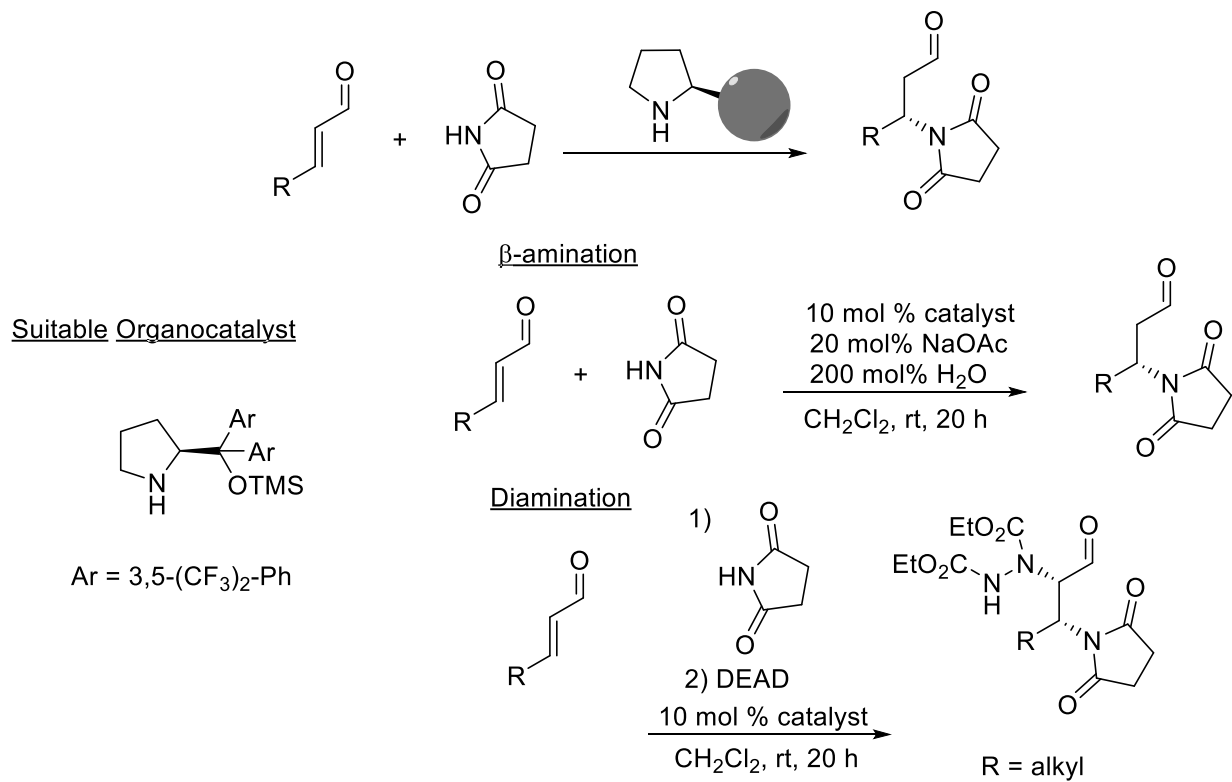


Chen, Y. K.; Yoshida, M.; MacMillan, D. A. C.; *J. Am. Chem. Soc.* **2006**, *128*, 9328-9329

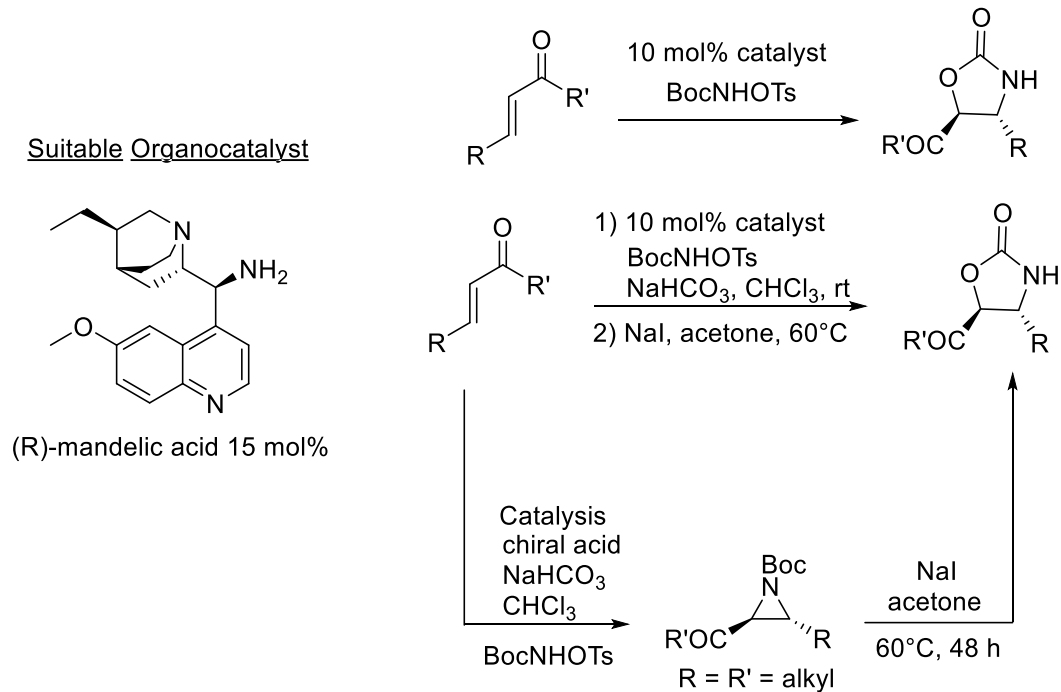
Figure III-XVI: Organocatalytic conjugate addition of carbamates to α,β unsaturated aldehydes

Work within the Jørgensen group highlighted the activation of α,β unsaturated systems with secondary chiral amines towards incorporation of commercially available nitrogen sources. This research focused around the incorporation of amines and diamines to α,β unsaturated systems, in very few steps to give access to enantioenriched products as precursors for further synthesis. Initial work focused on addition of an amine at the β position masked as succinimide. Incorporation of the chiral catalyst was experimentally proven to be necessary for β amination due to formation of the activated α,β iminium complex that facilitated 1,4 addition. Initial observations in this approach to β amination resulted in incorporation of DEAD as an electrophilic nitrogen source that was captured in the presence of the in-situ generated enamine. DEAD has been observed in literature as an α -amination source in α -functionalization. DEAD addition under these reaction conditions was influenced by the steric nature of the enamine intermediate and resulted in *syn*-addition of both masked amines in moderate yield, and high ee.⁸⁶

Jørgensen's lab then furthered their contributions to the field of organocatalysis with their tandem asymmetric aziridination and expansion reactions. Building on their previous efforts towards β -amination and *syn*-diamination, the Jørgensen group demonstrated the formation of Boc-protected disubstituted aziridines from BocNHOTs, an α , β unsaturated ketone and a secondary amine. These aziridines were then converted *in-situ* to their corresponding oxazolidinones with the addition of NaI. Jørgensen's work identified the factors that influence the regiochemical outcome of the aziridine expansions and demonstrated that ring opening occurred exclusively at the α -carbon to the ester due to the generation of a larger δ^+ at that carbon over the β -carbon.⁸⁷ This discovery along selective activation of α,β unsaturated systems without conjugated aromatic groups, were the basis for one of our approaches towards derivatives of Agesamides A and B.



Jiang, H.; Nielsen, J. B.; Nielsen, M.; Jorgensen, K.A.; *Chem. Eur. J.* **2007**, *13*, 9068-9075

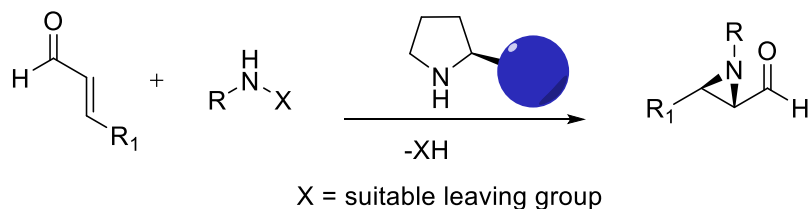


Cruz, D. C.; Sanchez-Murcia, P. A.; Jorgensen, K.A.; *Chem. Commun. J.* **2012**, *48*, 6112-6114

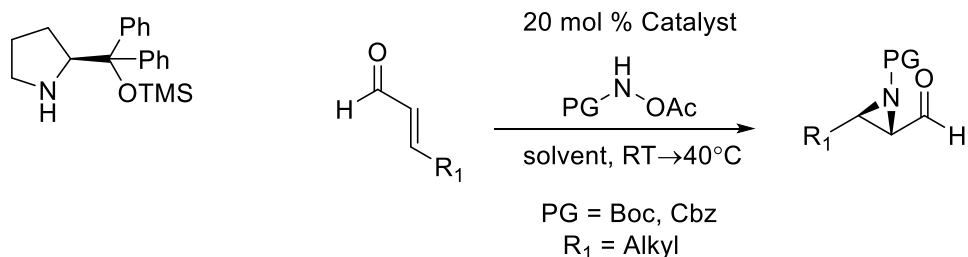
Figure III-XVII: Enantioselective deamination under organocatalytic conditions.

Our efforts combined the observations noted by the Jørgensen and MacMillan groups and focused on the development of a novel aziridination substrate which can be used on α,β unsaturated systems to yield the desired aziridine intermediates. The expansion of these aziridine intermediates towards derivatives of Agesamides A and B would then be explored. Previous publications exploited different functionalities of substituted hydroxyl-amine derivatives to evoke the formation of protected aziridines. The presence of chiral catalysts like chiral secondary amines have been used to make these reactions enantioselective towards aziridination.

This pioneering research was seen in the Cordova lab where they evolved the theory of iminium-enamine formation and catalysis displayed by MacMillan towards the highly enantioselective and diastereoselective aziridination of disubstituted α,β unsaturated aldehydes. The synthesis of their substituted hydroxyl-amine derivatives allowed for “nitrene mimics”. These systems allowed for initial nucleophilic attack of the α,β iminium complex resulting in an *in-situ* generated enamine that displayed the -OR leaving group forming an aziridine. Under the chiral environment induced by the catalyst, this initial nucleophilic addition and resulting enamine displacement occurred with facial selectivity. One of the key observations of this initial research highlighted the specificity of the secondary amine catalyst for product formation, diastereomer ratio and enantiomeric excess. Use of MacMillan’s stage 1 catalyst did not result in aziridination. Pyrrolidine based catalysts resulted in aziridine formation and highlighted the effect of R groups at the chiral center on the overall yield and stereoselectivity.⁸⁸⁻⁹¹



Suitable Organocatalyst

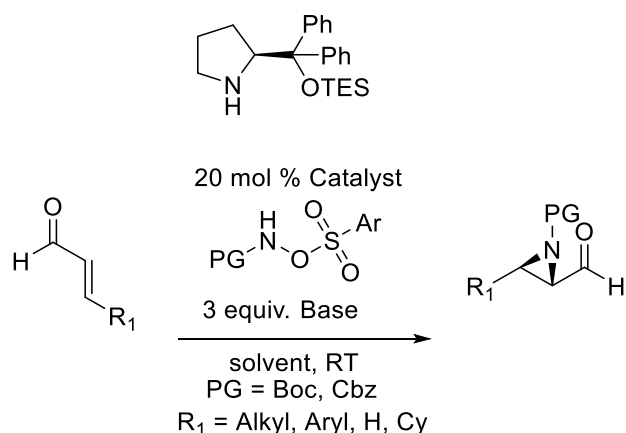


Vesely, J.; Ibrahem, I.; Zhao, G.; Rios, R.; Cordova, A. *Angew. Chem. Int. Ed.* **2007**, *46*, 778-781

Figure III-XVIII: Enantioselective aziridination of disubstituted aldehydes

Research done by Hamada and co-workers further evolved the experimental observations seen by the Cordova group. Hamada and co-workers further probed the mechanism behind the aziridination and identified that the conjugate base -OAc played a key role in product formation acting as a proton sponge after nucleophilic attack of the functionalized hydroxylamine on the iminium complex. Modification of the initial silyl group reported by Cordova was done to improve catalyst stability in the reaction. Coupled with those discoveries was their modification to the -OR leaving group for better displacement. These key changes allowed for them to increase the substrate scope beyond what was initially reported, allowing for aziridination of monosubstituted and aromatic conjugated α,β unsaturated aldehydes. Both these transformations were noted in literature to be difficult.⁹²

Suitable Organocatalyst



Arai, H.; Sugaya, N.; Sasaki, N.; Makino, K.; Lectard, S.; Hamada, Y. *Tetrahedron Lett.* **2009**, *50*, 3329-3332

Figure III-XIX: Enantioselective aziridination of monosubstituted and aromatic α,β unsaturated aldehydes.

These examples and their transformations became the basis of the approach towards synthesis of aziridine precursors for analogs of Agesamides A and B. Building on the foundation of the MacMillan group we proposed that the use of secondary amine catalyst would activate α,β unsaturated systems towards β -addition of a nitrogen nucleophile similarly to the work of the Jørgensen group. The favorable results of the Cordova and Hamada respectively have demonstrated the potential for functionalized hydroxylamines to form aziridines on these activated iminium systems. We proposed that modification of the N-functional group on the hydroxylamine to an indole derivative would allow the formation of an indole acyl aziridine. Based on the later works in the Jørgensen group that displayed ring opening via an S_N2 reaction in the presence of NaI; we proposed that this intermediate could be expanded to the six-membered ring and diamination product through closure by the indole nitrogen.⁹³⁻⁹⁴

Key Intermediate

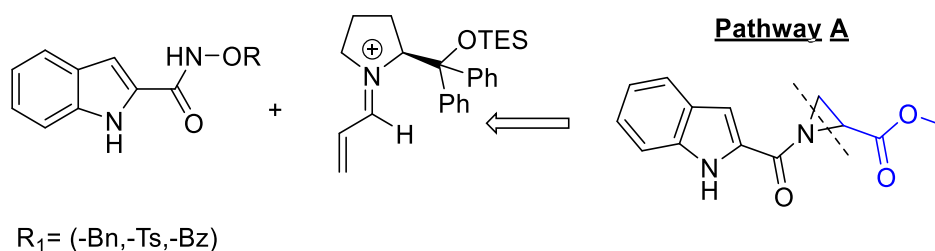
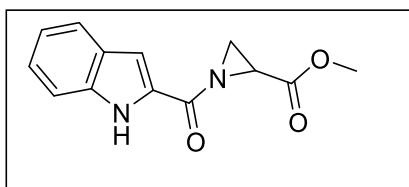
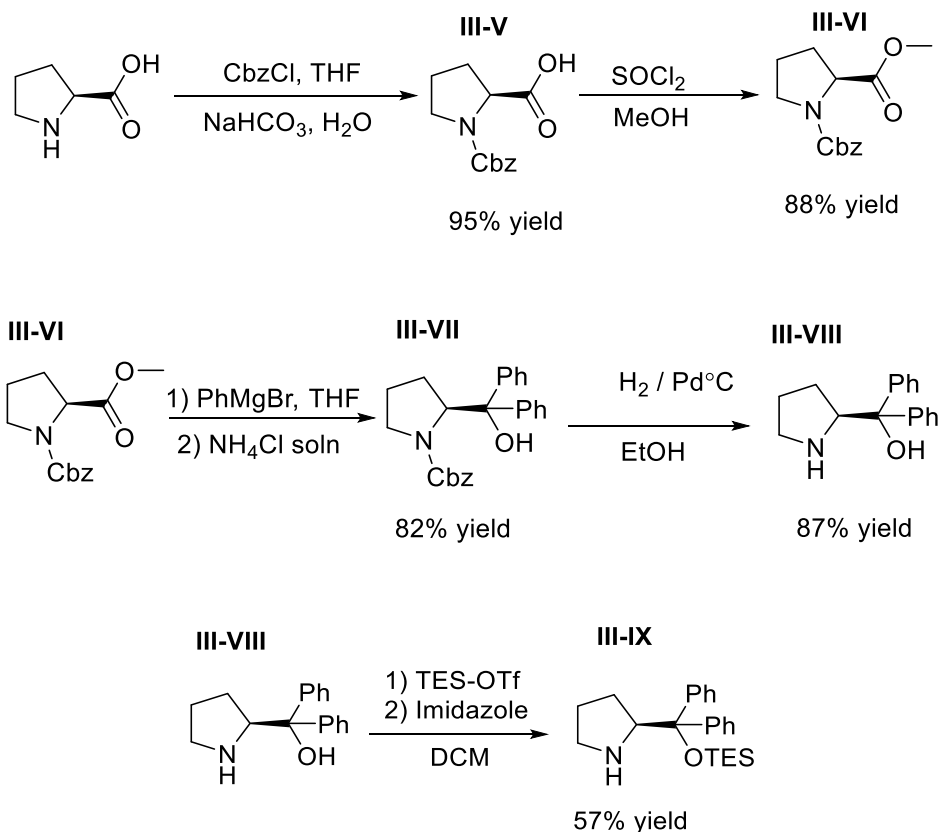


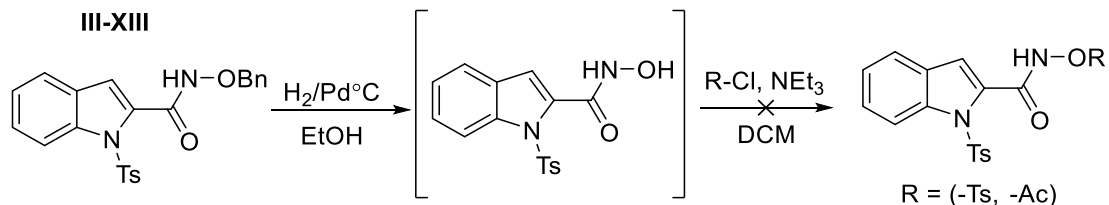
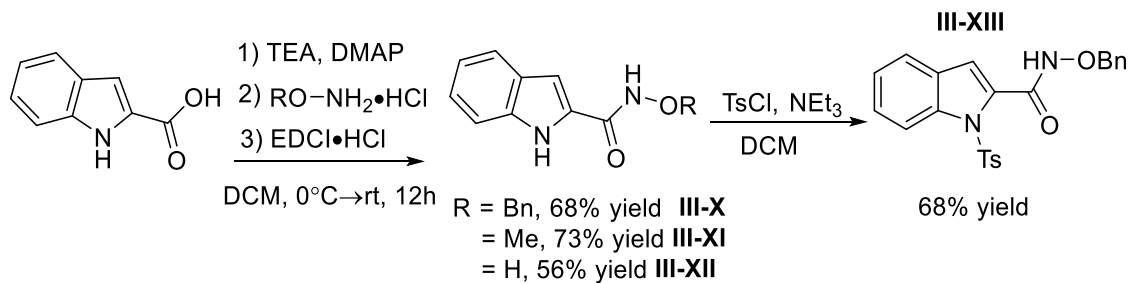
Figure III-XX: Approach towards desired aziridine intermediate.

The enantioselectivity for the aziridination is induced from the chiral secondary amine. This catalyst was accessed in five steps from the commercially available L-proline. Synthesis of the other enantiomer calls for the use of D-proline. Proline was protected with Cbz-Cl to produce Cbz-protected Proline. Activation of the carboxylic acids to form the acyl chloride in the presence of SOCl₂, stirring in MeOH resulted in the formation of the methyl ester. To this ester phenyl magnesium bromide, a Grignard reagent was added to produce the tertiary substituted alcohol, after which the Cbz protecting group is removed by hydrogenation to yield the chiral secondary amide. The final functionalization is the silyl alcohol protection, various silyl groups have been used depending on substrates so the precursor to this structure is the desired product. Selective silylations will allow access to different chiral catalyst derivatives to test overall enantioselectivity in the presence of functionalized hydroxylamides.



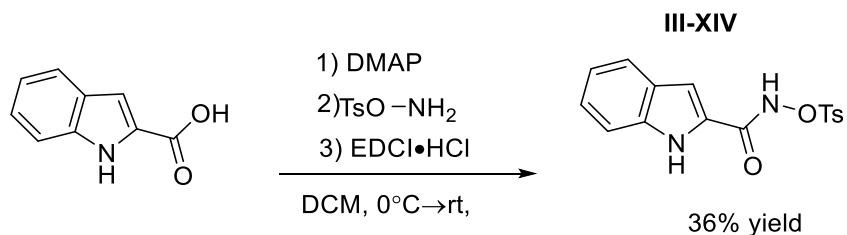
Scheme III-VI: Synthesis of the chiral secondary amine catalyst.

With the desired chiral secondary amine catalyst obtained, the synthesis of functionalized N-hydroxy-1H-indole-2-carboxamides began using EDCI conditions, and different O-R functionalized hydroxylamines. The indole nitrogen of resulting protected N-hydroxy-1H-indole-2-carboxamides was then tosylated. Deprotection of O-R group like the benzyl group under hydrogenation conditions produced N-hydroxy-1-tosyl-1H-indole-2-carboxamide. Any attempts to further functionalize the OH of the hydroxyamide lead to complete decomposition of the starting material.



Scheme III-VII: Pathway to desired Indole-derivative.

The inability to access 1-tosyl-N-(tosyloxy)-1H-indole-2-carboxamide, lead to the synthesis of the desired intermediate through the EDCI coupling of 1H-indole-2-carboxylic acid with O-Ts protected hydroxylamine.⁹⁵



Scheme III-VIII: Synthesis of desired indole derivative.

This intermediate was accessed at the same time as work in approach 3 was being pursued and identified that this pathway would access the desired product. Further explanation of the factors that concluded this are below.

Approach 3 – Controlled expansion of carbonyl aziridines to form fused ring intermediates

This approach focused on the development and optimization of all downstream reactions after the aziridination. This was done to ensure that after the methodology has been developed, all other synthetic transformations would systematically occur without incident under optimized reaction conditions.

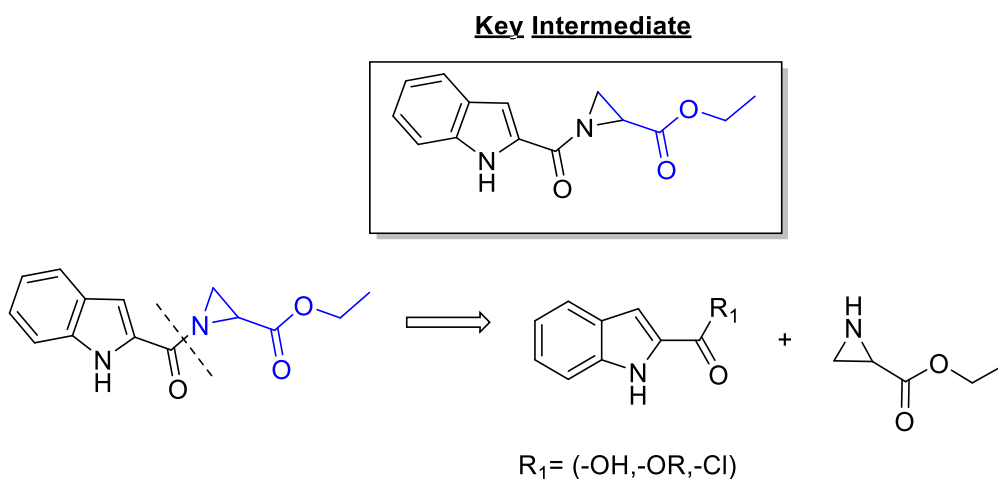
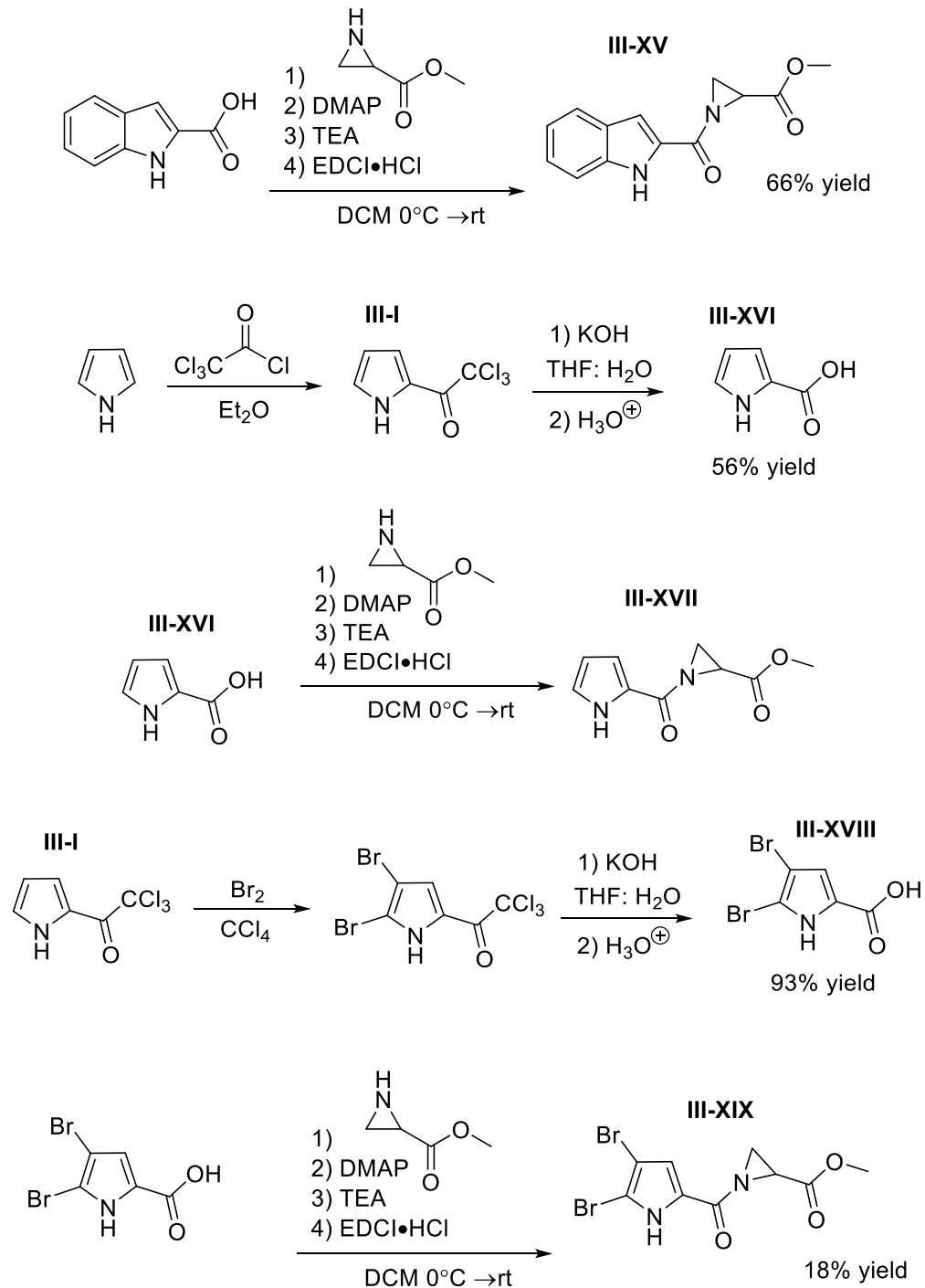


Figure III-XXI: Alternative approach to accessing the desired aziridine intermediate.

To better explore these reaction conditions, it was imperative to access this indole-2-carboxaziridine and other carboxaziridine intermediates. Therefore indole-2-carboxylic acid was coupled to aziridine-2-carboxylic acid methyl ester, to give methyl 1-(1H-indole-2-carbonyl)aziridine-2-carboxylate. EDCI coupling of pyrrole-2-carboxylic acid to aziridine-2-carboxylic acid methyl ester gave methyl 1-(1H-pyrrole-2-carbonyl)aziridine-2-carboxylate. The coupling of 4,5-dibromo-1H-pyrrole-2-carboxylic acid to aziridine-2-carboxylic acid methyl ester occurred to give methyl 1-(4,5-dibromo-1H-pyrrole-2-carbonyl)aziridine-2-carboxylate in low

yield. This highlighted the reduced reactivity of the dibromo-abduct in comparison to the other carboxylic acids towards EDCI coupling reactions.⁹⁵



Scheme III-IX: Synthesis of desired aziridine intermediates by EDCI coupling.

Development of controlled aziridine ring expansion was then explored. Tepe group research has previously identified a trend in aziridine ring opening with expansion of imidoaziridines favoring ring opening at the more electropositive carbon of the strained three member aziridine ring. Therefore the intermediates from the EDCI coupling reactions were designed to take advantage of this observation. In the presence of 2,6 Lutidine·HCl salt, the conj. acid the imidoaziridine of ethyl-3-phenylaziridine carboxylate expanded to 2-imidazolines. It was proposed that one of the major mechanisms for product formation required that first protonation of the aziridine nitrogen occur followed by ring expansion to give the imidazoline.

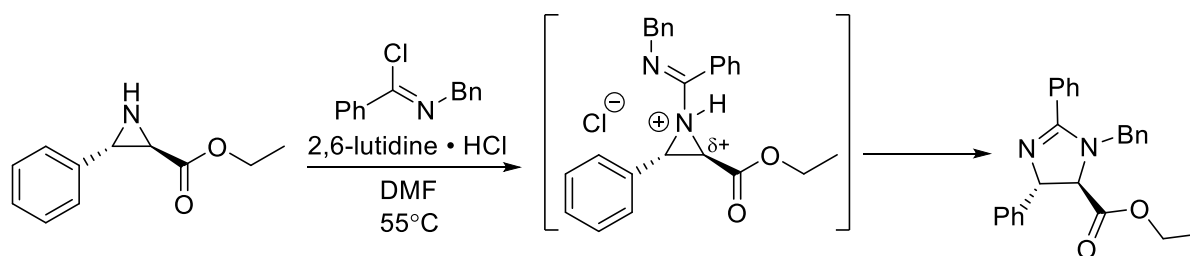


Figure III-XXII: Expansion of activated aziridines to give imidazolines.

The current hypothesis was that the proposed protonation of the intermediate carbonyl aziridine's nitrogen would behave in a similar manner to the protonated imidoaziridine. The buildup of positive charge on the carbon next to an ester, a strong electron withdrawing group would facilitate ring expansion from the indole nitrogen to yield the desired regioisomer. The expanded scaffold would then be transformed to natural products in a few steps.

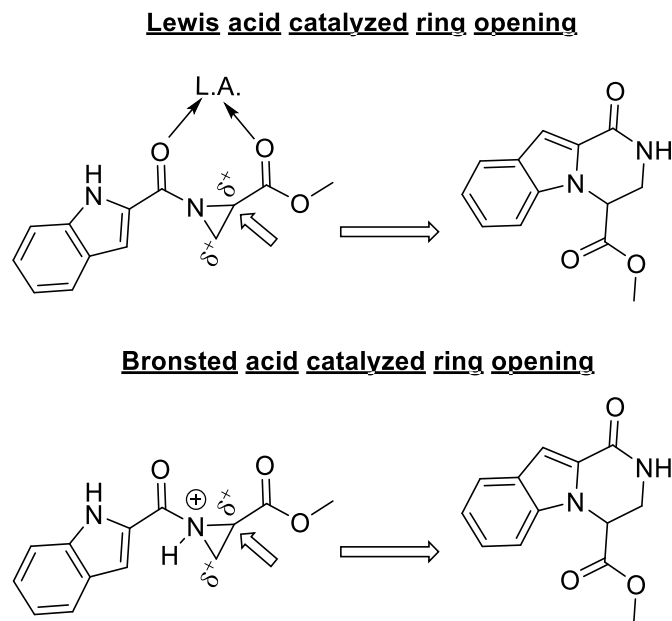


Figure III-XXIII: Proposed methodology for controlling ring opening of aziridine intermediates towards accessing desired 6,5,6 fused core.

Heine like ring expansions have been shown by Heine and workers to also yield oxazolines but in systems involving the incorporation of aziridine-carboxamides only cyclized ureas were formed. The nitrogen outcompeted the oxygen in the formation of cyclic ureas. Under this premise it was expected that even if there were mixtures of expansion products based on the formation of a 5-membered ring versus a 6-membered ring that the desired intermediate would be obtained in larger yield.⁹⁶⁻⁹⁷

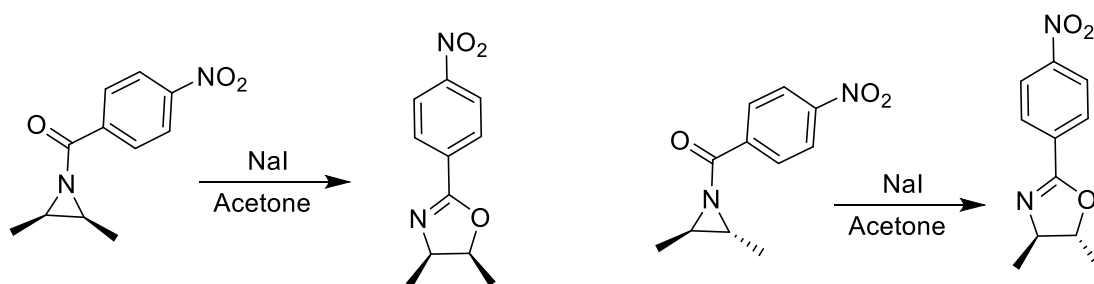
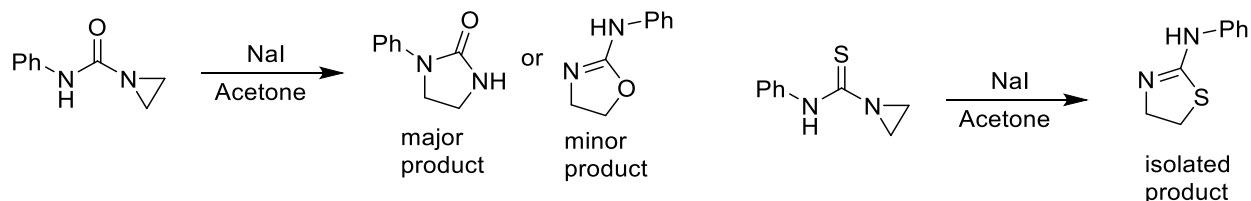


Figure III-XXIV: Heine ring expansion of aziridines to yield oxazolines and imidazolines.

Figure III-XXIV cont'd



King, D. C.; Portland, L. A.; Heine, H. W. *J. Org. Chem.* **1966**, *31*, 2662-2665
Kenyon, W. G.; Johnson, E. M.; Heine, H. W. *J. Am. Chem. Soc.* **1961**, *83*, 2570-2574

With that premise in hand experimental conditions for ring expansion were explored. Since acidic conditions have yielded the desired regioisomer in past aziridine expansions within the group for imidazolines, acidic conditions were first screened for their ability to yield the desired intermediate. Literature precedence has identified Lewis acids for their ability to expand N-functionalized aziridines to their β -amino- α -chloro carboxylate systems.⁹⁸

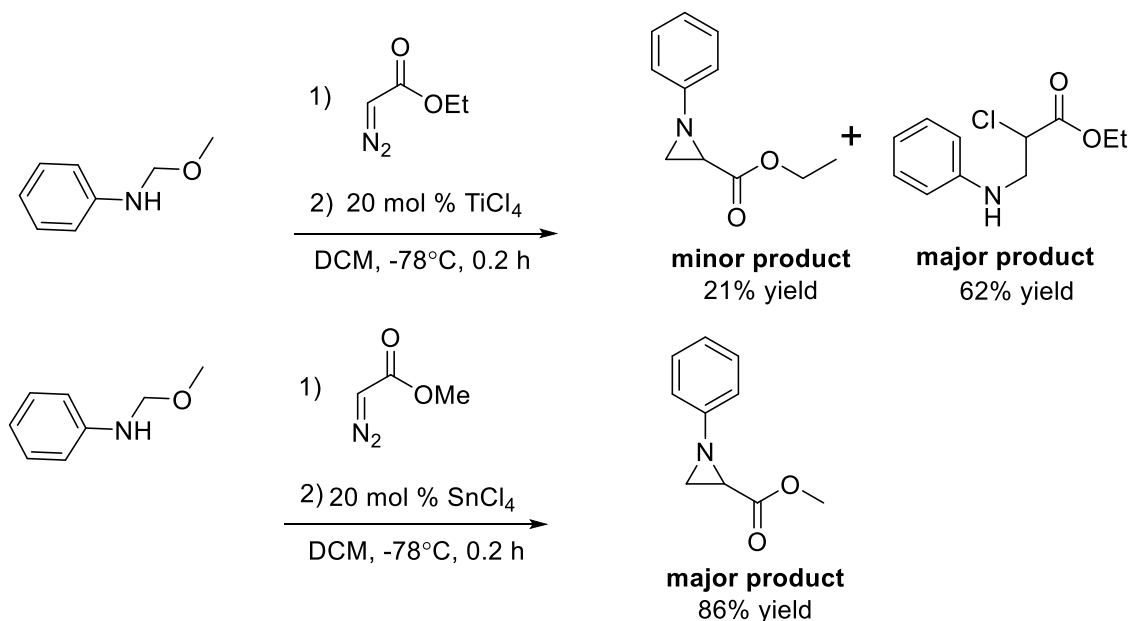
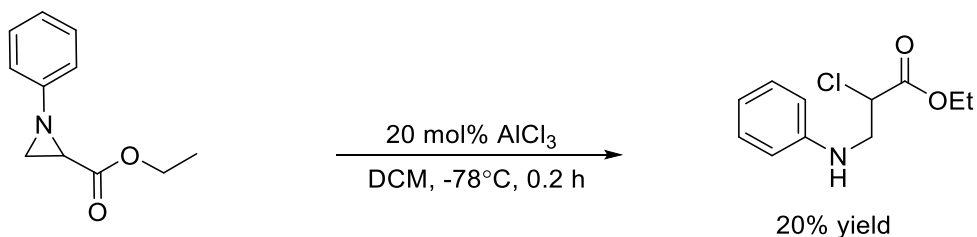


Figure III-XXV: Effect of Lewis acids on aziridine ring opening.

Figure III-XXV cont'd



Hyun-Joon, H.; Jang-Min, S.; Kyung-Ho, K.; Young-Gil, A.; Oksoo, H. *Tetrahedron* **1998**, *54*, 851-858

Yongun, K.; Hyun-Joon, H.; Hoseop, Y.; Baek, K. L.; Won, K. L. *Tetrahedron* **2006**, *62*, 8844-8849

To further probe this Lewis acid mediated expansion, methyl 1-(1H-indole-2-carbonyl)aziridine-2-carboxylate was first introduced to Ti(OiPr)₄. Titanium (IV) isopropoxide, is a strongly oxyphilic Lewis acid and titanium been shown to coordinate to the oxygen in amide and sequester them as ligands. The introduction of this Lewis acid was done to coordinate to the oxygen of the carboxaziridine according to previous literature reports. This coordination would in turn cause the donation of the aziridines lone pair electrons into the carbonyl of the carboxamide resulting in a buildup of positive charge at the carbon adjacent to the ester in the starting material. This would then catalyze the regiocontrolled ring opening towards the desired intermediate. Coordination with the carboxaziridine oxygen to the titanium Lewis acids was also theorized to reduce ring expansion for the formation of the side product, the 5 membered oxazoline ring.⁹⁹

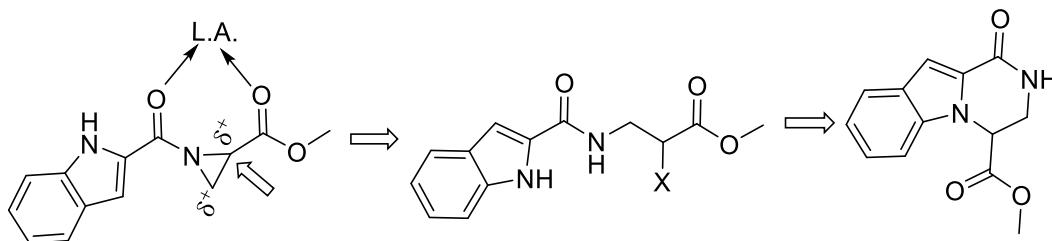
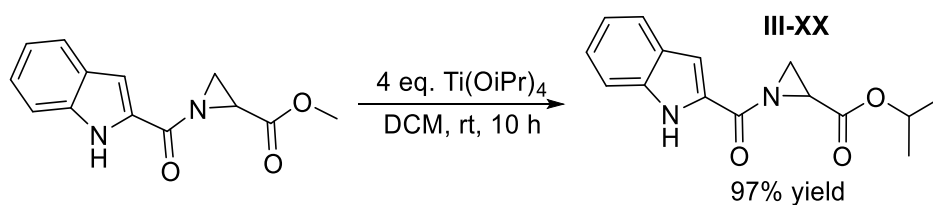


Figure III-XXVI: Proposed coordination of Lewis acid to access desired regioisomer with ring opening.

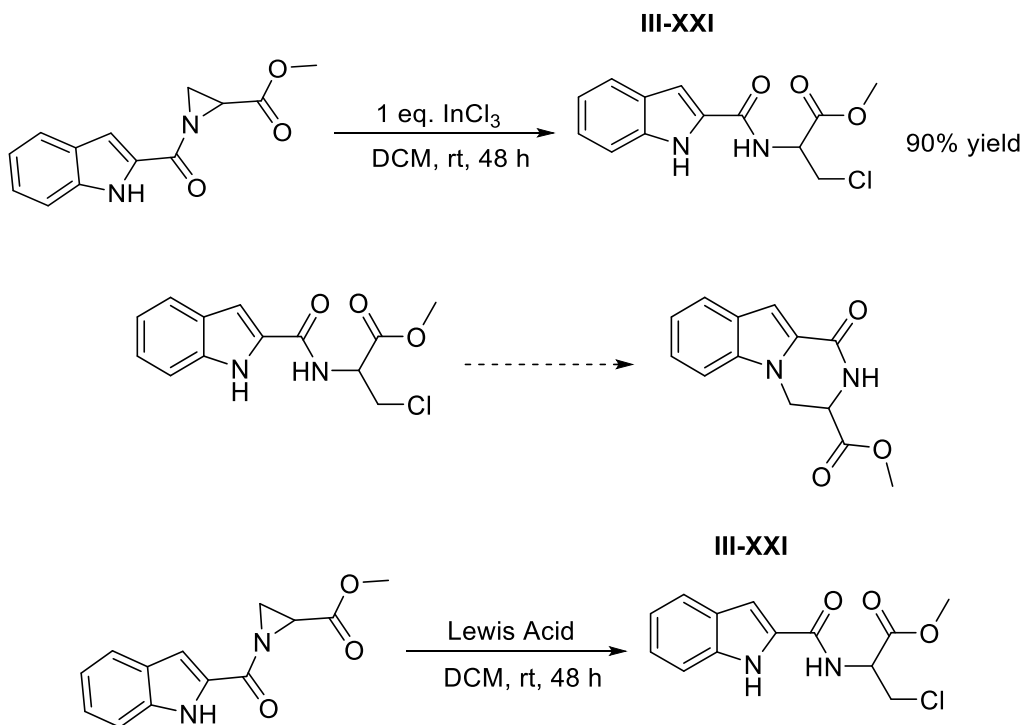
Upon addition the Lewis acid coordinated to the ester carbonyl of the aziridine instead of the amide carbonyl. Once coordinated to the ester, the side product of carbonyl ring opening to the 5 member oxazoline or the desired intermediate was not observed. Instead the trans-esterified product was isolated in high yield. This was due to ligand migration of the isopropoxide to yield isopropyl 1-(1H-indole-2-carbonyl)aziridine-2-carboxylate.



Scheme III-X: Transesterification with alkoxide ligands on Lewis acids.

Indium (III) chloride was used in another attempt towards ring expansion. Addition of the Indium (III) resulted in ring opening of the aziridine, but neither the cyclized oxazoline or desired intermediate was observed. Instead after coordination to the starting material there was migration of a chloride anion to the most sterically accessible carbon, the distal carbon of the aziridine. This was proven after workup when the methyl 3-chloro-2-(1H-indole-2-carboxamido)propanoate was isolated in great yield. Unfortunately, this intermediate if cyclized through the indole nitrogen would give the wrong regiochemistry of the desired cyclic intermediate. Other Lewis acids were

screened to verify if the regiochemistry of the ring opened product was unique to indium (III) chloride. They showed the same trend of ligand migration to the distal carbon and ring opening to the undesired regioisomer in great yield.¹⁰⁰



Scheme III-XI: Ring opening of the aziridine in the presence of a Lewis acid to wrong isomer

<u>Lewis acid</u>
InCl ₃
TiCl ₄
AlCl ₃
ZnCl ₂

Table III-II: Lewis acids screened for regioselective ring opening of acylated aziridines.

Approach 4- Brønsted acid catalyzed ring opening of carbonyl aziridines

Since the coordination of the Lewis acids promoted the formation of the disfavored product, through ligand migration, Brønsted acids then became the focus to attempt product formation. Full protonation of the aziridine nitrogen was theorized to force the buildup positive charge at the carbon alpha to the ester and would therefore focus ring opening either by the carbonyl of the carboxaziridine or the indole nitrogen.

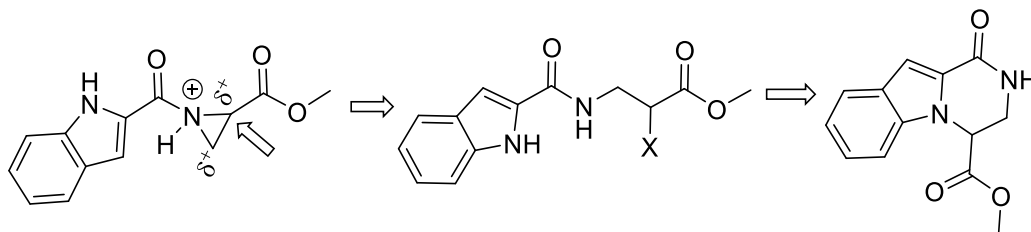
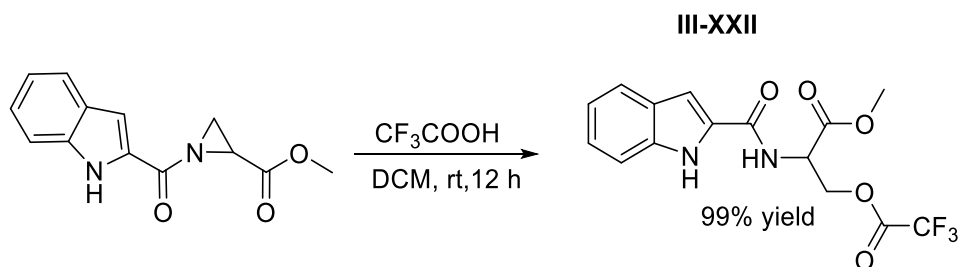


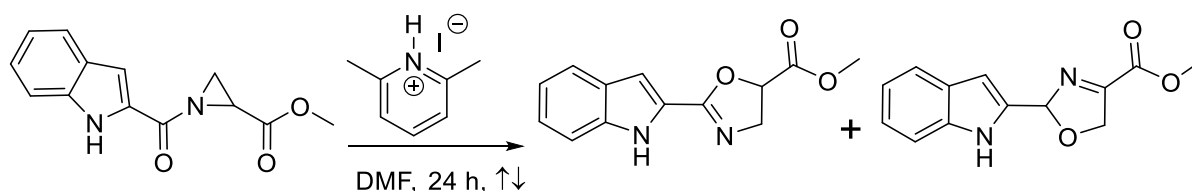
Figure III-XXVII: Proposed Brønsted acid activation to access desired regioisomer with ring opening.

In the presence of trifluoroacetic acid, the only product observed was the incorporation of the trifluoroacetic acid to the undesired regioisomer of the ring opened product. This was confirmed experimentally with HSQC.



Scheme III-XII: Ring opening of the acylated aziridine to wrong regioisomer.

In the presence of 2,6-Lutidine·HI salt, a weaker acid in comparison to trifluoroacetic acid, the products observed were a 1:1 mixture of cyclized oxazoline products, that were an inseparable mixture by chromatography.



Scheme III-XIII: Non-selective expansion of aziridine to oxazolines.

Another approach focused on intramolecular ring closure. The starting material was dissolved in a solution of EtOH: H₂O (1:4) and refluxed. Inspiration for this approach was noted from literature that highlighted the selective activation of oroidin towards cyclization through the pyrrole N-1 nitrogen to yield cyclo-oroidin. The optimized conditions for that cyclization were refluxing the molecule in polar protic solvent as opposed to the addition of strong acid. The

application of strong acid lead to olefin activation and ring closure but by the carbonyl oxygen instead.

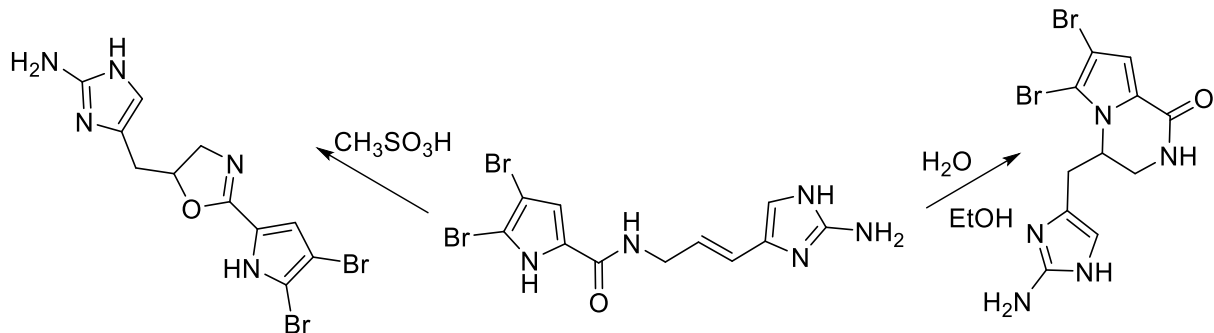
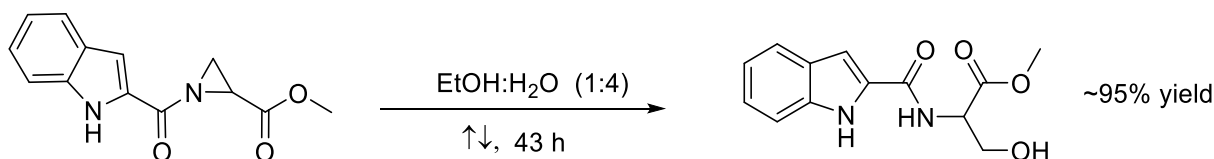


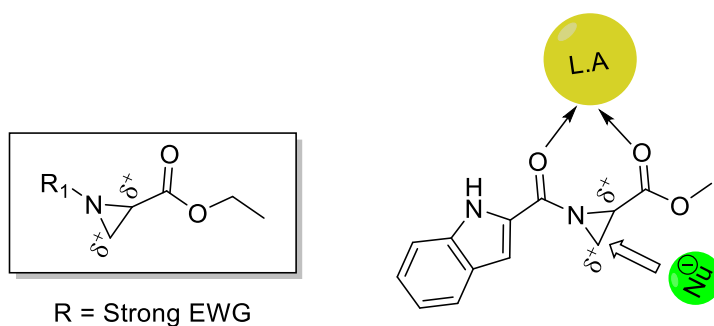
Figure III-XXVIII: Explanation of difference in stereochemistry based on acidity.

Since strong acidic conditions yielded the wrong regioisomer for the past expansions, the premise here was that milder conditions might yield the formation of the desired cyclic intermediate. Upon heating with polar solvent, the starting material was consumed to form what mostly resembles, methyl (1H-indole-2-carbonyl)serinate by both H-NMR, and C-NMR.



Scheme III-XIV: Proposed product of ring opening of aziridine in water.

The experimental results have shown that incorporation of a Brønsted acid or Lewis acid have led to the formation of the undesired regioisomer of the intermediate. This was due to coordination to both the amide carbonyl and the ester which cause a partial build up in charge in the aziridine ring. Coordination also makes the two-position of the aziridine sterically encumbered so the sterically accessible three position is preferentially attacked to release the buildup of positive charge and that results in the undesired regioisomer.



Yongeun, K.; Hyun-Joon, H.; Hoseop, Y.; Baek, K.; Won, K.L.; *Tetrahedron*, **2006**, 62, 8844-8849

Figure III-XXIX: Explanation behind expansion of intermediate to undesired regioisomer.

Aziridine ring opening does offer a unique opportunity to access the desired cyclic indole intermediate, however that expansion will be heavily reliant on finely tuned experimental conditions to afford the correct regiochemistry. To this effort, other approaches were exploited to access the desired 6,5,6 fused ring core intermediate.

Approach 5 – Acyl chloride ring opening of methyl 1-benzylaziridine-2-carboxylate

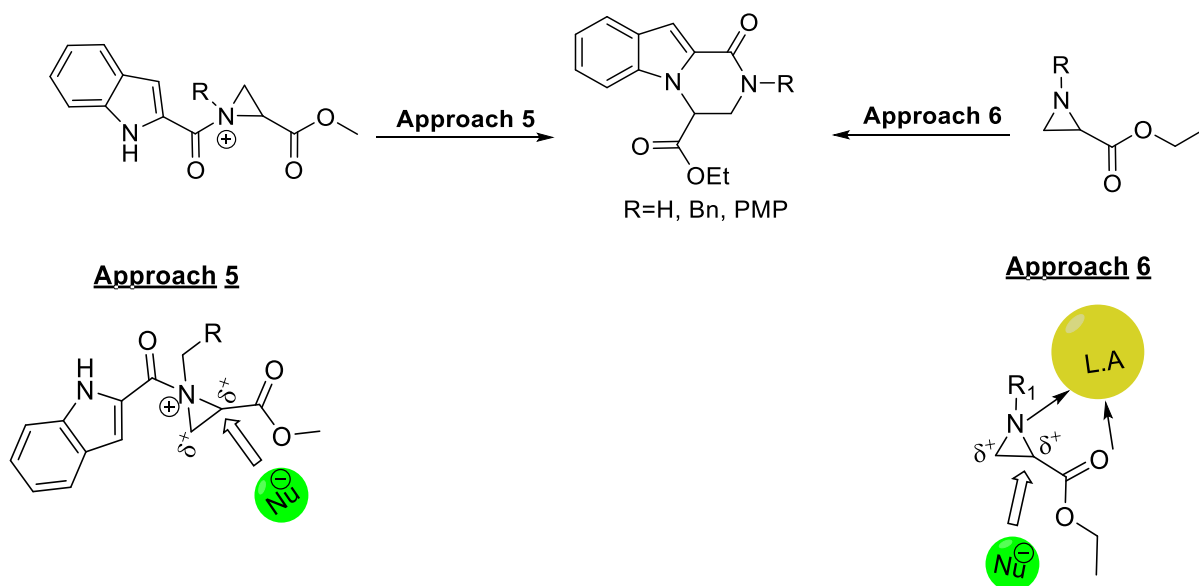
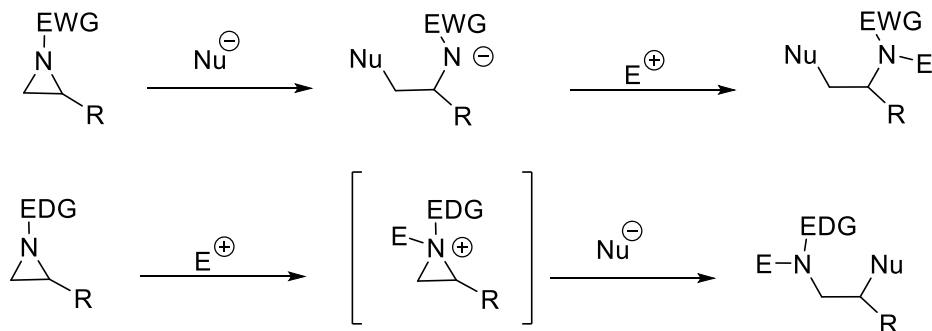


Figure III-XXX: Modified approach to regio-controlled ring openings of aziridines.

Approach 4 noted the problems observed in previous attempts of controlling the regiochemistry of the desired intermediates needed towards the successful expansion to the 6,5,6 fused core for the analog systems. The change in regiochemistry, as shown by experimental results as well as seen in some examples in literature has been attributed to the electron density of the aziridine intermediate. The regiochemical outcome was based on the R-group placed on the aziridine nitrogen. Masking the aziridine as an amide, directly changed the electronics of the strained 3-membered ring, instead of being electron rich, the strong EWG depleted the electron density of the 3-membered ring which contributed to the difference in regioselectivity. When introduced to a Lewis acid, there was a buildup of positive charge to both carbons in the strained 3-membered ring and steric accessibility to release this gradual buildup of positive charge became the major contributing factor to intermediate formation over electronics and resulted in the undesired regioisomer. When the aziridine was protected with an EDG, the strained 3-member ring was still electron rich and when introduced to an acyl chloride, acylation placed a formal positive charge on the 3-membered ring. While it does increase the buildup in positive charge at both carbons in the aziridine, this full positive charge directed the incoming nucleophile to the carbon, alpha to the ester with electronics being the driving factor over sterics, giving the desired α -chloro regioisomer.¹⁰⁰



Hyun-Joon, H.; Jang-min, S.; Kyung-Ho, K.; Young-Gil, A.; Oksoo, H; *Tetrahedron*, **1998**, *54*, 851-858
 Yongeun, K.; Hyun-Joon, H.; Hoseop, Y.; Baeck, K. L.; Won, K. L. *Tetrahedron* **2006**, *62*, 8844-8849

Figure III-XXXI: Methods of controlling regiochemical outcome of aziridines.

Synthetic redesign exchanging of the R-group on the aziridine nitrogen from an EWG, as the amide to an EDG like N-benzyl was done. Based on literature to an electron rich protected aziridine, once acylated with 1H-indole-2-carbonyl chloride, should force ring expansion towards accessing the desired intermediate below.¹⁰¹

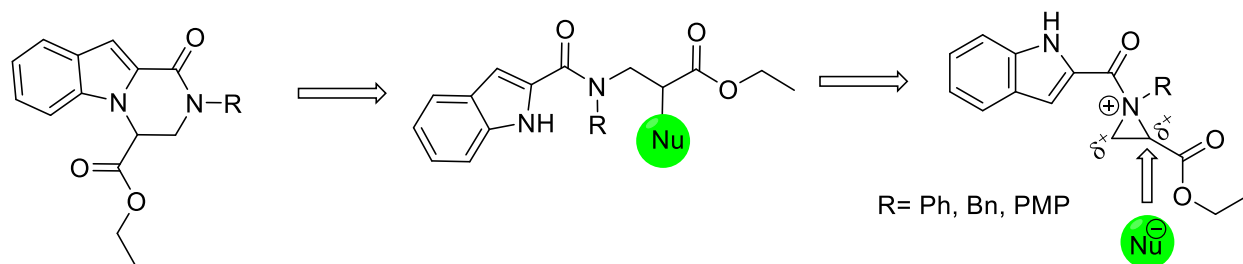


Figure III-XXXII: Modified approach to regio-controlled ring openings of aziridines.

With this understanding, the initial acyl chloride and lead aziridine compounds have been synthesized, to probe the overall ring opening and intermediate formation. By separating the aziridine formation and ring opening from the indole, any contribution by the amide carbonyl towards the formation of the undesired regioisomer was omitted. We proposed that the regiocontrolled expansion of aziridines through approach 4 or 5 would result in the α -chloro

intermediate. The resulting ring closure would give the 6, 5, 6 fused core with indole. This methodology would then be applied for the synthesis of a 5, 6 fused core with pyrrole to give Agesamides A and B and other synthetic analogs respectively.

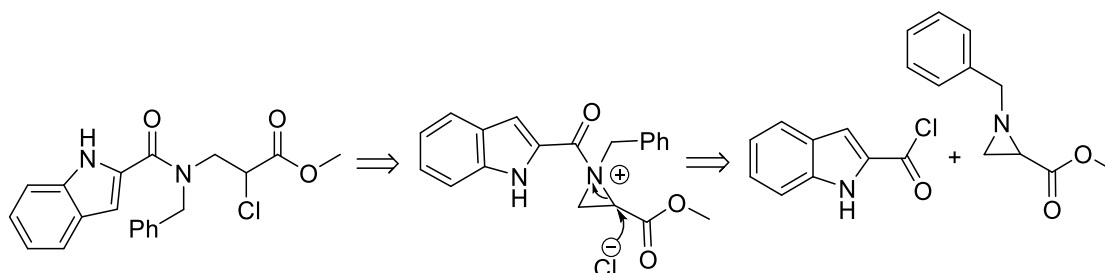
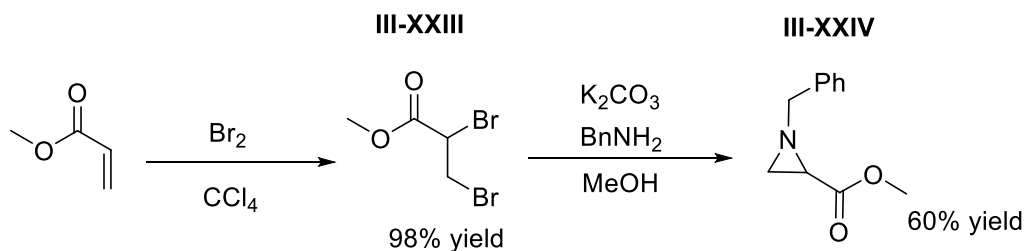


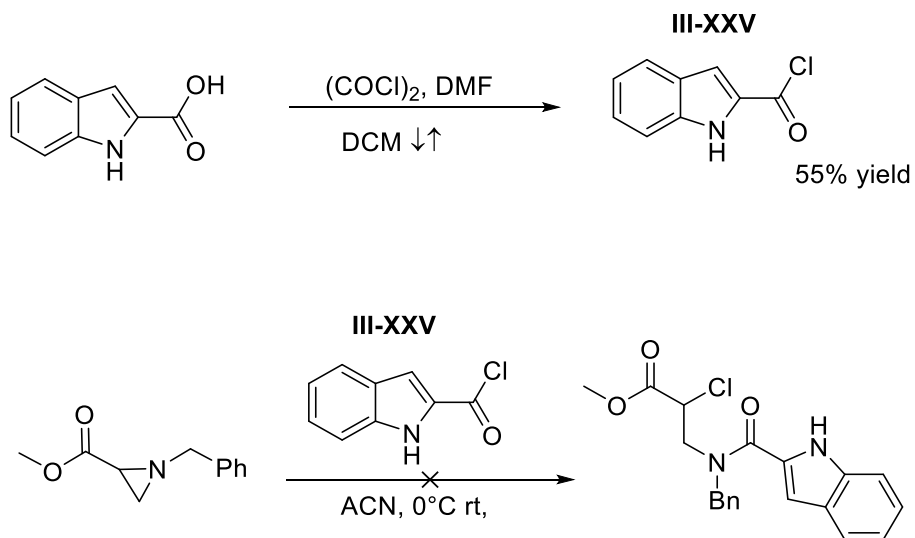
Figure III-XXXIII: Modified approach to regio-controlled ring openings of aziridines

Methyl 1-benzylaziridine-2-carboxylate was synthesized with the hypothesis that replacement of the EWG with an EDG would result in the expansion to desired regioisomer. EDG's increase the nucleophilicity of aziridine nitrogen and cause the overall 3-membered ring to be electron rich as opposed to electron poor with EWG installed on the nitrogen. This resulted in the aziridine acting as a nucleophile and when acylated in the presence of 1H-indole-2-carbonyl chloride was hypothesized to give the desired expansion product.¹⁰²

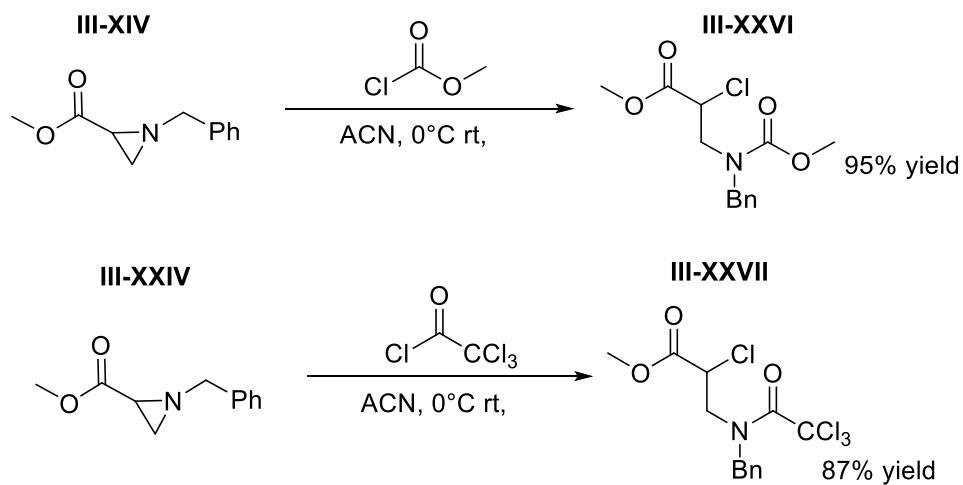


Scheme III-XV: Accessing derivative to test hypothesis for ring opening.

Scheme III-XV cont'd



Although the consumption of both starting materials occurred, the reaction did not proceed to the formation of the desired regioisomer. To understand where the reaction had failed, trial expansions of the aziridine were attempted to measure its nucleophilicity towards acylation and expansion.



Scheme III-XVI: Regiocontrolled ring opening of benzylated aziridines.

Addition of methyl chloroformate resulted in acylation and expansion to the desired regioisomer in excellent yields. Trichloroacetyl chloride addition to the aziridine resulted in full consumption of starting material to afford both regio isomers in a 13:1 ratio for the desired regioisomer. The minor formation of the undesired regioisomer was solely due to the difference in sterics of the acylated aziridine intermediate. The trichloroacylated intermediate was more sterically hindered and resulted in minor amounts of ring opening from the more accessible C₃ methylene. These expansions verified the nucleophilicity of the synthesized aziridine and confirmed the hypothesis that the desired regioisomer can be synthesized from aziridines bearing EDG groups. The results implicated that the reaction failure was due to 1H-indole-2-carbonyl chloride.

Approach 5 – Lewis acid ring opening of methyl 1-benzylaziridine-2-carboxylate

An installed protecting group, PMP-group or benzyl-group for example on the nitrogen, is electron rich enough promote aziridine ring opening under Lewis acidic conditions leading to the formation of the 3-amino-2-chloro-carboxylate ester. This intermediate can then be couple with 1H-indole-2-carbonyl chloride. With the protecting group still installed, the opportunity to close down through a 5-membered oxazoline is negated, allowing for closure to the 6-membered indole intermediate. This intermediate can then be used to access the desired indolo-Agesamide derivatives.

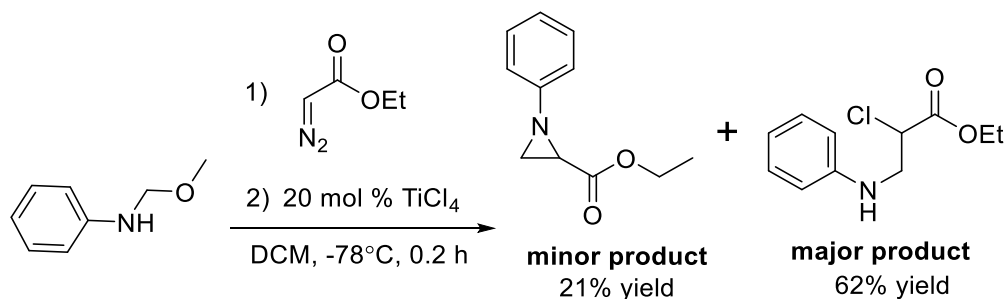
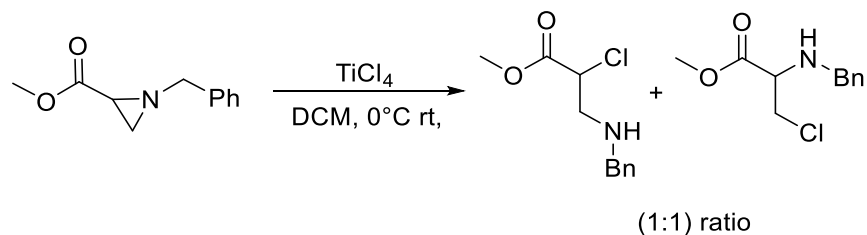


Figure III-XXXIV: Regioselective Lewis acid mediated ring opening



Scheme III-XVII: Results of Lewis acid ring opening of N-benzylated aziridines

Unfortunately, the expansion of N-benzylated aziridines resulted in a 1:1 ratio of both regioisomers when treated with TiCl_4 . Therefore other approaches to accessing the desired regiochemistry were pursued.

Approach 6 - N_1 and C_2 alkylation of pyrrole to α -chlorocarboxylates

The new route to access the desired scaffold was proposed from the α -chlorocarboxylates accessed from the ring opening reactions of aziridines in the presence of methyl chloroformate and trichloroacetyl chloride.

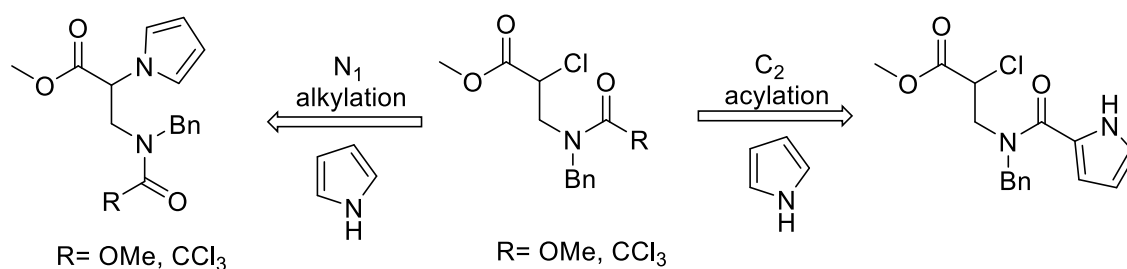


Figure III-XXXV: Alternative approach to accessing desired regiochemistry.

N_1 alkylation

Using the expanded intermediate, it was proposed that selective N_1 alkylation could be achieved under basic conditions. Deprotonation of pyrrole classically resulted with N-alkylation due to the

buildup of negative charge on the nitrogen of the pyrrole. Therefore deprotonation of pyrrole in the presence of the reactive intermediate was proposed to undergo N-alkylation.

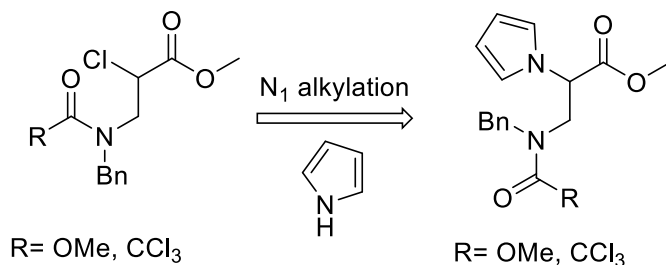
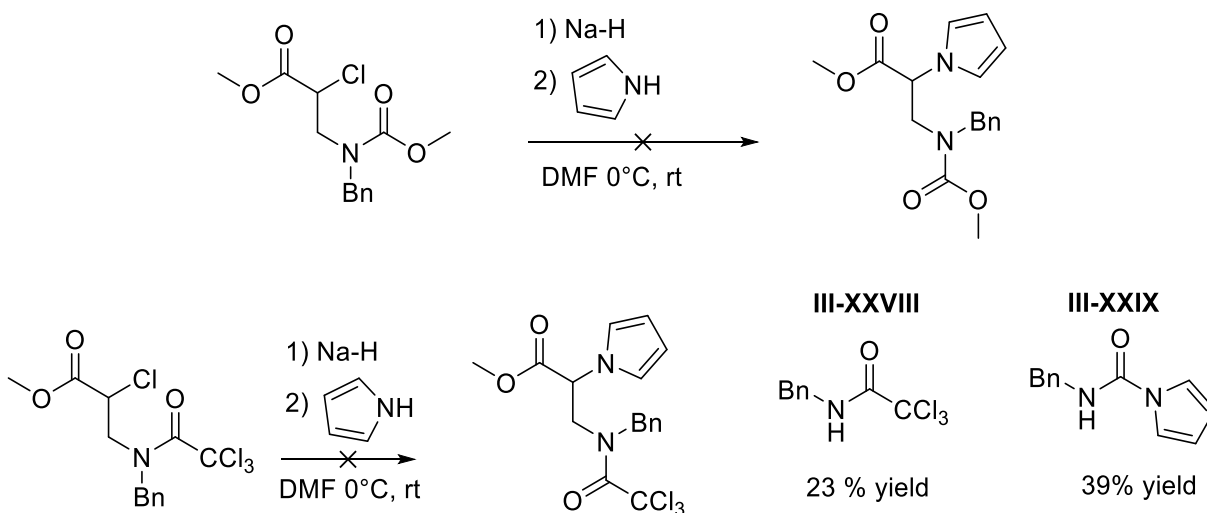


Figure III-XXXVI: Proposed pathway for N₁ alkylation.

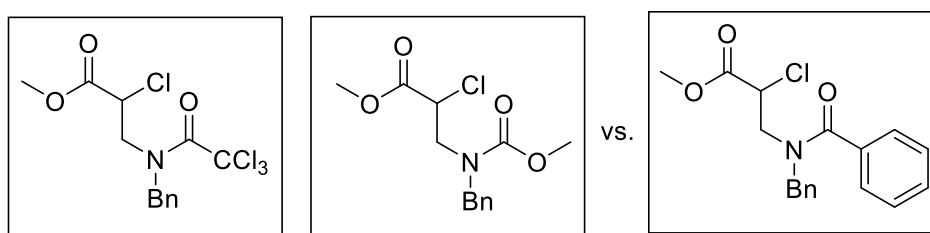


Scheme III-XVIII: Elimination products of proposed reaction.

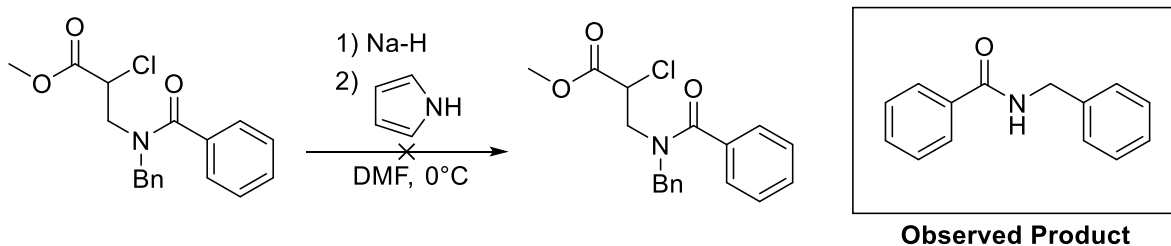
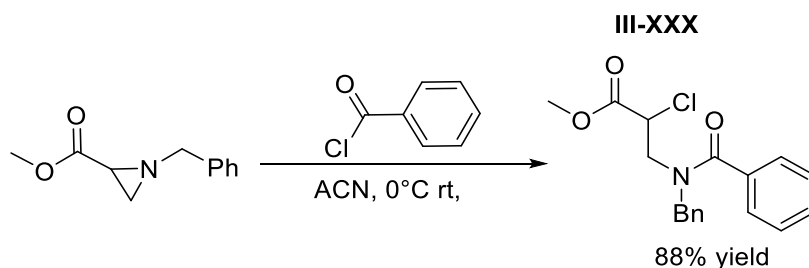
However, N₁ alkylation did not occur under basic conditions. Addition of the pyrrole to the carbamate under basic conditions resulted in complete decomposition. Addition of the pyrrole under basic conditions to the N-benzyl trichloroacetamide derivative resulted in elimination to form two side products, N-benzyl-2,2,2-trichloroacetamide and N-benzyl-1H-pyrrole-1-carboxamide. Identification of these side products suggested that the mechanism of action was the

elimination of the α -proton to give methyl 2-chloroacrylate, N-benzyl-2,2,2-trichloroacetamide and N-benzyl-1H-pyrrole-1-carboxamide respectively.

The observed elimination products of identified the functional group sensitivity to strongly basic conditions. To modify this acyl chlorides were used in aziridine expansions. The resulting amides are poorer leaving groups in comparison to their carbamate and trichloroamide counterparts. To this end methyl 3-(N-benzylbenzamido)-2-chloropropanoate was synthesized from the addition of benzoyl chloride.



Scheme III-XIX: Regioselective ring opening of N-benzyl aziridines by different electrophiles.



Scheme III-XX: Failed N_1 alkylation under basic conditions.

N₁ alkylation under basic conditions was attempted with methyl 3-(N-benzylbenzamido)-2-chloropropanoate. The E₂ elimination product was observed and identified that N₁ alkylation would not be possible under basic conditions.

C₂ acylation

Based on these findings, C₂ alkylation was explored next. Activation of the amide and carbamate under the conditions for the Bischler Napieralski reaction was proposed to acylate pyrrole at the C₂ position through the generation of the activated acylation reagent.

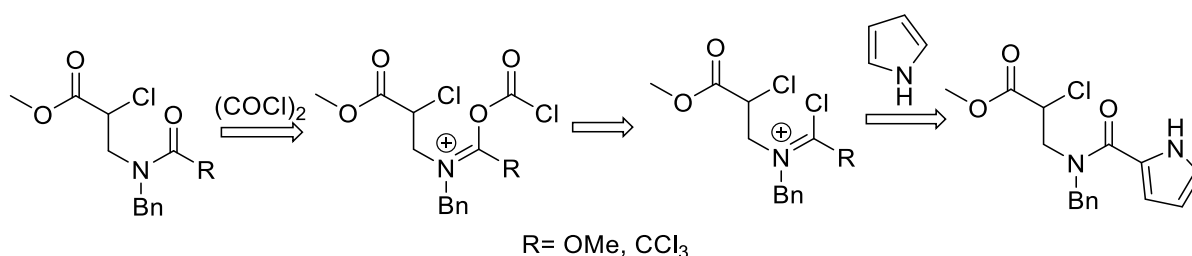
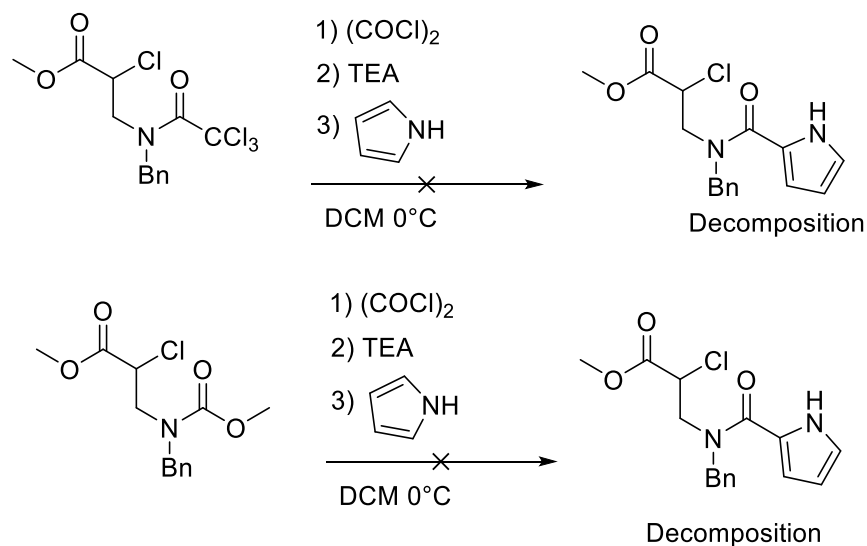
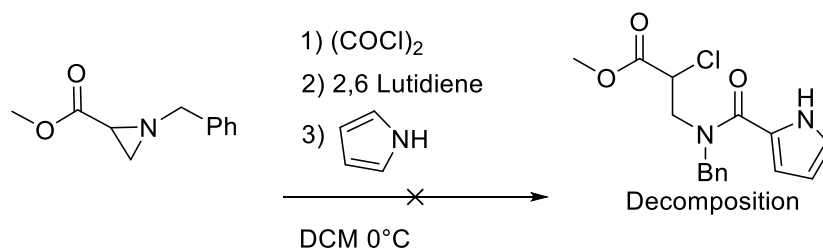


Figure III-XXXVII: Proposed pathway for C₂ alkylation of pyrrole.



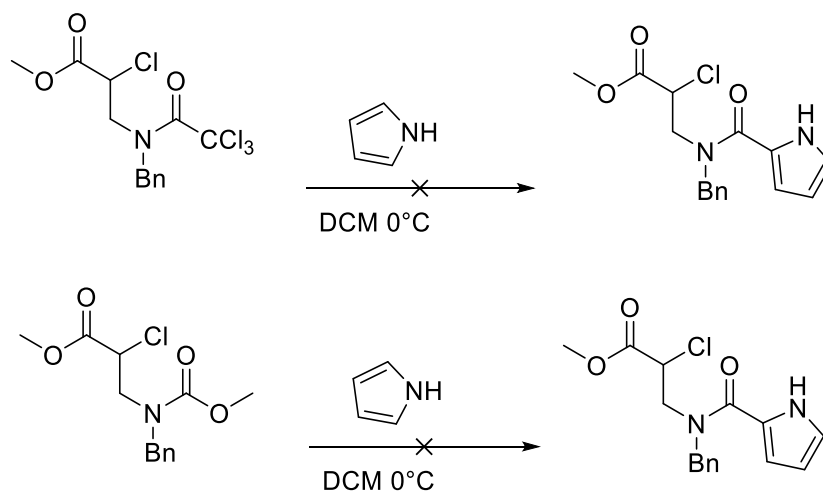
Scheme III-XXI: Failed C₂ alkylations of pyrrole.

Scheme III-XXI cont'd



Introduction of the pyrrole to the activated carbamate or the amide only resulted in decomposition. These initial results have highlighted the need for further exploration into milder methods of activating reagents to access the desired acylation. These results motivated the addition of just pyrrole to the carbamate and trichloroamide intermediates. It was speculated that pyrrole might undergo C_2 alkylation. Unfortunately pyrrole did not react with either intermediate and only starting material was observed.

Neutral conditions



Scheme III-XXII: Failed C_2 alkylations of pyrrole under neutral conditions.

Approach 7

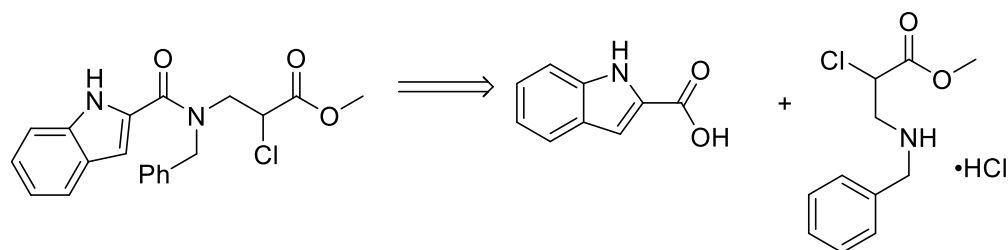
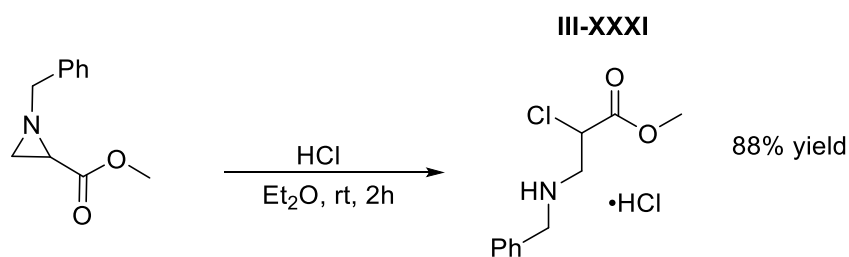


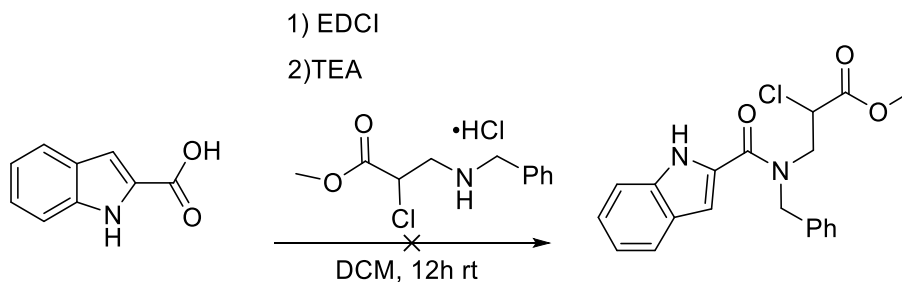
Figure III-XXXVIII: Proposed EDCI coupling to access desired regioisomer.

The experimental results of approach 6 identified that access to the desired intermediate for the 6, 5, 6 fused core may not be possible by N₁ or C₂ alkylation of pyrrole, due to the intermediate group's behavior under the reaction conditions. To circumvent this, it was proposed that milder methods of activation, ones without the use of strong acids and bases, could be used to access the desired intermediate through amide formation for the following ring closure. Carbodiimide coupling of carboxylic acids and amines result in amide formation under mild conditions and moderate to high yield. Because of this, it was proposed that the EDCI mediated coupling of indole-2-carboxylic acid to methyl 3-(benzylamino)-2-chloropropanoate HCl salt would access the intermediate.



Scheme III-XXIII: Regioselective ring opening of N-benzylated aziridines and failed coupling to indole-2-carboxylic acid.

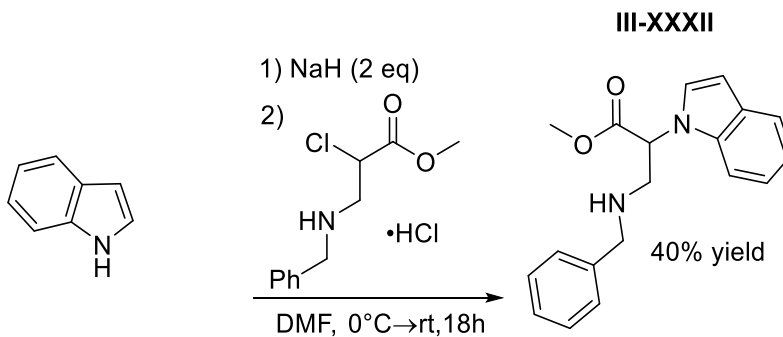
Scheme III-XXIII cont'd



EDCI mediated coupling failed to give the desired intermediate for ring closure and decomposition was observed. Accessing the HCl salt of methyl 3-(benzylamino)-2-chloropropanoate in high yields with the desired regiochemistry was identified another method of accessing the desired intermediate by combining aspects of the approach 6 with the intermediate of approach 7.

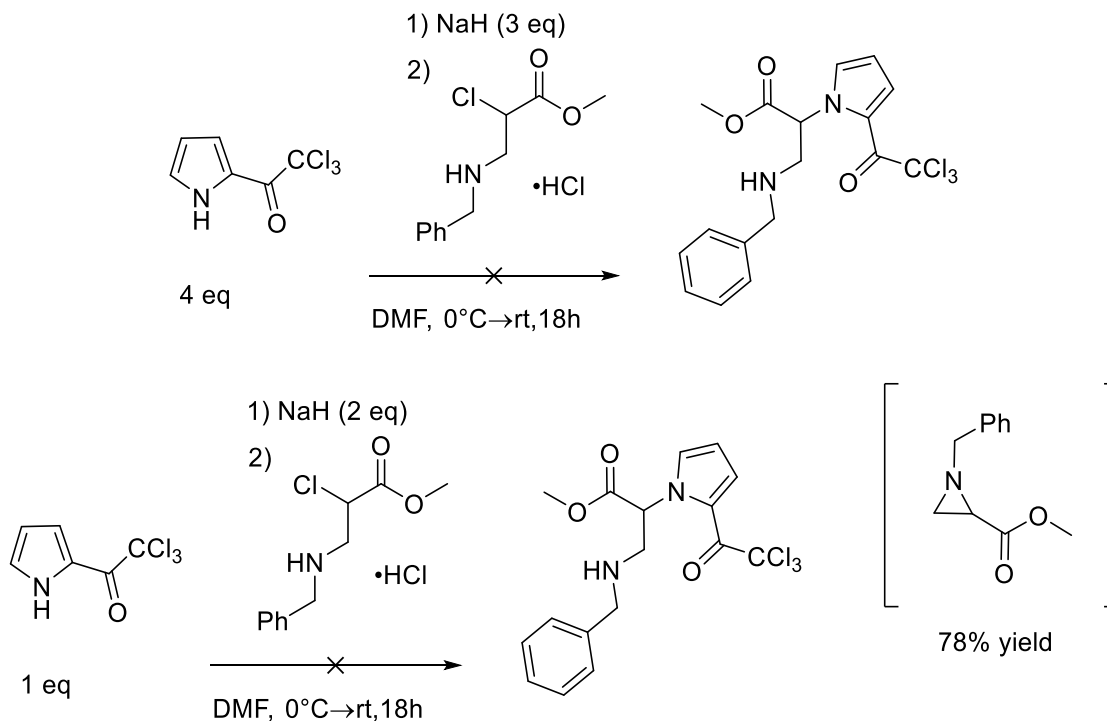
Approach 8

The functionalized amides and carbamates proved too labile for N₁ alkylation. The synthesis of methyl 3-(benzylamino)-2-chloropropanoate offered the opportunity to capitalize on the N-alkylation without the chance of elimination of the benzylated amine.



Scheme III-XXIV: N₁ alkylation of Indole under basic conditions.

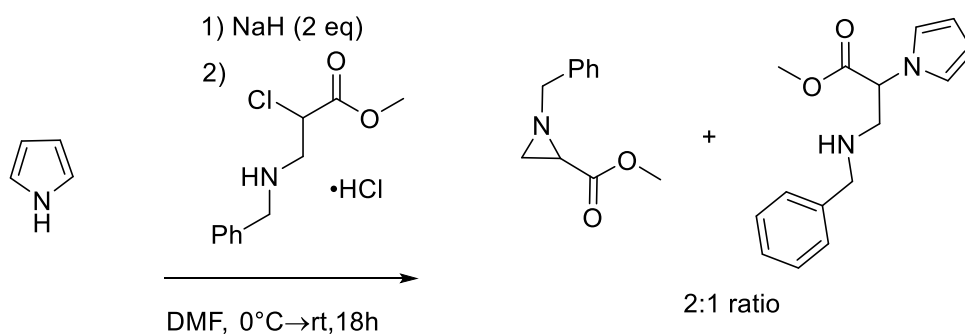
Isolation of the N-alkylated indole derivative confirmed the hypothesis that N-alkylation of the intermediate was possible. Based on that result, functionalized pyrroles were introduced under the same reaction conditions in an attempt to access the N-alkylated pyrrole intermediate.



Scheme III-XXV: Failed N₁ alkylations of 2-trichloroacetylpyrrole.

Exposure of the 2-trichloroacetylpyrrole to methyl 3-(benzylamino)-2-chloropropanoate under basic conditions did not result in product formation. Instead isolation of the methyl 1-benzylaziridine-2-carboxylate was observed in high yield. Based on this result it was concluded that the generated pyrrole anion, from deprotonation, was not nucleophilic enough to undergo alkylation. The decrease in nucleophilicity in comparison to indole was due to the presence of the trichloroacetyl group. This electron withdrawing group stabilized the generated anion, which made

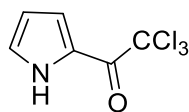
the molecule less nucleophilic. Therefore, intramolecular ring closure was the predominant reaction with the pyrrole acting as a base to quench the equivalent amount of acid generated by aziridine formation. Due to this result pyrrole was selected as the desired incoming nucleophile. The lack of a EWG would insure that the resulting negative charge from deprotonation of pyrrole would be more nucleophilic.



Scheme III-XXVI: Inseparable mix of products after N₁ alkylation of pyrrole under basic conditions.

Introduction of the pyrrole as the nucleophile resulted in N-alkylation of pyrrole only as the minor product in the presence of methyl 1-benzylaziridine-2-carboxylate, the major product. This reaction mixture could not be separated by column chromatography.

III-I



2,2,2-trichloro-1-(1H-pyrrol-2-yl)ethan-1-one:

Trichloroacetylchloride (23.166g, 127 mmol) was added to a flame dried flask with stir bar. 80 mL of anhydrous diethyl ether was added to the flask. The resulting solution was stirred vigorously while a solution of pyrrole (7.77 g, 16 mmol) in 60 mL in anhydrous diethyl ether was added dropwise by addition funnel over 1.5 h. The reaction was then stirred for an additional 4 h, before the reaction was quenched slowly with a solution of K_2CO_3 , (10.2 g, 73.8 mmol) in 10 mL of H_2O . The organic layers were separated, collected and dried over anhydrous Na_2SO_4 and stirred with activated charcoal for 10 minutes. The reaction was then filtered through celite to give an amber solution. This solution was concentrated in-vacuo and the addition of warm hexanes precipitated the product as grey crystals 66 % yield (16.3 g, 76.7 mmol).

Spectroscopy:

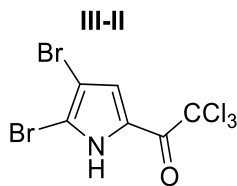
1H NMR (500 MHz, $CDCl_3$) δ 9.48 (s, 1H), 7.40 (ddd, $J = 3.9, 2.5, 1.2$ Hz, 1H), 7.18 (ddd, $J = 3.0, 2.5, 1.2$ Hz, 1H), 6.40 (dt, $J = 4.1, 2.5$ Hz, 1H).

^{13}C NMR (125 MHz, $CDCl_3$) δ 173.17, 127.03, 122.96, 121.12, 111.88, 94.90.

IR (FT-ATR) cm^{-1} : 3304, 3046, 1722, 1009

HRMS-ESI (m/z), calculated for $C_6H_5Cl_3NO$ ($M+H$) $^+$ 211.9437. Not stable to HRMS.

m.p.: 71.8-72.0°C



2,2,2-trichloro-1-(4,5-dibromo-1H-pyrrol-2-yl)ethan-1-one:

2,2,2-trichloro-1-(1H-pyrrol-2-yl)ethan-1-one (6.00 g, 28.24 mmol) was added to a flame dried round bottom flask and dissolved in 40 mL of concentrated Acetic acid. The resulting solution was stirred as a solution of Bromine (9.48 g, 59.31 mmol) in 80 mL of Acetic acid was added to the vessel, by addition funnel over 2.5 h. The solution's pH was adjusted to 6 by the addition of 300 mL of water. Grey-tan solids were precipitated, and collected by filtration to access the product 42% yield (8.8 g, 23.77 mmol)

Spectroscopy:

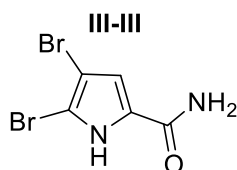
^1H NMR (500 MHz, CDCl_3) δ 9.69 (s, 1H), 7.36 (dd, $J = 3.0, 1.7$ Hz, 1H).

^{13}C NMR (125 MHz, CDCl_3) δ 171.84, 123.83, 122.91, 112.81, 102.40, 93.78.

IR (FT-ATR) cm^{-1} : 3295, 3003, 1713, 18961

HRMS-ESI (m/z), calculated for $\text{C}_6\text{H}_3\text{Br}_2\text{Cl}_3\text{NO}$ ($\text{M}+\text{H}$) $^+$ 367.7647. Not stable to HRMS.

m.p.: 135.5-136.2°C



4,5-dibromo-1H-pyrrole-2-carboxamide:

2,2,2-trichloro-1-(4,5-dibromo-1H-pyrrol-2-yl)ethan-1-one (2.0 g, 5.45 mmol) was added to a flame dried flask. Ammonium chloride was added as a solid (0.876 g, 16.38 mmol). Acetonitrile (15 ml) was then added to the vessel by syringe followed by 0.5 mL of H₂O. The resulting solution was vigorously stirred while Triethylamine was added by syringe (4.42 g, 43.66 mmol). The reaction was stirred at room temperature for 6 h. Evaporation of solvent gave the crude product which was extracted into chloroform, dried over anhydrous Na₂SO₄ and reduced under vacuum to give the product as a brown solid 68% yield (1.00 g, 3.71 mmol).

Spectroscopy:

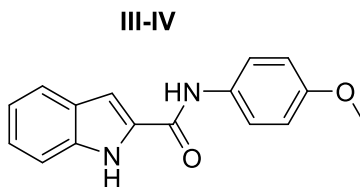
¹H NMR (500 MHz, DMSO-*d*₆) δ 12.63 (s, 1H), 7.59 (s, 1H), 7.17 (s, 1H), 6.90 (d, *J* = 2.6 Hz, 1H).

¹³C NMR (125 MHz, DMSO) δ 160.86, 128.64, 113.56, 105.09, 98.18.

IR (FT-ATR) cm⁻¹: 3312, 3297, 3254, 3011, 1687, 1015, 983.

HRMS-ESI (*m/z*), calculated for C₅H₅Br₂N₂O (M+H)⁺ 268.8769. Found 268.8745.

m.p: 300°C - Decomposition



N-(4-methoxyphenyl)-1H-indole-2-carboxamide:

Indole-2-carboxylic acid (1.98 g, 12.31 mmol) was added to a flame dried round bottom flask.

DCM was added to the flask by syringe and the resulting suspension was stirred as triethylamine

(1.25 g, 12.31 mmol) and DMAP (0.453 g, 3.69 mmol) was added. The solution was stirred at room temperature for 5 minutes before cooling to 0°C by ice bath. EDCI hydrochloride salt (3.07 g, 16 mmol) was added and the reaction was stirred for 12 h. The product precipitated out of solution and was filtered and titrated with Chloroform to give a pale solid 64% yield (2.1 g, 7.89 mmol).

Spectroscopy:

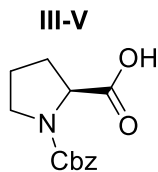
¹H NMR (500 MHz, DMSO-*d*₆) δ 11.70 (d, *J* = 2.1 Hz, 1H), 10.10 (s, 1H), 7.76 – 7.59 (m, 3H), 7.44 (dd, *J* = 8.2, 1.0 Hz, 1H), 7.38 – 7.32 (m, 1H), 7.19 (ddd, *J* = 8.2, 6.9, 1.2 Hz, 1H), 7.04 (ddd, *J* = 8.0, 6.9, 1.0 Hz, 1H), 6.99 – 6.85 (m, 2H), 3.73 (s, 3H).

¹³C NMR (125 MHz, DMSO) δ 159.83, 155.90, 137.14, 132.40, 132.09, 127.50, 124.03, 122.19, 122.08, 120.28, 114.28, 112.79, 103.85, 55.62.

IR (FT-ATR) cm⁻¹: 3284, 3265, 3012, 2986, 1693, 1126, 1013, 1005.

HRMS-ESI (m/z), calculated for C₁₆H₁₄N₂O₂Na (M+Na)⁺ 289.0953. Found 289.0961.

m.p: 135.6-136.2°C



((benzyloxy)carbonyl)-L-proline:

L-Proline (2.30 g, 20 mmol) was added to a flame dried flask. 400 mL of deionized H₂O was added to the flask followed by NaHCO₃ (1.682 g, 20 mmol). The solution benzyl chloroformate (3.41 g, 20 mmol) in THF (20 mL) was added to the flask dropwise by addition funnel. The solution was

stirred for 12 h at room temperature. The reaction was concentrated under vacuum and extracted into chloroform. The solution was washed with brine and then dried over anhydrous Na₂SO₄. The organic solution was reduced in-vacuo to get the product as an oil 95% yield (4.74 g, 19 mmol)

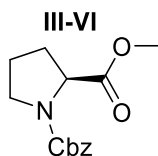
Spectroscopy:

¹H NMR (500 MHz, DMSO-*d*₆) δ 12.59 (s, 1H), 7.50 – 7.13 (m, 5H), 5.18 – 4.90 (m, 2H), 4.20 (ddd, *J* = 37.0, 9.0, 3.6 Hz, 1H), 3.40 (dddd, *J* = 17.7, 15.5, 7.4, 3.3 Hz, 2H), 2.29 – 2.06 (m, 1H), 2.04 – 1.70 (m, 3H).

¹³C NMR (125 MHz, DMSO) δ 174.40, 174.09, 154.39, 154.08, 142.97, 137.40, 137.38, 129.29, 129.09, 128.94, 128.84, 128.77, 128.72, 128.47, 128.24, 128.04, 127.91, 127.45, 127.05, 126.84, 79.64, 66.34, 66.33, 63.32, 59.33, 58.78, 47.18, 46.64, 46.58, 30.88, 29.84, 24.36, 23.45

IR (FT-ATR) cm⁻¹: 3052, 3002, 2976, 1752, 1703, 1105, 1023, 1006.

HRMS-ESI (*m/z*), calculated for C₁₃H₁₆NO₄ (M+H)⁺ 272.0899. Found 272.0893.



1-benzyl 2-methyl (S)-pyrrolidine-1,2-dicarboxylate:

((benzyloxy)carbonyl)-L-proline (4.75 g, 19.06 mmol) was added to a flame dried 250 mL round bottom flask, and was dissolved in anhydrous methanol (60 mL). 0.5 mL of DMF was added to the reaction and the reaction vessel was cooled the 0°C by ice bath. The solution was stirred vigorously as SOCl₂ (3.4g, 28.6 mmol) was added dropwise to the reaction vessel over 10 minutes. The reaction was brought to room temperature and stirred for 12 h. The reaction was concentrated

and extracted into CHCl₃, washed with a 10% Na₂CO₃ solution and dried over Na₂SO₄. The solution was concentrated to give the product as a clear oil 88% yield (4.39 g, 16.67 mmol)

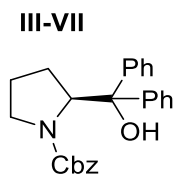
Spectroscopy:

¹H NMR (500 MHz, CDCl₃) δ 7.52 – 7.07 (m, 5H), 5.32 – 4.84 (m, 2H), 4.38 (ddd, *J* = 27.6, 8.6, 3.7 Hz, 1H), 3.75 (s, 1H), 3.68 – 3.38 (m, 3H), 2.38 – 2.12 (m, 1H), 2.12 – 1.78 (m, 3H).

¹³C NMR (125 MHz, CDCl₃) δ 173.29, 173.14, 154.87, 154.28, 136.69, 136.60, 128.71, 128.65, 128.58, 128.55, 128.45, 128.39, 127.96, 127.91, 127.89, 127.78, 127.63, 126.97, 67.02, 66.95, 65.37, 59.16, 58.84, 52.27, 52.07, 46.92, 46.43, 30.93, 29.92, 24.33, 23.55.

IR (FT-ATR) cm⁻¹: 3024, 2994, 1741, 1699, 1568, 1474, 1032, 1003, 965.

HRMS-ESI (*m/z*), calculated for C₁₄H₁₈NO₄ (M+H)⁺ 264.1236. Found 264.1230.



benzyl (S)-2-(hydroxydiphenylmethyl)pyrrolidine-1-carboxylate:

1-benzyl 2-methyl (S)-pyrrolidine-1,2-dicarboxylate (4.0 g, 16.05 mmol), was added to a flame dried round bottom flask and dissolved in anhydrous THF. The reaction vessel was cooled to 0°C by ice bath before the addition of 1M PhMgBr solution (44.13 mL, 44.13 mmol). The reaction was stirred at 0°C until starting material was consumed and then reaction was quenched with the addition of 5 mL of saturated NH₄Cl solution. The reaction was reduced and extracted into CHCl₃ before washing with brine and drying over Na₂SO₄. The solvent was concentrated and

purified by column chromatography (1:9 EtOAc: Hexanes) to yield the product as a clear oil
82% yield (5.1 g, 13.16 mmol).

Spectroscopy:

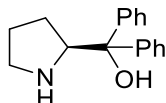
^1H NMR (500 MHz, CDCl_3) δ 7.56 – 7.14 (m, 15H), 6.04 (s, 1H), 5.21 (d, J = 12.2 Hz, 1H), 5.15 – 5.04 (m, 1H), 4.98 (dd, J = 8.9, 3.7 Hz, 1H), 3.65 – 3.33 (m, 1H), 3.02 (s, 2H), 2.12 (dq, J = 13.4, 8.8 Hz, 1H), 2.03 – 1.85 (m, 1H).

^{13}C NMR (125 MHz, CDCl_3) δ 146.26, 143.53, 136.50, 128.52, 128.15, 128.07, 127.91, 127.79, 127.62, 127.49, 127.23, 127.19, 81.64, 67.49, 66.15, 47.85, 29.70, 22.97.

IR (FT-ATR) cm^{-1} : 3389, 3003, 2954, 1698, 1574, 1056, 1012, 983.

HRMS-ESI (m/z), calculated for $\text{C}_{25}\text{H}_{26}\text{NO}_3$ ($\text{M}+\text{H}$) $^+$ 388.1913. Found 388.1935.

III-VIII



(S)-diphenyl(pyrrolidin-2-yl)methanol:

benzyl (S)-2-(hydroxydiphenylmethyl)pyrrolidine-1-carboxylate (1.0 g, 2.58 mmol) was added to a 100 mL flame dried round bottom flask. 20 mL of anhydrous MeOH was added to the flask. Pd^0C was added to the reaction vessel and the reaction was placed under a hydrogen atmosphere. The reaction was stirred until all starting material was consumed. The solution was filtered to remove the Pd^0C and the filtrate was reduced to give the product as a fine white powder 87% yield (0.568 g, 2.24 mmol).

Spectroscopy:

^1H NMR (500 MHz, DMSO- d_6) δ 9.45 (s, 1H), 8.31 (d, $J = 12.7$ Hz, 1H), 7.68 – 7.59 (m, 2H), 7.53 – 7.47 (m, 2H), 7.31 (dt, $J = 15.0, 7.6$ Hz, 4H), 7.20 (dt, $J = 17.7, 7.3$ Hz, 2H), 6.55 (s, 1H), 4.87 (s, 1H), 3.11 (t, $J = 6.0$ Hz, 2H), 1.87 (tt, $J = 8.6, 5.1$ Hz, 2H), 1.85 – 1.71 (m, 1H).

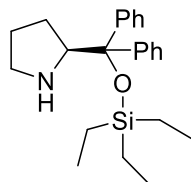
^{13}C NMR (125 MHz, DMSO) δ 145.48, 145.04, 128.82, 128.65, 127.62, 127.39, 126.25, 125.85, 77.52, 65.46, 47.13, 26.42, 24.49.

IR (FT-ATR) cm^{-1} : 3375, 3243, 3020, 2914, 1098, 1020, 997.

HRMS-ESI (m/z), calculated for $\text{C}_{17}\text{H}_{20}\text{NO}$ ($\text{M}+\text{H}$) $^+$ 254.1545. Found 254.1545.

m.p: 77.2-78.3°C

III-IX



(S)-2-(diphenyl((triethylsilyl)oxy)methyl)pyrrolidine:

(S)-diphenyl(pyrrolidin-2-yl)methanol (0.600 g, 2.37 mmol) was added to a 100 mL flame dried round bottom flask. 20 mL of anhydrous DCM was added to the flask and the reaction was cooled to 0°C and 2,6 lutidine was added by syringe (1.77 g, 16.58 mmol). After stirring for 5 minutes TESOTf (3.13 g, 11.84 mmol) was added and the reaction was stirred at room temperature for 8 h. The reaction was concentrated and purified by column chromatography (2.5:7.5 EtOAc: Hexane) to yield the product as an oil 57% yield (0.496 g, 1.35 mmol).

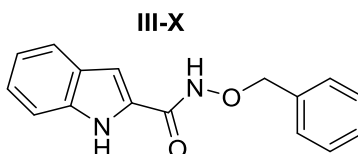
Spectroscopy:

^1H NMR (500 MHz, CDCl_3) δ 7.53 – 7.44 (m, 2H), 7.40 – 7.33 (m, 2H), 7.32 – 7.19 (m, 6H), 4.02 (t, $J = 7.3$ Hz, 1H), 2.83 (ddd, $J = 10.0, 7.5, 6.2$ Hz, 1H), 2.71 (ddd, $J = 10.1, 7.4, 5.6$ Hz, 1H), 1.76 (dd, $J = 8.5, 4.3$ Hz, 1H), 1.63 – 1.48 (m, 3H), 1.29 – 1.19 (m, 1H), 0.86 (t, $J = 7.9$ Hz, 9H), 0.36 (q, $J = 8.0$ Hz, 6H).

^{13}C NMR (125 MHz, CDCl_3) δ 146.65, 145.50, 128.82, 128.01, 127.51, 127.29, 126.92, 126.87, 82.87, 65.62, 47.24, 27.70, 25.11, 7.26, 6.49, 6.38.

IR (FT-ATR) cm^{-1} : 3241, 3066, 2984, 1592, 1128, 1053, 1039.

HRMS-ESI (m/z), calculated for $\text{C}_{23}\text{H}_{33}\text{NOSi}$ ($\text{M}+\text{H}$) $^+$ 368.2410. Found 368.2410.



N-(benzyloxy)-1H-indole-2-carboxamide:

Indole-2-carboxylic acid (2.00 g, 12.41 mmol) was added to a 100 mL flame dried flask. 20 mL of anhydrous DCM was added to the flask and the suspension was stirred while triethylamine (1.26 g, 12.41 mmol) was added to the flask. Benzyloxylamine HCl salt was added (1.98 g, 12.41 mmol). The reaction stirred for 5 minutes before cooling to 0°C by ice bath and the EDCI hydrochloride salt (2.38 g, 12.41 mmol) was added to the reaction. The reaction was warmed to room temperature and stirred for 10 h. The reaction was then washed with (2 X 15 mL) saturated NaCl solution and dried over anhydrous Na_2SO_4 . The organic layers were collected, concentrated to a crude solid and purified by column chromatography (3:7 Acetone:Hexanes) to give the product 68% yield (2.25g, 8.44 mmol).

Spectroscopy:

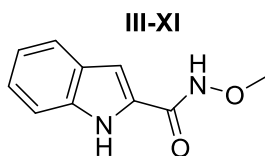
^1H NMR (500 MHz, DMSO- d_6) δ 11.80 (s, 1H), 11.69 (d, $J = 2.1$ Hz, 1H), 7.59 (dd, $J = 8.1, 1.1$ Hz, 1H), 7.49 – 7.31 (m, 6H), 7.17 (ddd, $J = 8.2, 6.9, 1.2$ Hz, 1H), 7.06 – 6.97 (m, 2H), 4.95 (s, 2H).

^{13}C NMR (125 MHz, DMSO) δ 160.18, 136.95, 136.33, 129.37, 129.20, 128.79, 127.34, 123.98, 122.04, 120.33, 112.74, 103.10, 77.79, 40.44, 40.27, 40.10, 39.94, 39.77, 39.60, 39.44.

IR (FT-ATR) cm^{-1} : 3265, 3228, 3017, 2964, 1675, 1564, 1469, 1105, 1058, 1022

HRMS-ESI (m/z), calculated for $\text{C}_{16}\text{H}_{15}\text{N}_2\text{O}_2$ ($\text{M}+\text{H}$) $^+$ 267.1134. Found 267.1141.

m.p: 156.9-160.4°C

**N-methoxy-1H-indole-2-carboxamide:**

Indole-2-carboxylic acid (2.00 g, 12.41 mmol) was added to a 100 mL flame dried flask. 20 mL of anhydrous DCM was added to the flask and the suspension was stirred while triethylamine (1.26 g, 12.41 mmol) was added to the flask. Methoxylamine HCl was added (1.03 g, 12.41 mmol). The reaction stirred for 5 minutes before cooling to 0°C by ice bath and the EDCI hydrochloride salt (2.38 g, 12.41 mmol) was added to the reaction. The reaction was warmed to room temperature and stirred for 10 h. The reaction was then washed with (2 X 15 mL) saturated NaCl solution and dried over anhydrous Na_2SO_4 . The organic layers were collected, concentrated to a crude solid and purified by column chromatography (3:7 Acetone:Hexanes) to give the product in 73% yield (1.72 g, 9.06 mmol)

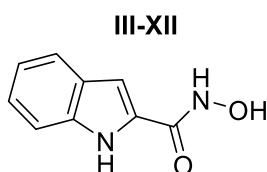
Spectroscopy:

^1H NMR (500 MHz, CDCl_3) δ 9.38 (s, 1H), 8.95 (s, 1H), 7.80 – 7.53 (m, 1H), 7.53 – 7.40 (m, 1H), 7.32 (ddd, $J = 8.2, 7.0, 1.1$ Hz, 1H), 7.17 (ddd, $J = 8.0, 7.0, 1.0$ Hz, 1H), 6.98 (s, 1H), 3.94 (s, 3H).

^{13}C NMR (125 MHz, CDCl_3) δ 136.38, 127.50, 127.14, 125.13, 122.24, 120.93, 111.98, 65.09.

IR (FT-ATR) cm^{-1} : 3254, 3208, 3002, 2987, 1695, 1564, 1467, 1112, 1069, 1045.

HRMS-ESI (m/z), calculated for $\text{C}_{10}\text{H}_{11}\text{N}_2\text{O}_2$ ($\text{M}+\text{H}$) $^+$ 191.0821. Found 191.0806.

**N-hydroxy-1H-indole-2-carboxamide:**

Indole-2-carboxylic acid (2.00 g, 12.41 mmol) was added to a 100 mL flame dried flask. 20 mL of anhydrous DCM was added to the flask and the suspension was stirred while triethylamine (1.26 g, 12.41 mmol) was added to the flask. Hydroxylamine HCl was added (0.862 g, 12.41 mmol). The reaction stirred for 5 minutes before cooling to 0°C by ice bath and the DCC (2.56 g, 12.41 mmol) was added to the reaction. The reaction was warmed to room temperature and stirred for 10 h. The reaction was then washed with (2 X 15 mL) saturated NaCl solution and dried over anhydrous Na_2SO_4 . The organic layers were collected, concentrated to a crude solid and purified by column chromatography (3:7 Acetone:Hexanes) to give the product in 56% yield (1.22 g, 6.95 mmol)

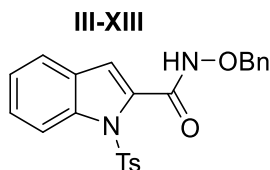
Spectroscopy:

^1H NMR (500 MHz, $\text{DMSO}-d_6$) δ 11.61 (s, 1H), 11.22 (s, 1H), 9.10 (s, 1H), 7.57 (d, $J = 8.0$ Hz, 1H), 7.39 (d, $J = 8.2$ Hz, 1H), 7.14 (q, $J = 6.3, 5.1$ Hz, 1H), 7.05 – 6.84 (m, 2H).

^{13}C NMR (125 MHz, DMSO) δ 160.06, 136.72, 129.95, 127.48, 123.58, 121.83, 120.17, 112.65, 102.04.

IR (FT-ATR) cm^{-1} : 3392, 3267, 3241, 3025, 1695, 1038, 1026.

HRMS-ESI (m/z), calculated for $\text{C}_9\text{H}_9\text{N}_2\text{O}_2$ ($\text{M}+\text{H}$) $^+$ 177.0664. Found 177.0710



N-(benzyloxy)-1-tosyl-1H-indole-2-carboxamide:

N-(benzyloxy)-1H-indole-2-carboxamide (1.5 g, 5.633 mol), was added to a flame dried 100 mL flask. 50 mL of anhydrous DCM was added to the flask by syringe. Triethylamine (0.684 g, 6.67 mmol) was added by syringe and the reaction was cooled to 0°C by ice bath before the addition of TsCl (1.127, 5.91 mmol). The reaction warmed to room temp and was stirred for 8 h. The reaction was washed with 2 X 20 mL saturated NaCl solution, the organic layers were collected and dried over anhydrous Na_2SO_4 . The solution was concentrated in-vacuo and purified by column chromatography (2:8 Acetone: Hexanes) to give the product as a purple solid 68% yield (1.61 g, 3.83 mmol)

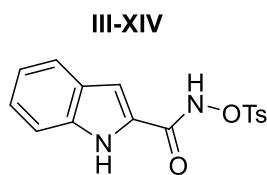
Spectroscopy:

^1H NMR (500 MHz, $\text{DMSO}-d_6$) δ 11.60 (d, $J = 2.3$ Hz, 1H), 7.89 – 7.71 (m, 2H), 7.54 (dd, $J = 7.9, 1.1$ Hz, 1H), 7.41 – 7.28 (m, 8H), 7.19 (ddd, $J = 8.3, 7.0, 1.2$ Hz, 1H), 7.09 – 6.97 (m, 1H), 6.64 (dd, $J = 2.2, 0.9$ Hz, 1H), 5.12 (s, 2H), 2.38 (s, 3H).

^{13}C NMR (125 MHz, DMSO) δ 146.33, 140.16, 138.32, 136.54, 133.16, 130.32, 128.80, 128.76, 128.62, 128.51, 127.20, 126.92, 124.60, 121.66, 120.44, 112.43, 106.49, 77.30, 21.68.

IR (FT-ATR) cm^{-1} : 3273, 3214, 3002, 2974, 1678, 1596, 1435, 1123, 1077, 1021.

HRMS-ESI (m/z), calculated for $\text{C}_{23}\text{H}_{21}\text{N}_2\text{O}_4\text{S}$ ($\text{M}+\text{H}$)⁺ 421.1222. Found 421.1222.



N-(tosyloxy)-1H-indole-2-carboxamide:

Indole-2-carboxylic acid (0.430 g, 2.67 mmol) was added to a 50 mL flame dried round bottom flask. 40 mL of anhydrous DCM was added to the reaction vessel and the suspension was stirred while DMAP (0.326 g, 2.67 mmol) was added by syringe. The reaction became homogeneous and O-tosylhydroxylamine was then added to the vessel (0.500 g, 2.67 mmol). The reaction was stirred at room temp for 10 minutes and then cooled to 0°C by ice bath. EDCI HCl salt was then added to the reaction vessel (0.512 g, 2.67 mmol) and the reaction stirred for 12 h. The solution was washed with saturated NH_4Cl solution (2 x 30 mL). The organic layers were collected and dried over anhydrous Na_2SO_4 and reduced in vacuo to give the crude product that was purified by column chromatography (2:8 Acetone:Hexanes) as a pale yellow solid 36% yield (0.320 g, 0.969 mmol).

Spectroscopy:

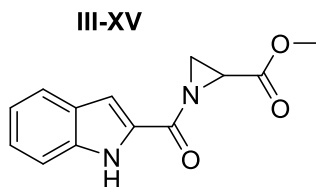
^1H NMR (500 MHz, $\text{DMSO}-d_6$) δ 12.29 (d, $J = 2.0$ Hz, 2H), 7.74 (dd, $J = 8.1, 1.1$ Hz, 2H), 7.59 – 7.44 (m, 3H), 7.36 (ddd, $J = 8.2, 6.9, 1.1$ Hz, 2H), 7.14 (ddd, $J = 8.0, 7.0, 1.0$ Hz, 2H), 2.48 (s, 3H).

^{13}C NMR (125 MHz, DMSO) δ 157.40, 139.09, 127.08, 126.67, 125.74, 123.21, 121.30, 113.30, 112.36, 40.44.

IR (FT-ATR) cm^{-1} : 3233, 3212, 3077, 2989, 1690, 1571, 1483, 1065, 1021.

HRMS-ESI (m/z), calculated for $\text{C}_{16}\text{H}_{15}\text{N}_2\text{O}_4\text{S}$ ($\text{M}+\text{H}$)⁺ 331.0753. Found 331.0764.

m.p.: 152.3-153.6°C



methyl 1-(1H-indole-2-carbonyl)aziridine-2-carboxylate:

Indole-2-carboxylic acid (1.77 g, 11 mmol) was added to a 100 mL flame dried round bottom flask. 40 mL of anhydrous DCM was added to the reaction vessel and the suspension was stirred while Triethylamine (1.12 g, 11 mmol) was added by syringe. The reaction became homogeneous and methyl aziridine-2-carboxylate was then added to the vessel by syringe (1.12g, 11 mmol) The reaction was stirred at room temp for 10 minutes and then cooled to 0°C by ice bath. EDCI HCl salt was then added to the reaction vessel (2.11 g, 11 mmol) and the reaction stirred for 12 h. The solution was washed with saturated NH_4Cl solution (2 x 30 mL). The organic layers were collected and dried over anhydrous Na_2SO_4 and reduced in vacuo to give the crude product that was purified by column chromatography (2:8 Acetone:Hexanes) as a pale orange solid 66% yield (1.77 g, 7.238 mmol)

Spectroscopy:

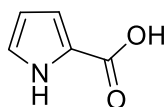
^1H NMR (500 MHz, $\text{DMSO}-d_6$) δ 11.91 – 11.78 (m, 1H), 7.67 (dd, $J = 8.1, 1.1$ Hz, 1H), 7.43 (dq, $J = 8.5, 1.0$ Hz, 1H), 7.25 (ddd, $J = 8.2, 6.9, 1.2$ Hz, 1H), 7.18 (dd, $J = 2.2, 1.0$ Hz, 1H), 7.07 (ddd, $J = 7.9, 6.9, 1.0$ Hz, 1H), 3.68 (s, 3H), 3.50 (dd, $J = 5.7, 3.1$ Hz, 1H), 2.83 (dd, $J = 5.8, 1.5$ Hz, 1H), 2.72 (dd, $J = 3.2, 1.5$ Hz, 1H).

^{13}C NMR (125 MHz, DMSO) δ 170.56, 169.03, 137.76, 130.40, 127.25, 125.30, 122.67, 120.71, 113.02, 107.46, 52.91, 35.25, 31.69.

IR (FT-ATR) cm^{-1} : 3301, 3054, 2978, 1738, 1699, 1126, 1059, 1032.

HRMS-ESI (m/z), calculated for $\text{C}_{13}\text{H}_{13}\text{N}_2\text{O}_3$ (M+H) $^+$ 245.0923. Found 245.0926.

III-XVI



1H-pyrrole-2-carboxylic acid:

2,2,2-trichloro-1-(1H-pyrrol-2-yl)ethan-1-one (4.00 g, 23.53 mmol) was added to a 100 mL round bottom flask. 40 mL of DI water was added to the reaction vessel followed by KOH (1.45 g, 25.88 mmol). The suspension was refluxed for 3 h after which the reaction pH was adjusted to pH = 2. Upon pH adjustment, the product precipitated out of the solution and was dried to yield the product as a red solid 56% yield (1.46 g, 13.14 mmol).

Spectroscopy:

^1H NMR (500 MHz, DMSO- d_6) δ 12.18 (s, 1H), 11.69 (s, 1H), 6.93 (td, $J = 2.7, 1.5$ Hz, 1H), 6.70 (ddd, $J = 3.9, 2.5, 1.5$ Hz, 1H), 6.11 (dt, $J = 3.6, 2.4$ Hz, 1H).

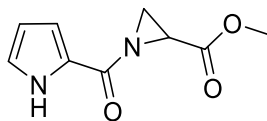
^{13}C NMR (125 MHz, DMSO) δ 162.30, 123.83, 123.31, 115.09, 109.71.

IR (FT-ATR) cm^{-1} : 3284, 3160, 3021, 2983, 1756, 1136, 1047.

HRMS-ESI (m/z), calculated for $\text{C}_5\text{H}_6\text{NO}_2$ (M+H) $^+$ 112.0399. Found 112.0412

m.p.: 202.7-203.4°C

III-XVII



methyl 1-(1H-pyrrole-2-carbonyl)aziridine-2-carboxylate:

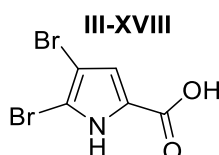
1H-pyrrole-2-carboxylic acid (1.10 g, 10 mmol) was added to a 100 mL flame dried round bottom flask. 40 mL of anhydrous DCM was added to the reaction vessel and the suspension was stirred while Triethylamine (1.164 g, 15.0 mmol) was added by syringe. The reaction became homogeneous and methyl aziridine-2-carboxylate was then added to the vessel by syringe (1.112 g, 11.0 mmol) The reaction was stirred at room temp for 10 minutes and then cooled to 0°C by ice bath. EDCI HCl salt was then added to the reaction vessel (2.88 g, 15 mmol) and the reaction stirred for 12 h. The solution was washed with saturated NH₄Cl solution (2 x 30 mL). The organic layers were collected and dried over anhydrous Na₂SO₄ and reduced in vacuo to give the crude product that was purified by column chromatography (2:8 Acetone:Hexanes) as an oil 62 % yield (1.2 g, 6.18 mmol).

Spectroscopy:

¹H NMR (500 MHz, DMSO-*d*₆) δ 11.87 (s, 1H), 7.03 (td, *J* = 2.5, 1.4 Hz, 1H), 6.81 (dt, *J* = 3.6, 1.6 Hz, 1H), 6.18 (dt, *J* = 3.9, 1.9 Hz, 1H), 3.67 (s, 3H), 2.74 – 2.55 (m, 2H).

¹³C NMR (125 MHz, DMSO) δ 169.20, 125.44, 125.01, 115.19, 110.15, 52.80, 34.80, 31.46.

HRMS-ESI (*m/z*), calculated for C₉H₁₀N₂O₃ (M+H)⁺ 195.0770. Found 195.0759.



4,5-dibromo-1H-pyrrole-2-carboxylic acid:

2,2,2-trichloro-1-(4,5-dibromo-1H-pyrrol-2-yl)ethan-1-one (3.90 g, 10.53 mmol) was added to a 100 mL round bottom flask. 40 mL of DI water was added to the reaction vessel followed by NaOH (0.768 g, 13.69 mmol). The suspension was refluxed for 3 h after which the reaction pH was adjusted to pH = 2. Upon pH adjustment the product precipitated out of the solution and was dried to yield the product as a purple solid 93% yield (2.62 g, 9.74 mmol).

Spectroscopy:

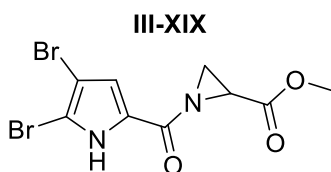
^1H NMR (500 MHz, DMSO- d_6) δ 13.16 – 12.59 (m, 2H), 6.82 (s, 1H).

^{13}C NMR (125 MHz, DMSO) δ 160.69, 125.43, 117.25, 107.18, 99.16.

IR (FT-ATR) cm^{-1} : 3214, 3151, 3096, 2967, 1165, 1052.

HRMS-ESI (m/z), calculated for $\text{C}_5\text{H}_4\text{Br}_2\text{NO}_2$ (M+H) $^+$ 267.8609. Found 267.8685.

m.p.: 293.3-293.8°C



methyl 1-(4,5-dibromo-1H-pyrrole-2-carbonyl)aziridine-2-carboxylate:

4,5-dibromo-1H-pyrrole-2-carboxylic acid (2.15 g, 8 mmol) was added to a 100 mL flame dried round bottom flask. 40 mL of anhydrous DCM was added to the reaction vessel and the suspension was stirred while Triethylamine (0.930 g, 9.2 mmol) was added by syringe. The reaction became homogeneous and methyl aziridine-2-carboxylate was then added to the vessel by syringe (0.890

g, 8.8 mmol) The reaction was stirred at room temp for 10 minutes and then cooled to 0°C by ice bath. EDCI HCl salt was then added to the reaction vessel (2.30 g, 12 mmol) and the reaction stirred for 12 h. The solution was washed with saturated NH₄Cl solution (2 x 30 mL). The organic layers were collected and dried over anhydrous Na₂SO₄ and reduced in vacuo to give the crude product that was purified by column chromatography (2:8 Acetone:Hexanes) as a red solid 18% yield (0.510 g, 1.448 mmol).

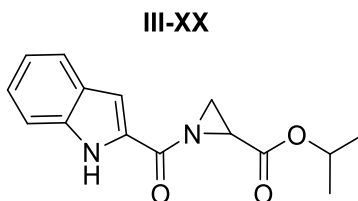
Spectroscopy:

¹H NMR (500 MHz, DMSO-*d*₆) δ 13.11 (s, 1H), 6.97 (s, 1H), 3.67 (s, 3H), 3.37 (dd, *J* = 5.8, 3.2 Hz, 1H), 2.72 (dd, *J* = 5.8, 1.5 Hz, 1H), 2.62 (dd, *J* = 3.3, 1.5 Hz, 1H).

¹³C NMR (125 MHz, DMSO) δ 168.95, 167.70, 127.35, 117.07, 108.94, 99.52, 52.90, 34.91, 31.67.

IR (FT-ATR) cm⁻¹: 3261, 3082, 2974, 1738, 1685, 1144, 1093.

HRMS-ESI (*m/z*), calculated for C₉H₉Br₂N₂O₃ (M+H)⁺ 350.8090. Found 350.8115.



isopropyl 1-(1H-indole-2-carbonyl)aziridine-2-carboxylate:

methyl 1-benzylaziridine-2-carboxylate (0.103 g, 0.4 mmol) was added to a 50 mL flame dried round bottom flask. 10 mL of anhydrous DCM was added by syringe to the reaction vessel and the solution was cooled to 0°C by ice bath before the addition of Titanium (IV) Isopropoxide (0.568 g, 2.0 mmol). The reaction stirred for 2 h after which the reaction was quenched with the addition

of saturated NaCl. The suspension was washed with DCM (3 X 30 mL). The organic layers were collected, dried over anhydrous Na₂SO₄ and concentrated to give the product as a yellow oil 97% yield (0.1099 g, 0.383 mmol).

Spectroscopy:

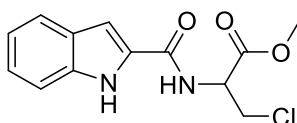
¹H NMR (500 MHz, CDCl₃) δ 9.74 (s, 1H), 7.68 (dq, *J* = 8.1, 1.0 Hz, 1H), 7.45 (dq, *J* = 8.4, 1.0 Hz, 1H), 7.32 (ddd, *J* = 8.3, 6.9, 1.1 Hz, 1H), 7.23 – 7.19 (m, 1H), 7.14 (ddd, *J* = 8.1, 6.9, 1.0 Hz, 1H), 5.04 (hept, *J* = 6.3 Hz, 1H), 3.36 (dd, *J* = 5.6, 3.2 Hz, 1H), 2.87 (dd, *J* = 3.3, 1.4 Hz, 1H), 2.74 (dd, *J* = 5.6, 1.4 Hz, 1H), 1.30 – 1.06 (m, 6H).

¹³C NMR (125 MHz, CDCl₃) δ 171.12, 167.59, 137.14, 129.81, 127.41, 125.72, 122.59, 120.89, 112.28, 108.11, 69.85, 36.20, 30.85, 21.66, 21.54.

IR (FT-ATR) cm⁻¹: 3236, 3002, 2967, 1739, 1683, 1182, 1063, 1033.

HRMS-ESI (*m/z*), calculated for C₁₅H₁₇N₂O₃ (M+H)⁺ 273.1240. Found 273.1263.

III-XXI



methyl 3-chloro-2-(1H-indole-2-carboxamido)propanoate:

methyl 1-benzylaziridine-2-carboxylate (0.103 g, 0.4 mmol) was added to a 25 mL flame dried round bottom flask. 10 mL of anhydrous DCM was added by syringe to the reaction vessel and to the resulting solution Indium (III) Chloride (0.0265 g, 0.12 mmol) was added. The reaction stirred at room temperature until all starting material was consumed (48 h) and the reaction was washed with saturated NaCl solution (3 X 15 mL). The organic layers were collected, dried over anhydrous

Na₂SO₄ and reduced in-vacuo to give the crude product as an oil. Column chromatography (2:8 Acetone: Hexanes) yielded the product as a yellow oil 90% yield (0.101 g, 0.360 mmol).

Spectroscopy:

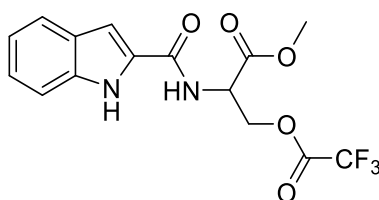
¹H NMR (500 MHz, CDCl₃) δ 9.63 (s, 1H), 7.72 – 7.66 (m, 1H), 7.47 – 7.41 (m, 1H), 7.32 (ddd, *J* = 8.2, 7.0, 1.1 Hz, 1H), 7.17 (ddd, *J* = 8.0, 7.0, 1.0 Hz, 1H), 7.12 (d, *J* = 7.5 Hz, 1H), 7.07 (dd, *J* = 2.2, 0.9 Hz, 1H), 5.25 (dt, *J* = 7.5, 3.3 Hz, 1H), 4.12 (dd, *J* = 11.4, 3.1 Hz, 1H), 4.06 (dd, *J* = 11.4, 3.4 Hz, 1H), 3.88 (s, 3H).

¹³C NMR (125 MHz, CDCl₃) δ 169.29, 161.38, 136.61, 129.42, 127.55, 124.97, 122.23, 120.84, 111.98, 103.68, 53.32, 53.28, 45.13.

IR (FT-ATR) cm⁻¹: 3287, 3196, 3055, 2943, 1738, 1695, 1208, 1084.

HRMS-ESI (*m/z*), calculated for C₁₃H₁₄ClN₂O₃ (M+H)⁺ 281.0694. Found 281.0735.

III-XXII



methyl N-(1H-indole-2-carbonyl)-O-(2,2,2-trifluoroacetyl)serinate:

methyl 1-benzylaziridine-2-carboxylate (0.103 g, 0.4 mmol) was added to a 25 mL flame dried round bottom flask. 10 mL of anhydrous DCM was added by syringe to the reaction vessel and to the resulting solution Trifluoroacetic acid (0.046 g, 0.4 mmol) was added. The reaction stirred at room temperature until all starting material was consumed (4 h) and the reaction was reduced in-

vacuo to give the crude product as an oil. Column chromatography (2:8 Acetone: Hexanes) yielded the product 99% yield (0.141 g, 0.394 mmol).

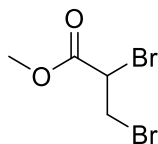
Spectroscopy:

^1H NMR (500 MHz, $\text{DMSO-}d_6$) δ 11.66 (d, $J = 2.1$ Hz, 1H), 9.07 (d, $J = 7.7$ Hz, 1H), 7.69 – 7.55 (m, 1H), 7.47 – 7.33 (m, 1H), 7.23 – 7.13 (m, 2H), 7.03 (ddd, $J = 7.9, 6.9, 1.0$ Hz, 1H), 4.97 (td, $J = 7.7, 4.5$ Hz, 1H), 4.82 (dd, $J = 11.2, 4.6$ Hz, 1H), 4.69 (dd, $J = 11.2, 7.7$ Hz, 1H), 3.68 (s, 3H).

^{13}C NMR (125 MHz, DMSO) δ 169.60, 161.75, 156.88, 156.54, 137.06, 130.85, 127.33, 124.17, 122.15, 120.33, 112.80, 104.05, 66.60, 52.91, 51.13.

HRMS-ESI (m/z), calculated for $\text{C}_{15}\text{H}_{14}\text{F}_3\text{N}_2\text{O}_5$ ($\text{M}+\text{H}$) $^+$ 359.0855. Found 359.0902.

III-XXIII



methyl 2,3-dibromopropanoate:

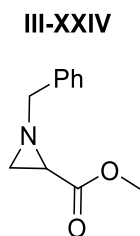
Methyl acrylate (2.58 g, 30 mmol) was added to a flame dried 250 mL round bottom flask. Anhydrous CCl_4 (60 mL) was added to the flask by syringe. Bromine (5.75 g, 36 mmol) was added slowly to the reaction by syringe over 10 minutes. The reaction was then heated to gentle reflux for 8 h to consume all starting material. The reaction was reduced in-vacuo to give the product as a beige oil 98% yield (7.2 g, 29.28 mmol).

Spectroscopy:

^1H NMR (500 MHz, CDCl_3) δ 4.45 (dd, $J = 11.4, 4.4$ Hz, 1H), 3.93 (dd, $J = 11.4, 9.9$ Hz, 1H), 3.85 (d, $J = 0.9$ Hz, 3H), 3.68 (dd, $J = 10.0, 4.4$ Hz, 1H).

^{13}C NMR (125 MHz, CDCl_3) δ 168.06, 53.40, 40.70, 29.59.

HRMS-ESI (m/z), calculated for $\text{C}_4\text{H}_7\text{Br}_2\text{O}_2$ ($\text{M}+\text{H}$) $^+$ 244.8815. Product not stable to HRMS conditions.

**methyl 1-benzylaziridine-2-carboxylate:**

K_2CO_3 (24.88 g, 180 mmol) was added to a flame dried 250 mL round bottom flask. Anhydrous MeOH (80 mL) was added to the flask and the suspension had methyl 2,3-dibromopropanoate (22.06 g, 90 mmol) was added as an oil to the vessel. The reaction was cooled to 0°C by ice bath. Benzylamine (75 mmol) was slowly added to the reaction by syringe over 5 minutes. The reaction was stirred at 0°C for 4 h before warming to room temperature and stirring for 14 h. The suspension was filtered and the filtrate was collected, reduced in-vacuo to give the crude product that was purified by column chromatography (3:7 EtOAc: Hexanes) to give the product as a clear oil 60% yield (8.6 g, 44.97 mmol)

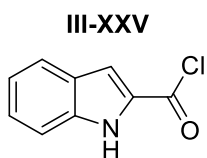
Spectroscopy:

^1H NMR (500 MHz, CDCl_3) δ 7.37 – 7.23 (m, 5H), 3.72 (s, 3H), 3.60 – 3.50 (m, 2H), 2.27 (dd, $J = 3.1, 1.1$ Hz, 1H), 2.22 (dd, $J = 6.4, 3.1$ Hz, 1H), 1.77 (dd, $J = 6.5, 1.1$ Hz, 1H).

^{13}C NMR (125 MHz, CDCl_3) δ 171.18, 137.65, 128.44, 128.07, 127.37, 63.92, 52.27, 37.35, 34.57.

IR (FT-ATR) cm^{-1} : 3033, 2961, 1735, 1149, 1062, 1037, 1024.

HRMS-ESI (m/z), calculated for $\text{C}_{11}\text{H}_{14}\text{NO}_2(\text{M}+\text{H})^+$ 192.1066. Found 192.1097.



1H-indole-2-carbonyl chloride:

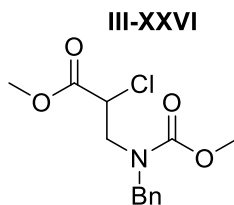
Indole-2-carboxylic acid (2.4 g, 14.89 mmol) was added to a 250 mL flame dried round bottom flask under inert atmosphere. 100 mL of anhydrous DCM was added to the flask. 0.15 mL of DMF was added to the reaction vessel. The reaction was cooled to 0°C by ice bath. The suspension was then vigorously stirred as Oxalyl chloride (5.76 g, 45.515 mmol) was slowly added to the reaction. Once the reaction became homogeneous it was refluxed for 2 h. The reaction was the reduced in vacuo to remove excess reagent and yielded the crude product that was flash columned to give the product as a pale-yellow solid 55% yield (1.47 g, 8.19 mmol).

Spectroscopy:

^1H NMR (500 MHz, CDCl_3) δ 8.88 (s, 1H), 7.75 (dq, $J = 8.2, 1.0$ Hz, 1H), 7.55 (dd, $J = 2.2, 0.6$ Hz, 1H), 7.45 – 7.41 (m, 2H), 7.21 (dt, $J = 8.0, 3.9$ Hz, 1H).

^{13}C NMR (125 MHz, CDCl_3) δ 159.92, 138.50, 129.49, 127.96, 127.05, 123.53, 121.83, 116.18, 112.24.

HRMS-ESI (m/z), calculated for $\text{C}_9\text{H}_7\text{ClNO}(\text{M}+\text{H})^+$ 180.0216. Product not stable to HRMS conditions.



methyl 3-(benzyl(methoxycarbonyl)amino)-2-chloropropanoate:

methyl 1-benzylaziridine-2-carboxylate (0.200 g, 1.046 mmol) was added as an oil to a 25 mL flame dried flask. 5 mL of anhydrous ACN was added by syringe and the reaction was cooled to 0°C by ice bath. Methyl chloroformate (0.098 g, 1.046 mmol) was added by syringe and the reaction was stirred at 0°C for 2 h. The reaction was concentrated to yield the product as a clear oil 95 % yield (0.298 g, 0.994 mmol).

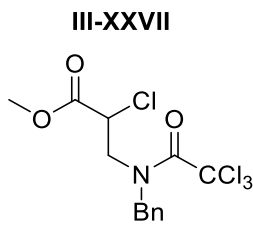
Spectroscopy:

¹H NMR (500 MHz, CDCl₃) δ 7.36 – 7.29 (m, 2H), 7.29 – 7.21 (m, 2H), 7.18 (d, *J* = 7.5 Hz, 1H), 4.73 – 4.46 (m, 3H), 3.82 – 3.68 (m, 7H), 3.58 (dq, *J* = 14.5, 7.2, 6.6 Hz, 1H).

¹³C NMR (125 MHz, CDCl₃) δ 168.99, 168.91, 156.95, 156.81, 137.13, 137.07, 128.70, 128.51, 128.38, 128.07, 127.92, 127.65, 127.56, 127.17, 53.80, 53.67, 53.18, 53.11, 53.07, 52.45, 52.04, 51.77, 50.88, 49.68.

IR (FT-ATR) cm⁻¹: 3106, 2998, 1743, 1704, 1692, 1589, 1471, 1158, 1103, 1045, 1003.

HRMS-ESI (*m/z*), calculated for C₁₃H₁₇ClNO₄ (*M*+*H*)⁺ 286.0849. Found 286.0897.



methyl 3-(N-benzyl-2,2,2-trichloroacetamido)-2-chloropropanoate:

methyl 1-benzylaziridine-2-carboxylate (0.207 g, 1.082 mmol) was added as an oil to a 25 mL flame dried flask. 5 mL of anhydrous ACN was added by syringe and the reaction was cooled to 0°C by ice bath. 2,2,2 trichloroacetyl chloride (0.197 g, 1.082 mmol) was added by syringe and the reaction was stirred at 0°C for 2 h. The reaction was concentrated and purified by column chromatography (3:7 EtOAc: Hexanes) to yield the product as a clear oil 87% yield (0.350 g, 0.941 mmol).

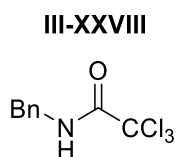
Spectroscopy:

¹H NMR (500 MHz, CDCl₃) δ 7.43 – 7.29 (m, 3H), 7.29 – 7.19 (m, 2H), 5.28 – 5.13 (m, 1H), 5.06 (dd, *J* = 16.6, 4.5 Hz, 1H), 4.85 (q, *J* = 6.5, 6.0 Hz, 1H), 3.91 (dt, *J* = 12.0, 5.3 Hz, 1H), 3.78 (d, *J* = 4.6 Hz, 3H), 3.62 – 3.50 (m, 1H).

¹³C NMR (125 MHz, CDCl₃) δ 168.55, 161.48, 134.60, 129.05, 128.21, 127.16, 92.52, 77.29, 55.27, 53.34, 52.22, 51.46.

IR (FT-ATR) cm⁻¹: 3058, 2967, 1744, 1659, 1582, 1133, 1047.

HRMS-ESI (*m/z*), calculated for C₁₃H₁₄Cl₄NO₃ (*M*+*H*)⁺ 371.9728. Found 371.9803.

**N-benzyl-2,2,2-trichloroacetamide:**

Sodium hydride (0.024 g, 0.558 mmol) was added to a flame dried 50 mL round bottom flask. Anhydrous DMF (5 mL) was added to the reaction vessel by syringe and the resulting suspension was cooled to 0°C. Pyrrole (0.034 g, 0.507 mmol) was added to the reaction vessel by syringe. The

reaction was stirred at 0°C for 1 hour before methyl 3-(N-benzyl-2,2,2-trichloroacetamido)-2-chloropropanoate (0.205 g, 0.507 mmol) was dissolved in 1 mL of anhydrous DMF and added slowly to the reaction vessel. The reaction stirred at 0°C for 1 h and was brought to room temperature and stirred for 12 h. The reaction was decanted into ethyl acetate (30 mL) and washed with 3 X 20 mL of 10% LiBr solution. The organic layers were collected dried over anhydrous Na₂SO₄ and reduced to give the crude product. The crude was purified by column chromatography to give the product in 23% yield (0.029 g, 0.117 mmol)

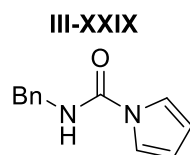
Spectroscopy:

¹H NMR (500 MHz, CDCl₃) δ 7.42 – 7.29 (m, 5H), 7.01 (s, 1H), 4.55 (d, *J* = 5.7 Hz, 2H).

¹³C NMR (125 MHz, CDCl₃) δ 150.90, 137.51, 128.93, 128.86, 127.89, 127.87, 127.70, 118.39, 111.98, 44.90.

IR (FT-ATR) cm⁻¹: 3295, 3082, 1654, 1563, 1069.

HRMS-ESI (m/z), calculated for C₉H₉Cl₃NO (M+H)⁺ 251.9750. Product not stable to HRMS conditions.



N-benzyl-1H-pyrrole-1-carboxamide:

Sodium hydride (0.024 g, 0.558 mmol) was added to a flame dried 50 mL round bottom flask. Anhydrous DMF (5 mL) was added to the reaction vessel by syringe and the resulting suspension was cooled to 0°C. Pyrrole (0.034 g, 0.507 mmol) was added to the reaction vessel by syringe. The reaction was stirred at 0°C for 1 hour before methyl 3-(N-benzyl-2,2,2-trichloroacetamido)-2-

chloropropanoate (0.205 g, 0.507 mmol) was dissolved in 1 mL of anhydrous DMF and added slowly to the reaction vessel. The reaction stirred at 0°C for 1 h and was brought to room temperature and stirred for 12 h. The reaction was decanted into ethyl acetate (30 mL) and washed with 3 X 20 mL of 10% LiBr solution. The organic layers were collected dried over anhydrous Na₂SO₄ and reduced to give the crude product. The crude was purified by column chromatography to give the product in 39% yield (0.04 g, 0.198 mmol).

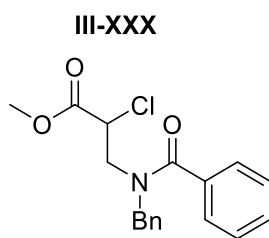
Spectroscopy:

¹H NMR (500 MHz, CDCl₃) δ 7.40 – 7.29 (m, 5H), 7.23 – 7.18 (m, 2H), 6.30 – 6.24 (m, 2H), 5.88 (s, 1H), 4.58 (d, *J* = 5.7 Hz, 2H).

¹³C NMR (125 MHz, CDCl₃) δ 150.90, 137.51, 128.93, 127.89, 127.70, 118.39, 111.98, 44.90.

IR (FT-ATR) cm⁻¹: 3312, 3025, 2974, 1664, 1670, 1598, 1472, 1024, 1018.

HRMS-ESI (*m/z*), calculated for C₁₂H₁₃N₂O (M+H)⁺ 201.1028. Found 201.1066.



methyl 3-(N-benzylbenzamido)-2-chloropropanoate:

methyl 1-benzylaziridine-2-carboxylate (0.200 g, 1.00 mmol) was added as an oil to a 25 mL flame dried flask. 5 mL of anhydrous ACN was added by syringe and the reaction was cooled to 0°C by ice bath. Benzoyl chloride (0.141 g, 1.0 mmol) was added by syringe and the reaction was stirred at 0°C for 2 h. The reaction was concentrated and purified by column chromatography (3:7 EtOAc: Hexanes) to yield the product as a clear oil 88% yield (0.274 g, 0.880 mmol).

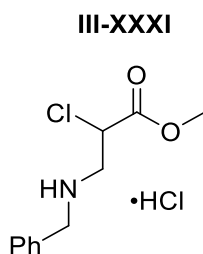
Spectroscopy:

^1H NMR (500 MHz, CDCl_3) δ 7.47 – 7.33 (m, 8H), 7.13 (d, $J = 7.4$ Hz, 2H), 4.94 (s, 1H), 4.68 (t, $J = 12.9$ Hz, 1H), 4.08 – 3.96 (m, 1H), 3.82 (s, 3H), 3.71 (dd, $J = 14.1, 7.8$ Hz, 2H).

^{13}C NMR (125 MHz, CDCl_3) δ 136.21, 135.53, 129.96, 128.95, 128.62, 128.29, 127.89, 127.00, 126.82, 77.26, 77.21, 77.00, 76.75, 54.89, 53.50, 53.24, 48.67.

IR (FT-ATR) cm^{-1} : 3058, 2977, 1742, 1695, 1588, 1102, 994, 954

HRMS: calculated for $\text{C}_{18}\text{H}_{19}\text{ClNO}_3$ ($\text{M}+\text{H}$) $^+$ 331.0978. Found 331.0988



methyl 3-(benzylamino)-2-chloropropanoate hydrochloride salt:

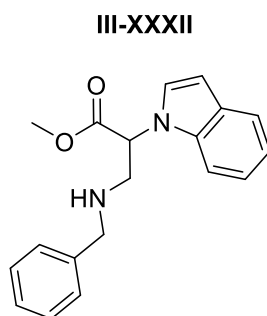
methyl 1-benzylaziridine-2-carboxylate (1.033 g, 5.4 mmol) was added as an oil to a 250 mL flame dried round bottom flask under inert atmosphere. 80 mL of Et_2O was added to the flask and the reaction vessel was cooled to 0°C by ice bath before the addition of 2.0 M HCl in Et_2O (27 mL, 54 mmol) by syringe. The reaction stirred at 0°C for 2 h. The suspension was filtered and the solid precipitant was collected and dried under vacuum to give the product as a white solid 88% yield (1.255 g, 4.75 mmol).

Spectroscopy:

^1H NMR (500 MHz, $\text{DMSO-}d_6$) δ 9.92 (d, $J = 15.3$ Hz, 2H), 7.65 – 7.49 (m, 2H), 7.49 – 7.32 (m, 3H), 5.17 (dd, $J = 8.2, 4.9$ Hz, 1H), 4.21 (s, 3H), 3.82 (d, 2H), 3.67 – 3.50 (m, 1H), 3.34 (td, $J = 13.5, 11.8, 7.8$ Hz, 1H).

^{13}C NMR (125 MHz, DMSO) δ 167.49, 131.87, 130.78, 129.50, 129.09, 53.92, 52.40, 50.81, 48.65.

HRMS-ESI (m/z), calculated for $\text{C}_{11}\text{H}_{16}\text{Cl}_2\text{NO}_2$ ($\text{M}+\text{H}$) $^+$ 228.0798 Found 228.0834.



methyl 3-(benzylamino)-2-(1H-indol-1-yl)propanoate:

Indole (0.134 g, 1.14 mmol) was added to a 50 mL flame dried round bottom flask under inert atmosphere. Anhydrous DMF (10 mL) was added to the flask by syringe. The reaction was cooled to 0°C by ice bath, before the addition of Na-H (0.096 g, 2.39 mmol). The reaction was stirred for 1 h before the addition of methyl 3-(benzylamino)-2-chloropropanoate hydrochloride salt methyl 3-(benzylamino)-2-chloropropanoate hydrochloride salt (0.300 g, 1.14 mmol) The reaction was allowed to come to room temperature and stirred for 10 h. The reaction was quenched with the addition of 5 mL of saturated NH_4Cl . The reaction was then extracted in EtOAc (40 mL) and washed with 10% LiBr solution (2 X 25 mL). The organic layers were collected, dried over anhydrous Na_2SO_4 and reduced in-vacuo to give the crude product that was purified by column

chromatography (2:8 Acetone:Hexanes) to give the product as a light yellow oil 40% yield (0.141 g, 0.456 mmol).

Spectroscopy:

^1H NMR (500 MHz, CDCl_3) δ 7.65 (dt, $J = 7.8, 0.9$ Hz, 1H), 7.40 – 7.29 (m, 3H), 7.29 – 7.19 (m, 6H), 7.15 (ddd, $J = 7.9, 7.0, 1.0$ Hz, 1H), 6.60 (d, $J = 3.3$ Hz, 1H), 5.24 (dd, $J = 8.2, 6.1$ Hz, 1H), 3.86 – 3.74 (m, 2H), 3.71 (s, 3H), 3.44 (dd, $J = 12.7, 6.1$ Hz, 1H), 3.33 (dd, $J = 12.7, 8.1$ Hz, 1H).

^{13}C NMR (125 MHz, CDCl_3) δ 170.42, 139.50, 136.32, 128.57, 128.47, 128.02, 127.17, 125.79, 122.02, 121.16, 120.04, 109.21, 102.99, 58.31, 53.37, 52.62, 49.66.

IR (FT-ATR) cm^{-1} : 3249, 3048, 2957, 754, 1574, 1054, 968, 874

HRMS-ESI (m/z), calculated for $\text{C}_{19}\text{H}_{20}\text{N}_2\text{O}_2$ ($\text{M}+\text{H}$) $^+$ 309.1610 Found 309.1626.

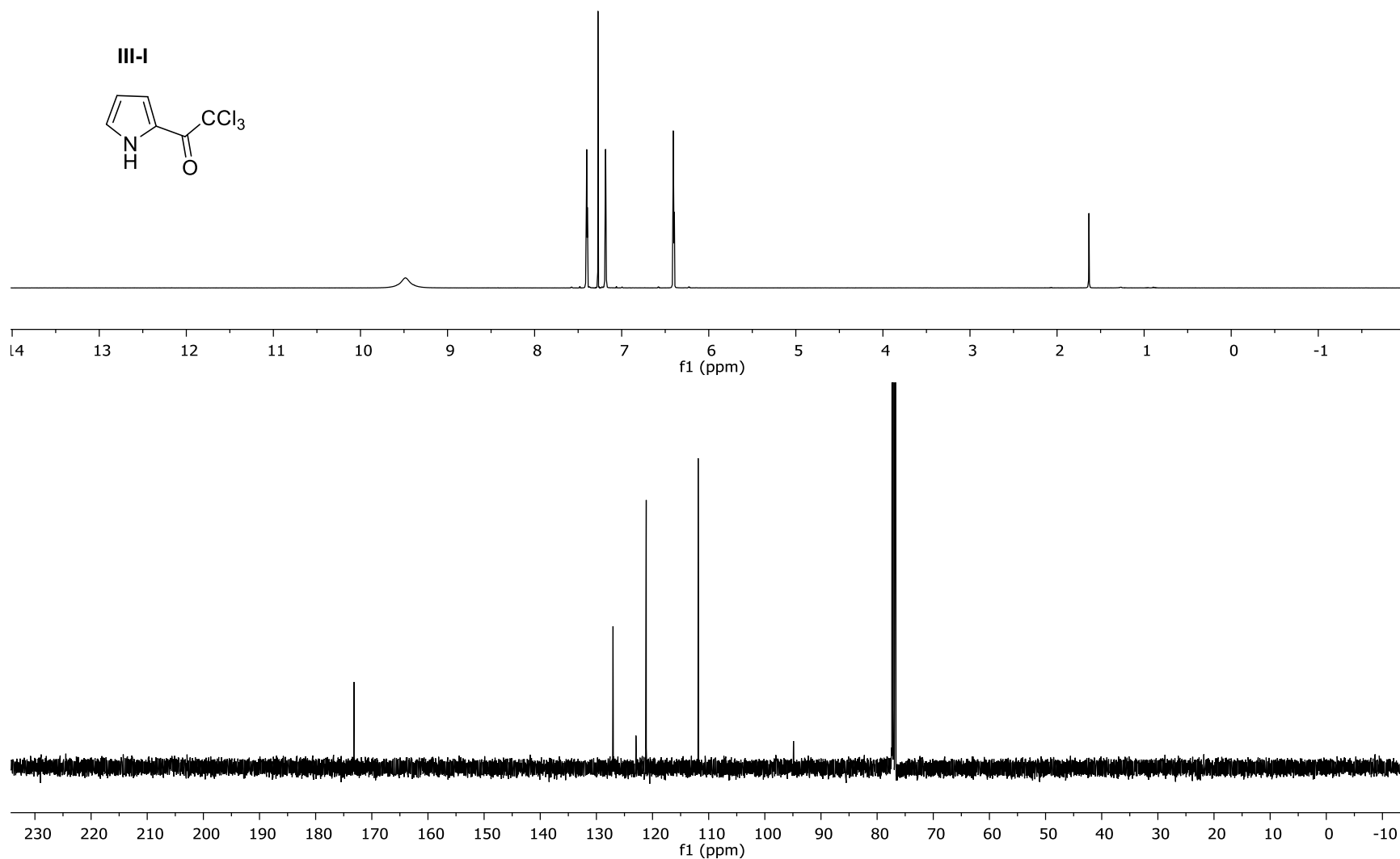


Figure III-XXXIX: The ^1H NMR and ^{13}C NMR for Compound **III-I**

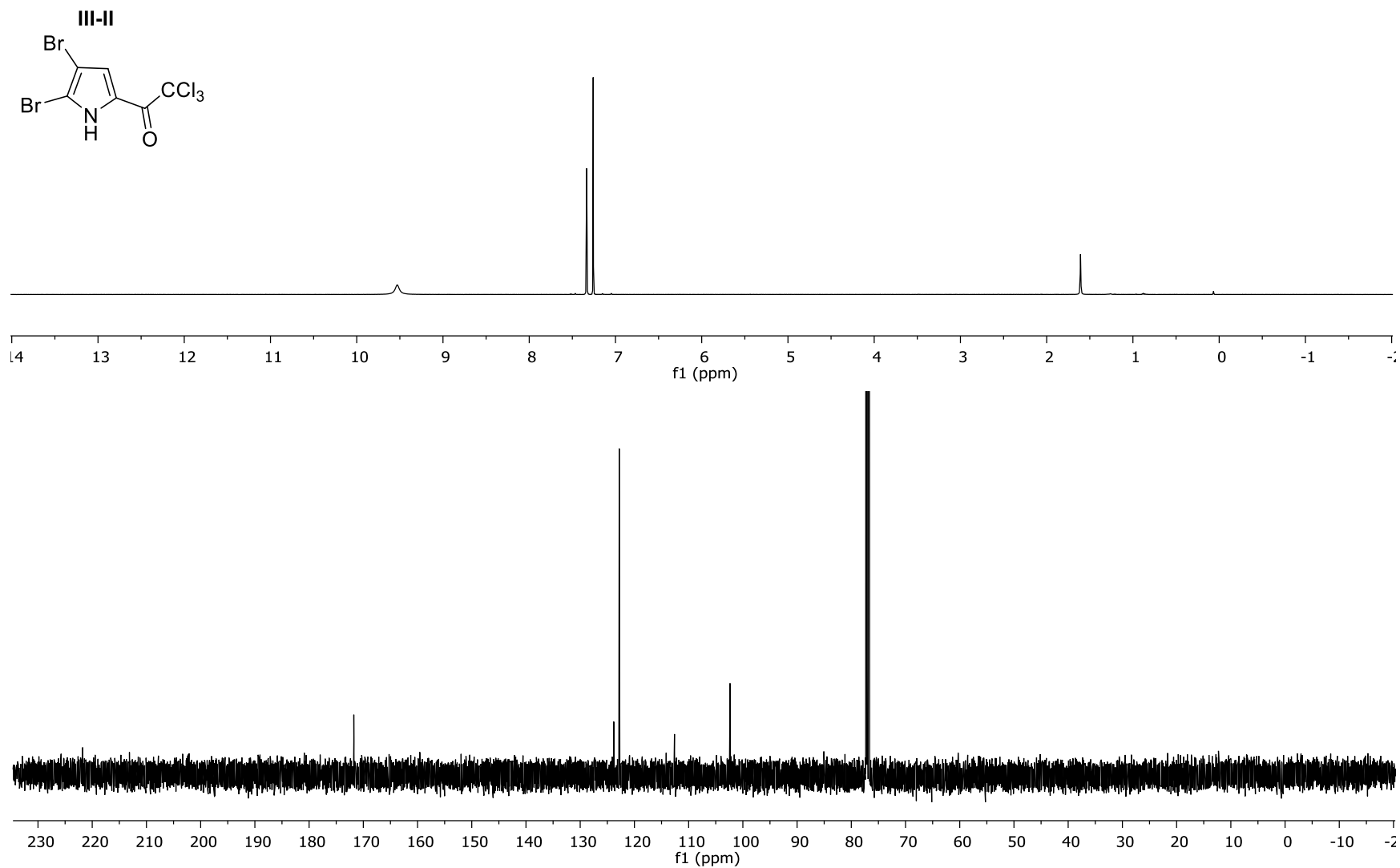


Figure III-XL: The ^1H NMR and ^{13}C NMR for Compound **III-II**

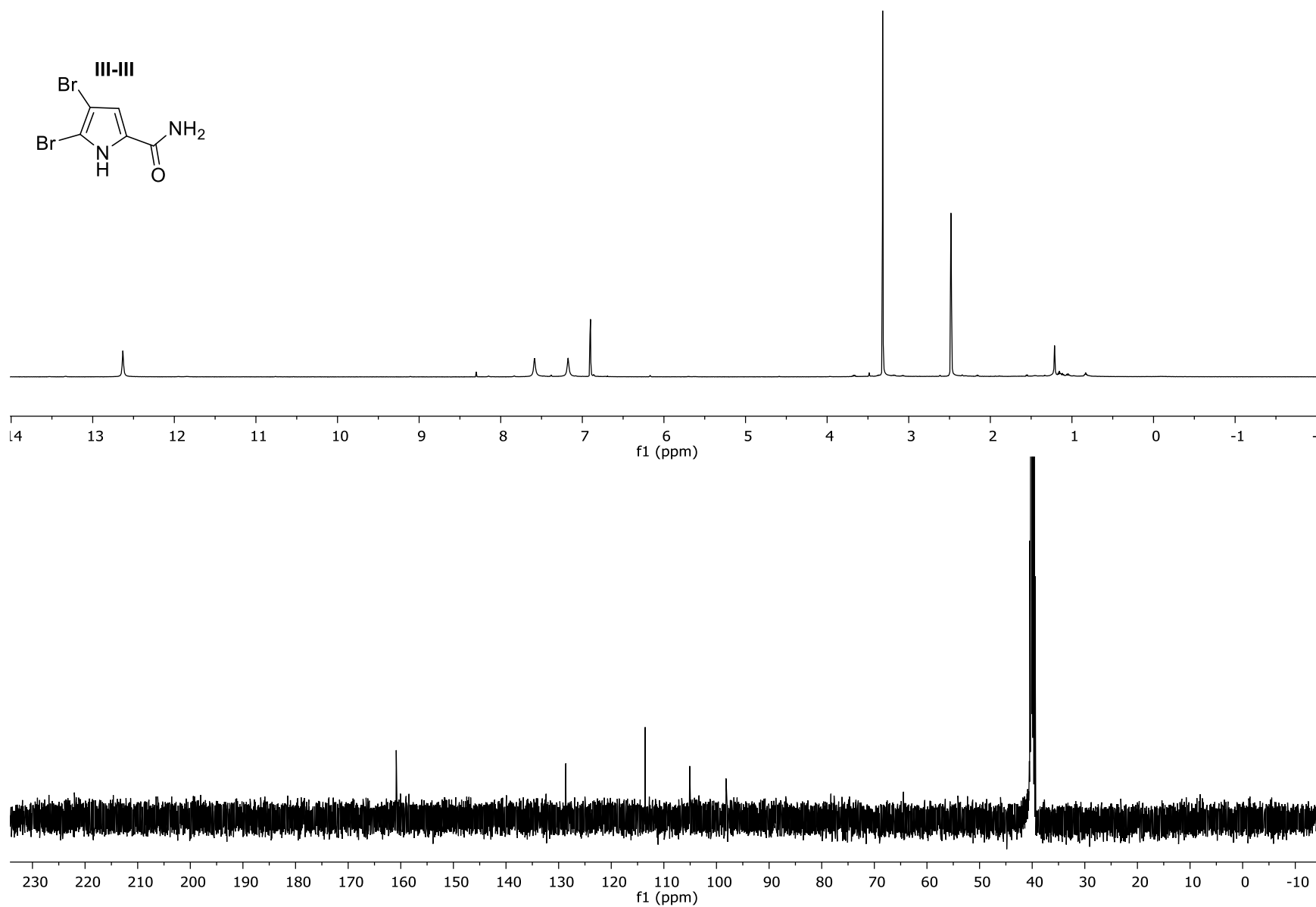


Figure III-XLI: The ^1H NMR and ^{13}C NMR for Compound **III-III**

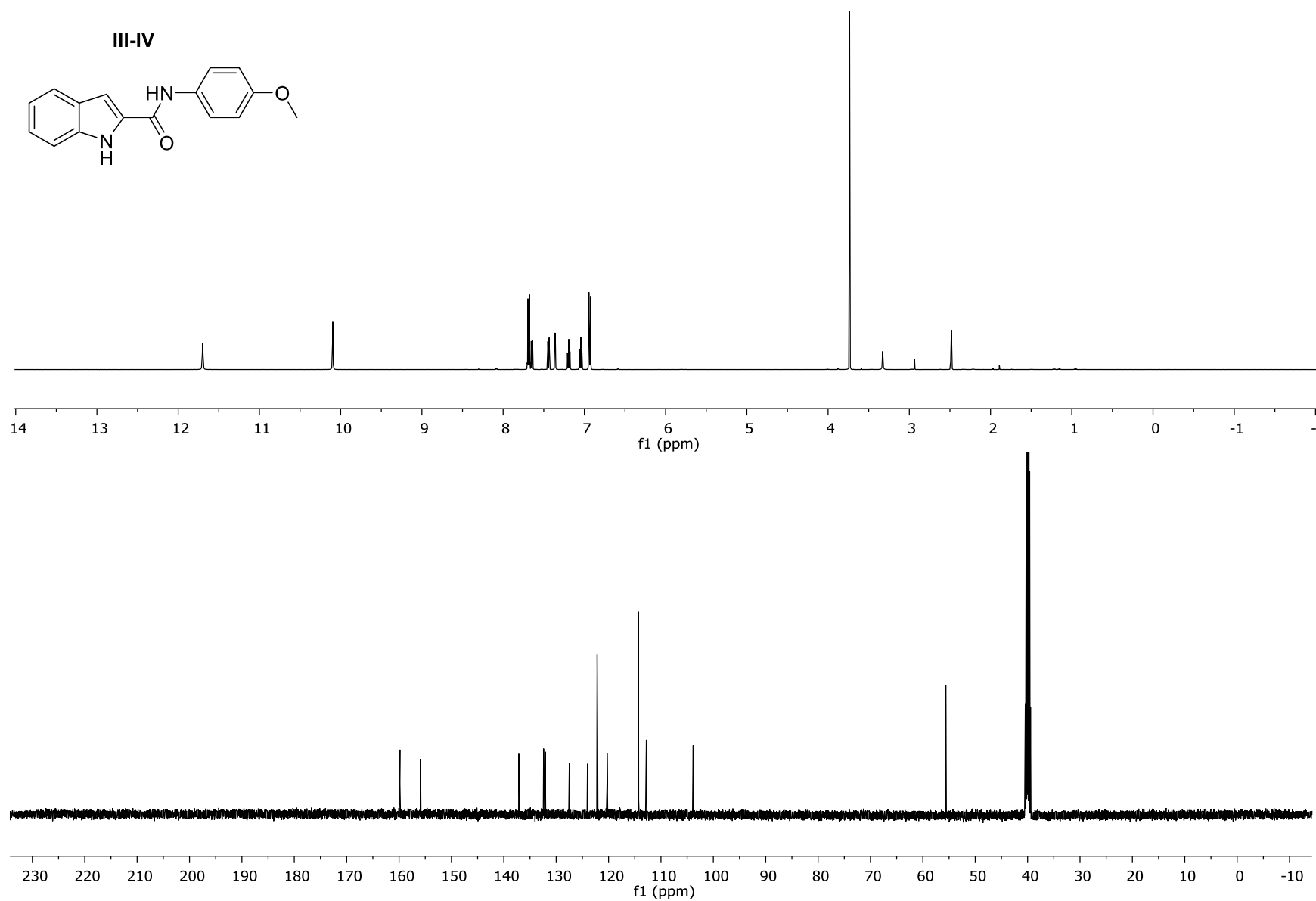


Figure III-XLII: The ¹H NMR and ¹³C NMR for Compound III-IV

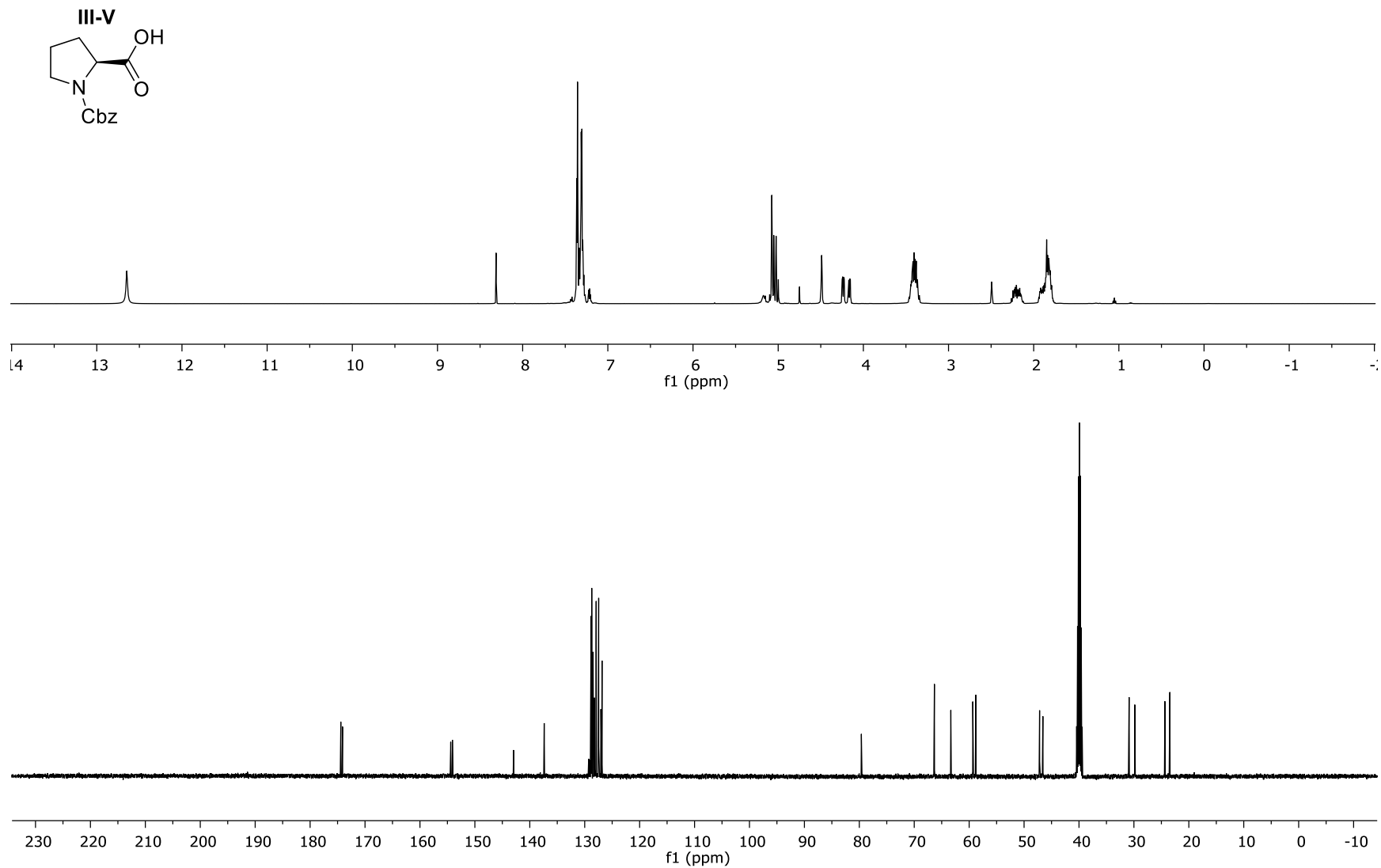


Figure III-XLIII: The ^1H NMR and ^{13}C NMR for Compound **III-V**

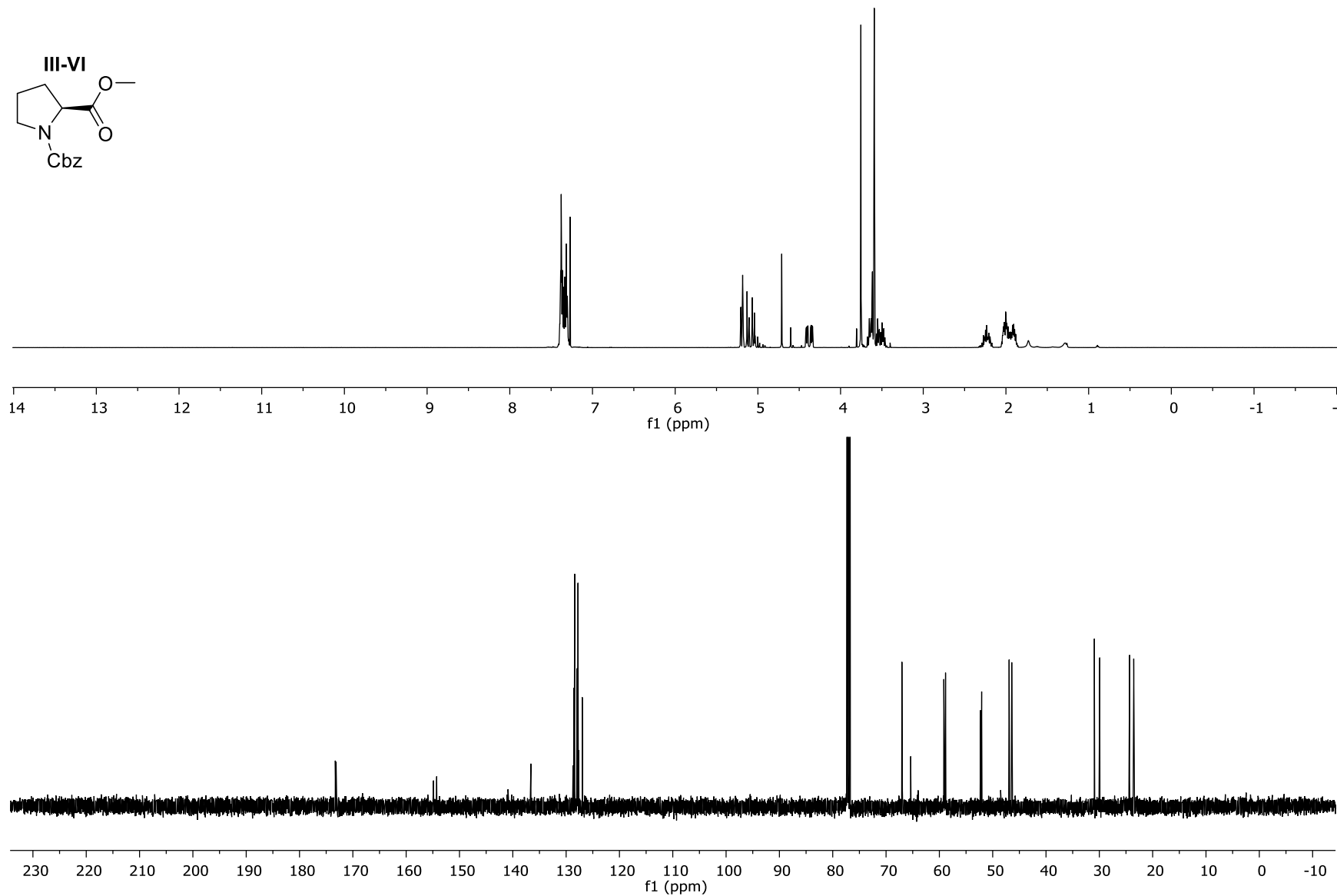
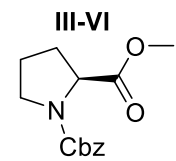


Figure III-XLIV: The ^1H NMR and ^{13}C NMR for Compound **III-VI**

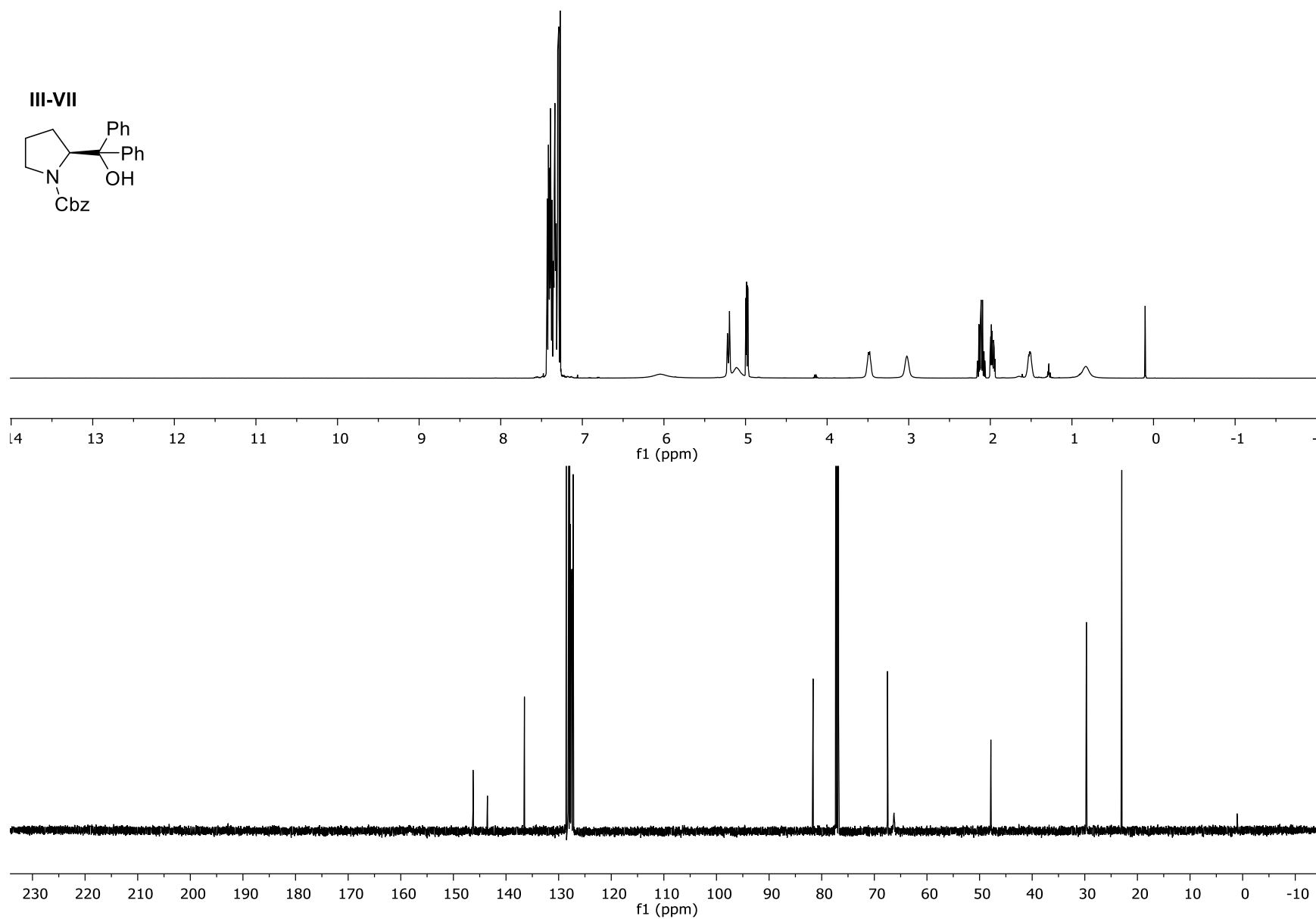


Figure III-XLV: The ^1H NMR and ^{13}C NMR for Compound **III-VII**

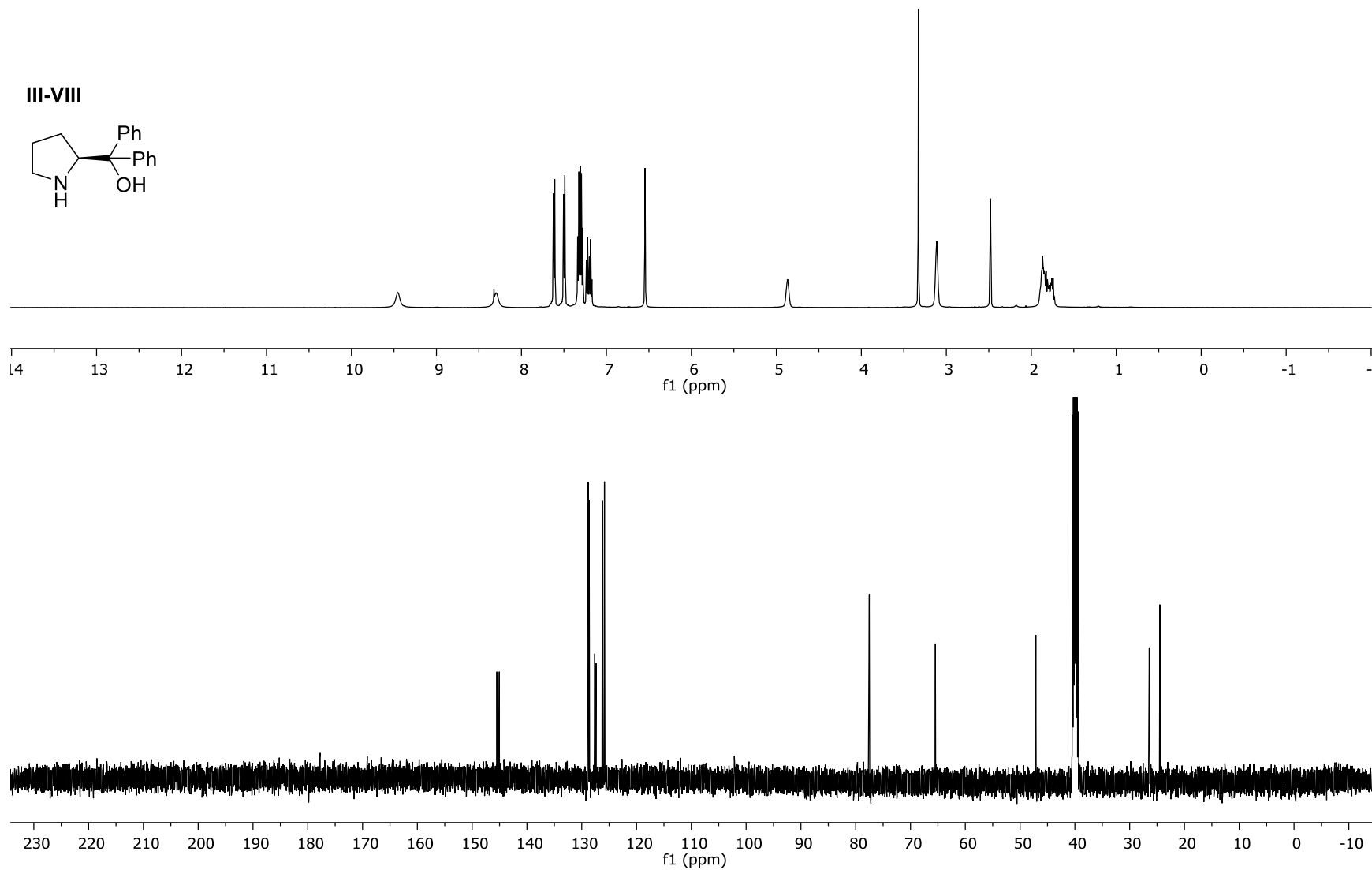


Figure III-XLVI: The ^1H NMR and ^{13}C NMR for Compound **III-VIII**

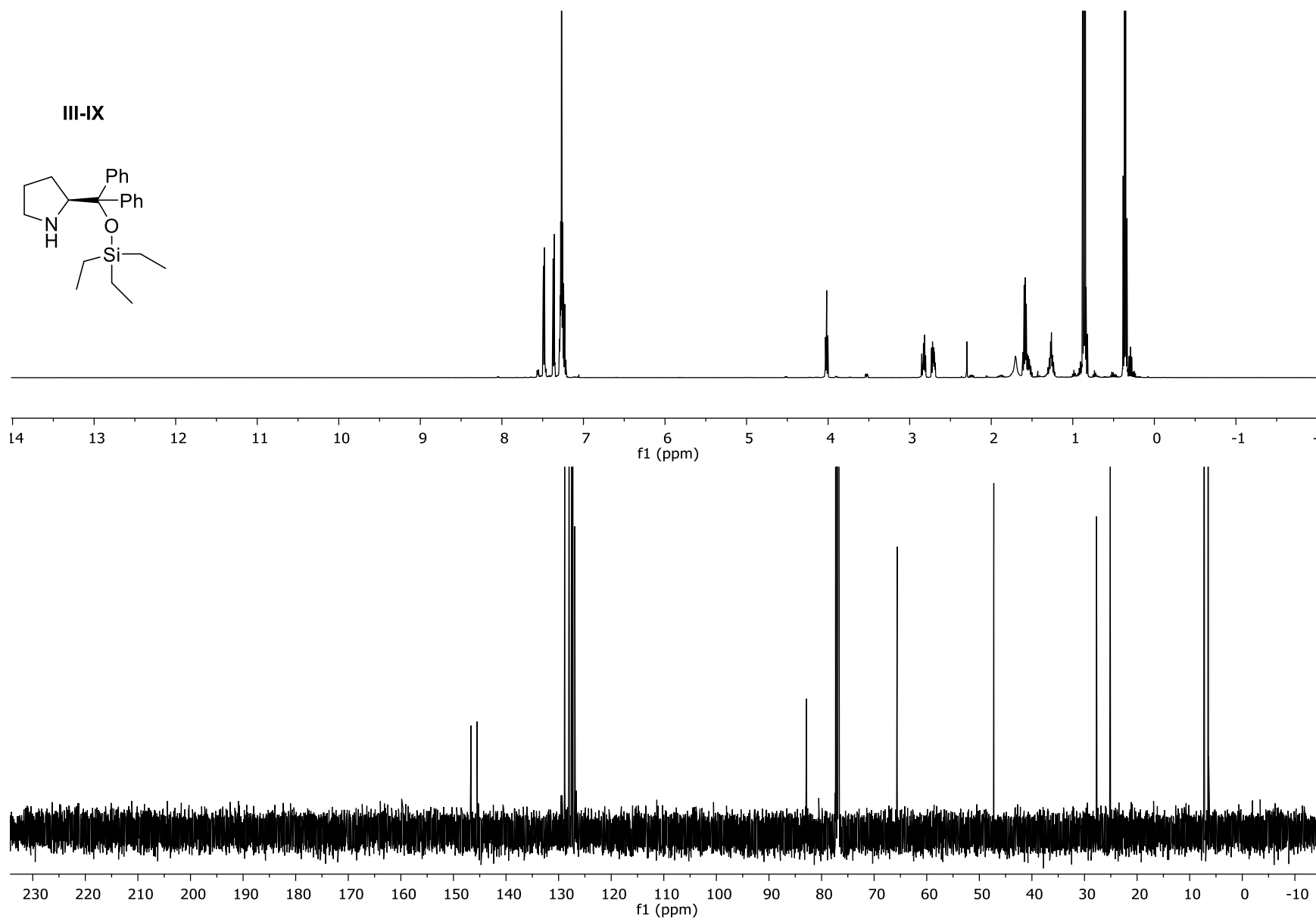


Figure III-XLVII: The ^1H NMR and ^{13}C NMR for Compound III-IX

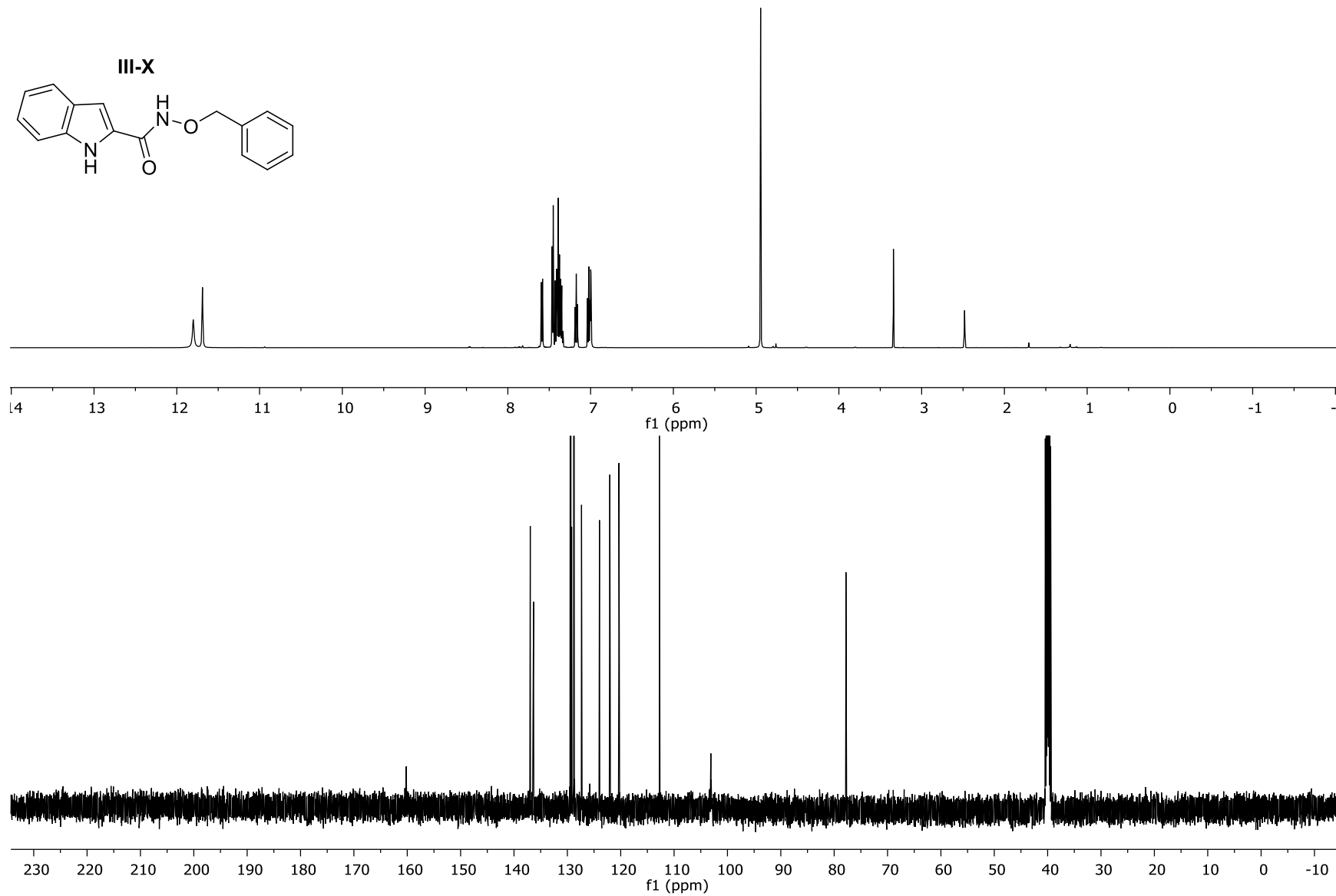


Figure III-XLVIII: The ^1H NMR and ^{13}C NMR for Compound III-X

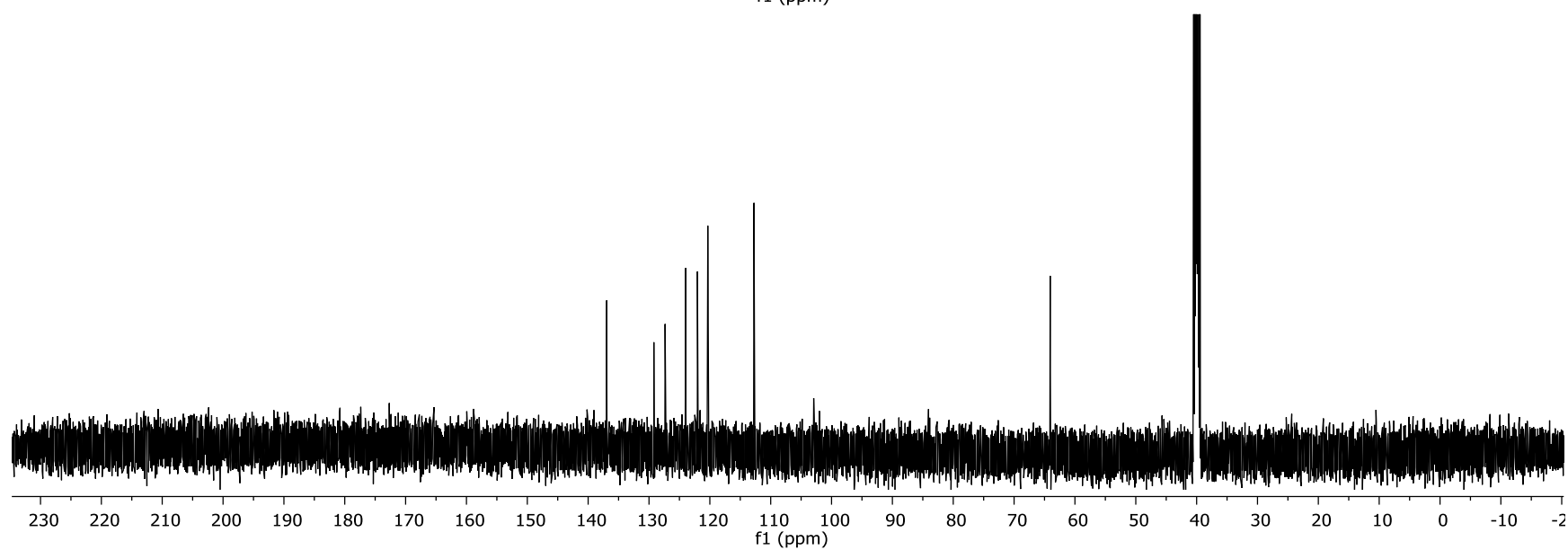
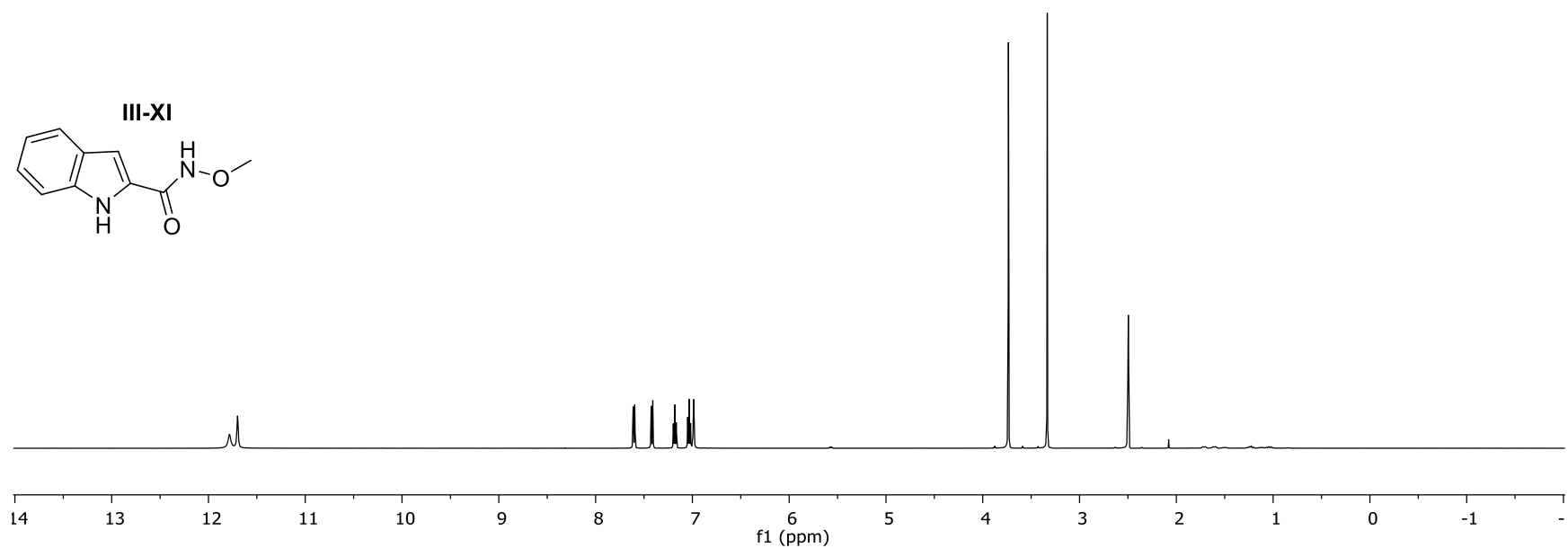
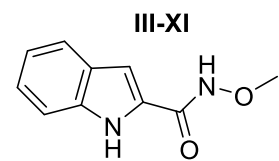


Figure III-XLIX: The ^1H NMR and ^{13}C NMR for Compound **III-XI**

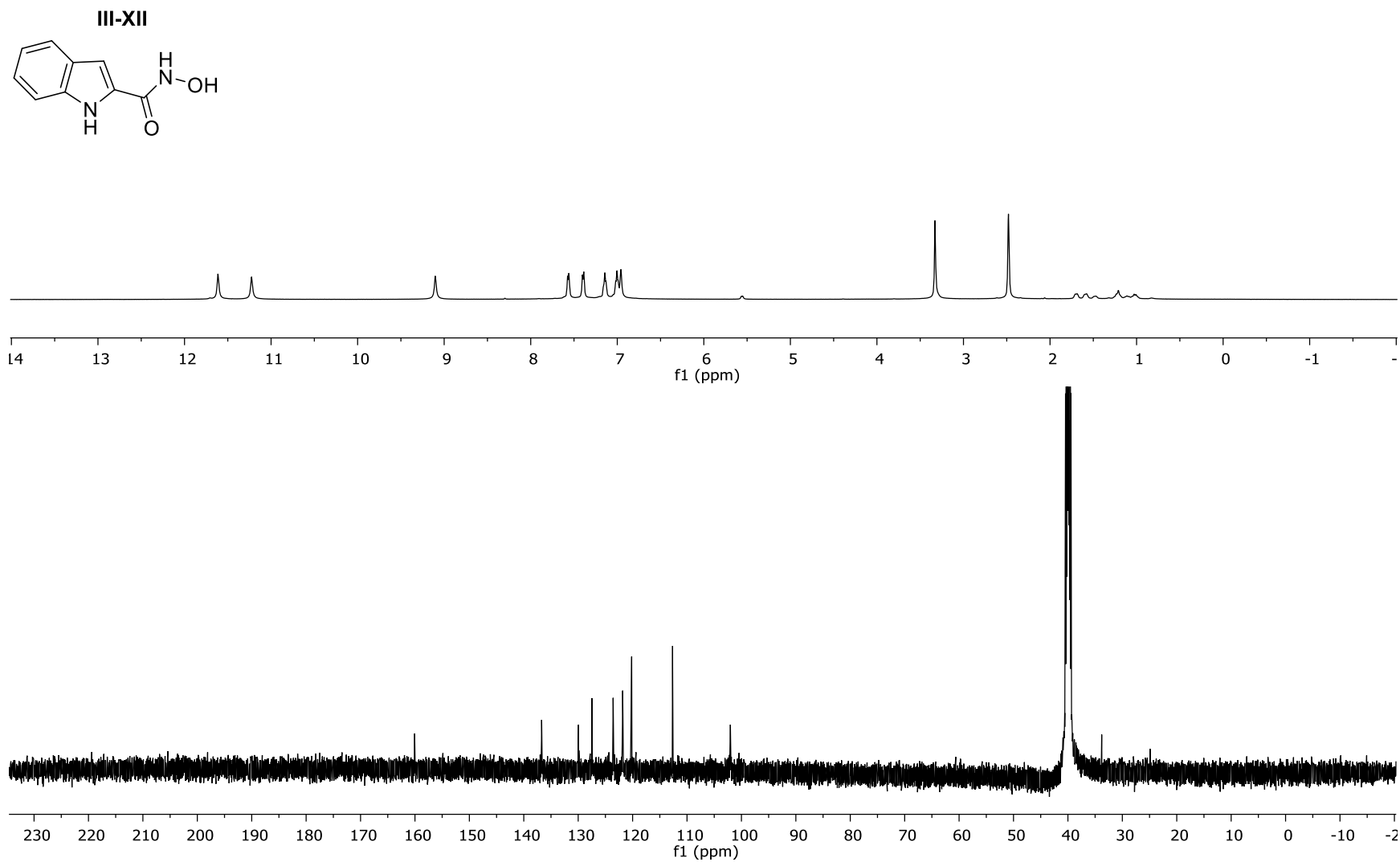


Figure III-L: The ^1H NMR and ^{13}C NMR for Compound **III-XII**

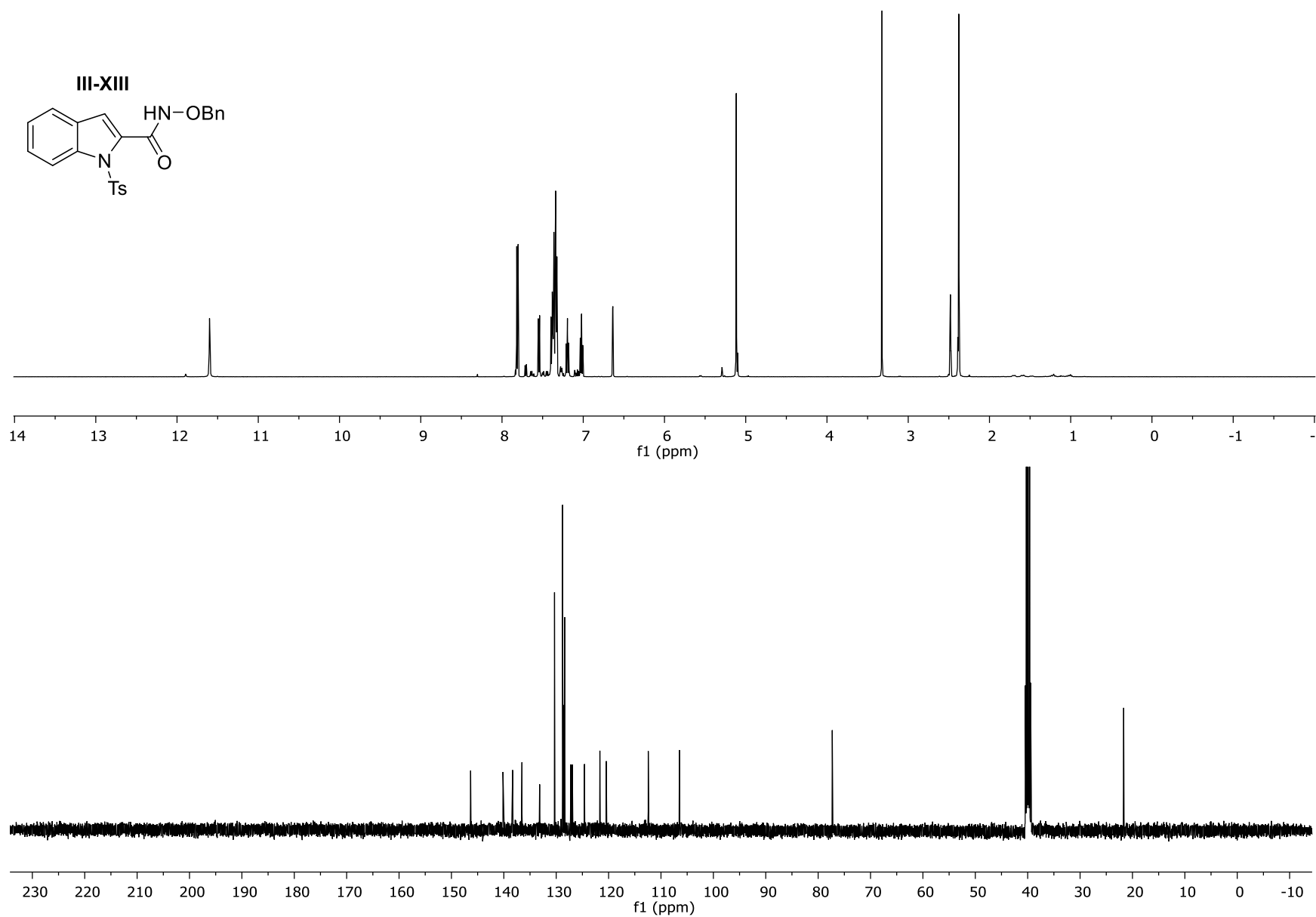


Figure III-LI: The ^1H NMR and ^{13}C NMR for Compound **III-XIII**

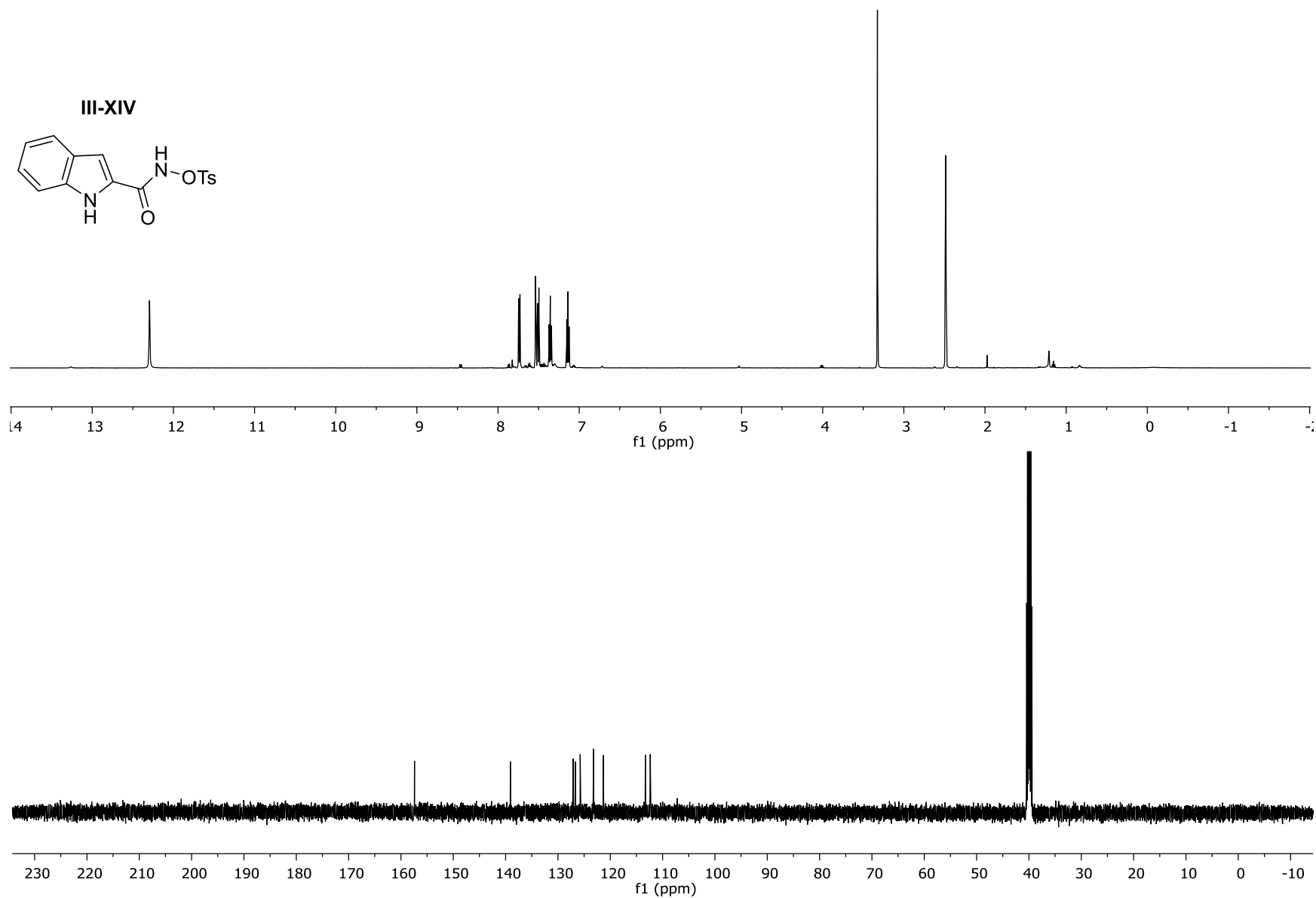


Figure III-LII: The ^1H NMR and ^{13}C NMR for Compound **III-XIV**

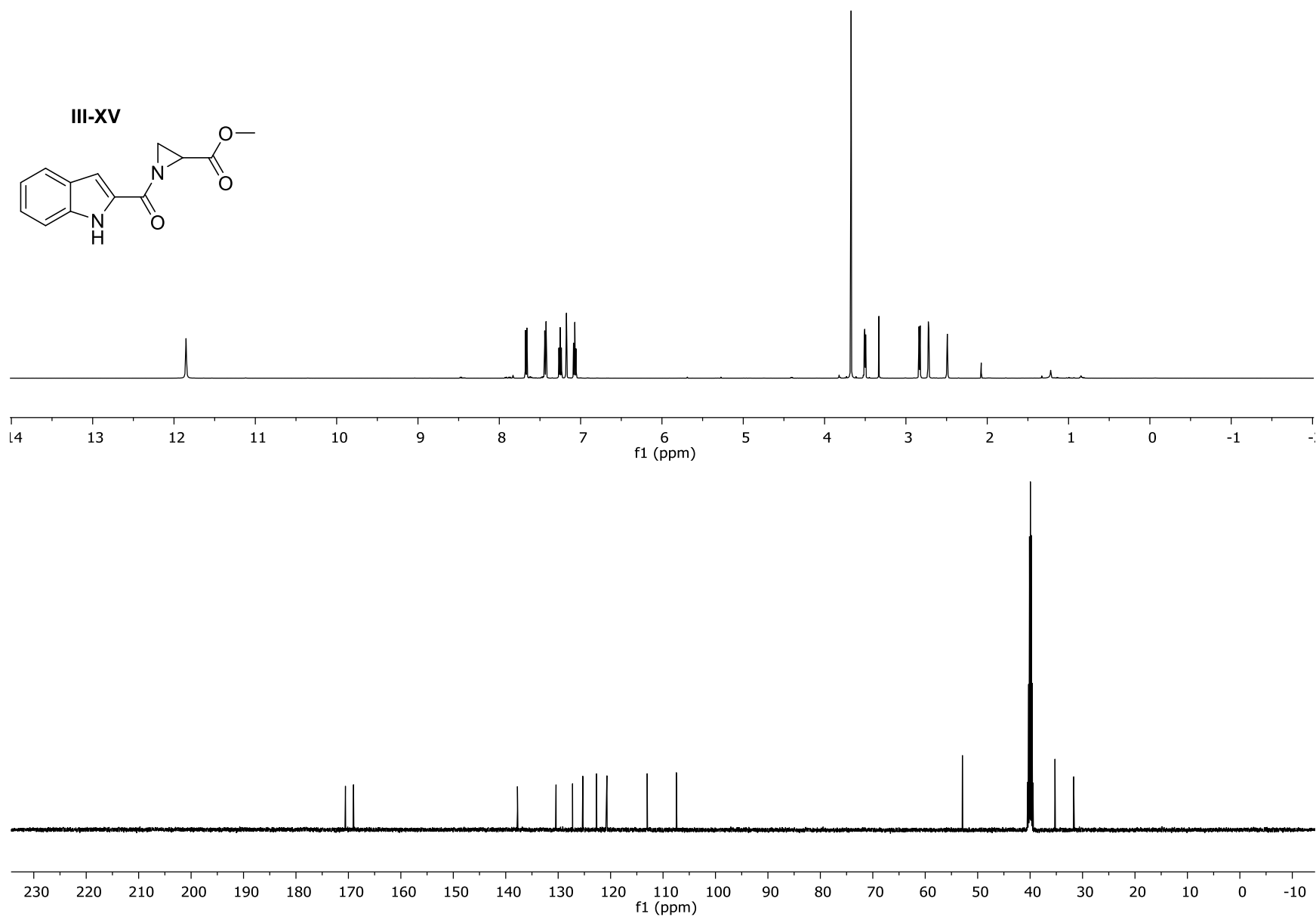


Figure III-LIII: The ^1H NMR and ^{13}C NMR for Compound **III-XV**

III-XVI

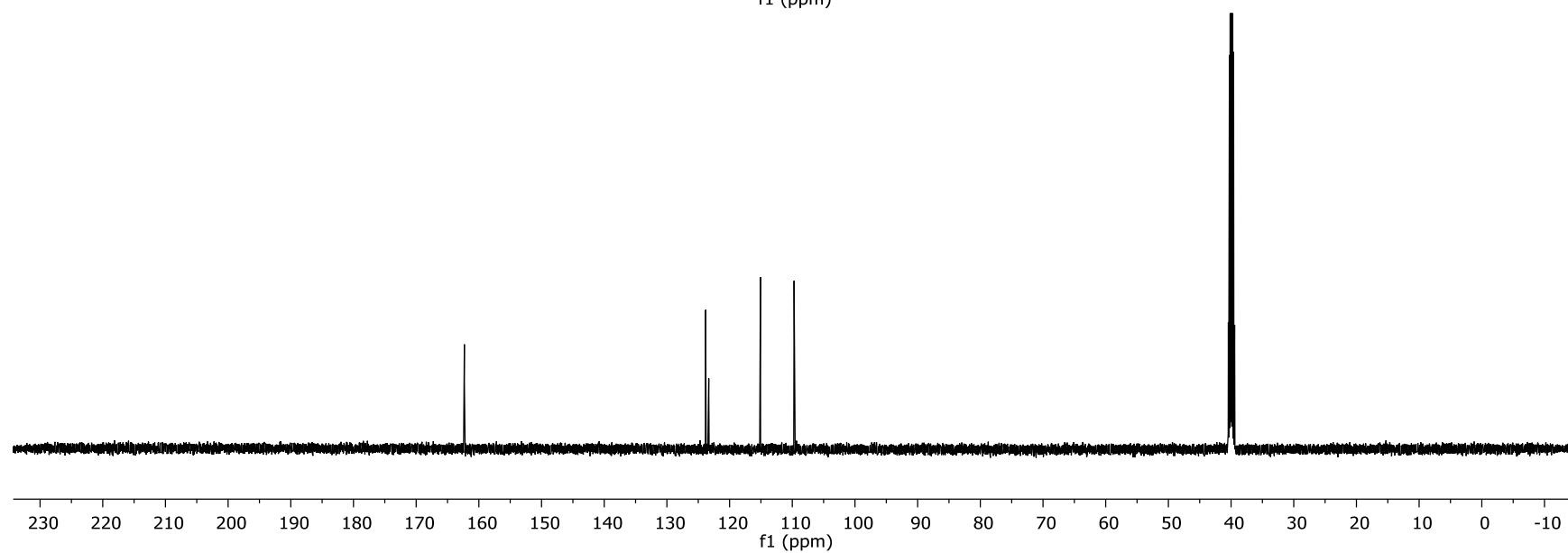
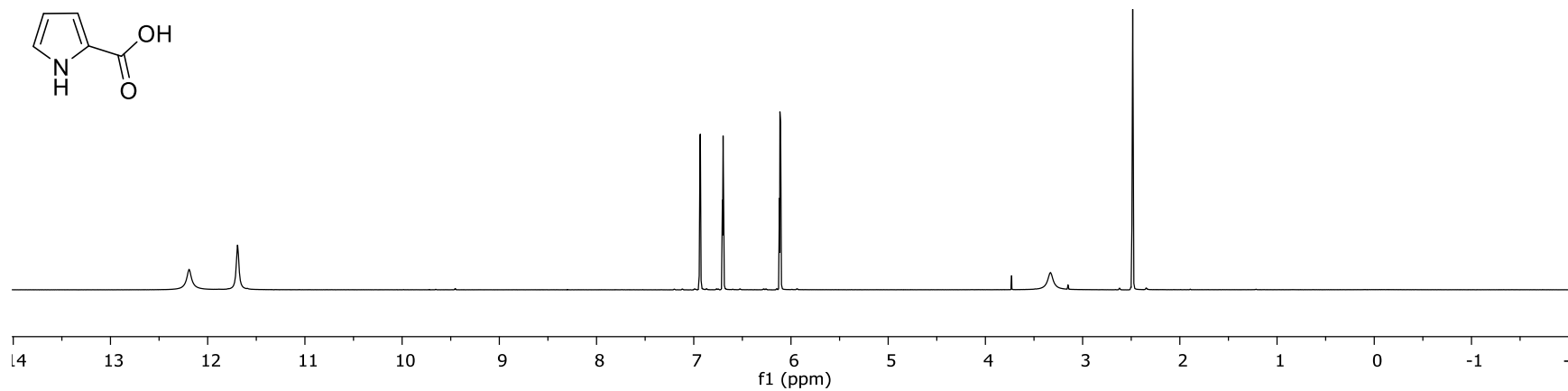
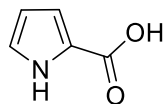


Figure III-LIV: The $^1\text{H NMR}$ and $^{13}\text{C NMR}$ for Compound III-XVI

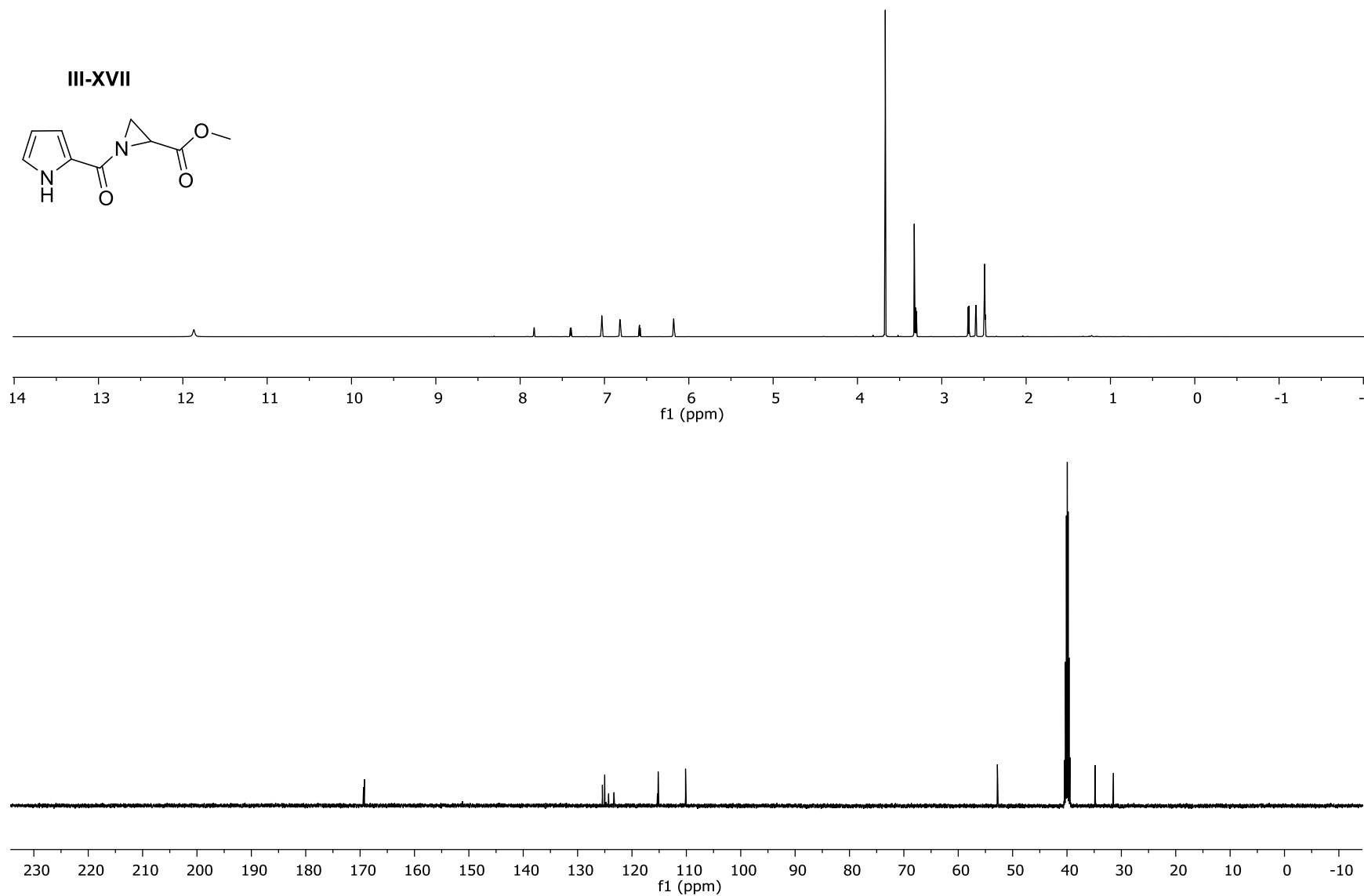


Figure III-LV: The ^1H NMR and ^{13}C NMR for Compound **III-XVII**

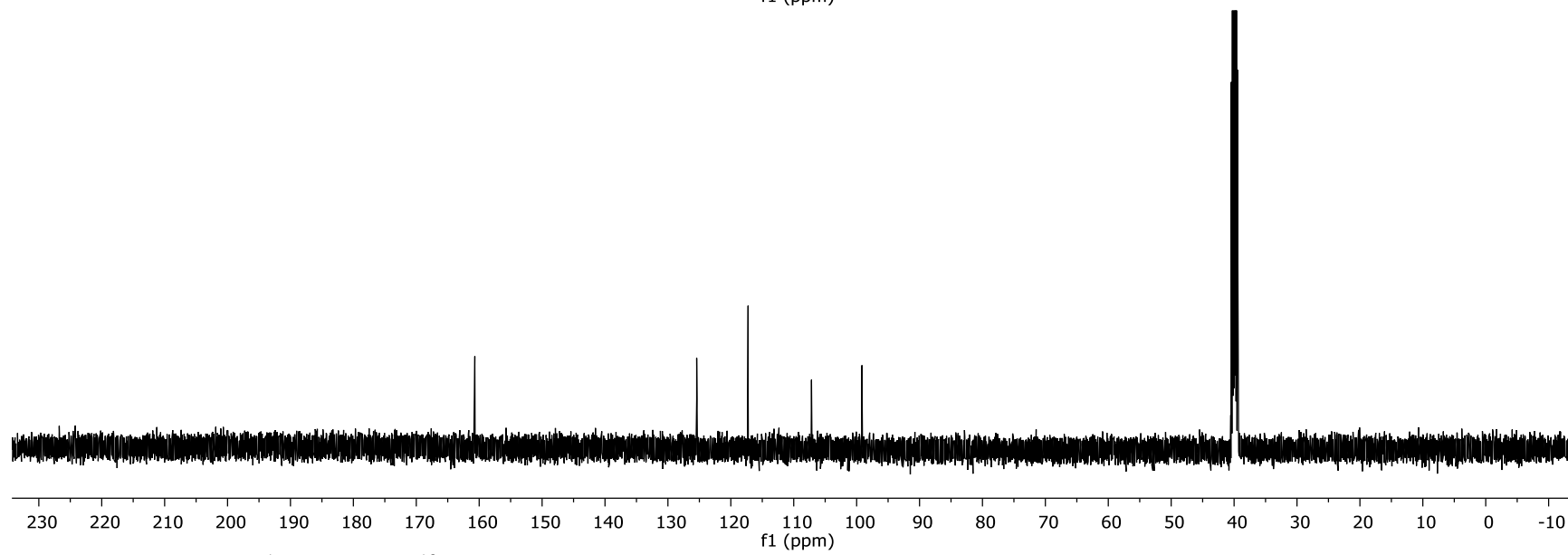
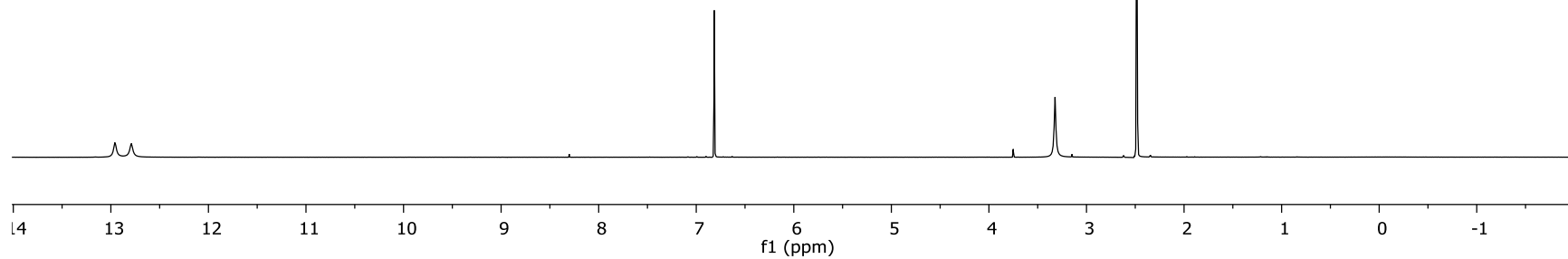


Figure III-LVI: The ^1H NMR and ^{13}C NMR for Compound III-XVIII

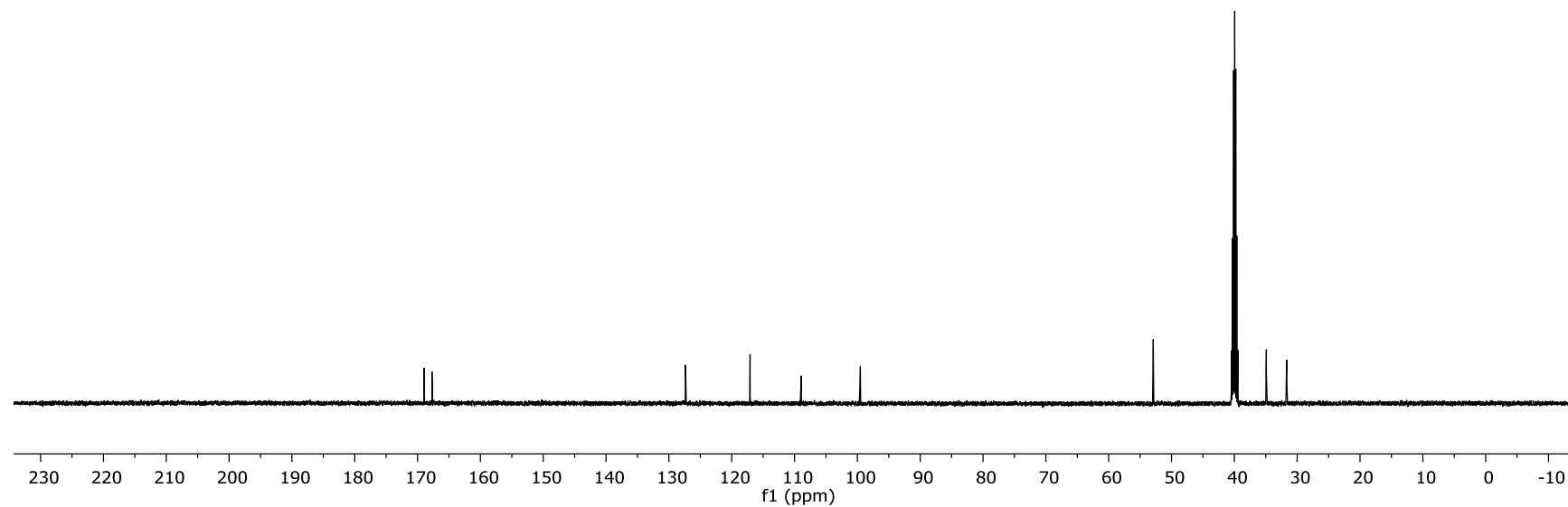
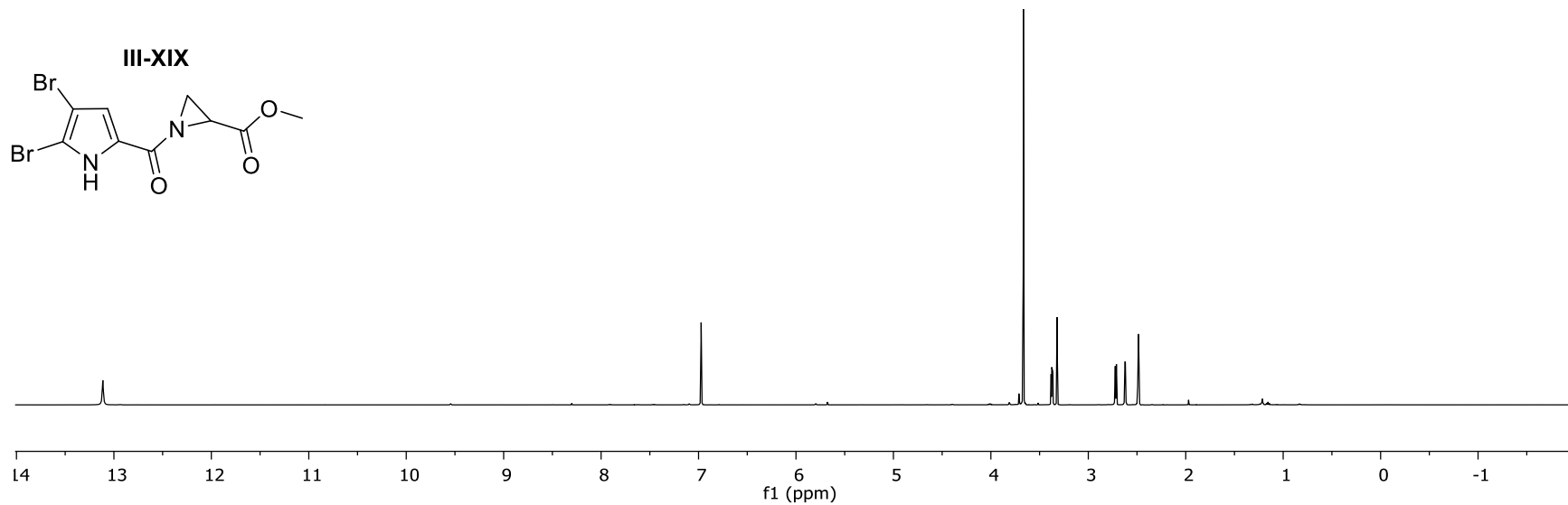
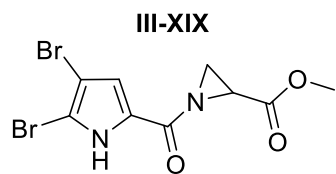


Figure III-LVII: The ^1H NMR and ^{13}C NMR for Compound **III-XIX**

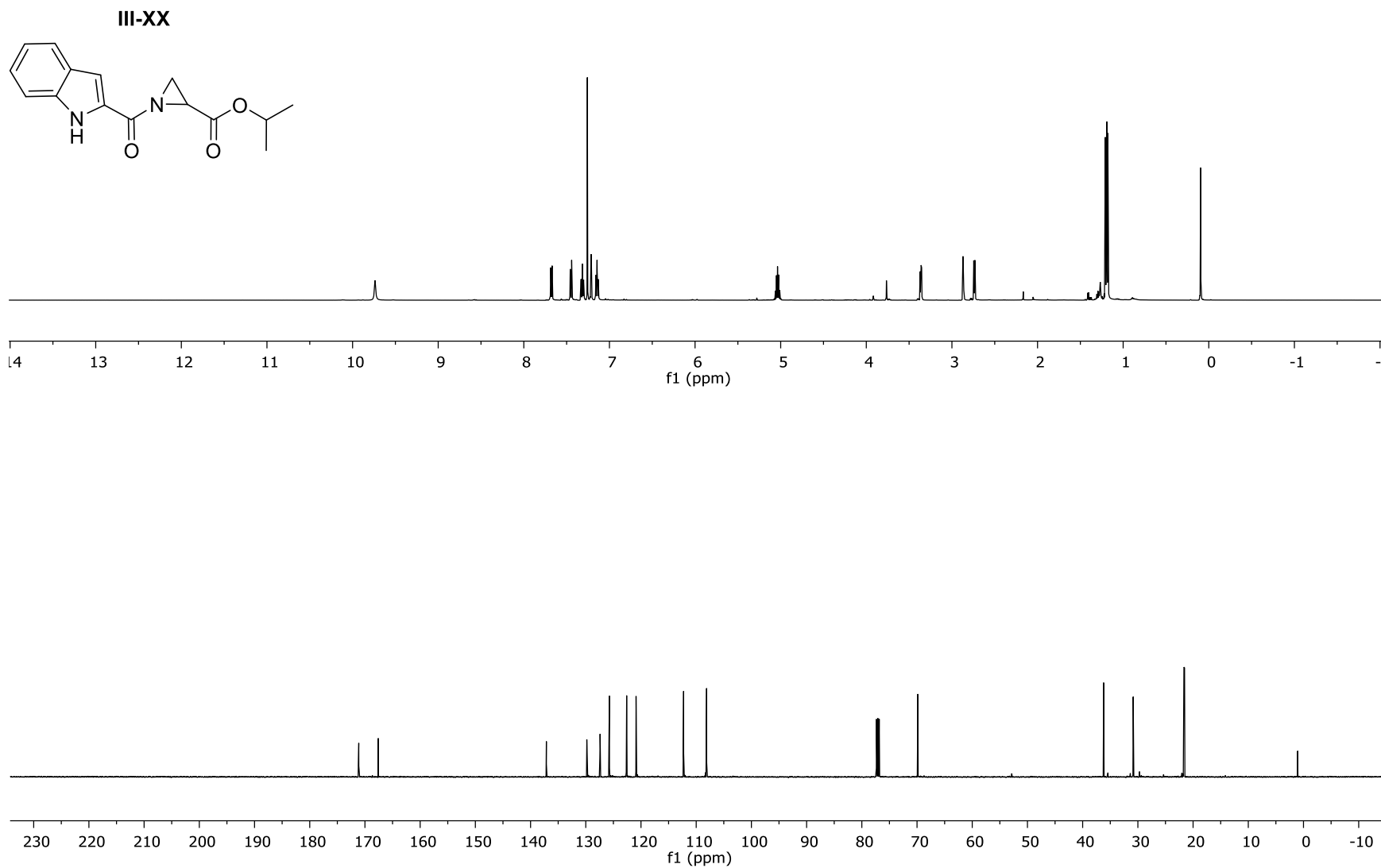


Figure III-LVIII: The ^1H NMR and ^{13}C NMR for Compound **III-XX**

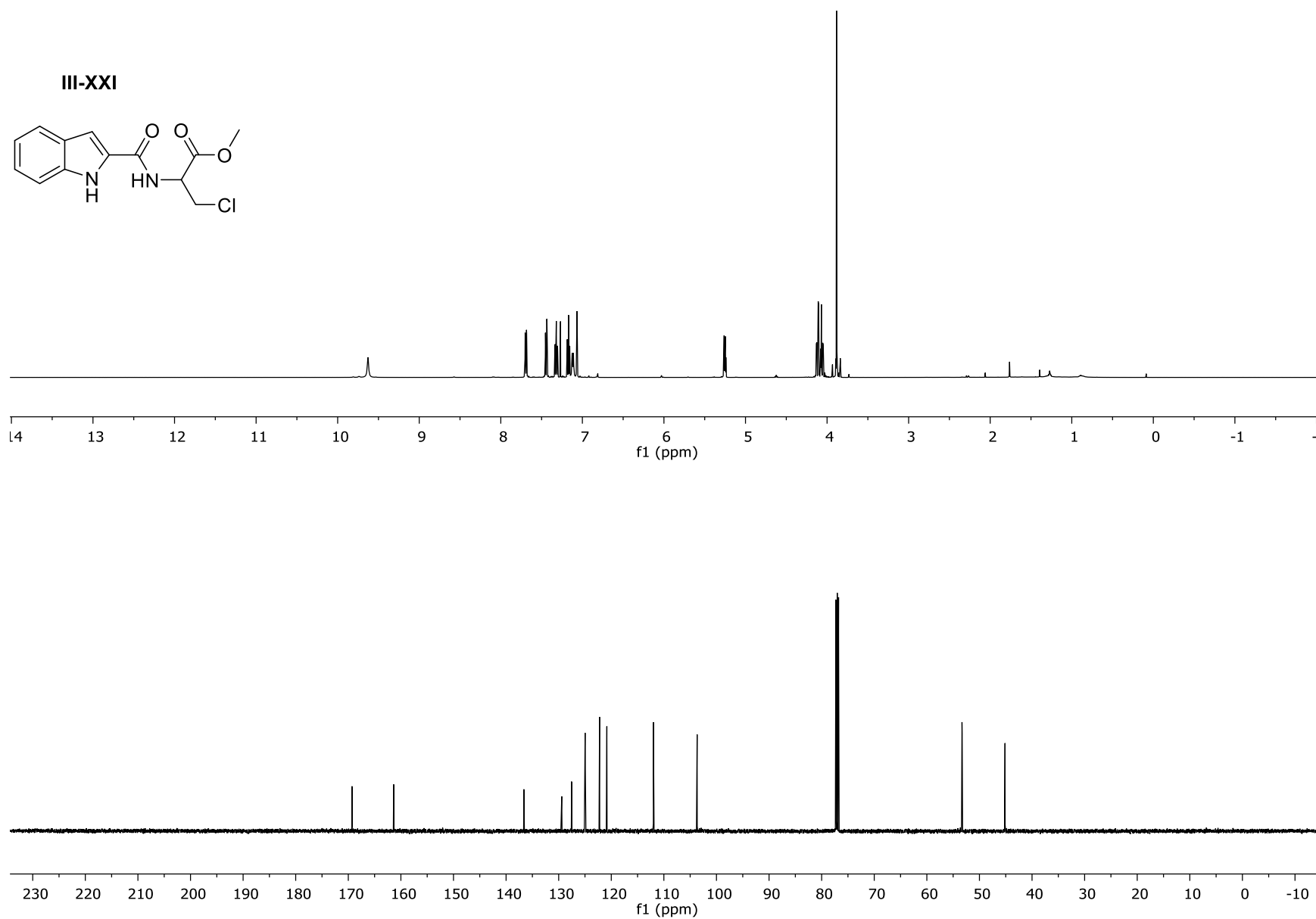


Figure III-LIX: The ^1H NMR and ^{13}C NMR for Compound III-XXI

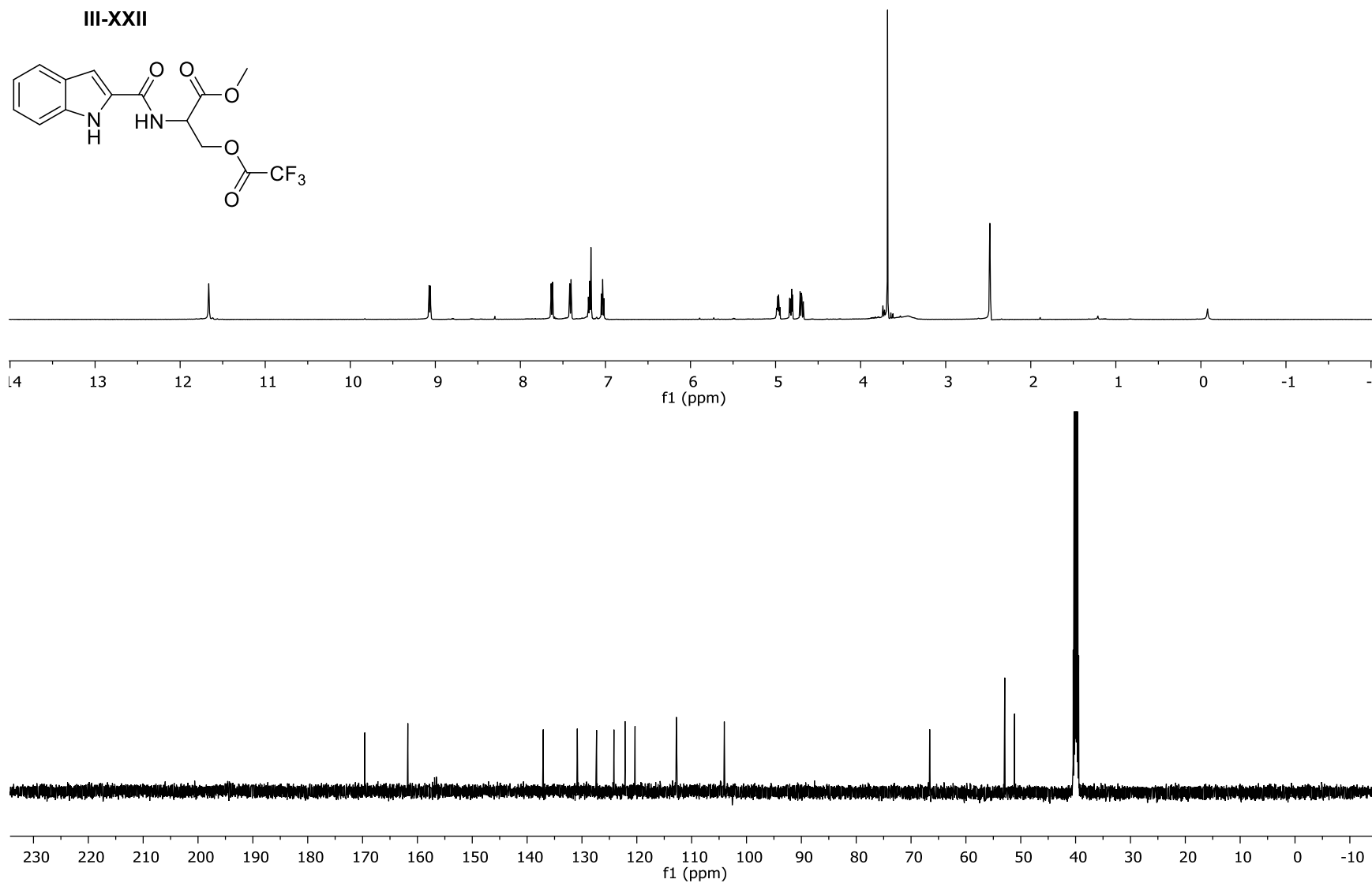


Figure III-LX: The ^1H NMR and ^{13}C NMR for Compound III-XXII

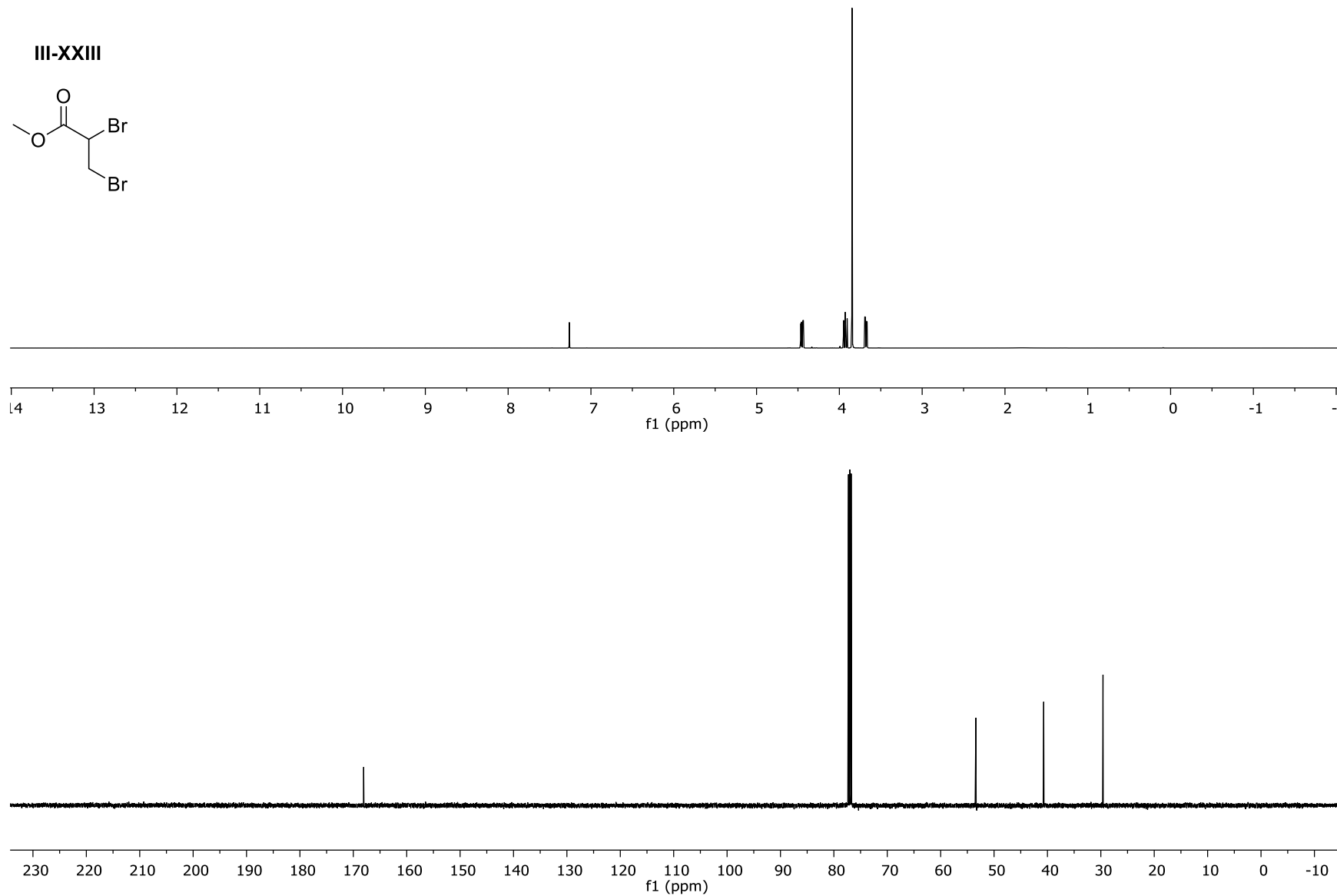


Figure III-LXI: The ^1H NMR and ^{13}C NMR for Compound III-XXIII

III-XXIV

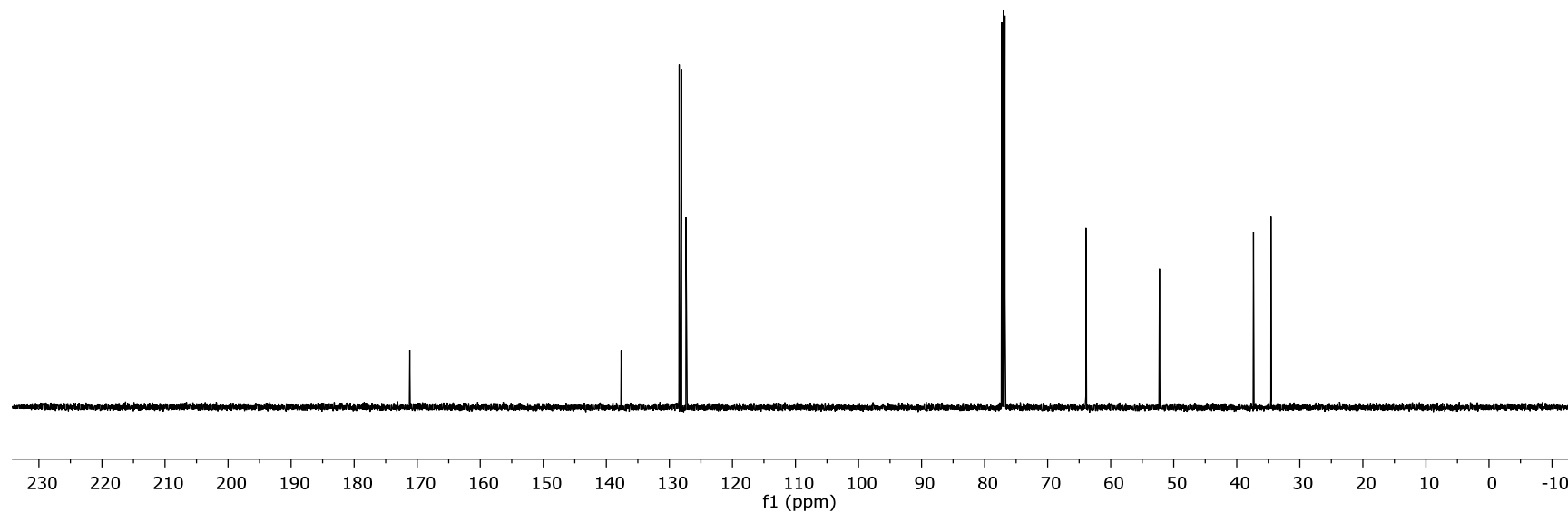
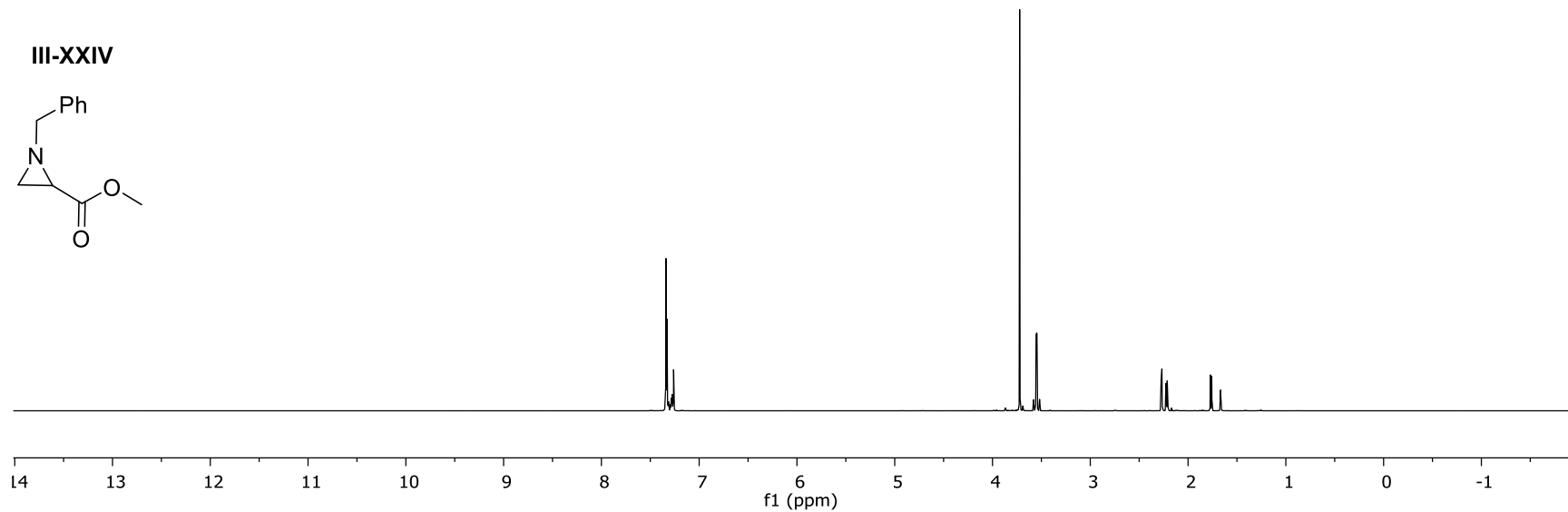
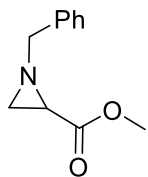


Figure III-LXII: The $^1\text{H NMR}$ and $^{13}\text{C NMR}$ for Compound III-XXIV

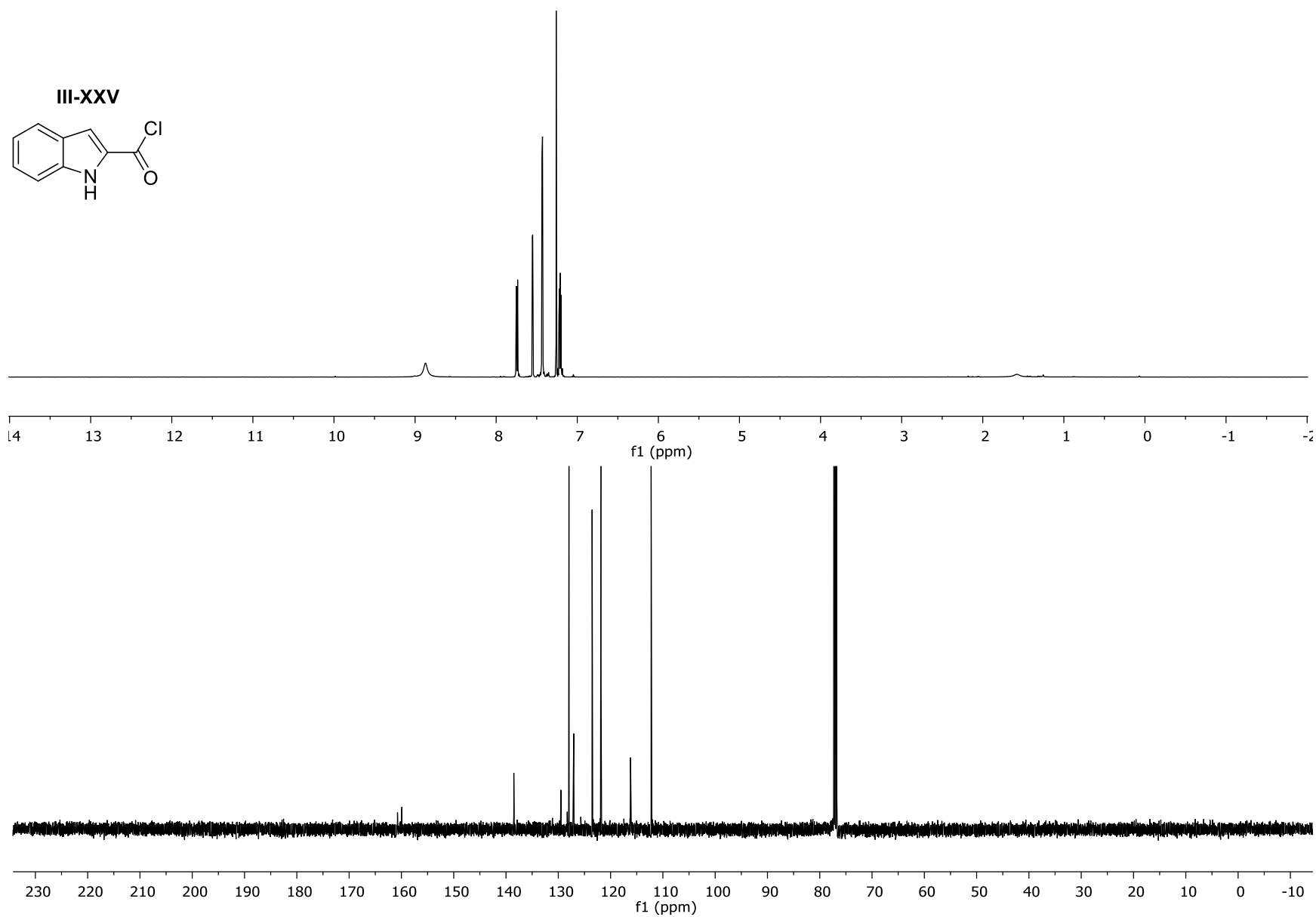


Figure III-LXIII: The ^1H NMR and ^{13}C NMR for Compound **III-XXV**

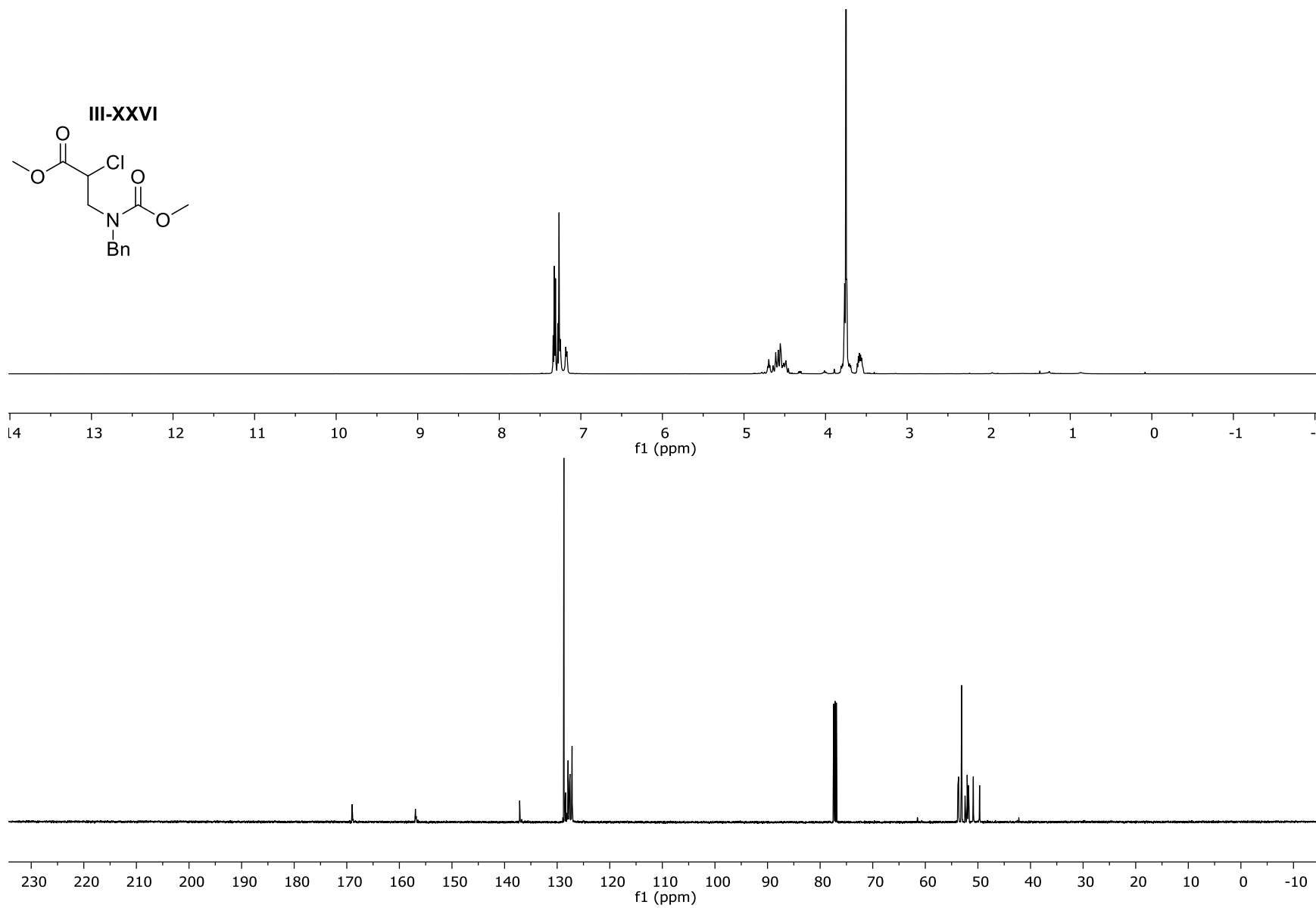


Figure III-LXIV: The ^1H NMR and ^{13}C NMR for Compound **III-XXVI**

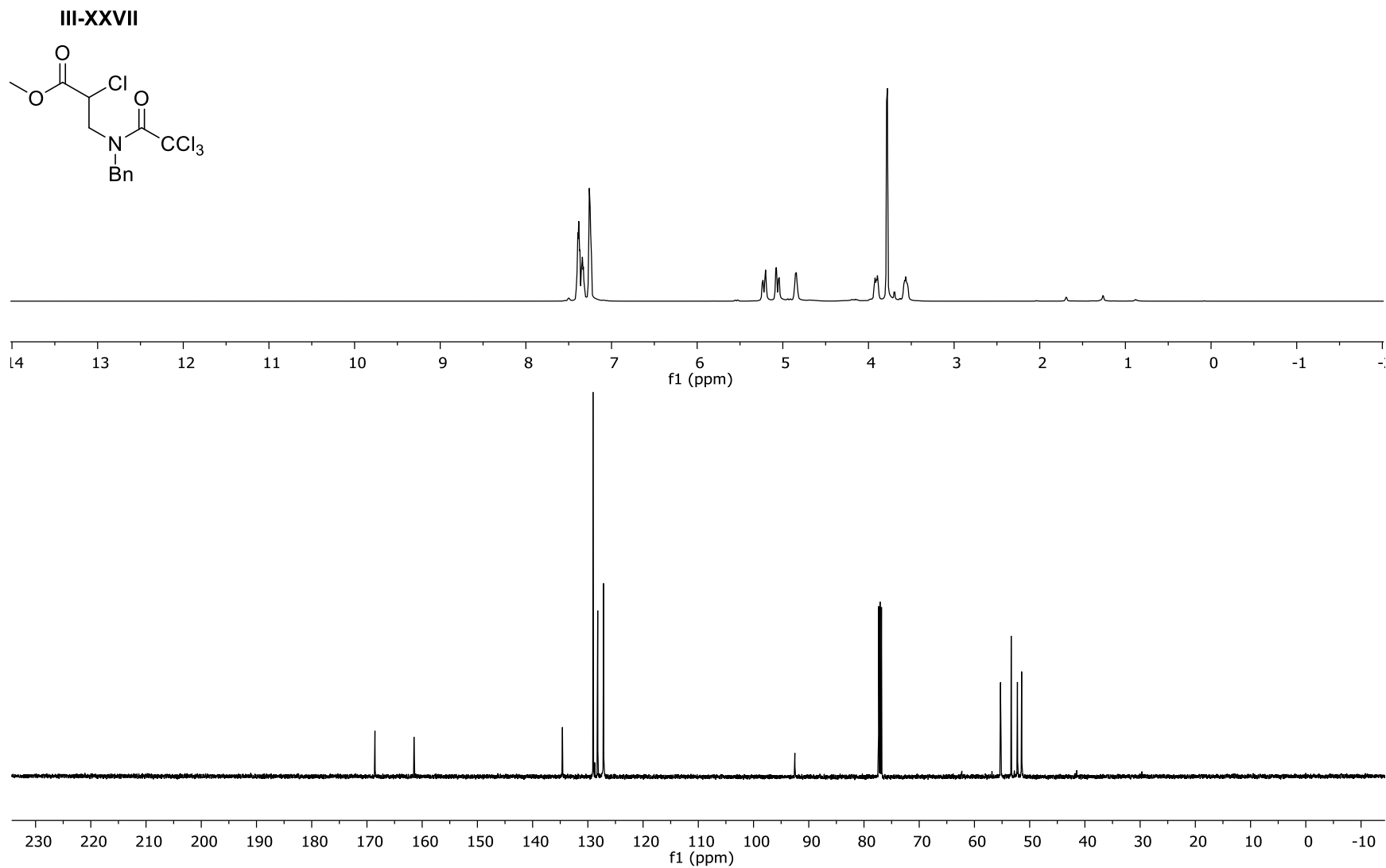


Figure III-LXV: The ^1H NMR and ^{13}C NMR for Compound **III-XXVII**

III-XXVIII

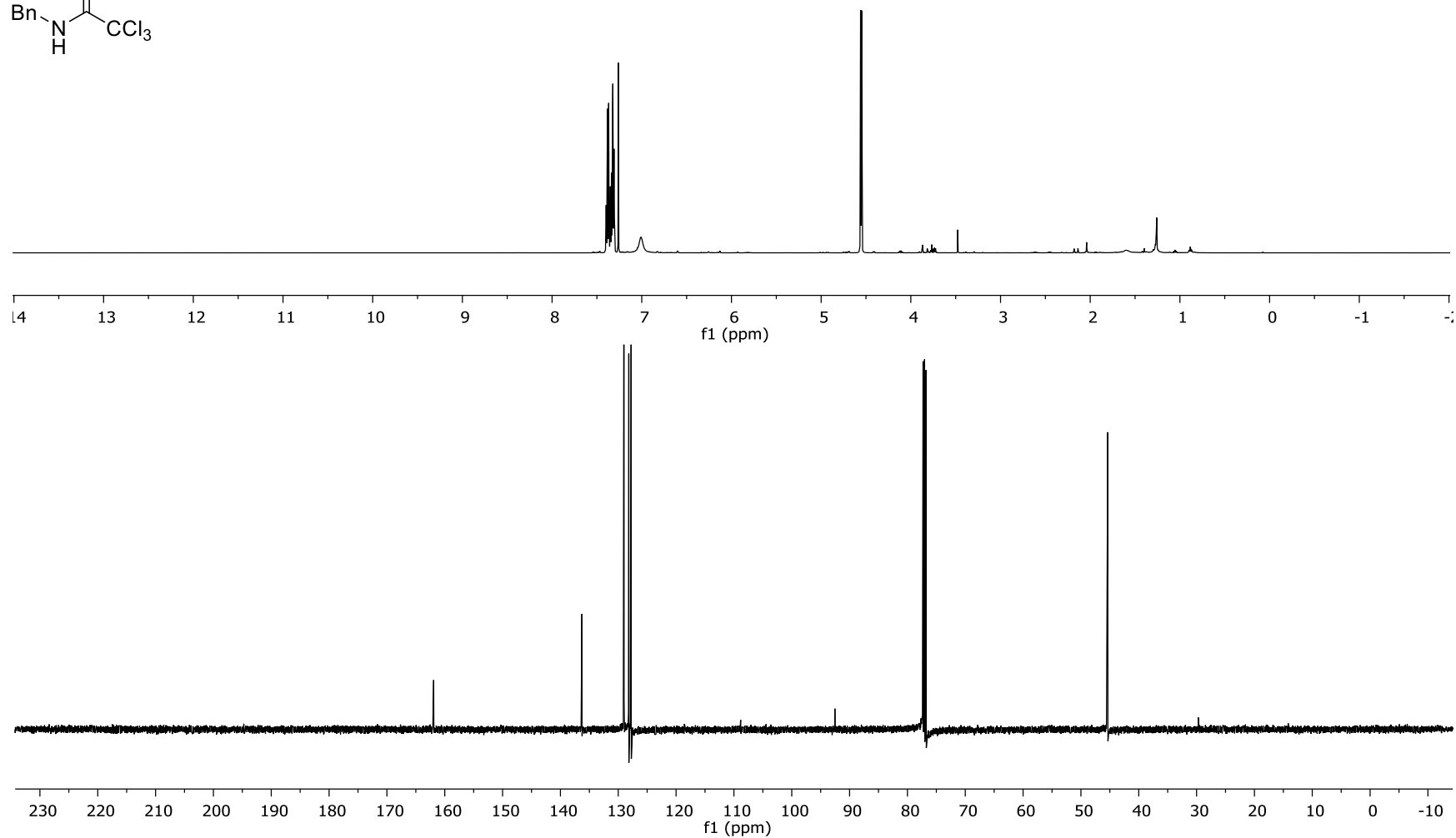
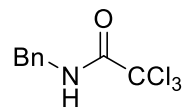


Figure III-LXVI: The ^1H NMR and ^{13}C NMR for Compound III-XXVIII

III-XXIX

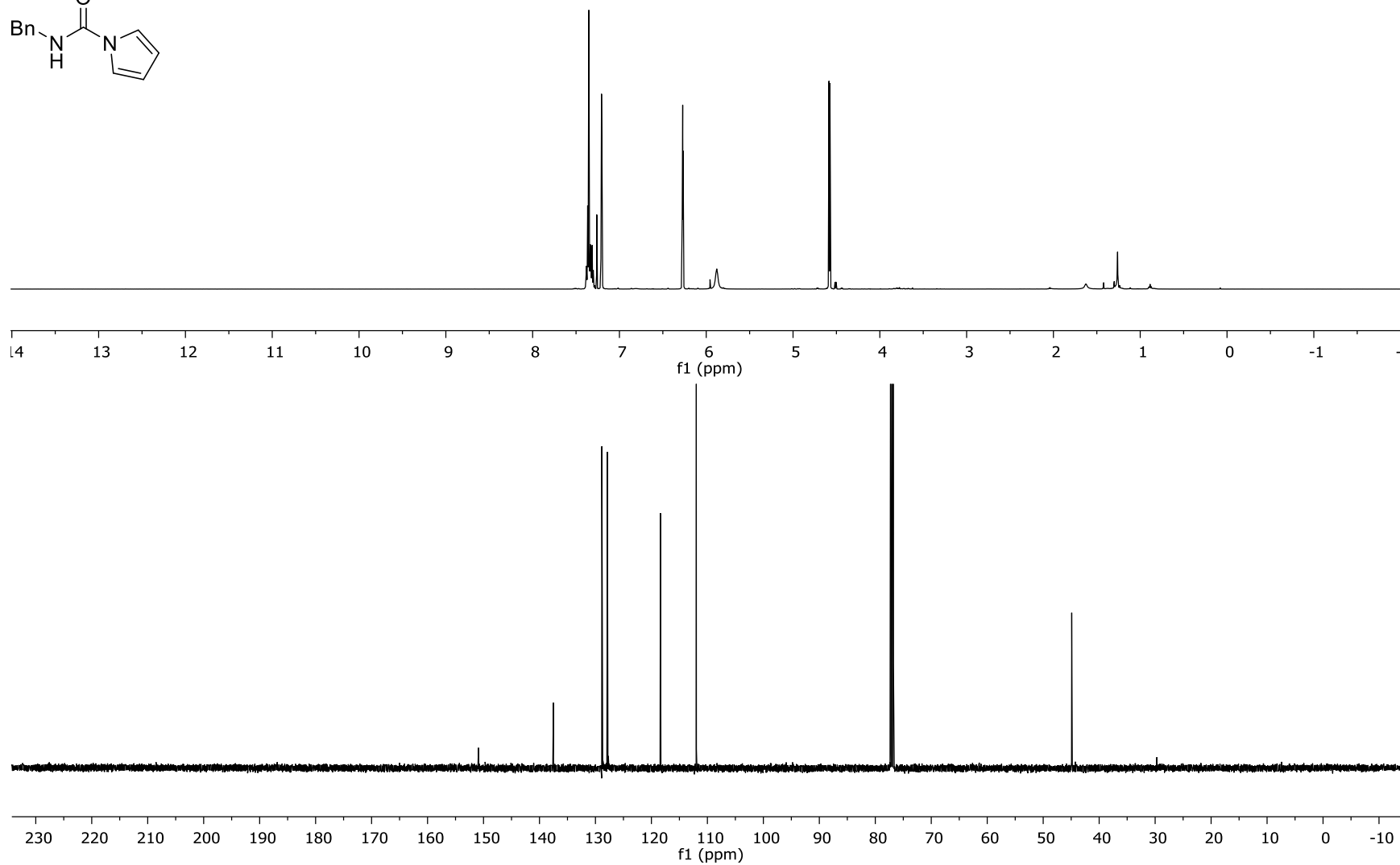
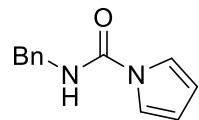


Figure III-LXVII: The ^1H NMR and ^{13}C NMR for Compound III-XXIX

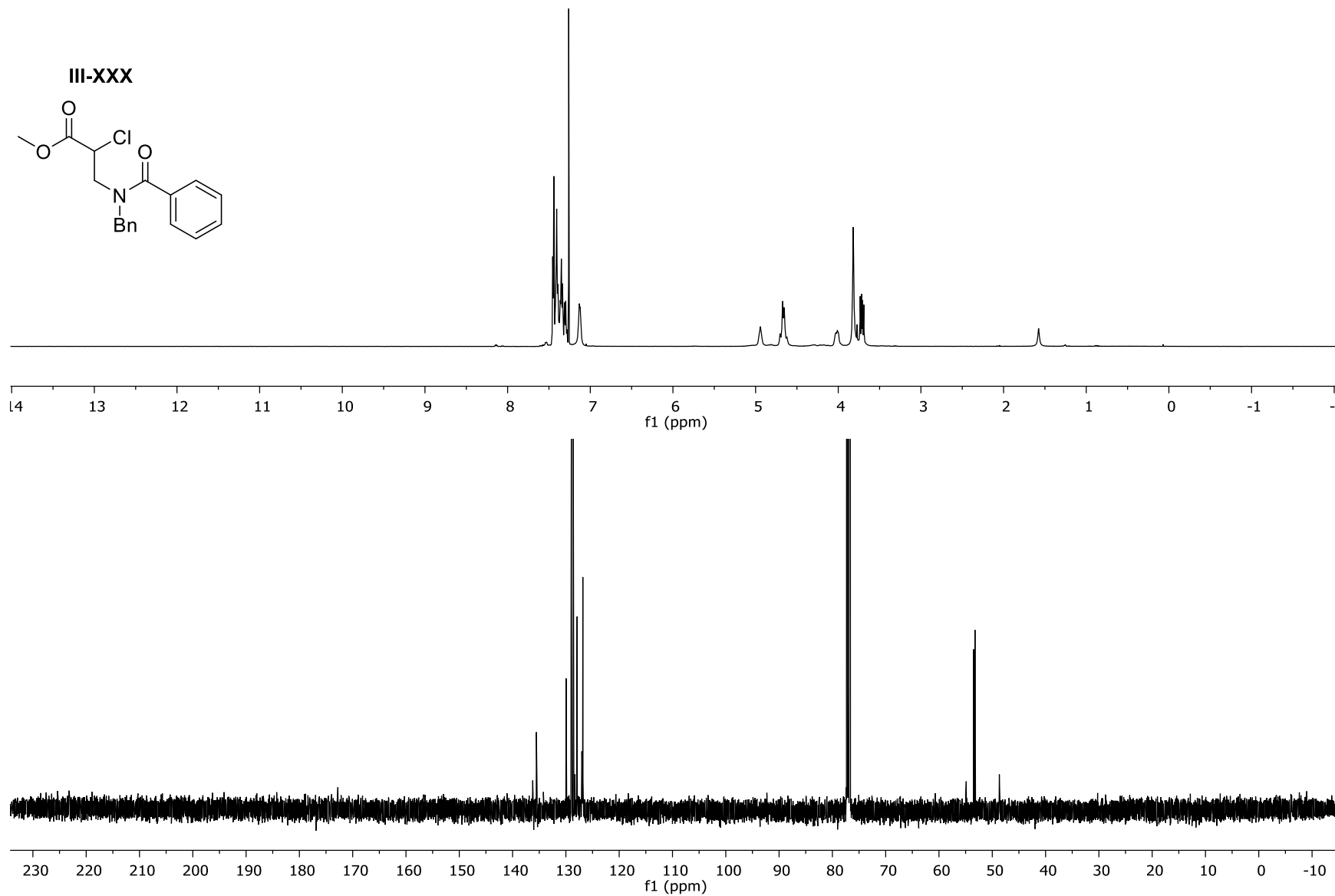
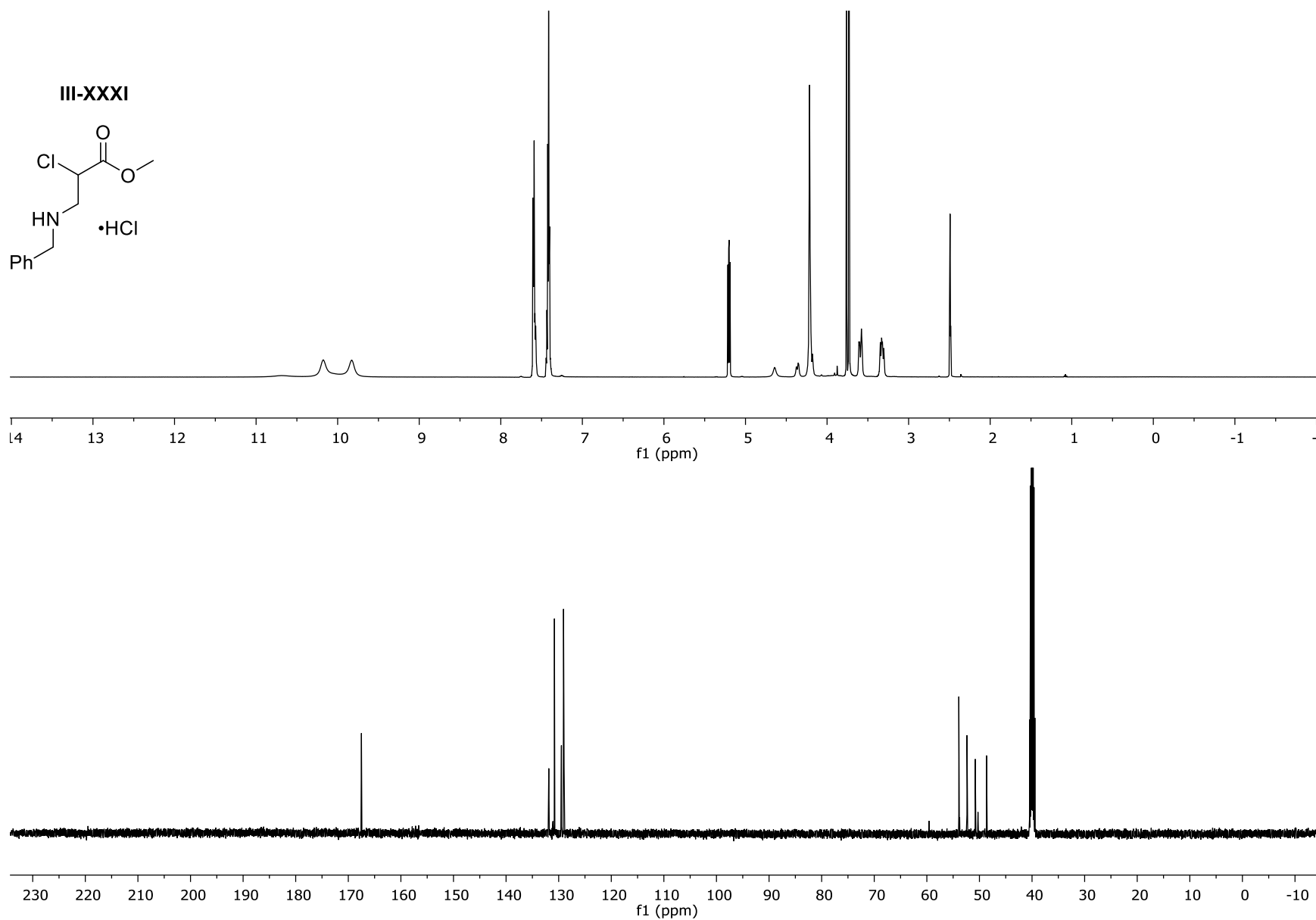


Figure III-LXVIII: The ^1H NMR and ^{13}C NMR for Compound **III-XXX**



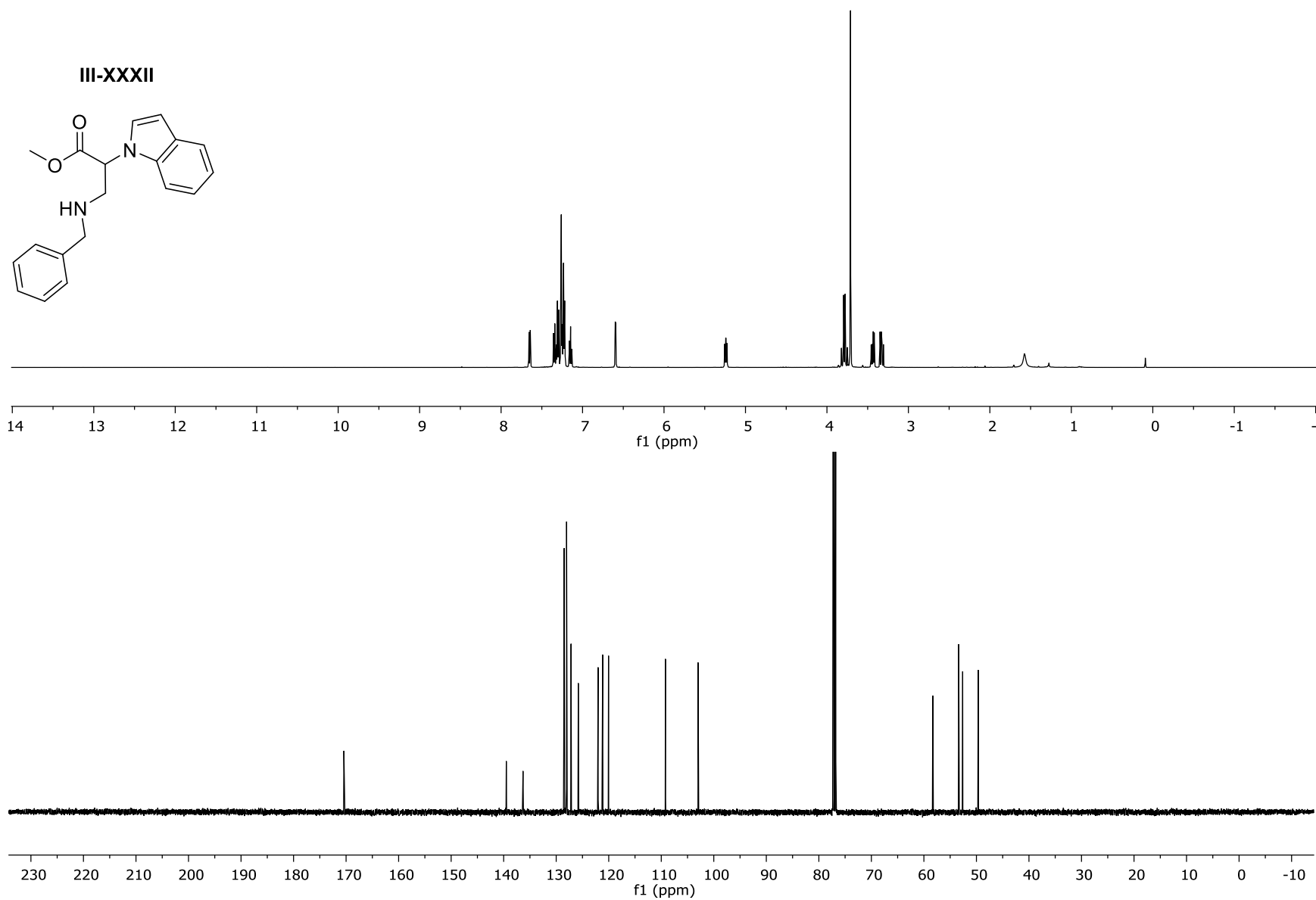


Figure III-LXX: The ^1H NMR and ^{13}C NMR for Compound **III-XXXII**

CHAPTER FOUR – OLEFIN ACTIVATION OF α,β UNSATURATED SYSTEMS

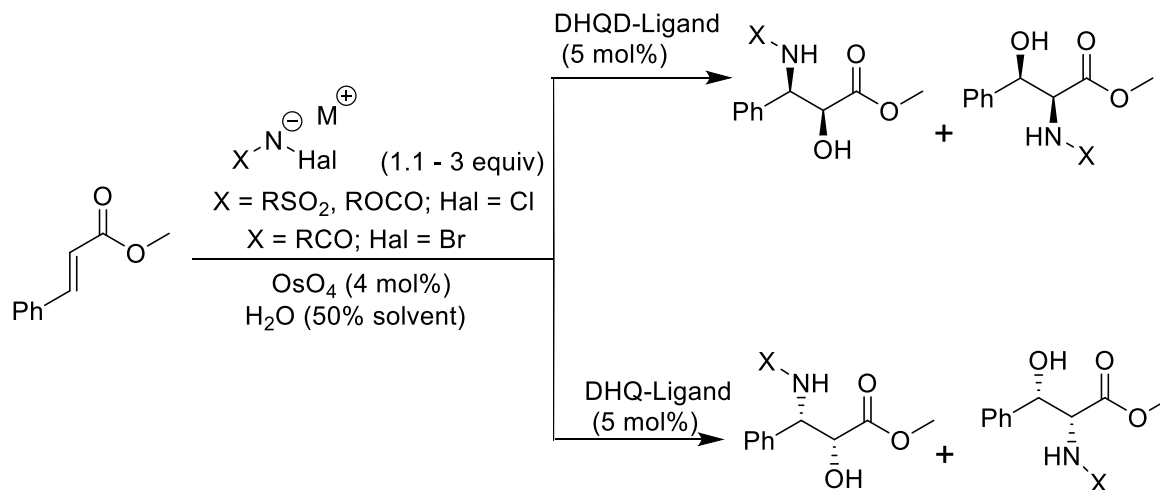
Recent publications and research within the Tepe group have both highlighted the relationship between activity in proteasome inhibitors and the substitution pattern of small molecule heterocycles. Based on these experimental results, it was proposed that further development of synthetic methodology was necessary to better access these scaffolds. Methodology development would give access to small libraries that could be quickly screened against various cell lines to identify reactive molecules. High throughput screening would also allow new avenues for research by identifying new diseases that the synthesized molecules are applicable to. Work in this chapter will highlight the methods approached to access these small molecules with work focusing around olefin activation. These reactive intermediates were approached to yield cyclized heterocycles. Initially it was proposed that methods of olefin activation can have multiple uses, accessing both heterocycles as well as giving access to aminoalcohols and diamines. Both of these systems can be accessed from the hydrolysis of heterocycles and offer an unique opportunity to access these problematic systems, in a few steps from cheap commercially available starting materials.

Innovation in the field of hydroxyamination and diamination, stems from the utility of the diamine and aminoalcohol functional groups, which are wide spanning due to them encompassing various subsets of both organic and organometallic chemistry. Natural product isolation continues to identify molecules from various families that possess the diamine or aminoalcohol motifs. The presence of these groups, in structurally diverse products continues to compel the development of novel retrosynthetic strategies and the advancement of synthetic methodology to afford the transformations, with functional group tolerance. Apart from this, direct functionalization allows

for new opportunities for ligand design, in forming metal-ligand complexes that can be used to perform unique transformations. The activity of isolated natural products or synthesized molecules have drawn focus to the growing need for continued methodology development towards diamination and hydroxyamination.¹⁰³⁻¹⁰⁴ The activity of many compounds is due to presence of these functional groups and are important pharmacophores utilized in efficacy modification, and drug synthesis. These reasons coupled with the wide array of commercially available olefin starting materials, and synthetically accessible olefins through Wittig chemistry have been responsible for the initial development of approaches towards olefin transformation. Throughout literature two common themes for olefin transformations are represented, direct and indirect functionalization, with both having pros and cons. Some of which are factors like functional groups and overall structural composition, to accessing this transformation that requires either the re-vamping of older ideas, or a new modern approach to address olefin activation.

One key example of the effort towards amino hydroxylation of olefins is seen in the sharpless asymmetric aminohydroxylation (SAA). In comparison to extensively studied transformations that yield identical heteroatom addition, the addition of two different heteroatoms is still a developing field. This is due to issues with controlling the regioselectivity and stereoselectivity of the product. Through the use of a d^0 transitional metal catalyzed pathway, reactions in the presence of chiral ligands cause the sequential transformation to aminoalcohols, via syn-addition, in moderate to good yields with high enantioselectivity. This reaction uses osmium tetroxide to generate an *in-situ* imidotrioxoosmium intermediate that undergoes a coordination and attack of the olefin species. This results in an osmium (VI) intermediate that is readily hydrolyzed to the aminoalcohol product. This transformation although powerful does possess limitations in its regioselectivity, enantioselectivity, and chemoselectivity. Mixtures of

regioisomers can occur within the isolated product of monosubstituted alkenes. The enantioselectivity of the reaction can be perturbed by the sterics of reactant molecules, and side reactions cause the formation of the diol product. The environmental effects and economic costs of transition metal mediated reactions as well as the metal's toxicity, give significance to development of alternative functionalization.¹⁰⁵⁻¹⁰⁹

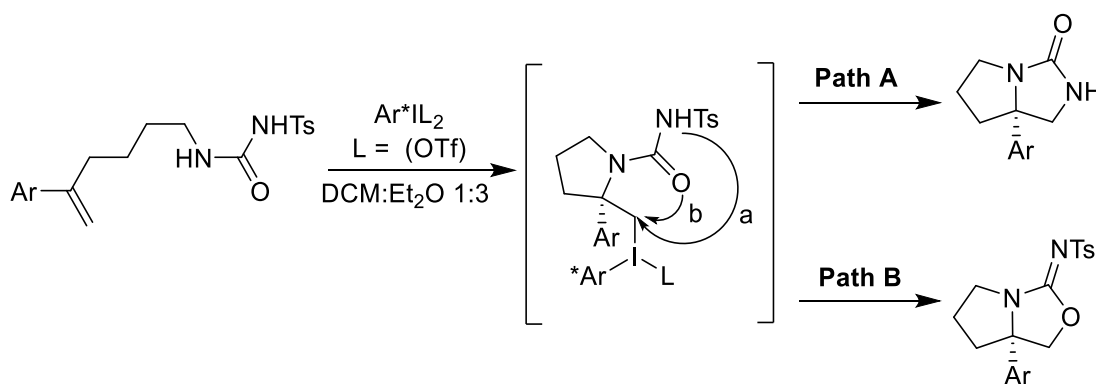


Li, G.; Chang, H. T.; Sharpless, K. B. *Angew. Chem.* **1996**, *108*, 449-452
 Li, G.; Chang, H. T.; Sharpless, K. B. *Angew. Chem. Int. Ed.* **1996**, *35*, 45-454

Figure IV-I: The sharpless asymmetric aminohydroxylation reaction.

The addition of hypervalent iodine reagents allow for olefin activation towards multiple carbon nucleophile bonds, under mild reaction conditions without the need for transition metal catalysis. These compounds operate by manipulating the hyper leaving group ability of iodine (III) compounds. These hypervalent iodine species can be generated from their iodine (I) counterparts. Incorporation of these highly electrophilic compounds is used by double displacement agents or bi-functional nucleophiles, to form aminoalcohols or diamines. Chiral iodine reagents cause asymmetric induction and result in overall stereoselective addition of the agent to the olefin. Tuning the sterics surrounding the iodine agent result in adjustments in the regioselectivity of the

reaction. Steric encumbrance around the iodine source creates a smaller overall pocket when forming the iodonium ion. This allows only small nucleophiles to displace the iodine reagent. One of the few drawbacks to applications of this method is the need of stoichiometric hypervalent iodine species to evoke the sequential transformation.¹¹⁰⁻¹¹¹



Farid, U.; Wirth, T *Angew. Chem. Int. Ed.* **2012**, *51*, 3462-3465

Figure IV-II: Hypervalent iodane mediated aminohydroxylation.

Another example is the formation of aziridines, which is a common method of an indirect transformation towards diamines and aminoalcohols. Aziridines offer a variety of synthetic applications towards nitrogen containing compounds and are valued in synthetic approaches based on their highly regioselective and stereoselective ring opening reactions. Formally nitrene like nitrogen sources have been used to functionalize olefins towards both metal and metal free aziridinations. Both methods tolerate electron rich, neutral and electron poor olefins transformations. Metal catalyzed aziridinations involve the formation of the reactive sulfonylimidoiodinane. This species in the presence of a catalytic transition metal produces a convenient nitrene source that ultimately results in aziridine formation. This reaction has been extensively studied, focusing on more efficient metal-aziridine systems towards asymmetric azidations, but still possesses drawbacks in its application. A large concern is the amount of PhI

that is produced as a side product that has to be oxidized to the iodane species with stoichiometric amounts of oxidant. The preparation and solubility of the imidoiodane species also hinders the overall application of this methodology towards large scale synthesis. Those coupled with the lack of function diversity in the overall imidoiodane species once generated has given rise to alternative methods of azirinidation. Iodine and CuI mediated processes have shown rapid reactivity towards formation of an iodonium species in the presence of Chloramine-T and an olefin that is then subsequently substituted to yield the desired aziridine. However, Chloramine T is only available as the trihydrate salt so reactions that require moisture free conditions are hazardous to this methodology due to Chloramine-T's explosive ability when thoroughly dried.¹¹²⁻¹¹³

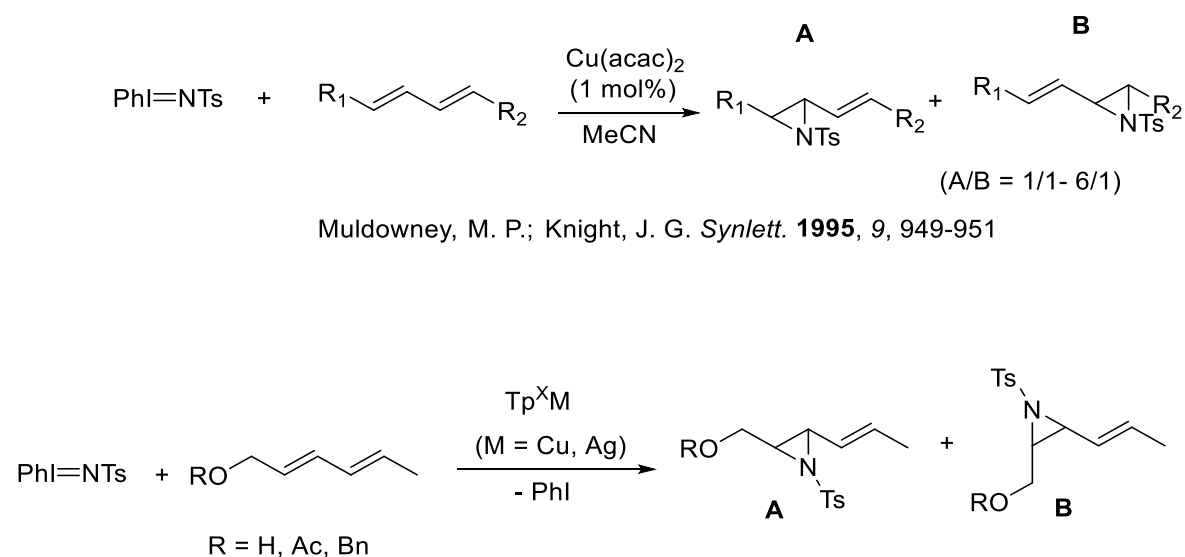
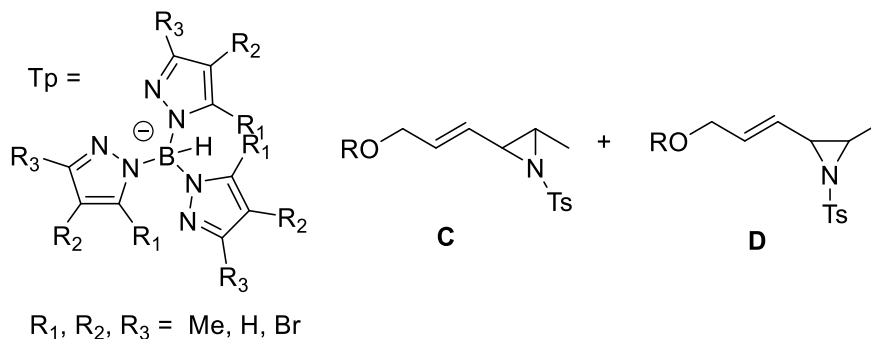


Figure IV-III: Copper-mediated N-tosylaziridination of olefins.

Figure IV-III cont'd



Llaveria, J.; Beltran, A.; Diaz-Requejo, M. M.; Matheu, M. I.; Castillon, S.; Perez, P.
J. Angew. Chem. Int. Ed. **2010**, *49*, 7092-7095

Current literature highlights two main approaches to invoke olefin functionalization of olefins to aminoalcohols and diamines. These methods either focused on strategic synthesis of key intermediates or the development of novel functionalization methodology.¹¹⁴⁻¹¹⁶ Either of these approaches would allow for activation and subsequent transformation of the olefin system. Both these approaches have been utilized within the Tepe lab. In one case, strategic synthesis of key intermediates afforded the desired transformation, through the formation of a bromonium intermediate. This was the key step in cyclic guanidine addition to access Dibromophakellin, one of the members of the highly sought after oroidon family of alkaloids.⁶⁵ This key intermediate was designed to mimic enamines in their nucleophilicity towards bromonium formation. Bromonium opening by a nucleophilic guanidine would result in product formation. Analysis of the product identified an alternative route to natural product synthesis in which the introduced guanidine being the strongest nucleophile, was brominated and sequentially attacked by the enamine double bond. Cyclization then produced the N-protected Dibromophakellin. The reactivity of both mechanisms for this product stem from the designed nucleophilicity of the intermediate. Efforts towards

accessing other members of the same alkaloid family, like Cylindridine-A using this approach are still of interest within the group.

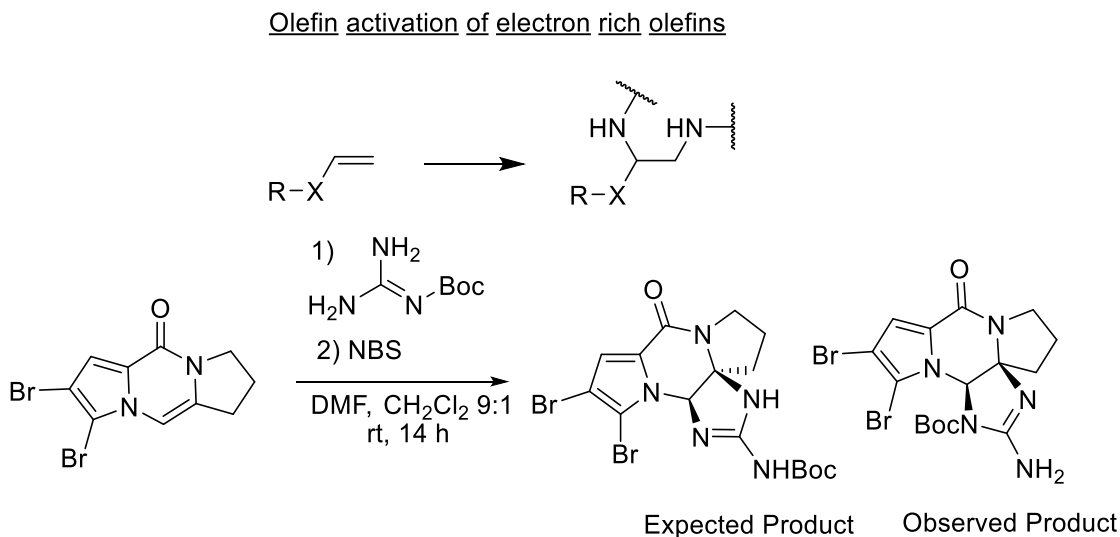


Figure IV-IV: Electron rich olefin diamination masked as 2-aminoimidazolines.

Alternative methodology for olefin functionalization is necessary to induce transformations to aminoalcohols and diamines when the system lacks electron donating groups, to increase its nucleophilicity. Motivated by the work of Heasley,¹¹⁷⁻¹¹⁹ the need for brominating reagents tuned for activity with neutral olefins was identified. Efforts within the group focused on the development of a bifunctional bromonium agent which could activate olefins with similar reactivity to styrene, an olefin with moderate activity. This NBS-like analog would allow delivery of a bromonium to the olefin and after which intermolecular opening by the imide nucleophile would result in an amino halogen intermediate. These systems can be further manipulated to access diamines and amino alcohols by halogen displacement under various conditions. The decreased reactivity in comparison to electron rich olefins, towards bromine capture and bromonium formation was countered by the addition of a catalytic amount of $\text{BF}_3 \cdot \text{OEt}_2$, which made the

brominating agent more reactive. Bromonium opening by the succinimide nucleophile resulted in the anti-addition product. Under neat conditions and heat, cyclization of one of the nitrogen's carbamate groups and subsequent demethylation resulted in the formation of 2-oxooxazolidines. These 2-oxooxazolidine compounds can be hydrolyzed under basic conditions to access aminoalcohols.⁷⁶

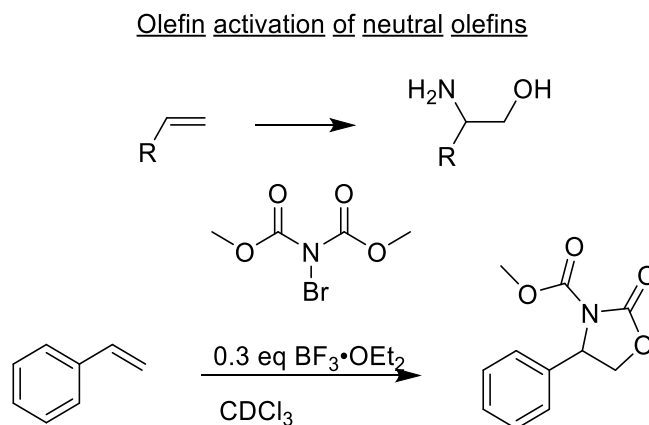


Figure IV-V: Aminobromination of neutral olefins.

In both cases either substrate, reagent electronics or sterics were manipulated to afford the desired reactivity that allowed for cyclization to products that contained the aminoalcohol or diamine motif. However, both cases allow the functionalization of only electron rich or neutral olefins. These techniques do not account for a key third situation, the activation of an electron withdrawn olefin, like α , β unsaturated olefin systems. I will discuss my progress towards the functionalization of electron withdrawn olefins, and conclude the attempts by the Tepe group toward olefin functionalization.

Olefin activation towards the synthesis of small molecule heterocycles as well as amino alcohols and diamines was spurred by the experimental results of Indolophakellin. Testing with

purified h20S identified that the activity of the compound was tied to the presence on the 2-aminoimidazoline core of the Indolophakellin structure.

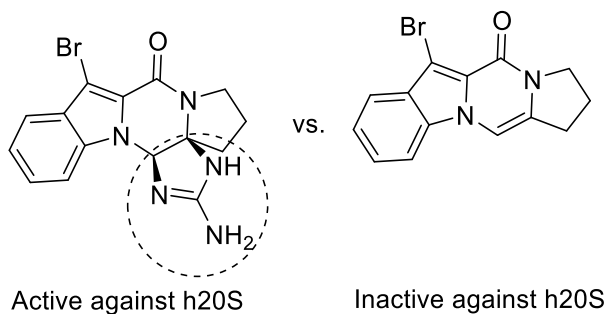


Figure IV-VI: Shows the difference in activity based on the presence of 2-aminoimidazoline core

This key observation motivated further research into designing another methodology to quickly access these 2-aminoimidazoline and similar cores on α, β unsaturated systems. With these synthetic analogs in hand, further research could be done to evaluate what functional groups would be necessary for potent inhibitors. It was proposed that a Baylis-Hillman like reaction would occur with α, β unsaturated system by either S_N2 or S_N2' displacement seen in the synthesis of Dibromophakellin and net the desired product.¹²⁰⁻¹²²

Baylis Hillman reaction

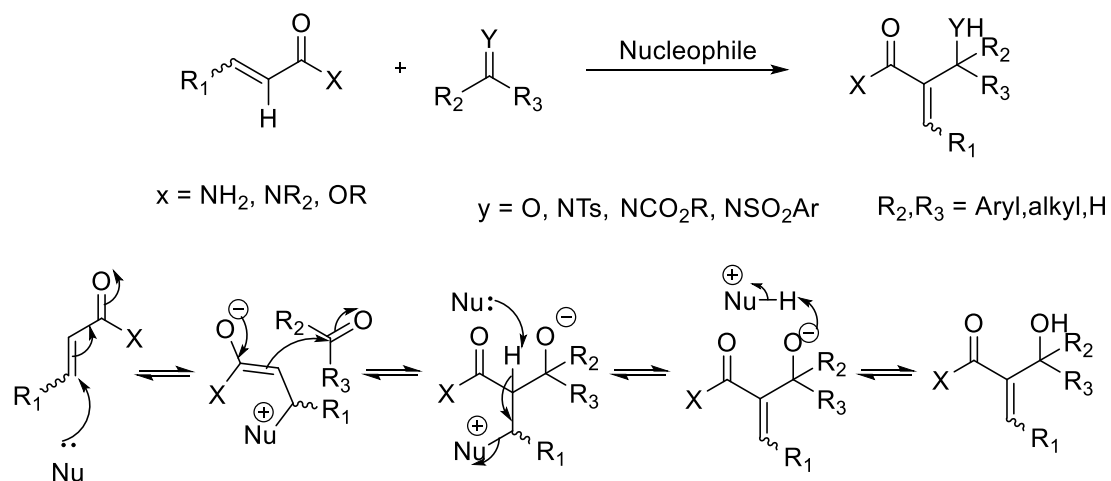
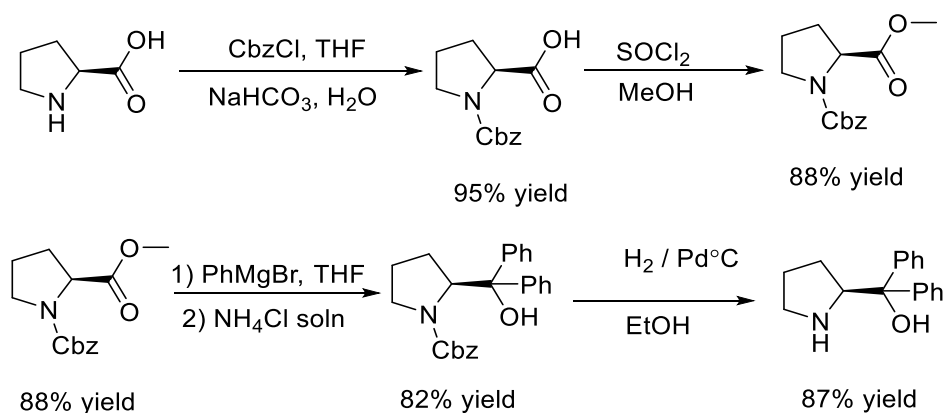


Figure IV-VII: The mechanism of the Baylis-Hillman reaction.

Previous work towards synthesizing derivatives of Agesamides A and B in chapter three focused on a 1,4 addition to an activated α,β iminium intermediates. The iminium intermediate was generated by the addition of acrolein to the secondary amine catalyst. The catalyst was accessed by the following synthetic steps.



Scheme IV-I: Chiral catalysis synthesis for asymmetric aziridination.

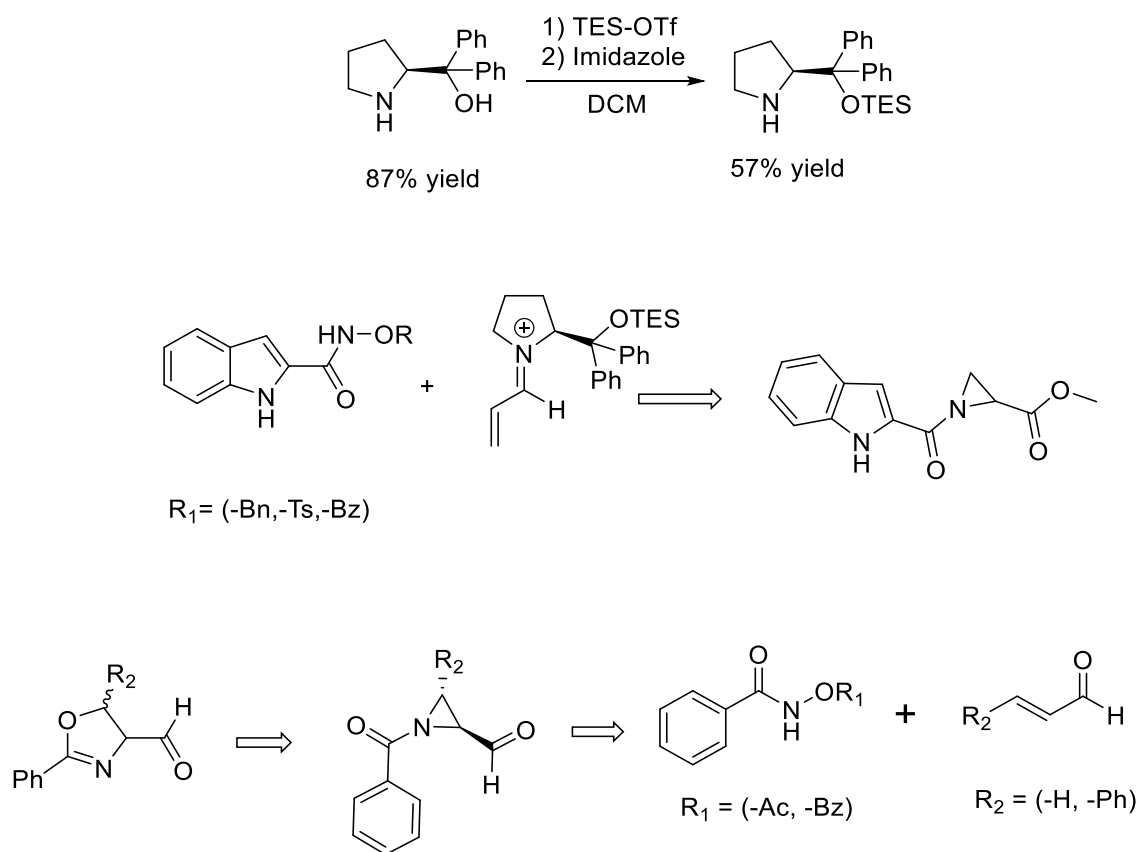
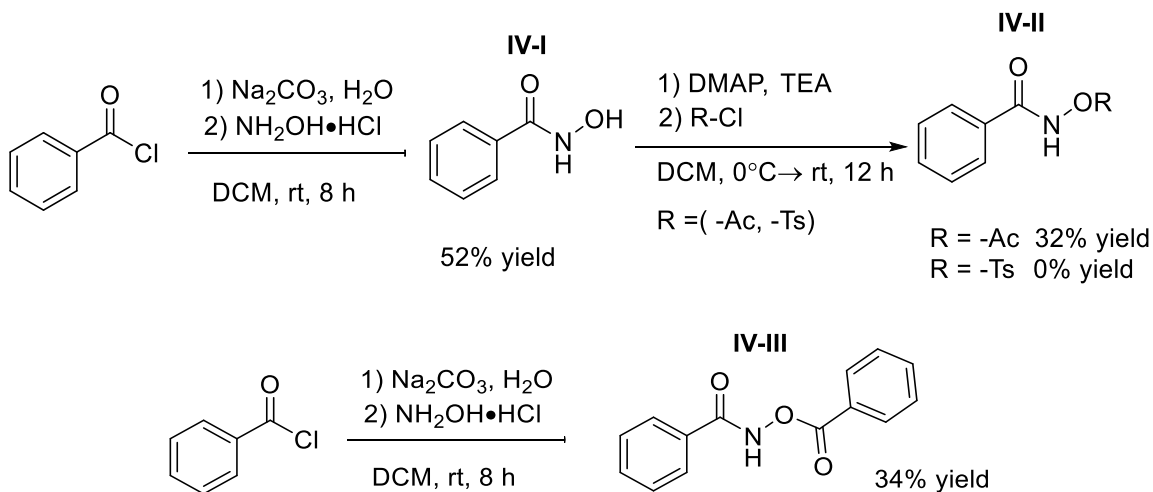


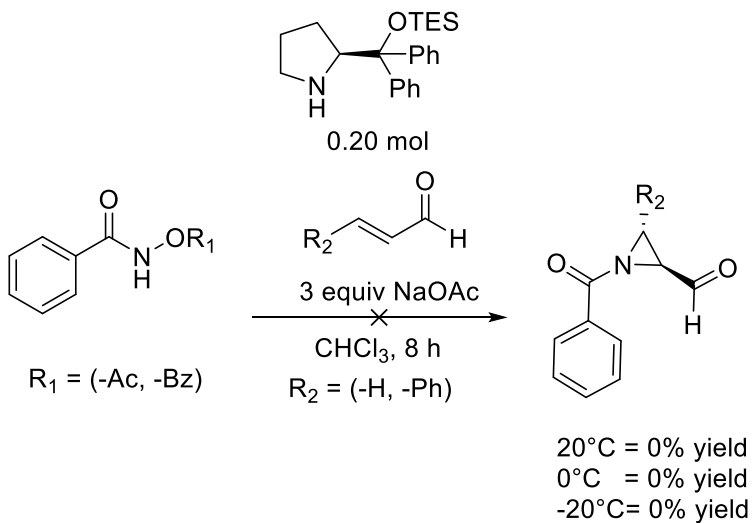
Figure IV-VIII: Proposed pathway towards 2-oxazoline formation

This expansion could not be probed because the synthesis of the tosylated starting material only resulted in decomposition. It was postulated that the reactivity of the -OTs group might be responsible for product degradation and decomposition. This result was further confirmed when the synthesis of N-tosylxybenzamide was attempted. Only decomposition was observed when tosyl protection of N-hydroxybenzamide was attempted. The -OTs group was proven to be too reactive and dimerization was suspected reason for decomposition. To better temper the reactivity of the leaving group N-acetoxybenzamide and N-(benzoyloxy)benzamide were both synthesized and used as substrates.



Scheme IV-II: Synthesis of -OR functionalized hydroxyamides.

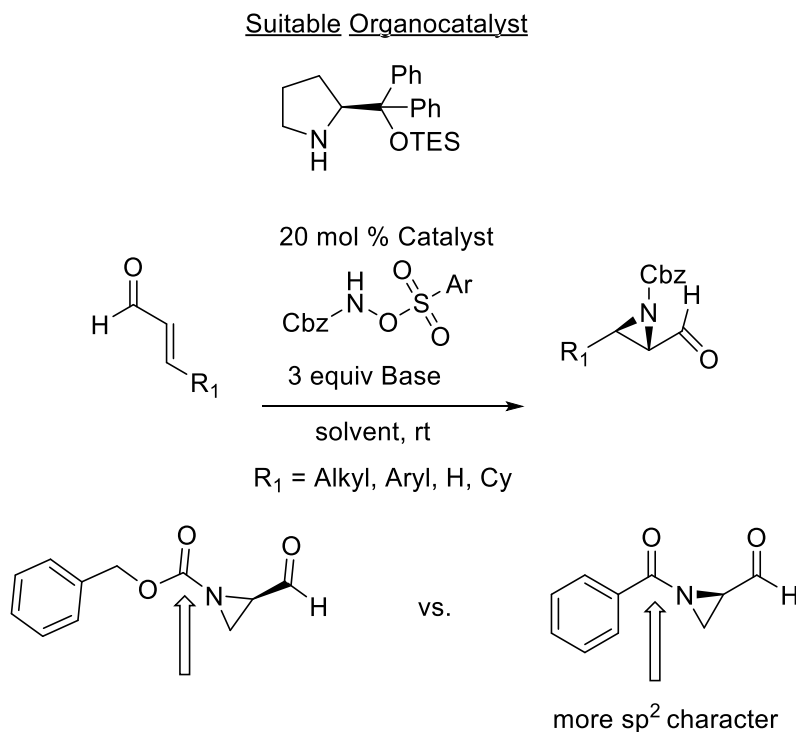
With the N-(benzoyloxy)benzamide decomposition of starting material occurred. N-acetoxybenzamide showed no product formation with only starting material being observed.



Scheme IV-III: Attempts at olefin functionalization using a chiral catalyst.

These results all point to a clear difference in the aziridine stability which is tied to protecting group on the aziridine nitrogen. The aziridine masked as the amide possesses more sp^2 character

with its lone pair being delocalized into the carbonyl carbon. This effect is lessened drastically due to the presence of the carbamate oxygen. This delocalization makes both carbons in the strained 3-member ring more δ^+ than its carbamate counterpart and prone to attack at either position. It's this aspect that is responsible for the decomposition that is observed when the reaction is completed.

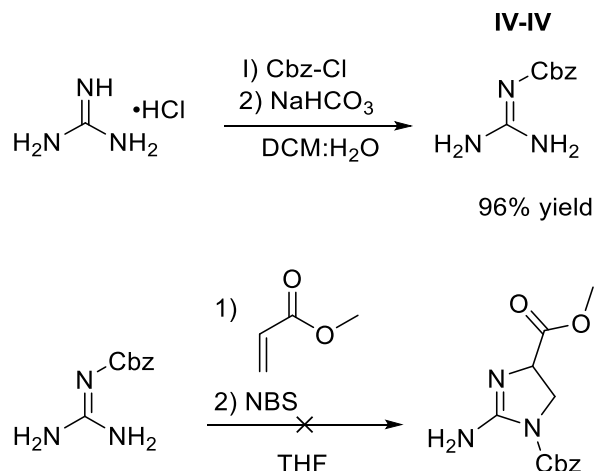


Arai, H.; Sugaya, N.; Sasaki, N.; Makino, K.; Lectard, S.; Hamada, Y. *Tetrahedron Lett.* **2009**, *50*, 3329-3332

Figure IV-IX: Displays difference in stability between aziridine structures.

Approach II

To further probe the mechanism of the desired transformation similar conditions to the successful cyclization of Dibromophakellin were applied. Guanidine was Cbz-protected and exposed to NBS in the presence of methyl acrylate.⁶⁵



Scheme IV-IV: Synthesis of Cbz-guanidine and attempted cyclization.

Addition of NBS to the solution of the Cbz-guanidine and methyl acrylate only resulted in decomposition. This was likely due to the dimerization of Cbz-guanidine with the brominated Cbz-guanidine.

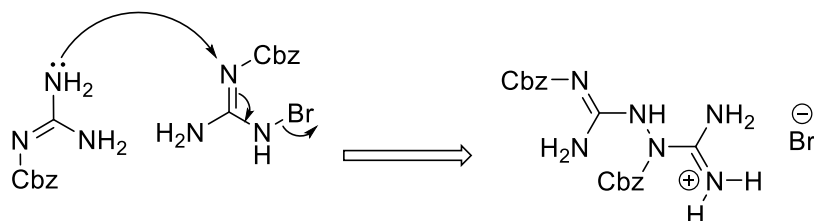
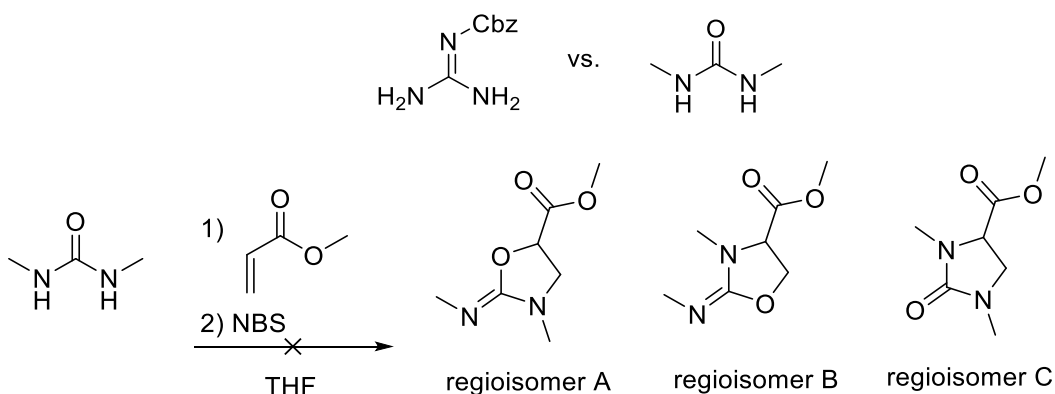


Figure IV-X: Identifies one pathway of dimerization of Cbz-guanidine.

To better develop the methodology for expansions 1,3-dimethylurea was selected as the new lead molecule in place of Cbz-guanidine. Both alkyl groups would aid in solubility and help with increasing its nucleophilicity but not to the extent of Cbz-guanidine. Because the nucleophilicity and basicity of 1,3 dimethyl urea is less than Cbz-guanidine the chance of dimerization was decreased.



Scheme IV-V: Identified that brominating and cyclization does not occur with only NBS.

Reacting 1,3 dimethylurea with an α,β unsaturated system like methyl acrylate in the presence of NBS resulted in no reaction. Lack of bromonium formation identified one of the major problems associated with activation α,β unsaturated systems, the lack of an electron-rich olefin to promote bromonium capture. This could be surmounted as shown in literature and a recent publication within the Tepe group through the generation of more reactive halonium source *in-situ*.⁷⁶

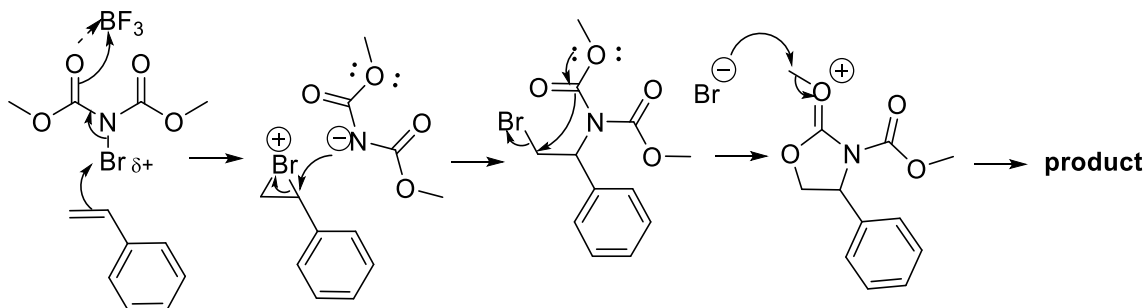
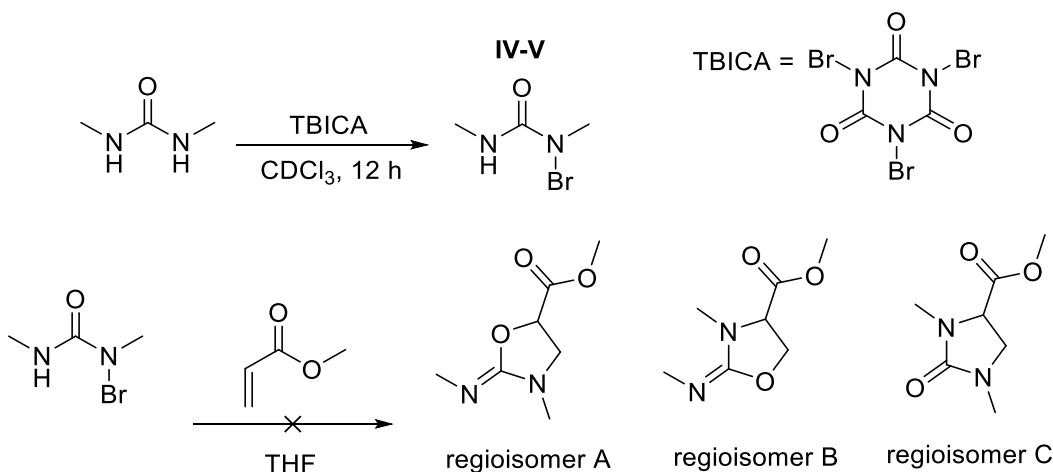


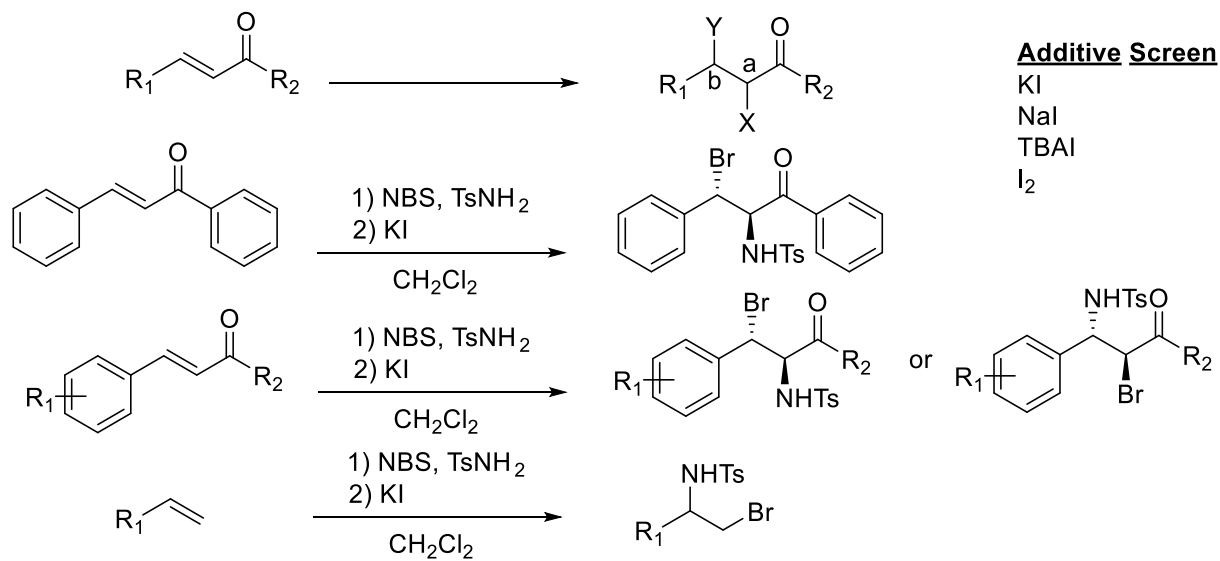
Figure IV-XI: Displays Lewis acid catalysis to form a more reactive Bromonium for cyclization.

The addition of the Lewis acid $\text{BF}_3 \cdot \text{OEt}_2$ resulted in the cyclization of the bromoimide reagent onto the starting material olefin. This resulted in an oxazolidinone. Pre-activation of the 1,3-dimethylurea was hypothesized to give access to more reactive NBS analog to catalyze cyclization. Synthesis of N-bromo-1,3-dimethylurea was done in the presence of TBICA.



Scheme IV-VI: Displays N-bromo-1,3-dimethylurea does not brominate methyl acrylate's olefin.

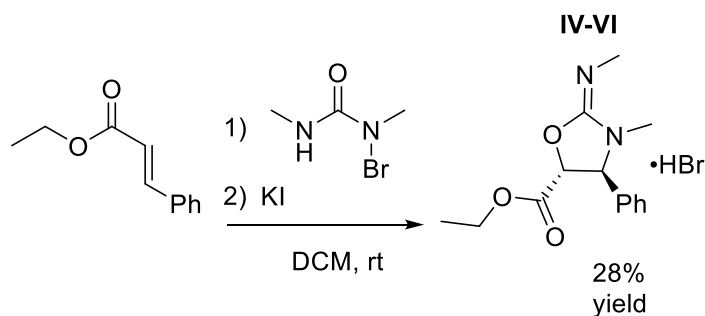
N-bromo-1,3-dimethylurea did not react with the starting material. This result furthered efforts towards finding other methods of olefin activation.^{79, 123-127} Probing literature identified queries of a few groups over understanding the catalytic addition of KI. It was observed that the addition of KI aided in amino halogenation of olefins.¹²⁸



Chen, Z.; Cao, J.; Wei, J. *Org. Biomol. Chem.* **2009**, 7, 3280-3284

Figure IV-XII: Shows catalytic KI aiding in aminobromination of an α,β unsaturated system.

Noting this result, KI along with other sources of Iodide were screened to identify which allowed olefin activation. KI generated the product with the highest yield. It also allowed for the addition of N-bromo-1,3-dimethylurea to ethyl cinnamate in low yields.



Scheme IV-VII: The cyclization of 1,3-dimethyl urea onto an α,β unsaturated system.

The low yields of the initial expansion lead to further modifications of the reaction conditions and replacement of the 1,3 dimethylurea with the more soluble nucleophile benzamide. Addition of benzamide, if it occurred under the same reaction conditions as the 1,3 dimethylurea would present a new methodology towards accessing oxazoline scaffolds for potential TB inhibitors. It would also still give access to amino alcohols by oxazoline hydrolysis.

New interest behind oxazoline scaffolds was driven by two factors, the desire to develop specificity for TB proteasome inhibition and the continued development of methodology to easily access amino alcohols from oxazoline hydrolysis. The current hypothesis focused on olefin activation as the key transformation towards accessing a diverse library of oxazoline compounds. Olefin activation of electron depleted olefins towards cyclization was the primary goal of the first stage of this research. The focus of this methodology was to use commercially available, inexpensive starting material as a feed stock to generate diverse oxazolines and their resulting amino alcohols for natural product synthesis, ligand design and biological testing.¹²⁹⁻¹³⁰ We proposed that an intermolecular cyclization of benzamide on α,β unsaturated esters could be accomplished in the presence of NBS and KI, like past results due to the generation of I-Br. This would act as the activating halonium source.

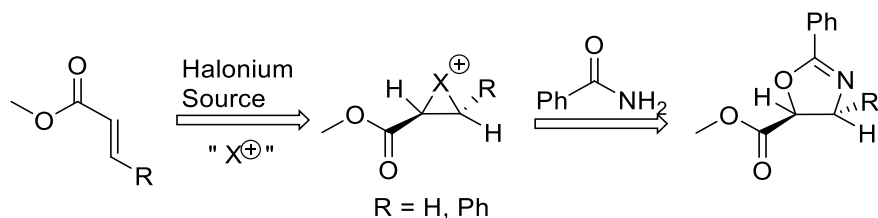
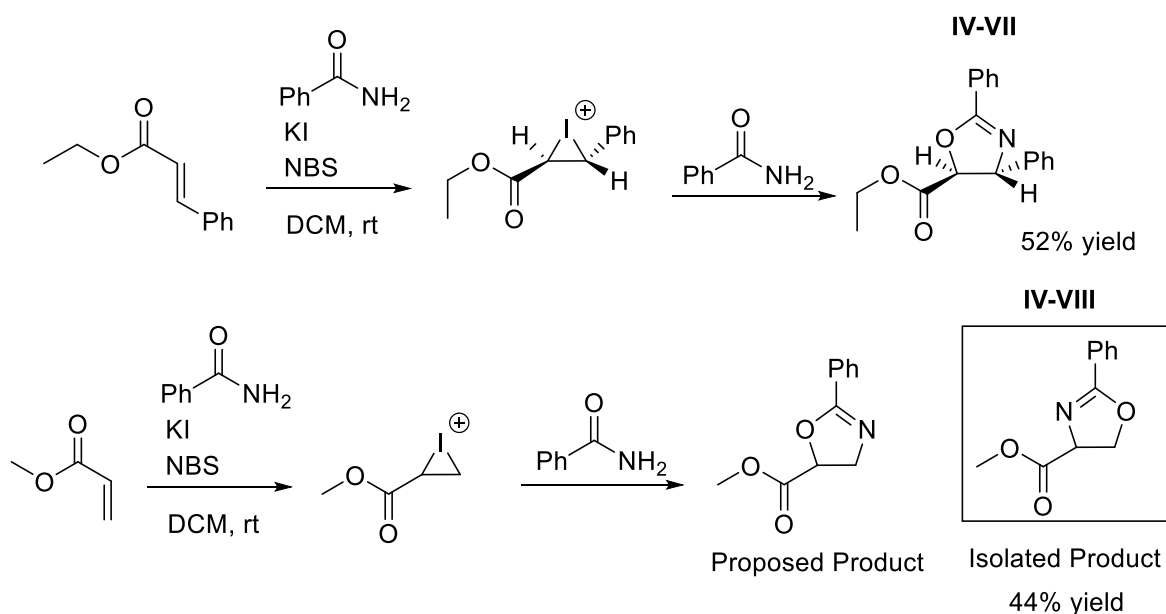


Figure IV-XIII: Proposed method of olefin activation in the presence of benzamide.

To test the experimental conditions necessary for inducing intermolecular cyclization, two α,β unsaturated esters, were selected as initial substrates and subjected to NBS and KI, in the presence of benzamide. The experimental results are seen below.



Scheme IV-VIII: Identified the difference in regiochemical outcome with olefin cyclization.

The difference in regiochemistry between the two isolated products was believed to be based on iodonium stability of the intermediates. The formation of the I-Br in the reaction flask afforded the generation of the iodonium by olefin capture, however the neighboring electronic effects of the substituents effect the regiochemistry of the expansion.¹³¹⁻¹³²

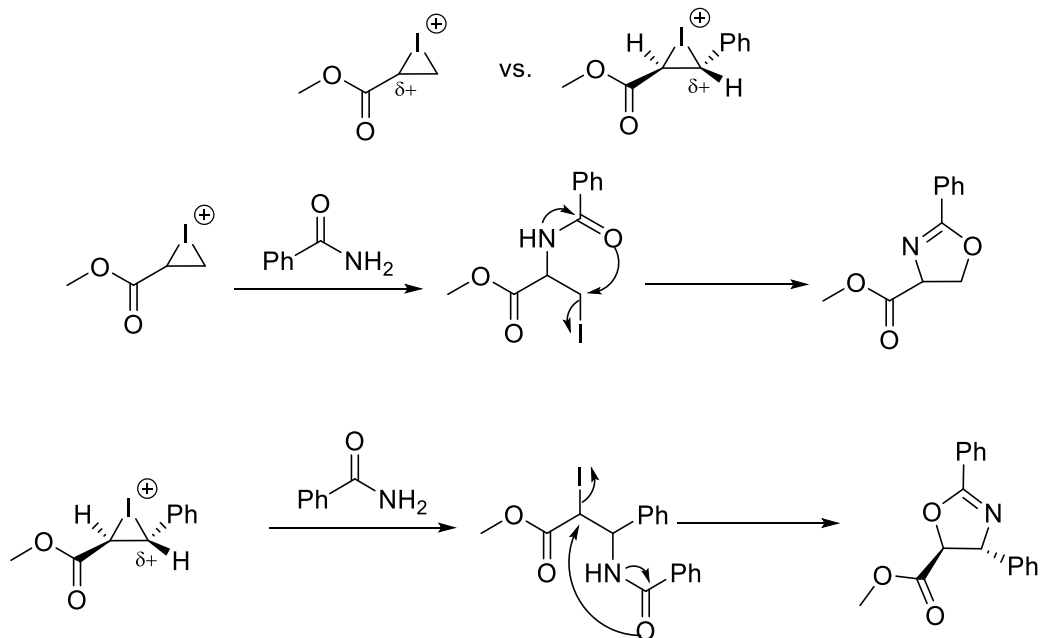


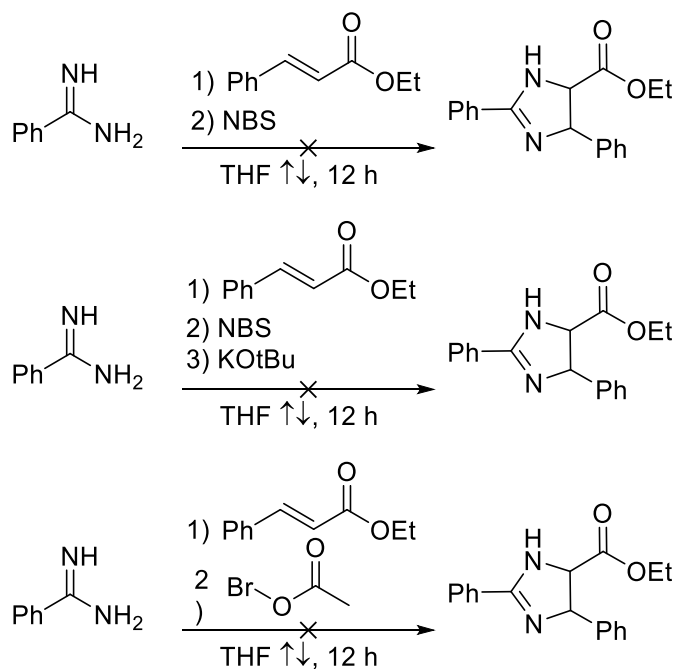
Figure IV-XIV: Explanation of the difference in regiochemistry based on intermediate stability.

The presence of the α -ester at C_2 in the iodonium of methyl acrylate caused the buildup of a larger partial positive charge at C_2 rather than the C_3 carbon, which resulted in regioselective ring opening by the amide nitrogen, followed by cyclization to give N alkylation at the ester's α -carbon. The iodonium of ethyl cinnamate produced the opposite alkylation product based on the presence of the benzyl group, which caused benzylic carbocation formation. This carbocation was quickly trapped by the incoming amide nucleophile and subsequent cyclization lead to O-alkylation at the ester's α -carbon.

The difference in regiochemistry of the two isolated products has offered a unique opportunity to further probe the mechanism of action in expansions of benzamide between mono and disubstituted α,β unsaturated esters. The cyclization results of benzamide on methyl acrylate have also introduced the possibility for regioselectivity in monosubstituted α,β unsaturated esters. Past chemistry involving the preformation of bromourea further support the formation of

the iodonium intermediate and also yield different regiochemistry based on the substitution of the starting α,β unsaturated ester.

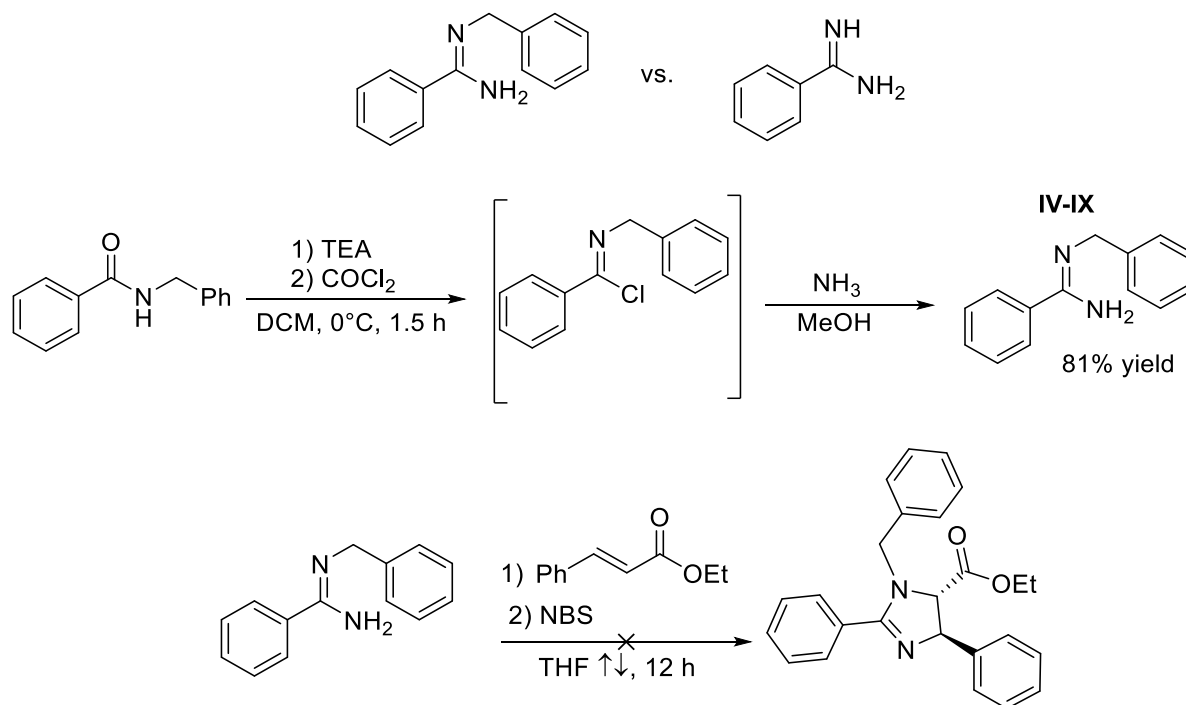
Based on those previous results that showed the cyclization of both benzamide and N,N-dimethylurea, we proposed that imidazolines may be accessed under similar bromination conditions by in the presence of benzamidine. These imidazolines could then be hydrolyzed to give diamines. Benzamidine hydrochloride salt was free based and treated to various brominating reagents in the presence of ethyl cinnamate. Bromination of benzamidine and resulting cyclization did not occur, instead just starting material was observed.



Scheme IV-IX: Depicts the failed bromination and cyclization of benzamidine under various conditions.

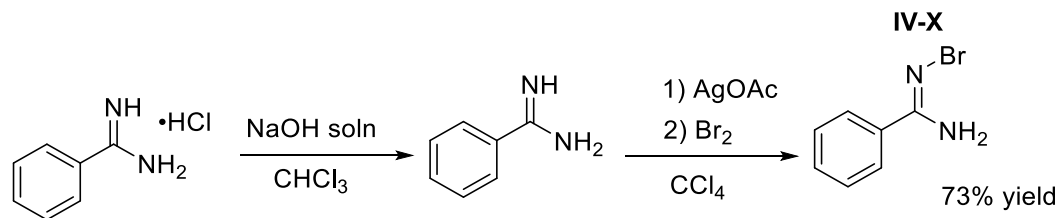
To probe whether the issue of solubility of the amidine was the reason behind reaction failure, N-benzyl benzamidine was accessed. The N-benzyl group was installed to better solubilize the

amidine and increase the nucleophilicity of the structure towards N-Br formation and resulting cyclization.



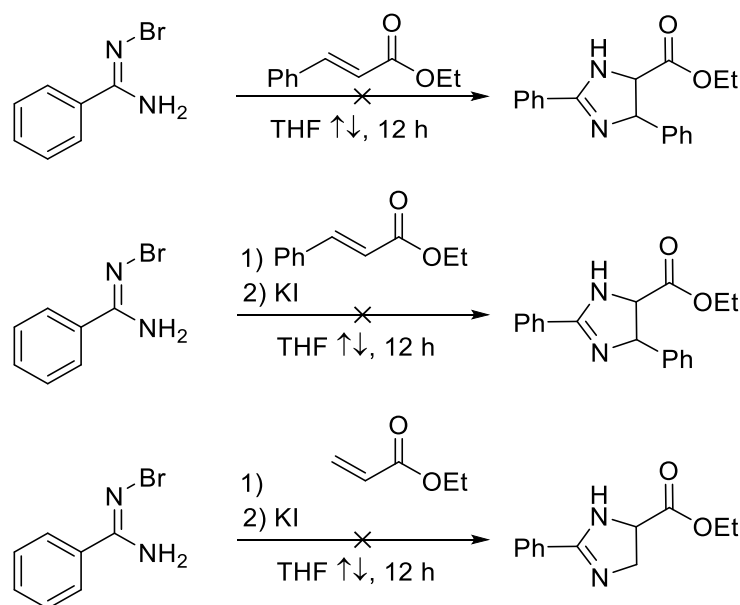
Scheme IV-X: Shows the failed cyclization of N-Benzylbenzamidine.

Incorporation of NBS with ethyl cinnamate in the presence of N-benzylbenzamidine resulted in decomposition. This was believed to be due to dimerization like with Cbz-guanidine and NBS. To better understand the mechanism of the transformation, the one pot reaction was separated into two steps, the bromination of benzamidines and the olefin activation to yield imidazolines. Benzamidines hydrochloride salt, was free based and then introduced to bromoacetate in carbon tetrachloride. After stirring for three hours the benzamidines bromide was precipitated over night with the addition of hexanes.¹³³ This brominating reagent was then screened for conditions to catalyze cyclization onto an α,β unsaturated olefin.



Scheme IV-XI: Synthesis of N-bromobenzamidine for olefin activation.

The addition of N-bromobenzamidine to ethyl cinnamate resulted in no reaction and recovery of starting material. Therefore, KI was added to the reaction to catalyze I-Br formation. The hypothesis was that with like benzamide, the *in-situ* formation of I-Br would result in cyclization of benzamidine.

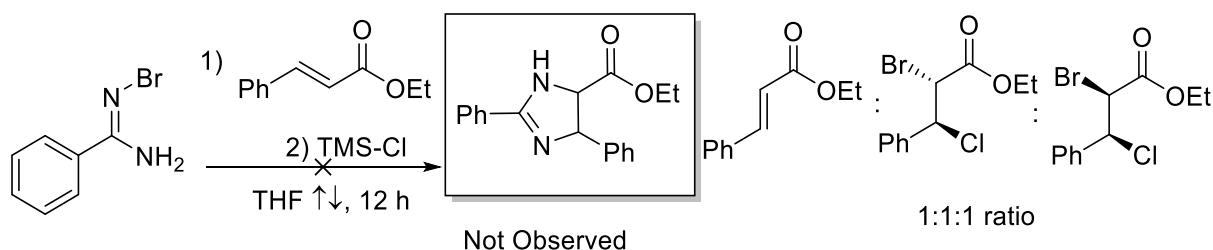


Scheme IV-XII: Failed cyclization of N-bromobenzamidine with methyl acrylate.

The addition of KI caused complete decomposition of the reactions and suggested that I-Br generation and cyclization is not compatible with the benzamidine substrate. Based on those

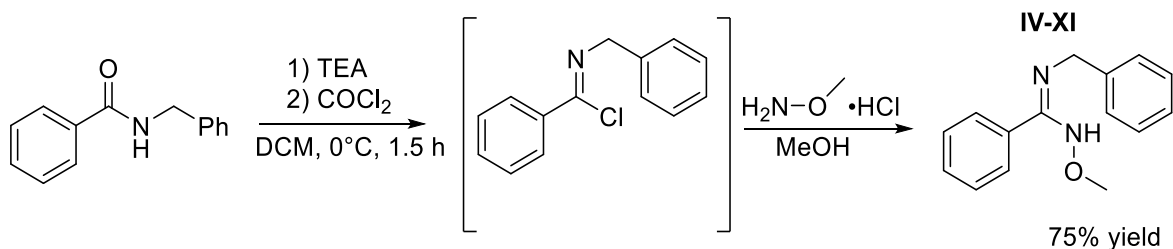
results, new methods of activation are necessary to create a more electrophilic brominating reagent from bromo-benzamidine, for resulting cyclization. Lewis acid activation was selected as a method of increasing the reactivity of bromo-benzamidine, for capture by an electron depleted olefin.¹³⁴⁻

135



Scheme IV-XIII: Lewis acid activation of N-bromobenzamidine.

Cyclization of benzamidine did not occur, but addition of the TMS-Cl did result in the activation of the brominating agent towards capture and opening with the chloride anion. Efforts towards the cyclization of ethyl cinnamate are still ongoing, but based on the intermediates observed, the project has evolved to also include functionalization of electron rich olefins with TMS-OTf. Triflates are better leaving groups than chlorides and this will be exploited to cyclize benzamidine. The observation of the dihalogenated intermediate implied that olefin activation occurred without benzamidine displacement and cyclization. This suggested that the benzamidine was not nucleophilic enough so efforts to synthesis other activated analogs of amidines were approached for accessing imidazolines. A more nucleophilic benzamidine, N-methoxy-N'-benzyl benzamidine was accessed from N-benzylbenzamide.



Scheme IV-XIV: Synthesis of N-methoxy-N'-benzyl benzamidine as new lead for olefin activation.

This molecule was pursued based on the behavior noted in the Baylis-Hillman reaction as well as other literature precedences for activated Michael addition. This molecule was designed as a “nitrene mimic” and was proposed undergo conjugate addition followed by enolate attack to yield an imidoyl aziridine. The strained ring system would then undergo an expansion to yield the desired imidazoline scaffold.

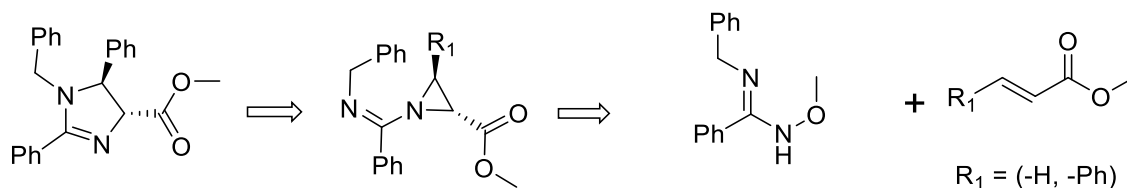
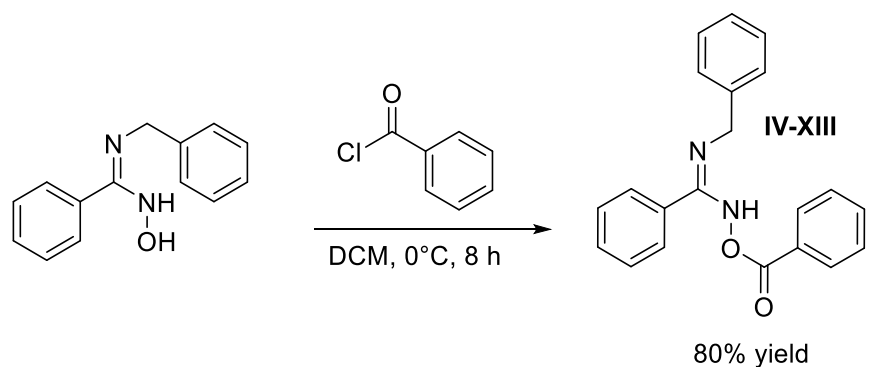
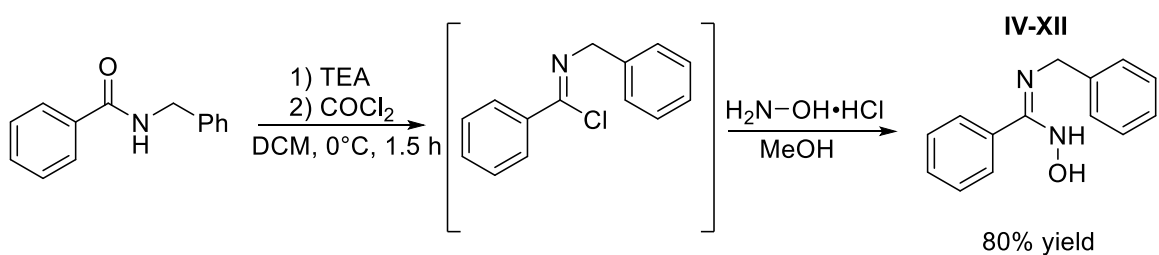
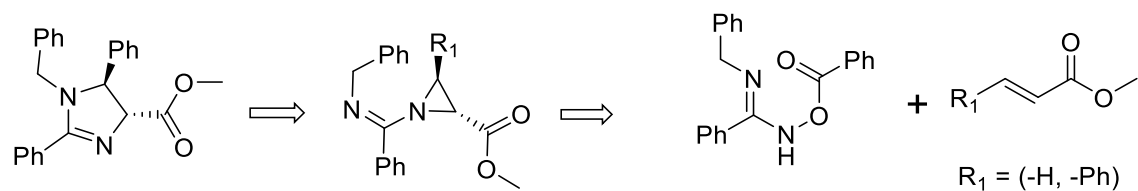


Figure IV-XV: Pathway to accessing imidazolines from activated benzamidines.

No reaction was observed under the nucleophilic or electrophilic reagent conditions. The leaving group potential was identified as the possible cause and the -OMe group was exchanged for a weaker base.



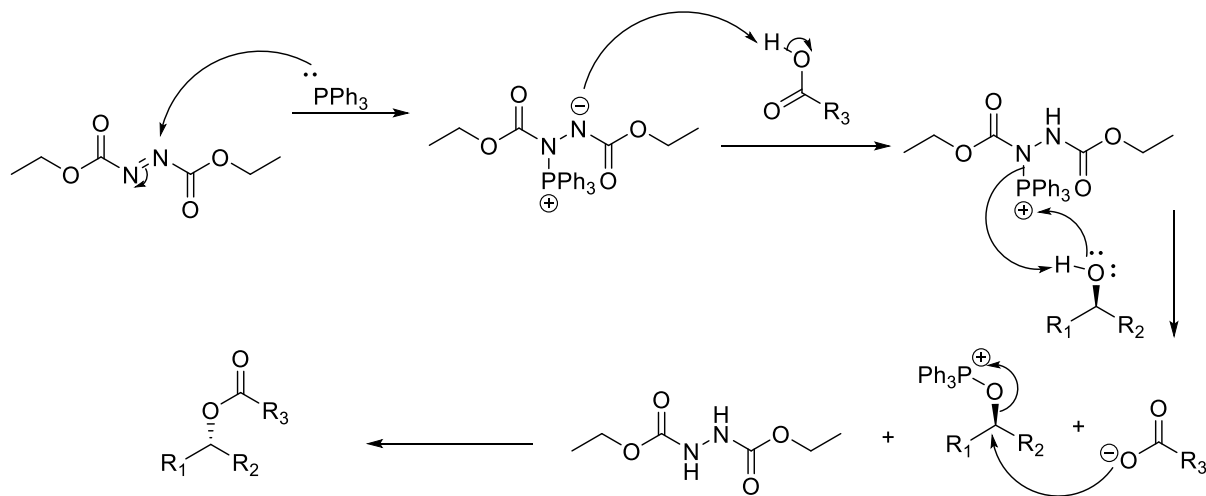
Scheme IV-XV: Synthesis of new lead compound for olefin activation towards imidazolines.

Replacement of the -OMe leaving group with an -OBz group increases the leaving group affinity of the substituent and the presence of the -OBz conjugate base may catalyze the reaction like noted with NaOAc. This substrate will be the leading reagent for imidazoline synthesis.

Approach 3 - Olefin activation through the formation of an Oxygen Phosphorous bond.

Along with reactions using I-Br generation, other methods to accommodate olefin activation were pursued through the activation of an Oxygen-Phosphorous bond. This approach to

olefin activation of α , β unsaturated systems was heavily influenced by named reactions like the Appel and the Mitsunobu reaction. These named reactions used the strength of the oxygen phosphorous bond to drive substitution reactions towards the formation of a variety of synthetic analogs with the inversion of stereochemistry on the chiral carbon center that initially attached to the activated oxygen. In the Mitsunobu reaction the presence of a strongly electron withdrawn dienophile catalyzes the overall transformation and substitution by the activation of phosphorous (III) to a phosphonium (IV) which promotes the attack of the generated alkoxide. Once the bonded to the phosphonium the driving force the overall substitution is the generation of phosphorous oxide (V) which activates the ipso carbon towards nucleophilic substitution with inversion of stereochemistry.¹³⁶

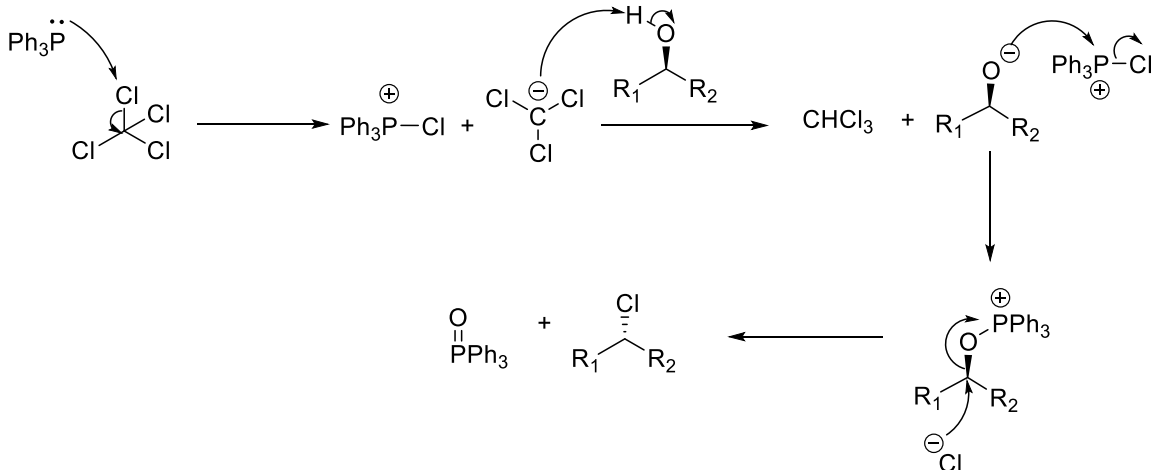


Fletcher, S. *Org. Chem. Front.* **2015**, 2, 739-752

Figure IV-XVI: The mechanism for the Mitsunobu reaction.

The Appel reaction involved the formation of alkyl chlorides from alcohol substrates through a mechanism similar to the Mitsunobu reaction. In the Appel reaction, addition of PPh₃ to a solution of CCl₄ promotes the abstraction of a chlorine atom from CCl₄, to activate the phosphorous (III) to the phosphonium cation and paired carbanion. In the presence of an alcohol,

the carbanion abstracts the acidic O-H proton to form the alkoxide that attacks the activated phosphonium. Once bound the driving force for the formation the phosphorous (V) oxide, facilitates the nucleophilic substitution of the ipso carbon by the only nucleophile present in solution, the chloride anion to give the desired product.¹³⁷



Denton, R. M.; Jie, A.; Aderiran, B.; Blake, A. J.; Lewis, W.; Poulton, A. M. *J. Org. Chem.* **2011**, *76*, 6749-6767

Figure IV-XVII: Mechanism for the appel reaction

Both of these methods involve attack of the ipso carbon, the goal of our chemistry is to use these thoroughly researched reactions towards the attack of the carbamate nitrogen, to access azidines and oxooxazolidine structures. To better probe the capability of this mechanism towards product formation, a number of nucleophiles were introduced to N-protected N-hydroxylamine in the presence of Phosphorous (III), before the Phosphorous was activated *in-situ*.

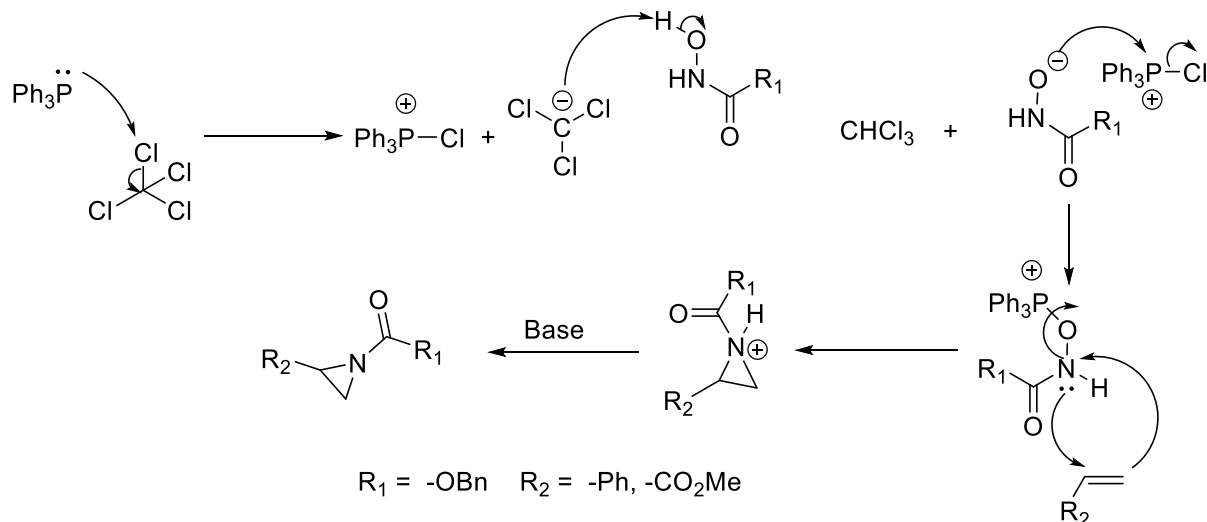
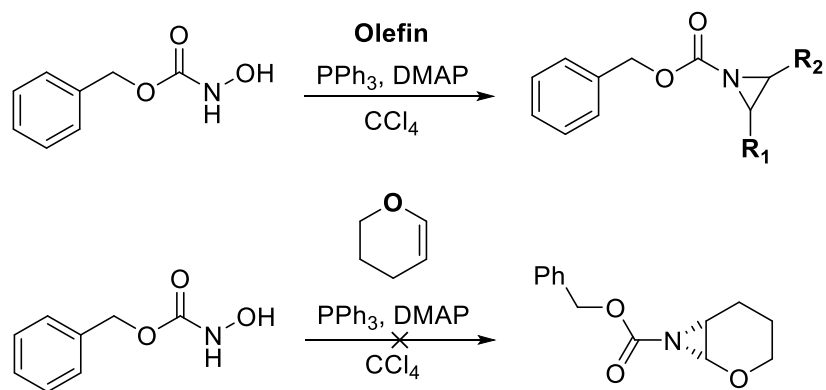


Figure IV-XVIII: Proposed mechanism for appel-like aziridination of olefins.

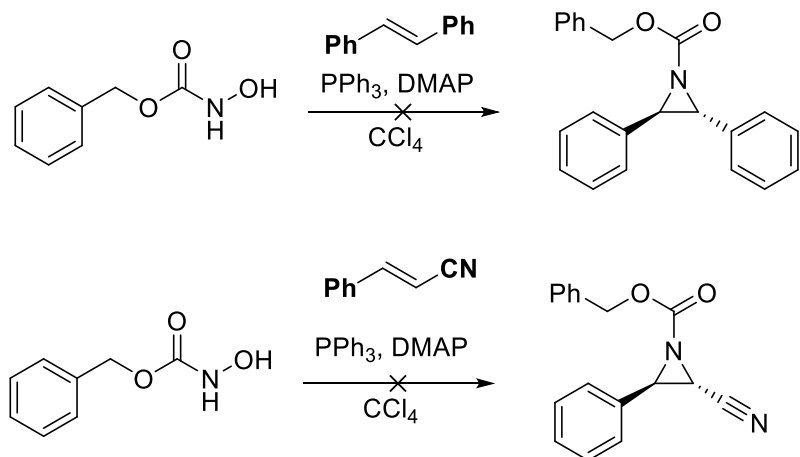
The initial screen for *in-situ* oxygen activation, showed no conversion towards the desired products in the presence of electron rich, neutral or depleted reactions, under the normal Appel conditions with PPh_3 and CCl_4 .

Approach 1 - Appel Reaction



Scheme IV-XVI: Attempted aziridination of olefins under appel conditions.

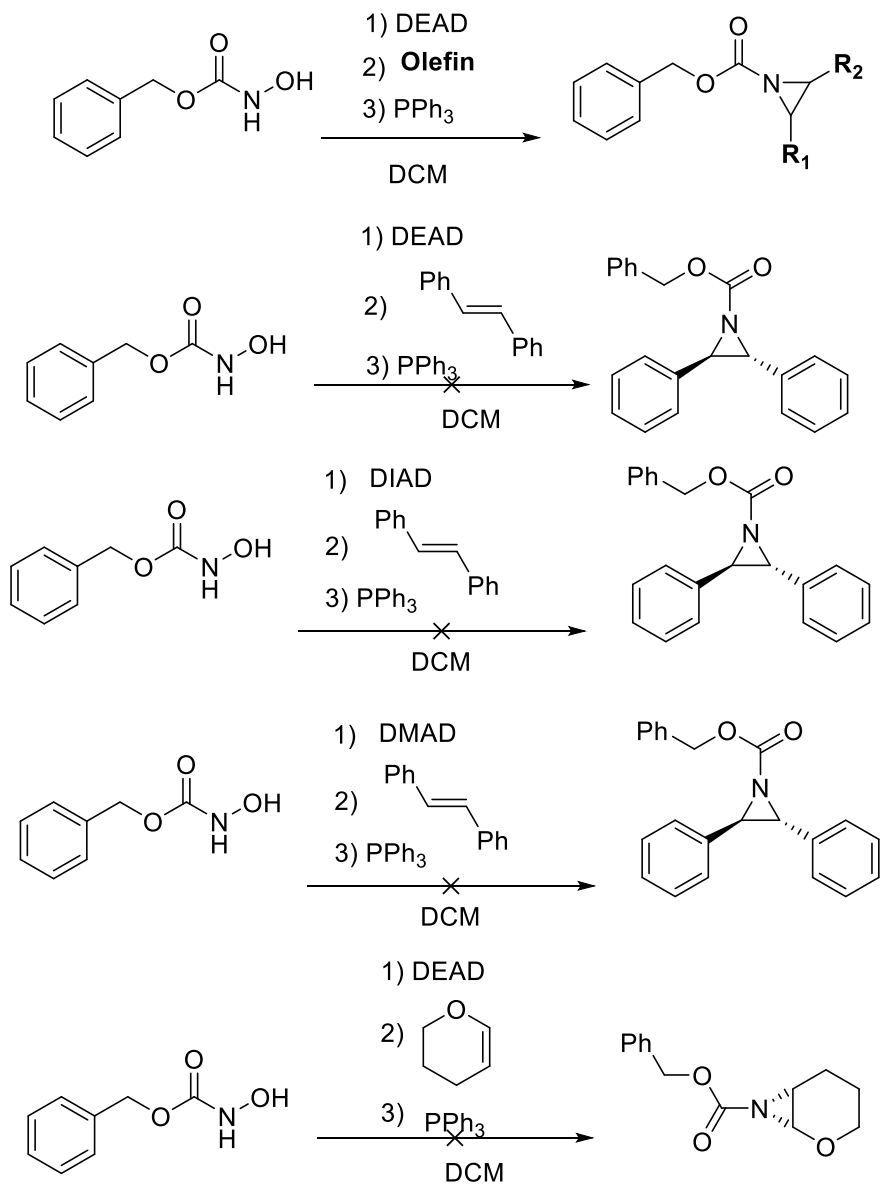
Scheme IV-XVI cont'd.



By targeting activation under Mitsunobu conditions, we eliminate the presence of the strong acid with the *in-situ* generated base of DIAD, DEAD and DMAD. The nucleophilicity of these nitrogens' is depleted in comparison to their cyclic and acyclic counterparts like TEA due the resonance with the carbamate carbonyl group. This allows for the opportunity for the incoming nucleophile to displace the activated oxygen and produce the desired aziridine.

To better probe this proposed transformation the following reactions were attempted, but only starting material was observed by TLC and NMR.

Approach 2 - Mitsunobu Reaction



Scheme IV-XVII: Attempts towards olefin activation using Mitsunobu conditions.

This led us to believe that the activation of the phosphorous is the key step in promotion of the initial oxygen-phosphonium bond. Therefore, to further gather information on this reaction the *in-situ* generation of the phosphonium from triphenyl phosphine was replaced with PPh₃·Br₂, an

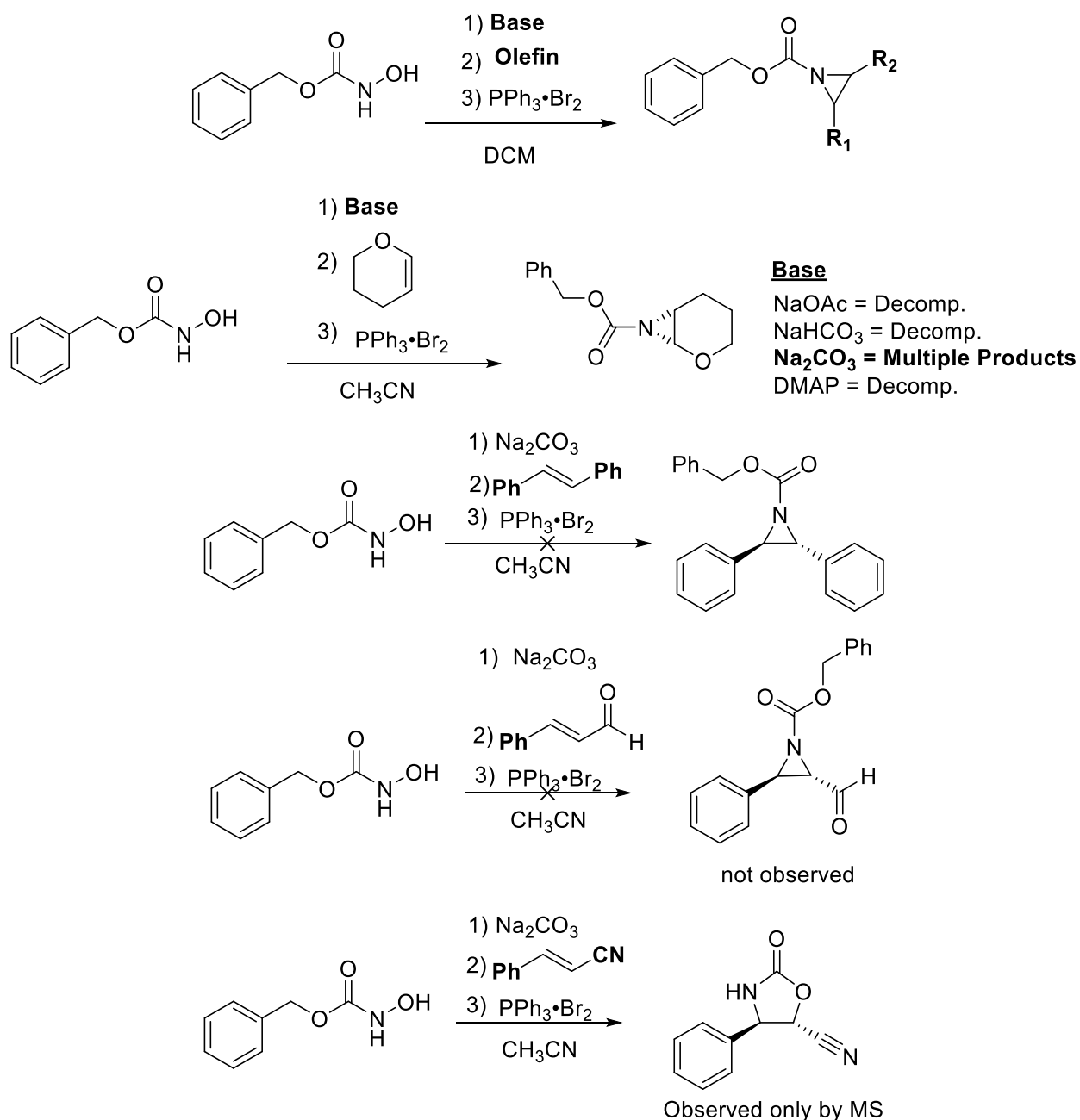
already activated phosphonium salt that is commonly used in literature towards the dehydration of urea to yield carbodiimides through the formation of phosphorous oxide. With this newly prepared phosphonium salt, the electron rich olefin in question was introduced to the dehydration reaction under various bases due to the formation of HBr as a side product in oxygen-phosphorous bond formation.

In the presence of the organic base DMAP, full decomposition of all starting materials was observed. This decomposition was attributed with the formation of the highly reaction N-N bond formation between DMAP and the carbamate nitrogen. N-N bonds are relative weak bond with a strength of 38.4 kcal that in the presence of the electron rich olefin promoted addition and further reactions towards no isolatable products. Decomposition was also observed when the reaction was carried out in the presence of sodium acetate (NaOAc). In the reaction with sodium acetate, generation of acetic acid (AcOH) after the initial hydroxy group activation resulted in highly acidic conditions that lead to full decomposition.

In the presence of the inorganic base Na_2CO_3 , the electron rich olefin did not decompose but showed enhanced reactivity towards the formation of many different olefins products through attack of the nitrogen. Attempted isolation of some of these products showed incorporation of the starting hydroxylamine towards C-N and C-O formation but the overall structural elucidation to the exact structures was impeded due to multiple products with the very similar R_f values.

Acknowledging that both DMAP and Na_2CO_3 contributed to the overall reactivity in the electron rich olefin, the next attempts towards product isolation were done in the presence of less reactive olefin nucleophiles. The hypothesis being that this would result in a more controlled addition of the nucleophile to the activated nitrogen.

Approach 3 - Dehydration Reaction

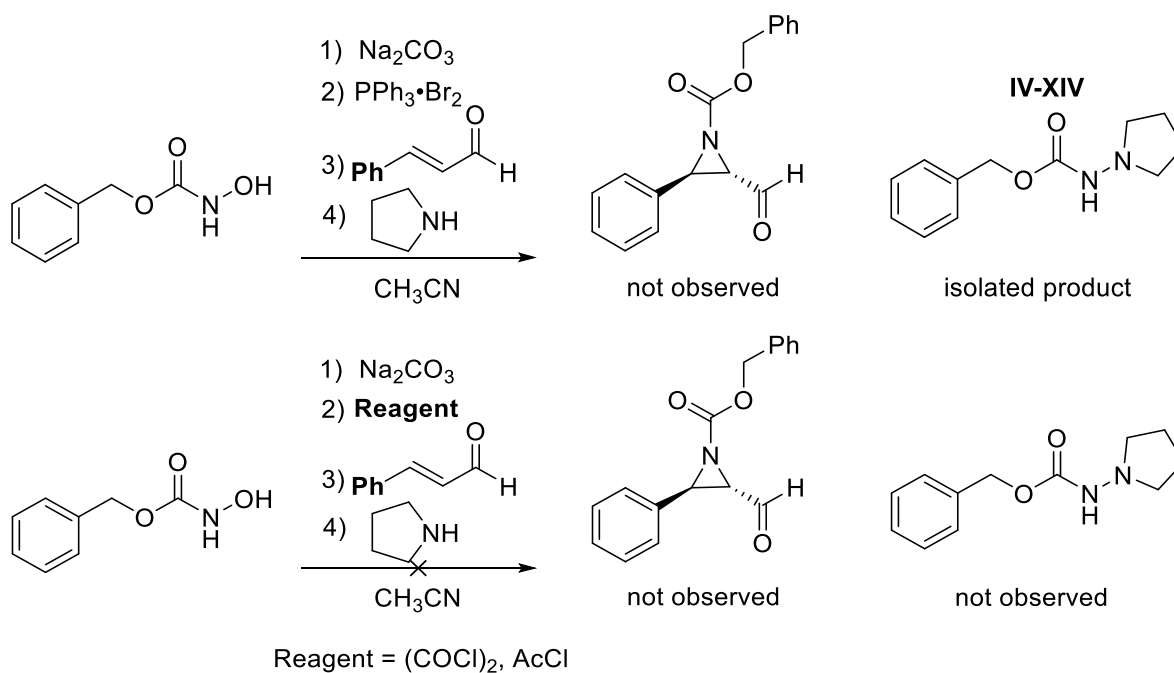


Scheme IV-XVIII: Attempted aziridination of olefins by dehydration of N-hydroxyamides.

Incorporation of the mixed bases with trans-stilbene resulted in the full consumption of the substrate by TLC but no compound was stable enough for isolation after column chromatography. The NMR revealed the isolated mass to be a decomposition product of the overall reaction. The

same result was observed when the substrate was changed to para-methoxystyrene. The only product observed by mass spec and crude NMR was that an electron withdrawn system cinnamionitrile under these reaction conditions in very low yield. The proposed transformation is accredited to a Baylis-Hillman mechanism. Attempts at solvent screening with the mixed base system to promote reactivity and denote solvent dependence on this pioneering chemistry did not yield the formation of the desired product.

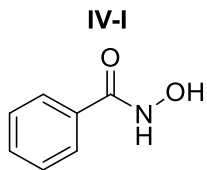
The isolation of a side product which identified nitrogen-nitrogen bond formation due to the high nucleophilicity shown by nitrogen bases. This is a feature that we are still modifying in the presence of electron rich olefins to promote product formation. When the reaction was attempted with either oxalyl chloride or acetyl chloride the same side product was not observed.



Scheme IV-XIX: Attempted aziridination of olefins by dehydration of N-hydroxyamides.

Failed isolation of the N-N bond coupled product when the activating reagent was changed, identified that the reaction was dependent on the presence of $\text{PPh}_3 \cdot \text{Br}_2$. The reaction was not

repeatable and verified that the dehydration pathway was not a viable candidate of olefin activation towards aminoalcohol or heterocycle formation.



N-hydroxybenzamide:

Hydroxylamine HCl salt (3.20 g, 46 mmol) was added to a 250 mL round bottom flask. 80 mL of DI water was added to the flask. To the stirring solution Na_2CO_3 was then added to the flask (6.5 g, 61 mmol). The reaction stirred for 0.5 h before being cooled to 0°C by ice bath. Benzoyl chloride (5.62 g, 40 mmol) dissolved in 60 mL of DCM was added to reaction flask over 2 h by addition funnel. The reaction then stirred for 16 h at room temperature. The organic layer was separated and dried over anhydrous Na_2SO_4 . The solution was concentrated in-vacuo and addition of hexanes followed by cooling at -20°C precipitated the product as a white solid 52% yield (3.27 g, 23.84 mmol).

Spectroscopy:

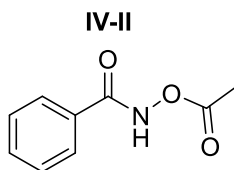
^1H NMR (500 MHz, $\text{DMSO}-d_6$) δ 11.21 (s, 1H), 9.03 (s, 1H), 7.78 – 7.69 (m, 2H), 7.57 – 7.48 (m, 1H), 7.44 (dd, $J = 8.3, 6.9$ Hz, 2H).

^{13}C NMR (125 MHz, $\text{DMSO}-D_6$) δ 164.63, 133.23, 131.58, 129.65, 128.82, 127.29.

IR (FT-ATR) cm^{-1} : 3421, 3315, 3065, 2985, 1678. 984

HRMS-ESI (m/z), calculated for $\text{C}_7\text{H}_8\text{NO}_2$ ($\text{M}+\text{H}$) $^+$: 138.0555. Found 138.0541.

m.p.: $120.0\text{--}120.4^\circ\text{C}$



N-acetoxybenzamide:

N-hydroxybenzamide (0.550 g, 4.01 mmol) was added to a 25 mL flame dried round bottom flask. 10 mL of anhydrous DCM was added to the flask by syringe. Triethylamine (0.487 g, 4.81 mmol) was added by syringe. The reaction was cooled to 0°C by ice bath before the addition of Acetyl chloride (0.286 g, 3.65 mmol). The reaction was stirred for 6 h, after which the solution was washed with saturated NaCl solution (2 X 10 mL). The organic layers were gathered dried over anhydrous Na₂SO₄ and reduced in vacuo to give the crude product as a clear oil. The crude was purified by column chromatography (2:8 Acetone:Hexanes) to give the product as a white powder 32% yield (0.230 g, 1.28 mmol).

Spectroscopy:

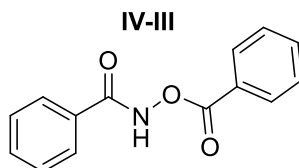
¹H NMR (500 MHz, CDCl₃) δ 9.61 (s, 1H), 7.84 – 7.78 (m, 2H), 7.60 – 7.53 (m, 1H), 7.49 – 7.41 (m, 2H), 2.28 (s, 3H).

¹³C NMR (125 MHz, CDCl₃) δ 169.15, 166.39, 132.81, 130.63, 128.83, 127.46, 18.41.

IR (FT-ATR) cm⁻¹: 3297, 3015, 2985, 1748, 1698, 1203, 1056

HRMS-ESI (m/z), calculated for C₉H₁₀NO₃ (M+H)⁺: 180.0660. Found 180.0690.

m.p.: 119.4-119.6°C



N-(benzoyloxy)benzamide:

Hydroxylamine HCl salt (3.20 g, 46 mmol) was added to a 250 mL round bottom flask. 80 mL of DI water was added to the flask. To the stirring solution Na₂CO₃ was then added to the flask (13.0 g, 122 mmol). The reaction stirred for 0.5 h before being cooled to 0°C by ice bath. Benzoyl chloride (11.25 g, 80 mmol) dissolved in 60 mL of DCM was added to reaction flask over 2 h by addition funnel. The reaction then stirred for 16 h at room temperature. The organic layer was separated and dried over anhydrous Na₂SO₄. The solution was concentrated in-vacuo and addition of hexanes followed by cooling at -20°C precipitated the product as a pale pink solid 34% yield (3.81 g, 15.79 mmol).

Spectroscopy:

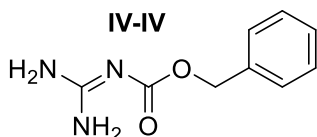
¹H NMR (500 MHz, CDCl₃) δ 9.77 (s, 1H), 8.20 – 8.11 (m, 2H), 7.93 – 7.84 (m, 2H), 7.75 (d, *J* = 7.7 Hz, 1H), 7.70 – 7.62 (m, 1H), 7.61 – 7.56 (m, 1H), 7.49 (dt, *J* = 11.9, 7.8 Hz, 3H).

¹³C NMR (125 MHz, CDCl₃) δ 165.30, 134.33, 132.83, 130.78, 130.06, 128.87, 128.74, 127.55, 126.52.

IR (FT-ATR) cm⁻¹: 3269, 3015, 1743, 1698, 1558, 1032, 981

HRMS-ESI (m/z), calculated for C₁₄H₁₂NO₃ (M+H)⁺: 242.0820. Found 242.0898.

m.p.:148.7-149.0°C



Cbz-guanidine:

50 mL of DI water was added to a 250 mL round bottom flask. Guanidine HCl salt (17.88, 187.2 mmol) was added to the solvent and the reaction was cooled to 0°C by ice bath before the addition of NaOH (8.3 g, 207.5 mmol) The reaction was stirred for 10 minutes at 0°C before the slow addition of Benzyl chloroformate (5.10 g, 29.95 mmol) dissolved in 40 mL of 1,4 dioxane by addition funnel. The reaction stirred for 10 h before washing with EtOAc (4 X 30 mL) to extract the product. The organic layer was dried over anhydrous Na₂SO₄ and reduced in-vacuo to give the product as a white solid 96% yield (5.548 g, 28.7 mmol).

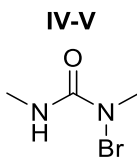
Spectroscopy:

¹H NMR (500 MHz, DMSO-*d*₆) δ 7.46 – 7.17 (m, 5H), 6.67 (s, 2H), 4.95 (s, 2H).

¹³C NMR (125 MHz, DMSO) δ 163.69, 163.47, 138.60, 128.66, 128.65, 128.47, 127.75, 127.69, 126.84, 65.23.

IR (FT-ATR) cm⁻¹: 3249, 3258, 3019, 2965, 1674, 1582, 1124

HRMS-ESI (m/z), calculated for C₉H₁₂N₃O₂ (M+H)⁺: 194.0930. Found 194.0916



1-bromo-1,3-dimethylurea:

Dimethylurea (0.212g, 2.4 mmol) was dissolved in dichloromethane (4 mL) and to that solution TBICA, Tribromoisocyanuric acid (0.351g, 0.96 mmol) was added. The reaction vessel was then covered with foil to prevent light exposure and the resulting mixture was allowed to stir for 24 h,

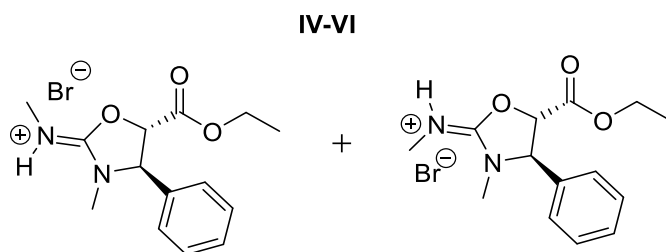
at 25°C. After which the reaction mixture was filtered, and the filtrate, a solution of the product, N-bromodimethylurea in dichloromethane was collected.

Spectroscopy:

^1H NMR (500MHz) (CDCl_3) δ : 5.58 (br, 1 H), 3.29 (s, 3 H), 2.73(d, 3 H)

^{13}C NMR (125MHz) (CDCl_3) δ : 160.08, 47.22, 44.58, 28.26, 26.29

HRMS-ESI (m/z), calculated for $\text{C}_3\text{H}_8\text{BrN}_2\text{O}$ ($\text{M}+\text{H}$) $^+$: 165.9745. Found 165.9978.



Z and E isomers of **ethyl 3-methyl-2-(methylimino)-4-phenyloxazolidine-5-carboxylate HBr salt**:

Dimethylurea (0.212g, 2.4 mmol) was dissolved in dichloromethane (4 mL) and to that solution TBICA, Tribromoisocyanuric acid (0.351g, 0.96 mmol) was added. The reaction vessel was then covered with foil to prevent light exposure and the resulting mixture was allowed to stir for 24 h, at 25°C. After which the reaction mixture was filtered, and the filtrate, a solution of the product N-bromodimethylurea in dichloromethane was collected. To this solution, Ethyl 3-phenylprop-2-enoate (0.405g, 2.3 mmol) was added dropwise by syringe (0.388 mL). Potassium Iodide (0.398g, 2.4 mmol) was then added and the reaction vessel was then covered with foil to prevent light exposure. The resulting mixture was stirred for 48 h at 25°C. The mixture was extracted with 20 mL of dichloromethane and washed with sat. NaCl solution (2 X 10 mL) and sat. NaHCO_3 solution (2 X 10 mL), and dried over anhydrous MgSO_4 , and concentrated to dryness *in vacuo*. The crude

material was then purified by flash chromatography (silica, 9.5:0.5 chloroform/methanol) affording the product as a red oil of (0.235 g, 6.85 mmol) in 28% yield

Spectroscopy:

^1H NMR (500 MHz) (CDCl_3): Mixture of Z and E isomers in a ratio of **5:1** ratio

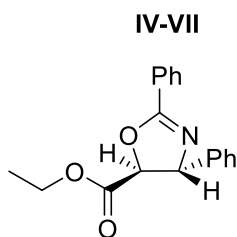
δ : 10.18 (s, br 1 H), 7.4-7.1 (m, 5 H) , 5.73.-5.71 (d, 1 H, $J = 10$ Hz), 4.95-4.87 (abq, 1 H), 4.46-4.44 (d, 1 H, $J = 10$ Hz), 4.28-4.14 (m, 2 H, $J = 7$ Hz), 3.25 (d, 3 H), 2.98-2.9 (d, 3 H), 1.28-1.20 (t, 3 H, $J = 7$ Hz)

^{13}C NMR (125 MHz) (CDCl_3) δ :167.401, 166.22, 158.33, 157.75, 135.02, 134.41, 130.23, 130.16, 129.98, 129.67, 129.33, 128.98, 127.08, 125.96, 83.34, 83.00, 68.40, 67.67, 63.07, 61.53, 32.55, 31.05 , 30.40, 30.34, 27.51, 27.10 14.25, 14.13

2D NOESY (500 MHz) (CDCl_3) δ :7.4-7.1*5.73-5.71 and 7.4-7.1*4.95-4.87

IR (NaCl, Neat): 3246, 3068, 2930, 1752, 1699, 1154, 1095, cm^{-1}

HRMS (LCMS) calculated for $\text{C}_{14}\text{H}_{19}\text{N}_2\text{O}_3^+$ ($\text{M}+\text{H}^+$): 263.14 Found: 263:1398



Trans-ethyl 2,4-diphenyl-4,5-dihydrooxazole-5-carboxylate:

Ethyl cinnamate (0.352 g, 2.0 mmol) was added to a 50 mL flame dried flask under inert atmosphere. 10 mL of anhydrous DCM was added to the flask by syringe. The solution was stirred vigorously while Benzamide (0.242 g, 2 mmol) was added as a solid to the flask followed by N-bromosuccinimide (0.355 g, 2 mmol). The vessel was wrapped in foil before the addition of KI

(0.332 g, 2.0 mmol). The reaction was then stirred at room temperature for 12 h before being extracted into ethyl acetate (30 mL). This organic solution was washed with saturated NaCl solution (2 X 25 mL), collected and dried over anhydrous Na₂SO₄ before being reduced to give a crude oil. This oil was purified by column chromatography (1.5:8.5 EtOAc:Hexanes) to yield the product as a yellow oil 52% yield (0.307 g, 1.04 mmol).

Spectroscopy:

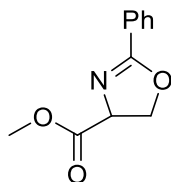
¹H NMR (500 MHz, CDCl₃) δ 8.13 – 8.06 (m, 2H), 7.57 – 7.50 (m, 1H), 7.49 – 7.32 (m, 7H), 5.90 (d, *J* = 7.6 Hz, 1H), 4.82 (d, *J* = 7.6 Hz, 1H), 4.33 (qq, *J* = 10.7, 7.1 Hz, 2H), 1.36 (t, *J* = 7.1 Hz, 3H).

¹³C NMR (125 MHz, CDCl₃) δ 170.91, 165.42, 139.68, 132.00, 128.94, 128.76, 128.65, 128.43, 126.94, 125.65, 83.24, 77.04, 61.93, 14.23.

IR (FT-ATR) cm⁻¹: 3021, 2985, 1741, 1689, 1586, 1163, 1012, 974

HRMS-ESI (*m/z*), calculated for C₁₇H₁₆NO₃ (M+H)⁺: 295.1208. Found 295.1198.

IV-VIII



methyl 2-phenyl-4,5-dihydrooxazole-4-carboxylate:

Methyl acrylate (0.860 g, 10 mmol) was added to a 50 mL flame dried round bottom flask under inert atmosphere. To this flask 5 mL of anhydrous DCM was added by syringe. This solution was stirred vigorously while Benzamide (0.242 g, 2 mmol) was added as a solid to the flask followed by N-bromosuccinimide (0.355 g, 2 mmol). The vessel was wrapped in foil before the addition of

KI (0.332 g, 2.0 mmol). The reaction was then stirred at room temperature for 12 h before being extracted into ethyl acetate (30 mL). This organic solution was washed with saturated NaCl solution (2 X 25 mL), collected and dried over anhydrous Na₂SO₄ before being reduced to give a crude oil. This oil was purified by column chromatography (3:7 EtOAc:Hexanes) to yield the product as a bright yellow oil 44% yield (0.181 g, 0.88 mmol).

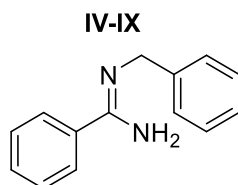
Spectroscopy:

¹H NMR (500 MHz, CDCl₃) δ 8.01 – 7.91 (m, 2H), 7.53 – 7.43 (m, 1H), 7.43 – 7.34 (m, 2H), 4.94 (dd, *J* = 10.6, 8.0 Hz, 1H), 4.68 (dd, *J* = 8.7, 7.9 Hz, 1H), 4.58 (dd, *J* = 10.6, 8.7 Hz, 1H), 3.80 (s, 3H).

¹³C NMR (125 MHz, CDCl₃): δ 166.33, 131.90, 128.57, 128.35, 126.82, 69.55, 68.50, 52.73.

IR (FT-ATR) cm⁻¹: 3046, 2915, 1721, 1684, 1575, 1260, 1037, 1028 984.

HRMS-ESI (m/z), calculated for C₁₁H₁₂NO₃ (M+H)⁺ : 206.0817. Found 206.0805.



N'-benzylbenzimidamide:

N-benzylbenzamide (1.267 g, 6 mmol) was added as a solid to a 100 mL flame dried round bottom flask under inert atmosphere. 50 mL of anhydrous DCM was then added to the flask by syringe. To the resulting solution Triethylamine (3.64 g, 36 mmol) was added by syringe. The reaction vessel was cooled to 0°C by ice bath before the slow addition of Oxalyl Chloride (0.914 g, 7.2 mmol) by syringe over 10 minutes. The reaction was then stirred at 0°C for 1.5 h before removal of the solvent under reduced pressure to give the crude imidoylchloride. 15 mL of 7 M ammonia in methanol, was then added to the crude product and the reaction was stirred at room temperature

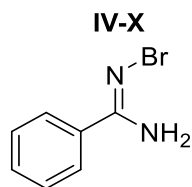
for 12 h. The solvent was removed under vacuum and the crude product was dissolved in EtOAc (35 mL). The organic solution was then washed with 1 M HCl solution and the aqueous layer was collected and basified to extract the product molecule in EtOAc (20 mL). The organic layer was then dried over anhydrous Na₂SO₄. The solvent was then removed in-vacuo to yield the product as a yellow oil 81% yield (1.02 g, 4.86 mmol).

Spectroscopy:

¹H NMR (500 MHz, CDCl₃-*d*) δ 7.64 – 7.53 (m, 2H), 7.47 – 7.32 (m, 7H), 7.31 – 7.24 (m, 1H), 5.39 (s, 2H), 4.54 (s, 2H).

¹³C NMR (125 MHz, CDCl₃) δ 138.93, 137.66, 130.13, 128.69, 128.67, 127.79, 127.77, 127.29, 126.07, 46.88.

HRMS-ESI (m/z), calculated for C₁₄H₁₅N₂ (M+H)⁺: 211.1235. Found 211.1389.



N'-bromobenzimidamide:

Silver(I) acetate (4.0 g, 23.97 mmol) was added to a 250 mL flame dried flask under inert atmosphere. To this 100 mL of CCl₄ was added by syringe. The resulting suspension was cooled to 0°C by ice bath. The vessel was then covered in foil before the addition of Bromine (3.82 g, 23.9 mmol). The reaction stirred for 25 minutes to generate Bromoacetate as a solution in CCl₄. The suspension was filtered in the absence of light and the solid was washed with 10 mL of CCl₄. The filtrate was collected and added to a round bottom flask containing Benzimidamide

as a solid (2.64 g, 21.98 mmol). The flask was covered in foil and the reaction stirred at room temperature for 3 h. 100 mL of Hexanes were added to the solution and the reaction was cooled at -20°C for 16 h to yield the product as a light yellow powder 73% yield (3.50 g, 17.6 mmol).

Spectroscopy:

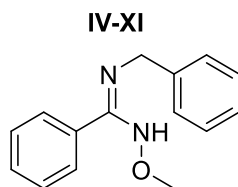
^1H NMR (500 MHz, CDCl_3) δ 7.66 (dt, $J = 7.1, 1.4$ Hz, 2H), 7.53 – 7.45 (m, 1H), 7.42 (dd, $J = 8.3, 6.8$ Hz, 2H), 5.62 (s, 2H).

^{13}C NMR (125 MHz, CDCl_3) δ 164.49, 132.39, 131.04, 128.79, 126.80.

IR (FT-ATR) cm^{-1} : 3254, 3233, 3010, 1687, 1582

HRMS-ESI (m/z), calculated for $\text{C}_7\text{H}_7\text{BrN}_2$ ($\text{M}+\text{H}$) $^+$: 198.9871. Found 198.9863.

m.p.:148.7-149.3°C



N'-benzyl-N-methoxybenzimidamide:

N-benzylbenzamide (1.52 g, 7.2 mmol) was added as a solid to a flame dried 100 mL flask. 20 mL of anhydrous DCM was added to the flask by syringe. Triethylamine (4.37 g, 43.2 mmol) was added to the flask by syringe. The resulting solution was cooled to 0°C by ice bath before the slow addition of oxalyl chloride (0.914 g, 7.2 mmol) over 10 minutes by syringe. The reaction stirred for 1.5 h before the solvent was removed in vacuo to yield crude imidoyl chloride. This tan solid was dissolved in 10 mL of anhydrous DMF. The resulting solution had methoxylamine HCl salt (1.20g, 14.4 mmol) added to it and was stirred at 55°C for 12 h. The reaction was extracted in EtOAc (50 mL). The organic layer was then washed with 10% LiBr solution (3 X 25 mL). The

organic layer was then washed with 1 M HCl solution and the aqueous solution was collected. This layer was basified to a pH of 12 by the addition of NaOH pellets and then washed with EtOAc (2 X 15 mL). The organic layers were collected and dried over anhydrous Na₂SO₄. The solvent was removed in-vacuo to yield the product as a brown oil 75% yield (1.29 g, 5.4 mmol).

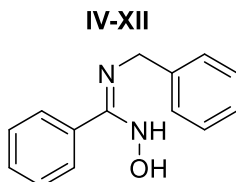
Spectroscopy:

¹H NMR (500 MHz, CDCl₃) δ 7.51 – 7.44 (m, 2H), 7.44 – 7.36 (m, 3H), 7.36 – 7.29 (m, 2H), 7.29 – 7.25 (m, 1H), 7.22 (ddt, *J* = 7.3, 1.2, 0.7 Hz, 2H), 5.61 (s, 1H), 4.23 (d, *J* = 6.7 Hz, 2H), 3.90 (s, 3H).

¹³C NMR (125 MHz, CDCl₃) δ 156.15, 139.51, 131.07, 129.61, 128.62, 128.50, 127.28, 126.87, 61.31, 47.56.

IR (FT-ATR) cm⁻¹: 3248, 3052, 2947, 1693, 1156, 1093

HRMS-ESI (*m/z*), calculated for C₁₅H₁₇N₂O (M+H)⁺: 241.1351. Found 241.1357



N'-benzyl-N-hydroxybenzimidamide:

N-benzylbenzamide (1.52 g, 7.2 mmol) was added as a solid to a flame dried 100 mL flask. 20 mL of anhydrous DCM was added to the flask by syringe. Triethylamine (4.37 g, 43.2 mmol) was added to the flask by syringe. The resulting solution was cooled to 0°C by ice bath before the slow addition of oxalyl chloride (0.914 g, 7.2 mmol) over 10 minutes by syringe. The reaction stirred for 1.5 h before the solvent was removed in vacuo to yield crude imidoyl chloride. This tan solid was dissolved in 10 mL of anhydrous DMF. The resulting solution had Hydroxylamine HCl salt

(1.00g, 14.4 mmol) added to it and was stirred at 55°C for 12 h. The reaction was extracted in EtOAc (50 mL). The organic layer was then washed with 10% LiBr solution (3 X 25 mL). The organic layer was then washed with 1 M HCl solution and the aqueous solution was collected. This layer was basified to a pH of 12 by the addition of NaOH pellets and then washed with EtOAc (2 X 15 mL). The organic layers were collected and dried over anhydrous Na₂SO₄. The solvent was removed in-vacuo to yield the product as a white solid 80% yield (1.30 g, 5.75 mmol).

Spectroscopy:

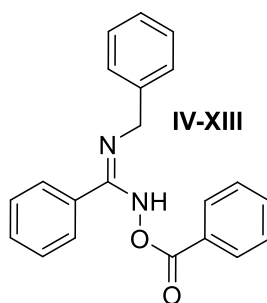
¹H NMR (500 MHz, CDCl₃) δ 7.51 – 7.33 (m, 5H), 7.36 – 7.28 (m, 2H), 7.32 – 7.22 (m, 1H), 7.26 – 7.16 (m, 2H), 5.76 (s, 1H), 4.25 (d, *J* = 5.7 Hz, 2H).

¹³C NMR (125 MHz, CDCl₃) δ 161.01, 156.51, 139.55, 131.15, 129.64, 128.59, 128.54, 128.43, 127.21, 126.78, 47.44.

(FT-ATR) cm⁻¹: 3416, 3358, 3054, 2942, 1658, 1573, 1029

HRMS-ESI (m/z), calculated for C₁₄H₁₅N₂O (M+H)⁺: 227.1184. Found 227.1179.

m.p.: 108.9-109.8°C



N-(benzoyloxy)-N'-benzylbenzimidamide:

N'-benzyl-N-hydroxybenzimidamide (0.75 g, 3.31 mmol) was added to a 50 mL flame dried flask under inert atmosphere. 20 mL of anhydrous THF was added to the flask by syringe. Triethylamine (0.670 g, 6.63 mmol) was added to the flask by syringe. The reaction was cooled to 0°C by ice

bath before the slow addition of Benzoyl chloride (0.466 g, 3.314 mmol) over 5 minutes. The reaction was then stirred for 8 h. The solvent was removed in-vacuo to yield the crude product which was extracted into 20 mL of CHCl₃, washed with saturated NaCl solution (2 X 15 mL) and dried over anhydrous Na₂SO₄. The solution was reduced in-vacuo to give the crude product that was purified by column chromatography (2.5:7.5 EtOAc: Hexanes) to yield the product as a white solid 80% yield (0.860g, 2.60 mmol).

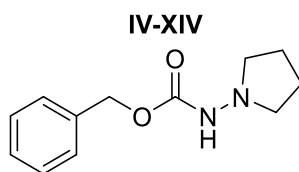
Spectroscopy:

¹H NMR (500 MHz, CDCl₃) δ 8.09 – 8.00 (m, 2H), 7.57 (dq, J = 7.5, 2.1, 1.7 Hz, 3H), 7.49 – 7.39 (m, 5H), 7.39 – 7.28 (m, 2H), 7.28 – 7.19 (m, 3H), 5.74 – 5.66 (m, 1H), 4.34 (d, J = 6.4 Hz, 2H).

¹³C NMR (125 MHz, CDCl₃) δ 164.02, 160.72, 138.55, 132.95, 130.51, 129.68, 129.53, 129.46, 129.11, 128.87, 128.60, 128.50, 127.70, 126.70, 47.90.

IR (FT-ATR) cm⁻¹: 3254, 3147, 2974, 1749, 1684, 1598, 1162, 1032.

HRMS-ESI (m/z), calculated for C₂₁H₁₉N₂O₂ (M+H)⁺: 331.1447. Found: 331.1447.



benzyl pyrrolidin-1-ylcarbamate:

Cinnamaldehyde (0.473 g, 3.59 mmol) was added to a flame dried 100 mL flask. 10 mL of anhydrous DCM was added to the reaction vessel by syringe. Triethylamine (0.431 g, 6.58 mmol) was added by syringe. The reaction was cooled to 0°C by ice bath and NaOAc (0.95 g, 8.97 mmol) was added to the reaction vessel. benzyl hydroxycarbamate (0.500 g, 2.99 mmol) was added to the reaction vessel as a solid. PPh₃·Br₂ (1.26 g, 2.99 mmol) was then added and the reaction was stirred

a 4°C for 10 h. After which the reaction was filtered and the filtrate was washed with 2 X 10 mL saturated NaCl solution, dried over anhydrous Na₂SO₄ and concentrated to give the product as a crude oil. The crude product was purified by column chromatography (2:8 EtOAc: Hexanes) to give the product 86% yield (0.566 g, 2.57 mmol).

Spectroscopy:

¹H NMR (500 MHz, CDCl₃) δ 8.86 (d, *J* = 24.1 Hz, 1H), 8.17 (s, 1H), 7.61 – 7.58 (m, 1H), 7.41 – 7.37 (m, 3H), 5.17 (s, 2H), 3.42 (dt, *J* = 24.9, 6.4 Hz, 4H), 1.99 – 1.70 (m, 4H).

¹³C NMR (125 MHz, CDCl₃) δ 155.10, 150.04, 137.06, 132.24, 129.86, 129.12, 128.72, 128.64, 128.59, 128.54, 128.44, 128.43, 128.30, 127.87, 126.98, 126.97, 66.71, 46.28, 45.84, 25.73, 24.97.

IR (FT-ATR) cm⁻¹: 3316, 3033, 1654, 1578, 1241, 1128, 1074.

HRMS-ESI (*m/z*), calculated for C₁₂H₁₇N₂O₂ (M+H)⁺: 221.1295. Found 221.1300.

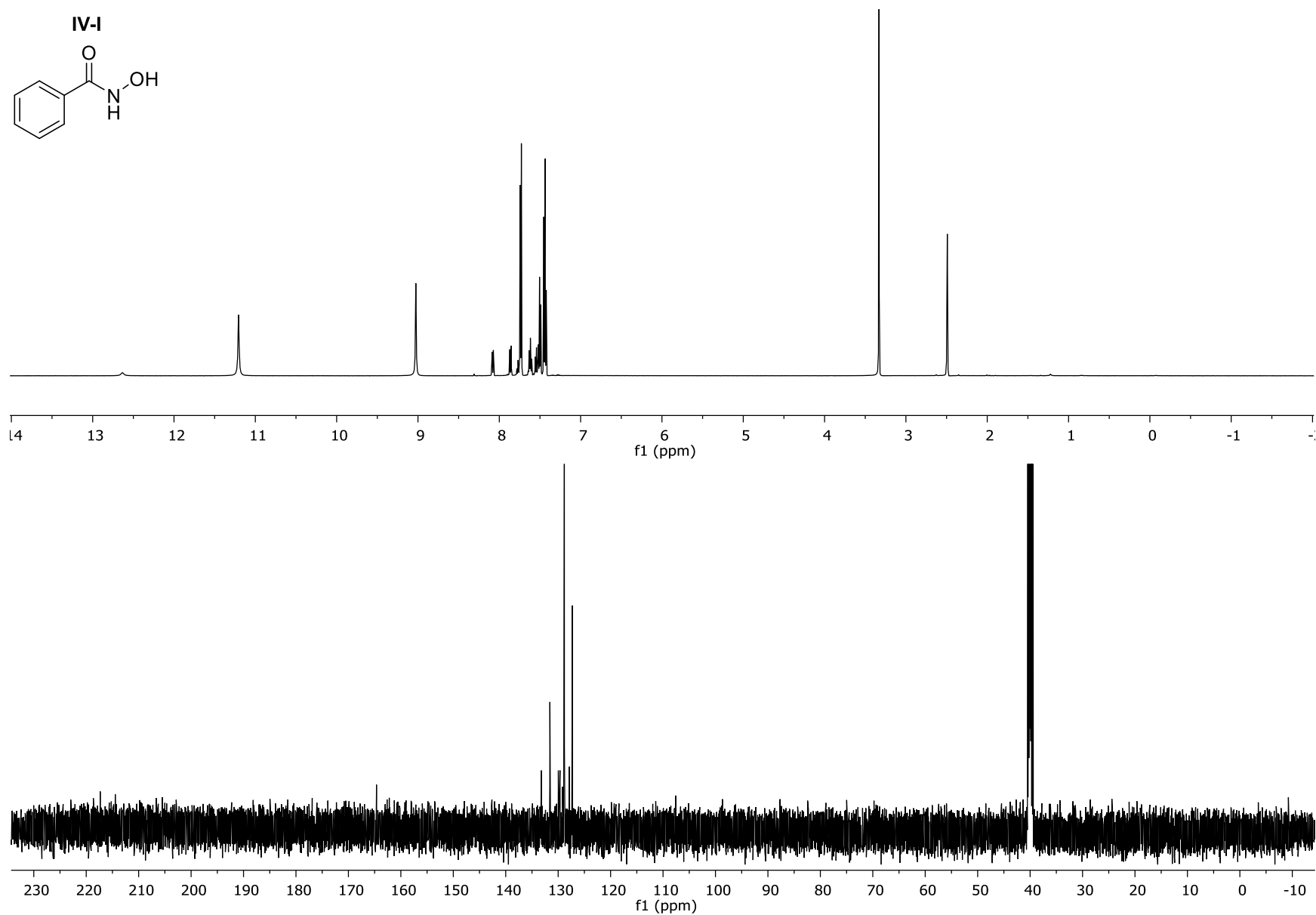
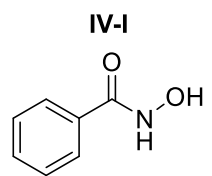


Figure IV-XIX: The ^1H NMR and ^{13}C NMR for Compound IV-I

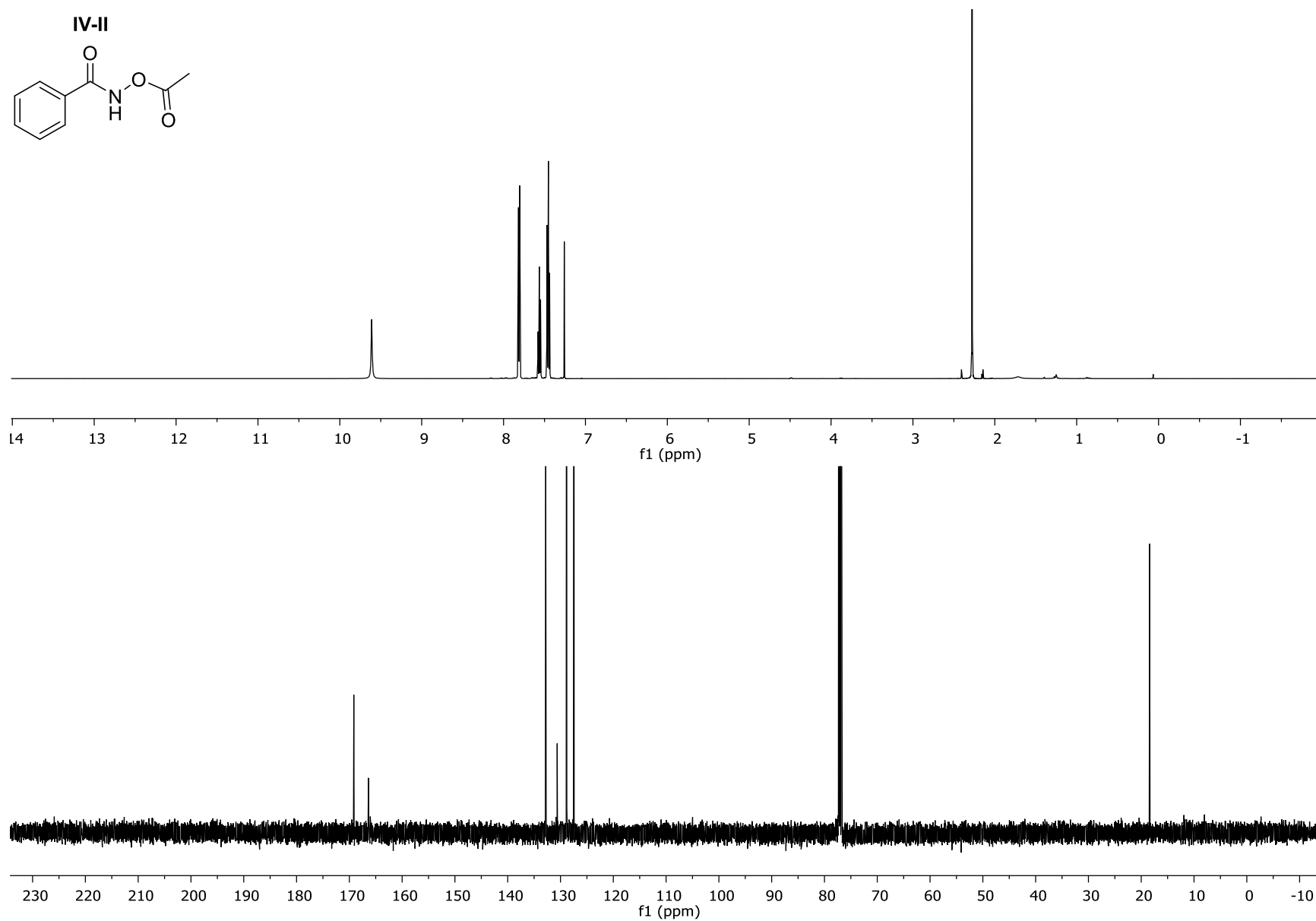
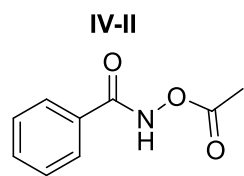


Figure IV-XX: The ^1H NMR and ^{13}C NMR for Compound IV-II

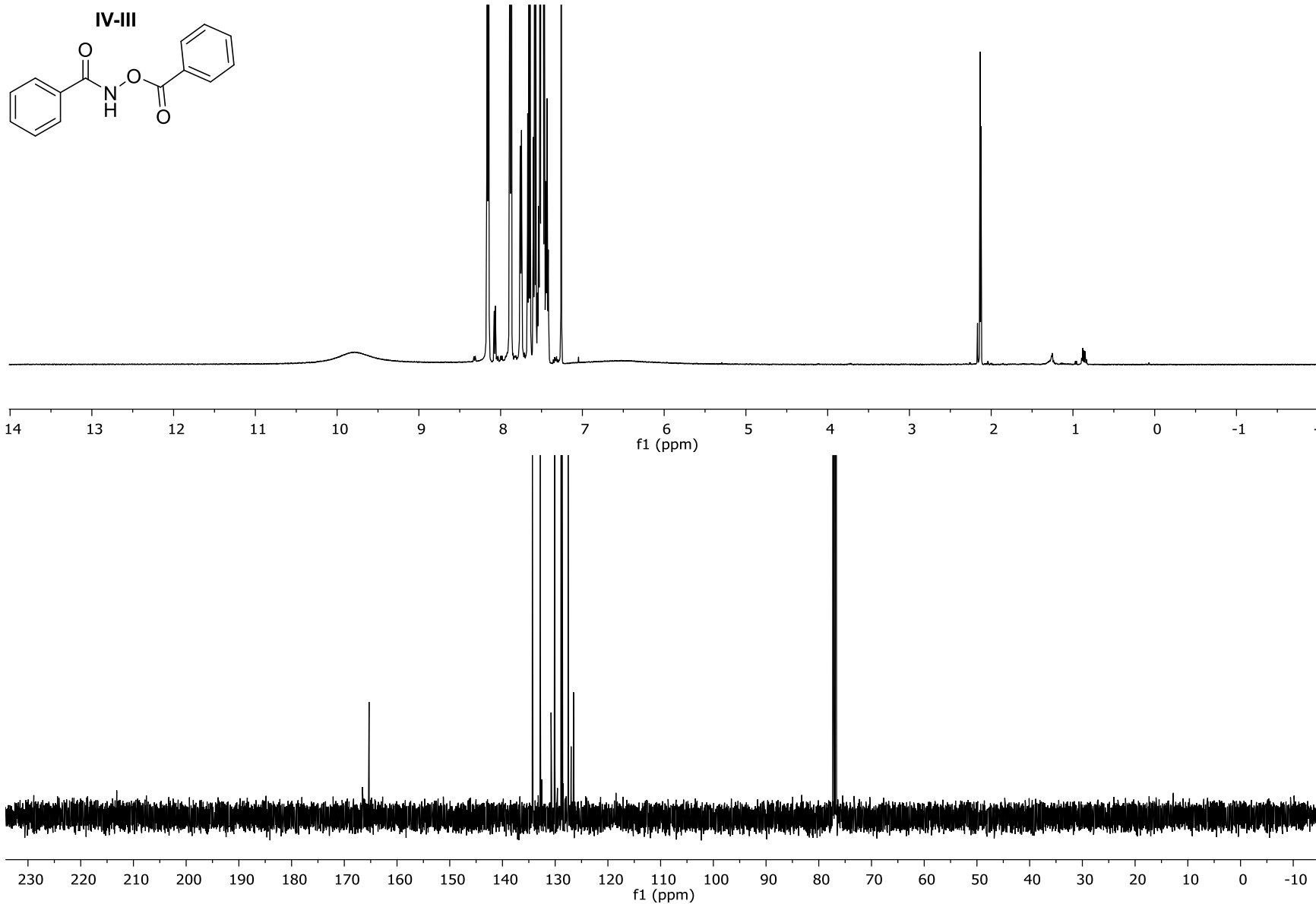


Figure IV-XXI-: The ¹H NMR and ¹³C NMR for Compound **IV-III**

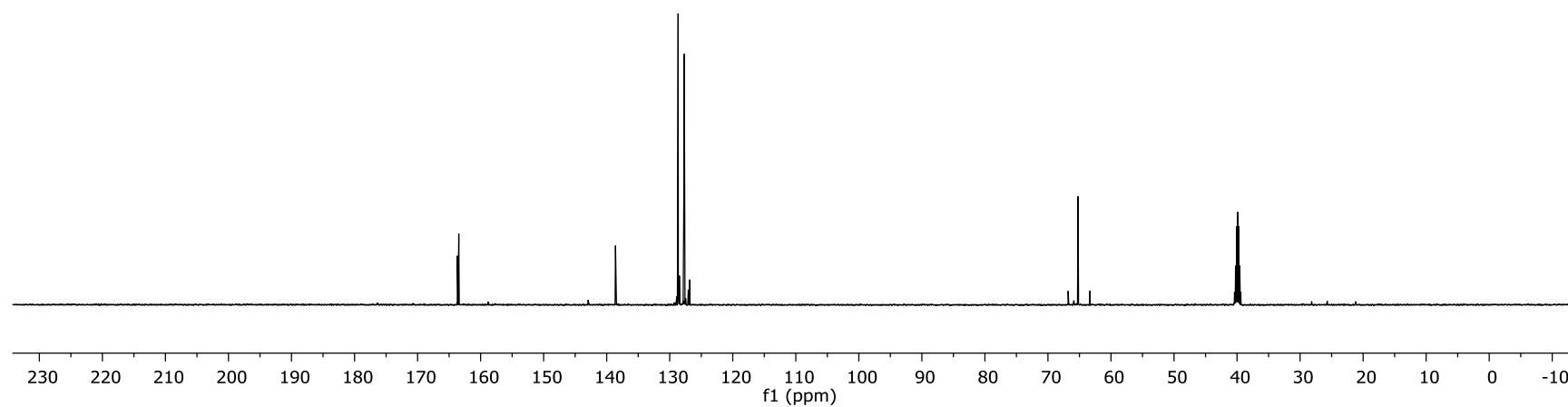
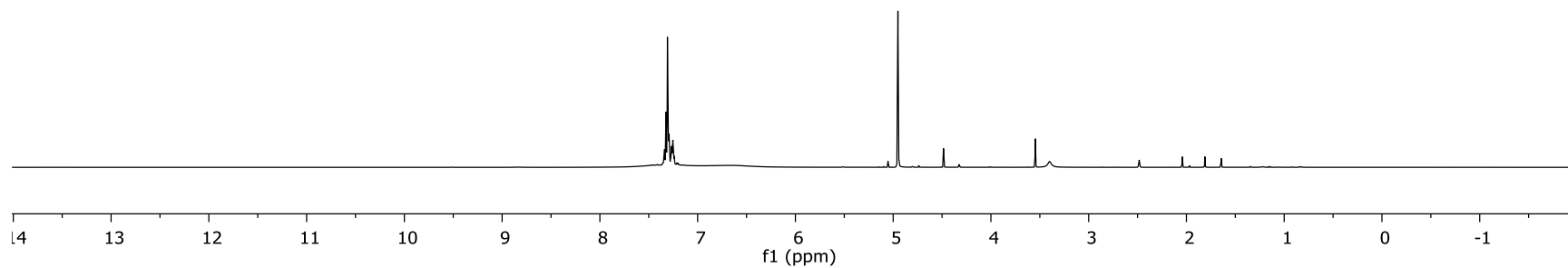
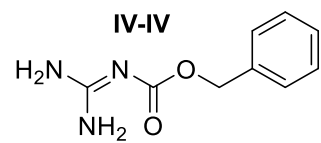


Figure IV-XXII: The ^1H NMR and ^{13}C NMR for Compound **IV-IV**

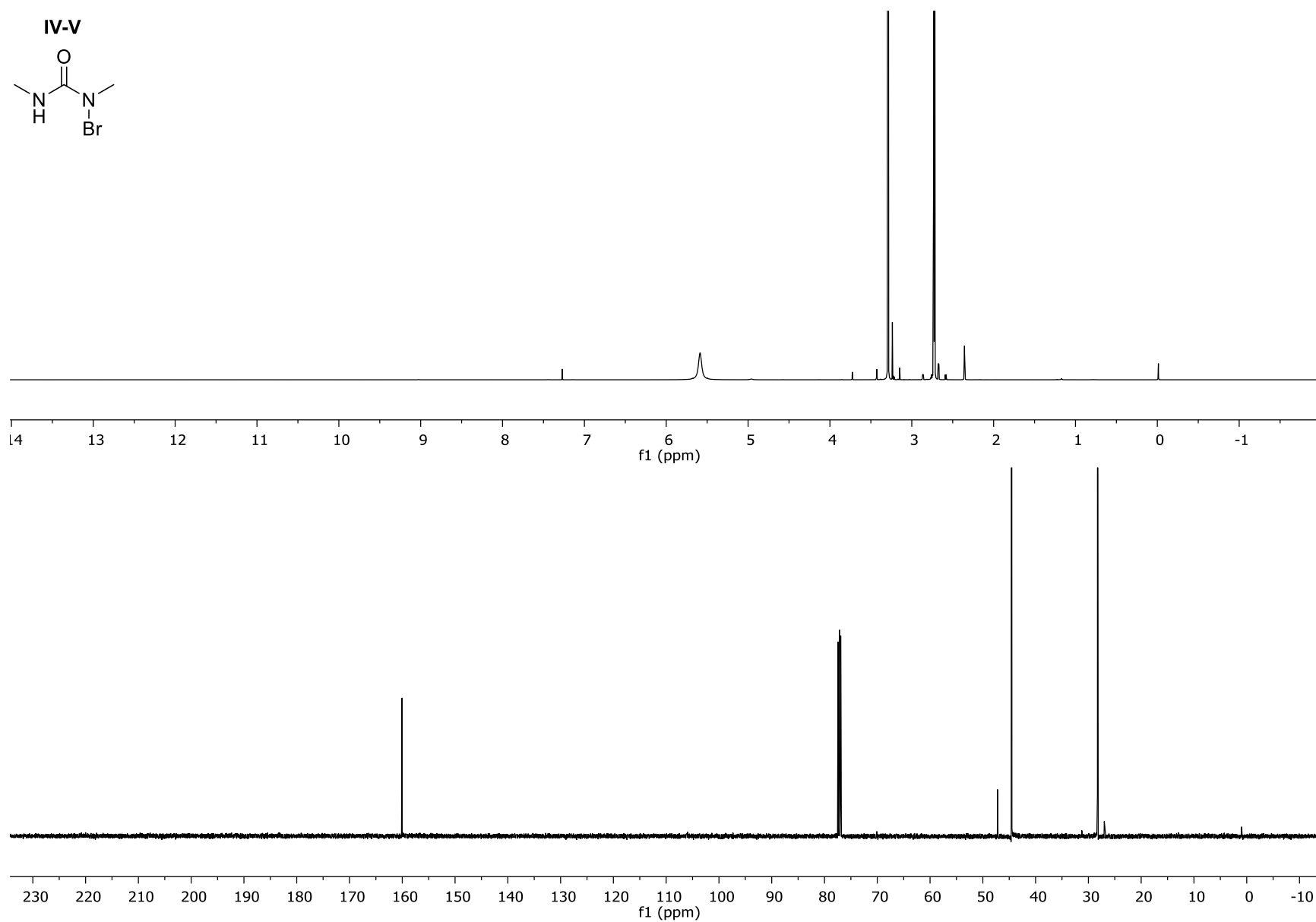
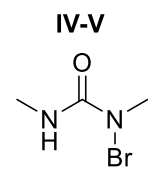


Figure IV-XXIII: The ^1H NMR and ^{13}C NMR for Compound IV-V

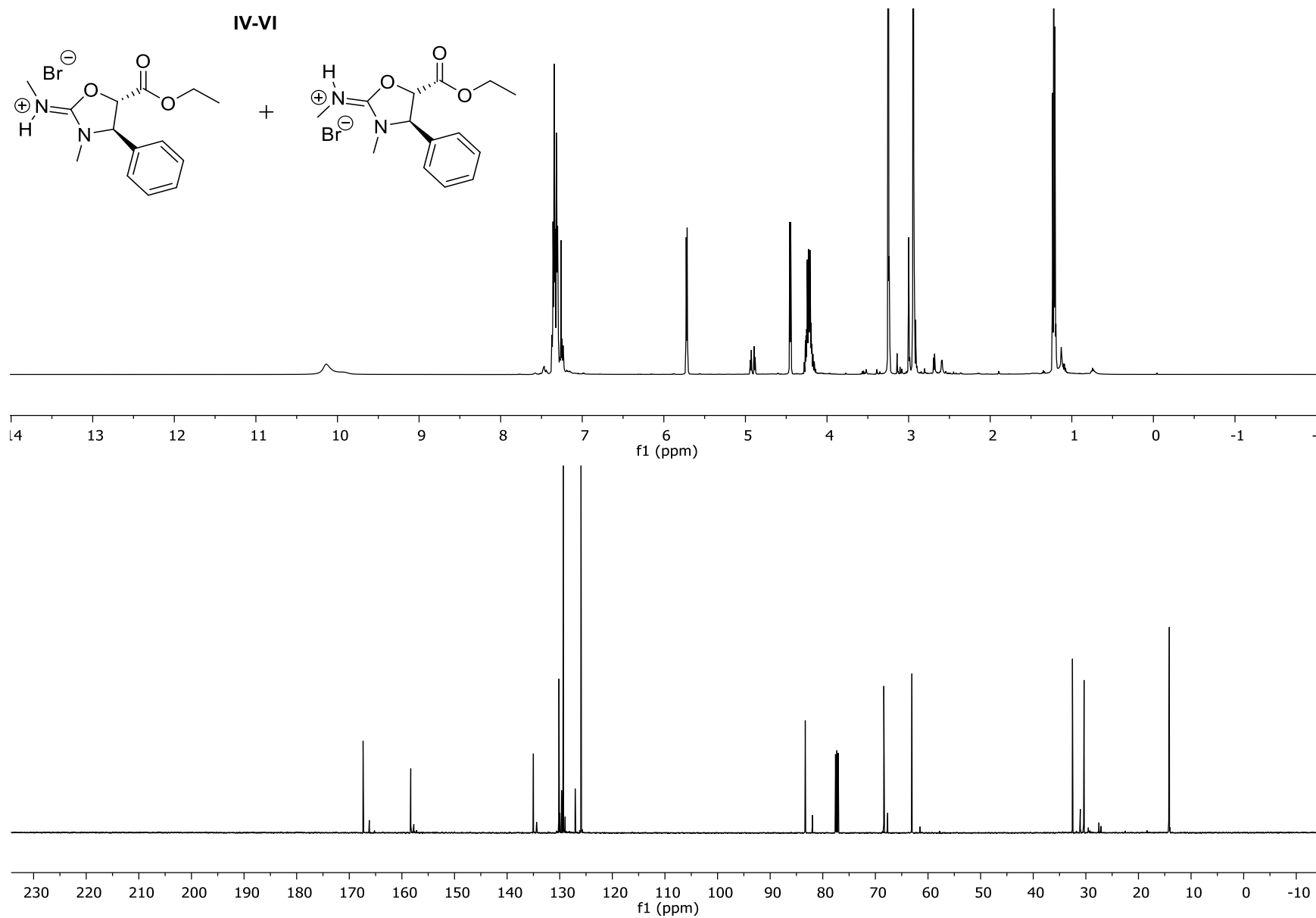


Figure IV-XXIV: The ^1H NMR and ^{13}C NMR for Compound IV-VI

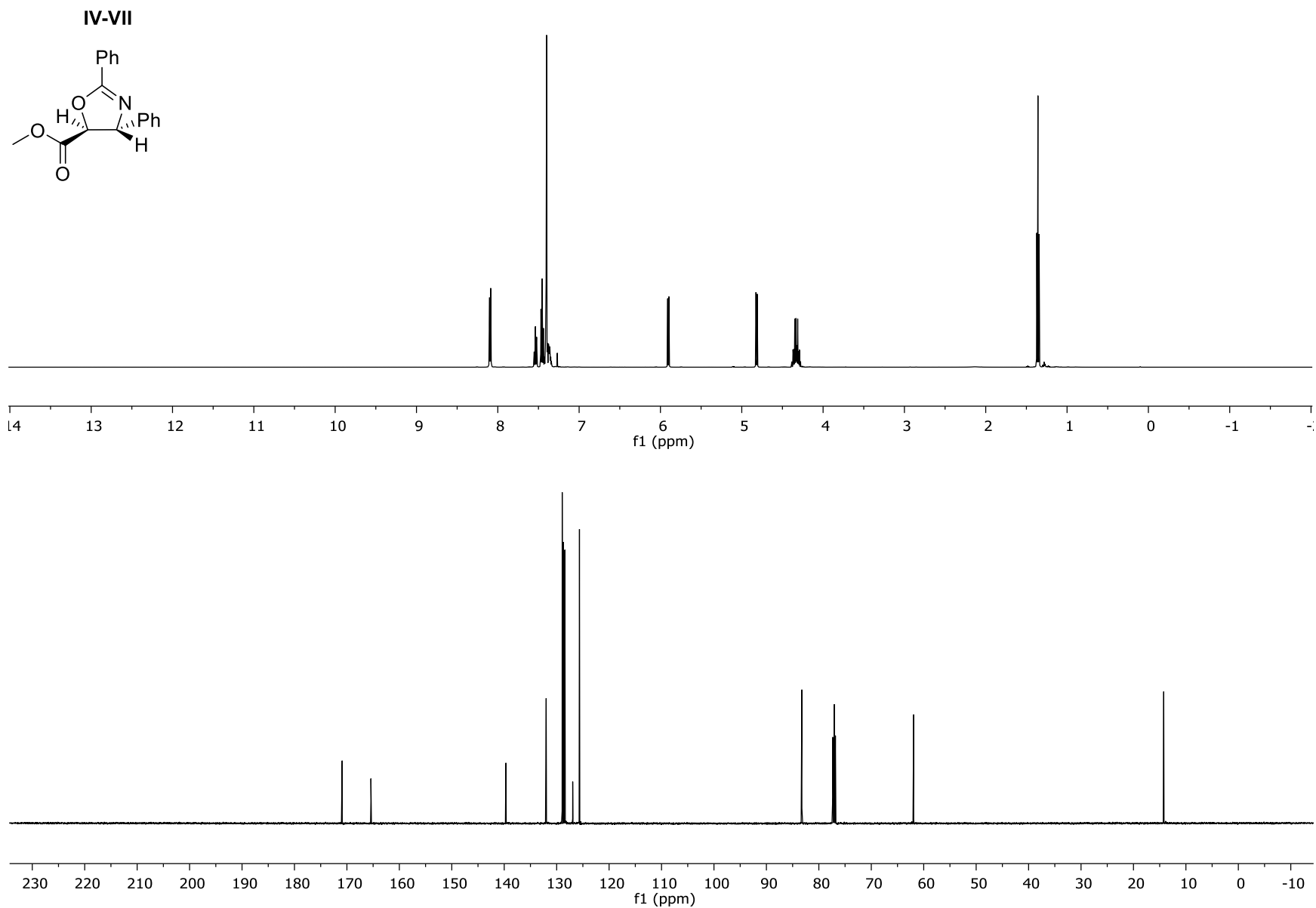


Figure IV-XXV: The ^1H NMR and ^{13}C NMR for Compound IV-VII

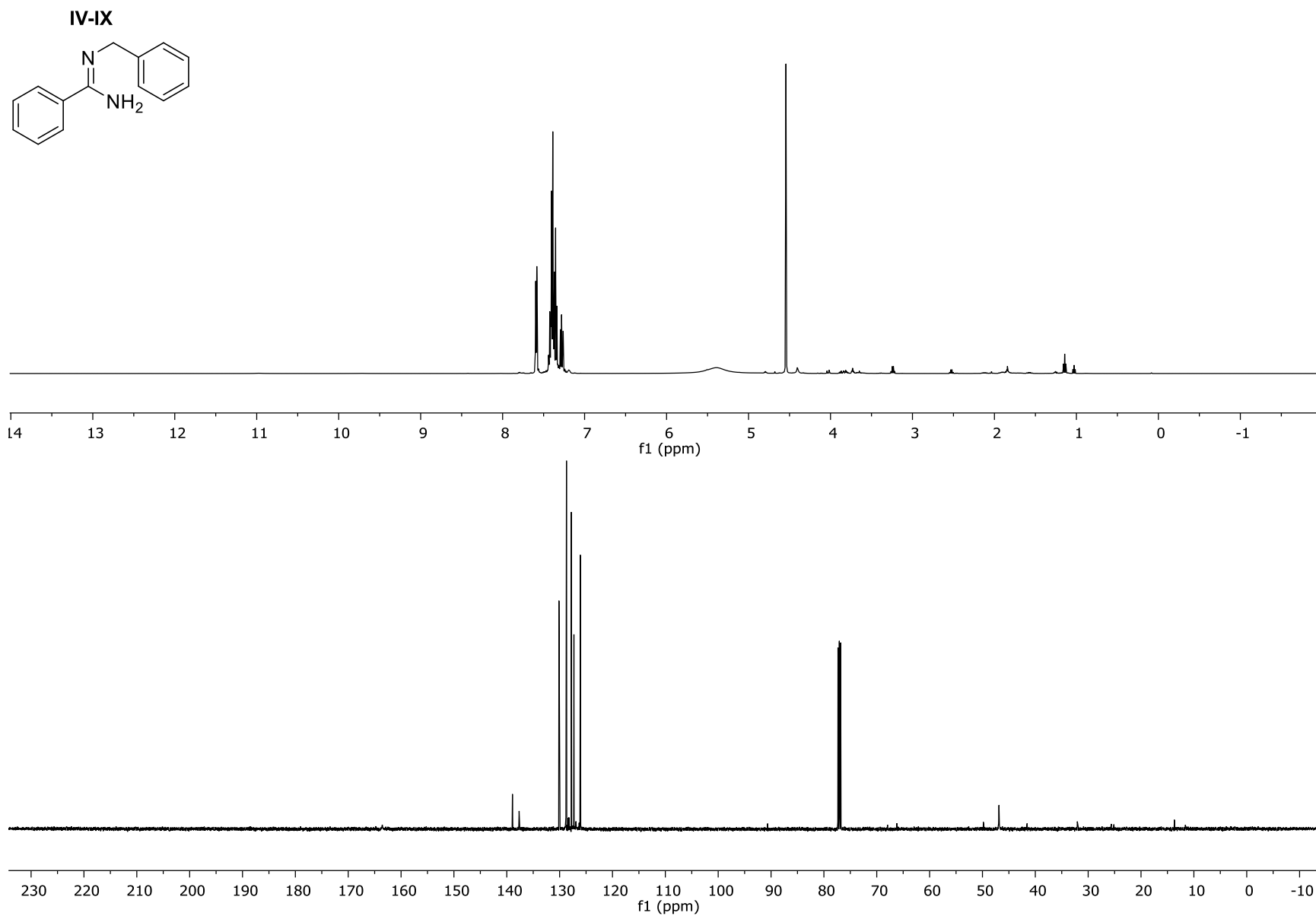


Figure IV-XXVII: The ^1H NMR and ^{13}C NMR for Compound IV-IX

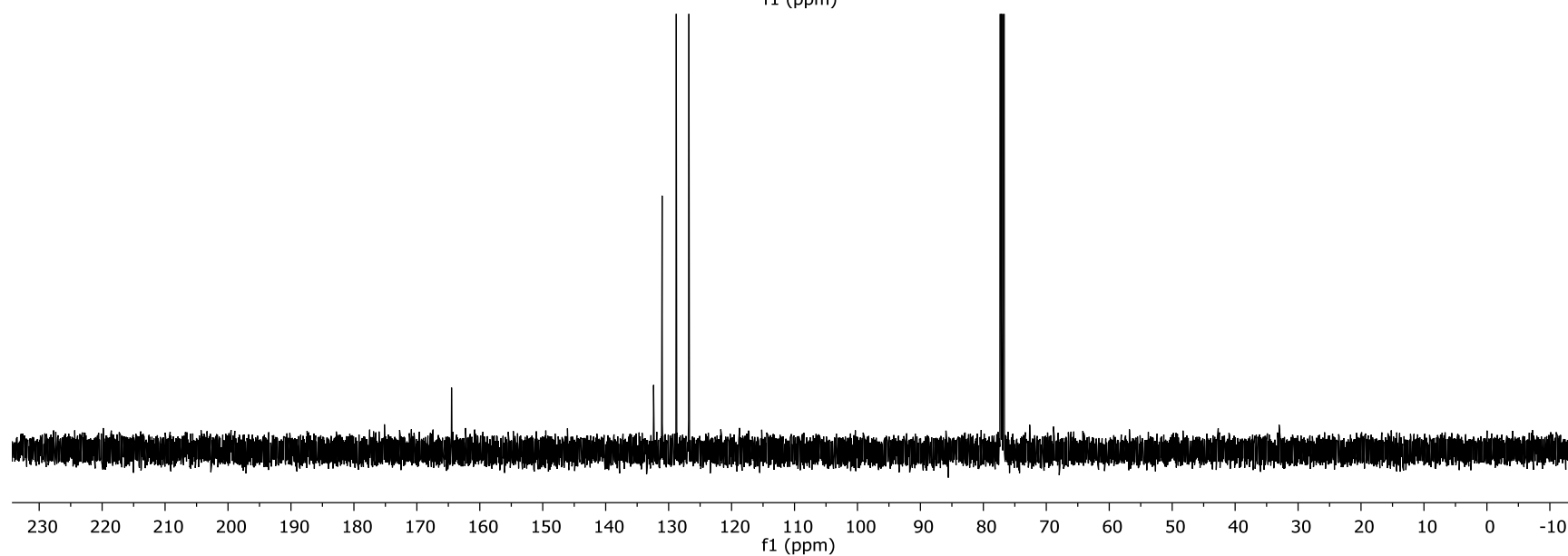
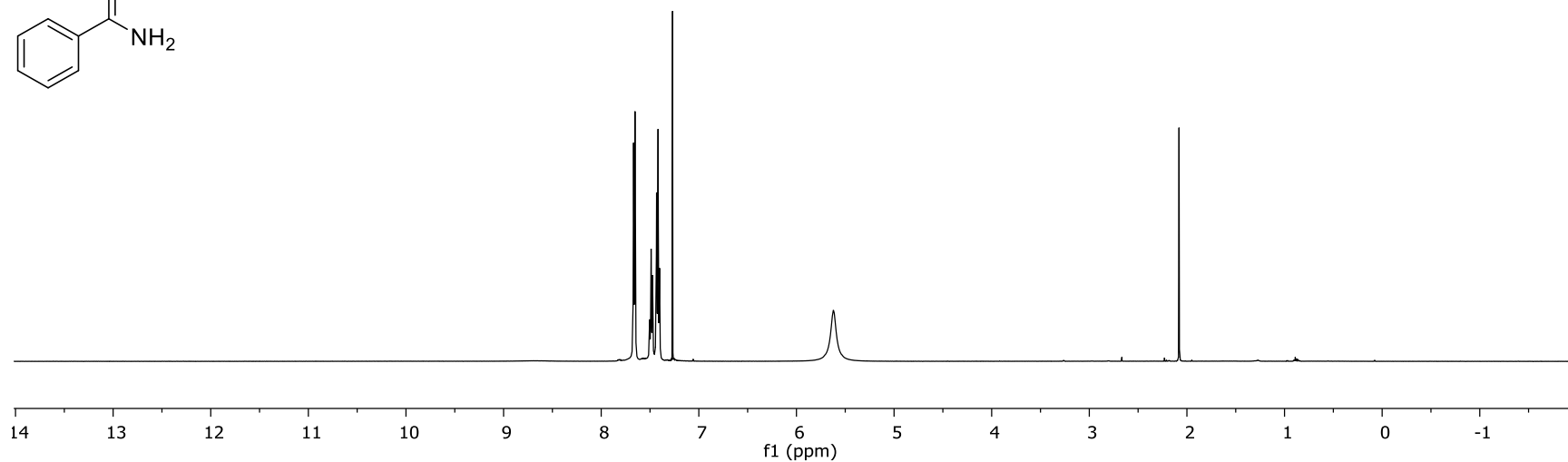


Figure IV-XXVIII: The $^1\text{H NMR}$ and $^{13}\text{C NMR}$ for Compound IV-X

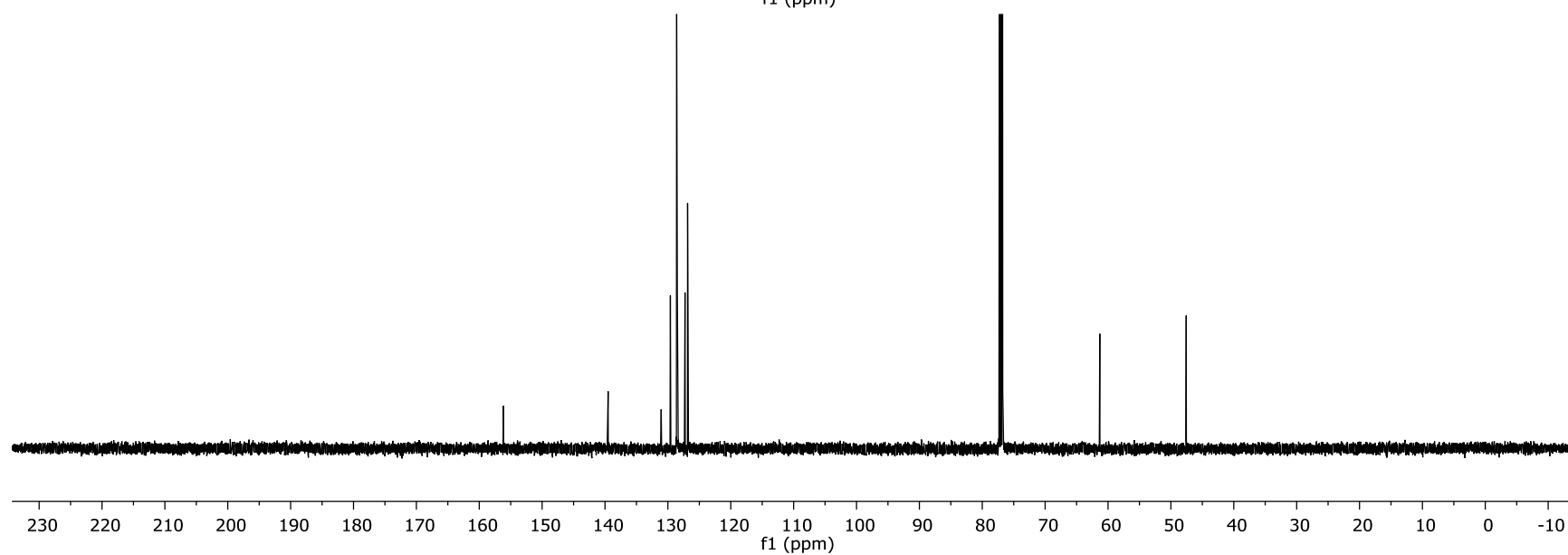
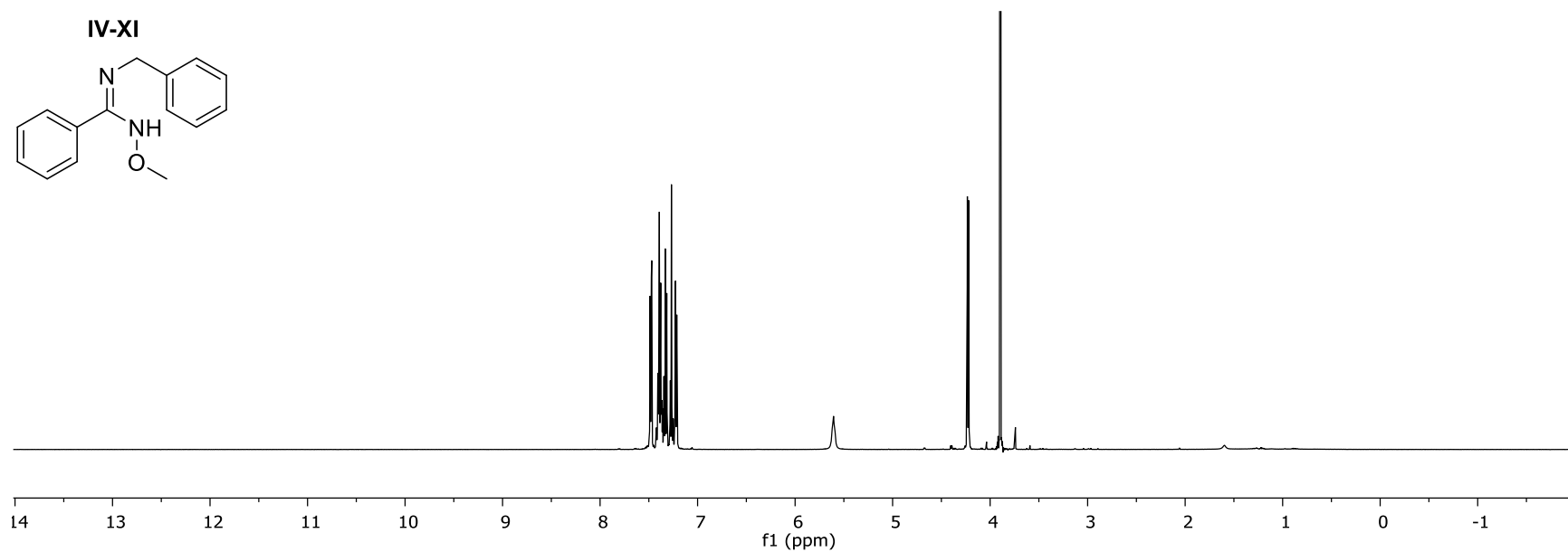
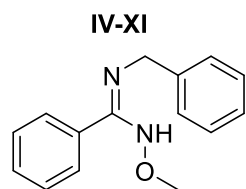


Figure IV-XXIX: The ^1H NMR and ^{13}C NMR for Compound **IV-XI**

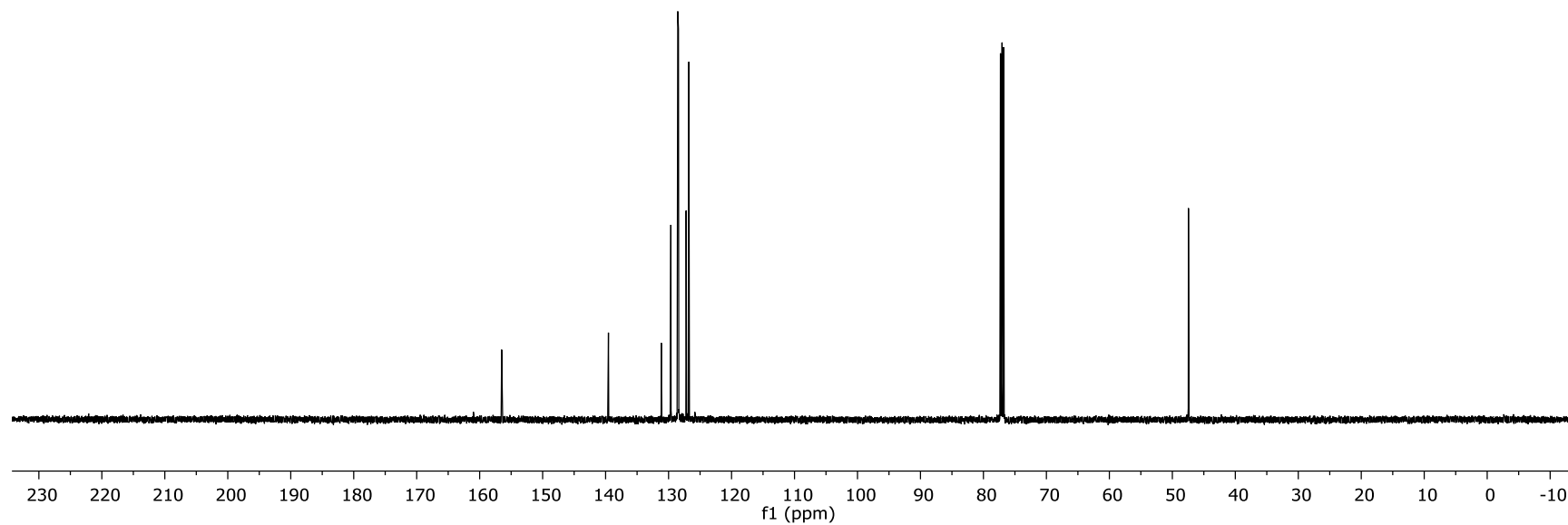
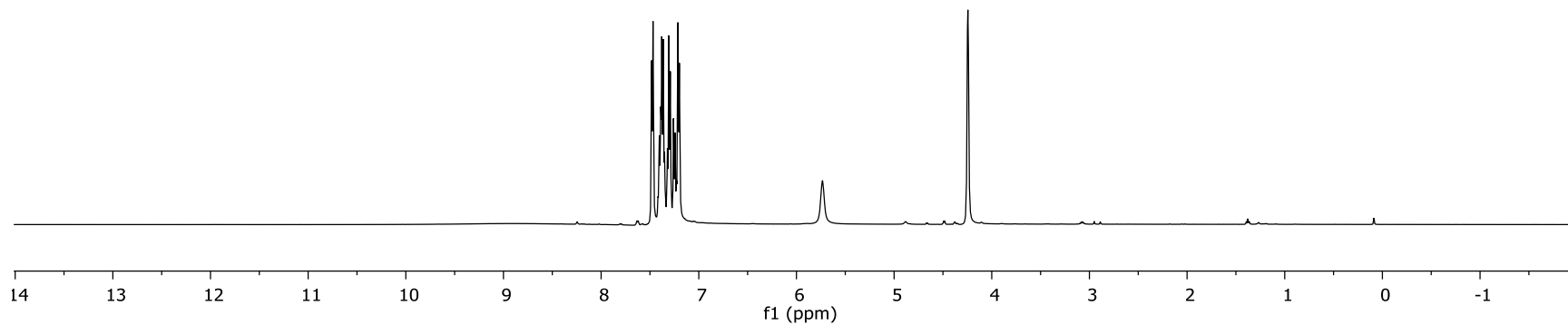
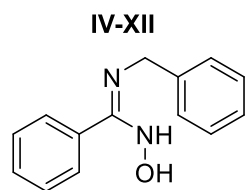


Figure IV-XXX: The ^1H NMR and ^{13}C NMR for Compound **IV-XII**

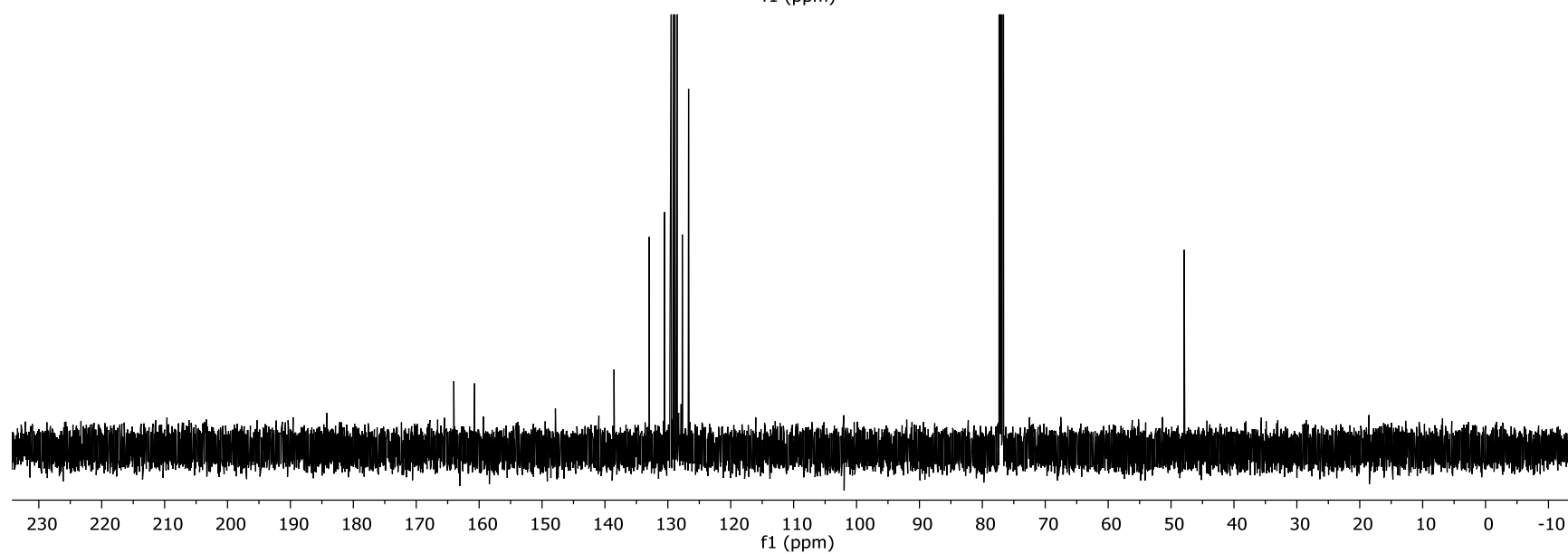
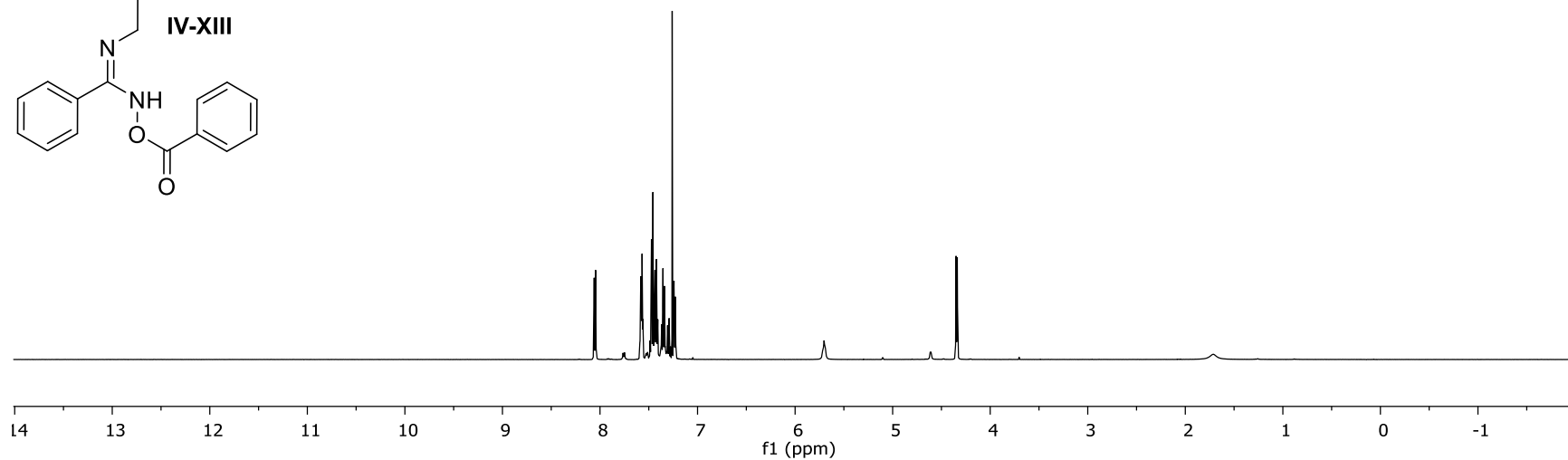
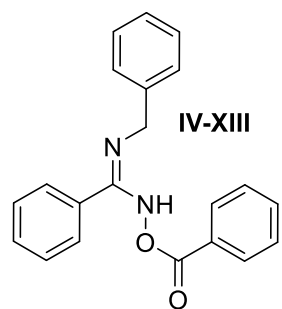


Figure IV-XXXI: The $^1\text{H NMR}$ and $^{13}\text{C NMR}$ for Compound IV-XIII

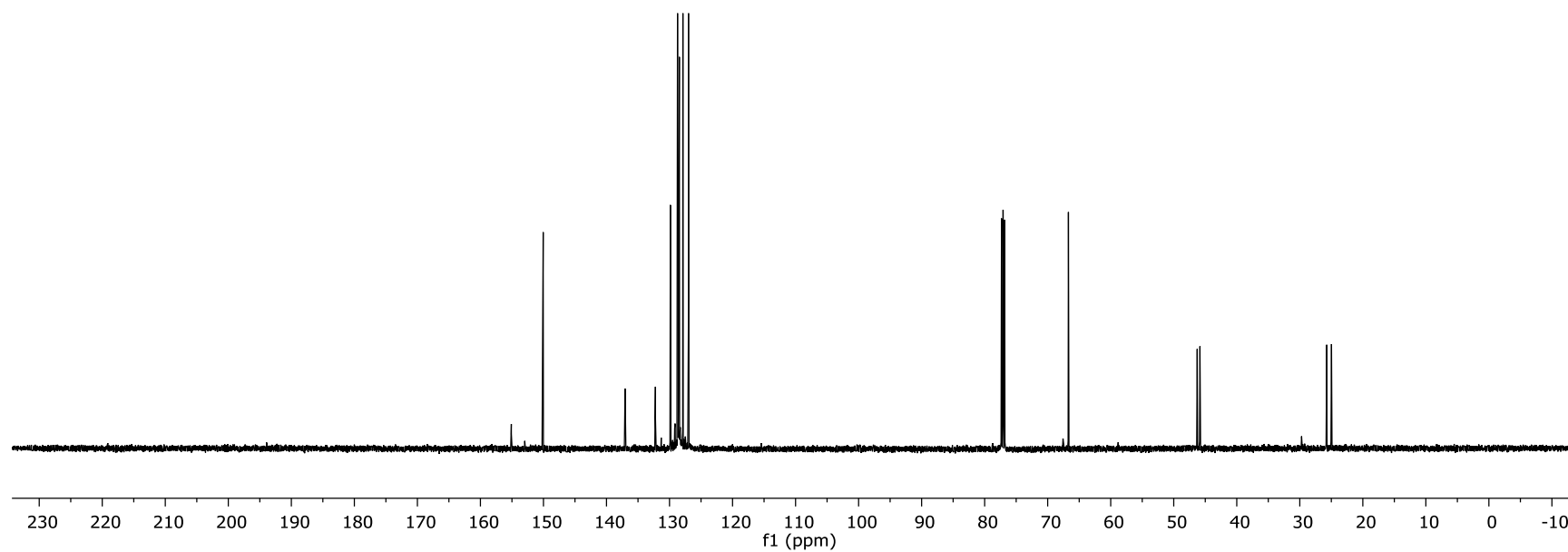
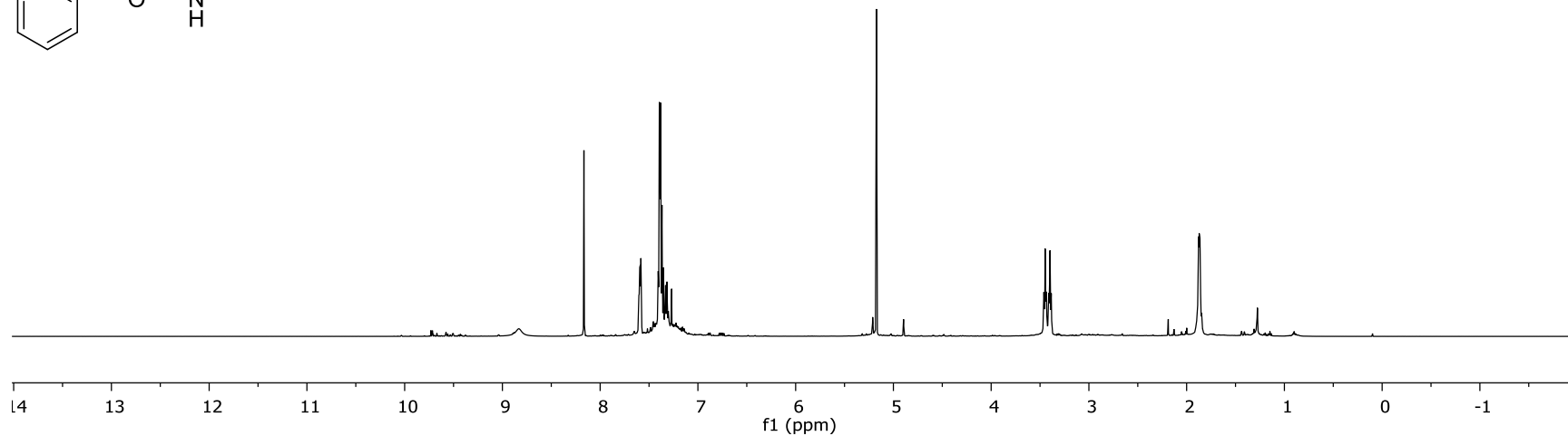
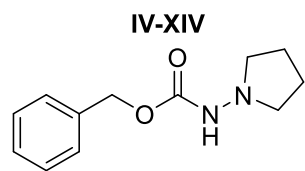


Figure IV-XXXII: The ^1H NMR and ^{13}C NMR for Compound IV-XIV

CHAPTER FIVE – CONCLUSIONS AND FUTURE WORK

In conclusion, my research within the Tepe group was focused around the design of new methodology towards accessing novel heterocyclic scaffolds for further evaluation as proteasome modulators. Initial biological evaluation identified imidazolines as h20s inhibitors. In this dissertation, we further demonstrated that the same imidazoline scaffolds can modulate both TB and h20s proteasomes. Through synthetic derivatization we have further developed the imidoyl aziridine expansion reaction to access a diverse library of imidazolines for biological evaluation. Our initial goals were to increase the potency of the imidazolines and identify the structural and electronic factors towards gaining specificity for the TB proteasome. Preliminary results have confirmed both goals. Probing the effect of electronic contribution to the potency of the 2-imidazoline identified the 4-methoxyphenyl derivative at the C₂ position as the most potent inhibitor. Further probing of the meta and ortho constitutional isomers of that molecule, resulted in less potent inhibitors and suggested that the electronic contribution isn't the only important interaction, atom orientation and location also plays a key role. This result was further supported by functionalization at the N₁ nitrogen of the imidazoline which had direct effects on the overall potency of the molecule. Computational modeling suggested that the steric effects of the N-1 group could be used to successfully anchor the molecule within the proteasome. This was experimentally confirmed with the cyclohexyl and cyclobutyl imidazoline derivatives. The changing of the substituent to a smaller group lowered the molecule's potency and does suggest that the sterics of the N-1 position are directly tied to reactivity. Probing the effect of substitution on specificity has identified two compounds with 3-fold selectivity for the TB proteasome over the h20s. Both

derivatives both employ the use of smaller functionalities at either the C₂ or N₁ positions result in inhibition of the TB proteasome while the potency in human 20s proteasome is greatly lessened.

Based on these results efforts were placed towards developing new methodology for imidazoline synthesis to enhance the specificity for the TB proteasome. Our hypothesis was that specificity for the TB proteasome could be enhanced based on accessing monosubstituted 2-imidazoline scaffolds. This was based on the specificity observed with disubstituted imidazolines with small N₁ and C₂ groups. This led to the discovery of the I-Br catalyzed pathway for oxazoline synthesis from α,β unsaturated esters. This reaction resulted in the addition of benzamide and 1,3-dimethyl urea across the starting olefin and identified the factors necessary for controlling the regiochemistry of benzamide addition. This hydrolysis of this heterocycle can lead to amino alcohol synthesis. Unfortunately, these experimental conditions were not compatible with amidines towards imidazoline synthesis. Further exploration led to sequential modification of amidine scaffolds have led to a new lead compound for exploring imidazoline synthesis from α,β unsaturated esters. This research will be continued by other students within the Tepe group. While pursuing olefin activation towards oxazolines and imidazolines, a new method for N-N bond formation was identified by the dehydration of Cbz-protected hydroxylamine in the presence of pyrrolidine. Future work within the Tepe group will focus around reproducing and furthering this reaction towards the synthesis of protected hydrazine molecules.

Agesamides A and B as well as synthetic analogs were attempted through regio-controlled ring opening of aziridine. It was hypothesized that ring opening would lead to the desired intermediate. Several attempts towards accessing the desired intermediates were pursued. With every iteration, the previous problems were addressed and fixed. The synthesis of these molecules was not completed. However, throughout this dissertation I have demonstrated that these problems

were addressed and fixed with every iteration, leading up to the successful N-alkylation of indole.
This research towards these molecules will be followed up on by other members of the Tepe group.

BIBLIOGRAPHY

BIBLIOGRAPHY

1. Liu, H.; Du, D.-M., Recent Advances in the Synthesis of 2-Imidazolines and Their Applications in Homogeneous Catalysis. *Advanced Synthesis & Catalysis* **2009**, *351*, 489-519.
2. Tyagi, R.; Tyagi, V. K.; Pandey, S. K., Imidazoline and Its Derivatives : An Overview. *Journal of Oleo Science* **2007**, *56*, 211-222.
3. Zhang, L.; He, Y.; Zhou, Y.; Yang, R.; Yang, Q.; Qing, D.; Niu, Q., A novel imidazoline derivative as corrosion inhibitor for P110 carbon steel in hydrochloric acid environment. *Petroleum* **2015**, *1*, 237-243.
4. Krasavin, M., Biologically active compounds based on the privileged 2-imidazoline scaffold: The world beyond adrenergic/imidazoline receptor modulators. *European Journal of Medicinal Chemistry* **2015**, *97*, 525-537.
5. S Regunathan, a.; Reis, D. J., Imidazoline Receptors and Their Endogenous Ligands. *Annu. Rev. Pharmacool. Toxicol.* **1996**, *36*, 511-544.
6. Ferm, R. J.; Riebsomer, J. L., The Chemistry of the 2-Imidazolines and Imidazolidines. *Chem. Rev.* **1954**, *54*, 593-613.
7. Dauwe, C.; Buddrus, J., Synthesis of Enantiopure C2-Chiral Amidines. *Synthesis* **1995**, *1995*, 171-172.
8. Neef, G.; Eder, U.; Sauer, G., One-step conversions of esters to 2-imidazolines, benzimidazoles and benzothiazoles by aluminum organic reagents. *J. Org. Chem.* **1981**, *46*, 2824-2826.
9. You, S.-L.; Kelly, J. W., Highly Efficient Enantiospecific Synthesis of Imidazoline-Containing Amino Acids Using Bis(triphenyl)oxodiphosphonium Trifluoromethanesulfonate. *Organic Letters* **2004**, *6*, 1681-1683.
10. Uchida, H.; Shimizu, T.; Reddy, P. Y.; Nakamura, S.; Toru, T., Solvent-Free Efficient Synthesis of 2,4,5-Triarylimidazolines from Aromatic Aldehydes and Hexamethyldisilazane. *Synthesis* **2003**, *2003*, 1236-1240.
11. Boland, N. A.; Casey, M.; Hynes, S. J.; Matthews, J. W.; Smyth, M. P., A Novel General Route for the Preparation of Enantiopure Imidazolines. *J. Org. Chem.* **2002**, *67*, 3919-3922.
12. Nakamura, S.; Maeno, Y.; Ohara, M.; Yamamura, A.; Funahashi, Y.; Shibata, N., Enantioselective Synthesis of Imidazolines with Quaternary Stereocenters by Organocatalytic Reaction of N-(Heteroarenesulfonyl)imines with Isocynoacetates. *Organic Letters* **2012**, *14*, 2960-2963.

13. Chen, J.-Q.; Yu, W.-L.; Wei, Y.-L.; Li, T.-H.; Xu, P.-F., Photoredox-Induced Functionalization of Alkenes for the Synthesis of Substituted Imidazolines and Oxazolidines. *J. Org. Chem.* **2017**, *82*, 243-249.
14. Hiyama, T.; Koide, H.; Fujita, S.; Nozaki, H., Reaction of N-alkoxycarbonylaziridines with nitriles. *Tetrahedron* **1973**, *29*, 3137-3139.
15. Ghorai, M. K.; Ghosh, K.; Das, K., Copper(II) triflate promoted cycloaddition of α -alkyl or aryl substituted N-tosylaziridines with nitriles: a highly efficient synthesis of substituted imidazolines. *Tetrahedron Letters* **2006**, *47*, 5399-5403.
16. Sharma, V.; Tepe, J. J., Diastereochemical Diversity of Imidazoline Scaffolds via Substrate Controlled TMSCl Mediated Cycloaddition of Azlactones. *Organic Letters* **2005**, *7*, 5091-5094.
17. Kahlon, D. K.; Lansdell, T. A.; Fisk, J. S.; Tepe, J. J., Structural–activity relationship study of highly-functionalized imidazolines as potent inhibitors of nuclear transcription factor- κ B mediated IL-6 production. *Bioorganic & Medicinal Chemistry* **2009**, *17*, 3093-3103.
18. Qu, K.; Fisk, J. S.; Tepe, J. J., Azomethine ylide mediated inversion of configuration of quaternary imidazoline carbon: converting trans- to its cis- imidazolines. *Tetrahedron letters* **2011**, *52*, 4840-4842.
19. Kuszpit, M. R.; Wulff, W. D.; Tepe, J. J., One-Pot Synthesis of 2-Imidazolines via the Ring Expansion of Imidoyl Chlorides with Aziridines. *J. Org. Chem.* **2011**, *76*, 2913-2919.
20. Gallastegui, N.; Groll, M., The 26S proteasome: assembly and function of a destructive machine. *Trends Biochem. Sci* **2010**, *35*, 634-642.
21. Borissenko, L.; Groll, M., 20S Proteasome and Its Inhibitors: Crystallographic Knowledge for Drug Development. *Chem. Rev.* **2007**, *107*, 687-717.
22. Almond, J. B.; Cohen, G. M., Almond JB, Cohen GM.. *The proteasome: a novel target for cancer chemotherapy. Leukemia* **16**: 433-443. 2002; Vol. 16, p 433-43.
23. Rentsch, A.; Landsberg, D.; Brodmann, T.; Bülow, L.; Girbig, A.-K.; Kalesse, M., Synthesis and Pharmacology of Proteasome Inhibitors. *Angew. Chem. Int. Ed.* **2013**, *52*, 5450-5488.
24. McConkey, D. J.; Zhu, K., Mechanisms of proteasome inhibitor action and resistance in cancer. *Drug Resistance Updates* **2008**, *11*, 164-179.
25. Amoils, S., The Mtb proteasome: an open and shut case. *Nat Rev Micro* **2006**, *4*, 325-325.
26. Hu, G.; Lin, G.; Wang, M.; Dick, L.; Xu, R.-M.; Nathan, C.; Li, H., Structure of the Mycobacterium tuberculosis proteasome and mechanism of inhibition by a peptidyl boronate. *Mol. Microbiol.* **2006**, *59*, 1417-1428.

27. Bode, N. J.; Darwin, K. H., The Pup-Proteasome System of Mycobacteria. *Microbiology spectrum* **2014**, *2*, 10.1128/microbiolspec.MGM2-0008-2013.
28. Azevedo, L. M.; Lansdell, T. A.; Ludwig, J. R.; Mosey, R. A.; Woloch, D. K.; Cogan, D. P.; Patten, G. P.; Kuszpit, M. R.; Fisk, J. S.; Tepe, J. J., Inhibition of the Human Proteasome by Imidazoline Scaffolds. *J. Med. Chem.* **2013**, *56*, 5974-5978.
29. Chowdhury, C.; Mukherjee, S.; Das, B.; Achari, B., Expedient and Rapid Synthesis of 1,2,3-Triazolo[5,1-c]morpholines through Palladium–Copper Catalysis. *J. Org. Chem.* **2009**, *74*, 3612-3615.
30. Busacca, C. A.; Bartholomeyzik, T.; Cheekoori, S.; Grinberg, N.; Lee, H.; Ma, S.; Saha, A.; Shen, S.; Senanayake, C. H., On the Racemization of Chiral Imidazolines. *J. Org. Chem.* **2008**, *73*, 9756-9761.
31. Evans, D. A.; Bilodeau, M. T.; Faul, M. M., Development of the Copper-Catalyzed Olefin Aziridination Reaction. *J. Am. Chem. Soc.* **1994**, *116*, 2742-2753.
32. Halfen, J. A.; Hallman, J. K.; Schultz, J. A.; Emerson, J. P., Remarkably Efficient Olefin Aziridination Mediated by a New Copper(II) Complex. *Organometallics* **1999**, *18*, 5435-5437.
33. Kantam, M. L.; Neeraja, V.; Kavita, B.; Haritha, Y., Cu(acac)₂ Immobilized in Ionic Liquids: A Novel and Recyclable Catalytic System for Aziridination of Olefins Using PhI=NTs as Nitrene Donor. *Synlett* **2004**, *2004*, 525-527.
34. Guthikonda, K.; Du Bois, J., A Unique and Highly Efficient Method for Catalytic Olefin Aziridination. *J. Am. Chem. Soc.* **2002**, *124*, 13672-13673.
35. Yoshimura, A.; Luedtke, M. W.; Zhdankin, V. V., (Tosylimino)phenyl- λ^3 -iodane as a Reagent for the Synthesis of Methyl Carbamates via Hofmann Rearrangement of Aromatic and Aliphatic Carboxamides. *J. Org. Chem.* **2012**, *77*, 2087-2091.
36. Kwong, H.-L.; Liu, D.; Chan, K.-Y.; Lee, C.-S.; Huang, K.-H.; Che, C.-M., Copper(I)-catalyzed asymmetric alkene aziridination mediated by PhI(OAc)₂: a facile one-pot procedure. *Tetrahedron Letters* **2004**, *45*, 3965-3968.
37. Sun, H.; Huang, B.; Lin, R.; Yang, C.; Xia, W., Metal-free one-pot synthesis of 2-substituted and 2,3-disubstituted morpholines from aziridines. *Beilstein Journal of Organic Chemistry* **2015**, *11*, 524-529.
38. Huang, C.-Y.; Doyle, A. G., Nickel-Catalyzed Negishi Alkylations of Styrenyl Aziridines. *J. Am. Chem. Soc.* **2012**, *134*, 9541-9544.
39. Ghorai, M. K.; Das, K.; Shukla, D., Lewis Acid-Mediated Highly Regioselective SN₂-Type Ring-Opening of 2-Aryl-N-tosylazetidines and Aziridines by Alcohols. *J. Org. Chem.* **2007**, *72*, 5859-5862.

40. Gandhi, S.; Bisai, A.; Prasad, B. A. B.; Singh, V. K., Studies on the Reaction of Aziridines with Nitriles and Carbonyls: Synthesis of Imidazolines and Oxazolidines. *J. Org. Chem.* **2007**, *72*, 2133-2142.
41. Hu, X. E., Nucleophilic ring opening of aziridines. *Tetrahedron* **2004**, *60*, 2701-2743.
42. Ghorai, M. K.; Das, K.; Kumar, A.; Ghosh, K., An efficient route to regioselective opening of N-tosylaziridines with zinc(II) halides. *Tetrahedron Letters* **2005**, *46*, 4103-4106.
43. Craig, R. A.; O'Connor, N. R.; Goldberg, A. F. G.; Stoltz, B. M., Stereoselective Lewis Acid Mediated (3+2) Cycloadditions of N-H- and N-Sulfonylaziridines with Heterocumulenes. *Chemistry – A European Journal* **2014**, *20*, 4806-4813.
44. Kokatla, H. P.; Thomson, P. F.; Bae, S.; Doddi, V. R.; Lakshman, M. K., Reduction of Amine N-Oxides by Diboron Reagents. *J. Org. Chem.* **2011**, *76*, 7842-7848.
45. Nyasse, B.; Grehn, L.; Ragnarsson, U., Mild, efficient cleavage of arenesulfonamides by magnesium reduction. *Chem. Commun.* **1997**, 1017-1018.
46. Alonso, D. A.; Andersson, P. G., Deprotection of Sulfonyl Aziridines. *J. Org. Chem.* **1998**, *63*, 9455-9461.
47. Sabitha, G.; Reddy, B. V. S.; Abraham, S.; Yadav, J. S., Deprotection of sulfonamides using iodotrimethylsilane. *Tetrahedron Letters* **1999**, *40*, 1569-1570.
48. Ankner, T.; Hilmersson, G., Instantaneous Deprotection of Tosylamides and Esters with SmI₂/Amine/Water. *Organic Letters* **2009**, *11*, 503-506.
49. Vedejs, E.; Lin, S., Deprotection of Arenesulfonamides with Samarium iodide. *J. Org. Chem.* **1994**, *59*, 1602-1603.
50. Ji, S.; Gortler, L. B.; Waring, A.; Battisti, A. J.; Bank, S.; Closson, W. D.; Wriede, P. A., Cleavage of sulfonamides with sodium naphthalene. *J. Am. Chem. Soc.* **1967**, *89*, 5311-5312.
51. Yadav, J. S.; Satheesh, G.; Murthy, C. V. S. R., Synthesis of (+)-Lycoricidine by the Application of Oxidative and Regioselective Ring-Opening of Aziridines. *Organic Letters* **2010**, *12*, 2544-2547.
52. Davis, O. A.; Hughes, M.; Bull, J. A., Copper-Catalyzed N-Arylation of 2-Imidazolines with Aryl Iodides. *J. Org. Chem.* **2013**, *78*, 3470-3475.
53. Horneff, T.; Chuprakov, S.; Chernyak, N.; Gevorgyan, V.; Fokin, V. V., Rhodium-Catalyzed Transannulation of 1,2,3-Triazoles with Nitriles. *J. Am. Chem. Soc.* **2008**, *130*, 14972-14974.
54. Clemens, N.; Sereda, O.; Wilhelm, R., Unexpected behaviour of tosylated and acetylated imidazolinium salts. *Organic & Biomolecular Chemistry* **2006**, *4*, 2285-2290.

55. Yang, H.-T.; Xing, M.-L.; Lu, X.-W.; Li, J.-X.; Cheng, J.; Sun, X.-Q.; Miao, C.-B., BF₃·Et₂O- or DMAP-Catalyzed Double Nucleophilic Substitution Reaction of Aziridinofullerenes with Sulfamides or Amidines. *J. Org. Chem.* **2014**, *79*, 11744-11749.
56. Havare, N.; Plattner, D. A., Oxidative Cleavage and Rearrangement of Aryl Epoxides Using Iodosylbenzene: on Criegee's Trail. *Helv. Chim. Acta* **2012**, *95*, 2036-2042.
57. Foelsche, E.; Hickel, A.; Hoenig, H.; Seuffer-Wasserthal, P., Lipase-catalyzed resolution of acyclic amino alcohol precursors. *J. Org. Chem.* **1990**, *55*, 1749-1753.
58. Cobb, J. E.; Cribbs, C. M.; Henke, B. R.; Uehling, D. E.; Hernan, A. G.; Martin, C.; Rayner, C. M., Triphenylphosphine. In *Encyclopedia of Reagents for Organic Synthesis*, John Wiley & Sons, Ltd: 2001.
59. Lansdell, T. A.; Hurchla, M. A.; Xiang, J.; Hovde, S.; Weilbaecher, K. N.; Henry, R. W.; Tepe, J. J., Noncompetitive Modulation of the Proteasome by Imidazoline Scaffolds Overcomes Bortezomib Resistance and Delays MM Tumor Growth in Vivo. *ACS Chemical Biology* **2013**, *8*, 578-587.
60. Lansdell, T. A.; Hewlett, N. M.; Skoumbourdis, A. P.; Fodor, M. D.; Seiple, I. B.; Su, S.; Baran, P. S.; Feldman, K. S.; Tepe, J. J., Palau'amine and Related Oroidin Alkaloids Dibromophakellin and Dibromophakellstatin Inhibit the Human 20S Proteasome. *J. Nat. Prod.* **2012**, *75*, 980-985.
61. Gautschi, J. T.; Whitman, S.; Holman, T. R.; Crews, P., An Analysis of Phakellin and Oroidin Structures Stimulated by Further Study of an Agelas Sponge. *J. Nat. Prod.* **2004**, *67*, 1256-1261.
62. Arndt, H.-D.; Riedrich, M., Synthesis of Marine Alkaloids from the Oroidin Family. *Angew. Chem. Int. Ed.* **2008**, *47*, 4785-4788.
63. Seiple, I. B.; Su, S.; Young, I. S.; Lewis, C. A.; Yamaguchi, J.; Baran, P. S., Total Synthesis of Palau'amine. *Angew. Chem. Int. Ed.* **2010**, *49*, 1095-1098.
64. Namba, K.; Takeuchi, K.; Kaihara, Y.; Oda, M.; Nakayama, A.; Nakayama, A.; Yoshida, M.; Tanino, K., Total synthesis of palau'amine. **2015**, *6*, 8731.
65. Hewlett, N. M.; Tepe, J. J., Total Synthesis of the Natural Product (±)-Dibromophakellin and Analogues. *Organic Letters* **2011**, *13*, 4550-4553.
66. Beck, P.; Lansdell, T. A.; Hewlett, N. M.; Tepe, J. J.; Groll, M., Indolo-Phakellins as β5-Specific Noncovalent Proteasome Inhibitors. *Angew. Chem. Int. Ed.* **2015**, *54*, 2830-2833.
67. Kuramoto, M.; Miyake, N.; Ishimaru, Y.; Ono, N.; Uno, H., Cylindradines A and B: Novel Bromopyrrole Alkaloids from the Marine Sponge *Axinella cylindratum*. *Organic Letters* **2008**, *10*, 5465-5468.

68. Imaoka, T.; Akimoto, T.; Iwamoto, O.; Nagasawa, K., Total Synthesis of (+)-Dibromophakellin and (+)-Dibromophakellstatin. *Chemistry – An Asian Journal* **2010**, *5*, 1810-1816.
69. Tsuda, M.; Yasuda, T.; Fukushi, E.; Kawabata, J.; Sekiguchi, M.; Fromont, J.; Kobayashi, J. i., Agesamides A and B, Bromopyrrole Alkaloids from Sponge Agelas Species: Application of DOSY for Chemical Screening of New Metabolites. *Organic Letters* **2006**, *8*, 4235-4238.
70. Patel, J.; Pelloux-Léon, N.; Minassian, F.; Vallée, Y., Total synthesis of (S)-(-)-cyclooroidin. *Tetrahedron Letters* **2006**, *47*, 5561-5563.
71. Papeo, G.; Frau, M. A. G.-Z.; Borghi, D.; Varasi, M., Total synthesis of (±)-cyclooroidin. *Tetrahedron Letters* **2005**, *46*, 8635-8638.
72. Mukherjee, S.; Sivappa, R.; Yousufuddin, M.; Lovely, C. J., Asymmetric Total Synthesis of ent-Cyclooroidin. *Organic Letters* **2010**, *12*, 4940-4943.
73. Patel, J.; Pelloux-Léon, N.; Minassian, F.; Vallée, Y., Syntheses of S-Enantiomers of Hanishin, Longamide B, and Longamide B Methyl Ester from L-Aspartic Acid β-Methyl Ester: Establishment of Absolute Stereochemistry. *J. Org. Chem.* **2005**, *70*, 9081-9084.
74. Trost, B. M.; Dong, G., Asymmetric Annulation toward Pyrrolo-piperazinones: Concise Enantioselective Syntheses of Pyrrole Alkaloid Natural Products. *Organic Letters* **2007**, *9*, 2357-2359.
75. Lee, S.-J.; Youn, S.-H.; Cho, C.-W., Organocatalytic enantioselective formal synthesis of bromopyrrole alkaloids via aza-Michael addition. *Organic & Biomolecular Chemistry* **2011**, *9*, 7734-7741.
76. Kuszpit, M. R.; Giletto, M. B.; Jones, C. L.; Bethel, T. K.; Tepe, J. J., Hydroxyamination of Olefins Using Br-N-(CO₂Me)₂. *J. Org. Chem.* **2015**, *80*, 1440-1445.
77. Schmuck, C.; Bickert, V.; Merschky, M.; Geiger, L.; Rupperecht, D.; Dudaczek, J.; Wich, P.; Rehm, T.; Machon, U., A Facile and Efficient Multi-Gram Synthesis of N-Protected 5-(Guanidinocarbonyl)-1H-pyrrole-2-carboxylic Acids. *Eur. J. Org. Chem.* **2008**, *2008*, 324-329.
78. Çetinkaya, Y.; Balci, M., Selective synthesis of N-substituted pyrrolo[1,2-a]pyrazin-1(2H)-one derivatives via alkyne cyclization. *Tetrahedron Letters* **2014**, *55*, 6698-6702.
79. Pace, V.; Vilkauskaitė, G.; Sackus, A.; Holzer, W., Highly efficient and chemoselective [small alpha]-iodination of acrylate esters through Morita-Baylis-Hillman-type chemistry. *Organic & Biomolecular Chemistry* **2013**, *11*, 1085-1088.
80. Ahrendt, K. A.; Borths, C. J.; MacMillan, D. W. C., New Strategies for Organic Catalysis: The First Highly Enantioselective Organocatalytic Diels–Alder Reaction. *J. Am. Chem. Soc.* **2000**, *122*, 4243-4244.

81. Paras, N. A.; MacMillan, D. W. C., The Enantioselective Organocatalytic 1,4-Addition of Electron-Rich Benzenes to α,β -Unsaturated Aldehydes. *J. Am. Chem. Soc.* **2002**, *124*, 7894-7895.
82. Huang, Y.; Walji, A. M.; Larsen, C. H.; MacMillan, D. W. C., Enantioselective Organo-Cascade Catalysis. *J. Am. Chem. Soc.* **2005**, *127*, 15051-15053.
83. Chen, Y. K.; Yoshida, M.; MacMillan, D. W. C., Enantioselective Organocatalytic Amine Conjugate Addition. *J. Am. Chem. Soc.* **2006**, *128*, 9328-9329.
84. Mangion, I. K.; Northrup, A. B.; MacMillan, D. W. C., The Importance of Iminium Geometry Control in Enamine Catalysis: Identification of a New Catalyst Architecture for Aldehyde–Aldehyde Couplings. *Angew. Chem. Int. Ed.* **2004**, *43*, 6722-6724.
85. Lelais, G.; MacMillan, D. W. C., Iminium Catalysis. In *Enantioselective Organocatalysis*, Wiley-VCH Verlag GmbH & Co. KGaA: 2007; pp 95-120.
86. Jiang, H.; Nielsen, J. B.; Nielsen, M.; Jørgensen, K. A., Organocatalysed Asymmetric β -Amination and Multicomponent syn-Selective Diamination of α,β -Unsaturated Aldehydes. *Chemistry – A European Journal* **2007**, *13*, 9068-9075.
87. Cruz, D. C.; Sanchez-Murcia, P. A.; Jorgensen, K. A., Formal asymmetric enone aminohydroxylation: organocatalytic one-pot synthesis of 4,5-disubstituted oxazolidinones. *Chem. Commun.* **2012**, *48*, 6112-6114.
88. Vesely, J.; Ibrahim, I.; Zhao, G.-L.; Rios, R.; Córdova, A., Organocatalytic Enantioselective Aziridination of α,β -Unsaturated Aldehydes. *Angew. Chem. Int. Ed.* **2007**, *46*, 778-781.
89. Rios, R.; Ibrahim, I.; Vesely, J.; Zhao, G.-L.; Córdova, A., A simple one-pot, three-component, catalytic, highly enantioselective isoxazolidine synthesis. *Tetrahedron Letters* **2007**, *48*, 5701-5705.
90. Deiana, L.; Zhao, G.-L.; Lin, S.; Dziedzic, P.; Zhang, Q.; Leijonmarck, H.; Córdova, A., Organocatalytic Enantioselective Aziridination of α -Substituted α,β -Unsaturated Aldehydes: Asymmetric Synthesis of Terminal Aziridines. *Advanced Synthesis & Catalysis* **2010**, *352*, 3201-3207.
91. Deiana, L.; Dziedzic, P.; Zhao, G. L.; Vesely, J.; Ibrahim, I.; Rios, R.; Sun, J.; Córdova, A., Catalytic Asymmetric Aziridination of α,β -Unsaturated Aldehydes. *Synfacts* **2011**, *2011*, 0900-0900.
92. Arai, H.; Sugaya, N.; Sasaki, N.; Makino, K.; Lectard, S.; Hamada, Y., Enantioselective aziridination reaction of α,β -unsaturated aldehydes using an organocatalyst and tert-butyl N-arenesulfonyloxycarbamates. *Tetrahedron Letters* **2009**, *50*, 3329-3332.

93. Fleischer, I.; Pfaltz, A., Enantioselective Michael Addition to α,β -Unsaturated Aldehydes: Combinatorial Catalyst Preparation and Screening, Reaction Optimization, and Mechanistic Studies. *Chemistry – A European Journal* **2010**, *16*, 95-99.
94. Hayashi, Y.; Gotoh, H.; Hayashi, T.; Shoji, M., Diphenylprolinol Silyl Ethers as Efficient Organocatalysts for the Asymmetric Michael Reaction of Aldehydes and Nitroalkenes. *Angew. Chem. Int. Ed.* **2005**, *44*, 4212-4215.
95. Han, S.-Y.; Kim, Y.-A., *Recent Development of Peptide Coupling Reagents in Organic Synthesis*. 2004; Vol. 60.
96. Heine, H. W.; King, D. C.; Portland, L. A., Aziridines. XII. The Isomerization of Some cis- and trans-1-p-Nitrobenzoyl-2,3-Substituted Aziridines. *J. Org. Chem.* **1966**, *31*, 2662-2665.
97. Heine, H. W.; Kenyon, W. G.; Johnson, E. M., The Isomerization and Dimerization of Aziridine Derivatives. IV. *J. Am. Chem. Soc.* **1961**, *83*, 2570-2574.
98. Ha, H.-J.; Suh, J.-M.; Kang, K.-H.; Ahn, Y.-G.; Han, O., A new synthesis of aziridine-2-carboxylates: Reaction of hexahydro-1,3,5-triazines or N-methoxymethylanilines with alkyl diazoacetates in the presence of lewis acid. *Tetrahedron* **1998**, *54*, 851-858.
99. Bucciarelli, M.; Forni, A.; Moretti, I.; Prati, F.; Torre, G., Regioselectivity of ring-opening reactions of optically active N-acetyl-2-methoxycarbonylaziridine. *Tetrahedron: Asymmetry* **1995**, *6*, 2073-2080.
100. Kim, Y.; Ha, H.-J.; Yun, H.; Lee, B. K.; Lee, W. K., Ring opening of 2-acylaziridines by acid chlorides. *Tetrahedron* **2006**, *62*, 8844-8849.
101. Ha, H.-J.; Jung, J.-H.; Lee, W. K., Application of Regio- and Stereoselective Functional Group Transformations of Chiral Aziridine-2-carboxylates. *Asian Journal of Organic Chemistry* **2014**, *3*, 1020-1035.
102. Wu, H.-H.; Sun, Y.-L.; Wan, C.-F.; Yang, S.-T.; Chen, S.-J.; Hu, C.-H.; Wu, A.-T., Highly selective and sensitive fluorescent chemosensor for Hg²⁺ in aqueous solution. *Tetrahedron Letters* **2012**, *53*, 1169-1172.
103. Donohoe, T. J.; Callens, C. K. A.; Flores, A.; Lacy, A. R.; Rathi, A. H., Recent Developments in Methodology for the Direct Oxyamination of Olefins. *Chemistry – A European Journal* **2011**, *17*, 58-76.
104. De Jong, S.; Nosal, D. G.; Wardrop, D. J., Methods for direct alkene diamination, new & old. *Tetrahedron* **2012**, *68*, 4067-4105.
105. Christie, S. D. R.; Warrington, A. D., Osmium and Palladium: Complementary Metals in Alkene Activation and Oxidation. *Synthesis* **2008**, *2008*, 1325-1341.
106. Nilov, D.; Reiser, O., The Sharpless Asymmetric Aminohydroxylation –Scope and Limitation. *Advanced Synthesis & Catalysis* **2002**, *344*, 1169-1173.

107. Wang, Z., Sharpless Aminohydroxylation. In *Comprehensive Organic Name Reactions and Reagents*, John Wiley & Sons, Inc.: 2010.
108. Kolb, H. C.; Sharpless, K. B., Asymmetric Aminohydroxylation. In *Transition Metals for Organic Synthesis*, Wiley-VCH Verlag GmbH: 2008; pp 309-336.
109. Masruri; Willis, A. C.; McLeod, M. D., Osmium-Catalyzed Vicinal Oxyamination of Alkenes by N-(4-Toluenesulfonyloxy)carbamates. *J. Org. Chem.* **2012**, *77*, 8480-8491.
110. Farid, U.; Wirth, T., Highly Stereoselective Metal-Free Oxyaminations Using Chiral Hypervalent Iodine Reagents. *Angew. Chem. Int. Ed.* **2012**, *51*, 3462-3465.
111. Brown, M.; Farid, U.; Wirth, T., Hypervalent Iodine Reagents as Powerful Electrophiles. *Synlett* **2013**, *24*, 424-431.
112. Knight, J. G.; Muldowney, M. P., Synthesis of N-p-Toluenesulphonyl-2-alkenyl Aziridines by Regioselective Aziridination of 1,3-Dienes. *Synlett* **1995**, *1995*, 949-951.
113. Llaveria, J.; Beltrán, Á.; Díaz-Requejo, M. M.; Matheu, M. I.; Castellón, S.; Pérez, P. J., Efficient Silver-Catalyzed Regio- and Stereospecific Aziridination of Dienes. *Angew. Chem. Int. Ed.* **2010**, *49*, 7092-7095.
114. Saikia, I.; Borah, A. J.; Phukan, P., Use of Bromine and Bromo-Organic Compounds in Organic Synthesis. *Chem. Rev.* **2016**, *116*, 6837-7042.
115. Lee, S.-H.; Yoon, J.; Nakamura, K.; Lee, Y.-S., Efficient Syntheses and Ring-Opening Reactions of trans- and cis-Oxazoline-5-carboxylates. *Organic Letters* **2000**, *2*, 1243-1246.
116. Williamson, K. S.; Yoon, T. P., Iron Catalyzed Asymmetric Oxyamination of Olefins. *J. Am. Chem. Soc.* **2012**, *134*, 12370-12373.
117. Heasley, V. L.; Louie, T. J.; Luttrull, D. K.; Millar, M. D.; Moore, H. B.; Nogales, D. F.; Sauerbrey, A. M.; Shevel, A. B.; Shibuya, T. Y., Effect of N-bromosuccinimide (NBS) and other N-brominating agents on the bromination of .alpha.,.beta.-unsaturated ketones in methanol. *J. Org. Chem.* **1988**, *53*, 2199-2204.
118. Heasley, V. L.; Spaite, D. W.; Shellhamer, D. F.; Heasley, G. E., Effect of a carbonyl group on the ring opening of a neighboring bromonium ion. *J. Org. Chem.* **1979**, *44*, 2608-2611.
119. Heasley, G. E.; Mark Janes, J.; Stark, S. R.; Robinson, B. L.; Heasley, V. L.; Shellhamer, D. F., Boron trifluoride promoted reactions of n-haloelectrophiles with alkenes. *Tetrahedron Letters* **1985**, *26*, 1811-1814.
120. Basavaiah, D.; Veeraraghavaiah, G., The Baylis-Hillman reaction: a novel concept for creativity in chemistry. *Chem. Soc. Rev.* **2012**, *41*, 68-78.

121. Octavio, R.; de Souza, M. A.; Vasconcellos, M. L. A. A., The Use of DMAP as Catalyst in the Baylis-Hillman Reaction Between Methyl Acrylate and Aromatic Aldehydes. *Synth. Commun.* **2003**, *33*, 1383-1389.
122. Shi, M.; Jiang, J.-K., Amendment in Titanium(IV) Chloride and Chalcogenide-Promoted Baylis-Hillman Reaction of Aldehydes with α,β -Unsaturated Ketones. *Tetrahedron* **2000**, *56*, 4793-4797.
123. Manarin, F.; Roehrs, J. A.; Gay, R. M.; Brandão, R.; Menezes, P. H.; Nogueira, C. W.; Zeni, G., Electrophilic Cyclization of 2-Chalcogenealkynylanisoles: Versatile Access to 2-Chalcogen-benzo[b]furans. *J. Org. Chem.* **2009**, *74*, 2153-2162.
124. Chen, Z.; Wen, H.; Li, W.; Zhou, J.; Hu, J.; Xia, W., One-Pot Synthesis of 2-Oxazolines from Ethyl α -Cyanocinnamate Derivatives with N-Bromoacetamide. *J. Heterocycl. Chem.* **2014**, *51*, 794-802.
125. Chen, Z.-g.; Xia, W.; Wen, H.; Wang, D.; Li, Y.-n.; Hu, J.-l., Synthesis of 2-oxazolines from ethyl α -cyanocinnamate derivatives with acetamide and N-bromosuccinimide. *Chemical Research in Chinese Universities* **2013**, *29*, 699-705.
126. Wu, X.-L.; Wang, G.-W., Aminohalogenation of Electron-Deficient Olefins Promoted by Hypervalent Iodine Compounds. *Eur. J. Org. Chem.* **2008**, *2008*, 6239-6246.
127. Wu, X.-L.; Xia, J.-J.; Wang, G.-W., Aminobromination of olefins with TsNH₂ and NBS as the nitrogen and bromine sources mediated by hypervalent iodine in a ball mill. *Organic & Biomolecular Chemistry* **2008**, *6*, 548-553.
128. Wei, J.-f.; Zhang, L.-h.; Chen, Z.-g.; Shi, X.-y.; Cao, J.-j., KI-catalyzed aminobromination of olefins with TsNH₂-NBS combination. *Organic & Biomolecular Chemistry* **2009**, *7*, 3280-3284.
129. Frump, J. A., Oxazolines. Their preparation, reactions, and applications. *Chem. Rev.* **1971**, *71*, 483-505.
130. Gant, T. G.; Meyers, A. I., The chemistry of 2-oxazolines (1985-present). *Tetrahedron* **1994**, *50*, 2297-2360.
131. Fujita, M.; Kitagawa, O.; Suzuki, T.; Taguchi, T., Regiocontrolled Iodoaminocyclization Reaction of an Ambident Nucleophile Mediated by Basic Metallic Reagent. *J. Org. Chem.* **1997**, *62*, 7330-7335.
132. Woo, J. C. S.; MacKay, D. B., Diastereoselective isothiourea iodocyclization for manzacidin synthesis. *Tetrahedron Letters* **2003**, *44*, 2881-2883.
133. Ahmad, S. M.; Braddock, D. C.; Cansell, G.; Hermitage, S. A.; Redmond, J. M.; White, A. J. P., Amidines as potent nucleophilic organocatalysts for the transfer of electrophilic bromine from N-bromosuccinimide to alkenes. *Tetrahedron Letters* **2007**, *48*, 5948-5952.

134. Guanti, G.; Narisano, E.; Banfi, L., DIASTEREOSELECTION IN TRIMETHYLSILYL TRIFLUOROMETHANESULFONATE CATALYZED REACTION OF SILYL KETENE ACETALS WITH IMINES. *Tetrahedron Letters* **1987**, 28, 4331-4334.
135. Hunt, P. A.; May, C.; Moody, C. J., Iodocyclisations of allyl- amidines and-ureas. *Tetrahedron Letters* **1988**, 29, 3001-3002.
136. Fletcher, S., The Mitsunobu reaction in the 21st century. *Organic Chemistry Frontiers* **2015**, 2, 739-752.
137. Denton, R. M.; An, J.; Adeniran, B.; Blake, A. J.; Lewis, W.; Poulton, A. M., Catalytic Phosphorus(V)-Mediated Nucleophilic Substitution Reactions: Development of a Catalytic Appel Reaction. *J. Org. Chem.* **2011**, 76, 6749-6767.